ANL-6797
Physics
(TID-4500, 26th Ed.)
AEC Research and
Development Report

ARGONNE NATIONAL LABORATORY
9700 South Cass Avenue
Argonne, Illinois 60440

INTERNATIONAL CONFERENCE ON NUCLEAR PHYSICS WITH REACTOR NEUTRONS, OCTOBER 15-17, 1963

(A Topical Conference of the American Physical Society)

Edited by
F. E. Throw

November 1963

Organizing Committee:

L. M. Bollinger
R. E. Coté
G. R. Ringo
R. K. Smither
F. E. Throw

This document is
PUBLICLY RELEASABLE
Barry Steele
Authorizing Official
Date: 2-7-07

Operated by The University of Chicago
under
Contract W-31-109-eng-38
with the
U. S. Atomic Energy Commission

DISCLAIMER

This report was prepared as an account of work sponsored by an agency of the United States Government. Neither the United States Government nor any agency Thereof, nor any of their employees, makes any warranty, express or implied, or assumes any legal liability or responsibility for the accuracy, completeness, or usefulness of any information, apparatus, product, or process disclosed, or represents that its use would not infringe privately owned rights. Reference herein to any specific commercial product, process, or service by trade name, trademark, manufacturer, or otherwise does not necessarily constitute or imply its endorsement, recommendation, or favoring by the United States Government or any agency thereof. The views and opinions of authors expressed herein do not necessarily state or reflect those of the United States Government or any agency thereof.

DISCLAIMER

Portions of this document may be illegible in electronic image products. Images are produced from the best available original document.

FOREWORD

The International Conference on Nuclear Physics with Reactor Neutrons was held at Argonne, Illinois, on 15—17 October 1963. It was sponsored by Argonne National Laboratory and was accepted as a topical conference by the American Physical Society. The abstracts of the contributed papers will be printed in the Bulletin of the American Physical Society.

The total registration was 207. Of these, 128 were physicists from other laboratories; 27 were from foreign countries. This relatively small group includes a high fraction of all experimental physicists who use reactor neutrons in nuclear physics experiments.

The subject matter of the conference was divided into five sessions. The opening session was concerned with the fundamental properties of the neutron. The papers on this topic, which were largely concerned with proposals for new and more refined experiments, indicate that experiments with thermal neutrons will in the future continue to be an important source of information about the fundamental properties of the neutron.

Sessions II and III and part of IV were concerned with neutron-capture gamma rays. These sessions were especially significant because they permitted a thorough survey of what is currently the most active area of nuclear physics performed with reactor neutrons. An indication of the intensity of the interest in neutron-capture gamma rays is that precision instruments and measurements were described by workers from Munich (Germany), Risø (Denmark), Studsvik (Sweden), Chalk River (Canada), Los Alamos, Livermore, and Argonne. With an effort of this magnitude, it is clear that the study of neutron-capture gamma rays is and will continue to be one of our principal sources of information about the nuclear level structure and decay schemes of heavy nuclides.

Although the discussion of measurements with precision instruments was the largest single topic covered by the conference, an impressively large number of papers showed that other kinds of experiments with neutron-capture gamma rays are also giving interesting results.

Examples are angular-correlation measurements on coincidence gamma rays, the study of spectra from targets with very low neutron cross sections, the study of spectra from resonant neutron capture, and measurements on the resonant scattering of capture gamma rays.

The final two subjects of the conference were neutron cross sections and fission. Although many experiments in both of these areas of research now make use of sources other than reactor neutrons, the papers presented at the conference showed that reactors continue to be the best source for many important measurements. For example, cross-section measurements on separated isotopes are best made with a fast-chopper time-of-flight neutron spectrometer. Similarly, the recent successful development (Munich) of a magnetic mass analyzer for fission fragments depends on the high intensity of fragments that can be produced with reactor neutrons.

In preparing this volume of Proceedings, editorial dabbling with the texts of the papers was kept to a minimum. If errors crept in despite the care taken, the editor offers his sincere apologies. In the interest of prompt publication, proof copies were not sent to the authors.

The scientific secretaries of the respective meetings checked the transcripts of the discussions with the participants. In a number of cases, the discussers quite thoroughly revised their statements in accordance with the announced desire that the Proceedings should "say what [each author] wishes he had said at the meeting." Consequently, some editing was required to preserve the connections between independently revised statements.

The scientific secretaries and the editor wish to express their thanks to all those who contributed manuscripts for this volume. Their courtesy and promptness were essential to the prompt publication. For the 100% cooperation, which we understand is quite unusual, we are most grateful.

Thanks are also due to Mr. W. G. Terry and Mr. George Kozuch of Leon M. Golding and Associates, Chicago — the court reporters who provided prompt transcripts for the discussions and many of the papers. Without them, this complete report would not have been feasible.

Finally, it is a pleasure to acknowledge the care and patience of the Physics Division secretaries who typed the multilith plates: Mrs. Kay M. Pemble, Miss Jo Miller, Mrs. Judy Miller, and Miss Barbara Baldwin.

TABLE OF CONTENTS

Session I. FUNDAMENTAL PROPERTIES OF THE NEUTRON — PAGE

I-1. THEORY OF FUNDAMENTAL PROPERTIES OF THE NEUTRON
R. M. Thaler. 2

I-2. THE NEUTRON-ELECTRON INTERACTION
V. E. Krohn. 15

I-3. PROPOSED EXPERIMENT TO OBSERVE n-n SCATTERING
C. O. Muehlhause. 21

I-4. SEARCH FOR PARTICLE-STABLE TETRANEUTRONS AND DINEUTRONS IN FISSION
J. P. Schiffer and R. Vandenbosch. 27

I-5. ACCELERATION OF FREE NEUTRONS UNDER GRAVITY
D. Paya, J. W. T. Dabbs, J. A. Harvey, and H. Horstmann. 30

I-6. MEASUREMENT OF THE POLARIZATION OF THERMAL-NEUTRON BEAMS BY MAGNETIZED MIRRORS
M. T. Burgy, G. R. Ringo, S. Ketudat, P. Rice-Evans, and S. Barkan. 35

I-7. THE MAGNETIC-MIRROR NEUTRON POLARIZER AT THE REACTOR "ISPRA 1"
M. Forte. 45

Session II. PRECISION MEASUREMENTS OF CAPTURE GAMMA-RAY SPECTRA — PAGE

II-1. APPLICATIONS OF NUCLEAR MODELS TO LOW-LYING STATES—SUMMARIES AND DEVELOPMENTS
Steven Moszkowski. 58

II-2. CAPTURE GAMMA DETERMINATION OF VANADIUM-52 STRUCTURE
D. H. White, W. John, and B. G. Saunders 79

II-3. ROTATIONAL AND VIBRATIONAL EFFECTS IN NEUTRON-CAPTURE GAMMA-RAY SPECTRA
R. K. Smither. 89

II-4,5,6. RISØ CURVED-CRYSTAL SPECTROMETER
O. W. B. Schult, B. P. Maier, U. Gruber, and R. Koch. 111

II-7. CAPTURE GAMMA RAYS FROM DYSPROSIUM
H. T. Motz and R. E. Carter. 133

II-8. BENT-CRYSTAL MEASUREMENTS ON GAMMA RAYS FROM NEUTRON CAPTURE IN INDIUM
W. John and R. W. Jewell. 143

II-9. INVESTIGATION OF NEUTRON CAPTURE IN SAMARIUM USING A HIGH-RESOLUTION CONVERSION-ELECTRON SPECTROMETER
E. Bieber. 148

PAGE

II-10. RECENT DEVELOPMENTS IN PRECISION DIFFRACTION MEASUREMENTS RELATED TO NEUTRON-CAPTURE γ-RAY SPECTRA

J. W. Knowles. 156

II-11. CAPTURE GAMMA RAYS AND NEUTRON BINDING ENERGIES

R. E. Carter and H. T. Motz. 179

II-12. NUCLEAR PHYSICS BY THE CHALMERS GROUP AT THE SWEDISH RESEARCH REACTORS

Sam Nilsson, R. Hardell, J. Rohlin, and B. Lundqvist. 183

Session III. OTHER EXPERIMENTS WITH CAPTURE GAMMA RAYS

III-1. THE COLLECTIVE MODEL IN RELATION TO NEUTRON-CAPTURE GAMMA-RAY SPECTRA

D. M. Brink. 194

III-2. PARTIAL WIDTHS FOR E1 GAMMA RAYS FROM NEUTRON RESONANCES AND THEIR RELATION TO THE GIANT RESONANCE. . .

R. T. Carpenter. 211

III-3. NEUTRON-CAPTURE GAMMA-RAY SPECTRA AND THE M1 GIANT RESONANCE

I. Bergqvist, B. Lundberg, and N. Starfelt 220

PAGE

III-4. GAMMA-RAY SPECTRA FROM RESONANCE NEUTRON CAPTURE IN THE TIN ISOTOPES

J. A. Harvey, G. G. Slaughter, J. R. Bird, and G. T. Chapman. 230

III-5. THERMAL NEUTRON CAPTURE IN D AND O^{16}

E. T. Jurney and H. T. Motz. 236

III-6. Withdrawn

III-7. STUDY OF THE NEUTRON-CAPTURE GAMMA RAYS IN Ca^{48}

Sol Raboy and C. C. Trail. 243

III-8. NEUTRON CAPTURE BY DEUTERIUM

C. C. Trail and S. Raboy. 247

III-9. $Cr^{53}(n,\gamma)Cr^{54}$ REACTION

M. R. Gunye and G. A. Bartholomew. 259

III-10. GAMMA-RAY ANGULAR CORRELATIONS IN Ca^{45}, Fe^{55}, Ni^{59}, Ni^{61}, and Ni^{63}

R. E. Coté, H. E. Jackson, Jr., L. L. Lee, Jr., and J. P. Schiffer. 270

III-11. VARYING THE ENERGY OF NEUTRON-CAPTURE GAMMA RAYS

G. Ben-David, B. Arad, and I. Pelah. . . . 271

III-12. NUCLEAR RESONANT SCATTERING OF THERMAL NEUTRON CAPTURE GAMMA RAYS

B. Arad, G. Ben-David, I. Pelah, and Y. Schlesinger. 275

PAGE

III-13. MEASUREMENT OF (γ,n) CROSS SECTIONS WITH NEUTRON-CAPTURE GAMMA RAYS

L. Green, R. R. Hurst, and D. J. Donahue 288

III-14. TOTAL RADIATION WIDTHS FOR s-WAVE AND p-WAVE NEUTRON CAPTURE IN Nb^{93}

H. E. Jackson. 294

Session IV. NEUTRON CROSS SECTIONS

IV-1. STATISTICAL PROPERTIES OF NUCLEAR STATES AND TRANSITIONS

Norbert Rosenzweig. 302

IV-2. DISTRIBUTION OF PARTIAL RADIATION WIDTHS

L. M. Bollinger, R. E. Coté, R. T. Carpenter, and J. P. Marion. 322

IV-3. RESONANCE NEUTRON COINCIDENCE CAPTURE GAMMA-RAY SPECTRA IN W^{184}

J. A. Moore, J. L. Friedes, R. E. Chrien, and H. Palevsky. 324

IV-4. FLUCTUATIONS IN PARTIAL RADIATION WIDTHS OF U^{239}

H. E. Jackson. 333

IV-5. RESONANCE REACTIONS AND THE NUCLEAR SHELL MODEL

R. H. Lemmer. 342

PAGE

IV-6. OPTICAL-MODEL INTERPRETATION OF NEUTRON STRENGTH FUNCTIONS

P. A. Moldauer. 358

IV-7. SPIN OF SOME LOW-ENERGY NEUTRON RESONANCES BY RESONANCE SCATTERING

F. Poortmans and H. Ceulemans. 363

IV-8. SMALL-SAMPLE TRANSMISSION MEASUREMENTS ON Pu^{241}, USING AN ELECTRON-LINAC PULSED-NEUTRON-SOURCE TIME-OF-FLIGHT SPECTROMETER

N. J. Pattenden and S. Bardsley. 369

IV-9. A TIME-SHARED COMPUTER-CENTERED DATA-COLLECTION SYSTEM AT THE BROOKHAVEN GRAPHITE RESEARCH REACTOR

R. E. Chrien, S. Rankowitz, and R. J. Spinrad. 376

IV-10. SLOW-NEUTRON CROSS SECTION OF He^3, B, AND Au; AND A He^3 PROPORTIONAL COUNTER FOR THE ABSOLUTE DETERMINATION OF NEUTRON BEAM INTENSITY

J. Als-Nielsen, A. Bahnsen, and O. Dietrich 384

IV-11. Withdrawn

IV-12. RADIOMETRIC DETERMINATION OF THE NEUTRON-CAPTURE CROSS SECTION OF 35-HR Rh^{105}

L. E. Glendenin and H. C. Griffin. 388

PAGE

IV-13. ANGULAR DISTRIBUTION OF GAMMA RAYS FROM (n,n'γ) REACTIONS PRODUCED BY FAST NEUTRONS FROM A REACTOR

R. D. Roberts and D. J. Donahue. 389

IV-14. COHERENT NUCLEAR SCATTERING AMPLITUDES AND CROSS SECTIONS AS DETERMINED BY NEUTRON-DIFFRACTION TECHNIQUES

M. H. Mueller, S. S. Sidhu, L. Heaton, R. L. Hitterman, and H. W. Knott. 393

IV-15. NMR OF SHORT-LIVED NUCLIDES BY POLARIZED NEUTRON CAPTURE AND β-DECAY ANISOTROPY

D. W. Connor, T. Tsang, and D. L. Davis. . . 397

Session V. THE FISSION PROCESS

V-1. THE THEORY OF FISSION

Lawrence Wilets. 406

V-2. STATISTICAL THEORY OF FISSION AND KINETIC ENERGY DISTRIBUTION

Peter Fong. 416

V-3. EXPERIMENTS ON FISSION USING THERMAL NEUTRONS

H. Maier-Leibnitz. 424

V-4. INSTRUMENTATION FOR FISSION-FRAGMENT ENERGY CORRELATION EXPERIMENTS WITH PILE-UP REDUCTION CAPABILITIES

C. W. Williams, H. W. Schmitt, F. J. Walter, and J. H. Neiler. 438

PAGE

V-5. CORRELATED FRAGMENT-ENERGY MEASUREMENTS FOR LOW-ENERGY NEUTRON-INDUCED FISSION

F. J. Walter, H. W. Schmitt, and J. H. Neiler. 441

V-6. EMISSION OF PROMPT GAMMA RAYS IN THE THERMAL-NEUTRON FISSION OF U^{235}

S. S. Kapoor and R. Ramanna. 449

V-7. DIRECT AND ABSOLUTE MEASUREMENT OF AVERAGE YIELD OF NEUTRONS FROM THERMAL FISSION OF U^{235}

A. DeVolpi and K. Porges. 450

V-8. NEW METHOD FOR THE DETECTION OF SHORT-LIVED FISSION PRODUCTS

D. Hovestadt and P. Armbruster. 455

V-9. INVESTIGATION OF QUASI-ADIABATIC ATOMIC COLLISIONS BY FISSION PRODUCTS

P. Armbruster, H. Specht, and A. Vollmer 464

Session I

FUNDAMENTAL PROPERTIES OF THE NEUTRON

Tuesday morning, 15 October 1963

Presiding: M. Hamermesh

Scientific secretaries:

G. R. Ringo
L. L. Lee, Jr.

I-1. THEORY OF FUNDAMENTAL PROPERTIES OF THE NEUTRON*

R. M. Thaler

Case Institute of Technology, Cleveland, Ohio

In preparing this talk for you, I began to write down what I expected to be a brief introduction. The introduction however, ran away with itself, and what I shall present here is that brief introduction cut down somewhat so that it will fit the allotted time. I present it with some trepidation, in the hope that it can serve as a preface to this conference. I feel as out of my element at this platform, denuded of both chalk and equations, as Gypsy Rose Lee felt when, in promotion of her novel she found herself speaking to a large audience: absolutely fully clothed.

Nuclear physics has become a venerable subject. Rutherford discovered the existence of the atomic nucleus in 1911, and the mass of nuclei was investigated by J. J. Thompson in 1913. For the next two decades or so, however, the nucleus was a charged particle at the center of the atom. These events predated the existence of most of the people in this room, and certainly preceded the professional existence of virtually everyone here. Attention was primarily focused in those years in the area now neatly labeled "atomic physics" in the undergraduate physics curriculum.

In order to explain the observation that $A \gtrsim 2Z$, it was hypothesized that the nucleus was composed of A protons and (A - Z) electrons. In 1931 Ehrenfest and Oppenheimer pointed out that N^{14}, which obeyed Bose-Einstein statistics, could not consist of an odd number of Fermi-Dirac particles (14 protons and 7 electrons). The following year (1932) the neutron was experimentally observed (Curie-Joliot and Joliot; Chadwick) and was tamed by Fermi and collaborators shortly thereafter (1934). These events mark the beginnings of that discipline which is now labeled "nuclear physics" in the undergraduate physics curriculum of a growing number of institutions.

---

*Invited paper.

On this basis, the neutron and proton were postulated as the fundamental constituents of nuclear matter by Heisenberg (1932). That this has proved a fruitful point of view can hardly be doubted. Thus in the years 1932-1934 nuclear physics took on its modern aspect. Further recent developments are sometimes also referred to as nuclear physics. Today these developments are most frequently called "elementary-particle" or just "particle" physics, to distinguish it from classical nuclear physics.

Thus we recognize that the history of nuclear physics begins with the neutron. However, the problem of β decay was a formidable obstacle to the acceptance of this postulate. Fermi solved this problem in 1934. Thenceforth the central problems of classical nuclear physics were two: (a) to determine the forces between nucleons primarily from nucleon-nucleon scattering experiments and (b) using this information, to calculate the static and dynamic properties of nuclei. Wigner (1933) showed us how to approach this problem, and demonstrated that the nuclear force was short ranged and strong within that range.

It took 25 years for there to be substantial further progress along that line. Within the last five years or so real progress was made on these problems (Signell-Marshak, Gammel-Thaler, Breit and collaborators). This work represents a significant measure of progress in the classical problem of nuclear physics. But what has emerged has been that this problem is essentially truly insoluble in its classic formulation. The pragmatic reason for this difficulty lies in the key phrase "off the energy shell." From the data on the scattering of nucleons from nucleons one may indeed construct a potential exchange dependence, spin dependence, etc. (or its equivalent — the V, S, or T, matrix) which fits the data. Such a potential cannot be unique however. Rather, at best we find a family of V, T, S matrices which coincide "on the energy shell" — i.e., for the case where the incident and scattered wave numbers are equal in magnitude.

However, a complete specification requires "off the energy shell" information and this cannot be gotten from elastic-scattering data alone. Further, in the nuclear-structure problem, "off the energy shell" contributions make significant contributions so that we can expect different results in our calculations from different models which fit the elastic-scattering data equally well. This is not a fatal defect, however, since the phenomenological description of the nuclear force then must simply be based on both nucleon-nucleon elastic-scattering data and the data on composite nuclei. However, it is not a prospect which gladdens the heart of even the most dogged theoretical physicist.

Historically we must now return to a parallel development. Soon after the central problem of classical nuclear physics was formulated in roughly the terms described above (in the early 1930's) Yukawa proposed a "meson" field theory analogous to the electromagnetic field theory — with the finite mass of the meson accounting for the short range of the nuclear force. The discovery in 1937 of particles of the expected mass was seen as a triumph for this idea. Now we know that these were the wrong kind of mesons — they were, of course, μ mesons. The right kind of mesons — π mesons — were not observed until 1947. Experiments with π mesons, particularly π-nucleon scattering, and their theoretical interpretation came even later (Fermi et al. 1954; Brueckner 1952; Chew 1953). During this period too, field theory, stimulated by the Lamb-Retherford experiment (1947) was developed into a full-blown discipline (Bethe 1947; Feynman 1949; Dyson 1949). However, the story, as we all know, does not have a happy ending. These developments which augured so well came grinding to a halt. A number of attempts have been made to calculate the nuclear force on a renormalized field-theoretic basis (Brueckner and Watson, Gartenhaus). These have met with limited quantitative success at best, although they do offer what appears to be a qualitatively correct picture. What then appeared to be a hopeful line of attack

which would allow us to calculate the nuclear force from first principles (and hence, among other advantages, circumvent the "off the energy shell" problem) did not finally live up to its promise.

New lines of attack are at present under investigation — about which more later. The picture I have just given you brings us up more or less into the latter part of the last decade, or the earliest part of this decade.

Let's talk about the neutron itself for a moment. What are its known properties? We know the mass of the neutron, its spin, its electric charge, its magnetic moment. These properties are rather well fixed — mass 939.505 MeV; spin $\frac{1}{2}$; electric charge 0. In fact a knowledge of these three properties is sufficient to much research in which the neutron is used as a tool—to study the structure of crystals, for example. But we know much more about the neutron. We give it a baryon number. We talk about the mass distribution and the charge distribution and the magnetic-moment distribution in the neutron. How can we know such things, or even talk about them? No one has ever identified a neutron directly through his five senses. The neutron is after all very much a mental construct. But putting aside very firmly the philosophical questions involved, we still find that we know the neutron or any other subatomic particle only through its interactions with other particles.

So I'd like to talk now about the properties of the neutron as a nucleon, in terms of its interactions. This is very much a field-theoretic approach, but one which requires that we know no field theory to discuss together.

Let's first categorize the various types of interactions of nature that we know about. In order of increasing strength these are: (1) GRAVITATIONAL INTERACTION, (2) WEAK INTERACTION, (3) ELECTROMAGNETIC INTERACTION, and (4) STRONG INTERACTION. Field theoretically we classify these interactions in terms of the strength of the coupling constant. The electromagnetic coupling constant is the familiar

$e^2/\hbar c = 1/137$. In fact the coupling constant represents the square of the fundamental natural unit of charge in dimensionless units. For the gravitational interaction we get a coupling constant of the order of 10^{-56}. The weak interactions are characterized by a coupling constant of the order of 10^{-14}. The electromagnetic coupling constant is 10^{-2}. The strong interactions have a coupling constant of the order of 10^{-1}.

Clearly the gravitational force is too weak to be of any practical interest (on the subatomic scale, of course) for some time to come. We do know experimentally that slow neutrons fall down and are no different in their interaction with the gravitational field than other material particles. We should very much like to know whether antiparticles fall "up" or "down." Such experiments are very difficult and, as the old saying goes, are "beyond the present state of the art." From the point of view of nuclear physics, we can simply say that gravitational forces simply do not exist.

Turning now to the weak interactions, we see that the weak interactions are very much stronger relative to the gravitational interaction than they are weak relative to the strong interactions. The relevant coupling constants are $\sim 10^{-1}$, $\sim 10^{-14}$, $\sim 10^{-56}$. You are all aware that this has been a very exciting field recently. The furor has now died down somewhat, but the field is still very much alive. The parity revolution culminated in the very beautiful paper of Feynman and Gell-Mann. I strongly recommend this paper to your attention. It is a true work of art! In this paper the old ideas of Fermi are reworked, in a manner suggested by parity-nonconservation, to reveal a new underlying simplicity. From the point of view of β decay, this represents a satisfactory solution which will stand indefinitely. The suggestions of the universal Fermi interaction and the conserved vector current are another matter which is under current investigation.

Again, however, from the viewpoint of the strong interactions, the weak interactions essentially never take place. This means, mainly that we never have to consider them together.

Now we come to the electromagnetic interactions. Here the story changes. The electromagnetic interactions are very much stronger than the gravitational and weak interactions and only slightly weaker than strong interactions. To emphasize this, I sometimes say that the renormalized mesic charge is only a factor of three or so greater than the electric charge. That is, the fact that $(e^2/\hbar c) \approx 1/137$ whereas $(g^2/\hbar c) \approx 0.08$ implies $e = 0.3\,g$. This implies, among other things, that it will not be possible to completely separate nuclear effects from electric effects. Sometimes this is useful to use, sometimes the reverse. One of the most familiar of such effects is the Coulomb-nuclear interference term in the scattering of charged particles.

Since the electron is a purely electromagnetic particle, in our present view of things, we shall talk first about the interactions of electrons with nucleons. First, what do the words "purely electromagnetic" mean? They mean that the interactions between electrons and other particles can be explained without the postulation of any forces other than electromagnetic forces. In this connection, then, the electron-neutron interaction is the most interesting phenomenon. The question to be answered experimentally is: is there a specific electron-neutron interaction beyond the purely electromagnetic one? You will hear more about that later in the program. Here we must, however, be very certain that we fully understand the nature of the electromagnetic interaction or we may fool ourselves. For example, Foldy pointed out many years ago that a small but important contribution arises in a careful relativistic treatment which may easily be overlooked in an intuitive nonrelativistic treatment. Further, such an interaction is far from necessarily at odds with our first comment about the pure electromagnetic nature of the electron. Our interpretation of such an interaction would be made in terms of the picture of the

neutron as being (part of the time, at least) a proton plus a negatively charged π meson. This is another example, then, of how the electromagnetic and strong interactions must be treated together.

Whatever the interpretation of the result in mesic terms, the hard fact remains that a specific electron-neutron interaction implies a distribution of charge in the neutron. The zeroth moment is the total charge. This is necessarily zero. Foldy has pointed out that the electron-neutron interaction specifically measures the second moment of the charge distribution. You will hear later this morning that the experiments yield a surprisingly small value for this second moment. This is really a surprise — since it implies that the charge distribution cannot be of the form we might expect. That is, it cannot be a positive core surrounded by a shell containing an equal amount of negative charge. If a substantial fraction of the fundamental charge is contained in this core, say 30%, then the value for the electron-neutron interaction would be much larger than measured, since the outside charge is weighted so much more heavily in the second moment. So from the electron-neutron interaction we have learned that either the charge distribution in the neutron is everywhere zero (for "zero" read "small"); or else that the charge distribution is complicated, consisting of at least an "up," a "down," and another "up."

The high-energy electron-scattering experiments of Hofstadter and collaborators at Stanford and R. R. Wilson and collaborators at Cornell have given us a new picture of the nucleons. These experiments forever banish the picture of the nucleons as point particles. From these scattering experiments, we may recover, with innumerable ifs and buts, the charge and magnetic-moment distribution in the nucleons. These distributions do not lead to a simple picture of the neutron. The neutron now appears to have a core of positive charge, surrounded by a region of negative charge, with, finally, a shell of positive charge outside the whole beast. It is interesting to note that this vast structure of experiment and analysis rests squarely on the shoulders of the measurement of the electron-neutron

interaction. Without the specific information that the second moment of the charge distribution was necessarily small, it would have been much more difficult to have determined a detailed picture of the charge distribution as a core of radius about $\frac{1}{2}$ F containing total charge ~ 0.3 e, a slightly greater amount of negative charge extending out to about 3 times that radius, and finally a shell of POSITIVE charge outside it all containing a few percent of e.

Another property of the nucleon that may be studied via the electromagnetic interaction is its electric polarizability. We speak primarily of the polarizability of the neutron only because the zero charge of the neutron makes its polarizability more readily accessible to measurement. Here the effect is that a charged particle near a neutron may induce in the neutron an electric dipole moment. The electric polarizability is a measure of how easily this may be accomplished. Notice how closely this is tied to the results we were just discussing. If the neutron were characterized by zero charge density everywhere, it could not be polarized. On the other hand, a knowledge of the charge distribution is not enough to yield the electric polarizability. Low-energy neutron scattering from nuclei leads to an upper limit for the polarizability. At present this is not an exciting result simply because the upper limit so determined is much greater than might be expected on meson theoretic grounds.

The point of view is clear. We believe we understand the electromagnetic interactions. Hence we may use the information we have gained in those studies as data relating to the strong interactions. We must now try to understand the measured electric-charge and magnetic-moment distributions (or equivalently the electric and magnetic form factors) in mesic terms. There are some interesting speculations about this which I hope to mention later.

Of course, you know there is a chance that everything I've said is all hooey — that there is a nonelectromagnetic neutron-electron force and that the zero result comes from cancellation between that and a second-moment contribution. This possibility is not taken very seriously right now.

The indisputable success of quantum electrodynamics leads us to take seriously any electromagnetic effects which we can predict. Polarization of the vacuum is such an effect. Briefly, a polarization of the vacuum arises from the existence of the electron-positron field, which, from the point of view of the potential energy, leads to a small additional term. This is the effect that accounts for the Lamb shift. It is also just barely observable in very-low-energy proton-proton scattering. (This, by the way, is an experimental problem which merits further work.) Again, though, our present expectations are that this effect is understood. It needs to be taken into account primarily to disentangle data primarily relevant to the strong interactions — subject always to the usually unstated assumption that more data on so fundamental a question is always welcome and our firmly-held theories will at once be abandoned when experiment proves them untenable.

We come now to the strong interactions. Here the mysteries multiply. In fact, at the moment it appears that strongly interacting particles breed like rabbits. It takes several pages to write them down and they tax the bounds of the Greek alphabet, even with sub- and superscripts. But for a while anyway, let's stick to nucleons — just old fashioned neutrons and protons.

I mentioned earlier that the classic problem of nuclear physics was to study the scattering of nucleons by nucleons in order to discover the force between them. Assuming for a moment that this has been successfully and uniquely accomplished, we have, from a fundamental point of view, found the data which the meson theory of nuclear forces must explain on a more fundamental basis. The situation is entirely

analogous to the one we discussed a few moments ago. From the electron-scattering data, we may assume we have found the electromagnetic structure of the nucleon in terms of the charge and moment distributions. It is now the business of the theory of strong interactions to explain these. In both cases it may very well turn out that the intermediate step of the phenomenological potential or distribution will prove an unnecessary detour and that the fundamental theory will deal directly with scattering amplitudes or form factors. In that case they serve only the function of helping us draw pictures; most of us visualize very much better in coordinate space than we do in momentum space.

In view of the emphasis I have placed on the relatively large strength of the electromagnetic interactions, it would be ludicrous for me to launch immediately into the theorist's Alice in Wonderland where the electromagnetic interaction can be switched off at will. So let's make the transition gradual by discussing the twilight zone where strong and electromagnetic interactions are both important.

We have already mentioned one such: vacuum polarization in p-p scattering. A precision determination of the p-p scattering length requires a suitable subtraction of this effect. If we are to study the charge independence of nuclear forces, all such effects must be treated with care. Back in the days when the specter of charged and neutral π mesons of differing mass did not haunt us, we could state this very simply. Charge independence of nuclear forces meant that, to within the restrictions implied by the exclusion principle, the forces between nucleons were identical except for electromagnetic effects. We might thus expect that the measured singlet scattering lengths in n-p and p-p scattering should coincide when corrected for electromagnetic effects. Schwinger in 1950 showed that the discrepancy that remained after correction for the Coulomb interaction vanished when the magnetic interaction was also taken into account. That reconciliation of the two scattering lengths became untenable with the introduction of the hard core (Salpeter 1953), since the magnetic interaction

contains a delta function centered at the origin. Recently, however, the new data on the electromagnetic structure of the nucleons has shed new light on the problem and a definitive calculation can be made. In brief, the final conclusion remains the same — the small residual discrepancies are of the order that could be explained by the pion mass difference, but that calculation is uncertain.

Incidentally, there is still need for much precision data on low-energy neutron-proton scattering (and high-energy too, for that matter). And blessed is he who does neutron-neutron scattering.

Charge independence leads to the idea of isotopic spin, and is central to our idea that neutron and proton are different aspects of the same entity, the nucleon. Any violation of this hypothesis which was not electromagnetic in origin would seriously affect the whole structure of elementary-particle physics.

In whatever time is left now, let's talk about the strong interactions in what we regard as a more fundamental way — that is, in terms of mesic theory. Earlier we mentioned in passing, as it were, the hopeful development of a field theory with the π mesons as the mediating particles. Experiments on pion-nucleon scattering (and their interpretation) a decade ago led us to the kind of understanding of the properties of mesic fields which should have sufficed for the calculation of the nuclear force. The nature of the field was clearly identified, and field theoretic techniques to handle the pseudoscalar field were sharpened. And in fact Brueckner and Watson (1953) emerged with a qualitatively correct picture of the nuclear force. But there it stopped.

The reason is not hard to see. Field theory, even in its renormalized form, is a perturbation expansion. That is to say, it is a power-series expansion in the coupling constant. Let us assume that the field theory is completely correct in all its details. None the less, the series may not converge. We are very used to this sort of thing. Suppose for a moment that we had solved a certain problem in a series expansion

in ϵ, and had gotten the result $1 - \epsilon + \epsilon^2 - \epsilon^3 + \epsilon^4 \ldots$ as a result. And suppose further that in the problem at hand $\epsilon = 2$. The series $1 - 2 + 4 - 8 + 16 - 32 + \cdots$ shows no tendency toward yielding a useful answer. Now Sommerfeld might have done the same problem, say, in parabolic coordinates and found the answer in closed form to be $1/(1 + \epsilon) = 1/3$ for $\epsilon = 2$. On the other hand, for $|\epsilon| \ll 1$ the series and closed-form solution coincide. In fact, all we needed to get the answer $1/(1 + \epsilon)$ from the series $1 - \epsilon + \epsilon^2 - \epsilon^3 \cdots$ was the added information that the series represented an analytic function of ϵ, and we could have gotten the closed-form answer from the series by analytic continuation.

The point of this illustration, I think, need not be belabored. The only place we have had trouble with field theory has been for the strong interactions. Quantum electrodynamics has been most successful; the theory of the weak interactions gives us no trouble.

As an aside, let me hasten to add that I do not think the difficulties with the perturbation treatment of field theory are as simple minded as my illustration. Dyson, I believe, has shown that there is reason to suspect the quantum electrodynamics does not converge — so that the perturbation series may be more in the nature of an asymptotic or semiconvergent series — the first umpteen terms of which sum to an approximation to the function, but which finally diverges.

What I have tried to do is give a brief motivation for all the work in analytic properties or dispersion theory which has so occupied the attention of theorists of late. Field theory works when the coupling constant is small enough. For the weak interactions the leading term suffices.

Field theory has not been entirely unsuccessful in the nuclear-force problem either. Speaking in terms of potentials, an unnecessary but visually useful device, the lowest order term in the perturbation expansion gives the so-called one-pion-exchange term, which is simply our old friend the Yukawa potential with range given by the pion mass and

strength given by the coupling constant. Since the contributions of all higher order terms is of shorter and shorter range, it is possible to isolate the one-pion contribution by looking at angular-momentum states sufficiently high that the angular-momentum barrier screens out the shorter range contributions. This sort of study, by Moravcsik and other collaborators of Chew at Livermore, showed us that the nucleon-nucleon scattering data were indeed completely consistent with our meson-theoretic ideas as to the nuclear force.

Here an accident of nature made the problem extra hard. The pseudoscalar character of the mesons made the one-pion-exchange term very much less important relative to the two-pion-exchange term than would have been the case for a scalar theory. This meant, in practice, that little information relevant to nuclear physics could be gained from a study of the leading term in the perturbation expansion.

I recall Feynman having remarked, with justifiable pride in his achievements, that we now know everything about the WEAK interactions and nothing about the STRONG. I should like here to maintain — not entirely facetiously — that we know just as much. Namely, in both cases we only know definitely the lowest order contributions. The hooker is that for the weak interactions the lowest order term suffices.

With the expansion of the number of strongly-interacting elementary particles, new and even more interesting problems arise. About these, time will permit not even the briefest of remarks. I want to point out, however, that these phenomena cannot be ignored in low-energy nuclear physics. We have already mentioned the example of the neutron-electron interaction, in which a purely relativistic effect is being measured at very low energies. The charge distributions of the nucleons are explained in terms of the ω and ρ resonances. The percent D state of the deuteron is very strongly affected by mesic exchange currents. Low-energy neutron scattering is affected by the production of virtual charged pions.

On this note I close. Thank you for your patience.

I-2. THE NEUTRON-ELECTRON INTERACTION*

V. E. Krohn

Argonne National Laboratory, Argonne, Illinois

I would like to discuss the reasons for our continuing interest in the measurement of the electron-neutron interaction with low-energy neutrons. I will briefly mention the connection with the theory of nucleon structure and with the high-energy electron-scattering experiments which investigate nucleon structure. Then I will discuss the various methods which have been used to measure this interaction with low-energy neutrons.

When the first measurements of the electron-neutron interaction became available in the late forties, as the previous speaker has mentioned, most theorists were surprised that the result was as small as it turned out to be. Then Foldy pointed out an effect, not previously appreciated, which seemed to account for the entire observed interaction all by itself. Since the Foldy term has already been discussed at some length, I will merely point out the magnitude of this term. In order to do this, I will adopt the usual convention, which is to talk about the electron-neutron interaction in terms of the potential which would give it, if that potential were effective over a sphere having a radius equal to the classical radius of the electron. Then the Foldy effect is -4080 eV.

Measurements, even to this date, have not definitely established a difference between the Foldy term and the total interaction, although it is obvious that there ought to be a difference. There is apparently a fortuitous cancellation of the second moment of the intrinsic charge distribution of the neutron.

As far as the electron-scattering measurements are concerned, as Professor Thaler has pointed out, these give greater detail about nucleon structure than is obtained from the electron-neutron

---

* Invited paper.

interaction alone, and recently these measurements have led to determinations of the low-energy electron-neutron interaction with uncertainties somewhat smaller than the magnitude of the effect. However, it would appear that for some time to come the scattering measurements will not give the value of the electron-neutron interaction with a precision comparable to that which can be achieved with low-energy neutrons. Since this result is obviously a severe test of any detailed theory of nucleon structure, there is good reason to seek the most precise and reliable experimental value that can be obtained from experiments involving low-energy neutrons.

Let me now discuss briefly the various methods used to measure the electron-neutron interaction with low-energy neutrons. One of these was first used by Havens, Rabi, and Rainwater. It involves transmission measurements on liquid metals. I should mention that, as is the case with the other two methods, this method looks at the scattering amplitude rather than the cross section. In the total cross section for the scattering of neutrons by an atom there is, in addition to the term involving the square of the nuclear scattering amplitude, a term which comes from the coherent scattering of neutrons by the electrons and the nucleus of an atom. This term is proportional to the nuclear scattering amplitude, the electron-neutron scattering amplitude, and the form factor (structure factor) of the atom. By making measurements at low energy where the form factor is fairly large and at higher energies where it is almost negligible, one obtains a difference which is primarily attributed to the electron-neutron interaction. The energy range of interest in this experiment is from about 0.1 V to around 8 or 10 V. At the lower energy, in addition to the electron-neutron term, one has a small term associated with diffraction in the liquid metal, and this has to be calculated and taken into account.

The first experiments were done with liquid lead and subsequently more precise results were obtained with bismuth. I think it is unfortunate that lead was not included in the precise work. The most accurate result by this method was obtained by Melkonian, Rustad, and Havens. It is -4340 ± 140 eV. The authors state that this result does not definitely establish a difference from the Foldy term.

Another method was used by Hughes, Harvey, Goldberg, and Stafne. These authors took advantage of the fact that at an interface between bismuth and liquid oxygen, the difference in the indices of refraction of these materials for neutrons is largely contributed by the electron-neutron scattering amplitude. They did critical reflection experiments with low-energy neutrons to establish the magnitude of this difference and used transmission measurements at higher energies to determine the small contribution of the nuclear amplitudes to the difference. This method has the advantage that one does not have a correction for diffraction in a liquid metal. The result obtained from this experiment was -3860 ± 370 V. This result was, I believe, the most precise available at the time it was published.

One objection to these two measurements standing alone is that both of them depend in about the same way on the assumption that the coherent scattering amplitude of bismuth is practically constant in the range of neutron energies from near thermal to about 10 eV. I think it desirable to obtain results depending on different nuclear scattering amplitudes in order to minimize the possibility that the results may be affected by serious systematic error. Thus, our interest in further measurements comes mainly from a desire to improve the reliability of the results with respect to systematic error, rather than to reduce the rather small uncertainties present in the experiments of Melkonian et al.

The third experimental method was first used by Fermi and Marshall and is the one which we are now pursuing in an attempt to obtain precise results. In this experiment, one looks at the fore-and-aft

asymmetry in the scattering of neutrons by an atom. This asymmetry comes from the term discussed in connection with the first experimental method, the coherent scattering of neutrons by the electrons and the nucleus of an atom. It is proportional to the two scattering amplitudes and to the atomic form factor which is a function of the scattering angle.

I like to think of the over-all measurement as a determination of the difference between the observed asymmetry in the scattering and the asymmetry which must be associated with the motion of the center of mass of the scattering system. In order to calculate the asymmetry associated with the motion of the center of mass, one must know the temperature of the scattering gas and the spectrum of the neutrons. In addition, to be precise one must do a separate calculation for each isotopic mass and must weight the results in proportion to the isotopic scattering cross sections and abundances in order to obtain a result which applies to a natural mixture of isotopes. Consequently we plan to measure the scattering cross sections of the isotopes of the noble gases. Noble gases are selected for the asymmetry measurements in order to avoid the effects of molecular diffraction and in order to have atoms of zero magnetic moment.

We have established that results for the electron-neutron interaction can be obtained from argon, krypton, and xenon. In addition, the measured asymmetry of neon will be used to test the calculation of the asymmetry associated with the motion of the center of mass.

Another area where we feel we must concentrate our effort if we are to obtain greater precision is the purification of the gases used in the scattering-asymmetry experiments. Hydrocarbons have much higher cross sections than the noble gases and exhibit very large fore-and-aft asymmetries. Hence, it is important to achieve very high purity and to show that impurities are not affecting the results.

Hopefully, when we are finished we will have results from three different elements so that the possibility of systematic errors affecting the results will be minimized. Also, the fast-chopper group here at Argonne is considering measurements by the first method discussed, with liquid lead as well as bismuth, but an effort to perform this experiment has not been started.

* * *

J. A. HARVEY, Oak Ridge National Laboratory: Do you worry about a small electric charge in the neutron affecting your scattering experiment? I mean, something as small as 10^{-12} electron charges could possibly give you some asymmetry. Or do you trust the theory that it is absolutely zero? I would also like to make a statement on the neutron-electron interaction with the mirror technique. We did make a small correction for the change of the bismuth amplitude from low energies to 10 eV based on the parameters of the higher energy resonances. You pointed this out as one possible weakness.

KROHN: I would say in connection with the charge, that if a discrepancy develops when additional precise data are available, perhaps one could start worrying about this. For the moment, we have not considered it.

In connection with your other remark, I did not mean to imply that I think something is wrong, but that there might be; and this would presumably be caused by unknown resonances.

A. I. YAVIN, University of Illinois: I wish to make a comment about an experiment which could be done sometime in the future. It is related to the paper which we have just heard and to the possibility mentioned in the previous paper that there might be a nonelectromagnetic e-n force which somehow cancels out in electron-neutron scattering. Most low-energy electron-neutron experiments have been done up to now with neutrons impinging on electrons in target atoms. There is also

the opposite approach of scattering electrons from neutrons in deuterium, but the binding energy of the deuteron as well as the interference from the proton make such investigations useful mainly at high energies, where still there might be some screening present.

I am thinking of a new technique of scattering electrons from free neutrons. In fact this technique would enable investigations of both e^--n and e^+-n interactions, thus contributing to the solution of the question of whether or not there is a nonelectromagnetic force between the electron and the neutron. Such a technique involves the use of a neutron-gas target and a beam of electrons or positrons impinging on it. High interaction rates can be achieved either by the utilization of a high-flux steady-state reactor in conjunction with a storage ring for electrons and positrons, or by the use of pulsed reactors and properly matched bunched beams of electrons. Multitraversal of the target enhances the interaction rate in the first method, whereas beam bunching and reactor pulsing achieves a similar effect in the second method. I do not expect that such experiments could be done today, but I would not be surprised if they become feasible in a year or two.

I-3. PROPOSED EXPERIMENT TO OBSERVE n-n SCATTERING*

C. O. Muehlhause

National Bureau of Standards, Washington, D.C.

A measure of the n-n scattering cross section at thermal energies would be of interest in that it would yield directly the zero-energy n-n singlet scattering amplitude for comparison with the n-p and p-p singlet amplitudes. It should be feasible to make this measurement using a high-flux ($\gtrsim 10^{14}/cm^2 sec$) steady-state reactor in which a well evacuated internal collimating beam duct ($\sim 10^{-8}$ torr) passes through the high-flux region.[1]

The duct is tapered and stepped and it begins and ends in nearly field-free space, i.e., it passes through the entire reactor structure including the biological shield. A thermal-neutron detector is placed outside the reactor on the axis of the duct and is located beyond the point where it could view the walls of the duct as shown in Fig. 1. Under these

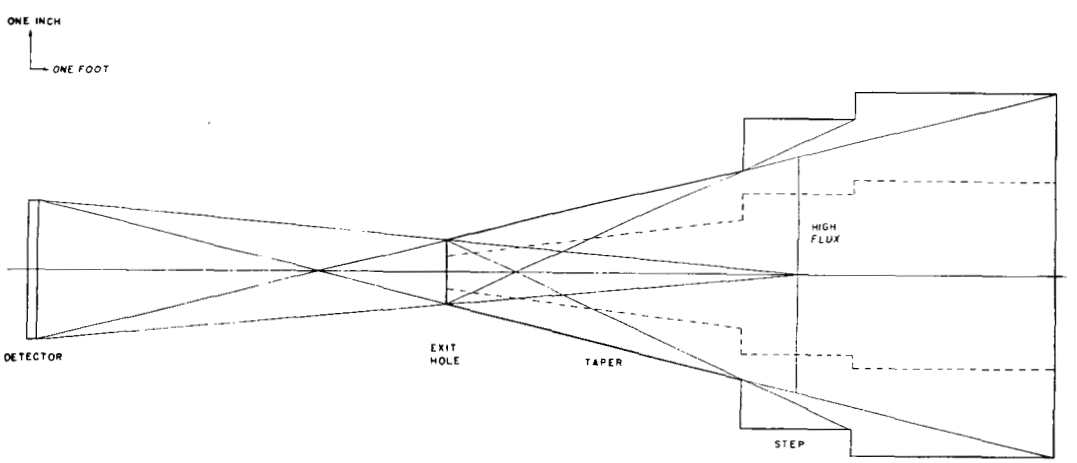

Fig. 1. Geometry of duct and detector arrangement proposed for the NBSR.

*Invited paper.

[1] C. O. Muehlhause, National Bureau of Standards Circular NBS 7583, NBSR-8, "Thermal n-n Scattering" (unpublished NBS report, 1963).

conditions, except for window scattering, only neutrons which scatter from other neutrons can reach the detector. The stepped section shown is over the most intense region of flux (i.e., over the core) and requires at least one internal scattering for background neutrons to exit from the collimator. The step and taper restrict epithermal neutron streaming along the duct.

The effect in question (n-n) varies as the square of the flux or power of the reactor and also as the fourth power of the duct diameter. In a particular arrangement proposed for the NBSR wherein the through-core portion of the tube is about 5 in. × 9 in., the expected signal should be between 5 and 10 counts/min. In addition to the geometrical factors involved, the estimate is based on the work of Ilakovak et al.[2] in which an n-n amplitude value of -22 F is given. The n-n effect can be calibrated by introducing a known quantity of some simple scattering gas (e.g., helium) into the system. The effect is also identifiable by varying the power of the reactor and analyzing for the square component of signal.

In realizing the above arrangement, the principal technical problems appear to be (1) fabrication of the duct to the precision required, (2) fabrication of the duct with a minimum of welds or seals, (3) measuring the pressure in the high-flux region, and (4) obviating, if necessary, the effect of deep outgassing by radiation in the walls of the duct ($\sim 10^{-10}$ to 10^{-11} torr liters/sec required).

* * *

S. KAPLAN, Lawrence Radiation Laboratory: Would you care to comment on the feasibility of doing this sort of experiment with, say, a pulsed reactor where you might be able to get possibly 100 times the flux you are talking about, but where I suspect there might be transient effects

[2] K. Ilakovac, L. G. Kuo, M. Petravic, and I. Slaus, Phys. Rev. 124, 1923 (1961).

that would affect your accuracy?

MUEHLHAUSE: Yes, that is another way that could very well succeed in doing it. I have a few general comments on it. I have calculated what one would expect in the way of neutrons emitted per pulse, say by the present advanced type of pulsed reactor, and it is of the order of one or possibly two counts per pulse. So one would have to run many of these in order to gain the statistics.

The big advantage you would have is that the background problems, and so on, would be negligible; but you would have to monitor the flux and the flux-time spectrum carefully.

I failed to stress here one other thing somewhat in relation to this. I pointed out that the effect sought is close to proportional to the square of the flux. Even more important is the size of the beam hole that you can manage to put through a reactor. The effect goes with the fourth power of the radius of that beam hole — basically because the square comes into determining the volume of neutrons scattering neutrons, and the next square power has to do with the solid angle that defines that source. It is more important to put a big fat hole through a reactor if you can do it than it is to go up in power. The only trouble is, if you attempted to do the experiment say at 10^{13} with a big hole, where in principle you would have maybe more signal than you would have in the smaller hole at 10^{14} or 10^{15}, your vacuum problem would then become inordinate.

H. MAIER-LEIBNITZ, Technischen Hochschule, Munich: The idea of measuring the neutron-neutron cross section has been known for quite a long time, and I would really like to know what accuracy do you want for that experiment to be useful. I mean, we had thought that 10% would not be enough. We thought it should have been something of the order of 3%.

MUEHLHAUSE: Yes, that is my feeling about it, having talked to the theoretical people. Perhaps Dr. Thaler could comment on this.

R. M. THALER, Case Institute of Technology: I would be interested in even a 10% experiment, particularly if it was widely different from our expectations.

MUEHLHAUSE: It has to be a few per cent to be worthwhile — the more accurate the better, especially as these other measurements become more accurate.

LYLE B. BORST, State University of New York at Buffalo: What value of the cross section did you assume in your calculation?

MUEHLHAUSE: I assumed just for purposes of calculation the result of Ilakovac, scattering amplitudes of -22 F. That gives rise to an entirely reasonable cross section of 61 barns. I put this in for lack of anything better. If it drops to 20 barns, things would be that much more difficult. The signal would fall. If it should be 100 barns, that would be all right.

R. K. SMITHER, Argonne National Laboratory: I have heard speculation on occasion about using two atomic bombs simultaneously exploded.

MUEHLHAUSE: That would be an interesting experiment. It would give the scattering at 14 MeV which would have some complications to it. That is, it would not be the zero-energy value but quite a worthwhile thing.

SMITHER: Are the fluxes reasonable to expect good counting rates?

MUEHLHAUSE: Yes. You have to detonate two bombs that are roughly the order of a kilometer apart. You dig tunnels at hundreds of dollars a foot through mountains, and they come together, and you make a T and you go another kilometer away and then you go boom! There are enough 14-MeV neutrons here to swamp the detector. It is quite easy to do.

A. I. YAVIN, University of Illinois: It seems to me that you could increase the neutron-neutron interaction rate and decrease the background from gas scattering by cooling the neutrons to, say, liquid-helium temperature.

MUEHLHAUSE: Right. That would be the situation if you hold the flux invariant, you would lower v_0 by the square root of the temperature. This would give a factor of 10 or more and that would emphasize the effect. That would be very desirable. It is just another complicated technological thing to try to do.

B. I. SPINRAD, Argonne National Laboratory: I would like to make a comment on the pulsed-reactor technique. It is not a thing used very much because the slowing-down time lengthens the pulse very appreciably, and the integrated steady-state flux in the reactor is greater than that you get from the pulses. However, I would like to ask what high-flux steady state, if you could achieve it for a few minutes, might satisfy you?

MUEHLHAUSE: What are you thinking of, 10^{16}?

SPINRAD: 10^{16} or 10^{17}.

MUEHLHAUSE: At 10^{16} you would have 50 to 100 thousand counts/min. If that went on for 2 min, you would get maybe 100 000 counts. That sounds pretty good. You would want to do this a few times.

M. HAMERMESH, Argonne National Laboratory: I did not understand the answer to the question about the accuracy and knowledge of σ_{nn}. I don't understand why a few per cent is good enough. What you have to do is see whether there is a deviation from the corresponding thing in the mirror interaction in the σ_{pp} for example. The 3% is nice to have, but that is a poor argument.

THALER: The better it is, the better off we are of course. What we really want is something which meets the precision of the p-p experiment.

HAMERMESH: But aren't there other experiments where if there were a violation of charge independence beyond some figure it would already have shown up; what is that figure?

R. SEGEL, Argonne National Laboratory: 3% from the O^{14} decay.

THALER: Let me make a remark about that. Namely, the scattering amplitude is practically infinity, so that a small change in this scattering amplitude would in fact represent a very small effect in the rest of the nuclear physics. For example, thinking in terms of potentials, a change of a few per cent in the depth or range would make an enormous change in the scattering amplitude here, so that these numbers would

indicate that less than a few per cent deviation from charge symmetry in nuclear reactions and so on is not as relevant as it might seem. In short, this amplitude is quite sensitive to the n-n potential and this is why even a 10% measurement might be of interest.

I-4. SEARCH FOR PARTICLE-STABLE TETRANEUTRONS AND DINEUTRONS IN FISSION*

J. P. Schiffer and R. Vandenbosch†

Argonne National Laboratory, Argonne, Illinois

[Since a report of this work has already been published— J. P. Schiffer and R. Vandenbosch, Phys. Letters 5, 292 (1963)—only the abstract of this paper is given here.]

Recent high-energy experiments have suggested the possibility of a particle-stable tetraneutron. If such a nucleus does in fact exist, there is no apparent reason why it should not be observed in fission. We have searched for it, using the hypothetical reactions $N^{14}(n^4,n)N^{17}$ and $Al^{27}(n^4,t)Mg^{28}$ as detectors. Assuming n^4 cross sections to be similar to alpha-particle cross sections, we can set a limit of no more than 10^{-8} tetraneutrons per fission. Since a dineutron could also produce Mg^{28} by the reaction $Al^{27}(n^2,p)Mg^{28}$ we can set a similar limit for dineutrons. The observed frequency of alpha particles and tritons in fission is 5×10^{-3} and 2×10^{-4}, respectively. It seems reasonable to conclude that on the basis of our results alone the existence of these particles is not very likely.

* * *

R. C. BLOCK, Oak Ridge National Laboratory: About what lifetime would you estimate for the tetraneutron? Would it get out of the fission event and get to your target?

SCHIFFER: Well, the lifetime is that of beta decay. Its lifetime could be milliseconds, minutes, or even hours. It depends upon the precise energy of the state, which, of course, is not known.

PETER AXEL, University of Illinois: Did you make any estimate or use any model of the fission process to decide how many of your tetraneutrons should come out compared with the alphas?

---

*Presented by J. P. Schiffer.

†Now at the University of Washington, Seattle, Washington.

SCHIFFER: Well, we guess that maybe something similar to the number of tritons might come out. We did not do any calculations.

AXEL: I don't know that they can be done, but evidently the alpha particle comes out as favorably as it does because the fissioning nucleus will pay a big price for the alpha-particle binding energy. I was just wondering whether the alphas in fission are well enough understood so you can make some estimates.

SCHIFFER: Well, the binding energy of the triton is less than half that of the alpha, and the frequency is down only by a factor of 10. If you want to use this as an argument, one might say that the tetraneutron has zero binding energy and should be down by another factor of 10. It is way, way below that. It is 4 orders of magnitude down from the tritons.

PETER FONG, Cornell University: In the slow-neutron fission of U^{235} there are 2.5 neutrons emitted for each fission event. The 2.5 neutrons are divided between the two fragments. The chance for one fragment to emit four neutrons is very small. The chance of emission of a tetraneutron, if it exists, is thus very small in the fission process.

SCHIFFER: Yes, but in the same arguments, tritons and alpha particles are unlikely. All I am really competent to comment about are experimental results, and I do not see how any arguments of that sort would cut tetraneutrons by as large a factor as has been observed, which is five orders of magnitude below alpha particles.

FONG: Neutrons are emitted after the fragments are separated but the alpha particle is emitted in the process of fission.

SCHIFFER: Well, there is a difference, but why wouldn't tetraneutrons be emitted the same as alpha particles or tritons are at any stage in the fission process.

FONG: Well, in that case you can expect the emission of a tetraneutron in any nuclear reaction.

SCHIFFER: Certainly. But how would any one have observed them in other nuclear reactions?

FONG: So the fission process is used here because there are many events so that we can make an observation.

SCHIFFER: That's right.

FONG: Not for the fission process per se?

SCHIFFER: No, sir.

J. R. HUIZENGA, Argonne National Laboratory: I think Professor Fong is missing one point. There is some sort of weak evidence floating around about the kinds of neutrons emitted in fission. There are neutrons evaporated from the fragments, but I think the neutrons that Dr. Schiffer was talking about were another kind of neutron, namely, those that are dropped off at the time the two fragments separate. These neutrons are analogous to other kinds of particles which are emitted in the fission, namely, the alpha particles and the tritons.

One can tell whether the neutrons are evaporated from the flying fragments or not by looking at their direction; and the evidence is that about 90% of the neutrons in fission are evaporated from the flying fragments. But there still may be some 10% of the neutrons emitted in fission which come from the very fission act itself.

I think that this is where one possibly might see the tetraneutrons emitted.

I-5. ACCELERATION OF FREE NEUTRONS UNDER GRAVITY*

D. Paya,† J. W. T. Dabbs, J. A. Harvey, and H. Horstmann‡

Oak Ridge National Laboratory, Oak Ridge, Tennessee

Although the very elegant and accurate Eötvös experiments have shown the equivalence of the gravitational acceleration of neutrons and protons bound in nuclei,[1] only a single measurement has been made with free neutrons. The result of this measurement[2] was given as $g = 935 \pm 70$ cm/sec^2. The present experiment was carried out in the 180-m evacuated flight path at the Oak Ridge Research Reactor (ORR).

The transmission edges associated with the (100) and (002) lattice spacings in a polycrystalline Be filter may be used to define neutrons of velocities $v_i = h/m\lambda_i$, where $\lambda_i = 2d(100)$ or $2d(002)$. This method has the virtues of simplicity and high intensity. Figure 1 shows the arrangement of the experiment. The collimating slits were 0.008 in. high and

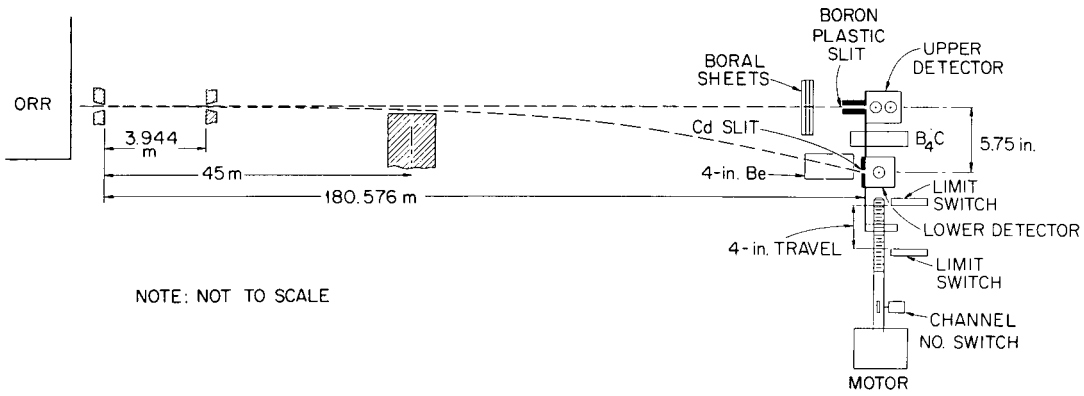

Fig. 1. Experimental arrangement.

---

*Presented by D. Paya.

†Visitor from CENS, Saclay (Seine-et-Oise), France.

‡Visitor from BCMN, Euratom, Geel, Belgium.

[1] R. H. Dicke, Scientific American 205, No. 6, 84 (June 1961).

[2] A. W. McReynolds, Phys. Rev. 83, 172 and 233 (1951).

were made from two boron steel plates about 2.5 in. long in the beam direction. The inner faces of the plates were coated with cast tetradecanoic acid ($C_{14}H_{28}O_2$). This material is useful for suppressing total reflection of neutrons at small angles.[3] The neutrons at 180 m were filtered by $\frac{1}{4}$ in. of Boral plus 0.060 in. of Cd into a "fast" beam which did not fall appreciably and by a 4-in.-thick Be block which gave the transmission edges mentioned above, and thus defined a "slow" beam which had fallen 5 — 6 in. The neutrons were detected by BF_3 proportional counters placed behind detector slits made as shown in Fig. 1. The upper slit was 0.226 in. high; the lower 0.257 in. high. The effective vertical separation of the two slits was 5.743 in. The entire assembly (counters, slits, and Be block) was oscillated vertically through a travel of 4 in. by a lead screw (32 thread/in.) at a rate of about 0.75 in./min. Each lead-screw revolution increased by one the address of the channel into which counts were stored in two halves of the memory bank of a 512-channel analyzer. Thus 128 channels correspond to the 4 in. travel. The first two quarters of the memory received lower detector counts during "down" and "up" travel, respectively; the second half was similarly used for the upper detector.

Since the counting rates in the lower detector were not large (200 c/min at the bottom of the travel), care was taken to reduce the background. The massive direct-line shield at 45 m, the B_4C shield between the upper-slit jaws and the lower counter, and a Cd wrapping around the lower counter were all found necessary. Upper detector backgrounds were taken through $\frac{3}{4}$ in. of Boral plus 0.060 in. of Cd; lower detector backgrounds were taken with 4 in. of Be plus 0.060 in. of Cd.

Figure 2 shows a typical upper-counter run; the data have been fitted by least squares to an isosceles triangle which is a good approximation to the expected function. The data represent the experimental resolution curve. The width at half maximum was 13 channels or $\frac{13}{32}$ in.

[3] I. R. Jones and W. Bartolini, Rev. Sci. Instr. 34, 28 (1963).

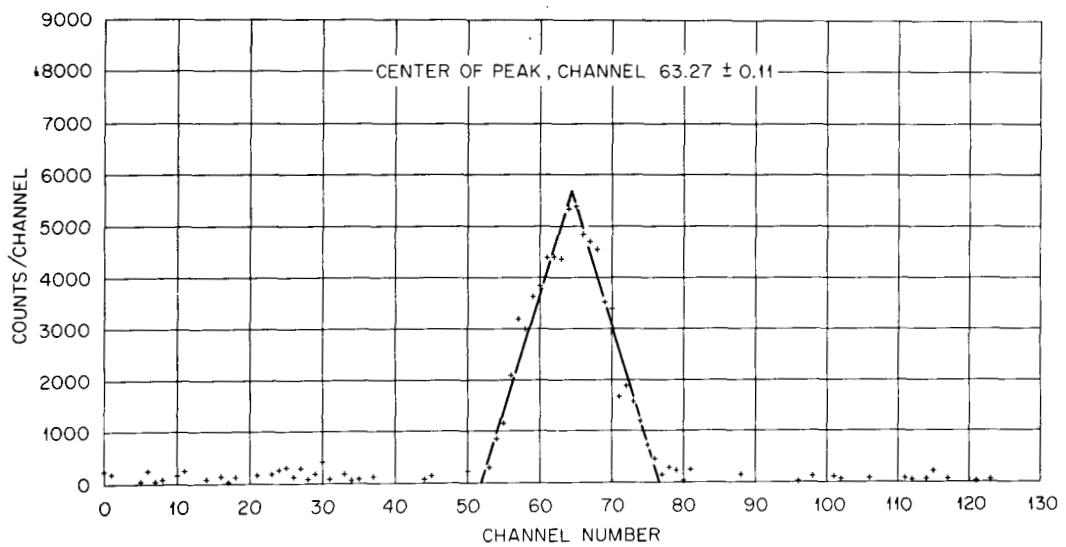

Fig. 2. Typical upper-counter run: Run 43-48, "fast" beam "up."

For the lower counter, a semitheoretical curve calculated by convoluting the resolution triangle with the result of the application of a stepped cross section to an expression approximating the lower-counter intensity distribution with the Be filter removed was used in the final analysis. Figure 3

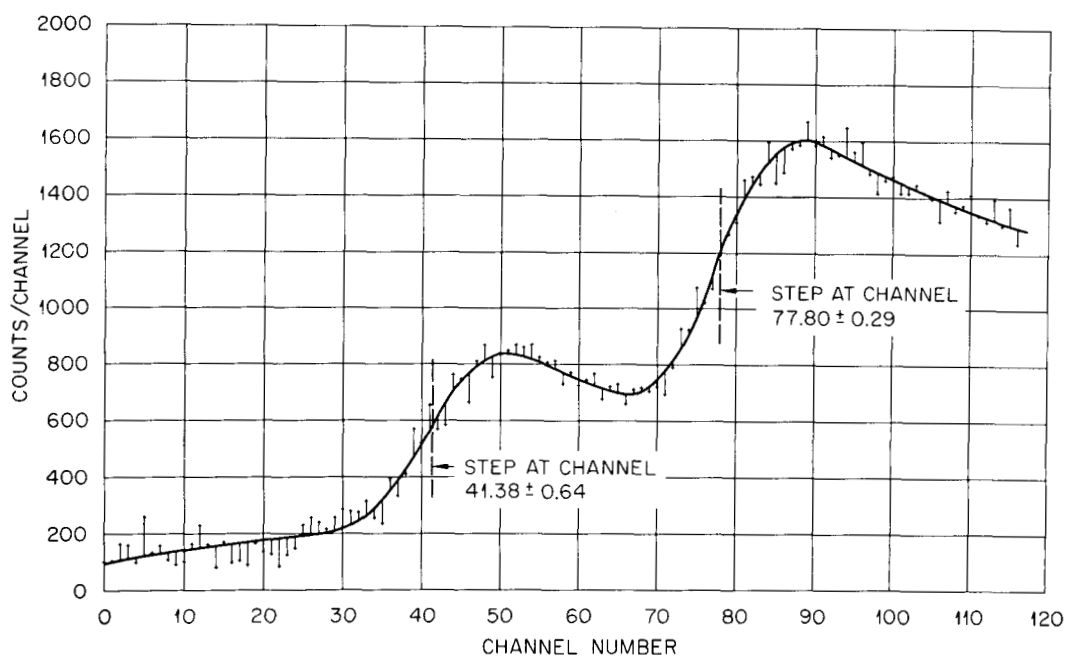

Fig. 3. Typical lower-counter run: gravity least-squares fit, Run 43, "down."

shows a typical lower-counter run; "up" corresponds to the lower channel numbers. The two transmission edges are clearly visible. The edge locations shown are those obtained from a preliminary[4] least-squares fit. Those counts to the left of the (002) edge were essentially all stray background counts and did not follow the open-beam distribution. The slope of the curve was therefore always permitted to take any value in this region. Table I gives the calculated results of a number of runs.

The values of λ_i were found to be 3.5780 Å and 3.9558 Å (± 0.0016 Å) from a detailed x-ray examination of the Be filter block actually used.[5] The fall of the neutrons passing through slits at horizontal locations 0, ℓ_1, and ℓ_2 is given by[2]

$$s = \frac{g}{2}\left(\frac{m\lambda}{h}\right)^2 (\ell_2^2 - \ell_1\ell_2). \qquad (1)$$

Using Eq. (1) and a suitable correction for the fall of the "fast" beam (about 0.005 cm), we find values for g as follows:

$$g(002) = 972 \pm 7 \text{ cm/sec}^2,$$
$$g(100) = 976 \pm 3 \text{ cm/sec}^2.$$

The local value of g, to a much higher accuracy, is

$$g(\text{local}) = 979.7 \text{ cm/sec}^2.$$

---

[4] See footnote a of Table I.

[5] The assistance of R. L. Sherman is gratefully acknowledged.

TABLE I. Calculated results.

Run No.	Duration (hr)	Center of fast peak (Channel No.)	(002) Step location (Channel No.)	(100) Step location (Channel No.)	(002) Net drop (cm)	(100) Net drop (cm)
43 down	25	65.34 ± 0.06	42.60 ± 0.64[a]	77.37 ± 0.29[a]	12.781 ± 0.051	15.413 ± 0.024
43 up	25	63.75 ± 0.07	40.36 ± 0.75	75.58 ± 0.46	12.731 ± 0.059	15.502 ± 0.037
45 down	20	66.84 ± 0.10	41.96 ± 0.53	78.94 ± 0.39	12.614 ± 0.042	15.547 ± 0.032
45 up	20	65.31 ± 0.08	40.44 ± 0.63	77.41 ± 0.40	12.614 ± 0.050	15.547 ± 0.032
57 down	24	65.83 ± 0.07	41.78 ± 0.53	77.92 ± 0.39	12.680 ± 0.042	15.547 ± 0.032
57 up	24	63.75 ± 0.12	41.68 ± 1.35	76.78 ± 0.62	12.835 ± 0.107	15.621 ± 0.050
58 down	4	65.96 ± 0.08	43.16 ± 1.43	77.34 ± 0.68	12.776 ± 0.114	15.489 ± 0.056

*These values differ from those shown in Fig. 3, which represents a preliminary analysis in which the slopes of the curve between channels 52 and 66 and above channel 90 were left free rather than forced to the theoretical value. The (002) difference is typical of this correction, but the (100) average correction was negligible.

I-6. MEASUREMENT OF THE POLARIZATION OF THERMAL-NEUTRON BEAMS BY MAGNETIZED MIRRORS*

M. T. Burgy, G. R. Ringo, S. Ketudat,† P. Rice-Evans,‡ and S. Barkan|

Argonne National Laboratory, Argonne, Illinois

Polarized neutrons are needed in several experiments in nuclear physics. One of these, which has been performed at Chalk River and here, is the measurement of the correlations between the directions of emission of the decay products of a decaying neutron and the spin of the neutron. This is perhaps the best test of weak-interaction theory in nuclear physics; its precision is limited at present by the accuracy with which we can measure polarization. In our first experiment this accuracy was approximately ± 8%.

The method we used to start with is shown in Fig. 1, which shows two magnetized mirrors (93% Co, 7% Fe) with the field magnetizing them parallel to the surface. The reflected polarized beam comes over to the analyzing mirror, set so that the grazing angle is the same as, or slightly smaller than, that at the first mirror. It reflects the beam again into a counter where the intensity I_p is measured with this polarized beam. Then one changes the conditions and makes another measurement on the polarized beam. This time a thin sheet of steel, unmagnetized or weakly magnetized in the guide field, depolarizes the beam before it strikes the second mirror. This gives a different intensity I_d coming off the analyzer; and the ratio $R = I_p/I_d$ gives one the polarization product P_1P_2 according to the formula

$$I_p/I_d \equiv R = 1 + P_1P_2. \tag{1}$$

---

*Presented by M. T. Burgy.

†Now at Chulalongkorn University, Bangkok, Thailand.

‡Now at Bedford College, University of London.

|Now at the University of Istanbul.

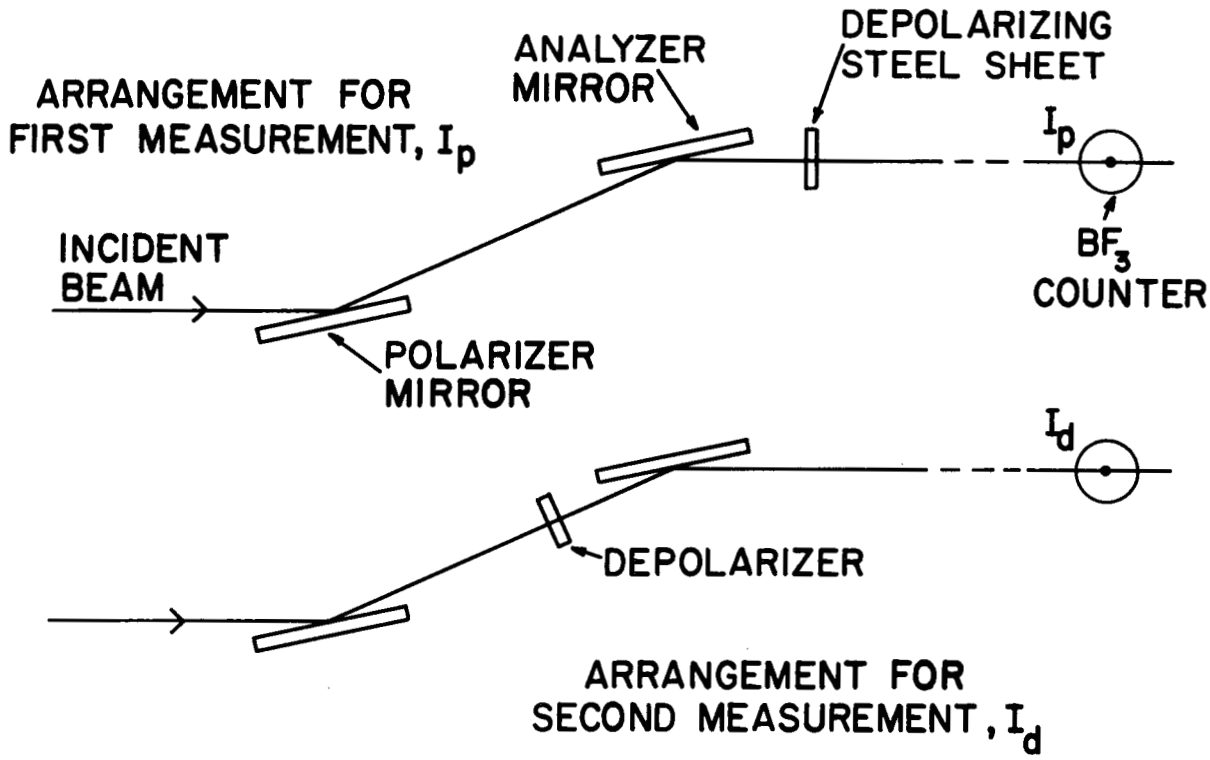

Fig. 1. Schematic representation showing the two conditions in which the neutron beam intensity is measured, giving I_p and I_d. The polarization product is obtained from these intensity measurements by the formula $1 + P_1 P_2 = R = I_p/I_d$. The magnetizing fields for the mirrors are normal to the plane of the figure.

Here, P_1 is the polarization of the beam reflected from the first mirror, and P_2 is the polarization that the beam reflected from the analyzer would have if the beam incident upon it were unpolarized.

There is a serious error in the use of this method which we did not realize when it was first proposed.[1] The magnetic domain structure of the steel sheet which depolarizes the beam makes the sheet magnetically inhomogeneous and produces small-angle scattering. Part of the beam which would hit the mirror if the sheet were not used is scattered away from the mirror. Thus there is some loss. Also, some neutrons strike the mirror at different angles than they would if the sheet were not used, and some that would have missed the mirror get scattered so that they do strike it.

[1] D. J. Hughes and M. T. Burgy, Phys. Rev. 76, 1413 (1949).

In almost all cases, there is a net change despite the partial compensation. Hence Eq. (1) is erroneous because it involves two effects instead of the single one considered theoretically. I should say that there is a large-angle scattering and absorption in the steel sheet too, and one expects to compensate for these by putting the steel sheet in the beam reflected from the second mirror during the measurement of I_p. It is placed fairly close to the mirror so that the neutrons scattered through large angles miss the counter. Thus the attenuation of the beam by capture and large-angle scattering in the steel sheet is very closely the same in the measurement of I_p and I_d.

The first step in correcting for the small-angle scattering is to make the counter large enough so that the region of uniform sensitivity is sufficiently broad. Then the neutrons scattered through small angles will still be counted during the measurement of I_p. There still remains the problem of correcting for the effect of small-angle scattering in the measurement of I_d.

Several years ago, a Russian group[2] investigated this source of error and proposed a method of correction in which one depolarizes the beam that is reflected from the first mirror and makes the two measurements I'_p and I'_d (corresponding to I_p and I_d) with this depolarized beam to get a measure of the contribution of the small-angle scattering. Then the ratio I_p/I_d obtained with the polarized beam can be multiplied by I'_d/I'_p to get the proper value of R. This corrected value of R is then used to get P_1P_2 according to Eq. (1).

However, the second steel sheet also spreads the beam and gives another perturbation. The Russian group proposed one method of minimizing the effect of the spreading of the beam from this second depolarizer. We tried another that we thought was an improvement — and for

---

[2] Abov, Beketov, Gul'ko, Ermakov, Krupchitskii, Taran, and Shatlovskaya, Pribory i Teknika Eksperimenta 4, 3 (July-August 1960). [English translation: Instr. Exper. Tech. 4, 571 (1961)] ; A. D. Gul'ko, Pribory i Teknika Eksperimenta 3, 40 (May-June 1961)[English translation: Instr. Exper. Tech. 4, 452 (1961)] .

for some time we were happy with it. But our method still has an error — as we found directly by replacing our polarizer mirror by a beryllium mirror which closely duplicated the geometrical relationships, the energy spectrum of the beam, the angular distribution, and so on, but gives a beam of zero polarization. However, our method gave $P_1P_2 \approx 0.03$. In the case of a high polarization, as when the polarizer is a cobalt mirror, this error in P_1P_2 would be approximately doubled, and we were trying to be more accurate.

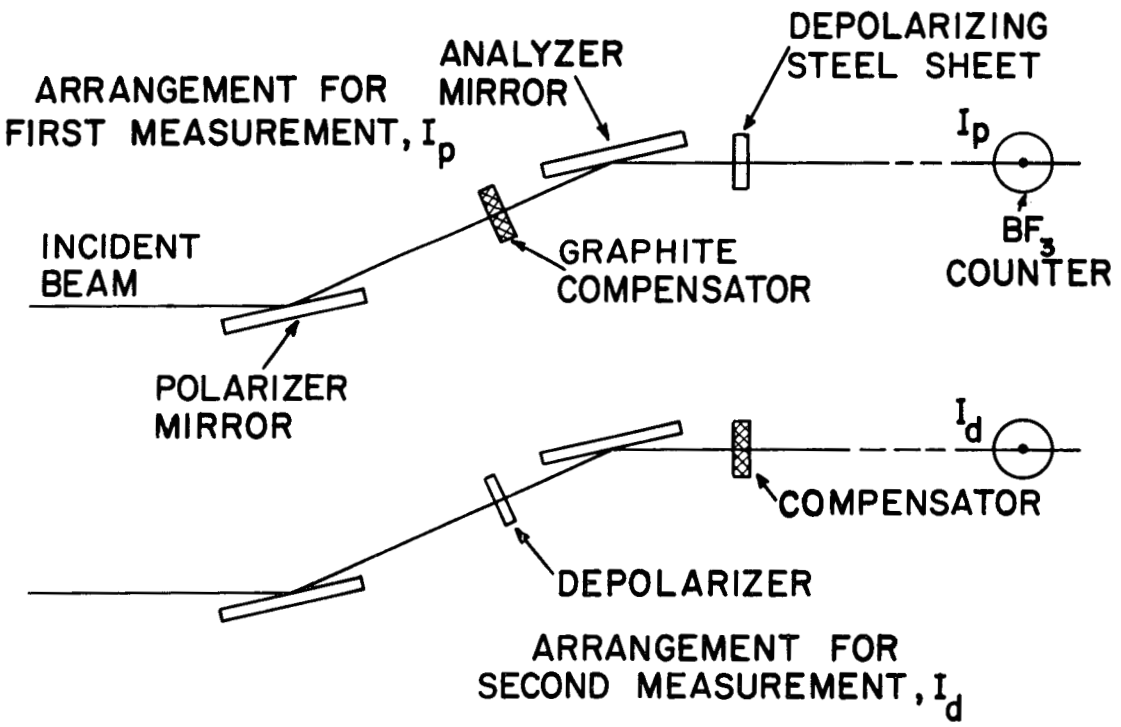

Fig. 2. Schematic representation showing the modification of the conditions shown in Fig. 1. Here a graphite sheet is used to compensate for the small-angle scattering in the steel depolarizer.

We have developed a method (Fig. 2) which, we think, gets around this trouble by having the beam spread all of the time in the measurement of both I_p and I_d. We accomplished this by putting a compensator which does a small-angle spreading of the beam in the measurement of I_p ahead of the analyzer. It gives the same spreading effect as

does the steel sheet, but it does not affect the polarization. A powder of a nonferromagnetic substance could be used, but we have found graphite convenient. Then I_p is measured with the graphite sheet in the beam between the two mirrors and the steel depolarizer in the beam reflected from the second mirror. In order to measure I_d, the graphite and steel sheets are interchanged. Thus, the difference in large-angle scattering and capture in the two sheets is compensated. One still relies on a sufficiently broad area of uniform sensitivity of the counter to avoid possible additional complications from the small-angle scattering. Now the only significant change between the case in which I_p is measured and the case in which I_d is measured is that the beam striking the second mirror is polarized in the first case and depolarized in the second case. Thus, we may expect to get the polarization product P_1P_2 from the two measurements.

Of course there is the problem of choosing a matching thickness of the graphite for the piece of steel used for the depolarization. To do this we used a beryllium mirror (giving a beam of zero polarization) in place of our cobalt polarizing mirror. The thickness of graphite that matches the steel depolarizer in its effect on the counting rate was found (and we assume this means it matches it in small-angle scattering). Now if, in practice, one wants to make the match when a cobalt mirror is the first mirror, a second steel depolarizer is used to depolarize the beam reflected from the first mirror; and the thickness of the graphite sheet is adjusted to match the effect of the first depolarizer (as with the beryllium mirror). This beam would be spread more than that from the beryllium mirror. We have found, however, that with this depolarized beam from a cobalt mirror we get the same thickness of graphite as a match for our first steel depolarizer as we got with the beryllium mirror. This indicates that the match is not very sensitive to the initial beam spread.

Figure 3 shows some relevant measurements of R, the ratio of the counting rate with the steel depolarizer removed to that with it in place (with a depolarized beam as a source). One sees that a straight line

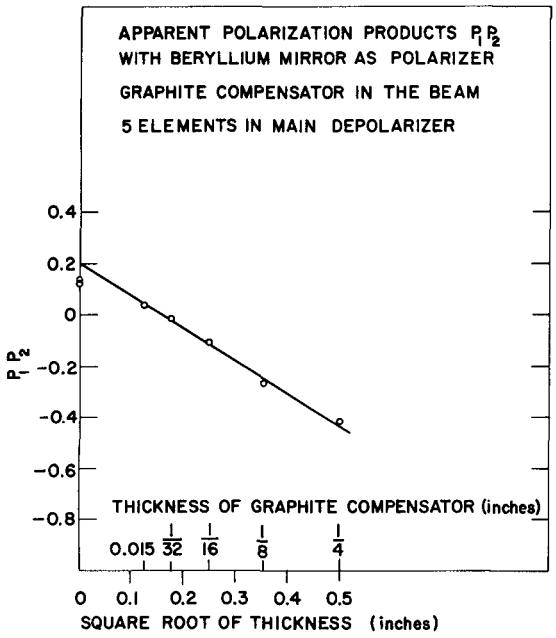

Fig. 3. The apparent polarization products $P_1 P_2 = R - 1$ obtained with a beam of zero polarization from a beryllium mirror as the polarizer, plotted as a function of the square root of the thickness of the graphite compensator. The ratio $R = I_p/I_d$ is obtained from measurements made in the manner shown in Fig. 2. The steel depolarizer consists of five elements, each 0.0045 in. thick. The thickness of graphite corresponding to $P_1 P_2 = 0$ (i.e., to $R = 1$) matches the depolarizer in its effect on the measured intensities from small-angle scattering.

is obtained when the apparent polarization products P_1P_2, given by measured ratios R (or, more strictly, R - 1) obtained with the beam of zero polarization, are plotted against the square root of the thickness. The points measured with the second depolarizer used to spread the beam fell on this line also. At zero thickness of the graphite, one does see that the point falls off the curve, indicating that at small thicknesses there is a transition through single and plural scattering and into multiple scattering as the thickness increases. From the line through the points, we find that a graphite compensator with a thickness of about 0.028 in. should match the steel depolarizer in small-angle scattering and give zero for the value of P_1P_2 obtained with the beryllium mirror. We had several specimens made with thicknesses near this value, and found one that matched the depolarizer very closely. We applied this method to the cobalt-iron alloy mirrors and got $P_1P_2 = 0.88$.

The principle of compensating for the small-angle scattering in a steel depolarizer may be applied to the correction method suggested by the Russian group, also. Here, the ratio R would be obtained with a graphite compensator in the beam reflected from the first mirror;

and the correction factor would then be gotten with the second depolarizing steel sheet replacing the graphite compensator.

Figure 4 shows what we call the "double-mirror arrangement," which should give a higher polarization. This has various advantages; in particular, we expect to get P_1 and P_2 with less uncertainty from a measured P_1P_2 product which is closer to unity. In this setup, we have arranged to get two reflections off the mirrors in the polarizer, and similarly for the analyzer. The offset of the mirrors and the spacing between them are chosen so that no beam can get directly through. Below, one can see the arrangement in larger scale. One can see that the mirrors are constructed from a thin layer of cobalt-iron on a copper backing.

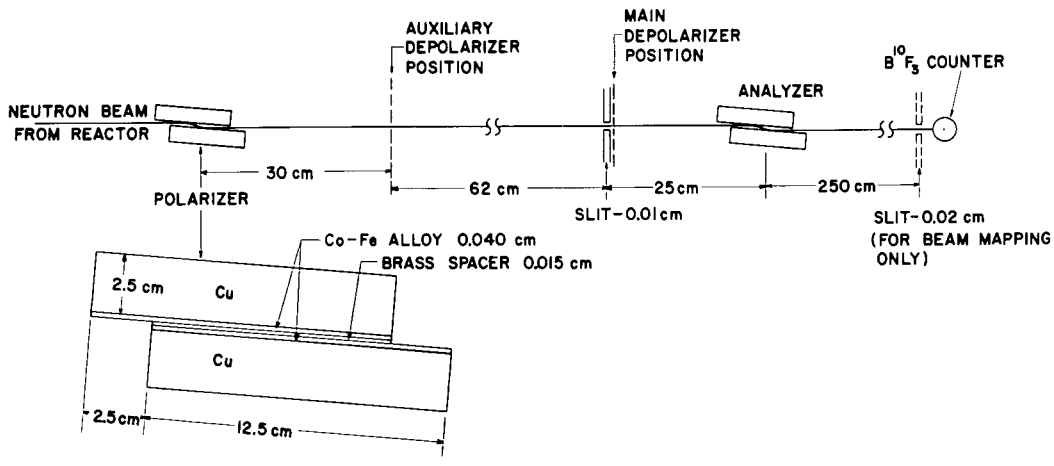

Fig. 4. Plan view of the arrangement with a double-mirror polarizer and double-mirror analyzer.

The advantage of this setup can be seen from the following considerations. Suppose that the reflectivities for neutrons in the two spin states relative to the field direction were in the ratio of ten to one for a single one of these mirrors. Then for a double reflection, the effective ratio of reflectivities is 100 to 1. The single mirror would give 81% polarization, and the two mirrors would give 98%. With a similar analyzer, one would get 0.96 for the polarization product. One might expect to get P_1 and P_2 separately with relatively small uncertainties, if such a high value were achieved.

However, we carried out this measurement, and only got about 0.90 — 0.91. I should say that we tried this double mirror arrangement and did most of our work with it using the other method of polarization measurement (the one without graphite compensators) and we got higher numbers there, in the range of 95 — 99% under various conditions. But then, when we corrected the method, this dropped down to about 91%, so we took a more critical look at our arrangement. With this high value of 0.88, obtained with the single-mirror arrangement, we should go up to what we got with the other method with the double-mirror arrangement. We decided that there must have been two errors in the old measurements which somewhat compensated. We think now that there are some effects of a few per cent from the transmission of the incident beam on the analyzer through the forward edge of the second mirror. The cobalt-iron alloy may not be near enough to saturation to avoid depolarizing the part of the beam that is transmitted, and this would be a defect of this arrangement. Moreover, we now believe the two mirrors are too close together and affect each other's magnetic flux, leading perhaps to horizontal (hence depolarizing) flux components. Our improvement of the polarization measurement has been a rather recent development so that our discovery of the defects in our double-mirror arrangement is very recent. We are undertaking modifications, which will control the beam so that the beam will use only the central part of each mirror in these pairs so that there will be no trouble from the edges. I am sorry I do not have data on that situation to give you though.

* * *

N. J. PATTENDEN, A.E.R.E., Harwell: I did an experiment similar to this in Brookhaven a few years back, but instead of using the mirror technique I used cobalt-iron crystal monochromators to produce the polarized beam. I also noticed this effect of small-angle scattering in the nonmagnetized sheet of iron. I was interested to see the thing pointed out again.

M. HAMERMESH, Argonne National Laboratory: What is the best polarization one can get now?

BURGY: Values of about 98% are claimed for the iron-cobalt crystal or magnetite crystals.

HAMERMESH: You mean using Bragg reflection?

BURGY: Yes, by Bragg reflection.

V. E. KROHN, Argonne National Laboratory: I wonder if you adequately emphasized the point of using the double mirror, which would be that with double reflection on both polarizer and analyzer you get (hopefully) a result close to 100% polarization. This is the result you must have if you are to determine the polarization of either one separately. So (hopefully) you want to establish that a double reflection in an analyzer means an analyzer with 100% polarization; then further measurements using this analyzer will be measurements of the polarization achieved by the polarizer, which may be a single mirror.

L. PASSEL, Brookhaven National Laboratory: In principle you can use three sets of polarizer-analyzer systems, and permute them, and get the polarization of any one in that way. This is often done with the iron-cobalt crystals. Is this reasonable in your case as well?

BURGY: Yes, it is, but this is something we have not carried out yet because this method of measurement, in which we have confidence, is a rather recent development. We have an extra complication in dealing with mirrors that you do not have with the crystals, namely, that we have a spectrum of wavelengths, and the measured result is actually an average of the product of P_1 and P_2 as a function of the wavelength over the spectrum. If there is much variation in that product, the average of the product would not factor into the product of the two simple averages of P_1 and P_2. If you work with the high-polarization case that you might get with double mirrors for both polarizer and analyzer, the difference should give a small error contribution, I think.

HAMERMESH: Does this mean that you perform the average over the spectrum of a product of two or a product of three, and they are not simply related?

BURGY: No, it is simply this. You determine P_1P_2; call that C. Now, mirror No. 2 and mirror No. 3 are used and you get $P_2P_3 = A$. And similarly $P_3P_1 = B$. Thus, formally, $P_1 = \sqrt{BC/A}$.

HAMERMESH: I think you are saying what I was trying to say — that these are really integrals over a spectrum so that this division is not correct.

BURGY: You assume that the average of the product equals the product of the averages. This will be better, I think, the closer the product is to unity throughout the range of the spectrum.

I-7. THE MAGNETIC-MIRROR NEUTRON POLARIZER AT THE REACTOR "ISPRA 1" *

M. Forte

EURATOM C.C.R. Ispra, Italy

Introduction

An apparatus producing a beam of polarized neutrons has been installed at the reactor Ispra 1. The polarization is obtained by the method of reflecting a slow-neutron beam on a magnetized Co-Fe mirror.

The beam is to be used, mainly, for capture gamma-ray experiments. The chosen method of polarization permits one to combine a high neutron intensity with a very small beam width, so that narrow targets can be conveniently used. This is especially important in some experiments with polarized neutrons in order to avoid target scattering effects which would result in depolarization.

To facilitate the investigation of nuclei with low capture cross section, care has been taken to obtain good beam purity and low background.

Mirror Material and Fabrication Method

At the surface of the magnetized mirror the refraction index must be larger or smaller than unity, according to the neutron spin state, so that total reflection of neutrons of one spin state can never take place. This condition is expressed, in terms of the average magnetic and nuclear coherent-scattering amplitudes, by $|a_n| \leq a_m$, where a_m will be proportional to the effective magnetic induction, taking into account that only a fraction of the atoms are oriented along the field.

Essentially, the only suitable magnetic materials are pure Co ($a_n = 0.28 \times 10^{-12}$ cm, $a_m \approx 2.5 \times 10^{-17}$ B cm, B in gauss) and Co alloys with some percent of Fe. Using pure Co involves some practical

* Read by title only.

difficulties. Indeed, to have satisfactory magnetic properties (not available with the normal hexagonal structure of Co) it is necessary to use cubic-structure Co, which can be formed by electroplating a thin layer on a copper backing.[1] The fabrication procedure, however, is not quite straightforward and the layer may be easily damaged by the polishing. Therefore, we preferred to use, as a starting material, a Co-Fe (Fe 6%) alloy, as it was successfully employed at Argonne.[2] With this material ($a_n = 0.32 \times 10^{-12}$ cm, $a_m \approx 2.5 \times 10^{-17}$ B cm), a magnetization $(B - H) \geqslant 13\,000$ gauss will fulfill the condition stated above.

We had available a hot-rolled sheet 0.6 mm thick and 11 cm high. In preliminary magnetic measurements, we found $(B - H) \approx 15\,700$ — 17 000 gauss at H = 100 — 350 gauss, in good agreement with the literature.[3] The polarizing mirror, 110 cm long and 11 cm high, has been assembled by aligning ten square mirrors. Each piece was made of an 11 × 11-cm square of Co-Fe sheet glued to a 2.5-cm-thick copper backing by means of type I "Araldite." The sheet surface to be glued was first prepared by sand blasting. Care was taken to obtain, as much as possible, a flat surface, so that after working the surface to an optical plane the sheet thickness remained sufficiently uniform to permit a uniform magnetization.

The optical work was performed by conventional techniques (grinding with abrasives and polishing with oxides, by means of a pitch lap). Each mirror was made flat within a few fringes. The polishing was not always satisfactory; indeed in almost all samples very fine scratches were visible under intense illumination, and sometimes slightly oxidized or opaque regions appeared.

The ten mirror segments are mounted on a single aluminum bar, as shown in Figs. 1— 3, so that an 8-cm-wide band of the mirror is

---

[1] D. J. Hughes and M. T. Burgy, Phys. Rev. 81, 498 (1951).

[2] M. T. Burgy, R. J. E. Epstein, V. E. Krohn, T. B. Novey, S. Raboy, G. R. Ringo, and V. L. Telegdi, Phys. Rev. 107, 1731 (1957).

[3] R. Bozorth, Ferromagnetism (D. Van Nostrand Co., Inc., Princeton, N. J., 1959).

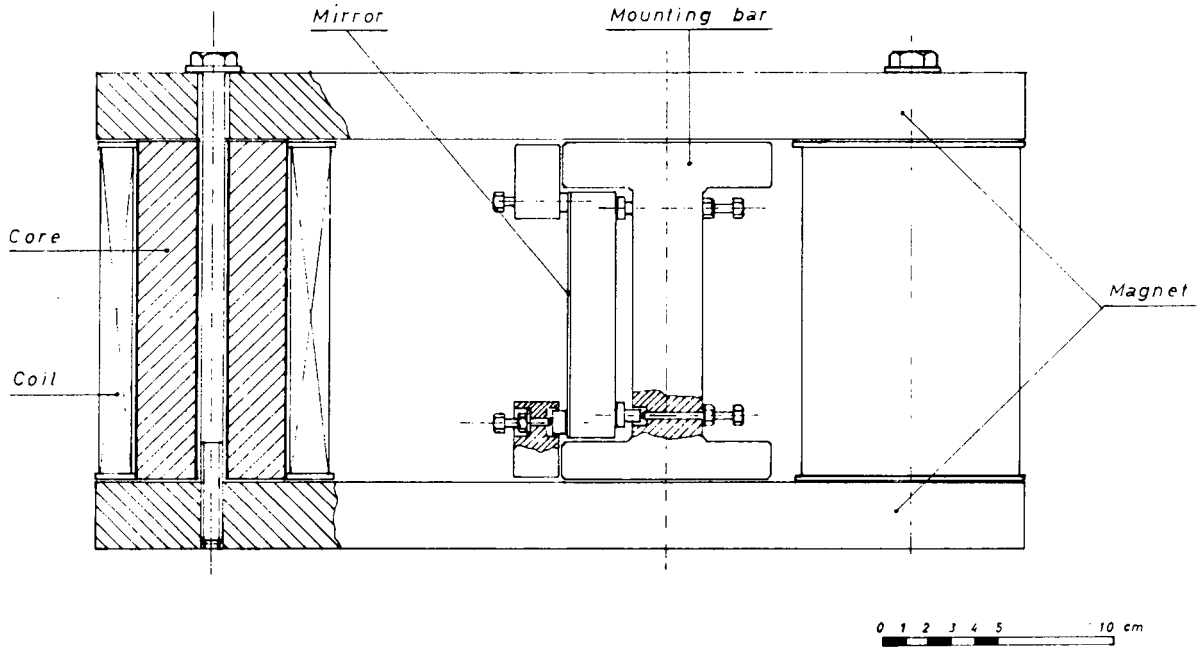

Fig. 1. Cross section of the mirror-mounting system and of the electromagnet.

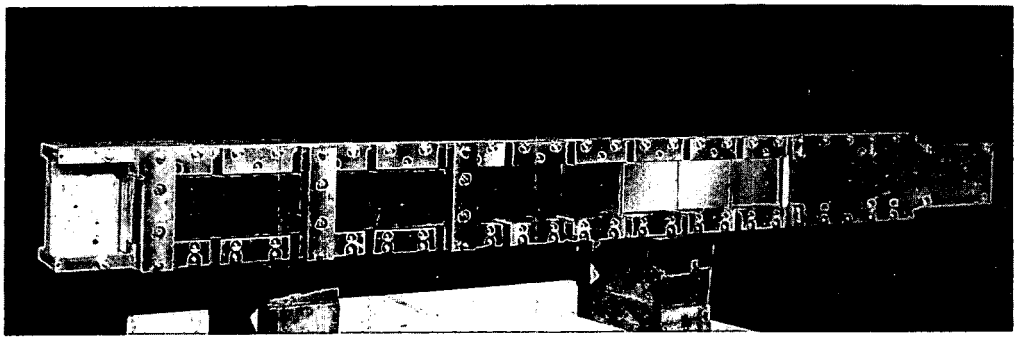

Fig. 2. Photograph of the mirror with collimators.

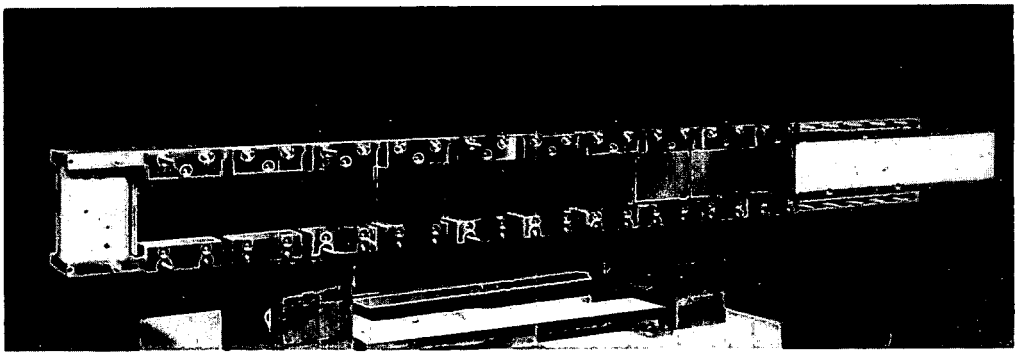

Fig. 3. Same as Fig. 3 except that the front collimating plates have been removed.

exposed to neutrons. The magnetization on this band is expected to be very high and uniform (as previously measured with the separate Co-Fe sheets).

The precise alignment of the ten segments was obtained with reference to three thin (50 micron diameter) wires stretched along the mirror very close to its surface. By observing the distance between each wire and its image, with the help of an optical micrometer, the position of each segment could be set with an accuracy probably better than 5 — 10 microns.

Description of the Apparatus

The general layout is shown in Fig. 4. A narrow thermal-neutron beam is obtained through a first stainless steel collimator plugged into the beam hole. The collimating slit has the following dimensions: length 150 cm, height 10 cm, input width 0.9 cm, output width 0.5 cm. The slit, which is closed at both ends by a 0.25 mm stainless steel window can be filled with water to shut off the beam. After passing through the 8-cm-high slit of the mechanical shutter, the beam is further collimated by a lead-bronze plate facing the first half of the mirror length. This latter collimation permits a minimum beam width, near the mirror center, of about about 1.5 mm. The separation between primary and reflected beam is finally accomplished by the output collimator made of a pair of lead-bronze plates fixed at the mirror end.

The mirror mounting bar, to which the collimating plates are fixed, is positioned in the gap of the electromagnet by means of micrometric screws. At the nominal 0° inclination, the mirror is aligned with one side of the collimating slit.

The electromagnet is made of two parallel Armco iron plates (poles) separated by six iron columns on which are wound coils. At the maximum supply power of 300 W, the mirror is in a magnetizing field of about 350 gauss.

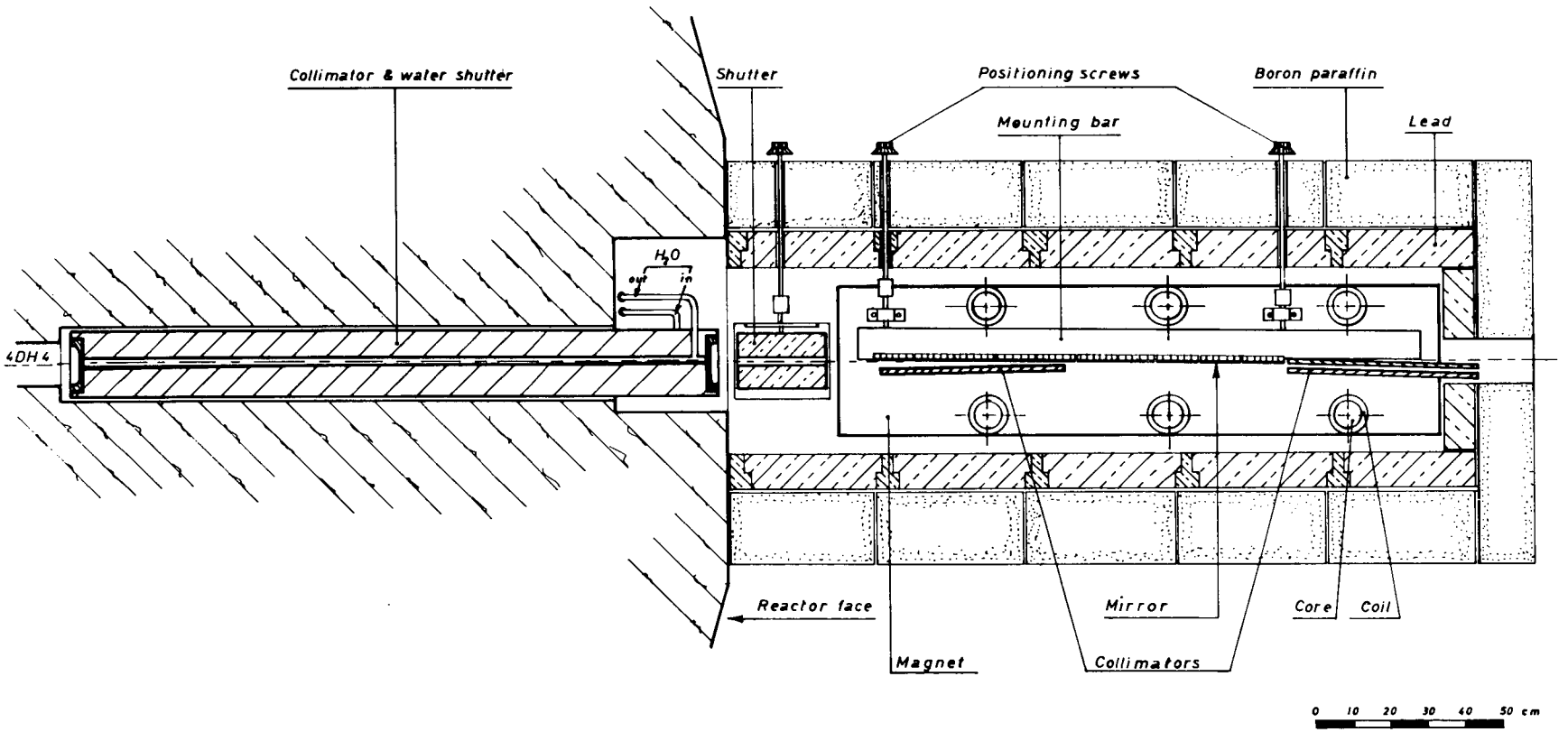

Fig. 4. General layout of the neutron polarizer.

The apparatus is mounted on a heavy concrete base and protected by a shielding tunnel consisting of a 10 cm inner lead wall and a 20 cm boron-paraffin (20% boron oxide) wall. The inner surface of the tunnel is lined with 0.5 cm boron-plastic sheet. This shielding was designed in order to provide a sufficient attenuation of both gammas and fast neutrons, with a least encumbrance. The outer dose levels, at 5 MW reactor power, are well below the MPL's adopted at Ispra, of 2.5 mrem/hr.

Some care was taken to reduce the stray radiations in the direction of the outgoing polarized neutron beam. Mainly, the walls of the slit of the mechanical shutter and the other collimating plates are made of a material (70% Cu and 30% Pb) having very high cross section both for fast neutrons and for gamma rays. Moreover, on their surfaces, thin coatings of boron and lithium compounds were suitably employed to minimize the production of high-energy capture gamma rays.

Beam Measurements

The following characteristics of the outgoing beam have been experimentally studied: (a) intensity, (b) polarization, (c) collimation and flux distribution, (d) ratio of fast to slow neutrons, and (e) gamma background. The measuring methods will first be described.

A detection efficiency of slow neutrons independent of the neutron spectrum (which varied with the mirror inclination, etc.) was needed. The absolute slow-neutron intensity was determined by detecting the 0.48-MeV gamma rays from a thick B target exposed to the beam. In connection with the polarization measurements, we have mainly used a BF_3 counter placed in a 20-cm-diameter paraffin cylinder enclosed in a Cd sheet. The detector was placed with its axis parallel to the beam height. The whole beam was admitted through a window in the Cd sheet.

The beam polarization was measured by means of a double-reflection experiment, using the so-called "shim method." The polarized beam reflected from the first mirror was made to reflect on a second mirror of the same kind and magnetized in a field of the same intensity and orientation (but, for practical reasons, the analyzing mirror was only 55 cm long). The intensity after the second reflection was measured. The beam impinging on the second mirror was then depolarized completely by inserting a 0.25-mm-thick Fe shim. The intensity ratio R with and without the shim is related to the intrinsic polarization of the two mirrors by $R = P_1 \cdot P_2 + 1$.

An accurate determination of the shim ratio was obtained after correcting for the secondary effects of the shim, such as absorption and small-angle scattering. The correction, directly measured by inserting a second identical shim across the beam already depolarized by the first shim, was of the order of 3 — 4%.

Measurement Results

The polarization was measured at the same time as the total intensity and the fast neutrons and gamma background, while the beam collimation and the mirror inclination were variously adjusted. The best compromise between neutron intensity and polarization, from a purely statistical point of view, corresponds to a maximum product $P\sqrt{I}$, which means a minimum measuring time (of the polarization-dependent effect) for a given statistical accuracy. From a practical point of view, however, the most stringent requirement is often to keep the background of fast neutrons and gamma rays at a reasonably low level.

We observed first that, while the inclination of the polarizing mirror varied between 8' and 13' the intensity changed by a factor of the order of 2, but the polarization was not significantly affected. The corrected shim ratio ranged between about 1.55 and 1.65, indicating a "probable" polarization, given as $\sqrt{P_1 P_2}$ from about 75 to 80%. At the

inclination of 7', below which the background was catastrophically increased due to direct transmission, the intensity was larger than 5×10^7 neutrons/sec.

For the next experiments on capture gamma rays, the mirror inclination was fixed at 12' the polarization at 80%, the intensity at about 3×10^7 neutrons/sec, and the ratio of fast to slow neutrons at about 10^{-2}. As previously observed, the polarization is not uniquely determined by the shim ratio. In our case, the value found for the latter permits the extreme limits 65% and 100% for the polarization that each of the two mirrors may be able to produce. Actually we presume that the imperfections to which the lack of complete polarization is due are rather equally shared by the two mirrors. To prove this, segments of polarizing and analyzing mirrors were variously interchanged, with no practical effects. Also the analyzing mirror was shifted to explore different beam sections, and its inclination was slightly varied; no change of the shim ratio larger than 5 — 6% was observed.

To search for a possible unequal magnetization of the mirrors, the magnetic fields on the polarizing and the analyzing mirrors were independently varied. For instance, increasing the field from 230 to 350 gauss had only the effect of raising the reflected intensity by several percent. According to these results, we believe it is rather safe to assume a polarization of 80% with an uncertainty of ± 10%.

The ratio of fast to slow neutrons reported above is the Cd ratio measured when using the BF_3 counter with a paraffin moderator. When measured with a bare BF_3 counter, having about a 10% efficiency to thermal neutrons, the Cd ratio was about 10^{-4}.

Measurements of the gamma intensity, made while the slow neutrons were stopped by a Cd shim, indicated a level of the order of 50 mR/hr in the beam path.

A qualitative picture of the neutron flux distribution over the beam cross section was obtained by exposing a normal photographic plate coated with a LiF layer (Fig. 5). As expected, the neutron flux is highly concentrated at small reflecting angles.

In some experiments it is very important to have a very narrow target from which neutrons may easily escape after a first scattering event that may cause depolarization. Therefore it was interesting to have a measurement of the total neutron intensity still available with a reduced width of the output collimator slit, including only the smaller reflection angles. The results (Fig. 6) indicate that a beam of 1.5—2 mm width may be conveniently used without serious loss of intensity.

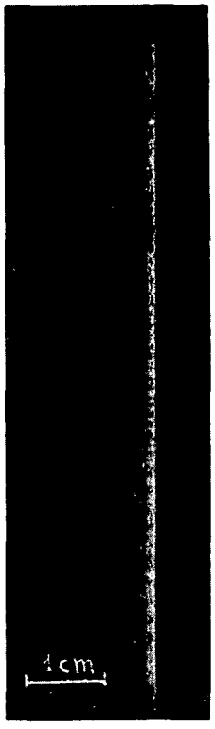

Fig. 5. A "radiograph" of the beam cross section.

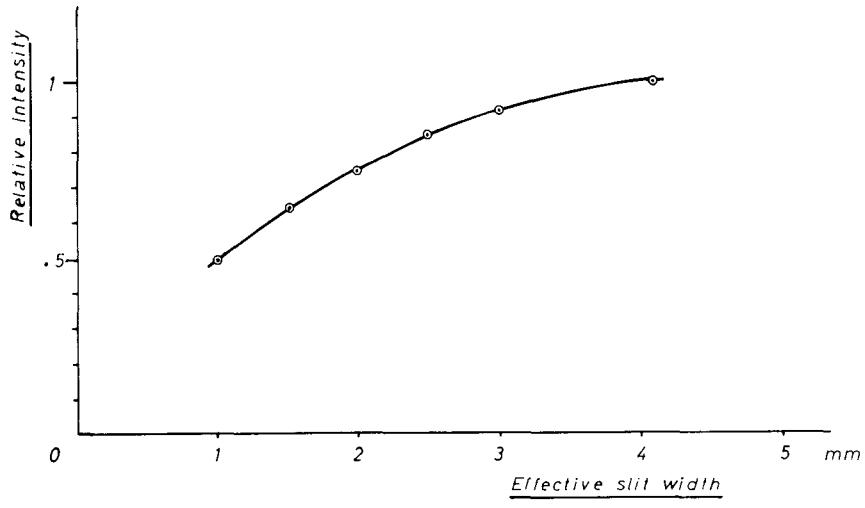

Fig. 6. Beam intensity vs collimation width.

Methods of Reversing the Spin Orientation

In order to measure polarization-dependent effects, as we plan to do with capture gamma rays, the most convenient method is to reverse the spin orientation while the detection system is left unchanged. Among possible methods of changing the spin orientation,[4] we have chosen the one of gradually turning a magnetic guide field along the beam, as shown in Fig. 7.

---

[4] K. Abrahams, O. Steinvoll, P. T. M. Bongaarts, and P. W. DeLange, Rev. Sci. Instr. 33, 5, 524 (1962).

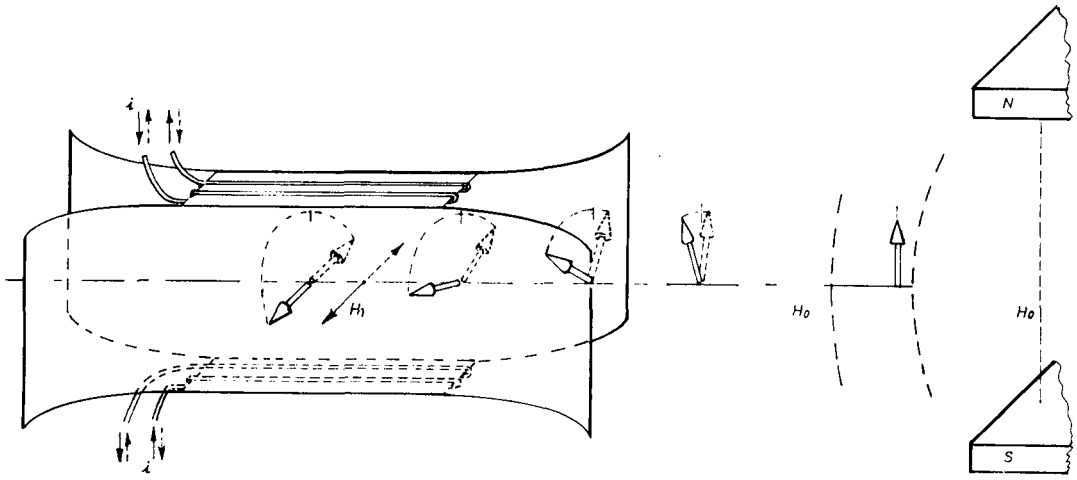

Fig. 7. Scheme of the device for neutron spin reversal.

A neutron traveling through such a field will see, in its own center-of-mass system, a rotating magnetic field. Provided that the field rotates slowly compared with the frequency of the Larmor precession, the spin will maintain the same orientation with respect to the turning field. More precisely, the neutron polarization will periodically vary like $1 - \frac{1}{2}\{\omega^2/[(\omega^2/4) + \Omega^2]\}\sin^2[(\omega^2/4) + \Omega^2]^{1/2}t$, where ω is the field frequency and Ω the Larmor frequency. In our case, guide fields of the order of a few gauss are turned over in a distance of a few tens of centimeters. Negligible depolarization ($<$ 1%) is expected at neutron velocities of, say, 3000 m/sec or lower. In the experimental device, schematically illustrated in Fig. 7, the field along the beam path is the resultant of the stray vertical field of the electromagnet of the polarizer and the horizontal field generated by a current in the magnetic box. Neutrons traveling to the center of the box (target position) will undergo a gradual 90° field turning. Reversing the magnetizing current of the box will effect a 180° reversal of the spin at the target position.

The proposed method has the following main advantages. The current to maintain the field in the magnetic box, which in our case is 5 — 10 gauss, can be conveniently low to be handled without

difficulties by an electronic programing device. It is easy to prevent the possibility that reversing the box field may influence the detectors. Indeed, when the box was magnetically shielded by two layers of 0.35-mm Mumetal sheet, the outside field variation was only a few hundredths of a gauss. It was verified that such a variation had very little influence on a standard scintillation counter, a 3 × 3-in. NaI(Tl) crystal directly coupled to a 3-in. Dumont 6363 photomultiplier, provided with moderate magnetic shielding.

The crystal window was very close to the side wall of the box. Co^{60} gamma rays were detected with the discriminator bias set at the center of the 1.33-MeV line, so that the counting rate was extremely sensitive to changes of the photomultiplier gain. However, the relative-counting-rate variations corresponding to periodic field reversals were within the statistical counting error of $\pm 2 \times 10^{-4}$. This corresponded to a gain stability of better than 10^{-5}.

Session II

PRECISION MEASUREMENTS OF CAPTURE GAMMA-RAY SPECTRA

Tuesday afternoon, 15 October 1963

Presiding: G. A. Bartholomew

Scientific secretaries:
R. K. Smither
D. S. Gemmell

II-1. APPLICATIONS OF NUCLEAR MODELS TO LOW-LYING STATES—SUMMARIES AND DEVELOPMENTS*

Steven Moszkowski

University of California, Los Angeles

In the last few years quite a bit of progress has been made in nuclear structure both theoretical and experimental. In my talk today, I would like to discuss three selected topics in which advances have been and are being made. These topics are (1) the effect of pairing on electromagnetic transitions, (2) some aspects of nuclear vibrational states, including the coupling of an odd particle to a vibrating core, and (3) the limitations of the shell model and the presence of unexpectedly strong collective motion in some light nuclei.

At this point I should remark that I will not restrict myself to those nuclei which can be reached by neutron capture. The talk will be a bit more general than that. I guess I also have to apologize that my talk will not deal with accurate energy calculations. Such things would come in, for instance, in studying rotation-vibration interaction in deformed nuclei, but this will be discussed elsewhere in this conference.

Now let me review the effect of pairing on electromagnetic transition rates. It is really an old problem. It was known already in 1950 that you have magnetic 2^4-pole transitions (M4) in which you have a change of 4 in the nuclear spin and a change in the parity. A number of these transitions occur for odd-A nuclei

---

*Invited paper.

with odd N or Z between 39 and 49, and also for odd N between 65 and 81. According to an extreme single-particle model, the transitions are $p_{1/2} \longleftrightarrow g_{9/2}$ and $h_{11/2} \longleftrightarrow d_{3/2}$, respectively. The presence of these "islands of isomerism" proved very important for the development of the nuclear shell model. One aspect of the transitions is that the lifetimes are expected to go like E^{-9}, and experimentally it was found that this was satisfied to a good approximation. The gamma-decay lifetimes range all of the way from the order of a second to a year. Furthermore, the lifetimes turned out to be not too far from those expected on the basis of a single nucleon making the transition.

Figure 1 will illustrate this point. This figure shows the

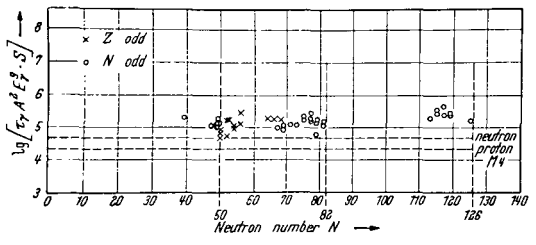

Fig. 1. Comparative lifetimes for M4 transitions. From D. Alburger, Handbuch der Physik (Springer Verlag, Berlin, 1957), Vol. 42, p. 93.

comparative lifetimes of the energy levels of these nuclei compared to the single-particle values, and you see they fluctuate only by factors of two or so.

It was remarkable that the single-particle model worked so well, and indeed rather puzzling because we know that this model is not expected to be so accurate. Now, according to the single-particle model, we will say that a nucleus like this can be described as follows: the nuclear spin is just the j of the last odd particle, and we could write the wavefunction as $\Psi = (j_1^{n_1})_0 (j_2^{n_2})_0\, j_{odd}$. This model implies that all of the states up to some energy are occupied, while all the states above it are empty. We know now, of course, that this is not quite right. In the last few years the so-called "quasi-particle" or "super-fluid" model of the nucleus has been developed in which we generalize the single-particle model to allow pairing correlations (correlation

between pairs of particles coupling to J = 0). Let me write down the wave function of an odd-A nucleus if one includes the pairing correlation. The wave function is written $\Psi = \prod_i (U_i + V_i j_i j_i^*)\, j_{odd}$, where j_i^* is the state conjugate to j_i. The pair of states j_i, j_i^* has a probability amplitude V_i of being occupied and U_i of being empty. The Fermi surface is now diffuse as indicated in Fig. 2. Here $P_i = V_i^2$ denotes

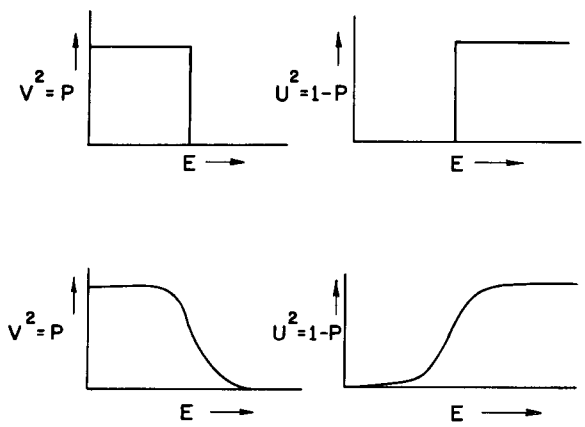

Fig. 2. U^2 and V^2 vs energy, exhibiting the diffuseness of the Fermi surface.

the average probability of occupation. The diffuseness measures the energy gap, which is closely related to the pairing energy, i.e., the even-odd mass differences.

I would like to make one remark here. With a wave function like this, the number of particles is not uniquely specified because (except for the odd particle) we have in each pair of states (j_i, j_i^*) either <u>two</u> nucleons or none. However, while there is some uncertainty in the number of particles, calculations have shown that the fluctuations in the number of particles are quite unimportant for getting over-all features.

Let me briefly discuss the effect of pairing on electromagnetic transition rates. This is really not new, but a very brief review. If we have a transition of a single particle, $j_i \rightarrow j_2$ (or hole, $j_1^{-1} \rightarrow j_2^{-1}$), we have $B = B_{sp}$, i.e., the single-particle value.

Now suppose, however, that we already have some

particles in the state j_2; then the transition would be $j_1(j_2^{n_2})_0 \rightarrow (j_2^{n_2+1})_{j_2}$. In this case B must be smaller than the single-particle value, because some of the states into which this particle could go in j_2 are already occupied. For this case it is reasonable that $R = B/B_{sp} = 1 - P_2 = U_2^2$. In fact, if shell j_2 is full, $P_2 = 1$ and this transition cannot occur at all. We can go beyond this. Suppose a small fraction of both shells j_1 and j_2 is occupied. In this case it is logical that $R = (1 - P_1)(1 - P_2)$.

However, this cannot be completely right. Suppose that both shells j_1 and j_2 were almost filled, i.e., suppose that $j_1^{-1} \rightarrow j_2^{-1}$. In this case it is well known that you will get exactly the same result as if holes are replaced by particles, and so in this case $R = P_1 P_2 = V_1^2 V_2^2$. In the quasi-particle it turns out that the transition amplitude R is the sum or difference of the amplitudes discussed above, i.e.,

$$R = (U_1 U_2 \pm V_1 V_2)^2 \qquad (1)$$

What I have tried to do is to give a plausibility argument for this result. The plus sign applies for magnetic transitions, the minus sign for electric transitions. This follows from rather simple considerations of time-reversal invariance.

Now suppose that the two states were very close together in energy, i.e., $V_1 = V_2$ and $U_1 = U_2$. Then $R = U_1^2 \pm V_1^2$. For magnetic transition, we find $R = 1$; the transition rate does not depend upon the number of particles in the shell. (This is for the same reason that magnetic dipole moments have the single-particle Schmidt values as we fill up a shell.) However, for an electric transition $R = (1 - 2P_1)^2$. The amplitude goes from 1 at the beginning of a shell to -1 at the end. Again, electric quadrupole moments have the same behavior—according to a jj-coupling model.

Now, the conclusion from this is that you would expect magnetic transition rates to deviate little from the predictions of the single-particle model, but electric transition rates to deviate quite strongly. This is in fact found and is really basically the reason why for M4 transitions one doesn't find much fluctuation in the reduced transition rates.

Figure 3 shows this point in slightly more detail. This is

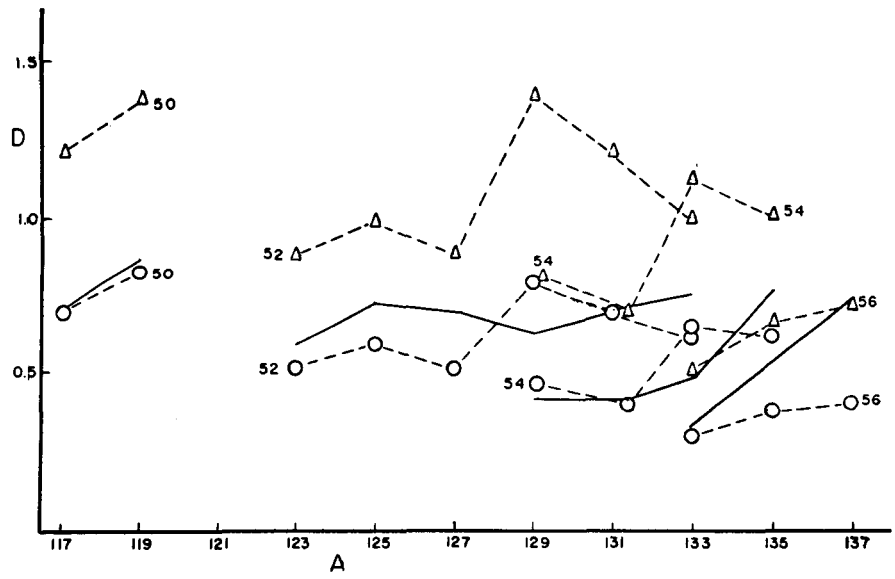

Fig. 3. Reduction factors for M4 $h_{11/2} \rightarrow d_{3/2}$ neutron transitions (from Ref. 1). The theoretical results are given by the solid lines while the experimental ratio of the transition probability to the single-particle value is given as triangles or circles connected by dashed lines with the assumption of the radius parameter of 1.0 and 1.1 fermi, respectively. The sequences are labeled by proton numbers.

taken from a recent preprint by Kisslinger and Sorenson.[1] What they have plotted here are these factors, except that their D is normalized slightly differently than my R; so D can be larger than unity. (By the

[1] L. Kisslinger and R. Sorenson, Office of Naval Research Technical Report 11, Department of Physics, Carnegie Institute of Technology, Pittsburgh, Pennsylvania.

way, the two dotted curves represent two different assumed nuclear radii, $1.0\ A^{1/3}$ and $1.1\ A^{1/3}$, respectively.) First of all, you see that the dotted lines and the solid lines follow each other fairly nicely. The second thing you see here is that the values of D are somewhat larger for 50 protons and decrease for 52, 54, and 56. However, they tend to increase with neutron number as N approaches the magic number 82. Some of the trends can be attributed to the inequality of V_1 and V_2. Kisslinger and Sorenson also consider the effect of quadrupole excitations in the wave function. (This is, of course, outside the model considered above.) These improve the agreement with experiment.

Let me just say a word about some other multipolarities. We have, for example, magnetic-dipole transitions and the same thing would apply there. At least in these N = 65-81 nuclei, some M4 transitions are followed by a $\frac{3^+}{2} \rightarrow \frac{1^+}{2}$ M1 transition. According to a single-particle model, they would be of the form $d_{3/2} \rightarrow s_{1/2}$. Now, this cannot occur in the simplest model because the magnetic pole can only flip the spins but not change the orbital motion. These are known as so-called "ℓ-forbidden" transitions; in fact it is known that such transitions are retarded relative to single-particle values, especially near closed shells, and reach a maximum rate in between. This is because deviations from this single-particle picture can take place easiest in the middle of a shell because particle effects and configuration mixing are strongest here.

Now, I should just mention something which will be discussed in much more detail during this conference by Bergqvist[2] and Harvey,[3] namely that some magnetic-dipole radiation can be actually

---

[2] I. Bergqvist, B. Lundberg, and N. Starfelt, paper III-3 presented at this conference.

[3] J. A. Harvey, G. G. Slaughter, J. R. Bird, and G. T. Chapman, paper III-4 presented at this conference.

enhanced relative to the predictions of the single-particle model. We are dealing here with transitions between members of a spin-orbit doublet, i.e., $g_{7/2} \rightarrow g_{9/2}$. These transitions have energies of several MeV, but occur strongly in some nuclei following neutron capture. This is an exciting development.

Now, let me just say a couple of words about electric transitions. Of course, you all know that many electric transitions are strongly enhanced relative to the prediction of the single-particle model because of the existence of collective motion, e.g., collective quadrupole excitation, etc. I will say something about these later.

According to the shell model there are, however, other kinds of electric transitions in which really a single particle changes its state. For example, let us take an example. In ${}_{48}Cd^{111}_{63}$ there is a transition of this type which can be identified with a single neutron jumping from an $h_{11/2}$ to a $d_{5/2}$ orbit. Such transitions have also been investigated theoretically recently by Kisslinger and Sorenson[1] and by Ikegami and Udagawa.[4] They have found that the transition rate is definitely reduced below the values expected for a single particle. Now, of course, an odd neutron acting by itself will not give off electric radiation. However you will get a polarization of the core to some extent; so the neutron should have an effective charge and you introduce an effective charge of the neutron $e_{eff} \approx 0.5-1$. Still, the transition rates experimentally found are much smaller than those predicted by the single-particle model.

Recently, it was shown, especially by Ikegami and Udagawa,[4] that the empirical rates for transitions of this type can be nicely accounted for by the quasi-particle picture (with inclusion of collective excitations). With the minus sign in Eq. (1), under

---

[4] H. Ikegami and T. Udagawa (preprint).

certain circumstances R will vanish. When one puts in the numbers, empirical U's and V's deduced from empirical positions of levels and pairing energies, one obtains reductions of 2 and even 3 orders of magnitude in the transition rates, in agreement with empirical trends.

In summary for this part of the talk, it seems that inclusion of the pair correlations in the nuclear wave functions of the nucleus, even in its first approximation, gives you a modification of the single-particle transition rates, which is at least in qualitative agreement with experimental trends.

The next part of my talk deals with vibrational states in spherical nuclei.

For even-even nuclei, the well-known quadrupole phonon model gives the states indicated in Fig. 4; the levels are equally spaced.

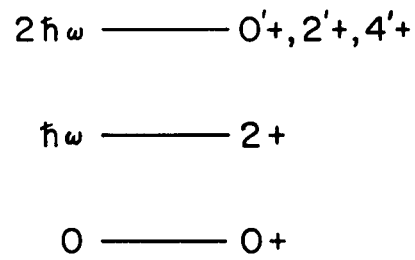

Fig. 4. Energy levels of spherical even-even nuclei according to the quadrupole phonon model.

Also, no E2 transition from the $2'^{+}$ state, to the 0^{+} ground state are predicted, and it is an old story, of course that a 2' state like this is found in many nuclei and you get a very weak cross-over.

Another remark that follows immediately from the model is that the values of B(E2) from any of these two-phonon states to the 2^{+} state are expected to be the same. We have B(E2, I' → 2) = 2 B(E2, 2 → 0).

I would like to discuss now some aspects of this model. Figure 5 shows the low-lying levels in three particular even-even nuclei of interest. In Ni^{62}, Sen Gupta and Van Patter[5] have found at least

[5] A. K. Sen Gupta and D. M. Van Patter, Phys. Rev. 131, 318 (1963).

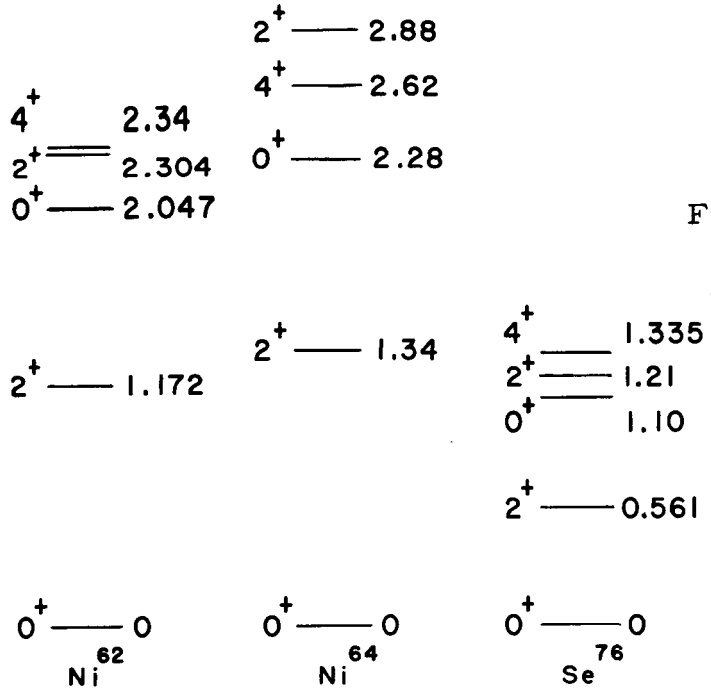

Fig. 5. Low-lying energy levels of Ni^{62} (Ref. 5), Ni^{64} (Ref. 8), and Se^{76} (Ref. 9).

three states that have the right spin to be members of the triplet, and these states have in fact been analyzed. Kerman and Shakin[6] have given a theoretical analysis for the splitting of the 2-phonon states, but this question is still open.[7] In Ni^{64}, states have recently been found by inelastic proton scattering at Oak Ridge.[8] Then there is Se^{76}, which I think is an interesting case, found by Douglas *et al.*[9] at Aldermaston. Here, we also know something about the electric-quadrupole transition rates. It is found experimentally that $B(4' \rightarrow 2) \approx 2\, B(2 \rightarrow 0)$ as

---

[6] A. K. Kerman and C. M. Shakin, Phys. Letters 1, 151 (1962).

[7] In a later talk at this conference, Brink (paper III-1 of this conference) will point out that the mechanism invoked by Kerman and Shakin (terms which depend on the 3rd and 4th power of the deformation) gives poor fits to the energies of the 3-phonon states in nuclei such as Sm^{150}.

[8] J. K. Dickens, F. G. Percy, R. J. Silva, and T. Tamura, Phys. Letters 6, 53 (1963).

[9] Douglas *et al.*, paper presented at the 1963 Asilomar Conference on Heavy Ions.

expected; but for the 0' and 2' states, the ratio is only about 1. This has not been explained yet. (In this nucleus one has to measure the transition rate going up, not down, because the states are excited by heavy-ion Coulomb excitation. The rates for the upward and downward transitions are related by elementary statistical factors.)

Well, I show this plot to stimulate your further thoughts about really trying to pin down states belong to the triplet. Of course, there is another well-known case which is a rather old story. In Cd^{114} not only were all three members of the triplet found but a couple of other states close by which must be other kinds of excitations.

Figure 6 shows another aspect of this which I think deserves some attention. Here are the most recent results for the

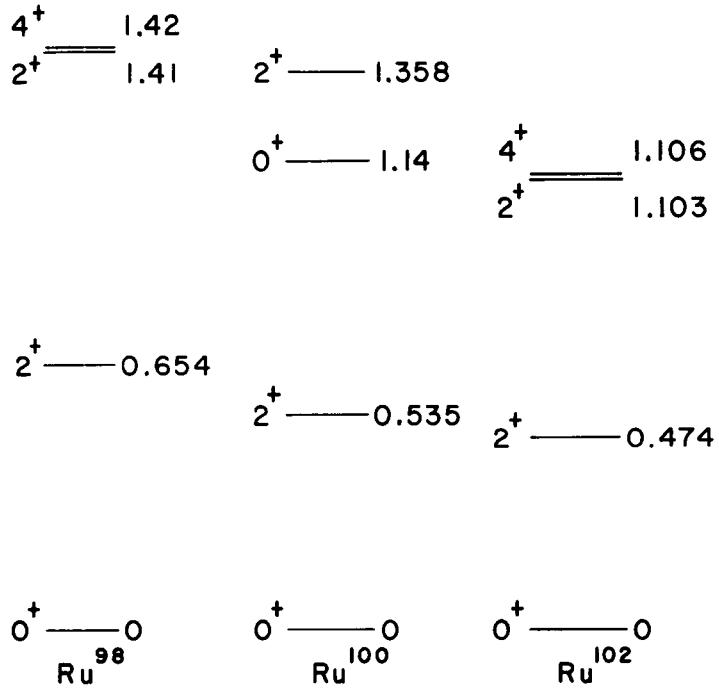

Fig. 6. Low-lying energy levels of Ru^{98}, Ru^{100}, and Ru^{102} (from Nuclear Data Tables and Born et al., Physica 29, 537, 1963.

isotopes of ruthenium. The point I would like to make is that for Ru^{98} and Ru^{102} one finds the $2'^{+}$ and $4'^{+}$ states; and for Ru^{100}, one finds the $0'^{+}$ and $2'^{+}$ states. I would like to stimulate further thought on the possibility of 0^{+} states in Ru^{98} and Ru^{102} as well as in other even-even nuclei in this region.

Here is another thing on which I am sticking my neck

out. There seems to be a tendency for the states to be ordered energetically as 0, 2, 4. (Let me however confess that I have been a little biased on all cases except one in Ni^{64}. In fact, there are also other cases besides Ni^{64} in which they are not ordered that way. However it would be nice to get further information on this.) I might say that a very naive theoretical model taking the quadrupole forces into account would not give you this order, but rather 0, 4, 2. Theoretically, it is difficult to get them ordered as 0, 2, 4. This is still an open problem.

Now, I would like to say something about odd-A nuclei in this region. This is an idea which was already introduced by Lawson and Uretsky[10] several years back, namely that if you have an odd-Z even-N nucleus you might regard it as a proton plus an even-even core.

Figure 7 shows the results of Vervier[11] on the isotopes

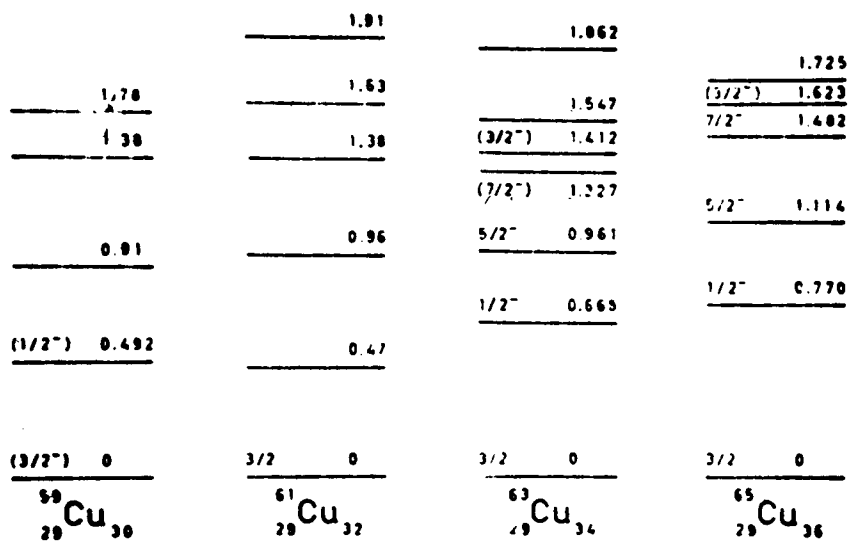

Fig. 7. Energy levels of odd-mass isotopes of Cu, Z = 29 (from Ref. 11).

---

[10] R. D. Lawson and J. L. Uretsky, Phys. Rev. 106, 1369 (1957); ibid. 108, 1300 (1957).

[11] J. Vervier, Nuovo Cimento 28, 1412 (1963).

of copper. The ground state is $\frac{3}{2}^-$ which can be identified with the odd proton in a $p_{3/2}$ state. The remaining even-even core has 0^+ in its ground state, but it can have a 2^+ excited state. You will then expect to get states in which you have not the single particle but the core excited; the angular momentum can couple to $\frac{1}{2}^-$, $\frac{3}{2}^-$, $\frac{5}{2}^-$, and $\frac{7}{2}^-$. Indeed, as can be seen, we have all four such states in Cu^{63} and Cu^{65}. There is one point that has already been made by Lawson and Uretsky[10] several years ago. The center of gravity of the four states in Cu^{65} is nearly the same as the energy of the 2^+ state of the "core" nucleus Ni^{64}. It is not clear however whether this is really as significant as was once thought.

More significant is this following fact. If one gets an E2 transition from one of the four states to the ground state, what happens is just that the core changes from 2^+ and 0^+. Thus, all of the B(E2, $I' \rightarrow \frac{3}{2}$) should be the same for the four cases.

Empirically, the B(E2) for these <u>are</u> nearly the same except for the $\frac{3}{2}^-$ excited state. Here the B(E2) is smaller. According to the simple model, this is not a sufficiently complete and accurate description of this nucleus. However, to make a long story short as Vervier points out,[11] both of the $\frac{3}{2}^-$ states have to be regarded as mixtures between 0-phonon and 1-phonon states (at least). But for the other states $\frac{1}{2}$, $\frac{5}{2}$, $\frac{7}{2}$ this may be a fair description.

All this may also hold for odd-neutron nuclei. Figure 8 shows the level schemes of nuclei with N = 29. Here the spins of these levels have not been pinned down sufficiently well to say anything for sure, but it would be nice to know to what extent the odd-particle-plus-core model has application in this region. (See the parenthetic remark in the comment by Schiffer in the discussion on this talk.)

Incidentally, there was one other point. Figure 7 showed that the order of excited levels was $\frac{1}{2}$, $\frac{5}{2}$, $\frac{7}{2}$, $\frac{3}{2}$. Except for the $\frac{3}{2}$

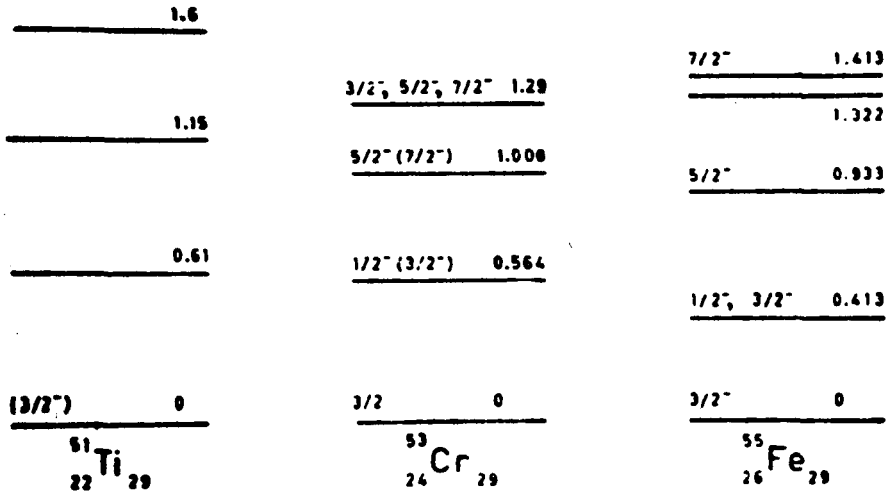

Fig. 8. Energy levels of odd-mass isotopes with N = 29 (from Ref. 11).

level, the levels occur in order of increasing J. I should point out to you that if one assumes a simple quadrupole interaction between the core and the particle, I believe one would get something like $\frac{1}{2}$, $\frac{7}{2}$, $\frac{3}{2}$, $\frac{5}{2}$. The observed order suggests the existence of some form of dipole-dipole interaction. What is this dipole-dipole interaction? It is still quite a mystery, and I think it is a fairly exciting problem to clear up. Of course the coupling between the $\frac{3}{2}^-$ levels pushes them apart so that the upper $\frac{3}{2}$ level moves upward (and above the $\frac{5}{2}$ and $\frac{7}{2}$ levels).

Another case is the odd nucleus Au^{197} where de Shalit[12] has made a similar analysis. Here the excited levels are in the order of increasing J: $\frac{1}{2}$, $\frac{3}{2}$, $\frac{5}{2}$, $\frac{7}{2}$.

Another example of this, I believe, is shown in Fig. 9. In the nucleus Tl^{203} (as well as the neighboring nucleus Tl^{205}) a pure quadrupole interaction between the core and the particle wouldn't give any splitting at all between these levels since the particle in the $s_{1/2}$ ground state has no quadrupole moment. The situation must be more involved, and again seems to suggest a dipole interaction. I might say

[12] A. de Shalit, Phys. Rev. 122, 1530 (1961).

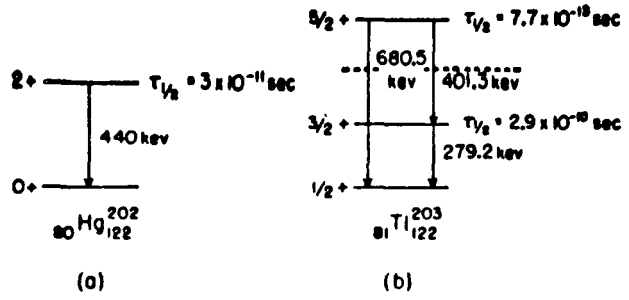

Fig. 9. Energy levels of Hg^{202} and Tl^{203} (from Ref. 12). The broken line shows the position of center of gravity of the $\frac{5}{2}^+$ and $\frac{3}{2}^+$ levels.

that Tl^{205} (which has a proton and two neutrons missing from the doubly magic nucleus $_{82}Pb^{208}_{126}$) has been fairly well explained both on the basis of a particle-core model and also a conventional shell model by Silverberg.[13]

Figure 10 shows that this situation might also arise in odd-N nuclei. Again, I think, it would be nice to look and see if there

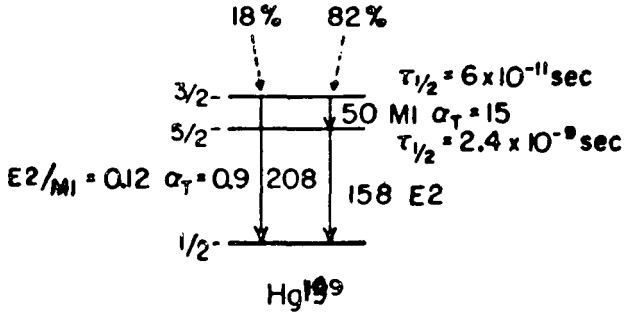

Fig. 10. Energy levels of Hg^{199} (from Ref. 12). The branching ratios refer to total transitions. (The 18% and 82% should be interchanged.)

cannot be more odd-N nuclei for which this picture of odd neutrons coupled with a core might have relevance. I think this may be a promising picture, though, of course, quite approximate. It may give us some more insight into nuclear structure.

The last part of my talk will be on a topic that may become something exciting in the near future. It deals with the possible predominance of collective effects even in regions of nuclei where they were not thought to be so important. Let me elaborate a little bit.

---

[13] L. Silverberg, Arkiv Fysik 20, 355 (1961).

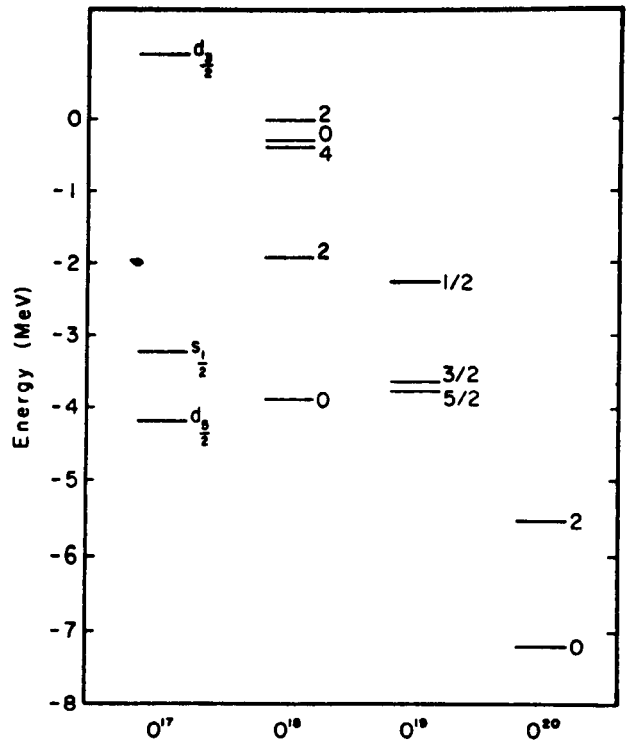

Fig. 11. Experimental energy levels of O^{17}, O^{18}, O^{19}, and O^{20} (from Ref. 14).

Figure 11 shows the experimental levels for the oxygen isotopes, taken from a recent paper by Dr. Pandya.[14] The positions of these levels can be quite nicely explained by conventional shell-model-type calculations in which one considers the neutrons outside of the closed-shell O^{16} core with reasonable internucleon forces.

Now it was shown by Pandya,[14] and also by Inoue and Arima[15] who made calculations on these isotopes (and also on Ne^{20}), that it is quite possible in this nucleus to fit the positions of most levels with reasonable interactions. However, it is difficult to fit the positions of the excited 0^+ state. This seems to be found in a number of other shell-model calculations too, e.g., in C^{12}.

---

[14] S. P. Pandya, Nucl. Phys. 43, 636 (1963).

[15] Inoue et al. (preprint).

Also, Flowers[16] has difficulty in fitting the position of the first excited 1^+ state in F^{18}. (Here the ground state is 1^+.) Perhaps the conventional shell model works well only for the lowest states of given spin and parity.

We know that when you get up to 10 MeV the shell model breaks down, i.e., excitations of closed shells become important. But now, apparently, even at lower energies there seems to be some trouble. This is very strongly supported by a recent communication by Bohr and Mottelson[17] who have looked at the B(E2) going from, say, this $0'^+$ state to the lowest 2^+ state.

Now, B(E2)'s, of course, strongly reflect collective quadrupole excitations. Consider for example the $2^+ \rightarrow 0^+$ transition in O^{18}. It would not occur at all if we accepted the shell models blindly because we have only two neutrons outside closed shells. As I have said before, however, we all know that you have to have some effective charge for the neutrons because of polarization of the core. If we take an effective charge of, say, 0.5, (a reasonable value in this region and also well understood theoretically), it can give a reasonable fit to this transition rate.

However, when it comes to the $0'^+ \rightarrow 2^+$ transition, one needs a tremendous effective charge (about 5e) to account for the observed rate.[17] In other words, this decay is almost two orders of magnitude larger than would be expected on the basis of a conventional shell model; apparently, when we get up to this $0'^+$ state, the

---

[16] B. H. Flowers and D. Wilmore (preprint).

[17] A. Bohr and B. R. Mottelson (private communication: Nuclear News, April 1963).

O^{16} core really starts to play a decisive role. A similar enhancement seems to occur also for the $0'^{+} \rightarrow 2^{+}$ transition in other nuclei such as Ca^{42}, Ge^{70}, and Ge^{72} (cf. Ref. 17). Also in O^{16}, a similar situation occurs. Here the $0'^{+}$ state is below the 2^{+} state and there is a large B(E2) between them. There is also a 4^{+} state higher up. The excitation energies are 6.1, 6.9, and 10.4 MeV, suggestive of a rotational band. This is supported by the observed ratios of E2 transition probabilities.

What I would like to do here is to suggest two things. Figure 12 shows the systematics of nuclei taken from a recent article

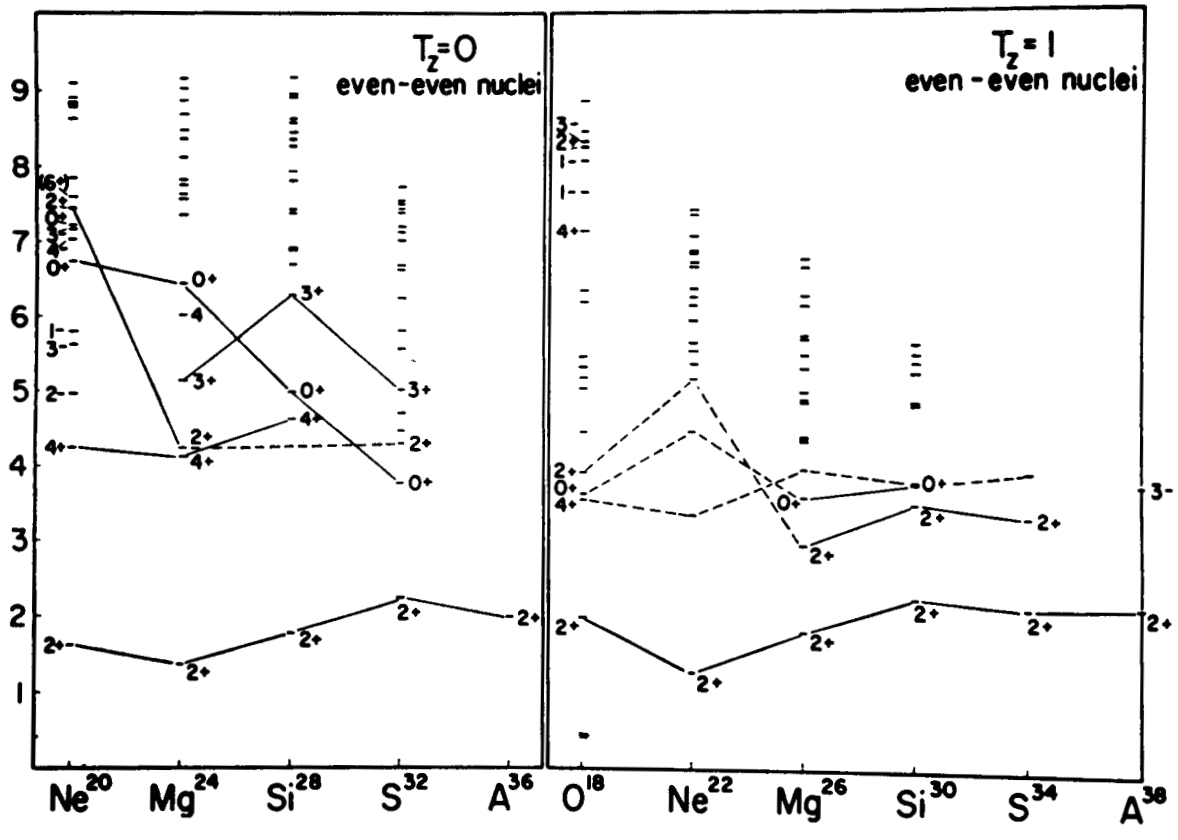

Fig. 12. Energy levels of even-even nuclei of the (s,d) shell, classified according to T_z, the z component of isotopic spin (from Ref. 18).

by Broude and Gove.[18] I would like to mention that you have excited 0^+ states here. It would be very nice to find out how large the B(E2) are for the $0'^+ \rightarrow 2^+$ transitions—how they vary as you go through a shell. Perhaps they are quite large.

Well, to finish, let me say that this is really not too surprising in a way. The core simply cannot be neglected. Apparently a "spherical" nucleus such as O^{16} or O^{18} is really spherical only for the lowest states, which you have seen from the success of the single-particle model. But perhaps at comparatively low excitation energies the core can get broken up and give tremendous collective effects. For example, the $0'^+$ state in O^{18} must contain[17] a large mixture of such configurations as $p^{-2}(sd)^4$. If one looks at the Nilsson model and allows for the breakup of the core, then this actually does not seem so unreasonable for the lowest states. You tend to get one kind of shape for the ground state, but you do not have to get high in energy before this shape is no longer stable; or you get a different shape, or alternatively you can get very little stability of spherical shape. So from the theoretical point of view, all this does not seem too surprising.

I would like to close this talk on one amusing note. In 1956 when Morinaga published a paper[19] dealing with a related problem, he pointed out that in some light nuclei you apparently do have something that looks like rotational bands. At that time, of course, transition rates were not known. But he looked at the ratios of energy spacings and identified certain groups of excited states as rotational bands. He

---

[18] C. Broude and H. E. Gove, Ann Phys. (New York) 23, 71 (1963).

[19] H. Morinaga, Phys. Rev. 101, 254 (1956).

assumed an α-particle model, and identified various bands with different configurations of α particles. Then in O^{16} the ground-state configuration is symmetric (i.e., the α particles are arranged in a tetrahedron) but in an excited state they tend more to be lined up. In a highly excited state they could even be lined up in a single row! This model was not taken very seriously at the time.

However, perhaps with the discovery of these large values of B(E2) there is at least something in Morinaga's picture we ought to consider, especially by those who do shell-model calculations. Apparently the idea of having those spherical shapes is fine in low states but the collective effects can become very important at already fairly low energies. There is quite a bit to be learned here.

Altogether, I have tried to outline a few special topics on nuclear models, which I think are exciting and susceptible to more experimental work. Thank you.

* * *

P. MOLDAUER, Argonne National Laboratory: I know how quite well established spin experiments have been made which give trouble with the quadrupole interaction. But some recent neutron-scattering experiments at Argonne by Smith are quite difficult to understand in terms of that spin assignment. The level order is perhaps something more like $\frac{7}{2}$, $\frac{1}{2}$.

MOSZKOWSKI: Well, that, of course would change my remarks. I took Vervier's spin assignments.

J. P. SCHIFFER, Argonne National Laboratory: Along the same line of spin assignments, I might mention that you showed three odd

nuclei, but with tentative spins. Now two of those nuclei are much better known. Bartholomew[20] has measured Cr^{53} by gamma-gamma correlations following neutron capture, and a lot of the spin assignments in Fe^{55} are now known definitely from (d,pγ) correlations.[21]

MOSZKOWSKI: How do they go?

SCHIFFER: Five or six spin are known. (These results suggest that the lowest three states are $\frac{3}{2}$, $\frac{1}{2}$, $\frac{5}{2}$, the same as for the Cu isotopes.)

MOSZKOWSKI: This is very nice. I would like to make another remark about this "odd proton or odd neutron plus core" model. I think at best it can only be semiquantitative, by the very nature of it. The energy required for the odd particles to go from one orbit to another is rarely very large compared with the energy required to excite the core. But I think it can at least be that much in many cases; and if we understand the limitations of this model it might well stimulate further experimental work (i.e., for determining the spins and transition rates).

K. K. SETH, Northwestern University: I would like to make a remark about evidence for the deformations in light nuclei around 70 or so. We know that in neutron scattering, especially in s waves, the effects of deformation show up. Back in 1956 and 1957, both ourselves and Bollinger found that similar splitting of the s-wave strength might be taking place. At that time we offered this addition, that it could be due to deformations. It is encourgaging to note that now there is reason to believe that reason for deformation may exist.

---

[20] G. A. Bartholomew and M. R. Gunye, Bull. Am. Phys. Soc. 8, 367 (1963).

[21] D. S. Gemmell, L. L. Lee, Jr., A. Marinov, and J. P. Schiffer, Bull. Am. Phys. Soc. 8, 523 (1963).

MOSZKOWSKI: Either a deformation or a sudden decrease in the stability of the spherical shape as you go into excited states.

SETH: As long as the particle sees such instability.

MOSZKOWSKI: It may be not a permanent deformation, but a vibration. It would be with a large zero-point motion $\langle \beta^2 \rangle$.

A VOICE: Chase actually did some computations with some guessed values of β^2. The spreading of the peak is the part of the experiment that he observed.

MOSZKOWSKI: That is very good.

R. LEMMER, Massachusetts Institute of Technology: This is a comment in connection with the "odd particle plus core". We tried another calculation on Cu^{63}, namely taking three quasi-particles and coupling them together by long-range interactions. If you do this, you get 15 states in the same energy range that you get 4. Now, when you analyze this and work out the B(E2) values, you find that even though you have ten energy levels, only four of them have strong B(E2) values. In that sense, you would still see 4 strong states electromagnetically.

MOSZKOWSKI: That is extremely fascinating. It bears on the point that I mentioned. Maybe a model such as the odd-particle-plus-core is only a very rough model. We know its limitations. If it makes any sense, it must really be (in a sense) derivable from a somewhat better description. What you are saying is that you actually get these states, but you also get other states.

LEMMER: That is right. These four states that are not really connected as a quartet, being coupled to a core, happen to have a strong B(E2). Why it gets strong, of course, is because some sort of coherent effects come in. It is hard to explain where they come from.

II-2. CAPTURE GAMMA DETERMINATION OF VANADIUM-52 STRUCTURE*

D. H. White, W. John, and B. G. Saunders

Lawrence Radiation Laboratory, Livermore, California

Vanadium-52 is an old friend around Lawrence Radiation Laboratory. It was first studied about three years ago by Commander Schwager who investigated some of the intermediate energy levels as well as the low-lying levels. More recently, in an attempt to learn more about its spin structure, we made some angular-correlation measurements. In the process, we measured some of the energies more carefully with the scintillation spectrometer, and found there seemed to be more structure than had previously been supposed.

At that point, we decided to attack the problem by use of the bent-crystal spectrometer which will be described in paper II-8 of this conference, as well as with a coincidence spectrometer.

Figure 1 is a schematic diagram of the thermal-neutron collimator and filter used for the scintillation spectrometer. On the left is the Livermore 2-MW tank-type reactor. It is light-water moderated. We have 3 in. of lead at the front end of the beam tube. The filter consists of a series of cores taken from quartz crystals. We have from three to five of them placed in the beam, depending upon how much background from reactor gammas we are willing to tolerate. We certainly are willing to tolerate more gamma background if we are doing coincidence work than if we are doing singles work.

*Presented by D. H. White.

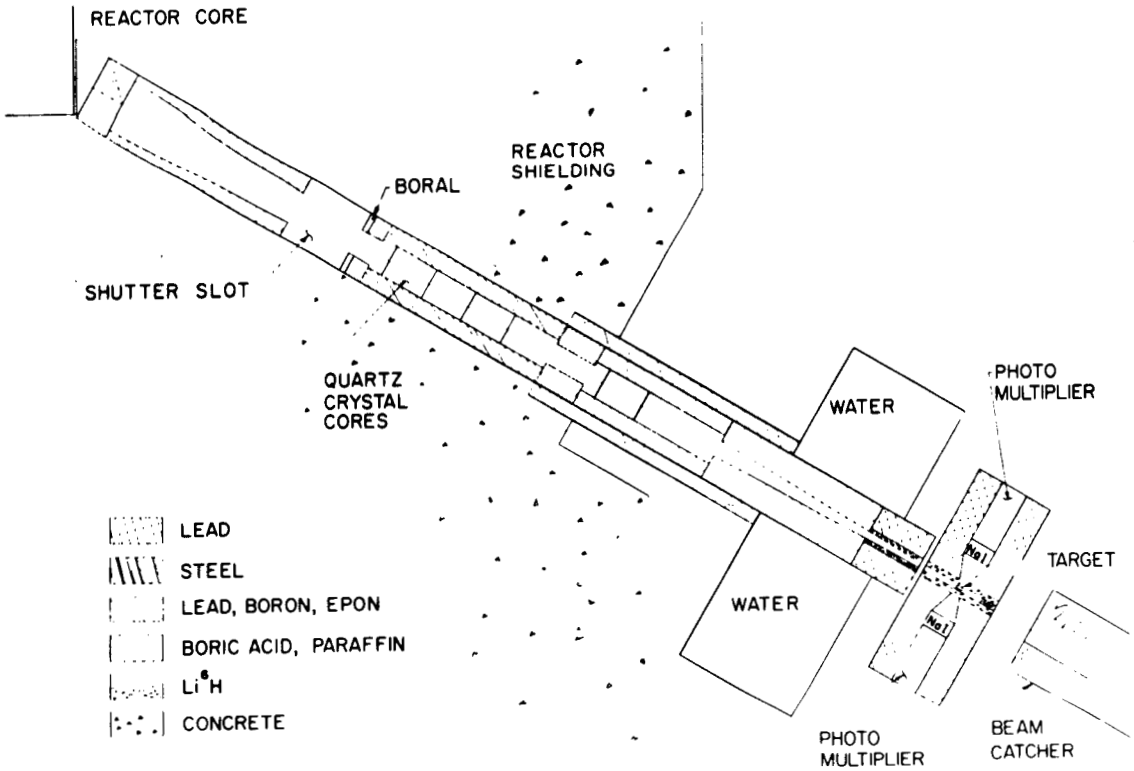

Fig. 1. Schematic diagram of the thermal-neutron collimator and filter used for the scintillation spectrometer.

I will comment on the way this filter operates. The theory is that a quartz crystal will scatter coherently those neutrons whose wavelengths are in the region of the crystal spacing, which would be around thermal energies. The point then is that if the neutron wavelength does not satisfy Bragg's law within the mosiac spread of the crystal, it will be transmitted in spite of a possibly high free-atom cross section.

Using approximately 2 ft. of crystalline quartz, we are able to get cadmium ratios of the order of 1000 to 10000, depending on what one means by a cadmium ratio. That is, we find that the ratio is very sensitive to the amount of cadmium placed in the beam, which shows that the neutron impurity is mostly in the neighborhood of electron volts. We feel that the very fast neutrons are for all practical purposes completely removed from the beam. However, the gamma intensity is still

something that has to be reckoned with.

You can gain an order of magnitude by liquid-nitrogen cooling, and in many cases it would be useful to do this. In fact, most people that use a quartz filter cool it. We have not found this necessary since we have sufficiently intense flux for our work so far.

The counters are shielded by a large lead assembly. We are using Li^6 to keep thermal neutrons out of the NaI crystals.

Figure 2 is a schematic diagram of the shielded apparatus

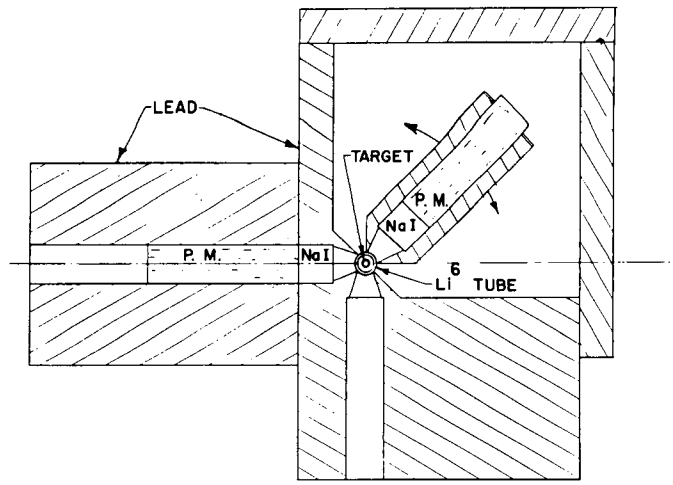

Fig. 2. Schematic diagram of the shielded apparatus for the correlation and coincidence measurements.

for the correlation and coincidence measurements. The movable arm can be rotated from 90° to 180°. We usually only use 90°, 135°, and 180° for our angular-correlation measurements. We use 2 × 2-in. crystals with the front face approximately 5 cm from the beam axis.

Figure 3 shows the low-energy V^{52} spectrum. The 1.43-MeV gamma following the beta decay of V^{52} represents 100% of the neutrons captured. We use it to calibrate the intensity of the other peaks. These peaks are at approximately 820, 640, 510, 425, 295, and 125 keV. We find that most of these are multiplets. A couple of them are fairly close multiplets.

In order to do coincidence work, we have used what I call the "double-window coincidence technique" depicted in Fig. 4. We set a wide window about the 125-keV peak to gate a multichannel pulse-height analyzer. We have a central window whose response is shown by the

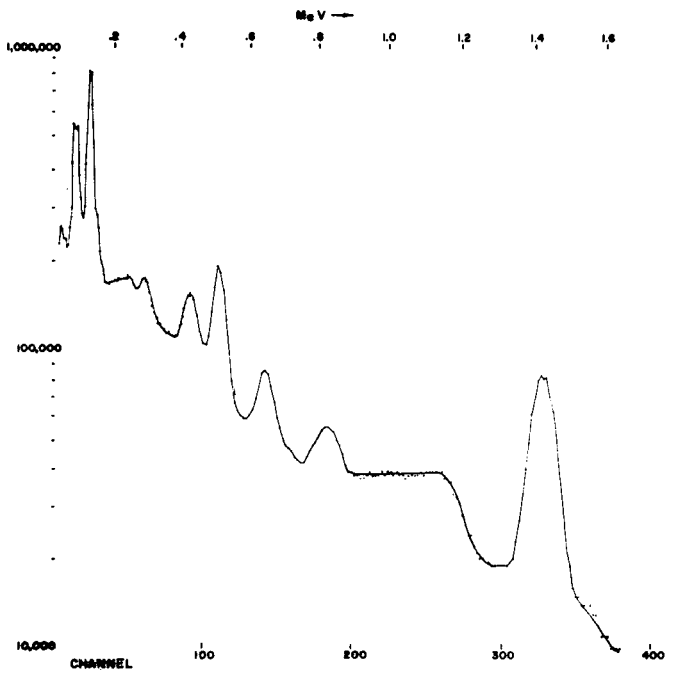

Fig. 3. Low-energy V^{52} spectrum.

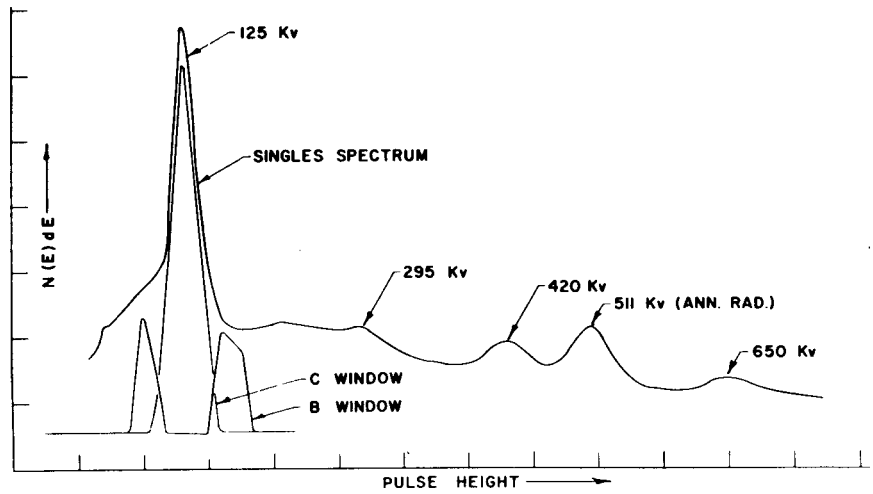

Fig. 4. The low-energy spectrum of V^{52}, presented as an illustration of the "double-window coincidence technique".

central peak. That gate routes the pulse from the other crystal into one subsection of the analyzer. If the count does not fall in the central window, the pulse goes into the remaining subsection. Now if the outer region is effectively twice the central region, the spectrum coincident

with only the outer windown represents the coincidence background. The difference between the two spectra represents the desired coincidence spectrum.

The results of the coincidence measurement are shown in Fig. 5. The upper curve shows the central-window coincidence spectrum.

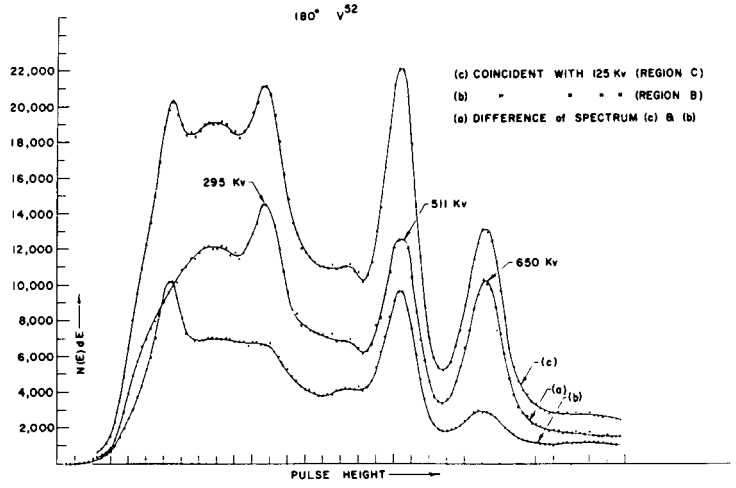

Fig. 5. The coincidence spectrum of V^{52}.

The lower curve shows the outer-window-only coincidence spectrum. The difference is the spectrum that we desire. You will notice that the residue of the 125-keV peak has now dropped out in the subtracted spectrum. This is an experimental way of showing that we set the window widths correctly. This is a part of an angular-correlation measurement, but it also shows fairly clearly that only the 295-keV peak and the 650-keV peak are in coincidence with the 125 peak. The 125 peak we now know is a doublet, 125 and 124 keV.

The capture gammas observed below 1 MeV are tabulated in Table I. Their energies have been determined from the bent-crystal spectrometer. The errors given are a combination of statistical errors and errors associated with the measurement asymmetries. The intensities in the central column here are intensities that have been determined from the scintillation spectrometer. Finally the separations into individual lines are based on relative intensities from the bent-crystal measurements. You will notice that the 125-keV doublet is quite close,

TABLE I. Vanadium-52 capture gammas (E < 1 MeV).

Energies[a] (keV)	Intensities[b] (per 100 neutrons captured)	
124.467 ± 0.028	19.4 ± 1.2	2.4 ± 0.3
125.004 ± 0.028		17.0 ± 1.4
147.871 ± 0.040	4.2 ± 0.3	
295.00 ± 0.06	2.5 ± 0.3	
419.50 ± 0.31	13.6 ± 1.0	5.0 ± 2.0
436.56 ± 0.26		8.6 ± 2.0
645.70 ± 0.09	14.7 ± 1.0	
793.3 ± 1.2	14.0 ± 1.0	4.0 ± 2.0
824.0 ± 1.8		6.0 ± 2.0
848.4 ± 1.1		4.0 ± 2.0

[a]Bent-crystal spectrometer.

[b]NaI scintillation spectrometer.

and impossible to separate with a scintillation spectrometer. There are also possibilities of a few very weak lines that we are now in the process of investigating.

The level scheme we propose is shown in Fig. 6. This scheme is consistent with all of the gammas that we see and with the coincidence work. We find the structure to be much more complicated than we anticipated before, eight levels being found below 1 MeV.

After determining this scheme, we looked for a 17-keV gamma and for a 22-keV gamma, using a thin cleaved NaI crystal with a beryllium window. We found a 16.7-keV gamma and measured its

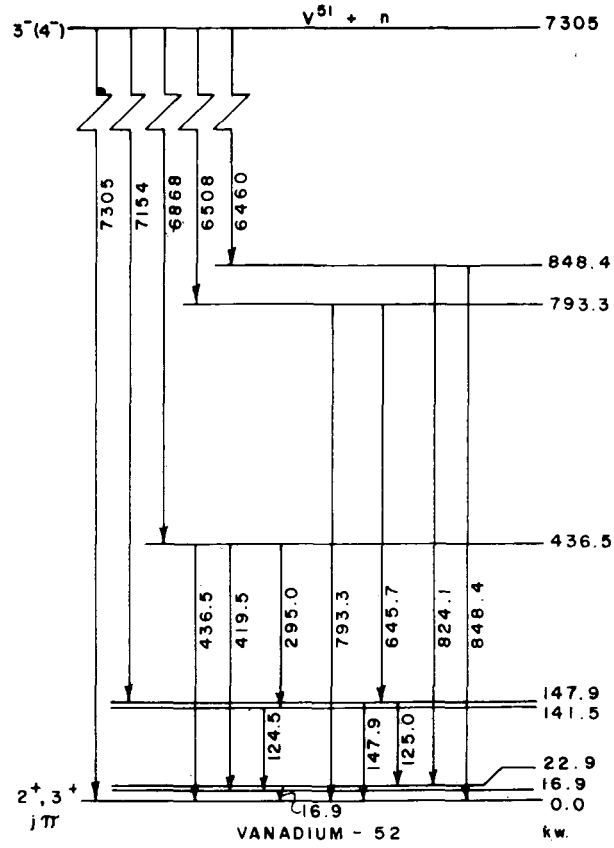

Fig. 6. Proposed level scheme for V^{52}.

energy quite closely. We did not find a 22-keV gamma. We believe there is a transition from the 22-keV level to the 17-keV level. Unfortunately the 6-keV gamma would be buried among the vanadium x rays.

The energies of the levels are given in the first column of Table II. The numbers in the next column are taken from Nuclear Data Sheets based on the work of Buechner and others who did the (d,p) work. We could not fit our results to the lower levels they find within the apparent precision. So I amused myself one morning by making my own analysis of one of their graphs which I took from a progress report. I came up with the numbers in the next column. I do not pretend to be better at analyzing their data than they are. Nevertheless, the fit is quite striking.

Finally, I will mention the numbers in the last column, inferred from Kinsey-and-Bartholomew's measurements of gammas from the capture state to the lower lying levels. These values are consistent

TABLE II. Low-lying V^{52} levels.

Present study (n,γ) (keV)	Buechner et al. (d,p)	Author's analysis of (d,p) results	Kinsey and Bartholomew (n,γ) capture-state decay
0.0	0	0.0	0
16.9			
22.9	21	21.0	
141.5	136		
147.9		147.5	151
436.5	431	435.2	437
793.3	787	793.2	797
848.4	841	847.9	(847)

with the levels that we propose, and we feel fairly confident that that level scheme is correct, although we have not finished the work yet.

Figure 7 represents some theoretical work done by Dr. Schwarcz of our laboratory, based on the shell model. Vanadium-52 has three protons in the $f_{7/2}$ shell and one neutron in the $2p_{3/2}$ shell, giving 24 shell-model states. As you will notice, if we take a potential of 30 MeV for the two-particle interaction, which seems to be consistent with other nuclei in the neighborhood, there are seven states below 1 MeV. We find eight. The question is still open. This has none of the sophistications mentioned by Dr. Moszkowski concerning core excitations; but we still are concerned with the question of where the other level comes from.

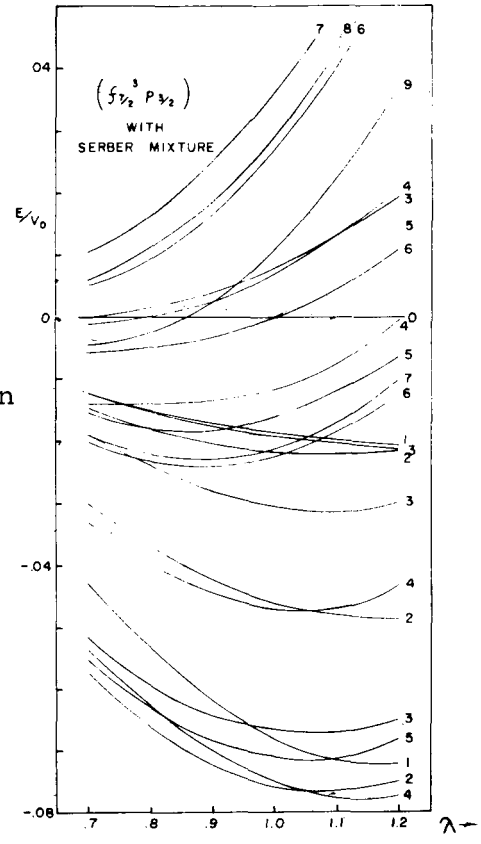

Fig. 7. Theoretical energy scheme for V^{52}, from a shell-model calculation by E. H. Schwarcz.

* * *

MOSZKOWSKI, University of California, Los Angeles: On your last remark, apparently the core excitation will come in when you go up to 3 MeV. When you have levels below 1 MeV, I do not think this will matter very much. Besides, all these levels are of different spin. One would expect that a conventional shell-model-type calculation can give pretty good fits here.

There is one thing that I am worried about, but it is a different point. In the shell-model calculations, there seems to be some evidence that to get detailed fits of the positions of the lower states, the tensor force may play a not insignificant role. That is something that I think Schwarcz may have to worry about.

WHITE: He tried several mixtures of the various exchange forces, and found that it was not sensitive to most of them.

G. BEN-DAVID, Israel AEC, Soreq Research Establishment, Rehovoth: Could you state what the neutron flux is at the target position?

WHITE: It was approximately 3×10^7 neutrons/cm^2 per second.

H. J. LIPKIN, Argonne National Laboratory: I have heard indications from some experimental work here at Argonne that $d_{3/2}$ hole states might be flitting around in the region, in the $f_{7/2}$ shells where these measurements have been taken.

WHITE: Well, you are talking about raising one of the nucleons out of the $d_{3/2}$ shell. I suspect that the excitation energy is too high to account for any low-lying states.

D. KURATH, Argonne National Laboratory: I had nothing to do with the experiment; but I do not see any of the specialists around here. I have heard some of the results. The ones about which I know are in the region of, say, the scandium isotopes, Sc^{43} and Sc^{45} and, further still, Sc^{48}—maybe in some titanium isotopes. In this region, they have found the $d_{3/2}$ comes close to 190 keV.

II-3. ROTATIONAL AND VIBRATIONAL EFFECTS IN NEUTRON-CAPTURE GAMMA-RAY SPECTRA*

R. K. Smither

Argonne National Laboratory, Argonne, Illinois

I. Introduction

Originally I had planned to talk about the application of the collective model to some recent experimental work performed here at Argonne. However, upon reviewing the program for this conference I find that the application of the collective model to the level schemes of specific nuclei will be presented in many of the forthcoming talks and thus the group will be adequately exposed to the rigors of applying theory to experiment for specific cases. I will therefore try to make my talk somewhat more general and discuss some aspects of the observed capture gamma-ray spectra which appear to be common to many nuclei. Some of these general features can be attributed to the collective properties of the nuclei while others appear to be of statistical origin.

II. General Survey

I shall base my remarks and conclusion on a set of Argonne experiments on eight nuclei. A summary of these nuclei appears in Table I. Starting from the left, the columns give the reaction (thermal neutron capture in Hf^{177}), then the excited nucleus (Hf^{178}), its basic type or classification (even-Z even-N), the character of its ground state (deformed), and finally the general properties of its

TABLE I. Salient features of the nuclei and associated level schemes recently investigated with the Argonne bent-crystal spectrometer.

Reaction	Excited nucleus	Type	Ground state	Level scheme
$Hf^{177}(n,\gamma) \rightarrow$	${}_{78}Hf^{178}_{100}$	Even-Z, even-N	Deformed	Rotational bands, ground state and excited states above 1 MeV
$Hf^{179}(n,\gamma) \rightarrow$	${}_{78}Hf^{180}_{102}$	Even-Z, even-N	Deformed	Rotational bands, ground state and excited states above 1 MeV
$Sm^{152}(n,\gamma) \rightarrow$	${}_{62}Sm^{153}_{91}$	Even-Z, odd-N	Deformed	Low-lying rotational bands overlapping the ground-state band
$Sm^{151}(n,\gamma) \rightarrow$	${}_{62}Sm^{152}_{90}$	Even-Z, even-N	Deformed	Rotational bands, ground state and excited states above 0.6 MeV
$Sm^{150}(n,\gamma) \rightarrow$	${}_{62}Sm^{151}_{89}$	Even-Z, odd-N	Deformed	Low-lying rotational bands overlapping the ground-state band
$Sm^{149}(n,\gamma) \rightarrow$	${}_{62}Sm^{150}_{88}$	Even-Z, even-N	Spherical	Mixed possible one-phonon and two-phonon vibrational states. Many unassigned levels above 1 MeV
$Te^{123}(n,\gamma) \rightarrow$	${}_{52}Te^{124}_{72}$	Even-Z, even-N	Spherical	Possible one-phonon and two-phonon states. Un assigned states above 1.2 MeV
$Cd^{113}(n,\gamma) \rightarrow$	${}_{48}Cd^{114}_{66}$	Even-Z, even-N	Spherical	Possible one-phonon and two-phonon states, with extra states at the two-phonon level and unassigned states above 1.5 MeV

level scheme. The level structures in the three even-Z even-N nuclei (Hf^{178}, Hf^{180}, and Sm^{152}) are quite similar, consisting of a well-developed ground-state rotational band up to 8^+ in the hafnium isotopes and up to 6^+ in the Sm^{152}. All these level schemes exhibit an energy gap of about 1 MeV (slightly lower in Sm, 0.6 MeV) above which there appear to be additional rotational bands based on excited states. This is the typical level scheme observed for deformed even-Z even-N nuclei. The two even-Z odd-N deformed nuclei (Sm^{153} and Sm^{151}) have level schemes characteristic of their type. Their level schemes contain many low-lying states of both positive and negative parities. These states can be interpreted as a number of overlapping rotational bands based on excited states with energies very close to that of the ground state. The last two nuclei (Te^{124} and Cd^{114}) exhibit level schemes characteristic of even-Z even-N, with spherical ground-state configurations. These are both close to the filled proton shell at 50 protons but quite far away from the closed neutron shells at 50 and 82. Both level schemes exhibit good candidates for one-phonon and two-phonon excitations, but at the three-phonon level the picture becomes clouded by many states with similar spins and parities. The ground state of the nucleus Sm^{150} appears to be right on the border between deformed and spherical, with the balance tipped to spherical. The first few states appear to fit the vibrational picture but again the picture becomes confused at the excitation energy of the three-phonon levels.

III. Example of Deformed Even-Z Even-N Nuclei

As an example of an even-Z even-N deformed nucleus, I will use the first nucleus on the list. Figure 1 is the level scheme

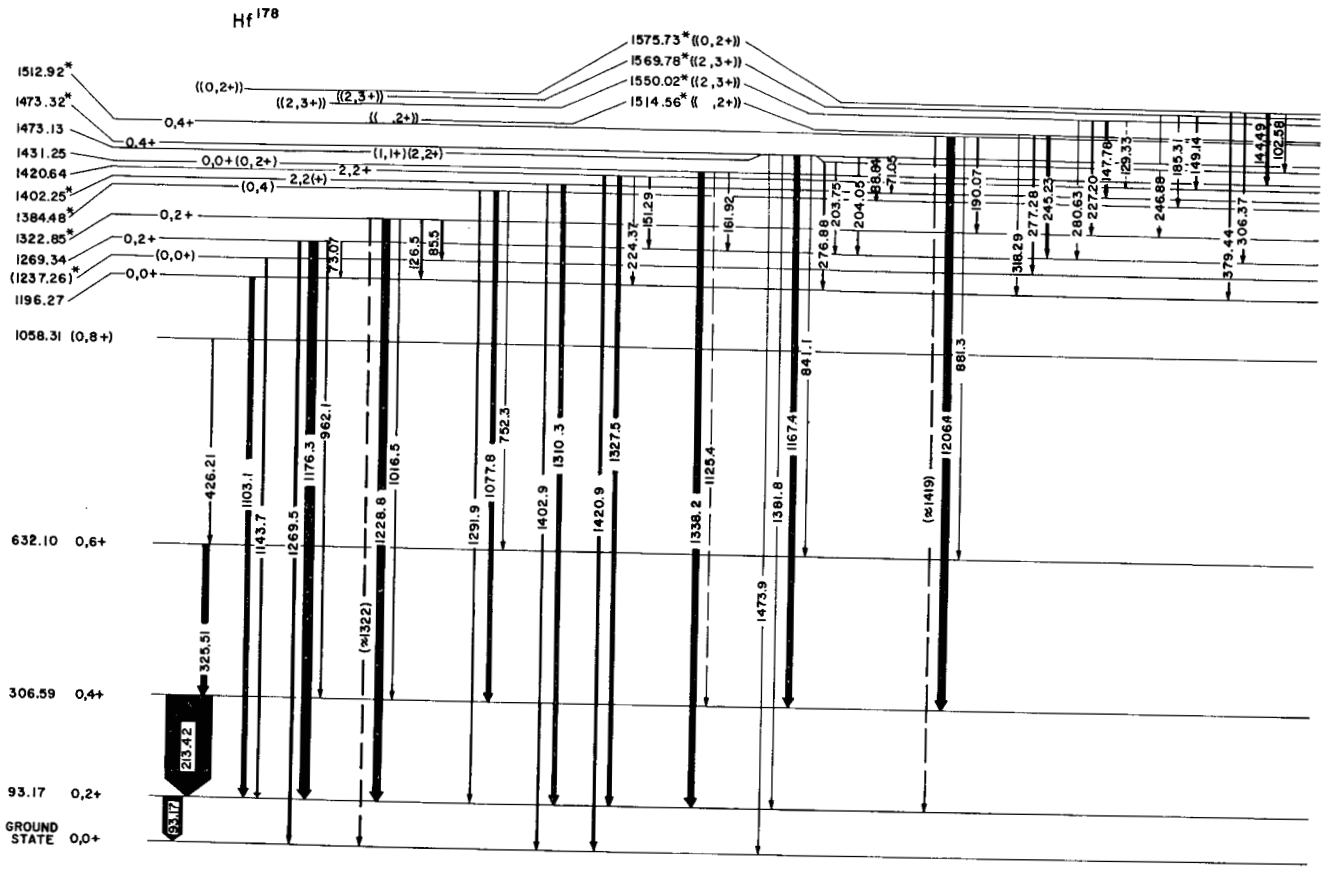

Fig. 1. Level scheme of Hf^{178} as deduced from the gamma-ray measurements made with the Argonne 7.7-m bent-crystal spectrometer. The energies of the levels and gamma rays are given in keV. The K value, spin, and parity of the level is given on the left in that order. The width of a line in the level scheme is meant to reflect the relative intensity of the gamma ray. The width scale used for the low-energy gammas between the upper states (energies between 1195 and 1575 keV) is four times that used for the gamma rays with energies between 1 and 2 MeV and for the ground-state band. No corrections have been made for internal conversion. An asterisk following the energy of a level indicates that this level has not been observed previously. The parentheses and double parentheses indicate uncertainty in the assignments.

of Hf^{178} which I have proposed on the basis of the precision gamma-ray measurements obtained with the Argonne bent-crystal spectrometer. In constructing a complicated level scheme of this type, one makes use of any additional information that can be obtained. This additional information may come from γ-γ coincidence and γ-γ angular-correlation studies, β-decay and conversion-electron experiments, Coulomb excitation, charged-particle reactions, etc. This additional information is not only helpful but essential if one is to make any sense out of these complicated gamma-ray spectra.

The level scheme we see here is typical of an even-Z even-N deformed nucleus with its K=0 ground-state rotational band with states 0^+, 2^+, 4^+, 6^+, 8^+, etc., the energy gap of approximately 1 MeV, then additional rotational bands. The level density above 1 MeV is somewhat higher than has been found in similar nuclei and will be reflected in the increased complexity of the γ-ray spectra, as we shall see. Another characteristic of an even-Z even-N deformed nucleus is the group of strong 1-MeV transitions which decay from the excited-state rotational bands to the ground-state rotational band. Although they are strongly retarded in relation to the low-energy transitions within the excited-state rotational band, they are still the strongest gamma rays in the spectrum. No gamma rays are shown decaying from the uppermost levels shown here. This does not mean that they are not present, but rather that the spectrometer was not sensitive enough to detect them. They are, however, at least a factor of ten less intense than the ones shown here. The level scheme shown in Fig. 1 does not suggest the complexity of the observed γ-ray spectra very well because the many closely spaced levels above 1.6 MeV are not shown.

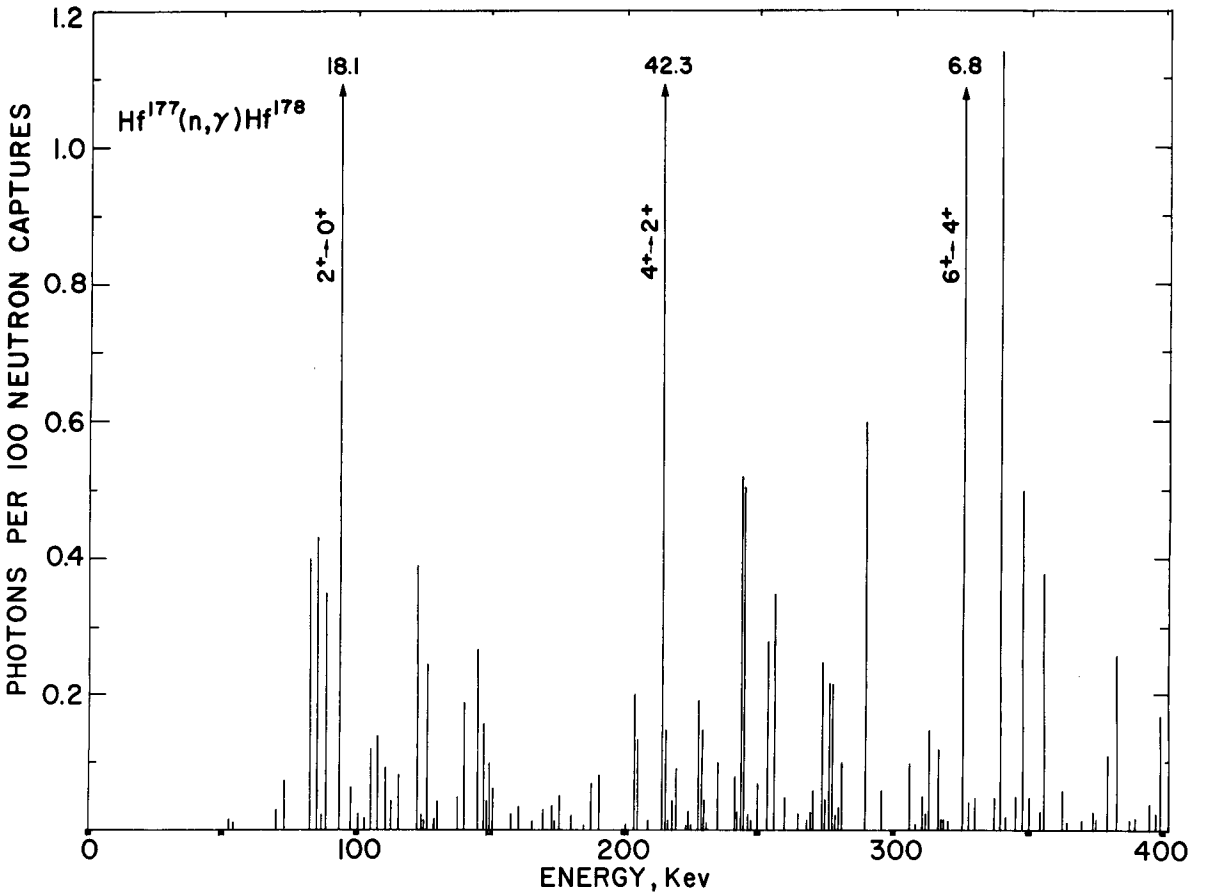

Fig. 2. Line graph of the $Hf^{177}(n,\gamma)Hf^{178}$ gamma-ray spectrum below 400 keV, observed with the Argonne 7.7-m bent-crystal spectrometer. The intensities of the gamma rays are given in photons per 100 neutron captures in Hf^{177}.

Figure 2 is a line graph of the gamma-ray spectrum below 400 keV as seen with the Argonne bent-crystal spectrometer. The intensity of the gamma ray is plotted vertically. The scale is in photons per 100 neutron captures. The energy of the gamma-ray is plotted horizontally, in keV. Both scales are linear. The measured spectrum continues up to 2 MeV with very little reduction in complexity.

I would like to discuss the distribution of the observed gamma rays as a function of their energy and intensity. This is difficult with a graph of this type because the details associated with the weak

transitions are lost in the forest of strong lines. In order to overcome this problem I have replotted the spectrum in a different manner in Fig. 3, in which each gamma-ray transition appears as a point on a

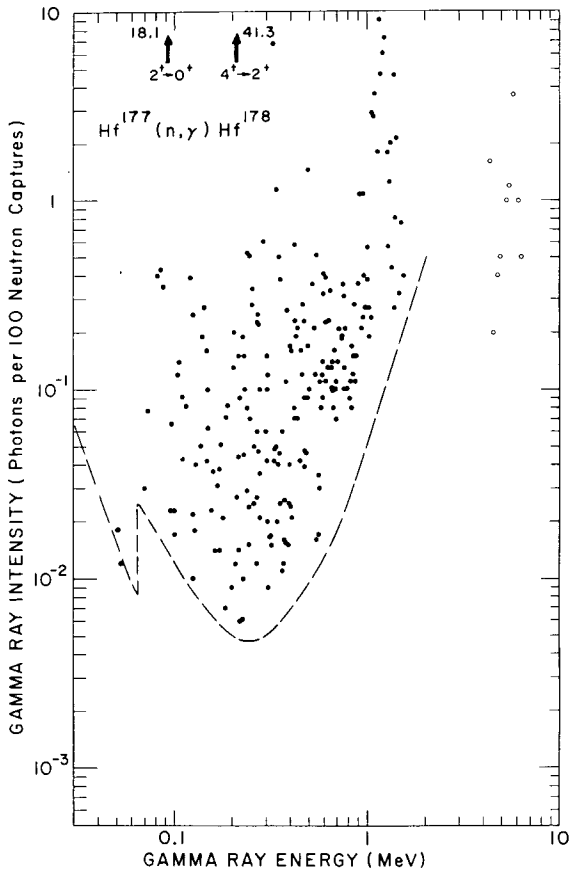

Fig. 3. A plot of log I_γ vs log E_γ for the gamma-ray spectrum from $Hf^{177}(n,\gamma)Hf^{178}$ as observed with the Argonne 7.7-m bent-crystal spectrometer (filled circles). The spectrum above 4 MeV (open circles) is a combination of the Compton-spectrometer work of Groshev and the pair-spectrometer work of Campion and Bartholomew. The vertical scale is the logarithm of the intensity of the gamma ray in photons per 100 neutron captures. The horizontal scale is the logarithm of the gamma-ray energy in keV. The intensity has not been corrected for conversion coefficients. The dashed curve indicates the minimum sensitivity of the bent-crystal spectrometer for this experiment.

log-log plot. The log of the intensity of the gamma is plotted vertically; the log of the energy of the gamma ray is plotted horizontally. The top

of the figure corresponds to an intensity of 10 photons per 100 neutron captures (a 10% line) and the bottom of the scale corresponds to a very weak line with an intensity of 5×10^{-4} photons per 100 neutron captures (one gamma per 2×10^{5} neutron captures). The dashed curve corresponds to the minimum sensitivity of the spectrometer during this experiment. The strong transition at 93 keV corresponds to the $2^{+} \rightarrow 0^{+}$ transition in the ground-state rotational band. The strong transition at 213 keV corresponds to the $4^{+} \rightarrow 2^{+}$ transition in the ground-state rotational band. In this figure we see the group of strong lines between 1.1 and 1.3 MeV that were identified in the level scheme as transitions from the levels of the excited-state rotational bands to the ground-state rotational band. They are very much stronger than anything else in the spectrum, except the transitions in the ground-state rotational band. This observed strength does not indicate that these gamma transitions are in any way enhanced but rather that the levels on which they originate are fed strongly from levels of higher excitation energy. This preferential population of low-lying excited-state rotational bands is not very well understood. It may be associated with K-forbiddenness in the gamma transitions. Another explanation may come from the mixing of the excited-state rotational bands. Appreciable amounts of mixing between the excited-state bands could enhance the gamma transitions between the excited-state bands in preference to transitions to the ground-state rotational band.

The distribution of gamma-ray transitions on the log I_{γ} - log E_{γ} plot (Fig. 3) is quite uniform and the large number of relatively strong low-energy gamma transitions is somewhat surprising. A sharp break in the intensity distribution occurs just below the energy

of the first excited state (93 keV). This sharp break in the distribution is present in all of the spectra of even-Z even-N nuclei I have examined to date. Many of these relatively strong, low-energy gammas appear in the level scheme (Fig. 1) as transitions between the levels of excited-state rotational bands. The deformations associated with these bands are similar to and less than the deformation associated with the ground-state rotational band. Rotational bands with similar or smaller deformations than the ground-state band will give rise to gamma-ray transitions with energies similar to or larger than those associated with the ground-state band. If this pattern is continued in the levels above 1.6 MeV, one would expect to find the observed break in the gamma distribution at the energy of the lowest energy transition ($2^+ \rightarrow 0^+$) in the ground-state rotational band. If these assumptions are true, then many of these relatively intense low-energy transitions are M1 and E2 transitions. They must be strongly enhanced as well, since they compete in most cases with the much more energetic (factor of 10) M1 and E2 transitions to the levels in the ground-state rotational band.

IV. Example of Spherical Even-Z Even-N Nuclei

The distribution of neutron-capture gamma rays associated with the level scheme of an even-Z even-N deformed nucleus (Fig. 3) is quite different from the spectrum observed for even-Z even-N spherical nuclei. This is evident from Fig. 4, which is a similar log I_γ vs log E_γ plot of the observed gamma-ray spectrum for $Cd^{113}(n,\gamma)Cd^{114}$. The absence of relatively strong low-energy transitions is quite evident in this figure. The long-dashed curve corresponds to the sensitivity of the spectrometer during this experiment. The lower,

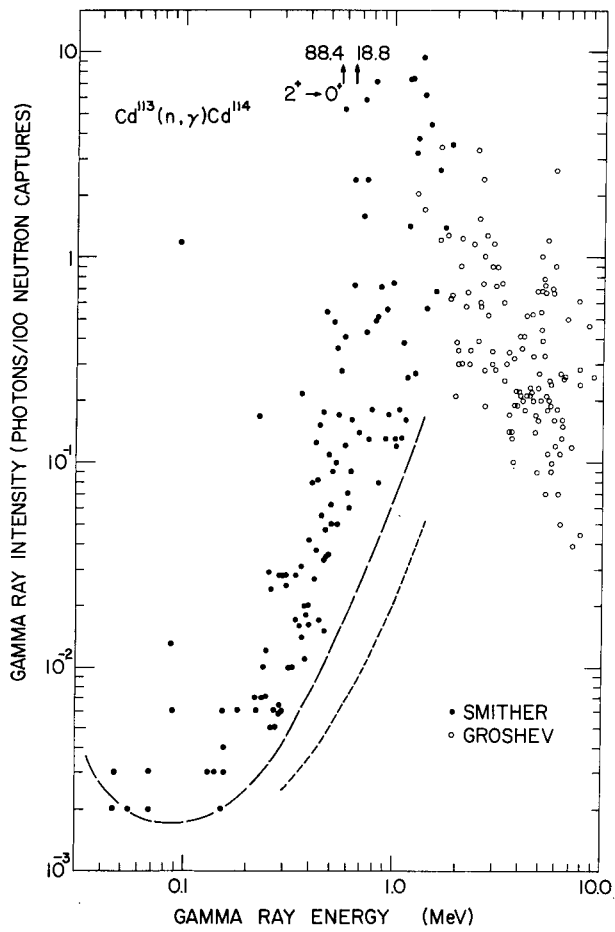

Fig. 4. A plot of log I_γ vs log E_γ for the gamma-ray spectrum of $Cd^{113}(n,\gamma)Cd^{114}$. The filled circles are the Argonne bent-crystal work; the open circles are the Compton-spectrometer work of Groshev. The gamma-ray intensity is not corrected for the conversion-electron process.

short-dashed curve corresponds to the present sensitivity of the spectrometer. These two lines were placed on the slide to emphasize the importance of the high sensitivity of the instrument for the investigation of spherical even-Z even-N nuclei.

Again, one observes a sharp break in the distribution of intensities just below the energy of the first excited state ($2^+ \rightarrow 0^+$) at 557 keV. Within the limitations of the distribution, the points (gamma transitions) appear to be evenly distributed in this plot. This even distribution will be observed in all the nuclei that I will discuss. Again, almost all of the strong transitions in the spectrum are believed to be E2 and/or M1 transitions.

One very strong (1.2%) low-energy gamma was observed at 95 keV. This strong low-energy gamma is believed to be an E2

transition. The theoretical conversion coefficient (K + L) for a 93-keV gamma is 1.9. The total intensity of this transition (γ intensity + conversion-electron intensity) is therefore 2.3%. The strength of this transition is 2—3 orders of magnitude stronger than any other transition of similar energy and is comparable in intensity to all but the five strongest lines in the spectrum. A strong line of similar energy was observed in the gamma spectrum of the other spherical even-Z even-N nucleus (Te^{124}) as well. The energy of this gamma ray (95 keV) is very close to the spacing between two levels whose energies are close to that predicted for the 2-phonon vibrational triplet. If this suggestion proves to be correct, then a similar explanation may be possible in the other two cases. Why a low-energy transition between two two-phonon states should be enhanced relative to the allowed transition to the 2^+ one-phonon state is not understood.

The level scheme of Cd^{114} is shown in Fig. 5. The ground state is 0^+. The first excited state is 2^+, which is consistent with the one-phonon state of the vibrational model. The groups of states occur at 2.2 times the energy of the first excited state and have spins of 0^+, 2^+, and 4^+. Any one of these states would be a good candidate for a member of the two-phonon vibrational triplet. The presence of five candidates for the vibrational triplet is disconcerting and suggests that something more complicated than the simple vibrational model will be needed to explain the level scheme. It is not surprising, therefore, to find very little evidence for a three-phonon vibrational quintet in the level scheme.

The average level spacing between 1 and 2 MeV is 100 keV. This is half that observed in the Hf^{178} level scheme and is not sufficient to explain the difference in the two gamma-ray spectra.

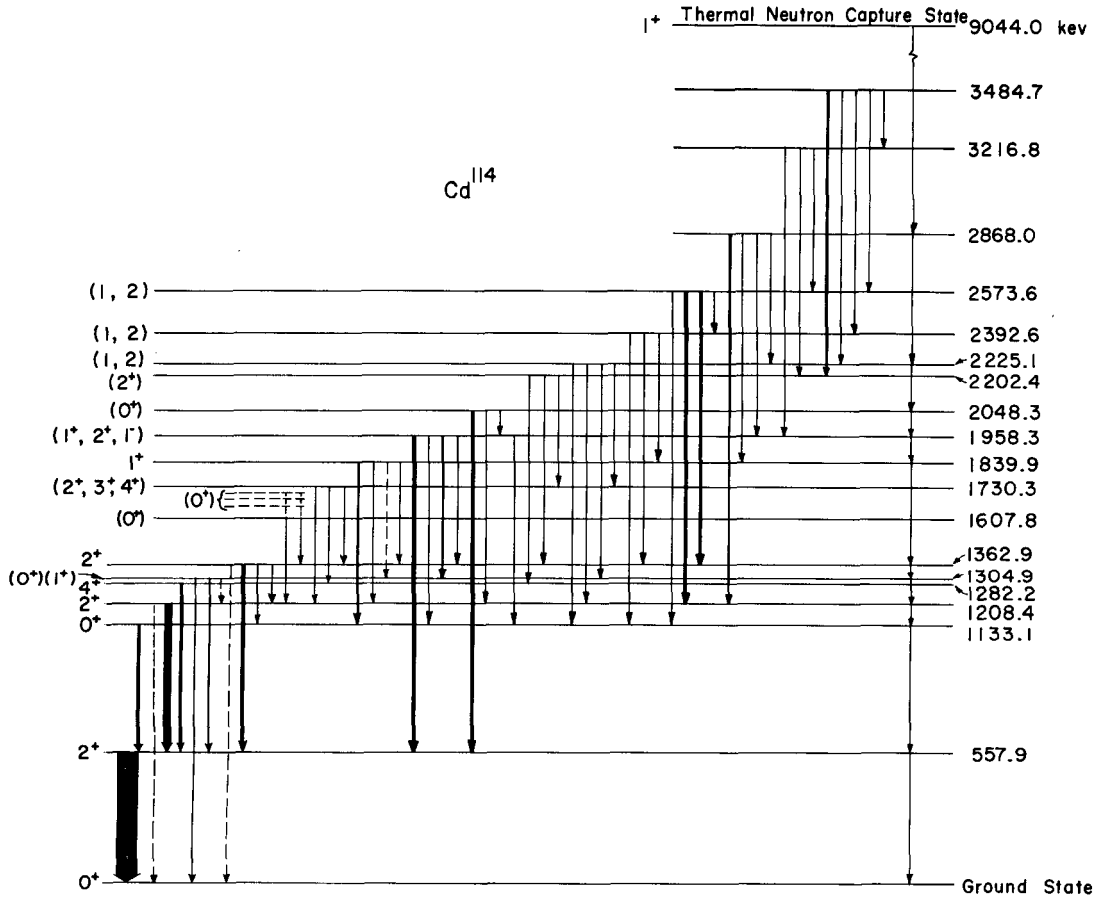

Fig. 5. Energy levels in Cd^{114} as determined from the precision energy measurements of capture gamma rays from $Cd^{113}(n,\gamma)Cd^{114}$ and coincidence measurements of associated gamma rays. The width of the line corresponds to the intensity of the gamma-ray transition.

Figure 6 is a log I_γ vs log E_γ plot of the spectrum from $Te^{123}(n,\gamma)Te^{124}$. The sensitivity of the instrument (dashed curve) severely limited the observed spectrum, but the salient features are still observable: (1) the break in the intensity distribution just below the energy of the first excited state ($2^+ \rightarrow 0^+$), (2) the absence of relatively strong low-energy gamma rays, and (3) the anomalously strong low-energy gamma at 100 keV.

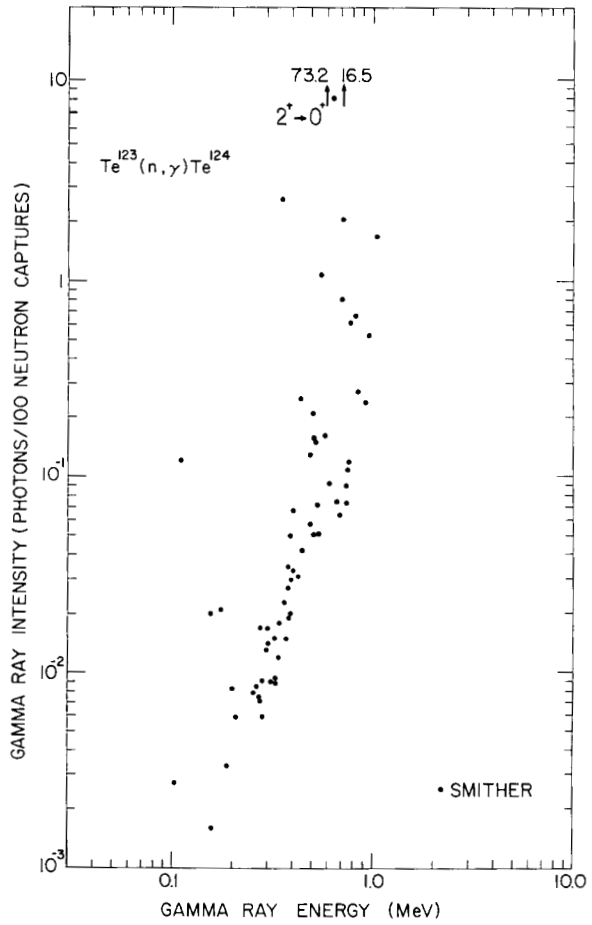

Fig. 6. A plot of log I_γ vs log E_γ for the gamma-ray spectrum $Te^{123}(n,\gamma)Te^{124}$ as observed with the Argonne bent-crystal spectrometer. The gamma-ray intensity is not corrected for the conversion coefficient.

V. Transition Region

We have just seen the striking difference between the gamma-ray spectra associated with deformed even-Z even-N nuclei and those associated with spherical even-Z even-N nuclei. I would now like to discuss the gamma-ray spectra associated with nuclei which fall in the transition region between the spherical and deformed nuclei.

As an example of this transition region, I will use the Sm isotopes: Sm^{152}, Sm^{151}, and Sm^{150} (Table I). The level scheme of Sm^{152} is rotational in character. It contains a well defined ground-state rotational band, an energy gap of 680 keV, and excited-state rotational

bands above this energy similar to those found in Hf^{178} (Fig. 1). Figure 7 is a log I_γ vs log E_γ plot of the observed gamma-ray spectrum

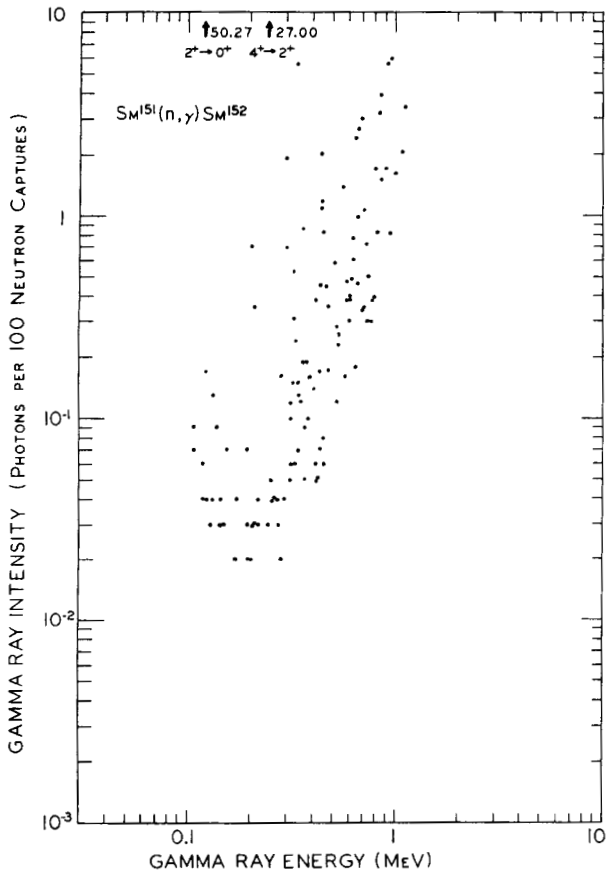

Fig. 7. A plot of log I_γ vs log E_γ for the gamma-ray spectrum of $Sm^{151}(n,\gamma)Sm^{152}$ as observed with the Argonne bent-crystal spectrometer. The gamma-ray intensity is not corrected for the conversion coefficient.

from $Sm^{151}(n,\gamma)Sm^{152}$. As in Hf, we observe many relatively strong low-energy transitions. Note the group of low-energy lines at the energy of the first excited state (122 keV). If these low-energy gamma rays can be associated with the lowest level spacing of excited-state rotational bands, as they appear to be, then the deformations associated with these bands are very similar to the deformation of the ground-state band.

Figure 8 is the level scheme of Sm^{151} as generated from the gamma spectrum [$Sm^{150}(n,\gamma)Sm^{151}$] observed with the bent-crystal spectrometer. The level scheme can be interpreted as a set of overlapping rotational bands whose lowest energy states are very close to

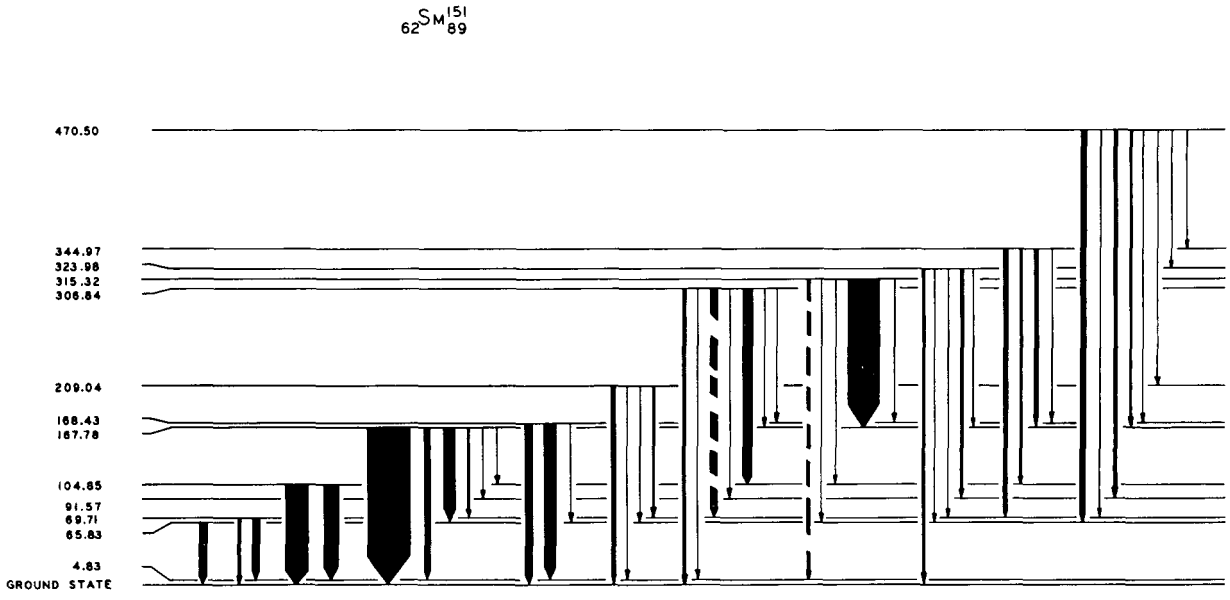

Fig. 8. The level scheme of Sm^{151} as defined by the Argonne bent-crystal work. The energy of the level is given in keV.

the ground state. Some of the strong lines are believed to be E1 while others are believed to be M1 and E2. The effect of this type of level structure on the observed gamma-ray spectrum is seen in Fig. 9, which shows the observed gamma spectrum for $Sm^{150}(n,\gamma)Sm^{151}$ on a log I_γ vs log E_γ plot. Note the large number of low-energy lines above 0.1%. About two-thirds of these relatively strong gammas are believed to be M1 or E2 transitions in low-lying rotational bands. The very strong enhancement of the M1 and E2 transitions relative to the competing E1 transitions suggests the collective character of this nucleus. Note the absence of a group of strong lines at 21 MeV. This feature of the spectrum is missing because the level scheme of Sm^{151} (an even-Z odd-N nucleus) does not have an energy gap as observed in even-Z even-N deformed nuclei. No break or structure occurs in the distribution of gamma rays (Fig. 9) because the deformations associated with the rotational bands (and thus the energies of the cascade gammas) vary widely from band to band.

As we move from Sm^{151} to Sm^{150}, the configuration of the

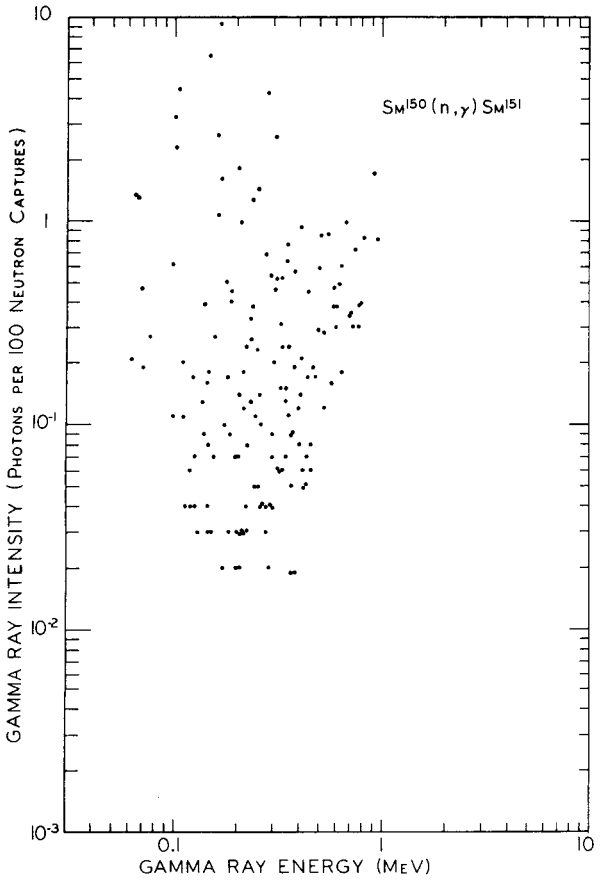

Fig. 9. A plot of log I_γ vs log E_γ for the gamma-ray spectrum of $Sm^{150}(n,\gamma)Sm^{151}$ as observed with the Argonne bent-crystal spectrometer. No correction is made for the conversion coefficients.

ground state changes from deformed to spherical in character. This transition is identified by the abrupt change in the energy of the first excited state (relative to Sm^{152}) and the suggestion of a two-phonon vibrational triplet structure at twice this energy. Figure 10 is the level scheme of Sm^{150} as suggested by the capture-gamma-ray work. This is a good example of what can be learned about a level scheme from neutron-capture gamma-ray experiments. The energies and intensities of the gamma rays are obtained with the bent-crystal spectrometer. The positions of the strong gamma rays in the level scheme are based on gamma-gamma coincidence experiments (filled circles and squares). The multipolarities and multipolarity admixtures, spins, and parities are obtained from γ-γ angular-correlation measurements (filled circles) and K-conversion coefficients. The precision gamma-ray measurements, gamma-gamma-coincidence measurements, and angular-correlation

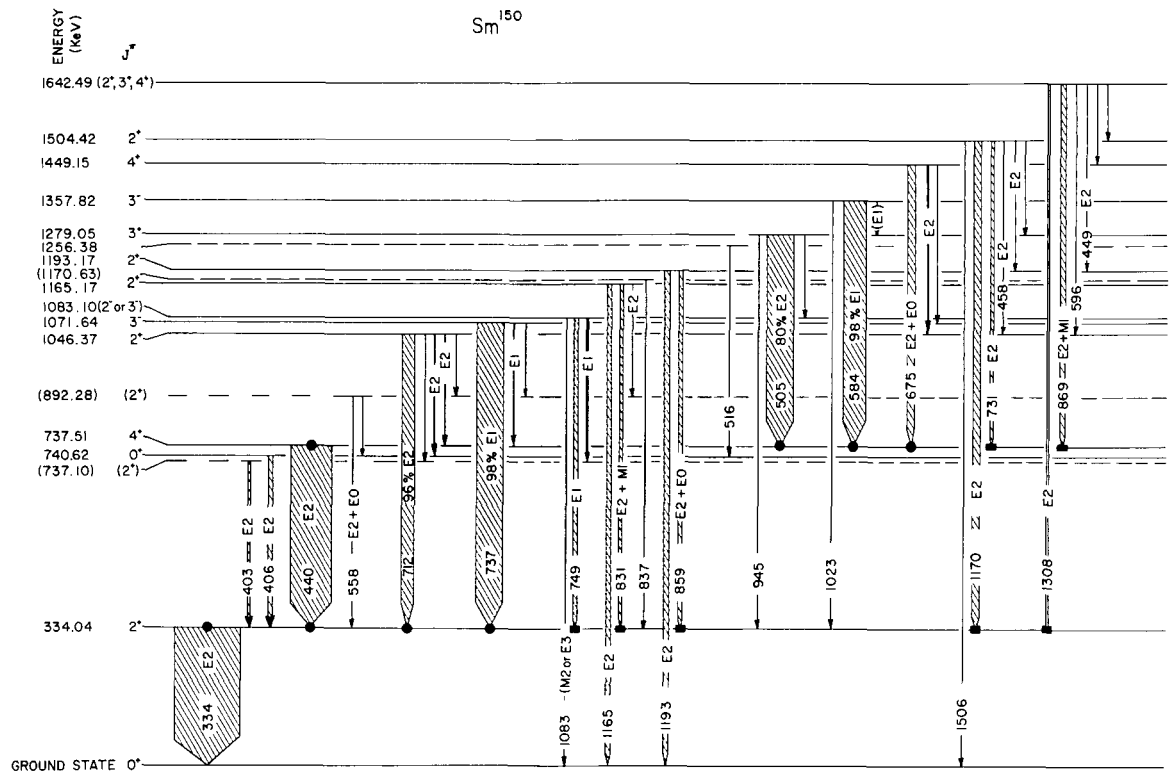

Fig. 10. Level scheme of Sm^{150} as defined by the bent-crystal measurements, γ-γ coincidence measurements, and γ-γ angular-correlation measurements performed at Argonne and used in conjunction with the conversion-electron measurements of Bieber in Munich and Groshev in Moscow.

measurements were performed here at Argonne. The K-conversion coefficients were obtained by combining the bent-crystal gamma-intensity measurements with the conversion-electron-intensity measurements of the Munich group and Russian group. In most cases, a unique determination of the spin and parity of the level results from this analysis. The precision of the energy measurement allows one to place many of the weaker gamma rays in the level scheme. The number of levels that can be added to a level scheme of this type is limited by the precision of the gamma-ray energy measurements. The number of possible combinations of gamma rays that may be used to suggest new levels increases with the square of the number of levels present. The chance of making an error

is therefore proportional to the square of the number of levels present. The probability of obtaining an accidential energy match is also proportional to the reciprocal square of the precision of the energy measurement. Thus the number of levels that can be generated from the capture-gamma-ray work is roughly proportional to the precision of the measurement. This is the main reason for the continued stress on the precision of these measurements. The average precision of the gamma-ray measurements in Fig. 10 is one part in 7000. With the present improvements in the instrument it now appears possible to obtain average precision of one part in 15 000 in similar experiments.

The level scheme of Sm^{150}, as shown in Fig. 10, is mixed in character. The low-lying excited states fit the vibrational picture with a 0^+ ground state, 2^+ first excited state, and a doublet or triplet at twice this energy with spins of 0^+, 2^+, and 4^+. Above 1 MeV the level scheme becomes much more complicated, with many states of similar spins and parities. The complexity of this level scheme precludes any simple application of vibrational theory in the region above 1 MeV. The three-phonon states, if present, will mix with other states of similar spin and parity and lose some (if not all) of their vibrational character. Nevertheless, a 3^+ state at 1279 keV and a 4^+ state at 1449 keV exhibit some of the expected characteristics of three-phonon vibrational levels. Their gamma transitions to the two-phonon levels are predominantly E2 transitions and their crossover transitions to the one-phonon first excited state are strongly inhibited in relation to the cascade transitions. The excitation energies of the two-phonon and three-phonon states are not simple multiples of the first excited states, but they increase uniformly. This may be related to the previously mentioned mixing with other

states having similar spins and parities. The lowest energy octopole vibrational level is a 3^- state. There are two 3^- states shown in the level scheme (Fig. 9) at 1071 and 1357 keV. The E3 transition to the ground state would be enhanced in the vibrational model and would constitute the best evidence available in the capture-gamma work for an octopole level. Neither of the above mentioned 3^- states has an observable ground-state transition so it is difficult to draw any conclusions.

Next I would like to call your attention to the two levels at 1165 and 1193 keV. The branching ratio between the ground-state transition and the transition to the first excited state is quite different from those of the other low-lying levels in that the intensity of the ground-state transition is comparable to that of the transition to the first excited state. These two levels would fit more readily into a rotational level scheme than into a vibrational level scheme. The mixed nature of the level scheme is reflected in the gamma-ray spectrum observed for the $Sm^{149}(n,\gamma)Sm^{150}$ reaction.

Figure 11 is a log I_γ vs log E_γ plot of the gamma-ray spectrum from $Sm^{149}(n,\gamma)Sm^{150}$ as measured with the bent-crystal spectrometer. The filled circles are the Argonne data; the open circles are the Compton-spectrometer work of Groshev et al. The distribution of gamma-rays is similar, both in density and in structure, to that observed for $Cd^{113}(n,\gamma)Cd^{114}$. The sensitivity of the instrument was greater in the Sm work than in the Cd work and thus many more of the weak gamma rays were observed. Again, a break in the intensity distribution is observed just below the energy of the first excited state, as was the case in all the other even-Z even-N nuclei. The strong low-energy line at 100 keV is present, but not as obvious as it was in Cd and Te.

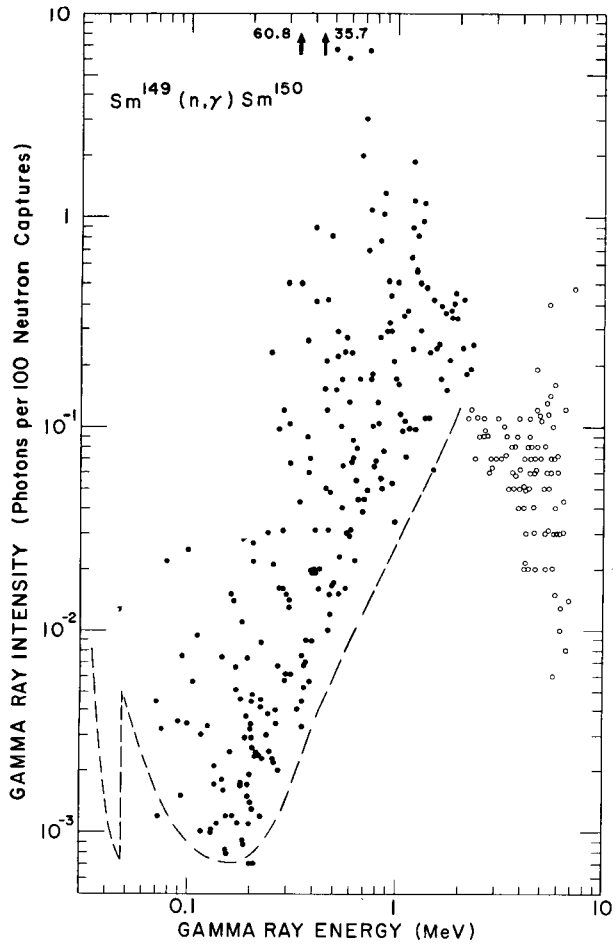

Fig. 11. A plot of log I_γ vs log E_γ for the gamma-ray spectrum from $Sm^{149}(n,\gamma)Sm^{150}$. The filled circles are the Argonne bent-crystal work. The open circles are the Russian Compton-spectrometer work.

V. Summary

In summary, neutron-capture gamma-ray spectra can be classified by the final nuclei. Spectra associated with deformed even-Z even-N nuclei are rich in relatively strong low-energy lines. One can therefore obtain considerable information with an instrument of limited sensitivity. The resolution of the instrument is at a premium, however, since one must resolve many gamma rays or groups of gamma rays with quite similar energies (e.g., the 1-MeV group in Hf). The collective model has been quite successful in predicting the observed results in these even-Z even-N deformed nuclei. This has stimulated considerable experimental and theoretical work in the field so that many new and

exciting results are expected.

The vibrational model has not been so successful in the even-Z even-N spherical nuclei. To date, all of the ground states (0^+) and the first excited states (2^+) investigated have been consistent with theory. The two-phonon triplet at twice the energy of the first excited state is suggested by one or two states in most of the cases investigated. The third state is often missing, and it is here that one expects the neutron-capture gamma-ray approach to be more successful. The selection rules for the population of a level following three or four cascade gamma-rays are much less restrictive than those found in β-decay studies or charged-particle reactions. The situation at the three-phonon level is still very confused (see Sm^{150} and Cd^{114}).

The experimental problem in even-Z even-N spherical nuclei is much harder than what is faced in deformed nuclei. Not only is high resolution necessary to resolve the complicated gamma spectrum but high sensitivity is necessary as well if very much of the low-energy spectrum is to be observed at all (compare Te with Hf).

The situation in the even-Z odd-N nuclei may prove to be the easiest to investigate with neutron-capture gamma rays because of the large number of strong, low-energy lines (Fig. 9) but considerable auxiliary information will be needed to interpret the complicated level schemes such as that in Fig. 8.

* * *

PETER AXEL, University of Illinois, Urbana, Illinois: I wonder if you could comment briefly on the extent to which your strong low-energy transitions are locatable at low-lying states, and whether you have any sort of order-of-magnitude figure for how much of the spectrum that people usually see is associated with low-lying states where presumably statistical calculations will work.

SMITHER: Yes. The level scheme of Sm^{150} shown in Fig. 10 contains about 50 gamma rays. This is 25% of the observed gamma-ray spectrum below 2 MeV. It includes, however, 80% of the gamma rays with intensities greater than 0.1%. Most of the unassigned transitions are weak low-energy transitions. In the level scheme of Hf^{178} (Fig. 1), there are 54 assigned gamma-ray transitions, which is also about 25% of the observed spectral lines with energies below 2 MeV. There are 81 gamma rays in the observed spectrum with energies below 300 keV. Twenty-eight of these gammas have intensities above 0.1%; 60% of them (intensity $\geq 0.1\%$) are in the Hf level scheme (Fig. 1) below 1.6 MeV. About 90% of the relatively strong lines in the level scheme of Sm^{151} are located below 0.5 MeV. Similar results are found in other nuclei. In summary, then, about 80—90% of the relatively strong low-energy lines are locatable in the level schemes below 2 MeV. The number of levels in the level scheme (and thus the number of gamma rays that can be associated with it) will depend on the accuracy of the experiment and the amount of additional information available. The level schemes mentioned above contain between 15 and 20 levels with 50 to 60 associated gamma rays assigned to the schemes.

II-4, 5, and 6. RISØ CURVED-CRYSTAL SPECTROMETER*

O. W. B. Schult, B. P. Maier, U. Gruber, and R. Koch

Laboratorium für Technische Physik der Technischen Hochschule München,

Research Establishment Risø

Towards the fall of 1960, one of the 7-in.-diameter tangential channels at the DR-3 reactor at Risø was offered to us by the Danish Atomic Energy Commission, especially by Professor Kofoed-Hansen. The high flux (6×10^{13} neutrons/cm^2 per sec) in the center of the beam hole caused us to use this facility for the measurement of neutron-capture gamma rays—an experiment which we had already done before, using a very small curved-crystal spectrometer at the FRM reactor at Garching near Munich.

The experience we gained from the Garching instrument proved to be very useful for the design of the new Risø spectrometer. The tremendous number of lines which we observed from Eu^{152} at Garching was the reason for high resolution to be the first requirement. The applicability of the Ritz combination principle demands that the relative energy determination of the detected lines should be as accurate as possible. Reasonable precision should be obtained during the automatic scanning of the spectrum. A small loss in luminosity was borne in order to make the whole apparatus as inexpensive and simple as possible.

---

*Presented by O. W. B. Schult. In the program of the conference, the subject of this paper was listed as three abstracts: II-4. Risø Curved-Crystal Spectrometer; II-5. Levels in Dy^{164} Populated after Neutron Capture; and II-6. Levels in Lu^{177} Populated after Neutron Capture.

High resolution was obtained by diffracting the gamma radiation from the 110 planes of a 4-mm-thick quartz lamina, which was bent between two steel blocks, the cylindrical surfaces of which were lapped by hand. The minimum reflex width was measured to be 7.2", corresponding to a resolution of 0.14% for the first-order reflex of 100 keV radiation. Actually only very few reflexes below 100 keV are measured in first order. For these reflexes the resolution is high enough to separate the single gamma lines. The main part of the spectrum is measured in second order. Strong reflexes can easily be measured in third order; and very intense lines are determined from the fifth-order reflexes, where the resolution for 100 keV radiation can be as high as 3×10^{-4}.

The sources normally contain only 50 mg of substance and have rather small dimensions (25 mm high, less than 0.2 mm wide, and 2—10 mm deep). Thus the average line width is 8—9".

The precise angular position of a reflex can be measured either absolutely or relative to a so-called reference line. The first technique is used for the determination of the energies of intense reflexes while the second method is applied to calculate the energies of weak reflexes using the recorder sheet and the precisely measured intense lines as reference lines.

When the spectrometer is operating with line sources, the angular orientation between the source and the spectrometer crystal must be sufficiently good. This means that the deviation of the source from its exact lateral position must be less than 3μ when the radius of curvature is of the order of 6 m. The source which is used for the measurement of neutron-capture gamma rays is usually located in the center of a long liner. Often it is suspended from a very light frame.

Therefore one cannot expect that the movement of the source is negligibly small. We have observed this movement at Garching. It is especially large (several seconds of arc) when the reactor is started or shut down. During operation at constant power, several hours after the reactor was started, the movement was found to be slow and irregular and of the order of a few tenths of a second of arc. This observation is in accordance with thermal effects giving rise to the movement. These dislocations can be eliminated to sufficient accuracy when the reflexes are measured point by point several times successively at both sides of the zero angular position. This procedure is followed for all strong reflexes observed at the Risø spectrometer and yields diffraction angles which are completely independent of the shape of the reflexes. The angle-measuring device is a theodolite with scale irregularities less than 0.1", which is suspended below the crystal and rigidly connected with the crystal table. This geometry is free of forces and allows, therefore, for the maximum precision.

All possible errors can be divided into two groups: accidental and systematic. Accidental errors appear in the angular values for the reflexes found during the successive measurement of a single gamma line at both sides of the angular zero point. Systematic errors can be avoided by a linearity test. This test was performed by measuring very intense x-ray and gamma lines in several orders (up to the ninth-order reflex). The test showed that the true energy E_γ of a transition must be calculated from the measured value E_m by use of the relation

$$E_\gamma = (1 - \alpha\,\phi)E_m \quad ,$$

where $\alpha \approx 3 \times 10^{-5}$/deg is independent of the energy.

The precision in the energy determination of the weak reflexes, which are calculated from the recorder sheet, is in principle limited by the source fluctuations. An angular accuracy of 1", being of the order of the angular fluctuations of the source, was considered to be a reasonable precision, allowing for a very simple mechanical solution of the automatic drive.

The spectrometer crystal and the theodolite rotate in a very precise wire-ball-bearing, which demands a very small momentum for its rotation. The detector and the whole shield are floating on an air bearing. As shown in Fig. 1, two stainless steel bands connect a colli-

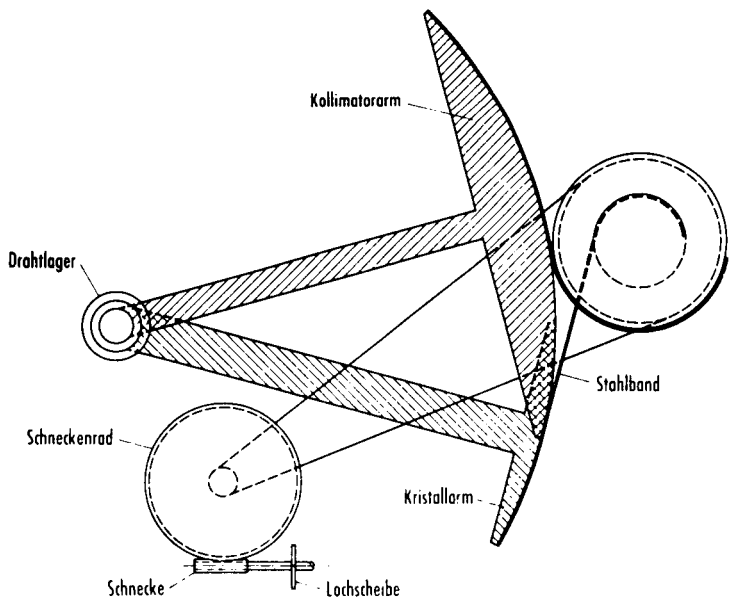

Fig. 1. Drive mechanism for Risø curved-crystal spectrometer.

mator arm and the crystal arm with two steel desks having the proper radii to keep the detector within ± 8" in the direction of the reflected beam (± 14" would have been sufficient because of the trapezoidal shape of the collimator. The steel disks are driven by a third band providing a 1:6 transmission between the disks and a worm wheel, which is rotated by a worm in connection with a special gear box. Lamps, photo-

resistors, and two disks with holes (mounted on the driving system of the spectrometer) produce signals every 10", 1', 10', and 1°. The linearity of this scale is better than 1", as could be tested with the theodolite.

The signals of the angular scale are recorded together with the photopeak counting rates of the first-, second-, and third-order reflexes, the total counting rate of the detector, and the monitor counting rate. The different orders are separated by subdividing the detector pulses in the ratios 1: 2: 3 and feeding these signals to three one-channel analyzers, which are operated in parallel. The correct channel height $E \propto 1/\phi$ is obtained from a very simple automatic mechanism. The discriminators transmit only pulses corresponding to the proper order of reflection. They are connected with counting-rate meters, each of which feeds one channel of the recorder, a 6-color point printer.

The source is suspended from a titanium tube (Fig. 2),

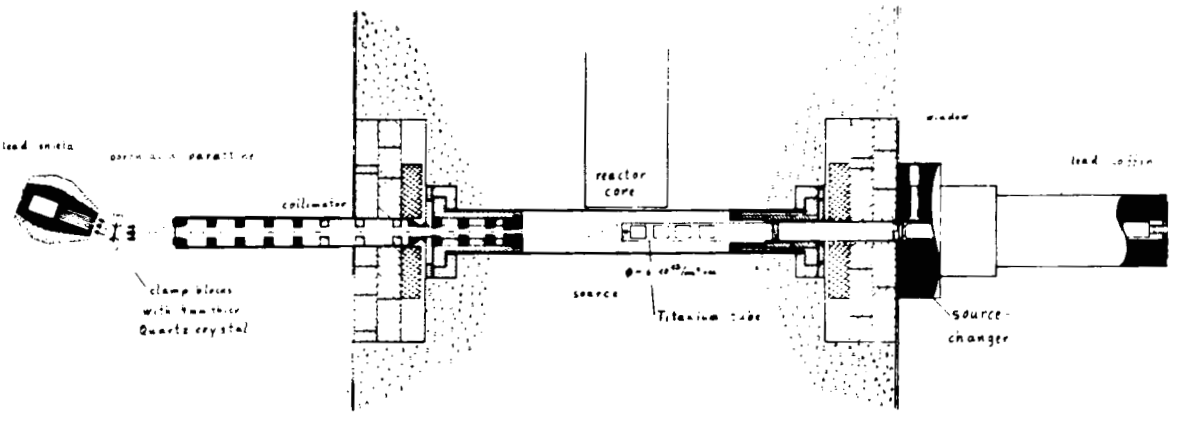

Fig. 2. Curved-crystal spectrometer at the DR-3 reactor at Risø, Denmark.

which is attached to the source-holder plug. This plug can be rotated around its axis and moved parallel to it in order to allow for the necessary alignment of the source. The lead coffin outside the reactor face serves as a shield during the source-change procedure. The very intense gamma

radiation originating from the source passes through a collimator which defines the beam falling on the crystal and acts as a shield against radiation coming from the reactor core, the aluminum liner, and the titanium tube. Only a Li_2CO_3 layer can be seen behind the source. The low background (at the end of the collimator, the γ background is 2 mR/hr and the fast-neutron background is 0.3 mR/hr) is essentially due to the sharp collimation, which was possible because of the choice of a small crystal window (15 cm^2). The reflected radiation passes through a tapered slit collimator which is 45 cm long, consisting of lead sheets 1 mm thick and 1 mm distant at the entrance. The detector (Fig. 3) is a

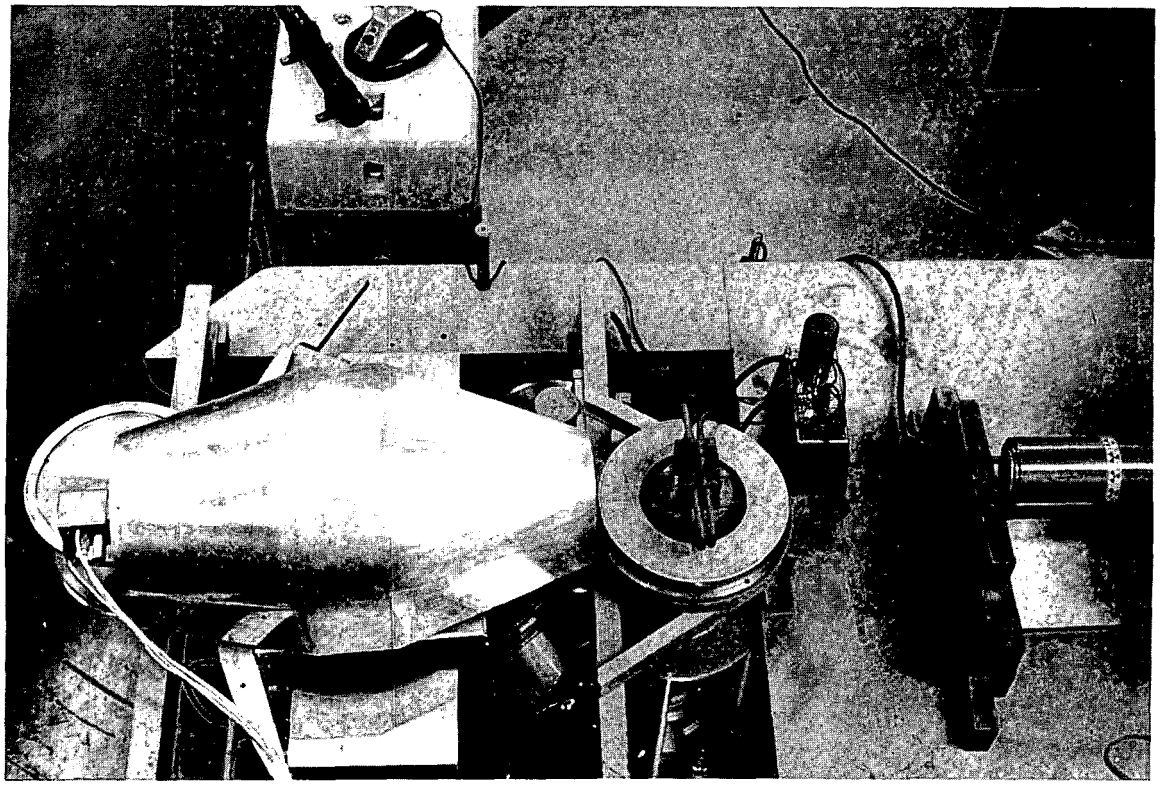

Fig. 3. Close-up view of curved-crystal spectrometer. The reactor is to the right.

2-in.-diameter scintillation counter with a thickness of 3 in., 4 in., or 4 mm. It is shielded by a 12-cm layer of lead plus 5 cm paraffin and

boric acid with a total weight of 0.4 tons. This shield is sufficient for the intended purpose. (For $\phi > 6^{\circ}$, the only background is that from the reactor hall, as shown in Fig. 4.)

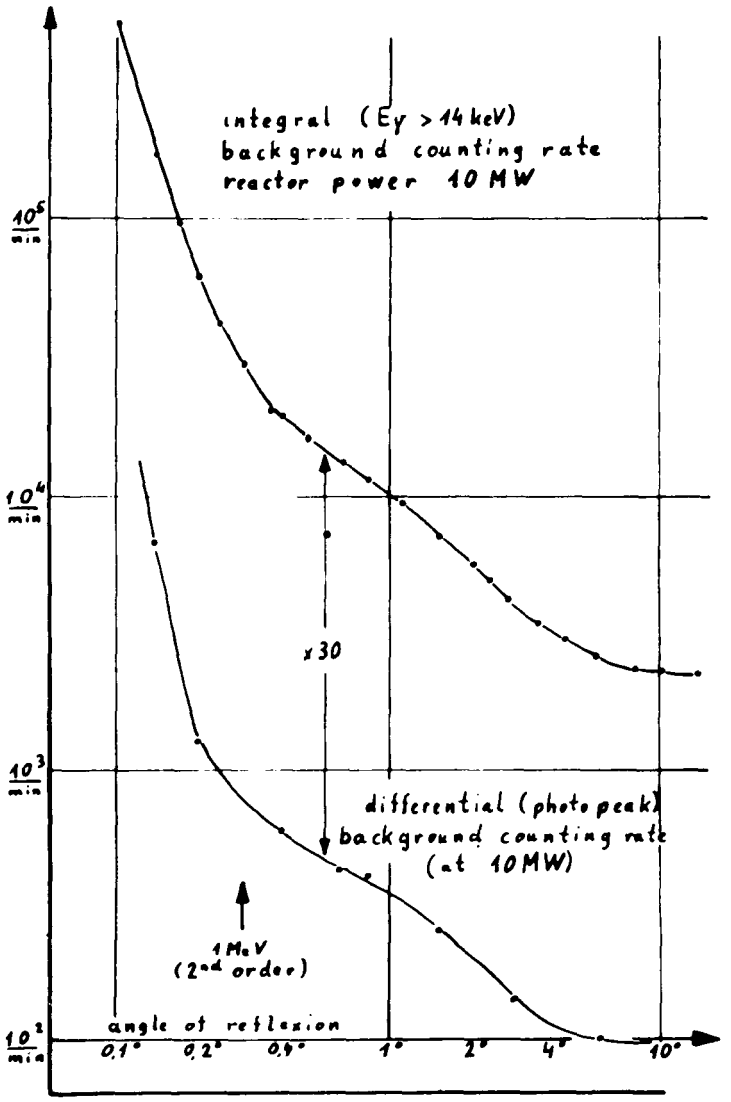

Fig. 4. A logarithmic plot of the background measured at the bent-crystal gamma-ray spectrometer at Risø.

The source is located 1 cm closer to the crystal than is ideal for very small diffraction angles. Therefore (and mainly because

of the small aperture of the crystal) the change in line width is negligible between $\phi = 0^{\circ}$ and $\phi = 5^{\circ}$, where high resolution is necessary. At 8° the width is only 14". Since only a few measurements need to be performed at still larger angles, the source is not moved during the measurement, although the construction of the source-holder plug allows one to make this adjustment if desired.

Relative intensities can be determined to an accuracy of 3—4% for a well-defined source geometry. Because the source depth is often 5—10 mm, large absorption corrections have to be made, implying a total error of 10—15% apart from statistics. Precise values of the absolute intensities of the strongest transitions as they can be obtained at the FRM, together with the numbers from the Risø spectrometer should allow for 5—8% data as long as the statistical error is small enough.

The over-all efficiency of the spectrometer is 3.5×10^{-8} for 411-keV radiation and a small source (Fig. 5). This number was measured with half of the maximum crystal window. The present crystal (since it has undergone twinning) allows only for the lower part to be used.

The minimum partial cross section is currently of the order of 10 mb at 100 keV. The energy accuracy is proportional to E_{γ}^{-1}. During standard measurements, a precision of $2—3 \times 10^{-5}$ is obtained for 100-keV lines. In extreme cases, this number could be decreased by a factor of 4, to yield 5×10^{-6} in relative energy determination at 100 keV.

Dy^{164}

For the determination of the neutron-capture gamma-

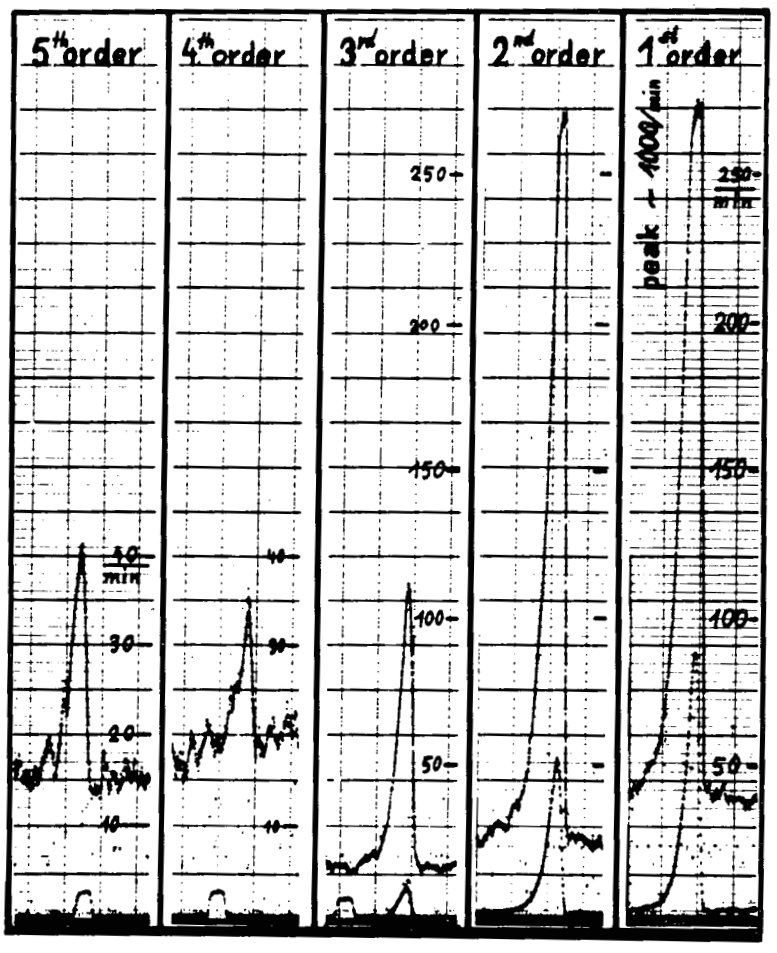

Fig. 5. Comparison of the first-, second-, third-, fourth-, and fifth-order reflections of the 411-keV gamma ray in Au^{198}. The source strength is 40 mC.

ray spectrum of Dy^{164}, a source of 43 mg Dy_2O_3 was irradiated in a thermal-neutron flux of $6 \times 10^{13}/cm^2$ per sec. The spectrum emitted from this sample (enriched 73% Dy^{163}, 10% Dy^{164}, 15% Dy^{162}, 2% Dy^{161}) was measured with the bent-crystal spectrometer at the DR-3 at Risø. Because of the very high cross section of Dy^{164}(2800 b) compared to that of Dy^{163}(120 b), most of the observed lines belong to Dy^{165}. The large number (about 220) of transitions found in this isotope Dy^{165} complicated the search for transitions occurring in Dy^{164}. Only 49 gamma lines between 40 and 970 keV could be attributed to this nucleus.

From the most intense low-energy lines corresponding to the $4^+ \rightarrow 2^+$ and $2^+ \rightarrow 0^+$ transitions in the ground-state rotational band (gsrb), the parameters A and B in the Bohr-Mottelson energy formula

$$E = AI(I + 1) - BI^2(I + 1)^2$$

were calculated as A = 12.2836(8) keV and B = 8.61(4) eV. From these numbers the energy of the 6^+ state was calculated to be 500.73(4) keV, which is 0.59 keV smaller than the experimental value [501.32(2) keV]. This value was found from the 259.09-keV line, which is considered as the $6^+ \rightarrow 4^+$ transition because its energy fits the calculated value as well as can be expected from a comparison with the neighboring even nucleus Dy^{162} and because its intensity decreases as is expected from a 2(-) or 3(-) compound state.

The energy difference of two very intense lines at 761 and 688 keV is equal to the energy of the ground-state transition; this leads one to assume a level at 761 keV. A transition of 519 keV, which can be fitted between this level and the 4^+ state of the gsrb defines the spin of the 761-keV level to be 2. The branching ratio of the transitions with energies of 761, 688, and 519 keV was measured as 0.75: 1.00: 0.015, in good agreement with the theoretical ratio 1.15: 1.00: 0.012 when the 761-keV level is regarded as the 2^+ gamma vibrational state (γvs). This agrees well with Yoshizawa's value of 770 keV for the 2^+ γvs, which he observed from Coulomb-excitation experiments.

Assuming that the moment of inertia in the gamma vibrational band is not very different from that in the gsrb, one can immediately conclude that the remaining very intense 754-keV line goes from the 3^+ γvs to the 2^+ level in the gsrb. Then a 586-keV transition to the 4^+ member of the gsrb is to be expected with an intensity 0.11 times

that of the 754-keV line. This transition was not observed because of a 6-times-stronger 584-keV line of Dy^{165}. Thus our measurement is in agreement with the assumption that the 3^+ γvs is at 828 keV.

From the spacing of the 3^+ and 2^+ γvs, the energy of the 4^+ γvs is calculated to be roughly 916 keV. Actually three transitions with intermediate intensity were found: an 843-keV line to the 2^+ and a 673-keV transition to the 4^+ level in the gsrb and a 154-keV line to the 2^+ γvs. The theory predicts three transitions to the 2^+, 4^+, and 6^+ levels in the gsrb with relative intensities 1.03: 1.00: 0.08. The observed branching ratio is 0.5: 1.00. The third weak 414-keV line to the 6^+ state could not be found because of a 300-times-stronger 414-keV transition in Dy^{165}.

The 154.18-keV transition between the 4^+ and 2^+ γvs (Fig. 6) allows for a sufficiently precise determination of the 5^+ γvs at 1025 keV. Two lines (782 keV and 523 keV) with relative intensities 1.00: 0.075 are expected from the theory. The 782-keV line was observed. The 523-keV transition is too weak to be detected.

The intensity of the strong 215-keV line demands that the line should go to the 2^+ or 3^+ γvs. With the help of the Ritz combination principle applied to the remaining lines, a few more states could be determined. The very small absolute error of the low-energy transitions fixes the distance between all levels around 1 MeV to a very high extent. Therefore the parameters A' and B' for the γvb were calculated as

$$A' = 11.181(6)\ \text{keV},$$

$$B' = 6.46\ (20)\ \text{eV}.$$

Furthermore the energy of the levels could be determined to better

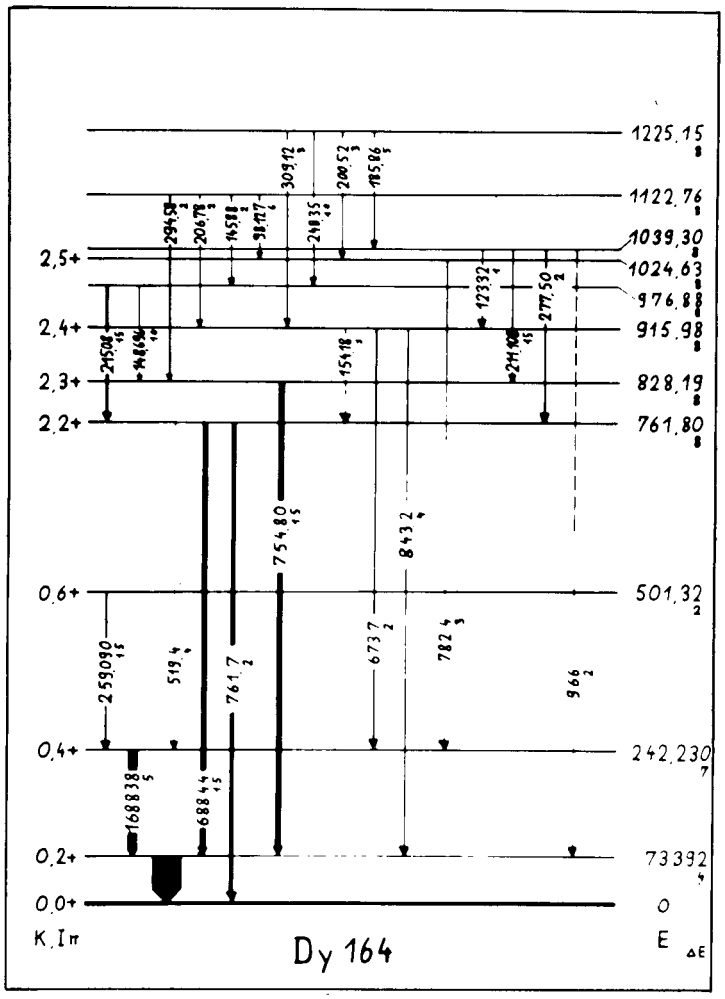

Fig. 6. Level scheme of Dy^{164} as derived from the bent-crystal measurement at Risø. The proposed spins and parities are given at the left and the energies of the levels are given at the right (in keV). The widths of the lines in the scheme reflect the intensities of the gamma transitions.

than 10^{-4} from all included transitions around 700 keV. The calculated distance between the 5^+ and 2^+ γvs is 262.76(7) keV, being a little less than the measured value 262.83(8) keV.

The unassigned levels at 976, 1039, 1122, and 1225 keV have a spacing which is 62.416(14), 83.466(18), and 102.37(2) keV—very similar to a rotational band with

$$A'' = 10.363(3)\ \text{keV}, \qquad B = -2.2(3)\ \text{eV},$$

and a spin sequence of 2, 3, 4, and 5. The calculated distance between the 4 and 5 states is 104.73(7) keV, differing by 2.4 keV from the experimental value. This difference seems to be quite large with respect to the small number B. The transitions between these levels and the γvs could be well understood (E1) if the parity of the new band is assumed to be odd. Then there remain three questions: (1) Why are the M1 transitions within the band not observed? (2) Why are the E2 transitions so weak? (3) Is the extremely faint (0.02 per 100 neutrons) 248.35-keV line then an accidental combination?

The 976-keV state is definitely a two-quasi-particle proton state. The rotational states superimposed on this level have to be considered as tentative.

The neutron states are expected at higher energies. From the neutron separation energy, the limit is about 1300 keV.

Two weeks ago I received a preprint from W. Neil and R. Sheline on "Levels in Dy^{164} from Deuteron Stripping and Inelastic Proton Scattering Experiments." It is interesting to compare their data with our results, which were obtained from measurement with the precise crystal spectrometer alone. Let us compare them in the energy region where Sheline's results and ours overlap. Sheline found levels at 72(2), 240(2), 503(3), 761(2), 827(5), 839(4), 919(3), 976(4), 1040(4), and 1157(5) keV (others at 1680 and at higher energies). The 72-, 240-, and 503-keV levels agree well with our gsrb. Sheline gives A = 11.95 keV and B $<$ 3 eV as an estimate. These values deviate a little from our numbers. It is, however, impossible to define the parameters A and (especially) B with reasonable precision as long as the levels are uncertain to 2 or 3 keV. The 761-keV state, which Sheline identifies as the 2^+ γvs, agrees excellently with our assignment.

The levels at 827 and 839 keV have not been resolved by Sheline. From his plot of the proton number (here 30/stripe) vs distance along the plate, I have tried to redetermine the energy of the center of these two lines. I found a value of 829(2) keV from an interpolation between the 761- and 919-keV states. The close agreement of this value with our energy, 828.19 keV, causes me to believe that there is only one state.

A further discrepancy is the 1040-keV level given by Sheline. He identifies this state with the 5^+ γvs. We consider the 1024-keV level as the 5^+ γvs. The 1157-keV level is atributed to the 6^+ γvs by Sheline. From our parameters A' and B' for the γvb, we calculate the energy of the 6^+ γvs to be 1153.2(2) keV, which is in good agreement with Sheline's 1157(5) keV. The agreement is still better when we consider that the calculated value is to be expected at a lower energy than the observed level (difference $\leqslant 1$ keV). This agreement is therefore a strong evidence for the 5^+ γvs at 1024 keV, as proposed by us.

Since Sheline does not expect appreciable excitation of two-quasi-particle proton states in the (d,p) reaction, the only explanation could be that Sheline's 1040(4)-keV should lie at 1024 keV. It is, however, necessary to mention that Sheline saw the 976-keV state, which seems not to be a collective level.

Lu^{177} Levels

Rotational states have been well established in the region of deformed nuclei, especially among the rare earths. The energies of these states agree with the levels calculated from the

equation

$$E = AI(I + 1).$$

A comparison of sufficiently precise experimental data with the values obtained from the above formula reveals deviations which can be accounted for by introducing the rotation-vibration interaction term. This is done in the Bohr-Mottelson energy relation

$$E = AI(I + 1) - BI^2(I + 1)^2.$$

Very precise energies of the transitions between rotational states, such as those that can be observed and measured with crystal spectrometers, allow for a test of the improved formula.

The gamma-ray spectra emitted after neutron capture ordinarily contain only a few transitions between the members of a rotational band in odd nuclei. This is due to the fact that the spin of the compound state is $\frac{1}{2}$. Consequently, only low-spin states will be populated with measurable intensity. It is evident that the efficiency of the energy relation can be tested best by experimentally determining as many states as possible in a rotational band.

A case in which this can well be done by neutron-capture gamma-ray studies is the odd-proton nucleus Lu^{177}. This case is exceptional in that the source, Lu^{176}, is an odd-odd nucleus which can, however, be easily used because of its large half-life (2×10^{10} yr). The ground-state spin of Lu^{176} is 7^-, allowing for a population of levels up to 17/2 in Lu^{177}. An 8.5-mg sample of enriched Lu^{176} oxide (74.5% Lu^{176}, 25.5% Lu^{175}) was enough to produce a total source activity of about 180 Curies because of the high cross

section (4000 b). A total of 220 lines with energies between 40 and 920 keV were found during the irradiation of this source with thermal neutrons (Fig. 7).

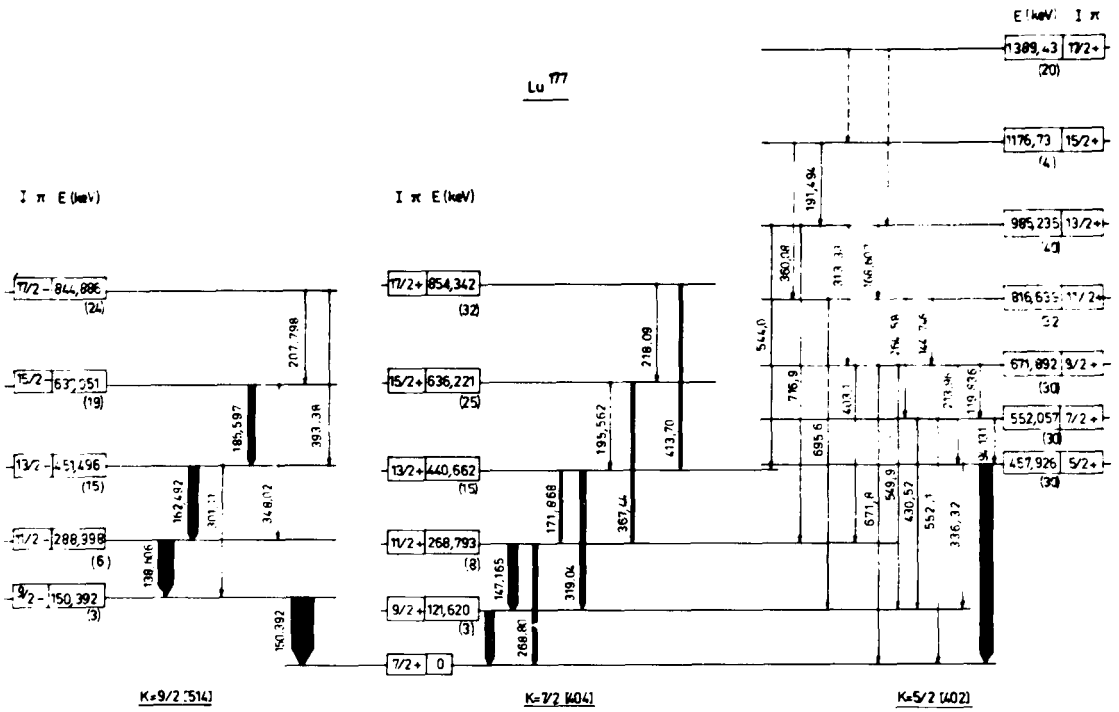

Fig. 7. The level scheme of Lu^{177} as defined by the bent-crystal measurements at Risø. The proposed spins, parities, and energies (in keV) are given to the left or right of each level. The K values and quantum numbers are given below each band.

The ground-state rotational band (K = 7/2 + [404] in Lu^{177} has been observed by O. B. Nielsen during decay studies. Part of the strongest transitions in the neutron-capture gamma-ray spectrum measured with the Risø spectrometer could clearly be attributed to the transitions between the lower six levels of this rotational band. The assignment was straightforward, where the very precise energies of the gamma lines proved to be very helpful.

The 150.3-keV line was found to be extremely intense. This is strong evidence for an E1 transition from another Nilsson state

to the ground state. The rather long half-life[1] of this state (1.2×10^{-7} sec) indicates a strong hindrance for the transition. This is in agreement with the assumption that the 150.3-keV level is identical with the K = 9/2 [514] state. This level and the first excited state of the rotational band superimposed on the [514] state have already been observed.[2] Apart from the very precise energies of these two transitions, we found six strong gamma lines corresponding to transitions depopulating the 17/2, 15/2, and 13/2 rotational levels in this band.

Application of the Ritz combination principle on the remaining strong transitions resulted in a third rotational band with a spin sequence 5/2, 7/2, 9/2, etc. In fact, such a band is to be expected from the Nilsson model predicting a K = 5/2 + [402] state at an energy of several hundred keV. The trivial requirement that the transition from the 5/2 level to the ground state should be stronger than the 7/2 → 5/2 transition demands the 5/2 level to be at 457.9 keV, corresponding to the single remaining line with sufficient intensity in the whole energy range.

Several transitions from the K = 5/2 levels to the K = 7/2 states are observed, as can be expected from their M1, E2 multipolarities.

From the very precise energies of the gamma lines, the parameters A and B in the Bohr-Mottelson energy formula were

---

[1] H. deWaard, Phil. Mag. 46, 445 (1956). This half-life was determined from the decay of Yb^{177}.

[2] Lines at 119 or 121.$\overset{7}{2}$ keV and at 146 or 150.$\overset{4}{2}$ keV were observed by J. Lindskog, T. Sundström, and P. Sparrman, Arkiv Fysik 23, 341 (1963) and by J. P. Mize, M. E. Bunker, and J. W. Starner, Phys. Rev. 103, 182 (1956). The latter also found three additional transitions at 1.24, 1.12, and 1.09 MeV.

TABLE I. Parameters A and B in the Bohr-Mottelson energy formula

$$E = A[I(I+1) - I_0(I_0+1)] - B[I^2(I+1)^2 - I_0^2(I_0+1)^2].$$

$[Nn_Z\Lambda]$	A (keV)	ΔA (keV)	B (eV)	ΔB (eV)	E_{γ_1}, E_{γ_2} (keV)	$\Delta E_{\gamma_{1,2}}$ (keV)
[404]	13.7855	0.0020	6.72	0.05	121, 620 147, 165	0.003 0.005
[514]	12.8543	0.0020	4.20	0.03	138, 606 162, 492	0.005 0.004
[402]	13.6533	0.0009	8.35	0.05	94, 131 119, 836	0.003 0.003

determined as shown in Table I. From these numbers the energies of the transitions between the higher members of the rotational band under consideration could be calculated. Table II compares these calculated energies with the measured values. The difference between the calculated and measured energies is very small and increases with I. In the $\frac{7^+}{2}$ and $\frac{5^+}{2}$ bands, the theoretical energies are smaller than the experimental ones. The deviation is less in the 7/2 band (B = 6.7 eV) and larger (a factor of 3) in the 5/2 band where B = 8.3 eV. In the 9/2 band, however, E_{theor} is larger than E_{exper}. The amount of deviation is larger than one would expect from the very small value of B (4.2 eV).

TABLE II. Comparison between the calculated and the measured values of the energies of the transitions between the higher members of the rotational band.

$(I+1) \rightarrow I$	$E_{\gamma,\,theor}$ (keV)	$\Delta E_{\gamma,theor}$ (keV)	$E_{\gamma,exper}$ (keV)	$\Delta E_{\gamma,exper}$ (keV)
		Band [404] $K = \frac{7^+}{2}$		
9/2 → 7/2	. . .	. . .	121.620	0.003
11/2 → 9/2	. . .	. . .	147.165	0.005
13/2 → 11/2	171.83	0.06	171.868	0.008
15/2 → 13/2	195.44	0.09	195.562	0.009
17/2 → 15/2	217.84	0.12	218.097	0.011
		Band [514] $K = \frac{9^-}{2}$		
11/2 → 9/2	. . .	. . .	138.606	0.005
13/2 → 11/2	. . .	. . .	162.492	0.004
15/2 → 13/2	185.72	0.06	185.597	0.009
17/2 → 15/2	208.20	0.08	207.798	0.008
		Band [402] $K = \frac{5^+}{2}$		
7/2 → 5/2	. . .	. . .	94.131	0.003
9/2 → 7/2	. . .	. . .	119.836	0.003
11/2 → 9/2	144.62	0.02	144.746	0.006
13/2 → 11/2	168.32	0.03	168.607	0.006
15/2 - 13/2	190.70	0.04	191.494	0.009
17/2 → 15/2	211.59	0.07	(212.846)	0.016

* * *

R. K. SMITHER, Argonne National Laboratory: In your level scheme of Dy^{164}, the lowest energy excited-state rotational band (K = 0) had strong transitions to the ground-state rotational band. A number of levels above this band have very weak transitions to the ground state. Would you care to comment on these states, and could you set an upper limit on the intensity of the missing transitions relative to the strong lines that you observed?

SCHULT: These unassigned states seem to correspond to two-quasi-particle proton states whose configuration I do not quite understand. I think there was one line going to the ground state and that it had a total intensity of only 1%, but we have not found any others. It is possible that there are weak transitions, but we have not observed them because our limit at this energy is roughly 0.6%.

SMITHER: I have found in the past that there often is a ratio of 10 or more in the relative intensity in similar situations. This is consistent with your work.

J. W. KNOWLES, Chalk River Nuclear Laboratory: Could you tell us something about the equipment? What is the mosaic width?

SCHULT: The mosaic width was measured to be less than 4", using a very small improvised spectrometer, only to test the width.

KNOWLES: Is this quartz?

SCHULT: Yes, it is quartz curved to 5.7 m. It is 4 mm thick; the reflection planes are the (110) planes having a grating constant of 2.5 Å. We have a line width of 7.2".

S. MOSZKOWSKI, University of California, Los Angeles: I am wondering if you have looked at all the higher order terms, i.e., the $I^3(I + 1)^3$ term, etc.

SCHULT: What we found is that when we use this very simple formula, $I(I + 1)$ and $I^2(I + 1)^2$, then we fit the first two transitions. Then on comparing the calculated and measured values, we usually find deviations at the higher transitions. These were nearly within our error for the [404] band of Lu^{177}, so the question about the third parameter is meaningless. But when, for example, you use the ground-state rotational band of Dy^{164}, then you get this parameter for the cubic term. I think we have B = 8 eV. We then find a clear difference between the calculated value and the measured value for the transition from the 6^+ level to the 4^+ level. We have also observed such a difference for Dy^{162}; and it is present in the other nuclei.

MOSZKOWSKI: Can you say anything systematic about that term?

SCHULT: I can say a little bit. Normally we find that the calculation gives a level a little below the experimental level. This means that the $-BI^2(I + 1)^2$ correction is too strong.

MOSZKOWSKI: That is what you would expect if you take $I(I + 1)$ only. You need something that makes the energies increase less rapidly with I, so you put in the $I^2(I + 1)^2$ term and it over-corrects a little.

SCHULT: That is true.

MOSZKOWSKI: Just to give a rough idea, can you make a rough dimensional sketch for the $I^3(I + 1)^3$ term? Would that be about the right order of magnitude—just roughly?

SCHULT: With the $I^3(I + 1)^3$ term, I can fit the third transition. But when I test it, I need a fourth transition which we do not observe in Dy^{164}, but only in Lu^{177}.

MOSZKOWSKI: Does it not make any improvement?

SCHULT: It does improve it; but the line energies must be very accurate for a comparison, and the cubed term is only of the order of 0.3 eV or much less. It is then a small difference, which might be left.

II-7. CAPTURE GAMMA RAYS FROM DYSPROSIUM

H. T. Motz and R. E. Carter

Los Alamos Scientific Laboratory, Los Alamos, New Mexico

The Los Alamos Compton spectrometer has some outstanding properties that are important to its use in determining energy levels of residual nuclei, which can be a great aid in nuclear spectroscopy. These may be briefly summarized as follows:

(a) The resolution is high and allows the clear separation of lines differing by some 30 keV at energies as high as 8 MeV.

(b) The linearity and stability of the instrument are also high enough that energy differences of well-resolved high-energy gamma rays can be determined in most cases to less than 1 keV, even up to 10 MeV.

(c) The spectral response is good enough that least-squares fitting of data is straightforward and results in a maximum exploitation of the above properties with high confidence and with realistic standard errors.

(d) The background is low and the sensitivity adequate so that transitions less than 1 per 1000 neutrons captured can be measured with varying accuracy when they are sufficiently well isolated.

The above characteristics permit the high-energy data obtained to be compared in detail with the low-energy capture spectra, with radioactive decay data, or with the corresponding (d,p) reaction.

The initial targets used with the instrument were nitrogen, beryllium, and sodium, which allowed the detailed determination of the line shape, the sensitivity, and the calibration by means of the well-known lines from the Na^{24} decay. The light-element reactions produce so few gamma rays that it was possible to derive closed decay schemes of high uncertainty. These will be discussed in a paper II-11 of this meeting under the title "Capture Gamma Rays and Neutron Binding Energies" and will not be discussed in detail here. Other work in our laboratory in 1960 involved the decay of the 1.2-min isomeric state of Dy^{165} to Ho^{165}, as well as the ground-state decay of the 2.3-hr Dy^{165}. These radioactive-decay studies gave some interesting information concerning a level that could not be fitted to the expected Nilsson assignments for Ho^{165}, and it was later determined that this level was from a gamma vibrational band in Ho^{165}. At the suggestion of Dr. M. E. Bunker,[1] we decided to examine the gamma-ray spectrum from natural dysprosium, which consists mostly of the capture in the reaction $Dy^{164}(n,\gamma)Dy^{165}$. The idea of this investigation was to confirm that the assumed 1.2-min isomer of about 108 keV in Dy^{165} has spin 1/2 as assumed in determining the spins of the daughter states in Ho^{165}. We expected to see a pair of lines going to the 1/2 state, believed to correspond to the Nilsson [521] orbital and to the first member (spin 3/2) of the rotational band some 50 keV above it, but just what in addition was

---

[1] F. P. Cranston, M. E. Bunker, and J. W. Starner, Bull. Am. Phys. Soc. 5, 255 (1960).

not known except from the initial work of Groshev. The spectrum that we observed is shown in Fig. 1. There was almost no information avail-

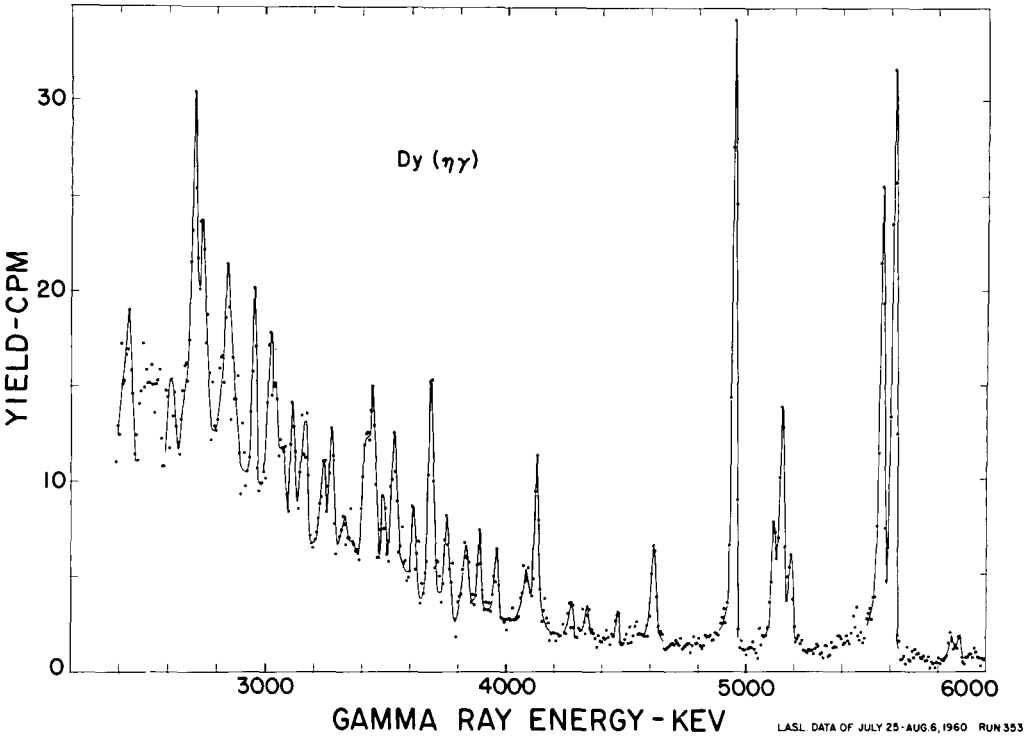

Fig. 1. High-energy gamma-ray spectrum from a 17-g sample of natural dysprosium in graphite. The lines at 3.7 and 4.95 MeV are from $C^{12}(n,\gamma)C^{13}$.

able at the time regarding the levels in Dy^{165}; the binding energy was not known to sufficient accuracy, so we could not reliably state that the pair of lines at 5.6 MeV (separated by 49.7 ± 0.4 keV) were indeed the sought pair. So the experiment was considered of no use for our immediate purposes and is shown[2] only as an illustration of how helpless a capture-

---

[2] H. T. Motz and R. E. Carter, Proceedings of the International Conference on Nuclidic Masses, Hamilton, Ontario, 1960, p. 299.

gamma-ray experiment can be even in determining binding energies when other information is not available. It is also an interesting example of how complicated rare-earth spectra can be and of why even higher resolution is desirable.

The situation remained dormant until the needed additional experiment was done independently in 1962 as part of the Florida State University (d,p) program in the deformed-nucleus region. This was the $Dy^{164}(d,p)Dy^{165}$ reaction observed by Shelton and Sheline.[3] The correspondence of the Q values observed in the (d,p) and the (n,γ) reactions is shown in Fig. 2 and is summarized for the higher transitions leading

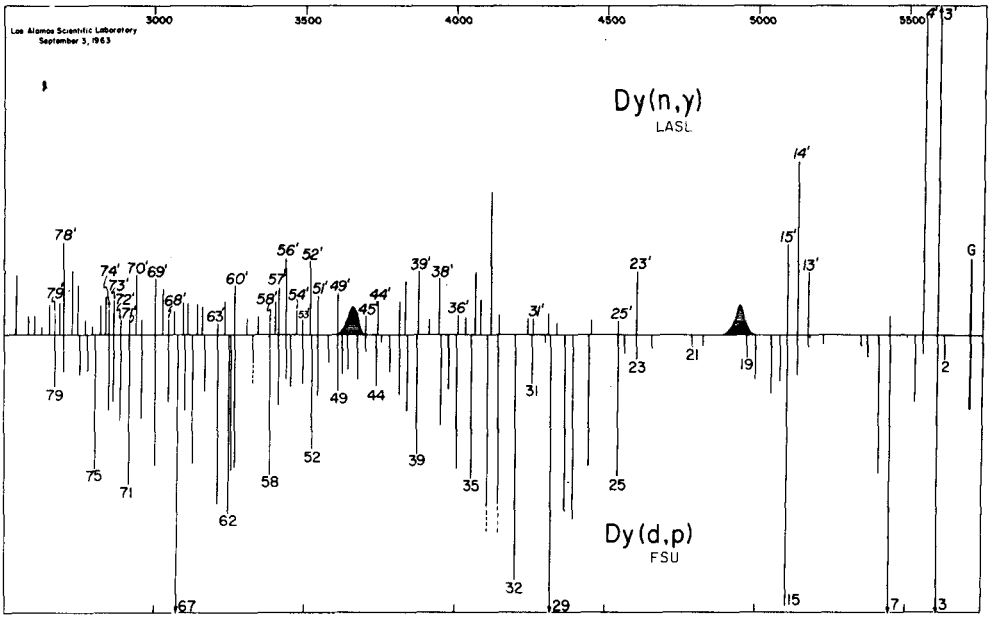

Fig. 2. Bar plot of Q values assigned to $Dy^{164}(d,p)Dy^{165}$ and $Dy^{164}(n,\gamma)Dy^{165}$, where the (d,p) values have been increaed by 2225 keV to allow a more direct comparison. The numbering sequence is chosen to be regular for the (d,p) peaks assigned to Dy^{165}, but only some of these index numbers are shown. The index number for an (n,γ) peak is shown when it is believed to correspond to a similar Q value for the (d,p). The unobserved ground-state Q value of 5715 keV is labeled "G". The peaks sketched at 3680 and 4950 keV for the (n,γ) cross section indicate that the $C^{12}(n,\gamma)C^{13}$ lines obliterate part of the spectrum.

[3] W. N. Shelton and R. K. Sheline, Bull. Am. Phys. Soc. 7, 569 (1962) and private communication.

to levels below 1.2 MeV in Table I. As can be seen from these presentations, the correspondence is surprisingly good and furnished the incentive and the information needed to re-examine Dy^{165}. We have confirmed our 1960 data with higher accuracy.

Two basic characteristics of the reaction mechanisms are important in the interpretation of these results. First, the thermal-capture spectrum is expected to be dominated by electric-dipole transitions which then excite states of spin-parity $\frac{1}{2}^-$ or $\frac{3}{2}^-$ since the target nucleus Dy^{164} is even-even and has spin-parity 0^+. Thus we would expect that the stronger high-energy lines belong to this limited class of final states, although the possibility of M1 transitions to positive-parity states cannot be ruled out, especially for the somewhat weaker lines. This can be quantitatively checked since the capture occurs almost completely in a resonance of known width. The (d,p) reaction, on the other hand, can transfer many units of angular momentum and thus excite states of much higher spin values. A most important added feature of the (d,p) reaction is that the differenctial cross section depends upon the characteristics of the deformed state. By means of the theoretical estimates for these differential cross sections, one can often determine from relative intensities of the (d,p) groups to what deformed states they might be assigned.

By a judicious combination of these properties, it has been possible to tentatively assign[4] some 27 levels to five Nilsson states and their rotational members and to two (K-2) gamma vibrational

---

[4] R. K. Sheline, W. N. Shelton, H. Motz, and R. E. Carter (to be published).

TABLE I. Preliminary values of the energies of the Dy^{165} levels.

Group No.	Excitation energy (keV) (d,p)	(n,γ)	Best value	Comments
1				Ground state; not observed.
2	84			
3	108.2	108.2	108.2	Reference level.
4	159.2	158.5	158.7	
5	181.1			
7	263	(262)		(n,γ) line prob. not from Dy^{164}(n,γ)
8a	295.8			
8b	302.7			
9	336.0			
10	359.4			
11	480			
12	522			
13	537	539.4		(d,p) line possible doublet
14	576	572.2		(d,p) line possible doublet
15	607	605.9	606	
16	629			
17	658			
18	710			
19	778			
20	885			
21	921			
22	1056			
23	1106	1103	1104	
24	1144			
25	1167	1167	1167	

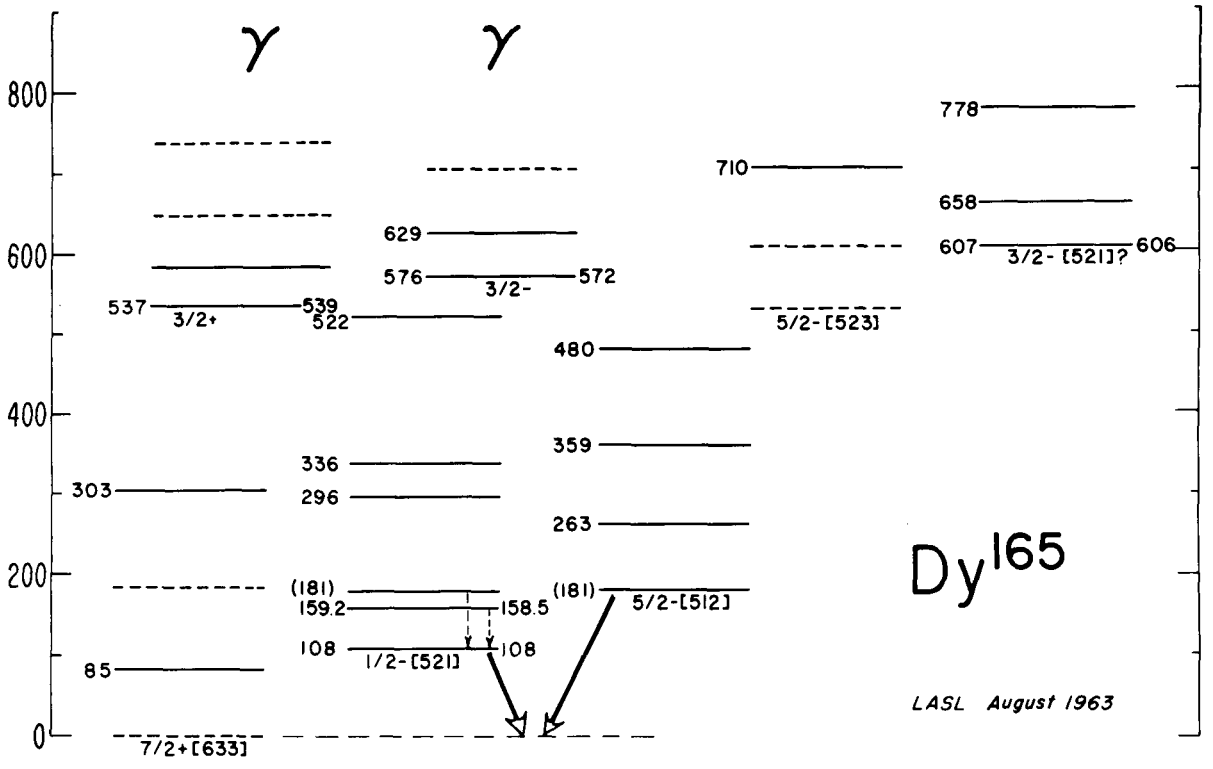

Fig. 3. Proposed level scheme and Nilsson assignments for Dy^{165}. Values on the left-hand side of a level are the excitation in keV from the (d,p) reaction (when observed); those on the right are from the high-energy (n,γ) transition (when observed). The reference state for all values is the 108-keV level which is the 1.2-min isomeric state. The dashed levels have not been observed in either the (d,p) or the high-energy (n,γ) spectra. The two K-2 gamma vibrational bands are believed to be associated with the orbitals above which they are drawn. The four low-energy transitions are observed with a scintillation spectrometer.

bands built upon two of these Nilsson states. These assignments are shown in Fig. 3, which gives the (d,p) excitation values on the left-hand side of an observed level and the (n,γ) excitation value on the right, when also observed. A dashed line indicates a level that is not observed in either the (d,p) or (n,γ) high-energy spectra but is inferred from the assigned level characteristics of the other band members. If these assignments to gamma vibrational bands are indeed correct, then they are the first such bands assigned to an odd-neutron orbital.

It should be noted that the 24 levels from the (d,p) reaction shown in Table I are from a set of some 79 corresponding to an excitation of up to 3 MeV. The eight gamma rays from Dy are similarly from a set of some 150. The data leading to the low-lying states shown in Fig. 3 constitute only a small fraction of the available information, and it is hoped that the decay scheme can be extended to somewhat higher energies—at least for the stronger transitions. It should be emphasized that the capture spectrum is obtained with a sample of natural dysprosium and that the weaker lines at high energies may be from other isotopes. Some of the strongest observed lines at low energies (below 1.5 MeV) are in fact from other isotopes.[5]

During the above work we received preliminary data[5] —a set of low-energy gamma-ray transitions from the Munich group working at Risø with a new curved-crystal diffraction spectrometer. We are now in the process of attempting to fit these very accurate gamma rays into our proposed level scheme to see if both the energy assignments and rotational character are consistent with the Risø energies and intensities. Also, we have just received coincidence information[6] on Dy^{165}, taken by John Neill at Brookhaven, which appears consistent with Fig. 3.

The very late timing of this work does not permit more than this brief progress report at this time. But this experi-

---

[5] O. W. B. Schult, B. P. Maier, and U. Gruber (private communication, August 1963).

[6] J. Neill (private communication, September 1963).

ment is an excellent example of many of the unavoidable features of neutron-capture gamma-ray spectroscopy, at least for the more complicated spectra. The ordering of the gamma rays is not known and, except for the high-energy gamma rays going to the first 1—2 MeV of excitation, cannot be even fitted together unless extremely high precision is available. But even this limited class of high-energy transitions does not lead to much useful information in itself. Similarly, the (d,p) reaction in itself is often incapable of making reliable assignments unless a complete angular-correlation experiment is done. But the combination of the results from several different experiments [low-energy spectra, high-energy spectra, coincidence spectra, and the (d,p) reaction] can lead to a mutually beneficial collaboration even for very complex spectra.

* * *

L. M. BOLLINGER, Argonne National Laboratory: You mentioned the statistical accuracy with which you could measure an energy difference. You stress that this was not a systematic error. What would you estimate your systematic error is in that case?

MOTZ: I think we would probably have two or three times that error in the case of Ti. This will be mentioned in the paper which Bob Carter will give, namely, that the nonlinearity of the instrument determines the systematic error. We really do not know the error at this time. We are neither optimists or pessimists, but it will be three times the error mentioned.

R. K. SMITHER, Argonne National Laboratory: There is still a need for the absolute energy calibration of these high-energy lines. Do you forsee any future advances that would enable you to pin down the absolute values of the high-energy gamma rays to this accuracy?

MOTZ: No. I think it can be improved; but the problem is with the nonlinearities of our instrument. This will also be discussed in Carter's talk (Paper II-11).

SMITHER: Do you feel that in the near future you will not be able to calibrate the nonlinearities?

MOTZ: If there were more light-element cases to check, or if we could derive an error curve from, say, 1 to 10 MeV which might be good to better than 0.5 keV, then we could make a correction to these values and use statistical errors. But that is not possible at this time.

P. AXEL, University of Illinois: I guess I am just a little confused as to why you want the absolute values. If you can get the differences, that is the only thing you need. How do you weight your points?

MOTZ: We have an integral number of counts. They are observed for each magnetic field setting or for each energy interval that we apply. Then we use the square root of the number of counts.

A VOICE: Do you have any values of χ^2?

MOTZ: Occasionally the value of χ^2 per degree of freedom is better than 1 (which is, of course, to be expected) but we will often accept a value as high as 5 or so for χ^2 per degree of freedom.

II-8. BENT-CRYSTAL MEASUREMENTS ON GAMMA RAYS FROM NEUTRON CAPTURE IN INDIUM*

W. John and R. W. Jewell

Lawrence Radiation Laboratory, Livermore, California

We have used a 2-m bent-quartz-crystal spectrometer to measure the energies (ranging from 85 to 1300 keV) of the gamma rays emitted from an indium target exposed to neutrons from the Livermore reactor. The experimental layout is shown in Fig. 1.

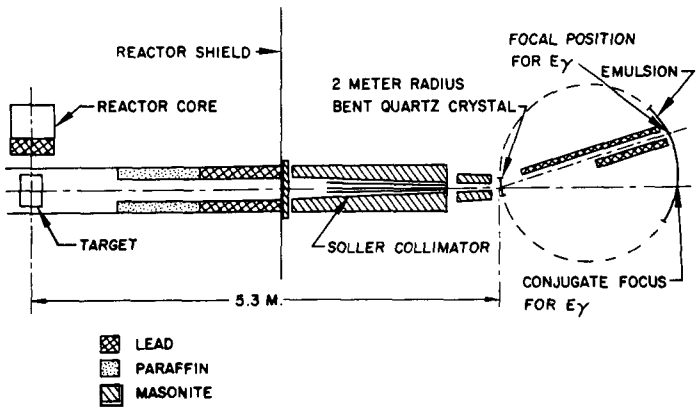

Fig. 1. Layout of bent-crystal spectrometer.

There is 7 in. of lead between the reactor core and the target which is situated in the through tube where the flux is approximately 6×10^{12} cm^{-2} sec^{-1}. The target consisted of high-purity foils of indium mounted in an aluminum holder. The gamma rays pass through a collimator fabricated of paraffin (for fast-neutron shielding) and lead. An absorber of 1-in. masonite has been found to be effective in reducing the fast-neutron background. The Livermore reactor is light-water moderated,

*Presented by W. John.

which results in a fairly large fast-neutron flux. Our spectrometer is operated in the Cauchois geometry, that is, with an extended source and a line focus on the Rowland circle. A Soller collimator situated here, made of steel plates, tapers towards the conjugate focus on the beam axis. The Soller collimator has been found useful for gamma rays in the high-energy end of our measurements, that is, above about 500 keV. I must mention that none of the indium measurements reported today were made with this Soller collimator, however.

The outer edges of the beam are finally defined by an adjustable lead collimator before the crystal. This slit is not moved during an experiment so that all of the gamma rays use the same portion of the crystal. This avoids possible line shifts due to imperfect bending of the crystal. Finally, another collimator is used to separate the diffracted beam from the direct beam. The focused line is detected with 600-μ Ilford G-5 emulsions mounted on glass. Whenever possible, we measure each line on both sides of the plate, that is, by reflecting the gamma rays from both sides of the crystal planes.

A typical line pattern is shown in Fig. 2. The calibration

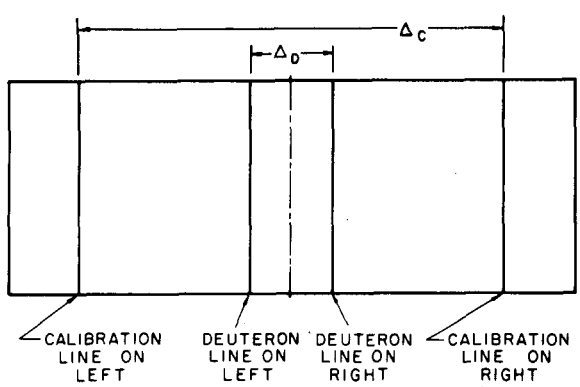

Fig. 2. Typical line pattern on the plate.

lines are obtained on both the left-hand and right-hand sides as well as the unknown, in this case the deuteron line. Then the separations of the lines are determined with an optical comparator. For this purpose we have recently used a comparator with electronic scanning of the type

invented by Tomkins and Fred. A rotating prism scans the line image across a photocell, first in one direction and then in the opposite direction. The setting is accomplished by matching the line profiles on an oscilloscope screen. A typical line can be located reproducibly to 1 μ, which is 0.1 sec of arc at 2 m. The data are entered on IBM cards and the calculations are made on the 7094 computer. The energy is calculated from Bragg's equation and the known energy of the calibration line. The standards include Ta and W x rays, the 100- and 150-keV gamma rays of W^{182}, the 412-keV line of Hg^{198}, and the annihilation radiation. The energy-wavelength conversion factor was taken from the 1955 adjustment of the fundamental constants by Cohen, Crowe, and DuMond. The most important standards were then W^{182}(100.107 keV), Hg^{198}(411.814 keV), and annihilation radiation (510.976 keV).

Most of the plates in this series were made with the (310) planes of quartz, with a line width of about 20 sec of arc. One plate was made with the $(10\bar{1})$ planes. These are the brightest planes in quartz but have a spacing about 3.5 times that of the (310) planes. This is partially compensated by the narrow line width. Ours is about 7 sec of arc. The $(10\bar{1})$ planes have bright higher order reflections also.

In all, about a dozen plates were obtained and measurements were made on 29 lines. The In gamma-ray energies (in keV) are 85.608(5), 90.94(4), 96.050(2), 110.75(2), 112.06(1), 112.45(1), 114.99(2), 122.00(5), 126.37(4), 140.44(2), 141.15(2), 155.27(2), 162.39(2), 171.07(2), 173.83(2), 175.09(6), 186.18(2), 196.60(3), 202.45(5), 272.97(3), 335.9(2), 376.3(3), 385.27)8), and 434.11(9). Six of these were previously seen at low resolution and assigned to

In^{116}. In addition, the following energies correspond to gamma rays previously assigned to Sn^{116}: 138.32(1), 417.2(1), 819.4(2), 1096.7(7), and 1293.4(6). The errors quoted include the error in the calibration lines (negligible for most of the lines), the errors from reading the plates, and an asymmetry error. If the plates were perfect, the line patterns would be symmetric about the center lines. Frequently they are not, and we assign an error assuming that one of the pair of unknown lines has been shifted. This asymmetry error is frequently the limiting error, especially if we do not have many plates containing the line in question.

By far the brightest was the 96-keV line and the error of 2 in 10^5 represents about the limiting accuracy we can get with the spectrometer. Very little work has been done on indium capture gammas. We have no decay scheme and, in fact, we have some difficulty even in assigning the gamma rays. Natural indium is 96% In^{115} with a capture cross section of about 200 b so that most of the gammas will be due to In^{116}. Six of the gammas we saw could be identified with energies previously reported by low-resolution experiments. In addition, five of the gamma rays correspond to gammas seen in Sn^{116} following β^- decay of In^{116}. Figure 3 shows the decay scheme taken from the Nuclear Data Sheets. The energies shown are from our work except for those in parentheses, which are from previous work. We have an internal check due to the cross-over transitions: 417.2 + 819.4 = 1236.6 and 138.32 + 1096.7 = 1235.0. The discrepancy is 1.6 keV. This probably indicates that the error quoted on the 1096-keV line is too small, this line being the most difficult to measure.

We hope in the future to obtain some relative intensities from densitometer measurements. However, other experiments will be necessary before any order can be made in the indium data.

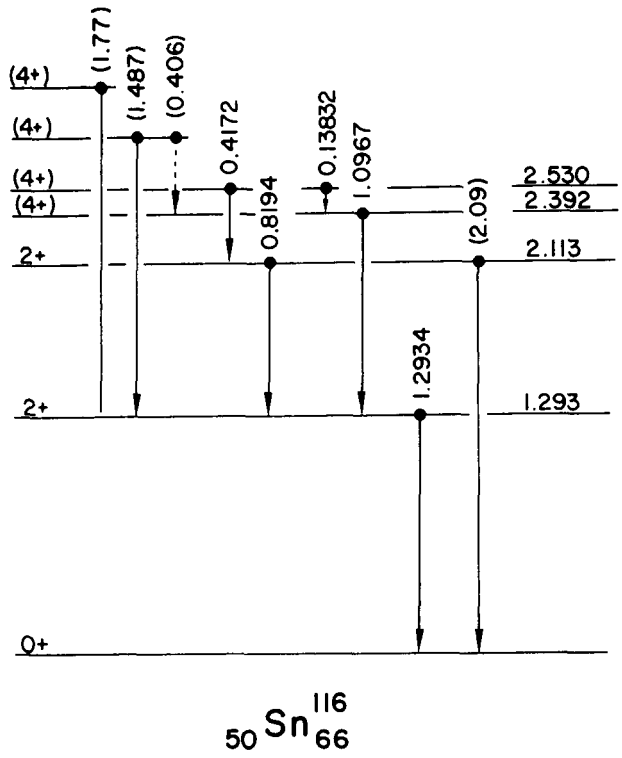

Fig. 3. Decay scheme of Sn^{116} (from Nuclear Data Sheets). The energies shown are from the present work, except for those in parentheses.

II-9. INVESTIGATION OF NEUTRON CAPTURE IN SAMARIUM USING A HIGH-RESOLUTION CONVERSION-ELECTRON SPECTROMETER*

E. Bieber

Laboratorium für Technische Physik der Technischen Hochschule München

In schemes of complicated neutron-capture decays, we have seen that even if you get a level scheme it will be quite without value for the theoretician if you do not assign spins to all of the levels. To get those, in many cases for the strong lines you will have available theoretical calculations—for instance, if you have rotational spectra. For some work you might draw conclusions from intensities, from lifetime measurements on some of those levels, and from correlation measurements when you can do those (i.e., whenever the lines are far enough apart so you can separate them by coincidences). You can use the (d,p) processes which give you levels and give you also spin assignments. And last, if you can do it, it is quite important to investigate conversion electrons; and there, of course, you would want, if possible, to have L_1, L_2, and L_3 ratios.

A few years ago we started working on conversion electrons, and we have used the principle which seems to be very useful generally. That is, whenever you want to do good work using neutrons, you should place the target where the neutrons are. That means you should come near the reactor.

---

*Presented by H. Maier-Leibnitz.

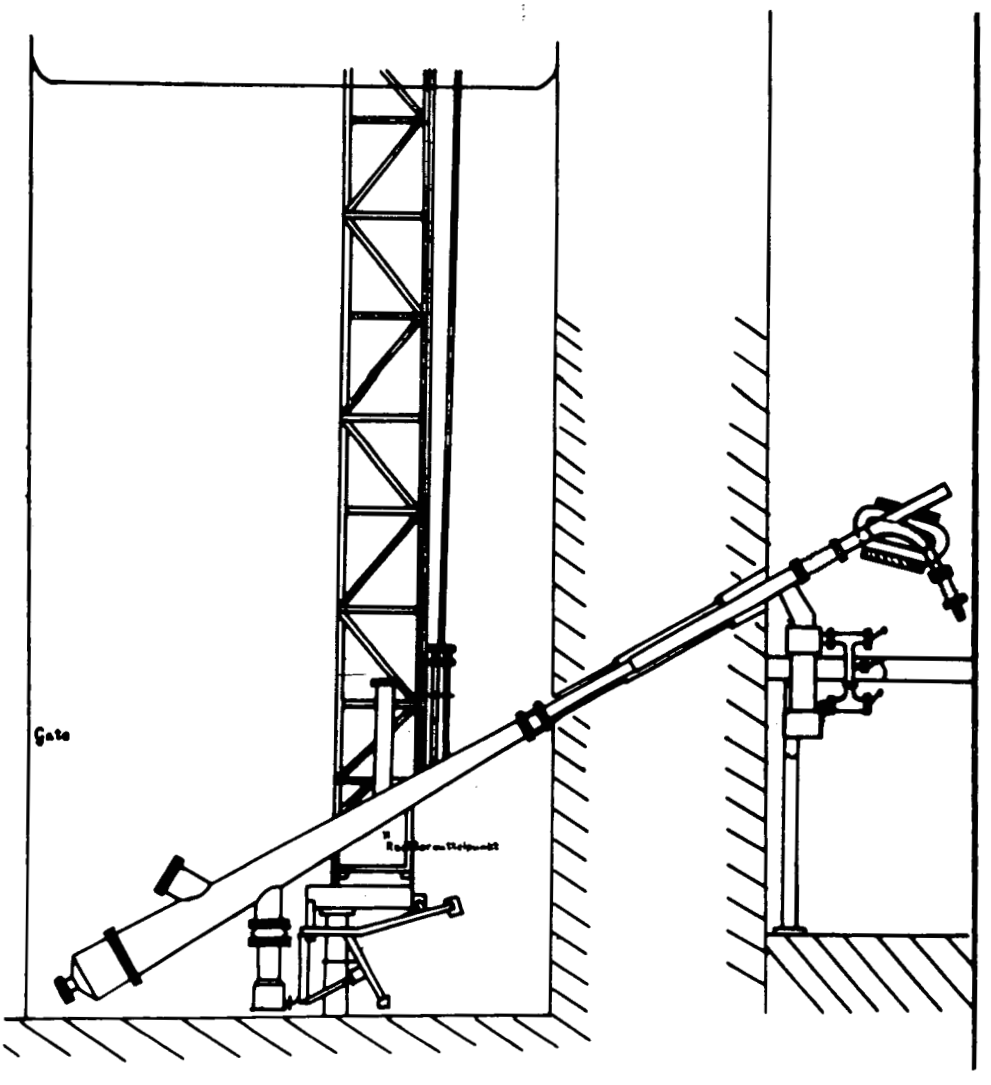

Fig. 1. Experimental arrangement. The reactor is in the tank to the left of the shielding wall.

Our arrangement is shown in Fig. 1. The reactor is in the tank to the left of the shielding wall. We have a very long and wide tube, 50 cm in diameter at the end. We do not get much background from here. We have good collimation in the reactor shield, and at the end we have a high-resolution double-focusing beta spectrometer. It is not very hard to do because we are actually using small angles, and the trick of it is the following.

If you were to lose intensity due to long distances you can

gain again by making your sample proportionately larger. So you get a resolution here of something like 10^{-3}, with targets which are as big as 1 × 5 cm.

To compare such an instrument with other instruments, I think it would be important to give something like a figure of merit, defined somewhat as follows. The best you can do is to put a thin sample of a certain area into the full flux of the reactor (near the lower left-hand end of the table), and then get out the conversion electrons produced there. So if you use any kind of arrangement, then from the number of conversion electrons you can conclude what that area would have been. The area could be proportional to the resolution you want. In our case, for comparison with other instruments, our area for a resolution of 10^{-3} is 10^{-5} cm^2.

Before discussing the background I will show you an example of what has been measured. Figure 2 shows the first spectrum of

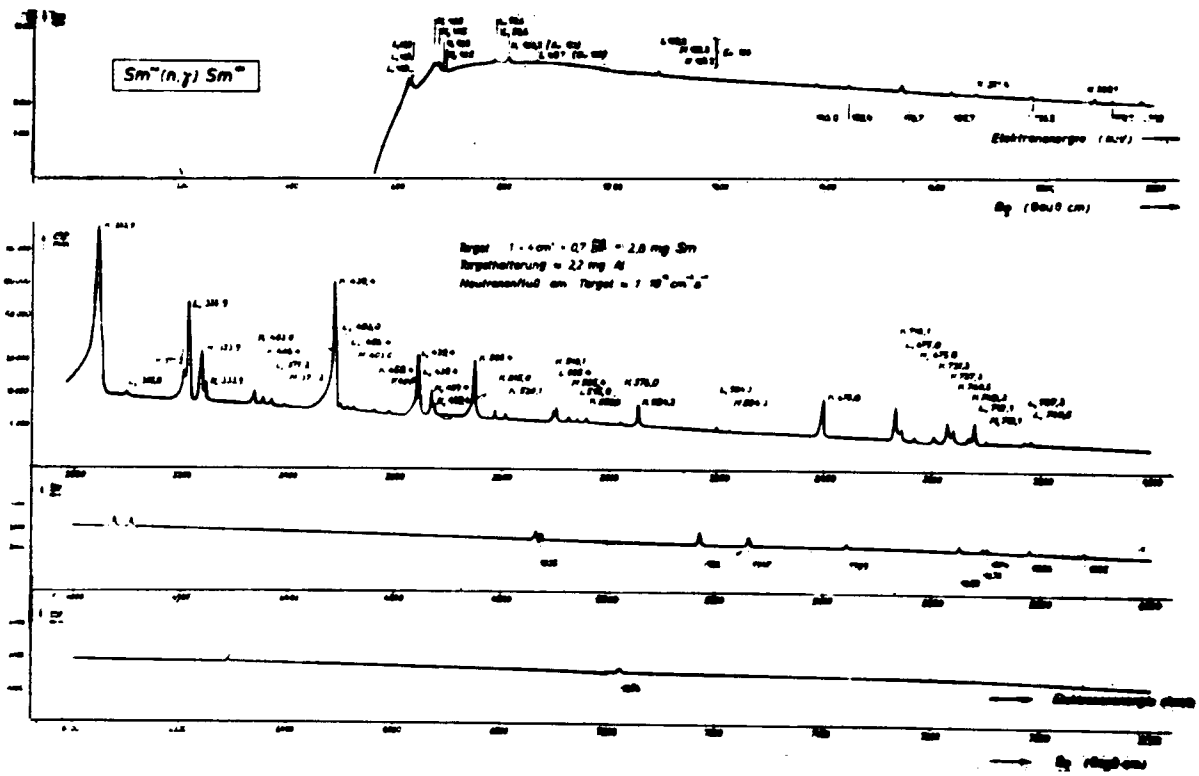

Fig. 2. Conversion-electron spectrum of samarium.

conversion electrons in samarium. The intensities of the strong lines at low energies are 10 to 30 times the background; and lines up to 1600 keV are about 10—20% above the background. These data have actually been used (I think) in the analysis which Dr. Smither gave on Sm^{150}.

As you can see quite well, if you use lower capture cross sections, then your background will ultimately limit your detection because the counting rates are always relatively high, still 4000/min. So the background is of the greatest importance for our measurements.

We have made an effort to reduce the background from the sample and sample holder. We have a 1-mg/cm^2 backing foil suspended on thin wires into the large tube so that the total weight that can be seen by the neutrons is about 4—5mg.

Figure 3 shows the background, again plotted logarithmically, as a function of the electron energy from 50 keV to 10 MeV. Most of the background comes from the production of secondary electrons in the sample, from gamma radiation from the wall, and from the reactor itself.

I would have liked to show you a more complete spectrum of samarium, but the main efforts recently have been toward improving our instrument both in background and in resolution; and I think today, after the old results have been used by others already, I will not discuss level schemes of samarium or things like that. Instead, I will show you recent progress obtained by stabilizing the magnetic field by 10^{-5}, and by improving the resolution. We now get much better

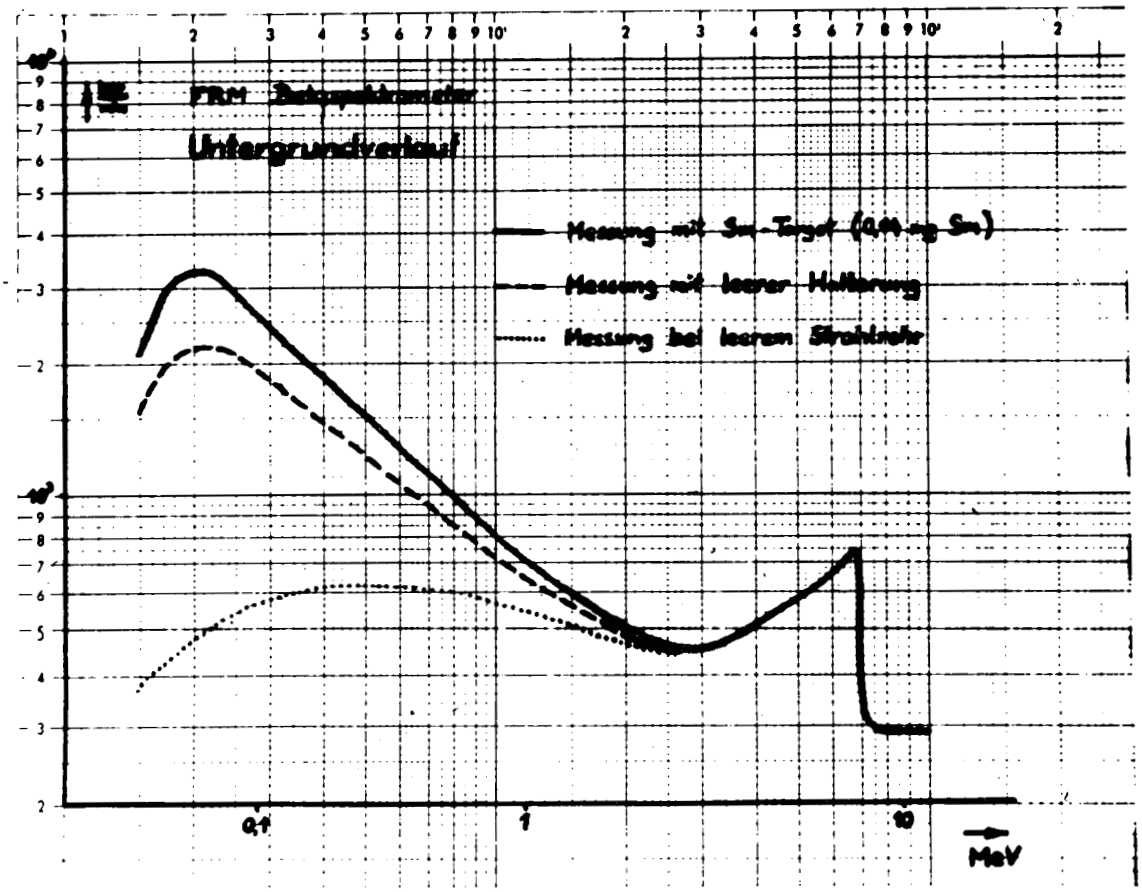

Fig. 3. Logarithmic plot of the background as a function of the electron energy from 50 keV to 10 MeV.

spectra. Figure 4 shows a portion of the samarium spectrum in more detail. You see the L line at 334 keV and the M and N lines.

In Fig. 5 you will see this portion again. You see that now the three L components at 334 keV are quite well shown. The same has been done down to less than 80 keV. We think that up to about 500 keV we can resolve the L structure quite nicely. I think that is all that I wanted to show you on that method. It is still in a rather early stage, and we do not have too many results. But I think it will supplement the other methods and it will be, in its accuracy and resolution, maybe the best method for some time to come in the region around 1000 keV.

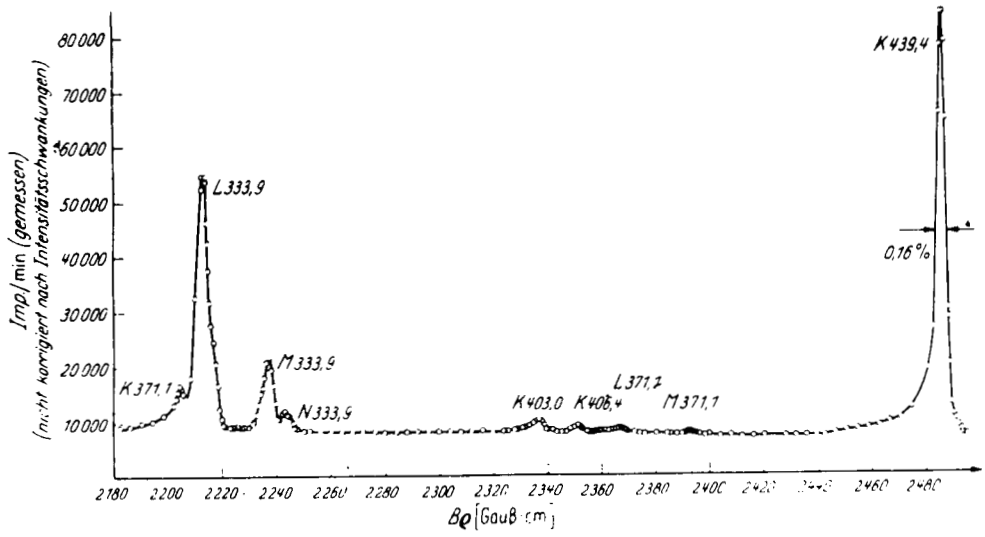

Fig. 4. Portion of the conversion-electron spectrum of Sm^{150}.

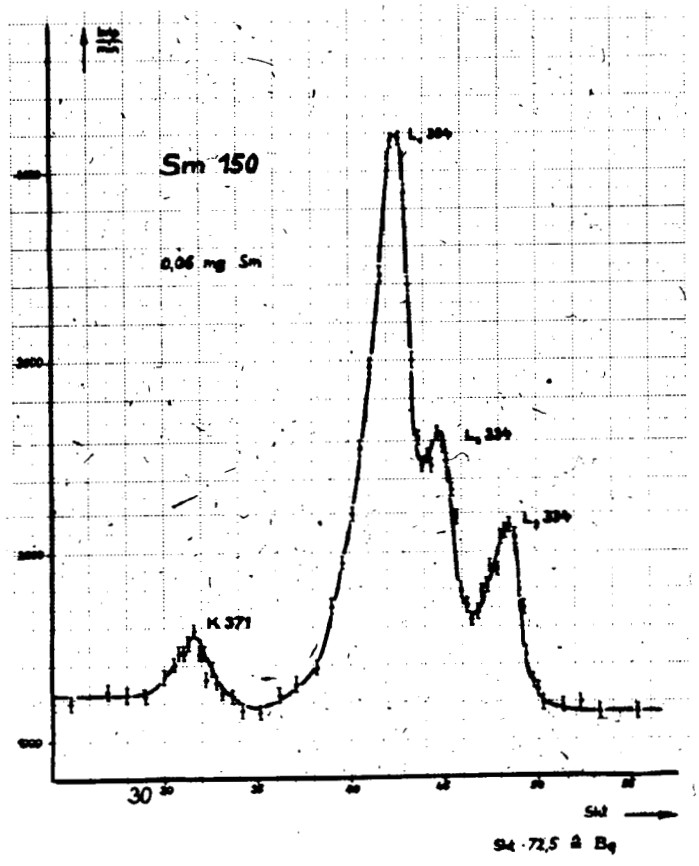

Fig. 5. The L_1, L_2, and L_3 lines in the conversion-electron spectrum of Sm^{150}.

* * *

L. B. BORST, State University of New York at Buffalo: Have you considered this as a method of measuring the beta decay of the neutron?

MAIER-LEIBNITZ: No. This tube was designed to measure the recoil-energy distribution of protons. That is why we have such a large volume—to get neutron decay around the reactor. We collect our recoil protons from a higher vacuum of course. We had a pump which could evacuate the part near the reactor down to 10^{-8} mm Hg; but after we had thought it out, theoreticians told us that unless these measurements were made as accurately as possible, it would not be worth while to do the experiment. So we switched over to the present experiment.

BORST: You are taking electrons out now. You will necessarily get electrons from neutron decay. How close are you to observing the beta-decay electrons?

MAIER-LEIBNITZ: I think that you could. I suppose it is a question of background. You would have to use a still better tube that would go farther down. Right now it is limited by the floor of the reactor tank. Protons would be much better, and much more interesting, too.

R. K. SMITHER, Argonne National Laboratory: One of the crucial problems you pointed out was that of sensitivity at 1 MeV. Could you give us a figure representing your minimum sensitivity at 1 MeV?

MAIER-LEIBNITZ: The sensitivity depends a little on energy. It would not be better than something like one barn for a line with 100% intensity—and even that may be optimistic. However, 1 MeV is a little easier than other energies.

II-10. RECENT DEVELOPMENTS IN PRECISION DIFFRACTION MEASUREMENTS RELATED TO NEUTRON-CAPTURE γ-RAY SPECTRA*

J. W. Knowles

Chalk River Nuclear Laboratory, Chalk River, Ontario

In recent years there has been considerable improvement in the energy resolution of neutron-capture γ-ray spectra. It is now practical to measure the complete spectrum with an energy resolution of $\leqslant 0.3\%$, using a crystal diffraction spectrometer to cover the range between 0.05 and 4 MeV and a Compton spectrometer for the range between 2 and 10 MeV. With this resolution much of the intensity of even very complex spectra, such as Gd^{156}, Gd^{158}, and Ta^{182}, can be resolved into individual γ rays. The precision for energy measurement averages between $1:10^3$ to $1:10^4$.

Attempts to construct decay schemes from these complex spectra have not been too successful (as shown by previous speakers). Hundreds of γ rays are resolved in one of these spectra but, perhaps, only 30% may be fitted into a level scheme—already established from other measurements such as (d,p) reactions, Coulomb excitation, β decay, or K capture. (Intermediate levels between the capture state and ground state are also obtained on the assumption that most of the high-energy γ rays decay from the capturing state.) If the precision of energy measurement is not better than $1:10^3$, it is nearly meaningless to construct additional decay

*Invited paper.

schemes from the remaining γ rays (70% of the resolved spectrum). For example, if one looks for correlations between the sums and differences of 100 γ-ray energies, one is dealing with 10^4 energy combinations. If the energy resolution is only 1: 10^3, there is a very high probability of chance correlation. In order that this situation be improved substantially, the precision of measurement should be increased by one or two orders of magnitude.

Activity at Chalk River has been directed towards increasing the precision of energy measurement of neutron-capture γ rays with a double-flat-crystal spectrometer. In particular, interest has centered on certain γ rays whose energy measurements give useful information relating the atomic constants. The precision attained in these measurements is between 1: 10^4 and 1: 10^5, depending on the conditions of measurement. In connection with these measurements, a number of new techniques were developed which may be found useful in the measurement of complex spectra.

It is not surprising that a double-flat-crystal spectrometer is found to be suitable for the comparison of γ-ray energies to high precision, since for more than thirty years such instruments have been used to compare x rays of energies[1-3] less than 100 keV with a standard error of a few parts in 10^5. A wavelength determination by the method of crystal diffraction is based on the Bragg

---

[1] A. H. Compton, Phys. Rev. 10, 95 (1917); A. H. Compton and S. K. Allison, X-rays in Theory and Experiment (D. van Nostrand Co., New York, 1943), 2nd ed., pp. 710-750.

[2] B. Davis and H. Purks, Proc. Natl. Acad. Sci. U.S. 13, 419 (1927).

[3] W. Ehrenberg and H. Mark, Z. Physik 42, 807, 823 (1927).

relation between wavelength λ, interplanar spacing d_H, and diffraction angle θ_B inside the crystal. The Bragg equation is

$$\lambda = 2d_H \sin\theta_B . \tag{1}$$

This equation also relates the wavelength outside the crystal to the external diffraction angle θ_B(the angle θ_B corresponds to the intensity in the peak of the diffracted line) to a precision of a few parts in 10^6, for diffraction by transmission through a crystal lamina with diffraction planes perpendicular to the incident surface. Since many measurements involve only a comparison of γ-ray energies or wavelengths, it is not necessary to know the crystal spacing d_H. The relative relationship is

$$\frac{E_2}{E_1} = \frac{\lambda_1}{\lambda_2} = \frac{\sin\theta_1}{\sin\theta_2} , \tag{2}$$

where E_1 and E_2 are the energies of two γ rays corresponding to wavelengths λ_1 and λ_2, respectively.

For γ rays with energy greater than a few hundred keV, the spectrometer resolution R can be expressed in terms of the diffraction line width W at half maximum intensity and the Bragg diffraction angle θ_B by the equation

$$R = \frac{\Delta E}{E} = \frac{\Delta\lambda}{\lambda} = \frac{W}{\theta_B} . \tag{3}$$

For a fixed width W, a smaller diffraction angle θ_B corresponds to a lower spectrometer resolution R. The resolution may vary from 0.5 to 0.01% depending on the γ-ray energy and the order of crystal diffraction.

The shape of the diffraction line is characteristic of crystal spectrometers. The line width W can be described as a function of a number of characteristic widths. The most prominent of these are a width W_f associated with the spectrometer geometry, the crystal mosaic width W_M associated with the angular distribution of imperfections in the crystals, and a width W_λ associated with the natural energy spread of the γ rays. If one had to define the line position in terms of line shape, it would be difficult to define the angular position of a diffracted line precisely.

However, the method of measurement with the crystal diffraction geometry (Fig. 1) circumvents this difficulty. A monochro-

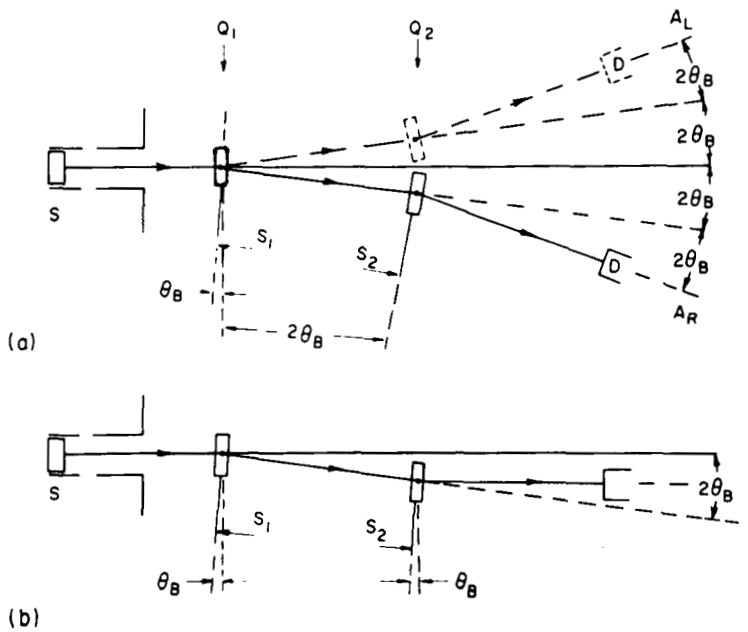

Fig. 1. The diffraction of radiation by the double-flat-crystal spectrometer with crystals arranged (a) in the antiparallel position and (b) in the parallel position.

matic γ ray diffracted to the right A_R and to the left A_L of the main beam has identical line shapes. The shapes are asymmetric with respect to the direct beam if they are determined by crystal imperfections (i.e., if $W \approx W_M$) but are symmetric with respect to the direct beam if the natural

energy spread of the radiation predominates (i.e., if $W \approx W_\lambda$). For a double-flat-crystal spectrometer, a width W_f associated with the spectrometer geometry can be made negligibly small by careful alignment of the diffracting crystals.[4] Line shapes which show the asymmetric character of the diffracted line resulting from crystal mosaic spread are shown in Fig. 2. These are the shapes[5] of the right and left lines of the

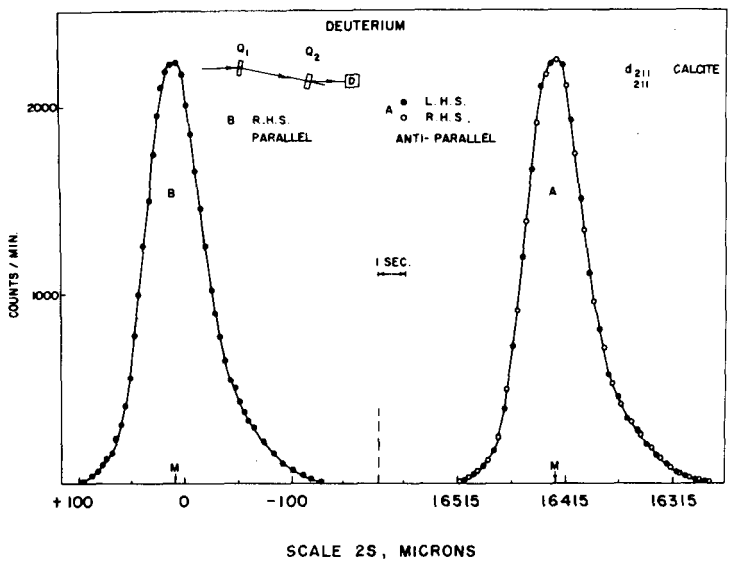

Fig. 2. The deuterium γ-ray line shape following diffraction from the (211), (211) planes of two calcite crystals. The line B, measured with the two crystals in the parallel position, has the same shape as the line A, measured with the two crystals in the antiparallel position. The right-hand curve (open circles) and left-hand curve (solid circles), plotted in microns on the standard scale, are superimposed relative to their common median M. The pronounced asymmetry in the wing of the lines is due to crystal imperfection. For these early measurements, the median is located to better than 2% of its width at half-maximum intensity.

---

[4] J. W. Knowles, Can. J. Phys. 37, 203 (1959).

[5] J. W. Knowles, Can. J. Phys. 40, 237 (1961).

2.224-keV gamma ray of deuterium diffracted from the (211, 211) planes of two calcite crystals. The angle $4\theta_B$ between these two lines is determined without interpretation of line shape from the separation of the line medians. In theory, the precision for this measurement depends only on the statistical count. The relative angular precision $\frac{\Delta W}{W}$ of a diffracted line is given by the approximate equation

$$\frac{\Delta W}{W} \approx \frac{\pm 0.33}{\sqrt{N}}, \tag{4}$$

so that for $N = 10^4$ counts the standard error is about 0.5% of the line width W. The corresponding uncertainty in the wavelength λ and energy E are given by

$$\frac{\Delta E}{E} = \frac{\Delta \lambda}{\lambda} = \frac{\Delta W}{\theta_B} \approx 0.33 \frac{R}{\sqrt{N}}. \tag{5}$$

The statistical precision is not usually attained in practice. The deviation from this ideal case may be expressed in terms of an uncertainty ΔW_s in angle. Equation (6), modified to include this uncertainty, becomes

$$\frac{\Delta E'}{E} \approx 0.33 \frac{R}{\sqrt{N}} + \frac{\Delta W_s}{\theta_B}. \tag{6}$$

Table I shows some of the most precise diffraction measurements made prior to 1959. The best angular precision $\Delta W_s = \pm 0.19$ sec was attained by Muller et al.[6] in their measurement of the 412-keV

[6] D. E. Muller, H. C. Hoyt, D. J. Klein, and J. W. M DuMond, Phys. Rev. 88, 775 (1952).

TABLE I. Precision γ-ray measurements with diffraction spectrometers.

Spectrometer description	Line width W (sec)	d_H (Å)	Resolution	Isotope	Best[f] measurement (keV)	Best fractional precision	Best angular precision, ΔW_s (sec)
DuMond (1947)	22	1.178	1.04	Cu^{64}	510.979 ± 0.067	± 1.3: 10^4 [b]	± 0.23
r_c = 200 cm[a]			0.84	Hg^{198}	411.801 ± 0.036	± 0.8: 10^4 [b]	± 0.19
quartz, d_{310}							
Beckman (1958)	15	1.178	0.57	Hg^{198}	411.770 ± 0.033	± 0.8: 10^4 [c]	± 0.19
r_c = 200 cm[a]	27		0.08	$La_{K\alpha 2}$	33.0340 ± 0.0004	± 1.2: 10^5 [d]	± 0.3
quartz, d_{310}	25		0.13	$Lu_{K\alpha 1}$	54.0698 ± 0.0009	± 1.7: 10^5 [d]	± 0.3
Knowles (1959)	2.7	3.028	0.5	Mg^{24}	1368 ± 1.	± 1: 10^3 [e]	± 0.46
double-flat-crystal calcite, d_{211}	1.6		0.6	Mg^{24}	2750 ± 3.	± 1: 10^3 [e]	± 0.30

[a] Here r_c = radius of curvature.

[b] These gamma-ray energies, 1 part in 10^4 greater than those originally quoted by Muller et al. (Ref. 6) in 1952, have been recalculated by use of the conversion relations of E. R. Cohen, J. W. M. DuMond, T. W. Layton, and J. S. Rollett, Revs. Modern Phys. 27, 363 (1955).

[c] P. Bergvall, Arkiv Fysik 16, 57 (1959).

[d] P. Bergvall, Arkiv Fysik 17, 125 (1960).

[e] The flat-crystal measurements, made prior to the development of the optical technique, have an angular precision comparable to that made with bent-crystal spectrometers (Ref. 4).

[f] A gamma-ray energy is calculated from its corresponding wavelength λ_s in x-units by use of the conversion relation $\lambda_s E$ = 12 372.44 ± 0.16 keV-xu [E. R. Cohen, J. W. M. DuMond, T. W. Layton, and J. S. Rollett, Revs. Modern Phys. 27, 363 (1955)]. A wavelength is measured relative to the average $(WK\alpha_1)_x$ x ray (208 573 ± 0.004 xu), which in turn refers to the standard $(MoK\alpha_1)_x$ x ray.

gamma ray of Au^{198}. The uncertainty ΔW_s in their measurement may be attributed to three sources: (a) insufficient sensitivity for angle measurement, (b) insufficient mechanical stability for angle measurement, and (c) a lack of knowledge of the relation between the scale used in the measurement and the diffraction angle θ_B.

The limit for precise measurement of a diffraction angle is considerably reduced for the parallel-beam flat-crystal spectrometer. For this instrument, the angular sensitivity is improved by using an optical device sensitive to angular changes of 0.02 sec of arc. (Recently this limit has been extended still further, to 0.001 sec of arc.) The 0.02-sec equipment used at Chalk River has been described, and is shown in Fig. 3.

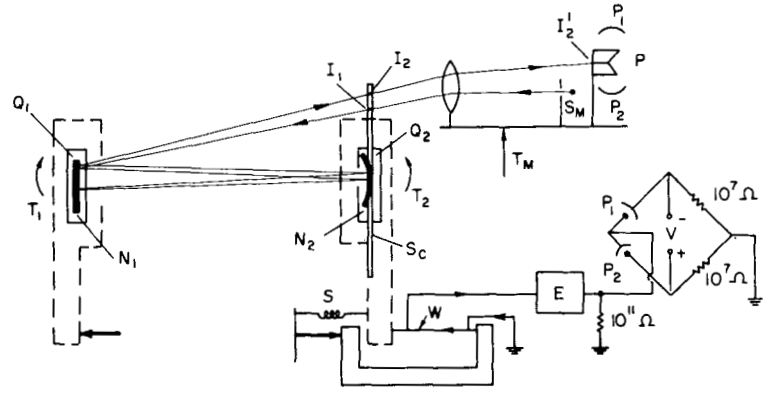

Fig. 3. A schematic drawing of the mechanical optical system used for measuring the relative angle between crystals Q_1 and Q_2. Mirror N_1 is an optical flat rigidly attached to crystal turntable T_1. Spherical mirror N_2 and standard scale S_c are similarly attached to turntable T_2. The focal length of mirror N_2 is twice the distance between the axes of rotation of T_1 and T_2. A traveling microscope T_M moves parallel to standard scale S_c and contains a line light source S_M. The light from this source focuses at I_1 and I_2 in the plane of the standard scale before and after reflection from the N_1, N_2 mirror system. The return image I_2 is again imaged at I_2' in the plane of the split prism P. The light balance is measured by photocells P_1 and P_2. The error signal controls a $\frac{1}{4}$-amp electric current flowing in a nichrome wire W. A change in current causes a change in wire temperature followed by a corresponding change in wire length so that the spectrometer arm T_2 rotates to balance the light image I_2' on the split prism.

To be of practical use, the improvement in angular sensitivity must be accompanied by a corresponding improvement in the mechanical stability of the spectrometer. A high degree of stability has been achieved with the flat-crystal spectrometer by the addition of feedback (Fig. 3). The angular position of the spectrometer arm T_2 is determined by the length of a 0.001-in.-diameter nichrome wire W, kept under constant tension by a spring. The length of the wire is determined by its temperature, which is held at about 200°C by passing through it an electric current of about 1 A. The strength of the current is proportional to a voltage produced in the photocell circuit by an unbalance of the light focused on the split prism P. The overall gain of the feedback system is 10^4. The system isolates the relative angular setting of the crystal turntables T_1 and T_2 from the external environment. The resultant angular stability is better than 10^{-3} sec of arc, a factor of 50 improvement over the same system without feedback.

The result of these two improvements has been to reduce the mechanical limitation on angular measurement so that the precision is limited in many cases only by statistical counts. This fact is illustrated in Fig. 4, which shows the matching of the right-hand and left-hand 171-keV gamma rays of Ta^{182}.

The accepted method for determining the angular distance between the right-hand and left-hand diffracted lines is to find, as mentioned previously, the line medians M and accept their separation as a measure of the separation of the two lines. This method allows easy calculation of the statistical precision, but it is

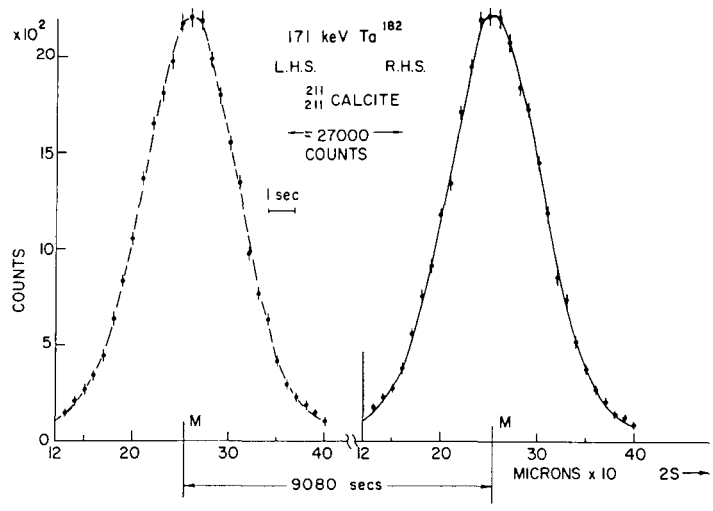

Fig. 4. The 171-keV gamma ray of Ta^{182}. This measurement is made by double-crystal diffraction from the (211, 211) planes of calcite crystals. The slight asymmetry results from a difference in mosaic structure between the diffracting crystals. The total count in each line is limited to 27 000 counts. M is the median position of each line.

insensitive to line shape and so gives no check on the accuracy of the measurement. Recently, an alternative method has been used. It consists in a least-squares fitting of the points of the right-hand 171-keV line shape to a Legendre polynomial with as many as 12 coefficients. The polynomial with coefficients so determined is matched to the left-hand curve for different values of the abcissa $\Delta\theta$. The sum of the squares of the deviations δ^2 of the left-hand line experimental points from the polynomial are plotted as a function of $\Delta\theta$ in Fig. 5. The minimum value, $\delta^2 = \delta_c^2$, determines the matching position. Simple considerations show that $\delta^2 = \delta_c^2 + \delta_s^2$, where under ideal conditions $\delta_c = \delta_s$, where δ_s is the statistical standard deviation for the two lines, and $\delta_s^2 = (\bar{m})^2 \Delta\theta^2$, where $(\bar{m})^2$ is the mean sum of the squares of the slopes of the diffracted lines. This mean sum is constant for small values of $\Delta\theta$ so that δ^2 has the parabolic shape shown at the lower left in Fig. 5. The square root of $(\delta^2 - \delta_c^2)$ plotted as a function of $\Delta\theta$

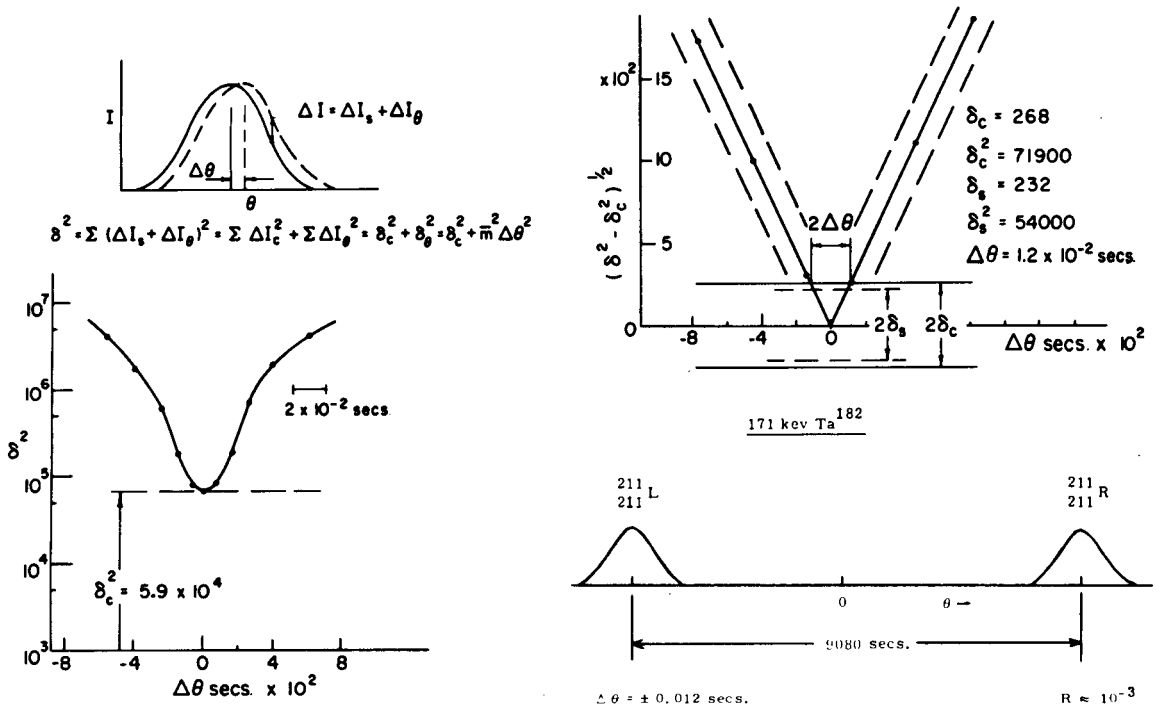

Fig. 5. The least-squares method of superposing the right-hand and left-hand gamma-ray shapes. The mean-square deviation δ^2 of the left-hand curve for varying overlap $\Delta\theta$ has a parabolic shape near $\Delta\theta = 0$ with minimum value $\delta_c{}^2$. This curve is replotted (upper right) as a graph of $(\delta^2 - \delta_c{}^2)^{1/2}$ against $\Delta\theta$. The standard deviation δ_s is calculated from the total number of counts under both lines. Corresponding to the diagram at the lower right, $\Delta E/E \approx \Delta\theta/\theta \approx \pm 1.4 \times 10^{-6}$ and $\Delta E = 0.24$ eV.

gives two intersecting straight lines, the upper right-hand graph in Fig. 5. The limit of error of these lines, indicated by the parallel dotted lines, is assumed to be equal to the root-mean-square deviation δ_c. The horizontal dotted lines show the theoretical standard deviation $\pm\,\delta_s$ based on the total counts. The standard error for $\Delta\theta$, based on δ_c, is thus $\pm\,1.2 \times 10^{-2}$ sec, 1/350 of a line width. The condition $\delta_c \approx \delta_s$ is confirmation of the degree of matching and stability of the measurement. The angular sensitivity $\pm\,\Delta\theta$ corresponds to a precision of measurement of $\pm\,1.4 \times 10^{6}$ for the 171-keV gamma ray diffracted from the (211,211) plane of calcite (lower right). The same method is

TABLE II. Fractional energy sensitivities of the double-flat-crystal spectrometer for various energies and orders of diffraction.

Order	Plane Calcite	Precision, $\Delta E/E$		
		0.20 MeV	2.0 MeV	4.0 MeV
1	211,211	1.4×10^{-6}	1.4×10^{-5}	2.8×10^{-5}
2	422,422	0.7	0.7	1.4
3	633,633	0.5	0.5	0.9

applicable to γ-ray measurements of higher energy. Table II lists the fractional energy sensitivities of the double-flat-crystal spectrometer at other energies and for different orders of diffraction.

Unfortunately, the superposition of lines does not in itself constitute a measurement of γ-ray energy. One must also determine the distance between two accurate reference points in the vicinity of the lines, and in addition transfer from the measurement scale to the angle scale with precision equal to that of the line comparison. Such transfers are always necessary since Bragg diffraction angles are not compared directly. What are compared are distances on the arcs of divided circles or linear distances tangential to the angular rotation of the diffracting crystals. With the double-flat-crystal spectrometer, angular position is expressed in terms of a linear separation 2S, the distance (measured on standard scale S_c) between the two foci I_1 and I_2 in Fig. 3 when diffracting from equivalent reference positions of the two lines. For diffraction at small angles from equivalent planes of two crystals, the standard scale separation 2S and Bragg diffraction angle θ_B are related by

$$2S = 16R_T\theta_B(1 + 13.39\ \theta_B^{\ 2}), \qquad (7)$$

where $R_T = 1117.747 \pm 0.009$ mm at $28.0 \pm 0.2^{\circ}C$ is the effective distance between the axes of rotation of the two crystal turntables.* This equation is believed accurate to a few parts in 10^5. The comparison of two widely separated angles from the corresponding measurements of length has not been satisfactorily solved where precision greater than 2—3 in 10^5 is required.

Systematic error may result from irregularities arising from imperfections in the optical system. However, these are expected to be negligible at small angles. For example, an error of 3 in 10^5 at a diffraction angle of 800 sec is only 1 in 10^6 at 200 sec. The effect would be negligible also in the wavelength comparison of two γ rays diffracted at large angles but with ray paths differing by only a few hundred seconds. This condition can be realized to minimize systematic error in the spectrometer geometry. It was first used in the determination of the relative angles of the deuterium and annihilation γ rays by diffracting the deuterium γ ray from different crystal planes. The method is illustrated in Fig. 6. Double diffraction from the (211,211) planes (Fig. 7) occurs at small angles while diffraction from the (844,844) planes occurs at angles 4 times as large. This latter ray path is within 10% of that of the annihilation radiation diffracted from the (211,211) planes. The counting rate decreases with increasing order of diffraction and is particularly low

---

*The determination of R_T is considered in detail in the original paper (Ref. 5).

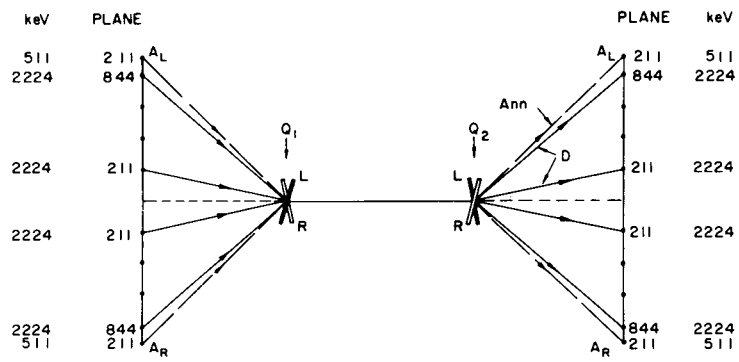

Fig. 6. A schematic drawing of the radiation paths for deuterium and annihilation γ rays following diffraction from different crystal planes of calcite used in the double-flat-crystal spectrometer. A_L, A_L and A_R, A_R represent double diffraction from crystals Q_1 and Q_2 to the left and to the right of the main beam, respectively, and L and R are the corresponding angular settings of the crystals.

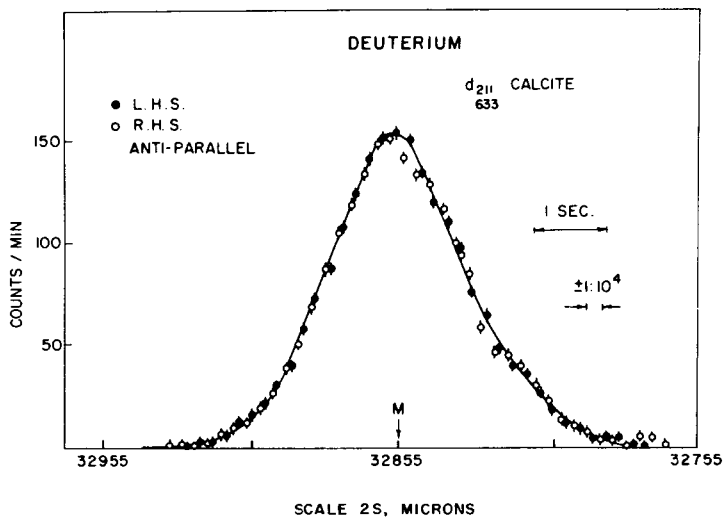

Fig. 7. The deuterium γ ray diffracted from the (211), (633) crystal planes of two calcite crystals set in the antiparallel orientations. The left-hand curve (closed circles) and right-hand curve (open circles) are plotted in microns on the standard scale relative to their common median M. The median is located to better than 3% of the width of the line.

for diffraction from the (844,844) set of planes(Fig. 8). In this latter case, it is the statistical count which determines the precision. Measurements of the energy of the deuterium γ ray following diffraction from different orders are plotted in Fig. 9 as a function of the standard

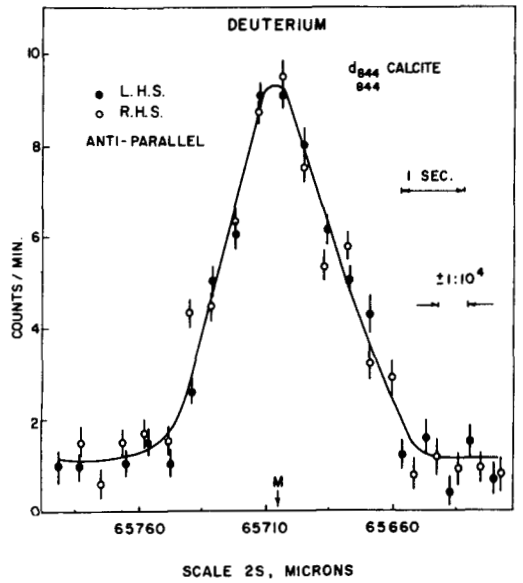

Fig. 8. The deuterium γ ray diffracted from the (844,844) crystal planes of calcite, the crystals being set in the antiparallel orientations. The left-hand curve (closed circles) and right-hand curve (open circles) are plotted in standard-scale microns relative to their common median M. The statistical count is not sufficient to define very precisely the shape of the lines, but it is sufficient to determine the median M (and therefore the superposition of the two diffracted lines) to better than 5% of their width at half-maximum intensity.

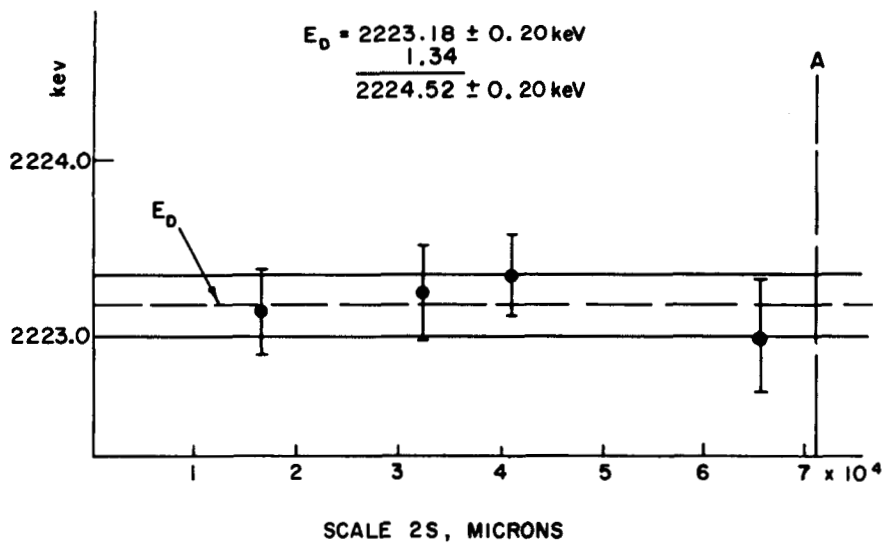

Fig. 9. The deuterium de-excitation γ-ray energy plotted as a function of the standard-scale separation 2S in microns. The angular position of the annihilation γ ray is given by the vertical broken line A. The vertical bars on the points are the probable errors of the measurement at each angle. The horizontal broken line is the arithmetic mean energy. The horizontal solid lines indicate the probable limits of error for this average measurement. However, the limit of error on the numerical value of the deuterium binding energy is the standard error.

scale distance 2S to show the consistency with changing angle. To estimate the deuteron binding energy, the energy of recoil (1.34 keV) of the deuterium nucleus after emission of the gamma ray is subtracted from the average energy of the deuterium gamma ray. The average precision of the deuterium energy measurement is 1: 10^4.

A further example of the use of multiple-order diffraction is the comparison of the wavelength $(\lambda_c)_x$ of the annihilation γ ray in terms of the standard $(WK\alpha_1)_x$. From such a measurement one may determine the ratio of the fine-structure constant α to the constant Λ for conversion from x units to milli-angstroms through the relation

$$(\lambda_c)_x \; \Lambda = \alpha^2/2R_\infty, \tag{8}$$

where R_∞ is the Rydberg constant.

The wavelength $(\lambda_c)_x$ has been measured in a number of ways.[7] ‡ The method which gives the highest precision with least possibility for systematic error is that which makes use of high-order crystal planes (Fig. 10). For this measurement, the 511-keV annihilation γ ray was compared with the neutron-capture γ ray of Ta^{182} at 171 keV; and in a separate experiment the 171-keV γ ray was compared with the internal conversion $(WK\alpha_1)$ x ray of W^{182}. The W^{182} is produced following β decay of Ta^{182}. These three radiations have energies in the ratio 9: 3: 1 to within a few percent. The 171-keV γ ray diffracted from the (211,211) planes of two calcite crystals is at nearly the same angle as that of the 511-keV

---

[7] J. W. Knowles, Can. J. Phys. 40, 257 (1961).

‡ The first measurement of $(\lambda_A)_x$ (Table III, row 1) required an absolute determination of the diffraction angle θ_B by use of Eq. (7).

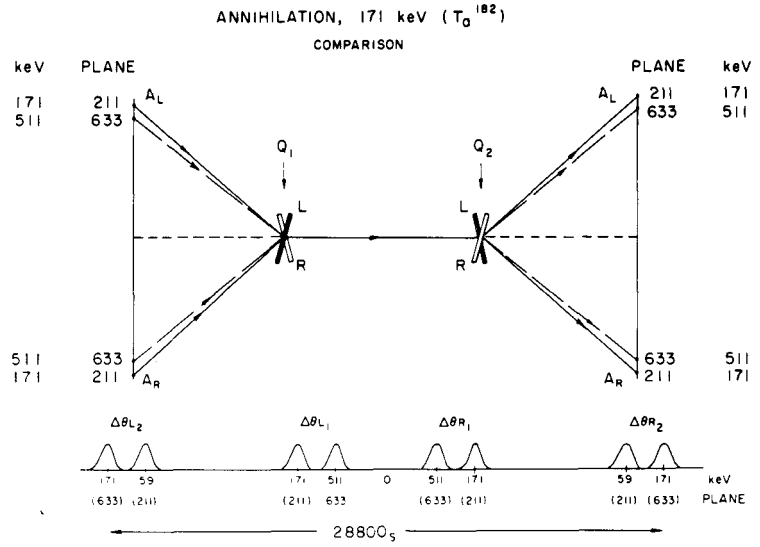

Fig. 10. A schematic drawing of radiation paths, to the right (A_R, A_R) and left (A_L, A_L) following diffraction from different crystal planes of the double-flat-crystal spectrometer. For these measurements the diffracting crystals Q_1 and Q_2 assume positions R, R, and L, L, respectively. The 511-keV gamma ray is diffracted from the (633,633) set of planes of calcite and the 171-keV gamma rays from the (211,211) planes. The diffracted γ rays, within a few percent, follow the same path. The angular differences $\Delta\,\theta_{L1}$ and $\Delta\,\theta_{R1}$ are measured in the comparison of the wavelengths of the 171- and 511-keV gamma rays. Equivalent measurements $\Delta\,\theta_{L2}$ and $\Delta\,\theta_{R2}$ are made in the comparison of the 171-keV gamma ray and the $WK\alpha_1$ x ray.

γ ray diffracted from the (633,633) planes; and similarly the 171-keV γ ray diffracted from the (633,633) planes nearly coincides with the $(WK\alpha_1)_x$ radiation diffracted from the (211,211) planes. Because of the natural broadening of the annihilation line (Fig. 11), it was necessary to measure all pairs of lines on both sides of the direct beam in order to eliminate effects of line shape. From these measurements is obtained the ratio $(9\lambda_c)_x/(\lambda WK\alpha)_x$ with standard error $\pm\ 1.5 \times 10^5$. The measurement is given in Table III, rows 2 and 3. This measurement is combined with the measurement of the energy ratio of the $(WK\alpha_1)_x$ and $(MoK\alpha_1)_x$ x rays obtained previously by Beckman et al.[8] with a standard error

[8] O. Beckman, P. Bergvall, and B. Axelsson, Arkiv Fysik 14, 419 (1958).

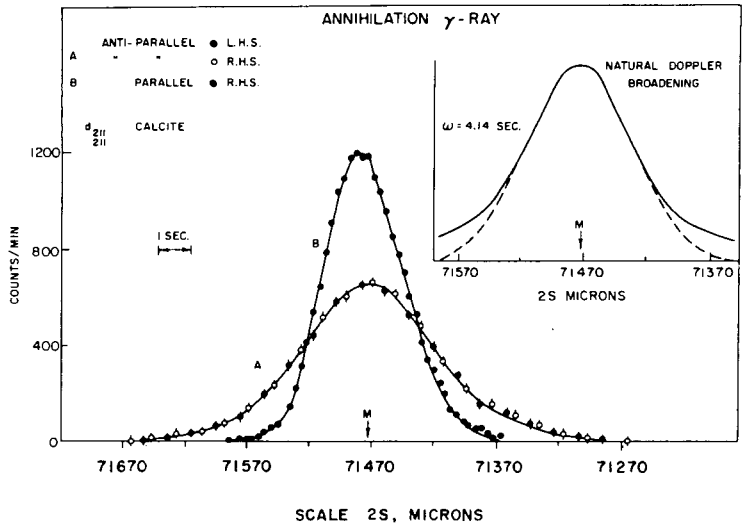

Fig. 11. The measured line shapes of the annihilation γ ray at 511 keV. Diffraction takes place from the (211,211) set of planes. The curve B is obtained by setting the two calcite crystals in the parallel position. In this position the spectrometer has zero energy dispersion, so that the line width is a measure of the perfection of the diffracting crystals. The curve A is the superposition of two diffraction lines measured to the right (open circles) and left (solid circles) of the direct beam. The points are plotted in microns with reference to their common median M. Curves A and B have the same area. The Doppler broadening of the annihilation γ ray, apparent in curve A, is "unfolded" by making use of curve B. The natural annihilation γ-ray shape obtained thereby is plotted in the inset. Its shape deviates from a Gaussian (the dotted line) in the wings; and its width at half maximum intensity is 4.14 sec of arc.

2: 10^5 and by Watson et al.[9] with a standard error 4: 10^5 to obtain a value for α^2/Λ. This value with a standard error 3.5: 10^5 agrees (within its error) with the value of α^2/Λ determined from the (1962) atomic constants.[10]

---

[9] B. B. Watson, W. J. West, D. A. Lind, and J. W. M. DuMond, Phys. Rev. 75, 505 (1949).

[10] E. R. Cohen, "Most Probable Values of the Physical Constants". Invited paper presented at the Symposium on Standards and Physical Constants, American Physical Society meeting, Washington, D. C., 1962. The paper is a summary of an analysis of the available data by DuMond, McNish, and Cohen.

TABLE III. Comparison of annihilation measurement with atomic constants.

Measurement[a]	Additional information	Annihilation wavelength $(\lambda_A)_x$ (xu)	α^2/Λ[b]
		$\times 10^{-3}$	$\times 10^{-10}$
(1) Absolute diffraction angle; precision 3: 10^5	(a) spacing of calcite in x units	24 212.99 ± 0.75	531 413.6 ± 15
θ_A = 7992.41 ± 0.30 microradians at 18.0°C	(b) Bearden comparison of calcite spacing with $(MoK\alpha_1)_x$ x ray.	24 212.46 ± 0.75	531 402.0 ± 15
(2) Measure of relative angles of annihilation γ ray and $WK\alpha_1$ x ray; precision 1.5: 10^5	(a) Beckman et al. (Ref. 8) comparison of $(WK\alpha_1)_x$ precision 2: 10^5	24 213.20 ± 0.62	531 418.2 ± 12
$9(\lambda_A)_x/(\lambda WK\alpha_1)_x$	(b) Watson et al. (Ref. 9) comparison of $(WK\alpha_1)_x$ with $(MoK\alpha_1)_x$; precision 4: 10^5	24 213.56 ± 0.96	531 426.1 ± 19
The annihilation wavelength in x units and α^2/Λ, calculated by use of the adjusted values of Λ and α^2.		24 212.14 ± 0.26	531 395.0 ± 5.8

[a] All limits of error are standard errors.

[b] Computed from $\alpha^2/\Lambda = 2R_\infty(\lambda_A)_x$, where the conversion constant from x units to milli-angstroms is $\Lambda = 1.002\,063 \pm 0.000\,006$, the Rydberg constant for infinite mass is $R_\infty = 109\,737.31 \times 10^{-8}$ cm^{-1} (precision 0.1: 10^6), and the fine-structure constant is $\alpha = (7.297\,20 \pm 0.000\,03) \times 10^{-3}$.

* * *

R. K. SMITHER, Argonne National Laboratory: One always likes to look ahead. Do you think the accuracy of measurements of this type can be pushed much farther?

KNOWLES: The final measurements that we have made are at least an order of magnitude better in precision than those shown in Table II. I feel that it is reasonable to hope that the precision of the scale-angle relationship can be improved by another factor of 10.

R. E. SEGEL, Argonne National Laboratory: Is there any obvious reason why such instruments are particularly suited for reactors; or could they be used on accelerators as well?

KNOWLES: The most obvious limitation at the moment is that the over-all efficiency of the spectrometer is 10^{-9} to 10^{-11}. This can be estimated very easily. The angle subtended by the first crystal, determined by the mosaic width and the vertical angle from the source in the reactor, is the most significant factor, about 10^{-8}. Another factor of 10 (or maybe 10^2) will be lost in diffraction from both crystals. This depends on the energy. At the lower energies the loss is only a factor of four, half on each crystal. Since at the higher energies the loss can be a factor of a few hundred, the over-all efficiency is often 10^{-10}.

SEGEL: I have never worked it out, but are the gamma rays from (n,γ) reactions in a reactor more intense than those from a target in the internal beam of a cyclotron?

KNOWLES: I think that the best efficiency you can obtain with a flat-crystal spectrometer is somewhere in the order of 10^{-7} to 10^{-8}. It is much better to go to a curved-crystal spectrometer

because its acceptance angle is better by two orders of magnitude.

H. MAIER-LEIBNITZ, Technischen Hochschule, Munich: May I ask who is making an effort, like we are doing at the present time, to build a better crystal spectrometer with as high an efficiency as possible—which might be 10^{-6} or even 10^{-5} in favorable cases. Do you coincide with us in work on that? Is anyone doing that besides us, please?

KNOWLES: As far as I know, nobody is doing this. A few years ago I suggested that this could be done: but we have not done it ourselves.

I might say that you might get efficiencies of the order of 10^{-5} with curved-crystal devices. This might be possible up to 1—2 MeV, but I think the resolutions of these devices would not be so high. They would be about 1%—maybe 0.5%.

SMITHER: Would you say a word on how you actually measured your angle—how you actually rotated your crystal and measured its angular position? You showed a compensating device.

KNOWLES: For the relative angle measurements we trusted our optical device implicitly. We located positions on the standard scale corresponding to the position of our light beam. We could observe these with our traveling microscope.

SMITHER: It was just a question of reading the scale?

KNOWLES: That's right; we just compared the ratio of the two distances between the right-hand and left-hand diffracted lines for two different gamma rays.

SMITHER: Do you use a linear distance scale?

KNOWLES: Actually it isn't quite linear because the sine and tangent of the angle are beginning to come in (even at small angles) when one is measuring to this precision. This variation from linearity is a small correction. The actual formula that we use is

$$2S = 16\, R_T \theta_B (1 + 13.39\, \theta_B^{\,2}),$$

where 2S is the distance between the two diffracted lines and R_T is an effective radius between the optical flat and the concave mirror. The diffracting crystals are fixed beneath these mirrors. The $\theta_B^{\,2}$ term is just a correction for the sine and the tangent of the angle. For small angles, 2S is just proportional to the angle. This formula is based on simple geometric considerations.

MAIER-LEIBNITZ: I have the idea that one of the very best things you could do is to use the best theodolite you can buy and measure the angle. People who use theodolites have done all they could for centuries to remove the inaccuracies. Wouldn't that be the simplest and best you can do?

KNOWLES: No, I think there is enough evidence now to show that many people in different laboratories are now managing to measure angles down to maybe a thousandth of a second of arc. The first such precision work was done by Jones at Aberdeen; and since 1926 he has been making angle measurements and improving on them. He has been able to make angle measurements that are at least ten times as good as ours. I should also mention people like Dicke, who are doing gravitation measurements. They have to measure small changes in angles with higher precision than ours.

O. W. B. SCHULT, Technischen Hochschule, Munich: A thousandth of a second is a fine number, but I think this number can only have meaning when one is interested in very small angles. Actually, when you have to measure an angle of 3—4° to a thousandth of a second, I think you run into terrible trouble. How long a time does it take to record your lines?

KNOWLES: It does not take as long as you would think. If you measure a million counts in a line (and you can do this on a strong line very quickly) and if you have a resolution of one part in a thousand, then you will have statistics sufficient to measure to one part in a million.

SCHULT: High precision is of essential advantage when you use the Ritz combination principle. Then it is, however, necessary to have high precision at all lines of interest. Therefore it is meaningless to measure a single line to such an accuracy when the others are bad.

KNOWLES: This is my point too. I deal with cases of a few lines which are measured to great precision. I think the point I would like to make is this: When it is necessary, you can make the precise measurements.

II-11. CAPTURE GAMMA RAYS AND NEUTRON BINDING ENERGIES

R. E. Carter and H. T. Motz

Los Alamos Scientific Laboratory, Los Alamos, N. M.

The Compton spectrometer at the Los Alamos Omega West Reactor[1,2] is designed to measure neutron-capture gamma rays above 0.5 MeV and is thus an excellent instrument to work in conjunction with data from low-energy diffraction instruments. For light nuclei the Compton spectrometer can measure essentially all of the spectrum since energy levels tend to be rather widely spaced; but for heavier nuclei it is necessary to complement the data with low-energy spectra from other sources. In order to determine spectroscopic details of energy levels it is essential to know the accuracy to which one can measure gamma-ray energies and their differences. This is required because it is not possible at this time to do high-resolution coincidence work and the best means of arriving at a decay scheme is primarily by energy correlations where one has $E_1 + E_2 = E_3$. Obviously, the certainty of such an energy-correlation approach for complex spectra improves greatly with decreased errors and must in any case involve the use of realistic error estimates. It has been pointed out that the most definite result of such an energy loop

---

[1] H. Motz, R. E. Carter, and W. D. Barfield, Pile Neutron Research in Physics (IAEA, Vienna, 1962), page 225.

[2] H. Motz and R. E. Carter, Proc. of the International Conference on Nuclidic Masses, edited by H. E. Duckworth (University of Toronto Press, Toronto, 1960), page 299.

comparison is that the sum is not equal. Even this fact is determined to a much higher certainty with increased accuracy. As an essential part of this program of spectroscopic information, one must then determine the linearity and reliability of the instrument, and binding-energy determinations result from such a study.

The spectrometer is essentially an iron-core double-focusing instrument of the Siegbahn-Svartholm type and has an inhomogeneous field. Such instruments are difficult to calibrate by means of complete field mapping and a one-point (or small area) field measurement is normally taken with a rotating coil as a measure of the entire magnetic field through which the electrons are deflected. If the field shape changes with current, then such a measurement is not adequate and a calibration nonlinearity will result. In the case of the Compton instrument, the angle of the back-scattered gamma ray is also involved in measuring the gamma-ray energy and an additional nonlinearity might enter from this added parameter.

All data are fitted with a least-squares program which imposes an additional complication in that this function does not exactly correspond to the true line shape. Deviations between the assumed and observed line shapes might then be a function of energy and give an additional source of nonlinearity. The analytic function that has been used for this work is a skewed Gaussian to which can be added a low-energy exponential tail. The width and skewness parameters have been determined for well-isolated single gamma rays throughout the energy scale and a plot of these parameters versus energy is assumed to be fitted by a smooth curve. The position of

the peak of the skewed Gaussian is taken as a measure of the energy and corresponds to the most probable focusing condition for maximum coincidence counting rate.

Because of great complexity and intercorrelations of these factors, we have taken an experimental approach to the determination of the over-all nonlinearity. This is possible because in several light-element reactions the spectrum affords stop-over and cross-over transitions which may be assumed to correspond to the same total energy —namely, the binding energy.

Table I shows the stop-over and cross-over comparisons

TABLE I. Transition energies (keV). The recoil energy is included in all cases. Errors are least-squares statistical errors only.

Nuclide	Stop-over	Sum	Cross-over	Diff.
Be^{10}	3367.3 ± 0.2 3443.6 ± 0.5	6810.9 ± 0.5	6809.6 ± 0.1	+ 1.3
	3367.3 ± 0.3 3443.4 ± 0.4	6810.7 ± 0.4	6810.1 ± 0.2	+ 0.6
C^{13}	1262.3 ± 0.5 3684.3 ± 0.3	4946.6 ± 0.6	4944.4 ± 0.4	+ 2.2
N^{15}	3533.2 ± 0.5 7300.1 ± 0.6	10833.3 ± 0.7	10832.8 ± 0.7	+ 0.5
	5268.8 ± 0.3 5562.6 ± 0.5	10831.4 ± 0.6	10833.6 ± 0.5	- 2.2
	5297.8 ± 0.4 5533.8 ± 0.4	10831.6 ± 0.5		- 2.0

for the relevant transitions from Be^{10}, C^{13}, and N^{15}. The differences in the sums versus the observed cross-over value (after recoil corrections) do not depend significantly on the calibration. But, having shown that the maximum nonlinear error is about 2 keV, one can then use a one-point calibration and obtain the binding energies as shown in Table II. The calibration point used for this work is the Chalk River

TABLE II. Neutron binding energies (keV).

Nuclide	LASL	Everling *et al.*	Diff.
Be^{10}	6810.4	6814.3 ± 2.1	- 3.9
C^{13}	4945.0	4947.0 ± 0.8	- 2.0
N^{15}	10832.3	10834.3 ± 0.9	- 2.0

value for the Mg^{24} line of 2753.98 ± 0.25 keV. The total errors in these values are not yet final and so are not quoted here. The differences shown in Table I allow the derivation of an error curve from which the maximum possible slope between various energy values gives the maximum error in energy differences that are determined from the spectrometer.

II-12. NUCLEAR PHYSICS BY THE CHALMERS GROUP AT THE SWEDISH RESEARCH REACTORS*

Sam Nilsson, R. Hardell, J. Rohlin, and B. Lundqvist

Chalmers University of Technology, Gotheburg, Sweden

Instruments at Reactor R1 ($\Phi_{th} = 2 \times 10^{12}$ neutron cm^{-2} sec^{-1})

A 1-m bent-quartz-crystal diffraction spectrometer is connected with the high-flux region by a pneumatic tube. Thanks to a special receiving station,[1] the recording of diffraction peaks can start 30 sec after pile-out. For measurements on activities with half-lives shorter than 1 hr, sample capsules of pure titanium instead of the conventional ones of aluminum proved to be necessary for the fulfillment of the background requirements.[2]

Precision energy determinations have been performed on short-lived isomeric transitions and of low-lying excited states in deformed nuclei.[3,4]

The most short-lived activity so far measured with this facility is the 1.2-min transition from the first intrinsic state in Dy^{165}.

---

[1] S. Nilsson, Nucl. Instr. and Methods 16, 89 (1962).

[2] R. Hardell and S. Nilsson, Nucleonics 20, 108 (1962).

[3] R. Hardell and S. Nilsson, Nucl. Phys. 39, 386 (1962).

[4] L. Persson, R. Hardell, and S. Nilsson, Arkiv Fysik 23, 1 (1963).

*Presented by Sam Nilsson.

The Bragg angle is determined by use of a precision theodolite (Model T3, Wild, Heerbrug, Switzerland) with a division interval of 0.2 sec of arc.

The spectrometer efficiency has been calibrated and the energy dependence of the peak reflectivity R has been found to be

$$R \propto E^{-2.26 \pm 0.02}.$$

Relative intensities of gamma lines can be determined with an accuracy of 10%.

A three-crystal pair spectrometer[5] was built to serve mainly as a complement to the diffraction spectrometers for the capture gamma studies described below. In order to achieve a high detection efficiency for the oppositely directed annihilation quanta escaping from the central crystal, the side crystals were made in the form of an annulus of NaI(Tl), 6 in. in diameter and 4 in. long with a $1\frac{9}{16}$-in. through-hole. The annular crystal is bisected and the two segments are optically isolated. Two photomultipliers are attached to each segment. Thanks to the close geometry, the spectrometer has a fairly small volume which facilitates the shielding.

Up to now the spectrometer has been used only with internal targets placed in a through reactor channel. The performance has been tested by investigations on gamma spectra from natural nickel, dysprosium, and calcium, and from a small enriched sample of Ca^{42}.

According to the efficiency determination of the spectrometer, typical required amounts of samples are as follows:

---

[5] S. E. Arnell and E. G. Nadjakov, Nucl. Instr. and Methods (in press).

Ni (σ = 4.8 b) 120 mg, Dy (σ = 950 b) 1.7 mg, Ca (σ = 0.43 b) 900 mg, and Ca^{42} (σ = 40 b; 28.3% enrichment) 40 mg.

The efficiency is 0.5% at 3 MeV and 1.6% at 10 MeV. The resolution width is about 5% at 1.5 MeV and 3% at 9 MeV.

A relative over-all efficiency could be defined as the number of counts per unit time in the peak of a certain gamma line for the same effective sample. The over-all efficiency thus found for the present spectrometer proved to be 1000 times that of the Michigan group[6] and about 100 times that of the Brookhaven group.[7]

The spectrometer will later be used also in coincidence with a single NaI(Tl) crystal spectrometer.

Instruments at Reactor R2 ($\Phi_{th} \approx 2 \times 10^{14}$ neutron cm^{-2} sec^{-1})

One double-flat-crystal spectrometer and one bent-crystal spectrometer[8] are both to be placed in front of the same horizontal through channel of the reactor. The spectrometer with two flat crystals (Fig. 1) is placed below the one with the bent crystal, as shown in the model (Fig. 2). The sample is placed in the center of the reactor channel close to the reactor core where the flux is about 2×10^{14} neutron cm^{-2} sec^{-1}. The sample is fixed to a carriage which

---

[6] P. A. Treado and P. R. Chagnon, Phys. Rev. 121, 1734 (1961).

[7] N. F. Fiebiger, W.R. Kane, and R. E. Segel, Phys. Rev. 125, 2031 (1962).

[8] S. Nilsson, Swedish Physics Conference, Lund, June 1961 [Arkiv Fysik 22, 427 (1962)].

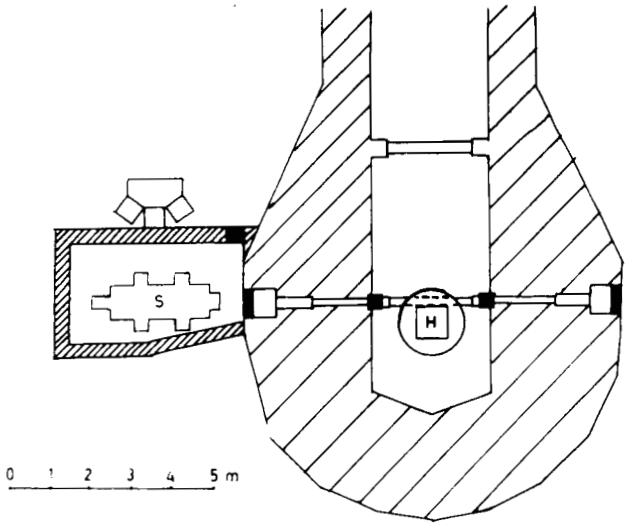

Fig. 1. Experimental arrangement (top view) of the double spectrometer assembly at the Research Reactor R2 at Gotheburg, Sweden. The spectrometers are located to the left of the reactor inside of a separate shield wall (heavily shaded area).

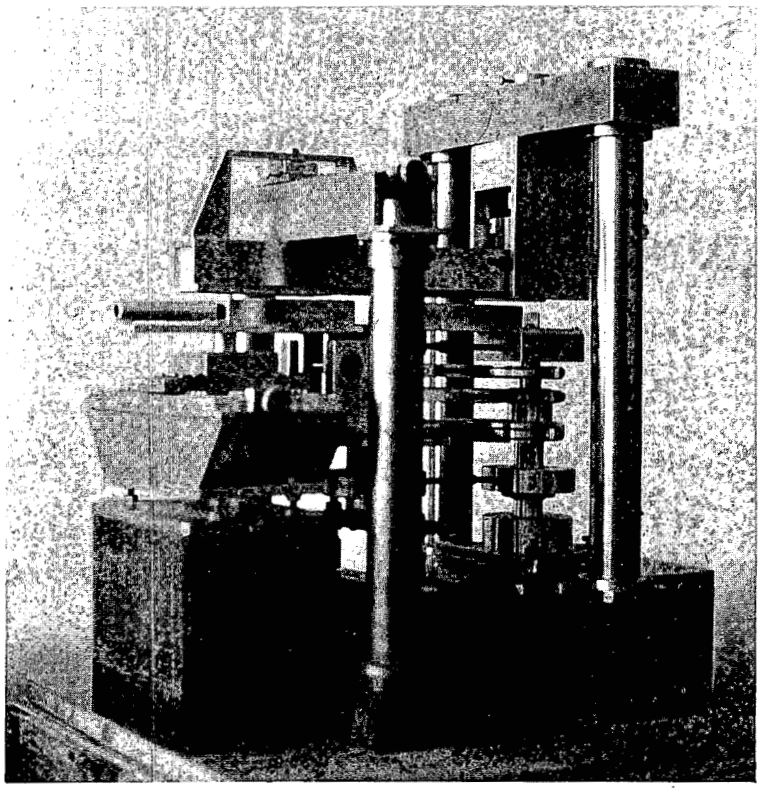

Fig. 2. A scale model of the double spectrometer assembly. The bent-crystal spectrometer is located above the double-flat-crystal spectrometer. The reactor will be to the right of the real spectrometer.

runs on a framework of aluminum pipe inserted from the opposite end of the channel. Thanks to the very low induced activity in the carriage made of titanium,[2] the sample exchange is fairly easy to perform. Both spectrometers have been designed on the requirement of maximum possible automatizibility by the most simple arrangements. We have chosen a pure mechanical system. Thus the rotational movement of crystals, slit collimators, and detectors in both spectrometers is coupled by thin steel bands running over precision-made circular wheels.

The double-flat-crystal spectrometer (Fig. 3) was built

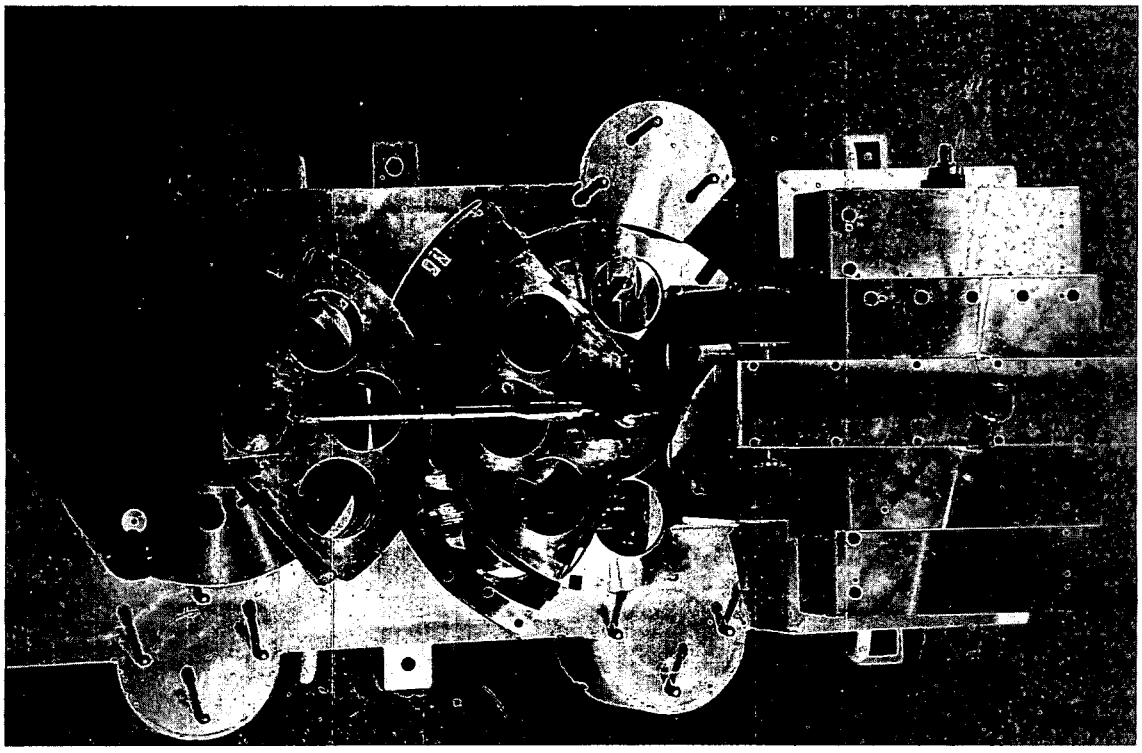

Fig. 3. Top view of double-crystal spectrometer with the two crystals removed to show the steel bands and disks which rotate the crystals. The reactor is to the right.

first and is now in use. The reason why this was built first is our close collaboration with the Münich group at Risø, Denmark which already has a bent-crystal spectrometer in use.

The mechanical coupling of the rotational movements proved to satisfy our demands in a first approximation. Thus the two flat crystals follow each other with an angle precision of better than 0.5 sec of arc over a rotational angle of ± 5°. Even the reproducibility is of the same quality. This means that the spectrometer can be automatized by very simple means, giving a sufficient accuracy in a first-order approximation. However, the most rigorous way to get a reliable automatization is to apply a device directly on the crystal axes (axis) which gives electrical pulses to a scale and/or printer. When recording the diffraction peaks point by point, the angular pulses are printed simultaneously with the gamma counts on the same strip.

A modified Michelson interferometer with photoelectric fringe counting (Fig. 4) has been developed for the conversion of angle into electrical pulses.[9] In order to avoid mechanical trouble in the

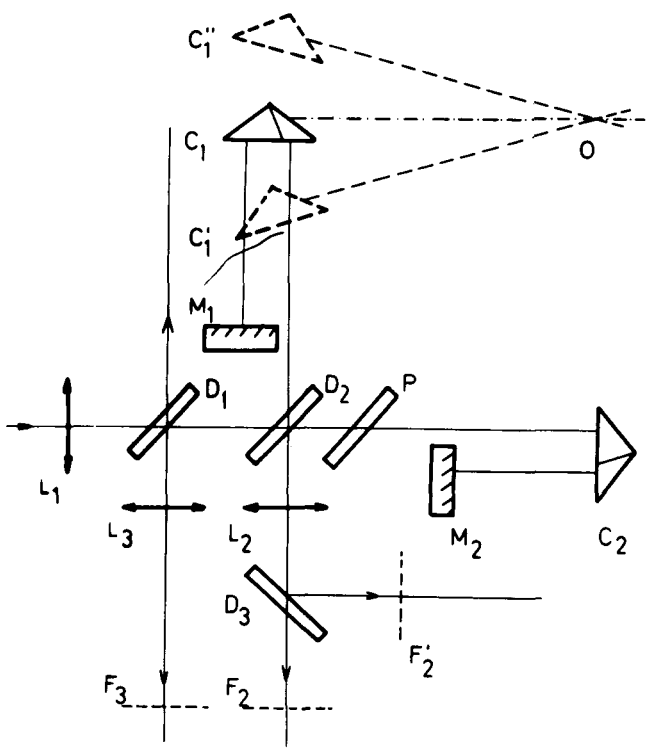

Fig. 4. Schematic diagram of the optical system to measure the rotation of the crystals. Here C_1 and C_2 are cube-corner prisms, M_1 and M_2 are plane mirros, D_1, D_2, and D_3 are beam splitters, and P is a compensating plate.

[9] J. Rohlin, Appl. Optics 2, 762 (1963).

transformation of the rotational motion of the crystal axis into an equivalent translational one, the plane mirrors in the Michelson interferometer were replaced by cube-corner prisms. Plane mirrors are used as end reflectors. The dependence of the optical path difference on the angles of adjustment of the interferometer components has been derived to a third-order approximation in the angle of inclination of the prisms. The sensitivity of the interferometer is 0.1 sec of arc over a range of 30°. This gives a wavelength accuracy of at least 1: 10^4 at 1 MeV when first-order reflection in the (502) planes of quartz is used.

The interferometer is made phase sensitive so as to be independent of backlash and vibrations of the system. Pulses from the two-phase detecting photomultipliers are fed into a two-directional scaler, which thus gives us the relevant number of fringe pulses.

The resolution of a double-flat-crystal spectrometer is determined exclusively by the quality of the diffraction crystals. The only purpose of the slit collimators is to shield the detector from the intense undiffracted gamma-ray beam. The lamellae in the present spectrometer are made of a Pb-Sb (6%) alloy. Three collimators with a total length of about 2 m give a collimation corresponding to a theoretical upper limit of energy of 20 MeV.

A 4-m bent-crystal spectrometer for decay studies[10] is being built on grants from the International Atomic Energy Agency, Vienna, for nondestructive analysis of irradiated fuel elements; but

---

[10] S. Nilsson, Swedish Physics Conf. Gothenburg, June 1963 (to appear in Arkiv Fysik).

it will also be used for pure nuclear spectroscopy. The spectrometer will be used in the so-called Johann geometry, i.e., with a line or strip source in order to make it possible to use enriched isotopes in milligram quantities. The spectrometer is expected to be ready in about half a year. It will be placed close to the high-flux reactor and connected with this by a fast rabbit system.

A permanent-field β-ray spectrograph. In resolution, precision, and efficiency, this instrument is comparable with the diffraction spectrometer. For decay studies we therefore found it advisable to complement the above-mentioned diffraction spectrometer with the β spectrograph, which will also be connected with the reactor by a pneumatic tube.

According to a technique[11] developed by Prof. Slätis at the Nobel Institute, Stockholm, electron intensities can be determined with an accuracy of about 5%. Even this corresponds well with the accuracy obtainable in a diffraction instrument. The 4-m bent-crystal spectrometer as well as the β spectrograph can in many cases also support the (n,γ) measurements with the diffraction spectrometers because in the low-energy region (0.03—2 MeV) covered by these instruments one very often has many lines emanating from radioactive nuclei.

* * *

J. W. KNOWLES, Chalk River Laboratories: I just want to say a few words about getting mechanical precision. We tried various

[11] H. Slätis, Arkiv Fysik 22, 517 (1962).

setups (most of them quite a bit simpler than this) to get mechanical precision to 0.01 seconds. One could obtain this all right, but you really did not get the 1-mil precision that you want until you introduce some sort of a feedback system. A great many of the temperature problems are solved if you make the feedback of the system high enough and part of that system is the arm of the spectrometer. I think a thing like that could very easily be added to the spectrometer.

NILSSON: The way it is built, it is a feedback system. It can tell us in which direction the crystals are rotated relative to each other.

KNOWLES: I was also going to ask where your interferometer is mounted with respect to the crystals. It seems to me that your flat mirrors and interferometer should somehow be made an integral part of your two flat-crystal assemblies. If they are even separated by a foot, we have found that one gets very suspicious of the angles between the optical system and the crystal system.

NILSSON: The picture that I showed was developed for one axis. Now we have to couple both of the cube-corner prisms to the two spectrometer axes. They give us the relevant rotation of the crystals relative to each other.

KNOWLES: A person who has had a lot of experience in this is Dr. Bearden at Johns Hopkins. For two years now they have had an interferometer operating with a flat-crystal spectrometer for x-ray measurements. He found that he had to make the device smaller and smaller. The whole device is about 6 in. across, and he had to mount the sensitive parts of his interferometer directly on his crystals or

effects such as people walking into the room or the temperature change resulting from people walking in the room would upset the measurements when you are measuring to a few parts per million.

NILSSON: We have not found any such dependence yet.

Session III

OTHER EXPERIMENTS WITH CAPTURE GAMMA RAYS

Wednesday morning, 16 October 1963

Presiding: G. Ben-David

Scientific secretaries:
S. Raboy
C. C. Trail

III-1. THE COLLECTIVE MODEL IN RELATION TO NEUTRON-CAPTURE GAMMA-RAY SPECTRA*

D. M. Brink

Clarendon Laboratory, Oxford

I would like to confess at the beginning of this talk that I am not really an expert in the field of neutron gamma-ray physics, and I would like to thank all those experts whom I have talked to and who have helped me arrange the talk that I am going to give this morning.

First, I would like to discuss estimates of partial radiative widths for electric-dipole, magnetic-dipole, and electric-quadrupole gamma-ray transitions emitted in the neutron-capture state and during the subsequent gamma-ray cascade. Estimates for these may be derived from formulae given by Blatt and Weisskopf or by Bartholomew in a review article in 1961. These single-particle estimates (in eV) are

$$\Gamma_B(E1) = 0.11\, A^{2/3}\, \epsilon^3\, D/D_0,$$

$$\Gamma_B(M1) = 0.021\, \epsilon^3\, D/D_0,$$

$$\Gamma_B(E2) = (1.2 \times 10^{-7})\, A^{4/3}\, \epsilon^5\, D/D_0.$$

In these formulae, ϵ is the energy of the gamma ray emitted, Γ is the partial radiative width, D is the spacing of the levels with the same spin and parity as the radiating state near the position of radiating state, and D_0 is the so-called spacing of single-particle levels (which, by convention, is taken to be 15 MeV).

I would just like to make a remark here that the estimate of Bartholomew differs from that of Weisskopf by a factor of $(2\ell + 1)$, where ℓ is the multipolarity of the gamma ray emitted; i.e., the Weisskopf value Γ_W is

$$\Gamma_W = (2\ell + 1)\, \Gamma_B,$$

*Invited paper.

where Γ_B is the Bartholomew value.

There are a number of effects which are important. Direct gamma-ray capture processes have been discussed by a number of people and they are important when the thermal-neutron capture state differs from the final state by a single-particle transition. I am not going to talk about direct capture this morning.

Recently, Professor Axel has promoted the idea of relating the gamma-emission matrix elements to gamma-absorption matrix elements by detailed balance and calculating these matrix elements by use of simple models for gamma-ray absorption. For example, for absorption of electric-dipole radiation, one has the giant-dipole model (first introduced by Goldhaber and Teller) where the incoming γ ray excites the nucleus in a mode in which the protons move against the neutrons — or the particle-hole model proposed by Castileo, Brown, Evans, and other people. The incoming photon excites the particle of the core into some excited state to produce a particle-hole state.

I will first discuss this idea in relation to electric-dipole radiation (the case treated by Axel); but the first part of the argument is quite general and applies also to magnetic-dipole radiation and electric-quadrupole radiation. Now, I imagine the nucleus in some state α, which may be a ground state or an excited state, and I place it in a varying electric-dipole field. What I am doing is just the classical theory of dispersion which is familiar from the very first days when one starts studying electromagnetic theory. I place the nucleus in this varying electric-dipole field and just investigate its response to the field. The response function consists of a dispersive part and an absorptive part. The dispersive part is related to the absorptive part by a dispersion relation so that if one knows the absorptive part then one can calculate the response function to the varying electric field.

If the radian frequency of the field is ω, then the energy absorbed from the field is

$$|A(\omega)|^2 X \epsilon \; g_a(\epsilon)\, d\epsilon \, .$$

Here $\epsilon = \hbar\omega$ (I prefer to work in energy units rather than frequency units; ϵ corresponds to the energy of the γ ray absorbed or emitted), $|A(\omega)|^2$ is the mean-square Fourier component of the applied field with radian frequency $\omega = \epsilon/\hbar$, the spectral function $g_a(\epsilon)$ is normalized by the relation

$$\int_0^\infty \epsilon \; g_a(\epsilon) = 1,$$

and X is a normalization constant.

The energy absorbed from the applied field may also be calculated from the matrix elements for transitions from the state a with energy E_a to states with energy $E_a + \epsilon$ and $E_a - \epsilon$ and the density of the states ρ in the neighborhood of these energies. The result is

$$X\, g_a(\epsilon) = |M_a(E_a + \epsilon)|^2 \rho(E_a + \epsilon) - |M_a(E_a - \epsilon)|^2 \rho(E_a - \epsilon). \quad (1)$$

The normalization constant X can be estimated by use of a sum rule for the matrix elements, namely,

$$X = \sum_\beta (E_\beta - E_a) |m_{a\beta}|^2.$$

This type of sum rule can often be calculated without detailed knowledge of the nuclear structure.

When ϵ is large enough so that $\rho(E_a + \epsilon) \gg \rho(E_a - \epsilon)$, the second term in the equation for $g_a(\epsilon)$ is small compared with the first and may be neglected. Thus,

$$|M_a(E_a + \epsilon)|^2 \rho(E_a + \epsilon) = X\, g_a(\epsilon). \quad (2)$$

This is an expression for the average of the square of a radiative matrix element. A partial radiation width can be calculated from it if the spectral function $g_a(\epsilon)$ is known.

When ϵ is small, both terms in Eq. (1) are important. As $\epsilon \to 0$

$$|M_a(E_a + \epsilon)|^2 \rho(E_a + \epsilon) \to X g_a(\epsilon) \left[\frac{2\epsilon}{\rho} \frac{d\rho}{d\epsilon}\right]^{-1}. \qquad (3)$$

It is a general result that $g_a(\epsilon) \to 0$ as $\epsilon \to 0$ so the average reduced width tends to a constant value for small ϵ (in practice, for $\epsilon \lesssim 1$ MeV).

A more accurate calculation should include spin effects. One finds that the ratio Γ/D should be almost independent of spin.

We are left now with the real problem of calculating the spectral function $g_a(\epsilon)$. This can never be done exactly, but simple nuclear models can give some idea of its shape. [In the Weisskopf estimates, $g(\epsilon)$ has a constant value.]

We know in the cases of E1 and E2 radiation that the absorption of radiation is closely connected with a collective motion of the nucleus. This suggests a model of the absorption process which leads directly to a simple analytic form for the spectral function $g(\epsilon)$. We assume that the collective motion is analogous to the motion of a damped harmonic oscillator. The oscillation is characterized by a natural radian frequency $\omega_0 = E_0/\hbar$ and a damping constant Γ, where $\Gamma/\hbar$ is a measure of the rate at which the energy in the collective mode is lost into "thermal" modes of motion of the nucleus. In this model, $g(\epsilon)$ has the Lorentz form

$$g(\epsilon) = \frac{2}{\pi} \frac{\epsilon \Gamma}{(\epsilon^2 - E_0^2)^2 + \epsilon^2 \Gamma^2} \qquad (4)$$

$$= g(\epsilon, E_0, \Gamma)$$

assumed by Axel in his paper. Putting in empirical values of Γ and E_0 and using the general theory, we obtain expressions for average partial radiative widths. In this model, $g_a(\epsilon)$ is the same for all states a. In a more general theory, the damping constant Γ would depend on the state a and the energy ϵ, but this dependence would be hard to calculate. In general, one would expect that $\Gamma_a(\epsilon)$ should decrease as ϵ decreases for a fixed a and increase with E_a for a fixed ϵ.

(a) E1 Radiation. If we assume that E1 absorption is dominated by the giant-dipole collective mode, then we should use formula (4) for the spectral function $g_\alpha(\epsilon)$ with E_0 and Γ chosen to fit the dipole resonance in the nucleus in question. When the state α is the ground state, the accuracy of (4) can be tested by analyzing photonuclear data. This has been done by Axel who concludes that it gives the general trends of the variation of photonuclear cross sections correctly. More recent experiments show some structure in the spectral function, a result which indicates that (4) is an over-simplification.

On the assumption that E_0 and Γ are independent of α and have the same values as in the ground state, the average value of a partial E1 width (in eV) is

$$\Gamma(E1) = 0.76\ A\ g(\epsilon)\,\epsilon^3\ D,$$

where D is the spacing of levels with the same spin and parity as the radiating state and $g(\epsilon)$ is given by Eq. (4). Axel, who put in empirical estimates for E_0 and Γ, obtains the approximate formula

$$[\Gamma(e1)/D] = (2.2\times10^{-5})\left(\frac{E}{7}\right)^5\left(\frac{A}{100}\right)^{8/3},$$

which should hold for energies near 7 MeV.

(b) E2 Radiation. One can do the same sort of thing for electric-quadrupole absorption. There are two possible types of collective modes. One knows that even-even nuclei in many regions have a vibrational spectrum with an excited state at about 0.5 MeV. This corresponds to oscillations of the nucleons outside closed shells. Another mode involves excitation of particles from one shell to other shells. This corresponds to a vibration of the core. One would expect higher frequency. One puts in estimates for the widths of these frequencies and one can calculate widths.

The first mode would contribute to the absorption of low-energy photons (of the order of 1 MeV or less) and the second mode would be important for the absorption of high-energy photons. In the high-energy region where the core vibrations produce an enhancement, the E2 partial width is estimated to be

$$\Gamma(E2) / \Gamma_B(E2) = 135\, D_0\, A^{1/3}\, g(\epsilon, E_0, \Gamma).$$

We do not know the position and the width of the quadrupole resonance. On the single-particle picture, the E1 giant-dipole resonance involves excitation of particles through one major shell and the E2 resonance involves excitation through two major shells. But residual interactions push the E1 resonance up and the E2 resonance down so that they may both occur at the same excitation energy. The E2 resonance would probably be wider than the giant-dipole resonance. The partial E2 widths may be enhanced by a factor of 100 or more in the resonance region, but they are still much smaller than E1 or M1 widths. I think that E2 radiation can be expected only between low excited states of nuclei where selection rules forbid or inhibit E1 or M1 radiation.

(c) M1 Radiation. The possibility of a giant M1 resonance has been suggested recently. On the basis of the quasi-particle picture, two processes seem to be important for γ-ray absorption. (i) Absorption of the M1 radiation by a quasi-particle. This process should be important for low-energy transitions ($\approx$ 1 MeV). (ii) Production of a quasi-particle pair. For this to occur the quasi-particle must have the same orbital angular momentum and opposite spin, i.e., $j_1 = \ell + \frac{1}{2}$, $j_2 = \ell - \frac{1}{2}$. For a given ℓ, the absorption spectrum has a maximum near the energy of the spin-orbit splitting between states j_1 and j_2. It should be important if the $j_1 = \ell + \frac{1}{2}$ state is almost full and the $j_2 = \ell - \frac{1}{2}$ state is almost empty, and is most important for states with large ℓ.

The effect should be strongest near a closed shell where the lower member of the highest orbital-angular-momentum state is full and the upper member is empty. We calculate the absorption on the assumption that all the M1 strength is concentrated in a width Γ about a mean energy E_0. We get for an average partial width

$$\Gamma(M1)/D = \frac{4}{9}(g_\ell - g_s)^2 E_0 \frac{\ell(\ell+1)}{2\ell+1} \frac{e^2}{\hbar c} \frac{1}{M^2c^4} \epsilon^3 g(\epsilon, E_0, \Gamma).$$

The single-particle estimate is

$$\Gamma_B/D = \frac{10}{4} \frac{e^2}{\hbar c} \frac{1}{M^2c^4} \frac{\epsilon^3}{D_0} .$$

The ratio of the two is

$$\Gamma(M1)/\Gamma_B(M1) = \frac{16}{90}(g_\ell - g_s)^2 E_0 \frac{\ell(\ell+1)}{2\ell+1} D_0\, g(\epsilon, E_0, \Gamma).$$

Here E_0 is the splitting between the states of the spin-orbit doublet, assumed to be the same as the resonance energy.

The maximum, enhancement, which occurs at $\epsilon = E_0$, is

$$\Gamma(M1)/\Gamma_B(M1) = \frac{32}{90\pi}(g_\ell - g_s)^2 \frac{\ell(\ell+1)}{(2\ell+1)} \frac{D_0}{\Gamma} .$$

If $\ell = 6$ and $\Gamma = 1$ MeV,

$$[\Gamma(M1)/\Gamma_B(M1)]_{max} \approx 20.$$

This estimate would be doubled in the lead region because both protons and neutrons contribute at the double closed shell.

The above formulae hold if the lower member of the spin-orbit doublet is completely filled and the upper member is completely empty. In a more general situation, it must be multiplied by a factor $(V_{j_1}^2 - V_{j_2}^2)$, where $V_{j_1}^2$ is the occupied fraction of the lower member

(j_1) of the doublet and $V_{j_2}^2$ the occupied fraction of the level j_2. When both levels are empty or both are filled, this factor is zero. (Here V_j is a parameter of the pairing-force model.)

At this point I would like to say that this estimate disagrees with the estimate that Dr. Harvey will put forward in paper III-4. His estimate is much larger than this; and it is for tin, which is not such a favorable case. I cannot understand how one can have enhancement as large as his. I think this point is important and should be discussed after his talk.

For the next ten minutes or so, I would like to change the subject completely and first talk a little about vibrational even-even nuclei. Professor Moszkowski said that such nuclei have a ground state with spin zero, first excited state spin 2, and then a triplet with spins 0, 2, 4 is expected. I am going to look at the three-phonon states which can have spins of 0, 2, 3, 4, and 6. I ask the question: Is it possible to locate some of these three-phonon states? So far as I know, up to date there has been no firm identification of the three-phonon states in any vibrational nuclei. Professor Moszkowski pointed out that the simple theory gives the two-phonon states an energy equal to twice that of the one-phonon state, and the three-phonon states have three times the energy of the one-phonon states. If one looks at nuclei, one finds the energy of the two-phonon states is not exactly double the energy of the one-phonon state, and hence the three-phonon states should also be shifted. Kerman and Shakin have given a theory of this shift. They describe this system by an anharmonic oscillator. They put in anharmonic terms which will make the distribution of levels different from that of the harmonic oscillator. This sort of thing was done quite a number of years ago by Wilets and Jean, and a number of other people, using special models. Kerman and Shakin put in cubic anharmonic terms and calculated in second-order perturbation theory. They get some relatively complicated formulae in terms of the parameters that come in here. One can simplify their

formulae quite a lot and generalize them also. If one has cubic and quartic anharmonic terms and calculates the cubic terms as far as second-order perturbation theory and the quartic terms to first order, then one can get some rather simple expressions for the shifts in these three-phonon states in terms of the shifts in the two-phonon states. These expressions are

$$\Delta E_0 = 3 \quad \epsilon_2 ,$$
$$\Delta E_2 = \frac{7}{5} \quad \epsilon_0 + \frac{4}{7} \quad \epsilon_2 + \frac{36}{35} \quad \epsilon_4$$
$$\Delta E_3 = \frac{15}{7} \quad \epsilon_2 + \frac{6}{7} \quad \epsilon_4 ,$$
$$\Delta E_4 = \frac{11}{7} \quad \epsilon_2 + \frac{10}{7} \quad \epsilon_4 ,$$
$$\Delta E_6 = 3 \quad \epsilon_4 .$$

In these equations, the numbers ϵ_0, ϵ_2, and ϵ_4, are the shifts of the positions of these two-phonon states from the energy $2\hbar\omega$ (i.e., from twice the energy $\hbar\omega$ which they would have on the perfect-oscillator model), and the ΔE's are the shifts of the three-phonon states.

One can try out this theory, theoretically, by trying to predict the positions of the Wilets-and-Jean three-phonon states in terms of the positions of their two-phonon states; and it really fits quite well. Then one can look at real nuclei, and I took first of all the case of osmium. — I forget which isotope. The low levels are I = 0, 2, 4, 6, and 8 — not really a rotational sequence. From the positions of the spin-two and spin-four levels it was possible to predict the position of the spin-six level since it depends only on the position of the spin-four two-phonon level. It fits to within about 30 keV, which is not really very good compared with the accuracy we talked about yesterday in rotational bands.

Then I thought that I would apply the formula to Sm^{150}. Figure 1 shows the level scheme of Sm^{150}, which comes from Groshev.

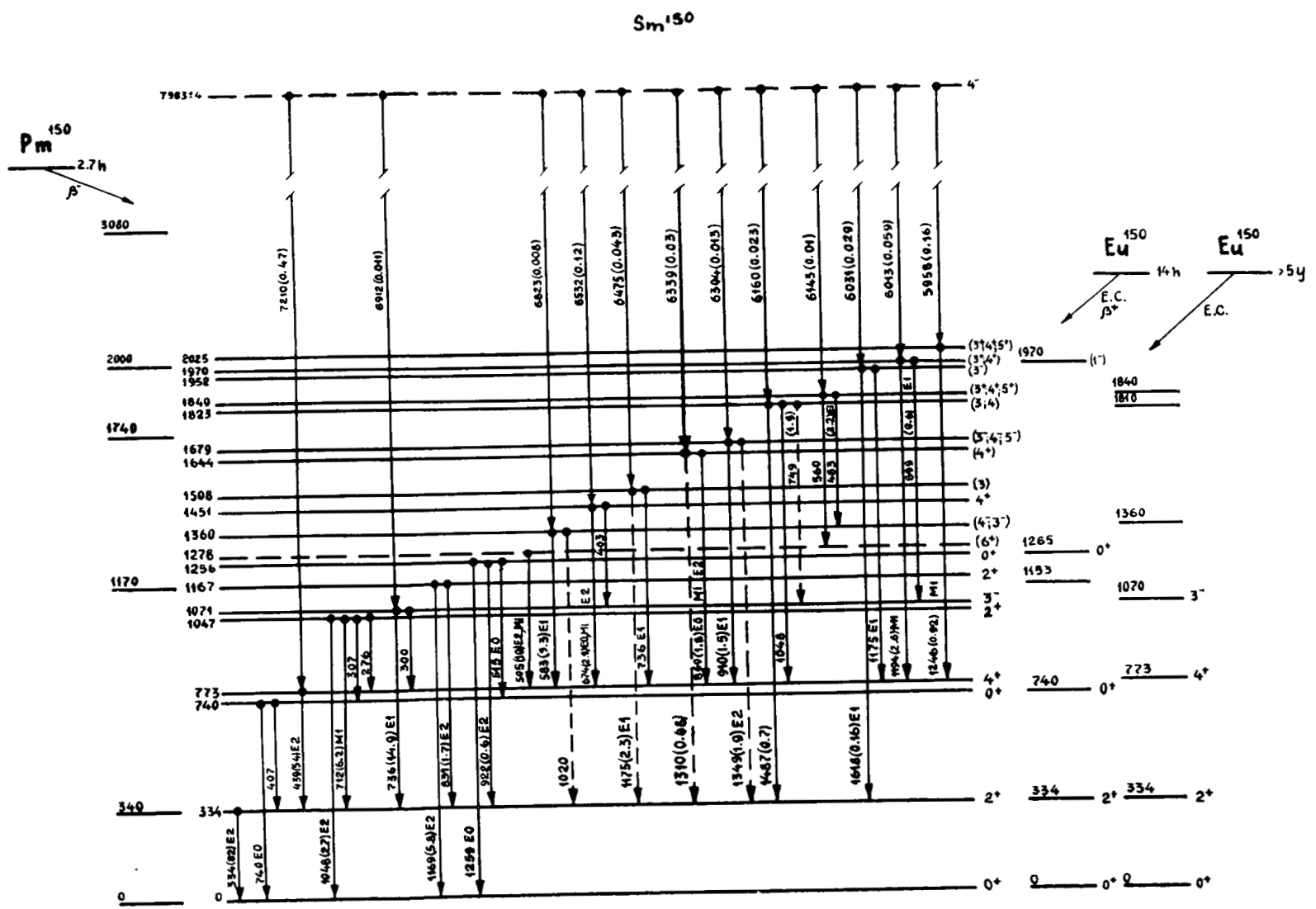

Fig. 1. Scheme of γ transitions of the Sm^{150} nucleus. [L. V. Groshev, A. M. Demidov, V. A. Ivanov, V. N. Lutsenko, and V. I. Pelekhov, Nucl. Phys. 43, 669 (1963), Fig. 4].

Higher up you can see spin-3^+ and spin-4^+ states, so I thought that I would apply these formulae to this case. I am afraid that the result was disastrous. I could not get my levels anywhere near where the levels are found there.

This theory gives such a nice formula, but I am afraid it does not really work. I think this is a bad omen for this type of nucleus, because any anharmonic calculation would give formulae which were rather like these. Hence I think that when one gets up as far as the "three-phonon" states, the theory of this vibrational nucleus is going to be difficult. On the other hand, I think it would be worth while to concentrate on one or two nuclei of this type and try to work them to death — i.e., really try experimentally to find these higher states, just to see if there is any simple feature there at all.

During the last two or three minutes of this talk I would like to discuss rotating nuclei, where the position is much better but still not really perfect. In a rotating even-even nucleus, the ground-state spin is zero and there is a ground-state rotational band; then there are various excited-state rotational bands built on some intrinsic excited states. Now, these intrinsic states may be β vibrations or γ vibrations, or they may be some sort of particle excitations. At this point I would like to mention one useful article by Gallagher and Soloviev in the Danish Journal, which discusses two quasi-particle states and tries to say, on the basis of the very simple theory, which two quasi-particle states one expects and what excitation energies they have. For people trying to interpret the spectra of even-even nuclei, it is a valuable document to have around.

Well, I have spent quite a bit of time in the past few weeks looking at Smither's results on Hf^{178}. I would just like to look at the spectrum (Fig. 2) for a minute. Even in this rotational nucleus, the level scheme does not really quite fit in with the simple model. It has the ground-state rotational band; and two K=0 bands based on 0^+

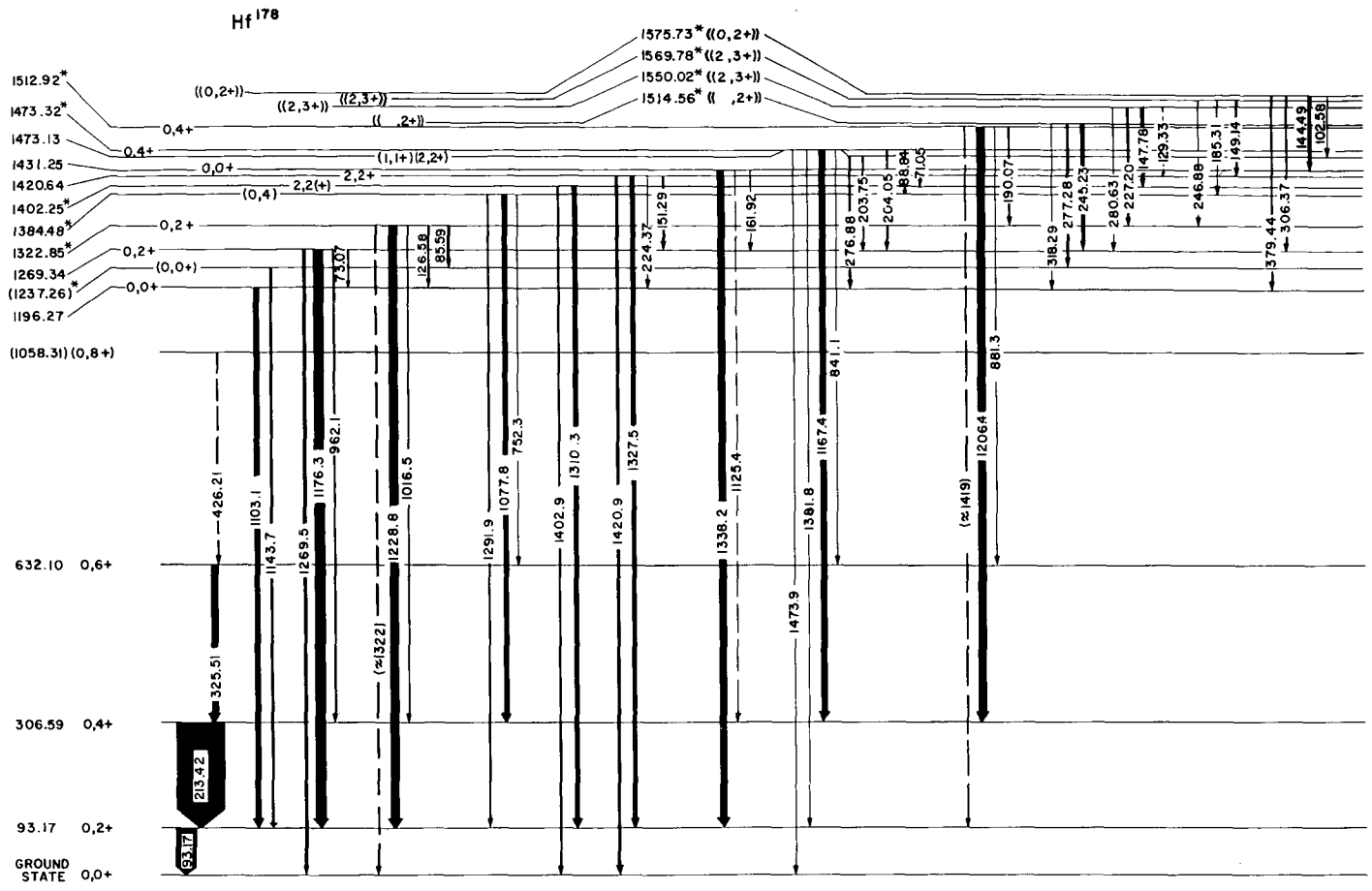

Fig. 2. Level scheme of Hf^{178} as deduced from the gamma-ray measurements made with the Argonne 7.7-m bent-crystal spectrometer. The energies of the levels and gamma rays are given in keV. The K value, spin, and parity of the level is given on the left in that order. The width of a line in the level scheme is meant to reflect the relative intensity of the gamma ray. The width scale used for the low-energy gammas between the upper states (energies between 1195 and 1575 keV) is four times that used for the gamma rays with energies between 1 and 2 MeV and for the ground-state band. No corrections have been made for internal conversion. An asterisk following the energy of a level indicates that this level has not been observed previously. The parentheses and double parentheses indicate uncertainty in the assignments. [R. K. Smither, Phys. Rev. 129, 1691 (1963), Fig. 5]

states at 1196 keV and 1237 keV have been suggested. Higher 2^+ and 4^+ rotational states have been seen, and in the case of the second band the spacings agree quite well with the predictions of the rotational model. On the other hand, the band based on the 1196-keV state is distorted and there may be strong mixing between the 4^+ states at 1384 keV and 1473 keV. The lower state might be mainly the ground state of a K=4 band with some of the K=0 band mixed in. If this were so, then the branching ratios would be characteristic of a K=0 band because transitions from a pure K= 4 band to the ground-state K=0 band would be forbidden. This is a simple situation in which branching ratios can give misleading assignments to the K quantum number because of band mixing. All such assignments must be checked by some independent method.

Smither also suggests two K = 2 bands based on 2^+ states at 1402 keV and 1420 keV. This is difficult to understand on the basis of the results of Gallagher and Soloviev. They have only one K=2 band, which they expect to come in at about 2.3 MeV. One K=2 band could be a γ vibration.

I would like to point out again that branching ratios may be quite useful for getting an idea of what the K values of the various bands may be, but they are not absolutely reliable because of band mixing. And if one gets results which do not seem to fit in with the other theoretical or experimental ideas, then the assignment should be tested by an independent method.

Then there is another very peculiar thing about this picture. There are some very strong transitions with between 6 and 12 gamma rays per 100 neutron captures. They come from states with energies up to 1513 keV; but from higher states there do not seem to be any other strong transitions. This is a very peculiar feature because it indicates that these low states must be populated in a very different way from the higher states. The intensity of the gamma ray depends not upon the transition probability to lower states but on the way these states are populated. There is this

strange discontinuity in the way they populate, which I think cannot be explained on purely a statistical argument about population of these states. So this is another problem which I hoped to be able to say something about but which I have not succeeded in understanding.

Now, just to finish this talk, I would like to say a word of encouragement for experimentalists. I think all the theory which I have talked about today is theory which can be applied directly by experimentalists and does not require complicated theoretical analysis. If one is going to explain, for example, the discontinuity in population of these excited states, then I am sure that the idea, when it is found, will be a relatively simple one and the sort of thing which does not require detailed theoretical analysis. So I would encourage experimentalists as well as theoreticians to try to solve this problem.

* * *

R. E. SEGEL, Argonne National Laboratory: Can you suggest a nucleus where the situation might be clear enough to look for the three-phonon states, i.e., where the other intrinsic states are not so low that they obscure the 3-phonon states.

BRINK: I think there are no nuclei where you tend to get the three-phonon states below the mess.

S. NILSSON, Studsvik, Sweden: I just happened to remember that Nilssen and Brayer in their initial paper mentioned the possibility of looking at the densities, just about the gap in even-even nuclei, to get some information about the difference in apparent forces for protons and neutrons. I am just wondering if you have taken this into consideration, where you could look at a spectrum of this type in Fig. 2. There should be some states emanating from quasi-particle states for comparison; so the spectra of this study would give something in the future when you get systematic information.

BRINK: Yes. I cannot see how it would explain any of these difficulties that appear in this sort of spectrum. Perhaps Smither has thought about this.

R. K. SMITHER, Argonne National Laboratory: One of my reasons for investigating the level scheme of Sm^{150} was the possibility of observing one or more three-phonon states in the level scheme. Sm^{150} is in the transition region between spherical and deformed nuclei. In this transition region, the energy of the first excited state (2^+) in even-Z even-N nuclei passes through a minimum. A similar minimum in excitation energy is observed for the two-phonon states. My hope was that the three-phonon states would also exhibit an energy minimum in the transition region and therefore be observable.

The other thing I would like to mention is that some of the spin assignments in Groshev's work differ from the assignments I have made on the basis of γ-γ angular-correlation work (Argonne) and conversion-electron work (Munich). In view of this difference, it would be interesting to repeat the comparison of the predicted position of the three-phonon states with the new assignments.

BRINK: After I heard your talk yesterday, I went home and recalculated the numbers. I had hoped your numbers would fit; but they did not.

SMITHER: The large variations in the population of different levels of the same spin and parity at about 1 MeV, which I observed in Hf^{178} (Fig. 1 of paper II-3 of this conference), appear to be present in the work of Dr. Schult as well. (See his level scheme for Dy^{164}, Fig. 6 of combined papers II-3, 4, and 5 of this conference.) Thus we are collecting more evidence for this effect. The level scheme of Hf^{180} (Table I of paper II-3 of this conference) shows similar variations in the populations of levels.

P. AXEL, University of Illinois: I want to comment on whether one can hope to explain why neighboring levels of the same spin and parity are populated differently by the gamma rays following neutron capture—that is, to explain why some 2^+ states are highly populated while others are not.

The situation is not dismal, particularly if experimental data can provide clues about refining the theory. Until now, we have all used the completely unwarranted implicit assumptions that every state in the nucleus has a giant-dipole resonance built on it and that the energy separation between each state and its giant resonance is the same. Only if these giant resonances and their energy structures were the same would one be warranted in using a universal single-valued function of energy to describe the gamma-ray transition probability between any two states. If these assumptions were warranted, the gamma-ray cascade could not distinguish between two neighboring 2^+ states.

But I think that the available data already tell us that one 2^+ state is quite different from another. This refutes the idea that all states have identical giant resonances. It would be very interesting to know where these assumptions break down, and possibly get information on parts of the giant resonances associated with excited states.

I would like to give an explicit example of possible refinements. Consider a model which attributes part of the width of the giant resonance to a coupling between the giant-dipole-excitation mode and, let us say, surface vibrations. This same model might imply that the giant-dipole resonance built on a vibrational 2^+ level has a different energy dependence, including some concentrations of strength in energy.

If the energy region in a nucleus reached by a captured neutron coincided with a peak in substructure of the giant-dipole resonance of some vibrational 2^+ state, this 2^+ state might receive much more gamma-ray intensity than its neighbors whose giant resonances might give contributions at different energies. Additional experimental data could help decide such questions.

I am not proposing this as a theory of giant resonances of excited states. Rather, I am suggesting that a theory is needed and that neutron-capture gamma-ray data might help, for example, by indicating which 2^+ states are favored. I realize that when you publish something with as much detail as Dr. Smither showed on his slide, the necessary data might be included. But I feel that if theoreticians are to be attracted to this problem, and if one expects them to use the data, the text should summarize some features appearing in the decay schemes. There has to be a paragraph that says, "Here are five 2^+ states which account for 40% of the radiation, and here are five other 2^+ states which have less than 1%." It is not enough to publish only a decay scheme, thereby requiring others to analyze it to rediscover how the percentages of primary transitions are distributed, how much goes directly to the first excited state, and so on.

BRINK: Yes, I did look at those low-energy gamma rays, and in this particular case it seems to me that these would account for perhaps 10% of the intensities of the high-energy gamma rays, but not anything like the whole intensity. Of course, direct transitions from the capture state seem to be rather unimportant.

G. A. BARTHOLOMEW, Chalk River Nuclear Laboratory: A $(2\ell + 1)$ statistical factor inserted by Blatt and Weisskopf was not included in the formulae used by Bartholomew, Ann. Rev. Nucl. Sci. 11, 259 (1961).

III-2. PARTIAL WIDTHS FOR E1 GAMMA RAYS FROM NEUTRON RESONANCES AND THEIR RELATION TO THE GIANT RESONANCE

R. T. Carpenter

State University of Iowa, Iowa City, Iowa

I would like to present to you what amounts to a survey of our existing experimental knowledge of E1 transition probabilities involving states near the neutron binding energy. Several kinds of experiments may yield this knowledge, each with its own advantages and limitations.

First of all there are the experiments wherein one examines the gamma-ray spectra following the capture of thermal neutrons. These measurements are no doubt the most extensive, covering as they do almost the entire periodic table. They have the further virtue of being relatively precise and, since only s-wave neutrons may interact at the low energies involved, one may unambiguously assign the multipolarities of gamma rays observed in the spectrum from independent knowledge of the spins and parities of the initial and final states. However, since only individual transition probabilities are measured, the values are members of the extremely broad Porter-Thomas distribution.[1] This means that the mean values of the transition probabilities are determined with 90% confidence only within about two orders of magnitude. This uncertainty is compounded by the fact that since the measurements are never made in the peaks of resonances, they are subject to interference effects. Taken together, these two phonomena severely limit the usefulness of individual thermal-neutron-capture results in a study of the characteristics of E1 transition probabilities.

Now the way to eliminate interference effects is to look in the peaks of neutron resonances; and the way to eliminate the effects of the

[1] C. E. Porter and R. G. Thomas, Phys. Rev. 104, 483 (1956); L. M. Bollinger, R. E. Coté, R. T. Carpenter, and J. P. Marion, Paper IV-2 (this conference).

Porter-Thomas fluctuations is to average over a large number of resonances. This can be done, for example, by looking at spectra resulting from capture of neutrons with a broad spread in energy in the region of a few kilovolts. However, by doing this one loses the uniqueness with which the multipolarity of the observed transitions may be specified. This is because p-wave interactions become important in the kilovolt region and because there is some reason to believe that M1 transitions may have intensities comparable to E1 transitions near the neutron binding energy.[2] Therefore, a transition observed to a particular final state would be an incoherent mixture of electric- and magnetic-dipole contributions.

A different class of experiments is suggested by the detailed balance result:

$$\frac{\langle \Gamma_i \rangle}{D} = \frac{E_\gamma^2}{2\pi^2 (\hbar c)^2 g} \langle \sigma_a \rangle \ .$$

Here $(\Gamma_i)/\hbar$ is the average probability of a transition from a level of spin J and excitation E_γ to the ground state, D is the average level spacing at energy E_γ for states with parity opposite to that of the ground state and with spin J, $\langle \sigma_a \rangle$ is the total absorption cross section for photons of energy E_γ, $g = (2J + 1)/[2(2I + 1)]$ for dipole transitions, and I is the spin of the ground state. Using this result one may obtain values of $\langle \Gamma_i \rangle / D$ from photoneutron cross-section measurements, photon elastic scattering measurements, photofission experiments, etc. Again these experiments effectively average over many excited levels so that the effects of interference and Porter-Thomas fluctuations are largely eliminated. However, again since M1 transitions may compete favorably with E1 transitions near

[2] I. Bergqvist, B. Lundberg, and N. Starfelt, Paper III-3 (this conference); J. A. Harvey, G. G. Slaughter, J. R. Bird, and G. T. Chapman, Paper III-4 (this conference).

the neutron threshold, their interpretation becomes ambiguous in this excitation region.

There remains one type of experiment which can in principle overcome all of the difficulties mentioned above while retaining most of the desirable features: namely, the study of spectra following capture in the peaks of individual resonances. Interference effects are obviously eliminated entirely in this type of experiment. Since individual states are involved, one may unambiguously assign the multipolarities of the transitions, a priori, from independent knowledge. Further, by averaging the results over many resonances the effects of the Porter-Thomas fluctuations may be reduced. Unfortunately, it is usually not possible to observe spectra in enough resonances to reduce these effects to an acceptably low level and the Porter-Thomas fluctuations remain the largest source of uncertainty in the experimental results.

A resonance-capture experiment of this type was completed by the author about a year ago and the results were described in an Argonne report.[3] I will not go into any of the experimental details at this time, but merely show the results: the solid circles in Fig. 1. The solid line in this

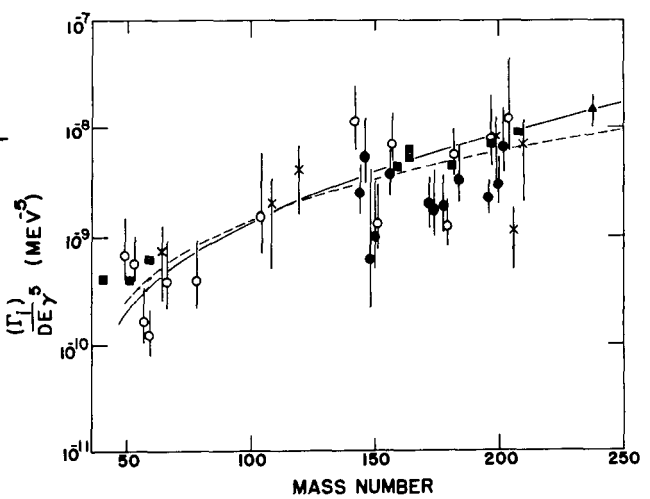

Fig. 1. Combined data showing the experimental E1 gamma-ray strength function. The solid circles show the resonance-neutron-capture results, the open circles are averages of thermal-neutron-capture results. The squares are from (γ, n) results. The crosses are from (γ, γ) results. The triangle is a photofission result. See text for an explanation of the two curves.

[3] R. T. Carpenter, Argonne National Laboratory Report ANL-6589 (1962).

figure is the prediction of the two-fluid hydrodynamical model[4] according to the approximation given by Axel.[5] The giant-dipole resonance parameters used were $E_g = 80\ A^{-1/3}$, $\Gamma_g = 5$ MeV. The factor E_γ^5 closely approximates the energy dependence predicted for $\langle \Gamma_i \rangle / D$ in the vicinity of 7 MeV excitation, so the plotted quantities are approximately independent of energy. (By removing the energy dependence in this way instead of using the complete hydrodynamical result, the plotted quantities do not depend explicitly on the giant-dipole resonance parameters.) The dashed curve shows the prediction of the more complete hydrodynamical expression[6,7] which takes into account the nuclear deformation and explains the observed splitting of the giant-dipole resonance in the region of deformed nuclei. In addition, E_g was taken as being given by $E_g = 50\ A^{-1/3} + 5.3$ which is of the form suggested by Carver and Peaselee[8] and which seems to more accurately fit the experimental data.

In addition to the unfortunately large residual effects of the Porter-Thomas fluctuations, as indicated by the error bars, these results suffer from the rather limited range of nuclei which may be investigated in this type of experiment. Therefore, an attempt has been made to extend the results to other mass regions by use of the results of the other types of experiments mentioned above. For example, to reduce the Porter-Thomas fluctuations and interference effects inherent in the thermal results, averages have been taken over results for adjacent nuclei, as well as for different transitions in the same nuclei. Data were included only if the spins and parities of both the initial state and final state were known from

---

[4] H. Steinwedel and J. H. D. Jensen, Z. Naturforsch. 5a, 413 (1950).

[5] Peter Axel, Phys. Rev. 126, 671 (1962).

[6] K. Okomoto, Progr. Theoret. Phys. (Kyoto) 15, 75 (1956).

[7] M. Danos, Nucl. Phys. 5, 23 (1958).

[8] J. H. Carver and D. C. Peaslee, Phys. Rev. 120, 2155 (1960).

independent experiments to be such as to permit E1 transitions. These averages[9,10] are shown as open circles in Fig. 1. The generally good agreement between these points and the resonance-capture points in the mass region where they may be directly compared may give us confidence that the extension outside this region is valid. In the case of the photonuclear results,[11] an attempt was made to discriminate against M1 transitions by considering points on the experimental $\sigma(\gamma, n)$ curves approximately 2 MeV above the neutron threshold. These points were read from published curves. The results are shown as solid squares in Fig. 1. Again, in all cases in which a direct comparison may be made, the agreement is quite satisfactory. This indicates that the procedure used does give a valid indication of the E1 strength function. Finally, the crosses in Fig. 1 are the results of an experiment on the elastic scattering of photons,[12] and the solid triangle is a photofission result.[13] The over-all consistency of all of these data is quite satisfactory and may be taken as good evidence that they are in fact representative of the E1 strength function.

It is apparent that the general trend predicted by the two-fluid hydrodynamical model is followed, but it is also apparent that there is some structure superimposed. It is my opinion that this is real. A plot of the total radiation widths measured for neutron resonances[14] shows a similar structure, only part of which is explained by structure in the nuclear level densities. It would seem that the data shown in Fig. 1 indicate that variations in the E1 strength function also contribute to the observed effect.

---

[9] L. V. Groshev, Atlas of Gamma-Ray Spectra from Radiative Capture of Thermal Neutrons (Pergamon Press, London, 1959).

[10] G. A. Bartholomew, Ann. Rev. Nucl. Sci. 11, 259 (1961).

[11] See E. G. Fuller and Evans Hayward in Nuclear Reactions, edited by P. M. Endt and P. P. Smith (North-Holland Publishing Company, Amsterdam, 1962), Vol. II, Chap. III.

[12] K. Riebel and A. K. Mann, Phys. Rev. 118, 701 (1960).

[13] J. B. Huizenga, K. M. Clarke, J. E. Gindler, and R. Vandenbosch, Nucl. Phys. 34, 439 (1962).

[14] L. M. Bollinger in Nuclear Spectroscopy, ecited by F. Ajzenberg-Selove (Academic Press, New York and London, 1960), Chapter III-E.

Finally, one may ask to what extent the single-particle estimate agrees with these data. Figure 2 shows the same data with the factor E_γ^3 taken as the energy dependence of $\langle\Gamma_i\rangle/D$. The solid curve in

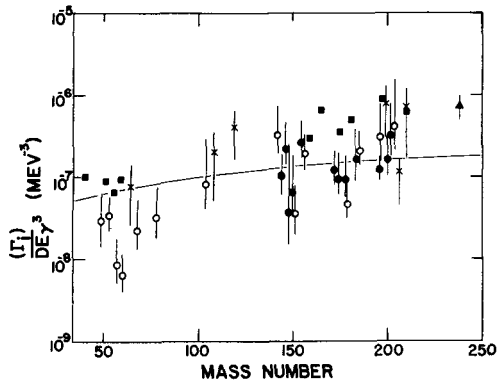

Fig. 2. The data treated according to the single-particle estimate. The symbols used have the same significance as for Fig. 1. The curve corresponds to D_0 = 10 MeV, if one includes a factor 1/4 for the effective nucleon charge.

this figure shows the predicted $A^{2/3}$ mass dependence and corresponds to[15] D_0 = 10 MeV and an effective nucleon charge of $\frac{1}{2}$. Over all, the data are in only somewhat worse agreement with the predicted mass dependence than are the points in Fig. 1. However it is no longer true that there is good agreement between the capture results and the results obtained using the inverse reactions. This may be taken as a clear indication that the energy dependence predicted for $\langle\Gamma_i\rangle/D$ (or, equivalently, for $\langle\sigma_a\rangle$) by the single-particle estimate is a poor approximation.

[15] John M. Blatt and Victor F. Weisskopf, Theoretical Nuclear Physics (John Wiley and Sons, New York, 1952), Chap. 12.

* * *

P. AXEL, University of Illinois: I would like to clarify a semantic problem. The distinction between what we are doing now and what used to be done is not the distinction between the hydrodynamic and the single-particle models. Although Dr. Brink's approach to this problem is more illuminating than the old approach, the old approach does not have to be thrown away. It might, therefore, be worth while to point out the difference between the previous procedure and the current procedure from the

point of view of this old approach, which is called here the single-particle model.

The starting point is the estimate which Weisskopf made to apply to transitions between two low-lying states, each of which was a good single-particle state. However, we are interested in transitions involving levels near 7 MeV in a nucleus, and must not unthinkingly apply the single-particle estimate. If you ask what the single-particle estimate has to do with states at 7 MeV, you realize that it would have direct relevance only if some particular single-particle E1 excitation had an energy of about 7 MeV.

Thus, you can ask whether the nucleus you are considering has a valence nucleon which would be excited strongly by electric dipole to a single-particle-model level near 7 MeV. Depending on the nucleus you consider, there might or might not be such a strong single-particle state near 7 MeV. If there were such a state, one would still have the problem of deciding over what energy range the levels in the actual nucleus contained part of the strength associated with this single state in the model.

However, independent of the valence nucleon, it is clear that heavy nuclei have of the order of 20 core nucleons which can make strong E1 transitions. Furthermore, all of these transitions correspond to energies between about 6 MeV and 9 MeV.

Therefore, the single-particle-model estimate of what dipole strength to expect in the energy region from 6 MeV to 9 MeV is not 1 Weisskopf unit. Instead, it is of the order of 50 Weisskopf units, as can be calculated by evaluating nucleon matrix elements by use of shell-model wave functions. The largeness of this estimate clearly indicates that refinements are needed. However, this is not a new worry because it is well known that the predicted strength has been pushed up in energy to the giant resonance.

In summary, the single-particle description of electric-dipole excitation near 7 MeV is completely inadequate— partly because many different single-particle excitations are possible and partly because the associated strength has been shifted strongly in energy to form the giant resonance. There is no reason to use the single-particle Weisskopf unit to try to describe a 7-MeV transition. When the single-particle model is refined to include particle-hole interactions, the shift of strength to the giant-resonance region seems to be explained. It seems quite likely that this refined model will also be able to account for the transition strengths observed near 7 MeV inasmuch as these strengths seem consistent with extrapolating the giant resonance to 7 MeV.

I think there remains the big question of how to treat electric-dipole transitions of 4 MeV, 3 MeV, 2 MeV, and 1 MeV. I do not think anyone yet knows how to do this; neither experimental evidence nor theoretical guidance is available. However, I do not think that anybody, including firm adherents to the single-particle or shell-model approach, would quarrel with the fact that the estimates of dipole strength obtained by extrapolating the giant resonance are quite similar to what is expected from the refined independent-particle theory including interactions. No one who has looked at the single-particle model critically in recent times has claimed that the gamma-ray strength function near 7 MeV should vary as the cube of the energy.

CARPENTER: Yes, I think it is amusing. The development of the theory was such that even though the hydrodynamical model was available at the same time the single-particle model was, and the principle of detailed balance was known for a half a century, it is only recently being appreciated.

AXEL: This reference to a fact which had been known for a long time but which has just been appreciated reminds me of one other thing. Known for not so long a time, but perhaps relevant, is the fact that the gamma-scattering data mentioned show additional substructure. When

you interpret data obtained in the region of neutron resonances, you should ask whether you may be in a peak or a valley of this gamma-ray-strength substructure. We have some substructure in elastic scattering of gamma rays. Although we do not know whether this substructure exists in all nuclei, we do not have any license to assume that there is a smooth energy dependence without bumps whose width is of the order of a few hundred keV. Certainly if there are peaks and valleys with widths of the order of a few hundred keV, there are ambiguities in data obtained in the neutron resonance region as well as in a lot of other experiments.

III-3. NEUTRON-CAPTURE GAMMA-RAY SPECTRA AND THE M1 GIANT RESONANCE*

I. Bergqvist, B. Lundberg, and N. Starfelt

Research Institute of National Defense, Stockholm, Sweden

It has generally been accepted that all strong γ rays from neutron capture in heavy nuclei are of the electric-dipole type. Calculations of the γ-ray spectra based on the statistical model and assuming the transition probability to be proportional to the cube of the photon energy have given results which differ considerably from the measured spectra in the mass regions $110 \leqslant A \leqslant 140$ and $180 \leqslant A \leqslant 200$. The purpose of this paper is to suggest that magnetic-dipole transitions in the nuclei in these mass regions may compete successfully with the E1 transitions because of the effect of an M1 giant resonance predicted by Mottelson.[1]

Figure 1 shows the gross structure of γ-ray spectra from neutron capture in some of the elements in the two mass regions mentioned.[2] The high-energy part of the spectrum becomes more intense as the closed neutron shells 126 and 82 are approached. Also shown are spectra calculated according to the statistical model. This calculation depends on the level density and the transition probability.

For the spectra in Fig. 1, the level-density formula of Newton was used and the level density for states of spin J was assumed to be proportional to $(2J + 1)$. However, Starfelt[3] has shown that the spectrum changes very little when different estimates of the level density are used.

---

*Presented by I. Bergqvist.

[1] B. R. Mottelson, Proceedings of the International Conference on Nuclear Structure, Kingston, edited by D. A. Bromley and E. W. Vogt (University of Toronto Press, Toronto, 1960), p. 525.

[2] I. Bergqvist and N. Starfelt, Nucl. Phys. 39, 353 and 529 (1963).

[3] N. Starfelt (to be published).

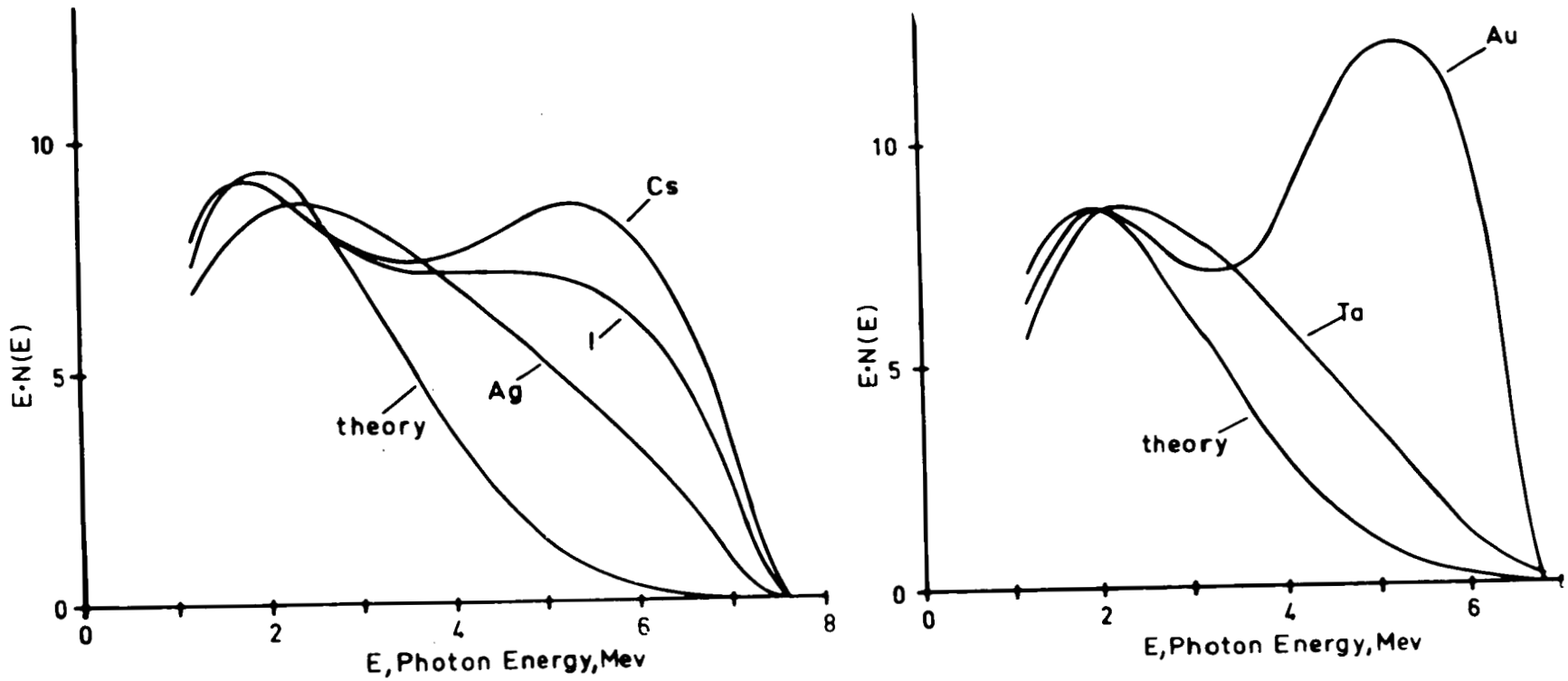

Fig. 1. Gross structure of the γ-ray spectra in the mass regions (a) $110 \leqslant A \leqslant 140$ and (b) $180 \leqslant A \leqslant 200$. The neutron energy was 20 keV in the experiments on the elements Ag to Cs and 15 keV for the Ta and Au. The spectra of Cs and Au calculated from the statistical theory are also shown (Ref. 2).

One must in fact assume a very high concentration of levels at 1 — 2 MeV excitation energy in Au in order to obtain agreement with experiments.

The partial radiation width $\Gamma_{\gamma i}$ for dipole transitions is given by

$$\Gamma_{\gamma i} = f \cdot E_{\gamma}^{3} \cdot D ,$$

where E_{γ} is the photon energy and D is the level spacing (near the capturing state) for levels of the same spin and parity as the capturing state. The factor f, which could be called the reduced γ-ray strength function, is in earlier calculations often assumed to be a constant. This was the case, for example, for the calculated spectra in Fig. 1. However, it is possible to obtain information about the γ-ray strength function from γ-absorption measurements. There are two main limitations to such a procedure. The first is due to the fact that in γ-absorption experiments only transitions from the ground state are studied. We have to make assumptions regarding excited states; in the following we will assume that for each excited state there exists a giant resonance of the same shape and of the same effective energy as that corresponding to the ground state. The second difficulty is connected with extrapolation of the giant resonance from higher energies, where there exist good data from experiments such as (γ, n) reactions, towards lower energies, which are of importance in the capture γ-ray spectra. Two analytical expressions have been used: one by Fuller and Hayward[4] and also by Axel[5] is the Lorentz line shape of the resonance, the other has been used by Lane and Lynn[6] for calcula-

---

[4] E. G. Fuller and Evans Hayward, Nuclear Reactions, edited by Endt, Demeur, and Smith (North Holland Publishing Co., Amsterdam, 1962), Vol. II.

[5] P. Axel, Phys. Rev. 126, 671 (1962).

[6] A. M. Lane and J. E. Lynn, Nucl. Phys. 11, 646 (1959).

tion of capture cross sections. Both of them are discussed in Ref. 3 in some detail. Results of a γ-ray calculation for Au by use of these expressions are shown in Fig. 2. It is obvious that these results do not suffice to explain the experiments for Cs and Au, for example, but possibly do for Ag and Ta.

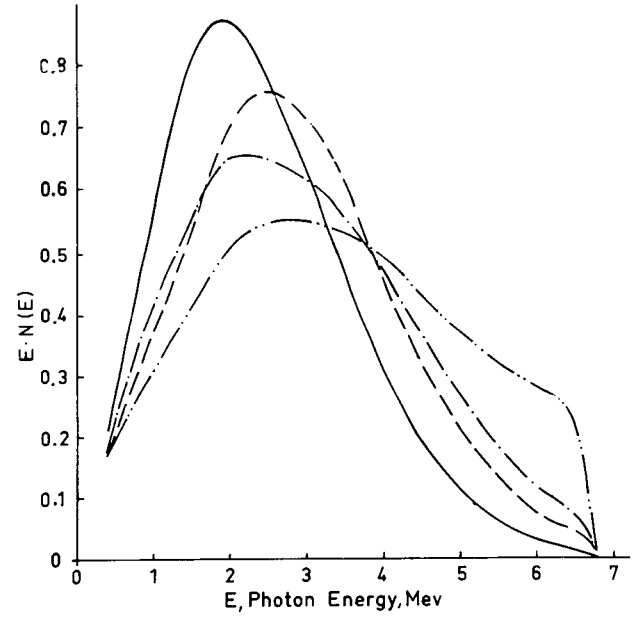

Fig. 2. Gamma-ray spectra for Au calculated taking into account the E1 giant resonance. The dashed curve represents the calculation using the Lorentz line-shape expression (Refs. 4 and 5) and the dot-dashed curves using the shape by Lane and Lynn (Ref. 6). For comparison, the spectrum calculated assuming the γ-ray strength function to be constant is also shown (solid line). A nuclear temperature T=0.7 MeV was used for calculating the spectrum giving the highest intensity of the high-energy γ rays. In the other three spectra, Newton's formula was employed.

It would then be reasonable to explore the effect on the capture γ-ray spectrum of the M1 giant resonance predicted by Mottelson. The position of this resonance should be given by the spin-orbit splitting in the g, h, and i shells. The neutron subshells $i_{13/2}$ and the proton shell $h_{11/2}$ are filled near Pb. M1 transitions can take place to the empty subshells $i_{11/2}$ and $h_{9/2}$ and the spin-orbit splitting is about 5.5 MeV. Close to the closed neutron shell 82, the subshells $h_{11/2}$ and $g_{9/2}$ are filled and the M1 resonance should be due to transitions to the empty subshells $h_{9/2}$ and $g_{7/2}$, respectively. In this case also, the splitting is expected to be about 5.5 MeV. In the calculations (Fig. 3)[3], the M1 giant resonance at 5.5 MeV was assumed to have the same shape as the E1 resonance. The width was assumed to be 1.5 MeV and the strength 1% of the E1 giant resonance, in agreement with the estimate of

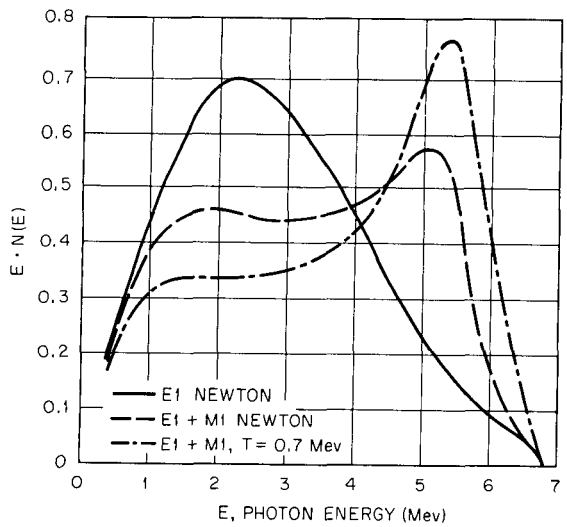

Fig. 3. Gamma-ray spectra for Au calculated taking into account the E1 and M1 giant resonances. The shape of the giant resonance as given by Lane and Lynn (Ref. 6) was used.

Blatt and Weiskopf.[7] It must be concluded that the inclusion of the M1 resonance at the expected resonance energy and with the expected strength is sufficient to obtain agreement with experiments. Furthermore, the variations with mass number of the strengths of the resonances dictated by the population of the $g_{9/2}$, $h_{11/2}$, and $i_{13/2}$ subshells are in agreement with the systematic variation of the experimental γ-ray spectra.

Recent experiments at high neutron energies seem to support the interpretation in terms of a peak in the γ-ray strength function at 5.5 MeV. The γ-ray spectra from the capture of neutrons at 1 MeV and 3.2 MeV in Ta and Au were measured (Fig. 4). On the assumption that the high intensity of the high-energy γ rays is due to a concentration of levels at an excitation energy of 1 —2 MeV, the bump in the spectrum should move with the neutron energy. Similarly, if the effect is due to the tail of the E1 giant resonance, the bump should also vary with the excitation energy and possibly the bump would be more pronounced since the excitation energy is closer to the E1 giant-resonance energy. It is obvious from Fig. 4 that the shape of the spectrum scarcely changes with neutron energy. The higher excitation energy only causes

[7] J. M. Blatt and V. F. Weisskopf, Theoretical Nuclear Physics (John Wiley and Sons, New York, 1952).

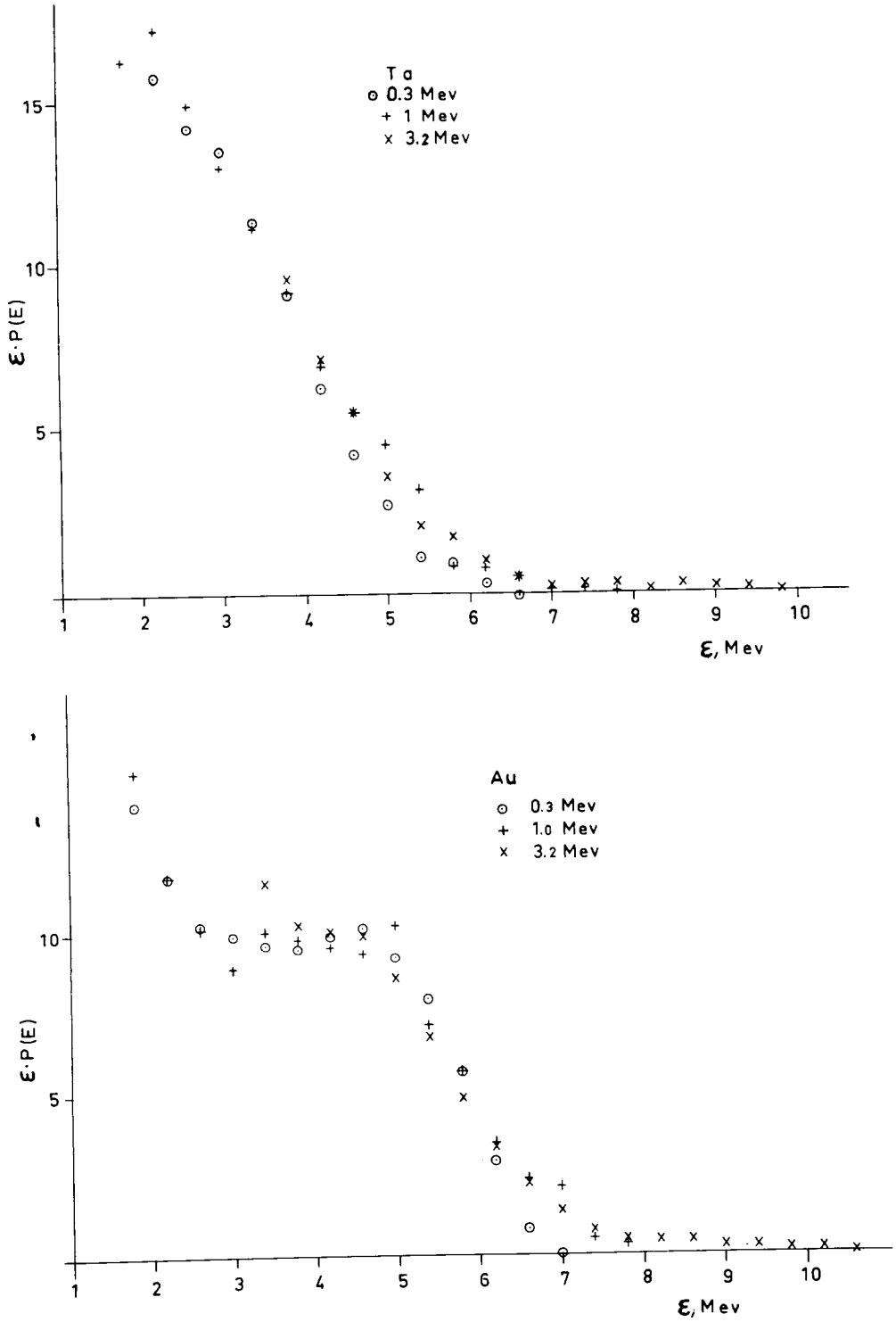

Fig. 4. Experimental pulse distributions $P(\epsilon)$ multiplied by the pulse height ϵ.

the spectra to tail off at a higher photon energy. Thus, the only reasonable conclusion so far is that the anomalous γ-ray spectra are due to a peak in the γ-ray strength function at an energy of about 5.5 MeV.

The experimental results of Harvey et al.[8] on γ-ray spectra from resonance capture in Sn isotopes show that M1 transitions corresponding to photon energies of about 6 MeV may well dominate in the spectrum. This supports the interpretation in terms of an M1 giant resonance.

---

[8] J. A. Harvey, G. G. Slaughter, J. R. Bird, and G. T. Chapman, paper III-4 of this conference.

* * *

J. JULIEN, Centre d'Etudes Nucleaires de Saclay: We have investigated the γ-ray spectrum of gold from neutron resonance capture. About 20 neutron resonances were studied. The intensity of the high-energy γ rays varies from resonance to resonance.

BERGQVIST: We have observed a difference between the spectrum from thermal-neutron capture and that from 15-keV capture which presumably represents average s-wave capture. Most of the difference could be attributed to a decrease of the intensity of the strong lines close to 6.25 MeV.

G. A. BARTHOLOMEW, Chalk River Nuclear Laboratory: In those results from thermal-neutron capture where the spins and parities are established, no strong transitions with known multipolarities have been identified as M1.

BERGQVIST: The only strong identified M1 transitions in these mass regions are those in tin isotopes that will be reported by J. Harvey and collaborators in the next paper (paper III-4). For all the other nuclei, we don't know whether the strong γ rays at about 5.5 MeV are of

E1 or M1 type. The bump in gold, for example, represents transitions to levels at about 1 MeV excitation energy of unknown spins and parities.

P. AXEL, University of Illinois: There is one thing about the curve that was just shown which I do not understand. The curve makes it seem as though there is a strong 5-MeV gamma ray; and if there were one, my guess would be that it is M1. But, where are the E1 transitions from neutron capture in the nucleus? Surely, from the gamma-ray strengths that we see when we do gamma reactions, there must be corresponding gammas in capture experiments. I do not understand why your experiment does not show any of these.

BERGQVIST: In Fig. 2, I showed the results from the calculation of γ-ray spectra by use of the Lorentz line shape of the E1 giant resonance. The spectrum has a maximum at 2 — 3 MeV and is tailing off towards higher energy. When the excitation energy is raised to 9 — 10 MeV, I expect that a similar calculation will show the same general shape of the γ-ray spectrum. Of course the tail will extend up to the maximum photon energy. I think this is also the case experimentally. In Fig. 4, the γ-ray spectra extend up to about 10 MeV, but the high-energy γ rays are not very intense.

AXEL: But I was asking about your data using 3-MeV neutrons in which you can excite 8-MeV states. Why don't you see the corresponding 8-MeV gamma rays?

BERGQVIST: We do see them; but they are weak.

AXEL: The E1 strength that has been shown to be at 8 MeV is stronger than your proposed M1 giant resonance.

BERGQVIST: That does not mean the magnetic giant resonance does not exist, but it does mean the E1 strength at 8 MeV is bigger. Those points show there is some.

AXEL: Yes, there is something, but not enough. The estimates indicate that the electric-dipole strength near 8 MeV is a few percent of the electric-dipole giant resonance. The magnetic-dipole giant

resonance you suggest is only about 1% of the giant electric dipole. These figures imply that there should be a few times the strength of the magnetic dipole appearing as E1 transitions near 8 MeV. There is no such strength near 8 MeV on your figure. Thus, there are two puzzles in that figure: What is at 5 MeV, and why isn't there something at 8 MeV?

BERGQVIST: I do not think there is any contradiction here. The quantity of importance in spectrum calculations is the product of transition probability and density of final states — not the transition probability alone. In order to fit the experimental data in gold, for instance, you have to assume another peak in the γ-ray strength function at about 5.5 MeV with a width of 1 — 2 MeV and an integrated strength of 1 — 2% of the known E1 giant-resonance strength.

R. T. CARPENTER, State University of Iowa, Iowa City: In the first place, I do not think there is necessarily a few percent of the total E1 strength left after you get out of the giant resonance at about 15 MeV. I do not think there is quite that much left below, say, 7 MeV.

AXEL: Are you arguing that I do not know how to extrapolate the resonance? Your experimental numbers, which agree well with my estimates, represent (near 8 MeV) a few percent of the total giant resonance.

CARPENTER: That may be. On the other hand, my numbers are in fair agreement with the average spectra that you get by a calculation of the first type he mentioned — the statistical kind of calculation. Presumably this is the calculation which agrees with the spectra shown in the figure except for this M1 bump.

AXEL: I hate to be controversial. I think that you are not necessarily going to throw light on the question of whether you are seeing M1 or E1 in the 5-MeV part of the spectrum by adjusting E1 transition rates to agree with the observed 1-MeV gamma rays. This adjustment implies a conviction that E1 transitions can be fitted with a smooth,

known, monotonic energy dependence from the giant resonance to 1 MeV. Nobody knows how to describe the 1-MeV gamma-ray transitions. When you calculate the gamma-ray spectrum, you assume that you know how 1-MeV and 2-MeV transitions behave. I think that you end up in those calculations by ignoring what is known about 8-MeV gamma rays and E1 transitions at neighboring energies in order to fit the lower energy gamma rays. This is a very dangerous procedure considering the present state of our knowledge.

D. M. BRINK, Clarendon Laboratory, Oxford: If I remember correctly, the predictions of the Axel formula and of the Weisskopf formula are almost the same for electric-dipole transitions with an energy of 7 MeV or so. Axel's estimate is about 100 times the Weisskopf estimate for the magnetic dipole. According to my calculations, the magnetic dipoles are enhanced by a factor of, say, 40 or 80 or so — maybe even a hundred. I would have thought that the magnetic-dipole transition strengths should be just about the same order of magnitude as the electric-dipole transition strength, I mean partial radiation width.

III-4. GAMMA-RAY SPECTRA FROM RESONANCE NEUTRON CAPTURE IN THE TIN ISOTOPES*

J. A. Harvey, G. G. Slaughter, J. R. Bird,† and G. T. Chapman

Oak Ridge National Laboratory, Oak Ridge, Tennessee

The gamma-ray spectra from neutron capture in individual resonances in samples enriched in the various tin isotopes have been studied with a large sodium iodide crystal. The seven abundant isotopes Sn^{116} to Sn^{124} had isotopic enrichments from 90 to 98% and each sample weighed about 35 g. Only 1—3 g of the isotopes Sn^{112}, Sn^{114}, and Sn^{115} were available with isotopic enrichments from 30—70%. The enriched tin isotopes were all in the metallic form. A 5-m flight path was used with the "fast chopper" spectrometer at the ORR, resulting in a neutron energy resolution width of about 15% up to 200 eV. This resolution is sufficient to resolve most of the resonances in these enriched samples up to about 400 eV. The 9 × 12-in. NaI crystal was shielded with 16 tons of lead and 2 tons of LiH to reduce the background.

The time-of-flight spectrum for gamma rays from the Sn^{124} sample producing pulses in a pulse-height gate from channels 74 to 87 (i.e., from about 4.9 to 5.9 MeV) is shown in the left-hand side of Fig. 1. The peak at channel 29 is the zero-time peak and the one at channel 73 corresponds to the 62-eV resonance. The pulse-height spectrum produced in the time interval from 68—78 μsec (i.e., the 62-eV resonance) is shown in the right-hand side of Fig. 1. The pulse-height spectrum has been corrected for background, which was taken with a B^{10} filter with a transmission of 2% at 62 eV. The background was about 10% of the peak at channel 83. The NaI crystal was calibrated with low-energy radioactive sources, the 4.4-MeV gamma ray from a PoBe source, and thermal-neutron-capture gamma rays from Pb, Fe, and N.

---

*Presented by J. A. Harvey

†Visitor from AERE, Harwell, England.

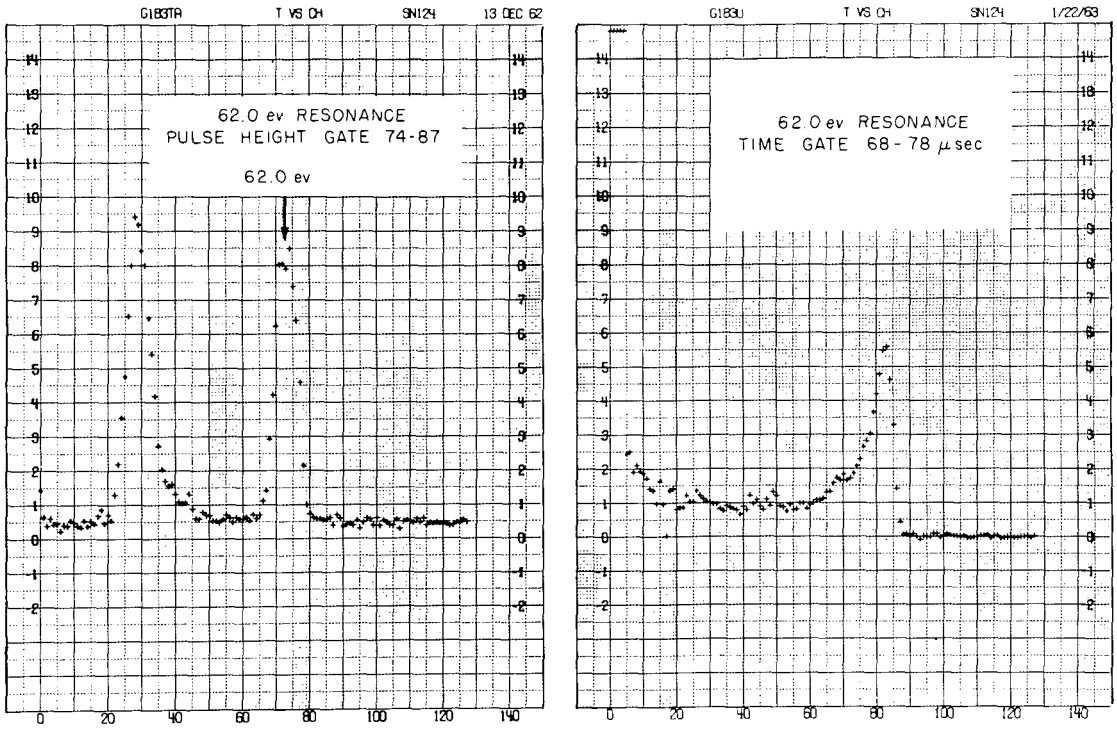

Fig. 1. Gamma rays from neutron capture in the 62.0-eV resonance of Sn^{124}. Left-hand graph: time-of-flight spectrum with the pulse-height gate from about 4.9 to 5.9 MeV. Right-hand graph: Pulse-height spectrum produced in the time interval from 68 to 78 μsec (the 62-eV resonance).

The relative strengths $[\Gamma_\gamma(E_\gamma)/\Gamma_\gamma]$ of the high-energy transitions from the tin resonances can be determined from the observed pulse-height distribution if the response matrix is known for the crystal (including the effect on the gamma rays of the fast-neutron shielding between the tin samples and the crystal). An approximate technique (accurate to within a factor of 2) was used to estimate the relative strengths of the high-energy transitions from the pulse-height spectra since a detailed unfolding program was not available. A summary of the results on the resonances which showed strong high-energy gamma rays is given in Table I. Some of these strong gamma rays comprise about 50% of the capture spectra. The gamma-ray energies are accurate to about 0.1 MeV.

TABLE I. Summary of strong M1 transitions from resonances in tin.

Isotope	D (eV)	E_γ (MeV)	E_n (eV)	$\nu_\gamma = \frac{\Gamma_\gamma(E_\gamma)}{\Gamma_\gamma}$	$\frac{k(M1)_{exp}}{E(M1)_{B\&W}}$	Parity of capturing state
Sn^{124}	400	5.65	62	0.50	540	-
		5.46	62	0.15	180	-
Sn^{122}	400	5.81	107	0.50	500	-or +
			260	0.19	190	-or +
Sn^{120}	200	6.05	427	0.13	140	probably+
Sn^{118}	180	6.48	46	0.36	570	probably+
			360	0.25	400	+
Sn^{116}	180	6.86	111	0.023	31	+
			148	0.22	290	probably+
Sn^{117}	25	9.3	39	~0.003	~11	+
		8.0	39	0.09	500	+
	25	9.3	{196}	0.05	200	probably+
		8.0	{201}	0.04	250	probably+

The average level spacings D were taken from Fuketa *et al.*[1] The spectra from resonance capture in the target nuclide Sn^{119} did not show strong high-energy gamma rays. The Sn^{112}, Sn^{114}, and Sn^{115} samples were too small for us to obtain significant resonance-capture data.

The low-lying excited states of the odd-A tin nuclides Sn^{117} to Sn^{125} are known to have the spins and parities $\frac{1}{2}^+$, $\frac{3}{2}^+$, and $\frac{11}{2}^-$ from the work of Kisslinger and Sorensen[2] and from (d, p) measurements.[3]

[1] T. Fuketa, F. A. Khan, and J. A. Harvey, Oak Ridge National Laboratory Report, ORNL-3425.

[2] L. S. Kisslinger and R. A. Sorensen, Kgl. Danske Videnskab. Selskab, Mat.-fys. Medd., No. 9 (1960).

[3] B. L. Cohen and R. E. Price, Phys. Rev. 121, 1441 (1961).

In Sn^{118} there is a 2^+ excited state at 1.22 MeV. Since most of the low-energy neutron resonances measured are much too strong to be p-wave resonances, the capturing state for the even-A target nuclides must be $\frac{1}{2}^+$; hence the high-energy transitions must be M1, E2, or of higher multipolarity. The strengths of the transitions (assuming M1) are computed from the formula

$$k(M1)_{exp} = \frac{\nu_\gamma \Gamma_\gamma}{E_\gamma^{\,3} (D \times 10^{-6})} ,$$

where $\nu_\gamma = \Gamma_\gamma(E_\gamma)/\Gamma_\gamma$, $\Gamma_\gamma = 0.11$ eV, E_γ is in MeV, and D is in eV.

The theoretical estimate of Blatt and Weisskopf as given by Bartholomew[4] is

$$k(M1)_{B\&W} = \frac{0.021}{D_0} = 1.40 \times 10^{-3} \qquad \text{for } D_0 = 15 \text{ MeV}.$$

The strengths of these M1 transitions (Table I) are hundreds of times larger than the theoretical estimate of Blatt and Weisskopf and more than ten times as large as the strongest M1 transitions[4] previously measured in this mass region.

The gamma-ray spectra from thermal-neutron capture have also been measured. On the assumption that thermal capture is due to s-wave neutrons, the M1 ground-state transition from capture in Sn^{117} is enhanced by a factor of 110 and by about a factor of 15 for the other isotopes.

Enhanced M1 transitions in this mass region have been postulated by Bergqvist et al.[5] to account for the gamma-ray spectra in this mass region. An M1 giant resonance with a resonance energy of

---

[4] G. A. Bartholomew, Ann. Rev. Nucl. Sci. 11, 259 (1961).

[5] I. Bergqvist, B. Lundberg, and N. Starfelt, paper III-3 of this conference.

about 5.5 MeV and 1.5 MeV wide, as predicted by Mottelson, gave good agreement with their data. This M1 giant resonance should occur at an energy corresponding to the spin-orbit coupling energy, which in the mass region of tin is the difference between the nearly filled $g_{9/2}$ shell and the empty $g_{7/2}$ shell.

* * *

I. BERGQVIST, Research Institute of National Defense, Stockholm: Did you also measure the radiation widths for these resonances?

HARVEY: Thank you for the question. We have transmission data on the enriched samples and have analyzed the 39-, the 45-, and the 62-eV resonances. A value of about 110×10^{-3} eV was obtained. This value, which I would say is good within about a factor of 2, is the one we used in the calculations.

BERGQVIST: Yes. The total radiation widths can fluctuate very much from resonance to resonance.

HARVEY: Right. When we get the samples back from Harwell, we will try to measure the radiation widths for all the resonances listed in the table.

P. AXEL, University of Illinois: I would like to ask a question of Dr. Bergqvist or the speaker about this. We have been told by theoreticians that maybe 1% of the electric dipole is an M1 giant resonance. Dr. Bergqvist told us that he has evidence for that resonance being at 5 MeV, and now you have evidence for it being at 9 MeV.

HARVEY: For the even-A isotopes, the gamma rays are from 5.5 to 6.5 MeV. Only Sn^{117} showed the 9-MeV gamma ray.

AXEL: But in this one case it was 100 times the single-particle M1 estimate, it is an M1, and it is at 9 MeV.

HARVEY: Right. But all the strong M1 gamma rays are always 5.5—6.5 MeV.

I would also like to comment on Carpenter's statement concerning the Porter-Thomas distribution. Small values from the

distribution are quite probable but the chance of getting a value 5 or 10 times the average is pretty small.

R. T. CARPENTER, State University of Iowa, Iowa City: If the resonance in Sn^{124} is a p-wave resonance, it must have an extremely large reduced neutron width.

HARVEY: If we assume that the p-wave level spacing is the same as the s-wave, it would give a p-wave strength function of 360×10^{-4}, which is rather large.

CARPENTER: You have one anomaly or another.

HARVEY: Yes, that is right.

cat ad HDC-5990; CONF-346-1 C-12-26-63

III-5. THERMAL NEUTRON CAPTURE IN D AND O^{16} *†

E. T. Jurney and H. T. Motz

Los Alamos Scientific Laboratory, Los Alamos, New Mexico

Thermal-neutron-capture cross sections of several low-Z target nuclei have recently been determined by direct observation of the capture-gamma-ray spectra. In particular, O^{16} and D have been examined, and detailed results will be given. Capture-cross-section measurements for other nuclei will be given in tabular form.

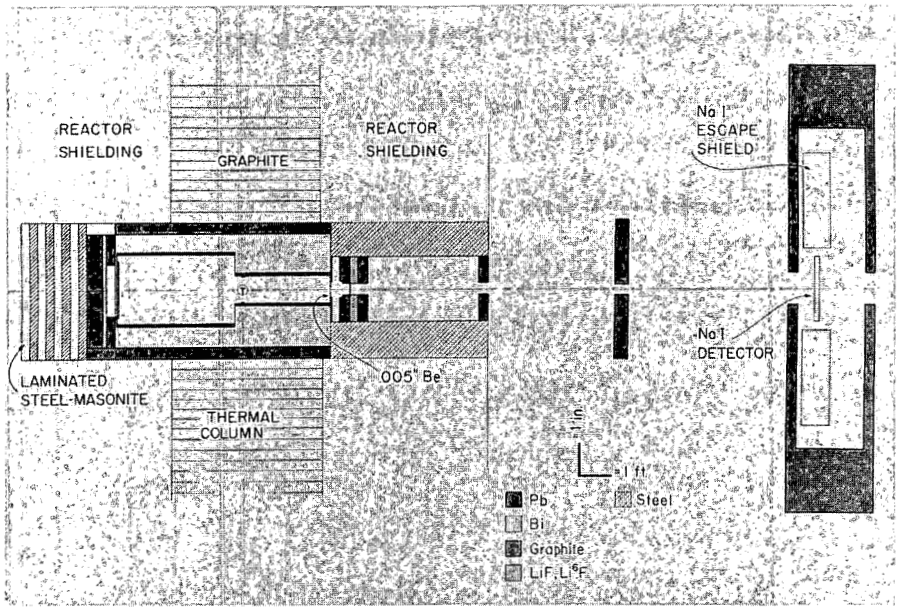

Fig. 1. Experimental arrangement at the Omega West reactor. Note the distorted scale. Target containers are placed at position T.

Figure 1 shows the experimental arrangement (note distorted scale). A $3\frac{1}{2}$-in. square cross section bismuth channel, with a $1\frac{1}{2}$-in. port along its long axis, has been installed transversely through the thermal column of the Los Alamos Omega West reactor, extending into the reactor shield at the far end, and joining to a γ-ray collimator

*Work performed under the auspices of the U.S. Atomic Energy Commission.

†Presented by E. T. Jurney.

at the near end. The collimator is removable to allow for easy insertion of targets to the position T at the center line of the thermal column, where the thermal neutron flux is about 2×10^{11} neutrons/cm^2-sec. Neutrons are excluded from the γ-ray beam by LiF and Li^6F filters. The end of the collimator is fitted with a 0.005-in. Be window and an O-ring seal so that the channel can be evacuated to remove the substantial $N^{14}(n,\gamma)$ source of background from air, or can be filled with gas to serve as a gas target. After further collimation, the γ-ray beam is detected with a NaI crystal 6-in. long by $2\frac{1}{2}$-in. in diam, placed inside an NaI annulus (12-in. long by 8-in. in diameter) operated in anticoincidence. The latter effectively suppresses escape pulses from the detecting crystal.[1] Backgrounds are low enough to permit detection of transitions corresponding to about 0.1 mb of capture in gas targets at 1 atm.

In order to get accurate relative line intensities and energies from a spectrum, a least-squares fitting analysis is made with an IBM-7090 computer. The fitted function is composed of two main parts: (1) A Gaussian component corresponds to the full-energy peak; above about 3 MeV an exponential "tail" is smoothed onto the low-energy side of the Gaussian. (2) One or more exponential terms can be combined with a constant term to fit the background continuum. This combination allows fits to be extended frequently to background-counting-rate ranges greater than a decade.

Two targets of D_2O having substantially different O^{17} and O^{18} enrichments were examined for lines from O^{16} capture. The spectra from the two targets were practically identical; one of them is shown in Fig. 2. The three lines attributable to O^{16} capture agree well in energy with three of the four expected from the known level scheme of O^{17}. The fourth is masked by a contaminating $H^1(n,\gamma)$ line. Contribution from

[1] C. C. Trail and S. Raboy, Rev. Sci. Instr. 30, 425 (1959).

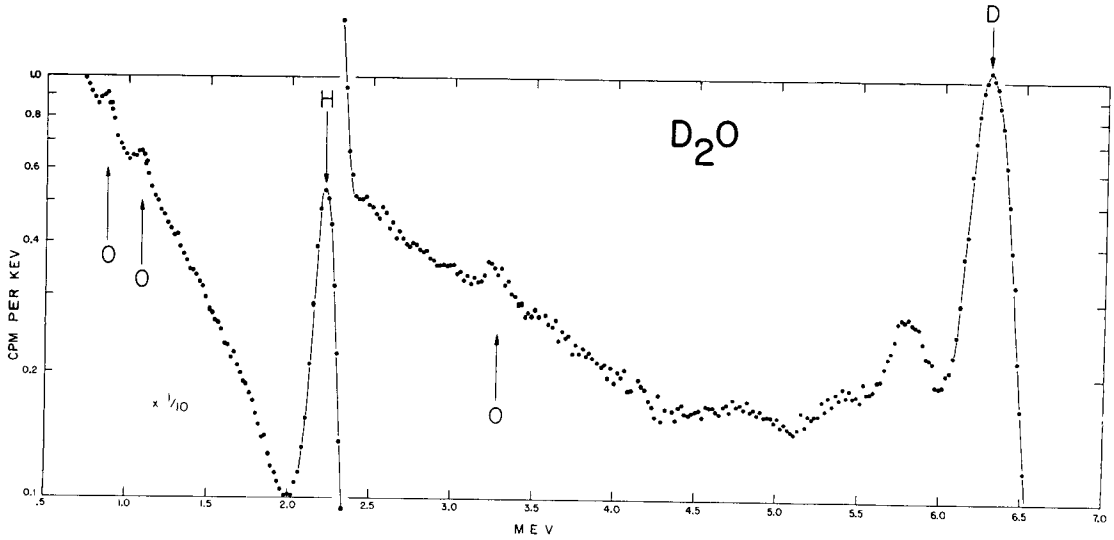

Fig. 2. Capture-gamma spectrum from a D_2O target. The strong hydrogen line is from about 200 ppm ordinary water contamination.

thermal-column background and from the source container have been subtracted.

In order to confirm the existence of the missing line, expected at about 2185 keV, a target of 1300 mm Hg of spectroscopically pure oxygen gas was introduced into the channel. Figure 3 shows the resulting spectrum. A slight mismatch in subtracting the thermal-column background evidently produced the dips in the wings of the 2185-keV line.

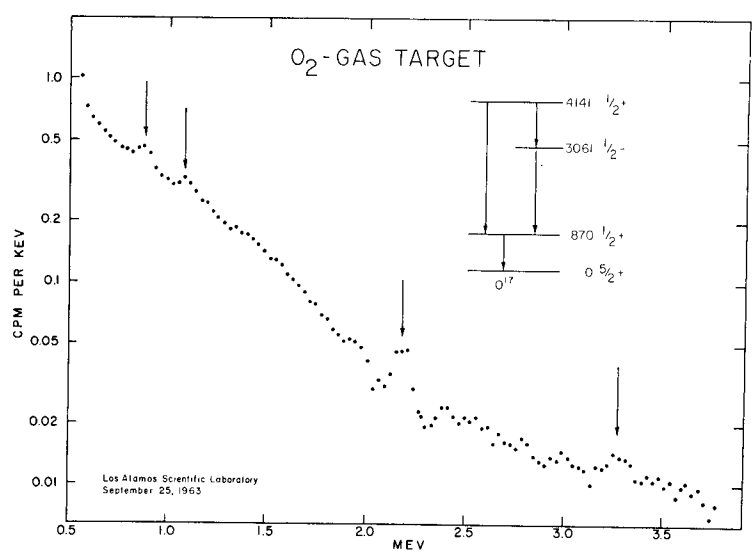

Fig. 3. Spectrum of $O^{16}(n,\gamma)$. The target was about 0.03 moles of O_2 gas.

The energies and intensities observed are consistent with the decay scheme for O^{17} shown in the figure. Although the ratio of the reduced transition probabilities for the 1090- and 3270-keV lines (E1/M1) is somewhat high at about 120, the intensities cannot be taken to be inconsistent with the accepted spin assignments.

Extraction of cross-section information from these data has been done in the following way. For the liquid D_2O targets, 1 ml of the 33-ml total of target material was replaced with ordinary water and the net increase in the intensity of the hydrogen line was measured. This gave the intensity from a known amount of "standard" in a counting geometry identical with that of the undiluted D_2O targets, which, with a curve of detector sensitivity vs energy, permitted calculation of the partial capture cross sections for each transition in the unknown spectrum. For gas targets, the sensitivity curve has been normalized to the hydrogen line (by use of a CH_4 target) to give partial capture cross sections directly for a known target pressure. The weighted mean of O^{16} capture cross sections for the three targets is 178 ± 25 μb.

Much of the error in these measurements comes from an insufficiently accurate detector-sensitivity curve. Thus, for the case of deuterium, Pb^{207} capture gives a more suitable standard than H^1 capture, since the sensitivity difference between the 6260-keV $D(n, \gamma)$ transition and the 7370-keV Pb^{208} ground-state transition is small, and since the Pb^{207} cross section is known well.[2] Figure 4 shows the relative intensity of the $D(n, \gamma)$ transition and the $Pb^{207}(n, \gamma)$ ground-state transition, from a target containing 6.1 g/cm^2 of D_2O and 1.4 g/cm^2 of natural lead. Part of what appears to be an abnormally large 1-quantum-escape peak below

---

[2] D. Jowett, S. K. Pattenden, H. Rose, V. G. Small, and R. B. Tattersall, in AERE R/R 2516, have measured the natural Pb capture cross section as 171 ± 2 mb. Our results show $\sigma_c(Pb^{204}) = (0.94 \pm 0.07)\,\sigma_c(Pb^{207})$, and $\sigma_c(Pb^{206}) = (0.043 \pm 0.001)\sigma_c(Pb^{207})$. Combining these data gives a value of $\sigma_c(Pb^{207}) = 709 \pm 10$ mb.

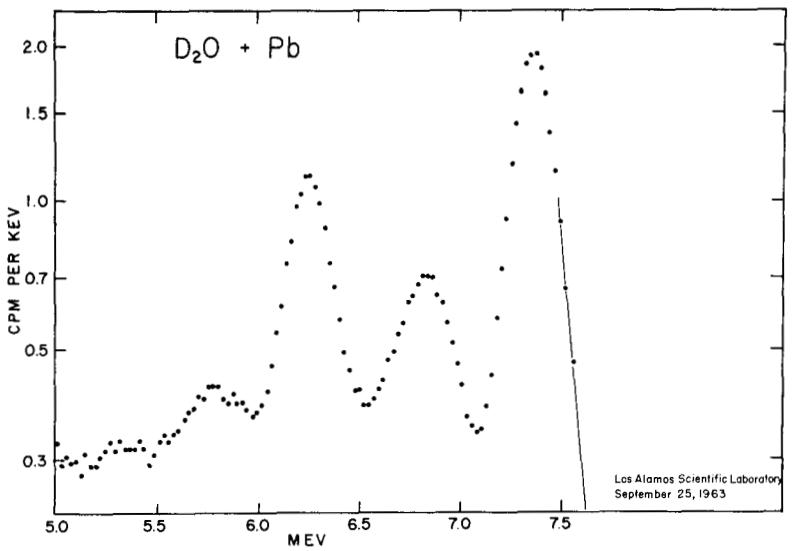

Fig. 4. Capture gamma-ray spectrum from a mixed target of D_2O and Pb. The peak at about 6.8 MeV includes both a one-quantum-escape peak from the 7.37-MeV Pb^{208} line and the 6.735-MeV ground-state transition in Pb^{207}.

the Pb line is the ground-state transition from $Pb^{206}(n,\gamma)$. After correcting for the small difference in detector sensitivity, the ratio of line intensities from Pb and D_2 capture yields a value of 0.60 ± 0.05 mb for deuterium capture.

The total capture cross section can also be deduced by summing the product of line energy times partial capture cross section over the entire spectrum and dividing the sum by the neutron binding energy. This approach has the advantage that no knowledge of the decay scheme of the capturing nucleus is necessary, but it assumes that no line of the spectrum is missed (e.g., through electron capture) and that contaminating lines are not present in the spectrum. Some of the cross sections (marked with an asterisk in Table I) have been arrived at in this way.

* * *

S. RABOY, Argonne National Laboratory: I would like to make two remarks, one of which is in question form. I would like to know if you calculated the cross section for your $D(n,\gamma)T$ reaction in terms of the $H(n,\gamma)D$ reaction. The relevant efficiencies of your scintillation counter for these gamma rays can be obtained by a Monte Carlo technique. I would be interested to see how this compares with your result referred

TABLE I. Thermal-neutron-capture cross sections from the direct observation of capture-gamma-ray spectra.

Target nucleus	σ_c (millibarns)	
	LASL	BNL-325 (2nd edition)
D^2	0.60 ± 0.05	0.57 ± 0.01
Be^9	9.2 ± 1.5[a]	10.0 ± 1[b]
O^{16}	0.178 ± 0.025	<0.2
C^{12} (CH_4 gas)	3.8 ± 0.4[a]	3.73 ± 0.02
N^{14}	75.0 ± 7.5[a]	80 ± 20

[a] Values not based on knowledge of the decay scheme.

[b] $\sigma = 7.5 \pm 1$ [Jarczyk et al., Helv. Phys. Acta 34, 483 (1961)]; $\sigma < 9$ [D. Jowett et al., Ref. 2.]

to the cross section of Pb^{208}.

My second remark is with reference to your $D(n,\gamma)T$ measurement referred to Pb^{208}. I would like to suggest a possible source of systematic error in your measurement. I think you had about 30 g of D_2O in your sample. The bulk of the captures in D_2O come after multiple scattering in the D_2O, so that the neutron flux seen by the D_2O is different from the flux seen by your plates of lead. I would like to suggest that this is a source of systematic error and, of course, it makes your measured cross section too large. After all, the capture cross section of about 0.5 mb competes with the scattering cross section of about 10 b.

JURNEY: First of all, we have referred the capture cross section of deuterium to hydrogen in much the same way as for the oxygen. The agreement is not as good as we would like, but we would like to blame this on the fact that we do not know the sensitivity correction quite well

enough to do this. It is a very broad energy region from 2.2 to 6.2 MeV. The correction, we think, is a matter of a factor of 2; that is, the sensitivity is different by a factor of 2.

H. MOTZ, Los Alamos Scientific Laboratory: I think that the pile-oscillator measurements which correct for multiple scattering would indicate that with our size of sample the correction is not comparable to the 10% error that we assigned to the cross section.

III-6. Withdrawn at the request of the authors.

III-7. STUDY OF THE NEUTRON-CAPTURE GAMMA RAYS IN Ca^{48}†‡

Sol Raboy and C. C. Trail

Argonne National Laboratory, Argonne, Illinois

We have a facility at Argonne for the study of the gamma rays that result from absorption of neutrons by various nuclei with very low cross section and/or by samples containing only small numbers of the atoms of interest.

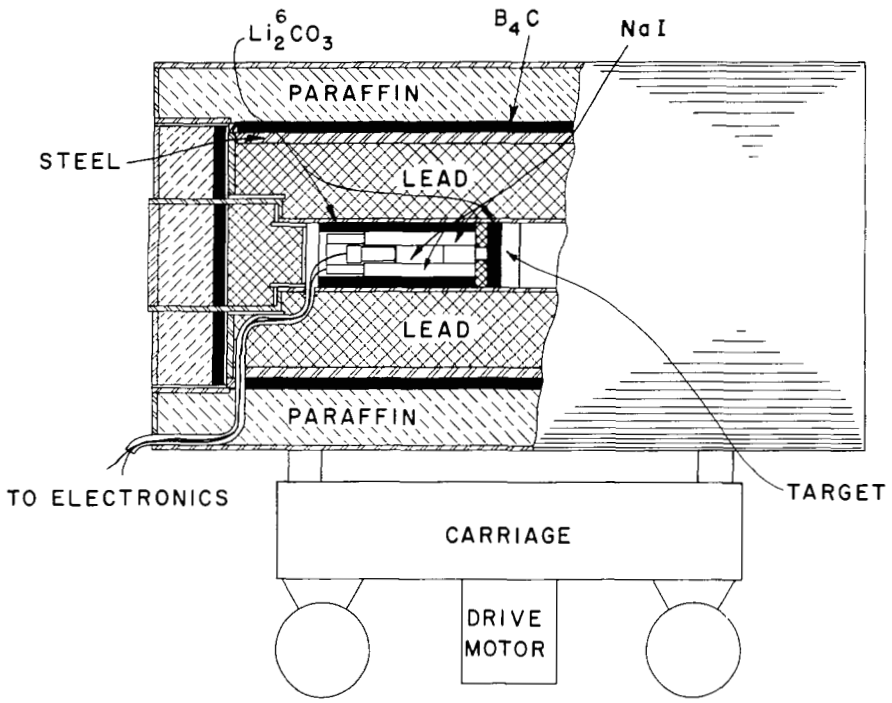

Fig. 1. Counter arrangement and shield for neutron-capture work.

Figure 1 shows our detecting arrangement. It consists of a cylinder of sodium iodide (2.5 in. in diameter and 6 in. long) within an annulus of sodium iodide (12 in. long and 8 in. in diameter), and the necessary photomultiplier tubes. There are two such counters in our system. They are enclosed in the 13-ton shield. I think we are outclassed by the

†Work performed under the auspices of the U.S. Atomic Energy Commission.

‡Presented by Sol Raboy.

Oak Ridge shield shown earlier. We have a slot in this shield through which our neutrons pass. The specimen to be studied is placed in the center of this slot so it can be seen by the two counters.

We have a homemade 2D coincidence system in which the output of one counter feeds into an analyzer with four channels of variable width; and the spectrum in coincidence with each of these channels is recorded in one of four banks of 128 channels in a 512-channel analyzer. The output of the second counter goes into the 512-channel analyzer when in coincidence with the output of any of the four variable windows.

We have started with 1 g of Ca^{48}, which is about 90% abundant in this sample. We estimate from the abundance and from the cross sections of the other calcium isotopes that 6% of our captures in this specimen are from Ca^{40} and about 6% in Ca^{42}; everything else is much smaller.

The neutron beam is very clean—free of γ-ray background—by virtue of being reflected from a 40-in. cobalt mirror borrowed from G. R. Ringo. The neutrons are almost entirely subthermal.

Figure 2 presents the singles spectrum of Ca^{48}. The γ ray at about 5.6 MeV represents the transition in Ca^{40}. The full-energy

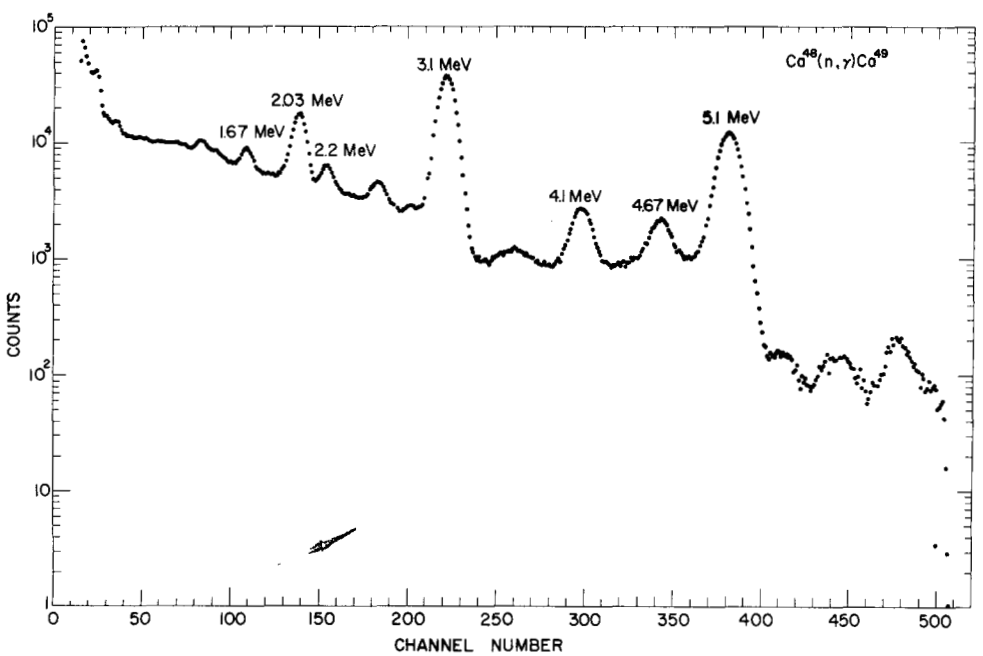

Fig. 2. Singles spectrum of $Ca^{48}(n,\gamma)Ca^{49}$.

jump at about channel 380 is 5.1 MeV, and the other two transitions that we have identified in Ca^{49} are at 3.1 and 2.03 MeV.

Now, Ca^{49} is β active with an 8-min half-life. By turning the beam off and observing the spectrum, we have decided that the 4.11-MeV peak is completely due to the 8-min activity and that part of the gamma ray at 3.1 MeV is also in the 8-min activity. We have interpreted this 4.6-MeV gamma ray as being a one-quantum escape from the 5.1-MeV transition.

We have studied this 8.8-MeV activity to see what we would have to subtract from the $Ca^{48}(n,\gamma)Ca^{49}$ spectrum. Figure 3 is the spectrum we obtained. We normalized it and subtracted it from the previous spectrum.

Figure 4 shows some coincidence work in which a window was set on the 3.1-MeV peak. We get the 2.1-MeV gamma ray in coincidence with this.

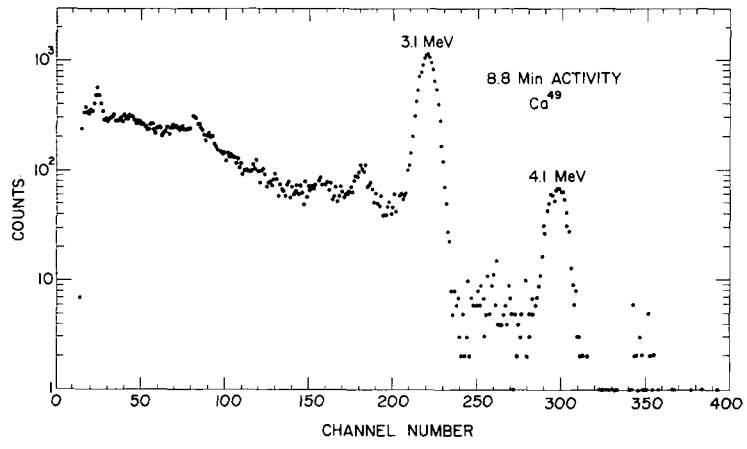

Fig. 3. Gamma-ray spectrum of the 8.8-min activity in Ca^{49}.

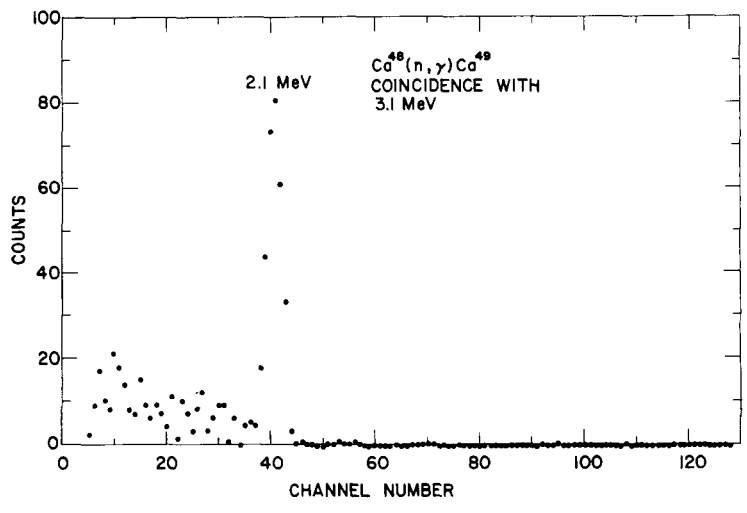

Fig. 4. Spectrum of all coincidences with the γ ray at 3.1 MeV.

Figure 5 shows the spectrum in coincidence with the 2.1-MeV peak. We get the 3.1-MeV peak and something at 2.2 MeV. If you remember from Fig. 2, there was a suggestion of something at 2.2 MeV.

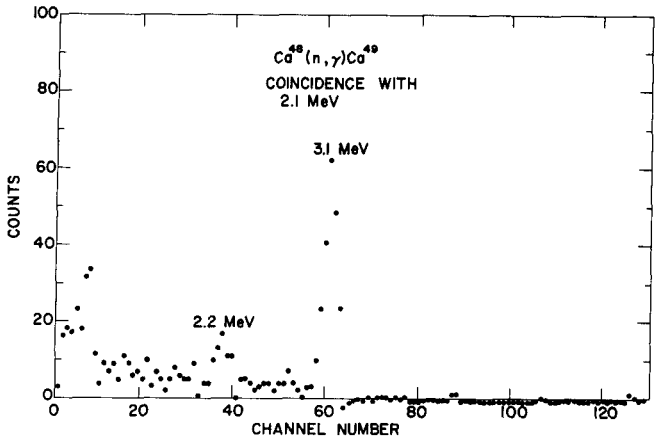

Fig. 5. Spectrum of all coincidences with the γ ray at 2.03 MeV.

At this time we think that parts of both the 2.1- and the 2.2-MeV peaks come from the $Ca^{40}(n, \gamma)Ca^{41}$. We are not sure of this yet. We have to study the other calcium isotopes to see what they look like so that we can make more sense out of this. Using our computer program, we can say at this time that the ratio of the 5.1-MeV intensity to the 3.1-MeV intensity is somewhere around 3.5:1.

III-8. NEUTRON CAPTURE BY DEUTERIUM* †

C. C. Trail and S. Raboy

Argonne National Laboratory, Argonne, Illinois

Some time ago it was pointed out by Blin-Stoyle and Feshbach[1] that the neutron-deuterium reaction was a particularly sensitive one for studying parity nonconservation in the strong interactions. They estimate that from this reaction one gets an enhancement factor of roughly 100. The type of experiment that they suggest is to measure the yield of the capture gamma rays as a function of the polarization of the incident neutron. Since we have an intense beam of polarized neutrons, we decided to look to see if this reaction was available to the experimentalist, even though the cross section is very small.

Heretofore the gamma ray has been seen[2] from capture in the moderating water of the reactor; no beam work has been reported. As a preliminary investigation with our sensitive gamma-ray spectrometer, our efficient shield, and our intense polarized beam, we would like to report on the capture cross section and the energy of the gamma ray from this reaction.

---

*Work performed under the auspices of the U. S. Atomic Energy Commission.

†Presented by C. C. Trail.

[1] R. J. Blin-Stoyle and Herman Feshbach, Nucl. Phys. 27, 395 (1961).

[2] B. B. Kinsey and G. A. Bartholomew, Phys. Rev. 80, 918 (1950).

We measured the energy of the neutrons rather crudely by a gold transmission technique, and found the energy of the neutrons to be 0.01 eV.

Figure 1 shows the spectrum we get from about 120 ml of heavy water with about 3% impurity of light water in a Teflon container.

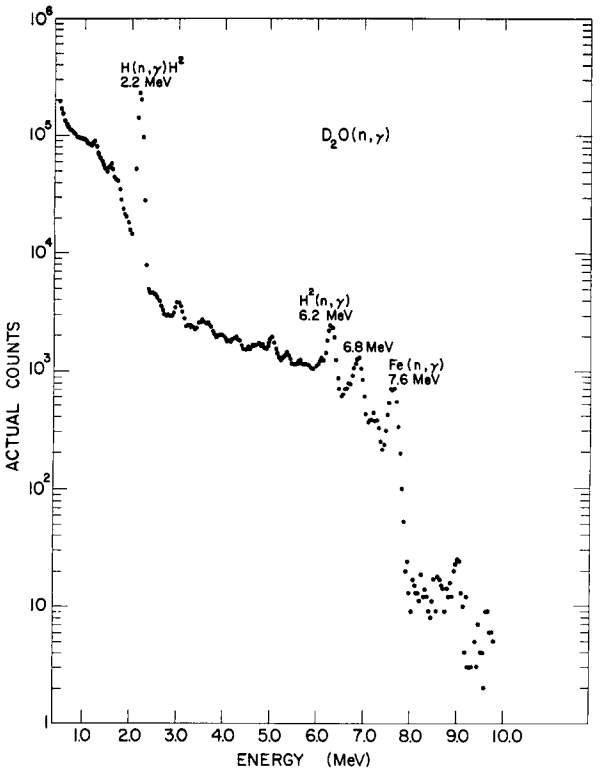

Fig. 1. The gamma-ray spectrum from neutrons incident on heavy water containing about 3% light water.

At 7.6 MeV we see an iron gamma ray from neutron capture by the shielding. The gamma ray of interest is at 6.2 MeV. A gamma ray at 6.8 MeV is always in our background and is somehow related to the fast-neutron contamination in the beam. The light-water gamma ray is at 2.2 MeV.

Our procedure is to take a background from light water and normalize it to the gamma rays from Fe, subtract it from the heavy-water spectrum, and make a least-squares fit to a Gaussian to get the parameters for the Gaussian describing the 6.2-MeV peak. We use a similar procedure with a sample of pure heavy water to get the parameters for the peak at 2.2 MeV. The results for a typical run are shown in

TABLE I. Parameters for the Gaussian-plus-background function

$$a_1 \exp\left[-\frac{(a_2 - x)^2}{a_3^2}\right] + a_4$$

for the two gamma rays. The parameters are determined by a χ^2-minimization fit to the data.

Gamma-ray energy (MeV)	a_1 (counts)	a_2 (channels)	a_3 (channels)	a_4 (counts)	χ^2 Calc.	χ^2 Expected
2.2	$(2.316 \pm 0.013) \times 10^5$	48.505 ± 0.006	1.701 ± 0.009	1152 ± 307	32	4
6.2	2044 ± 75	149.65 ± 0.09	3.14 ± 0.16	189 ± 65	6	7

Table I. For the two gamma rays it lists the amplitudes of the Gaussians, their peak positions, their widths, any residual backgrounds (assumed constant over the region of the fit), the calculated χ^2 and the χ^2 expected from the number of parameters, and the number of channels used. Whenever χ^2 was larger than expected, the errors have been increased.

Table II gives the ratio of $a_1 a_3$ for the gamma ray from

TABLE II. Ratios of the areas of the photopeaks of the gamma rays from neutron capture by hydrogen and deuterium. The uncertainty in the weighted average includes an estimate of the systematic error in the determination of the ratio.

Run No.	$(a_1 a_3)_D/(a_1 a_3)_H$
425	$(1.82 \pm 0.18) \times 10^{-2}$
426	$(1.63 \pm 0.11) \times 10^{-2}$
427	$(1.60 \pm 0.10) \times 10^{-2}$
428	$(1.62 \pm 0.12) \times 10^{-2}$
825	$(1.65 \pm 0.16) \times 10^{-2}$
826	$(1.59 \pm 0.08) \times 10^{-2}$
827	$(1.56 \pm 0.06) \times 10^{-2}$
828	$(1.71 \pm 0.13) \times 10^{-2}$
Weighted average =	$(1.61 \pm 0.11) \times 10^{-2}$

deuterium to that from hydrogen for each of 8 runs. The product $\alpha_1\alpha_3$ is proportional to the area under the Gaussian. The weighted average of these ratios is 1.61×10^{-2}. To get the ratio of capture cross sections, we have to correct for the attenuation of the gamma rays by the neutron shielding and sample, the relative abundances of the capturing nuclei, and the photoefficiency of the counter.

A Monte Carlo calculation showed that the ratio of the photoefficiencies was about 2.26 ± 0.11. The error includes an estimate of the possible systematic error of the Monte Carlo calculation, an error that is pretty hard to evaluate. We have made some effort to check the Monte Carlo calculation by looking at cascade gamma rays which are known to be in a 1: 1 ratio, but we have not been able to check this out as high as 6 MeV.

Before and after the neutron-capture experiment, the relative abundance of D and H was determined with an infrared spectrometer. The isotopic abundance of light hydrogen in the sample was found to be $(3.52 \pm 0.03)\%$. The amount of light water in the sample of heavy water used for background subtraction was $(0.40 \pm 0.01)\%$.

The errors associated with the determination of the ratios of the areas of the photopeaks, treated as systematic errors, amount to 7%. In addition, there is a 3% uncertainty in the relative attenuation of the gamma rays, 1% in the relative isotopic abundances, and 5% from the Monte Carlo calculation. The combination of these errors yields an uncertainty of about 10% in the ratio of cross sections.

Our result for the ratio of capture cross sections is $\sigma_D/\sigma_H = (1.06 \pm 0.11) \times 10^{-3}$. If we assume that the capture cross sections of both isotopes have the same energy dependence below thermal neutron energy and use[3] $\sigma_H = 332 \pm 2$ mb, then we find $\sigma_D = 353 \pm 35$ μb.

---

[3] S. P. Harris, C. O. Muehlhause, D. Rose, H. P. Schroeder, G. E. Thomas, Jr., and S. Wexler, Phys. Rev. 91, 125 (1953).

To measure the energy of the gamma ray, we used a sample of deuterated polyethylene with some light hydrogen as a contaminant. The two lines from neutron capture in graphite were also used for the energy calibration. Also, some iron wire was embedded in the sample of deuterated polyethylene to enhance the 7.6-MeV iron gamma ray so that it could be used as a standard. Figure 2 shows the gamma-ray

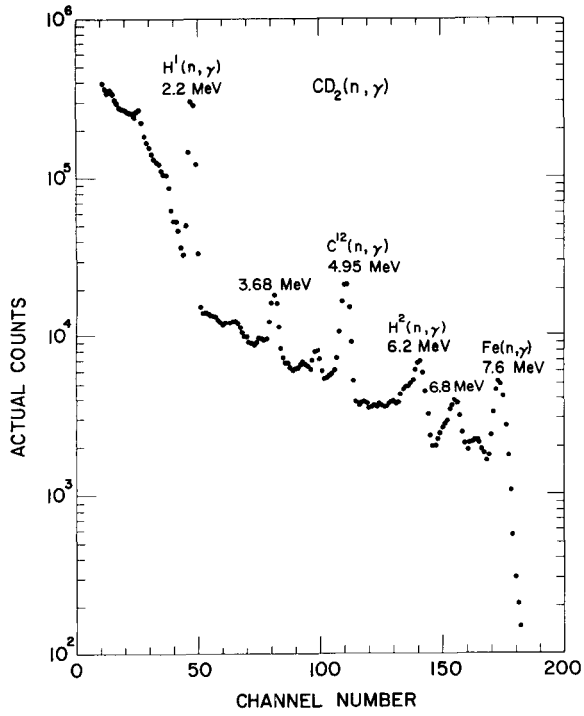

Fig. 2. The gamma-ray spectrum from neutrons incident on deuterated polyethylene which has a small impurity of mass-1 hydrogen and has an iron wire embedded in it

spectrum from the sample. The iron gamma ray is known[4] to about 4 keV. The lines from graphite are each known to 7 or 8 keV, and the energy of the gamma ray from capture by the photon is known[5] to approximately 2 keV. Other determinations of the deuteron binding energy are in disagreement with the value of Ref. 5, but we have found that our measurements reported here are insensitive to the value used for the deuteron binding energy.

---

[4] B. B. Kinsey and G. A. Bartholomew, Phys. Rev. 89, 375 (1953).

[5] J. E. Monahan, S. Raboy, and C. C. Trail, Nucl. Phys. 24, 400 (1961).

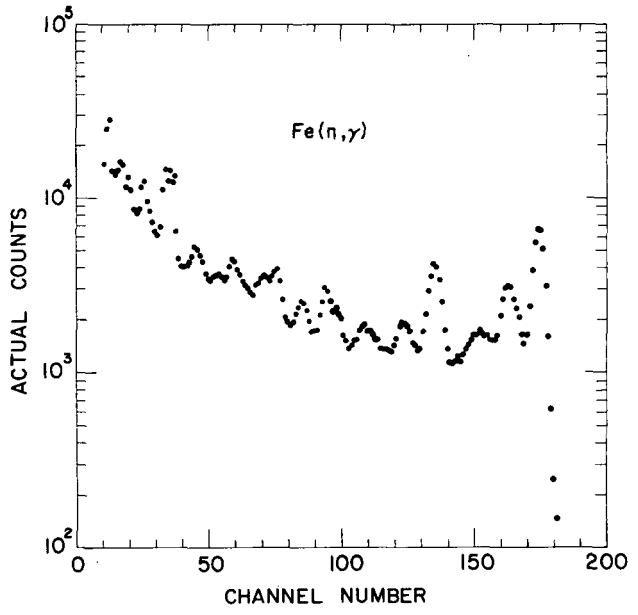

Fig. 3. The gamma-ray spectrum from neutron capture by iron.

Figure 3 shows the iron spectrum with the prominent 7.6-MeV line. Another line in the iron spectrum occurs very close to the deuteron capture line. By subtracting the iron spectrum, we get the unblemished deuteron-capture spectrum.

Table III lists the results obtained when we use two coun-

TABLE III. Summary of the determination of the energy of the gamma ray from neutron capture by deuterium.

Run No.	Energy of gamma ray (keV)
406a	6246.4 ± 4.4
406b	6242.6 ± 7.2
408a	6250.0 ± 2.2
408b	6251.6 ± 1.9

Weighted average: 6251 ± 2 keV

Recoil energy: 7 keV

Binding energy of neutron in triton: 6258 ± 2 keV

Mass values:[a] 6257.6 ± 0.5

[a]From Everling, König, Mattauch, and Wapstra, Ref. 6.

ters and split the memory of the 512-channel analyzer into 2 banks of 256, so that the two runs yielded four determinations. The latter determinations had a much smaller error. When we take a weighted average of the results, the latter numbers pretty well dominate the final result.

We obtain 6251 ± 2 keV for the energy of the gamma ray. If we add a 7-keV recoil energy, we get 6258 ± 2 keV for the binding energy. The mass value[6] is 6257.6 ± 0.5 keV. It is interesting to compare this result with other experimental numbers that can be combined to give this binding energy.

Table IV illustrates how one can combine the Q value

TABLE IV. A comparison of binding energies of deuterium [B.E.(D)] and tritium with the Q value for the $H^2(d,p)H^3$ reaction.

$$H^2 + H^2 \rightarrow H^1 + H^3 + Q$$
$$H^1 + n \rightarrow H^2 + B.E.(D)$$

$$H^2 + n \rightarrow H^3 + Q + B.E.(D)$$

Q:	4044 ± 5 keV[a]
Calculated B.E.(D):	2214 ± 5 keV
Measured B.E.(D):	2219 ± 2 keV (ANL)
	2224.52 ± 0.20 keV (Knowles)[b]

[a]Ref. 7.

[b]Ref. 8.

[6]F. Everling, L. A. König, J. H. E. Mattauch, and A. H. Wapstra, Nucl. Phys. 15, 342 (1960).

for the $H^2(d,p)H^3$ reaction with the binding energy of the deuteron to get the binding energy of the neutron in deuterium. The most recent determination of the Q value is the one at Wisconsin[7] where they obtained Q = 4044 ± 5 keV. If we subtract this from 6258, we get a deuteron binding energy of 2214 ± 5 keV.

Our measured value[5] is 2219 ± 2 keV. The number reported by Knowles[8] of Chalk River is 2224.52 ± 0.20 keV. Most of the other measurements actually group about this latter number. We find our number in better agreement with the systematics of light nuclei.

* * *

L. M. BOLLINGER, Argonne National Laboratory: The figures that you just saw remind me to make a comment to some of you who may be starting work in this area. You notice the iron line that showed up. This is an indication that one should avoid iron as the mortal sin because it gives trouble whenever it is used in shielding in the presence of neutrons. All the work that I know of here has been to some extent like that.

H. MOTZ, Los Alamos Scientific Laboratory: You mentioned that you added 3% light water to the heavy-water sample. Did you measure the dilution in the heavy water before adding this known amount?

TRAIL: Yes. This was done by an infrared spectroscopic measurement on the initial sample of heavy water.

---

[7] R. A. Douglas, J. W. Broer, Ren Chiba, D. F. Herring, and Edward A. Silverstein, Phys. Rev. 104, 1059 (1956).

[8] J. W. Knowles, Can. J. Phys. 40, 257 (1962).

MOTZ: It was the net amount of hydrogen that you added that was compared to D(n,γ)?

TRAIL: Right. The net amount of light water was (3.12 ± 0.03)%.

MOTZ: I do not understand the reason for the discrepancy in the measurements of the D(n,γ) cross section at this time. I do want to ask about the binding-energy measurement. You are surpassing yourself! Four years ago you claimed a part in 1000 at 2.2 MeV. Now you claim a part in 3000 at 6.2 MeV. What fraction of the line width is this 2-keV error from the deuterium line?

TRAIL: The 2-keV uncertainty represents about 1% of the full width at half maximum.

MOTZ: We have looked at individual line shapes with three central crystals over a broad range of energies, and we find none of these three crystals gives a purely Gaussian response at all energies. There is always a satellite, either on the low or high side. One can see at some energy range that this might blend with the peak. Now you are assuming a Gaussian response to a very high order.

TRAIL: Not entirely. If χ^2 is larger than one would expect, the errors are suitably increased.

MOTZ: I do not think that the number of points you have on a peak enable you to say that χ^2 over a broad range is really determining the sensitivity of the fit to the peak itself. How broad a range are you fitting?

TRAIL: I would say roughly that it usually is around a factor of 10 to 20 in intensity on each side of the peak.

MOTZ: You mean a factor of 10 or 20 in amplitude?

TRAIL: Something like that.

MOTZ: Well, I still think the centroid can be moved by an amount certainly comparable to 2 keV due to non-Gaussian shape.

TRAIL: If this shifts the binding energy, the shift in the $D(n,\gamma)$ line must be different from that in the calibration line. We have no evidence for such an effect.

MOTZ: That is what I am saying. The satellite can come and go if you go in the energy band from 2 to 6 MeV.

J. W. KNOWLES, Chalk River Nuclear Laboratory: Is there any systematic deviation between your two measurements of these binding energies and the latest measurements at other laboratories? Are you low by the same per cent?

TRAIL: Our deuterium measurement is 2219 ± 2 keV. We seem to be about 5 keV lower than other determinations. On the other hand, our measurement of the tritium gamma ray seems to be about 7 keV higher than that reported by Bartholomew and Kinsey, but these investigators report their number with about 8 keV uncertainty.

KNOWLES: There is no other way you can check the measurement?

TRAIL: It might be useful for us to measure our deuteron number again, but the agreement we get between our measurements and that derived from the Q value of $H^2(d,p)H^3$ gives us additional confidence in our number.

J. J. SCHMIDT, Kernforschungszentrum, Karlsruhe: What cross section do you assume at 0.01 eV to get the capture cross section?

TRAIL: We actually make the assumption that the capture cross sections for both hydrogen and deuterium vary in the same way from thermal, and the number that we report is based on the value of 332 ± 2 mb for the capture cross section of hydrogen.

O. W. B. SCHULT, Technischen Hochschule, Munich: I should like to put a question. What is the resolution for this line?

TRAIL: The resolution width is roughly 3%.

A VOICE: 3%? You get an energy precision of 3×10^{-4}. This means you have to determine the center of the line to 1%. What was the counting rate in that? What was the background?

TRAIL: The total number in the peak was of the order of 6000 to 8000, as I recall.

SCHULT: Let us assume that all of the reference lines are infinitely precise and that the multichannel analyzer is accurate to 2 in 10^4. I am surprised that you can achieve this precision.

TRAIL: I will fall back on the statistical anal ysis of the data. We use four lines to calibrate the analog-to-digital converter. We used the peak position of the lines to determine the parameters of a calibration curve; and in each case we make a χ^2 test of the fit.

W. JOHN, Lawrence Radiation Laboratory: I am one of the other people who measured this binding energy. I would say in his defense that the way he has analyzed the data looks reasonable to me. Probably the discrepancy is an experimental effect, but I would look at all these numbers in all these experiments, and I would say there is no possibility the binding energy of the deuteron could be so low.

III-9. $Cr^{53}(n,\gamma)Cr^{54}$ REACTION*

M. R. Gunye and G. A. Bartholomew

Chalk River Nuclear Laboratories

Pub lit. CRNE-316-4 C 1-20-64

Even-Z nuclei in the 2p1f shell tend to have neutron-capture γ-ray decay schemes dominated by a few very strong cascades which lend themselves to easy measurement with a γ-γ correlation apparatus. As a further incentive to studying this region, there has lately been a quickening of interest in the application of various models to level systems in this part of the table. Cr^{54} is among the even-even nuclei in this region which may be reached easily by the (n, γ) reaction. Previous capture-γ-ray studies with a separated Cr^{53} target were made by Kane, Fiebiger, and Fox[1] who studied coincidences and by White[2] who studied angular correlations of γ rays in the $Cr^{53}(n,\gamma)Cr^{54}$ spectrum. Our work parallels both of these and carries the spin measurements somewhat further.

In the present experiment the detectors were 3 X 3-in. NaI spectrometers. The target was 4.2 g of Cr_2O_3 enriched to 95.2% in Cr^{53}. The electronics included a fast-slow coincidence circuit, a pulse-adding circuit, and pulse-height stabilizers for each detector. With a neutron beam of about 10^6 neutrons cm^{-2} sec^{-1}, typical correlation measurements lasted one or two days for ordinary coincidences and one week or more for sum coincidences.

Figure 1 shows a sum-coincidence spectrum (low-energy portion) obtained with the sum gate set to select all two-step transitions from the capturing state to the ground state. The gate energy was $9.4 < E < 9.9$ MeV. Angular correlations at the angles 90° and 180° were measured for the γ rays at 0.84, 3.72, and 4.86 MeV. Most of the other

*Presented by G. A. Bartholomew.

[1] W. R. Kane, N. F. Fiebiger, and J. D. Fox, Phys. Rev. 125, 2037 (1962).

[2] D. H. White, Phys. Rev. 131, 777 (1963).

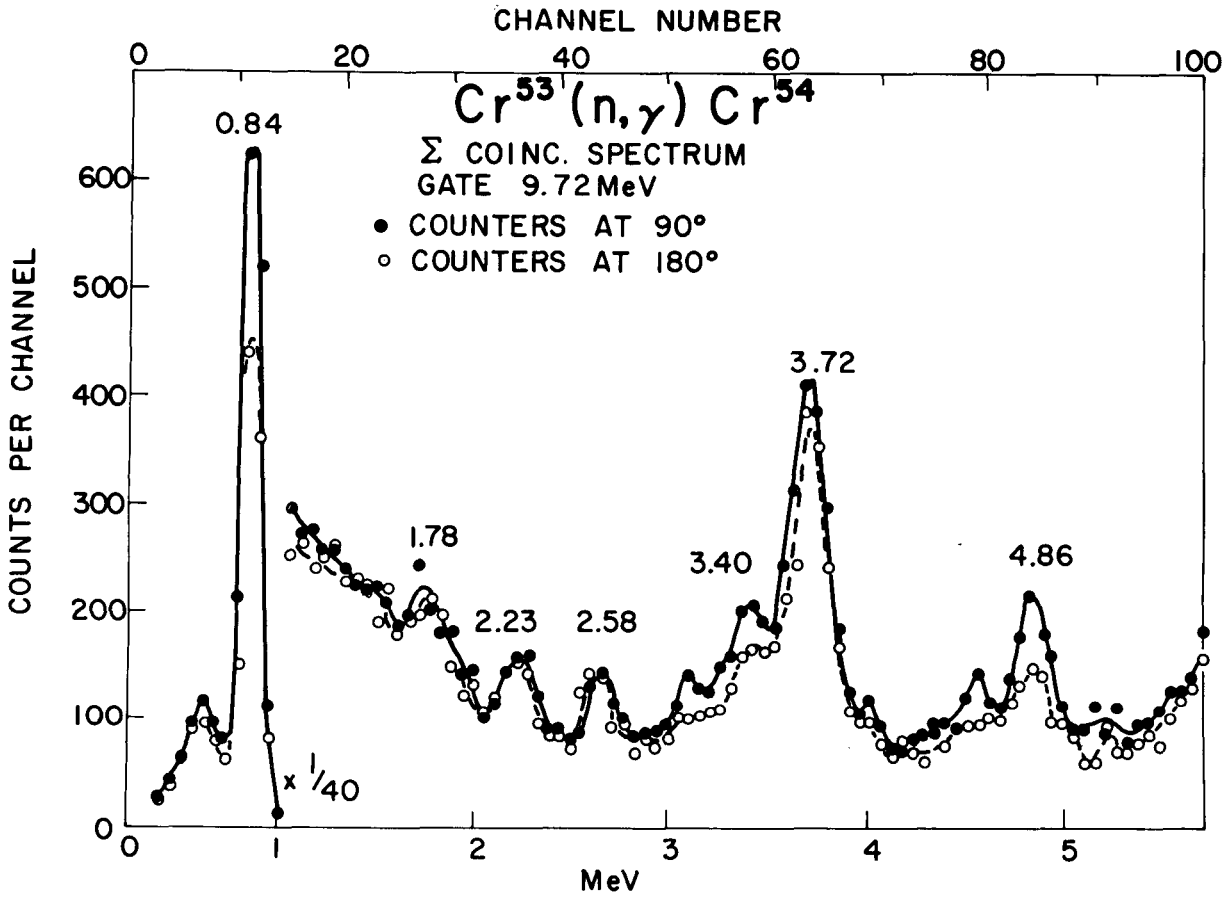

Fig. 1. Low-energy portion of the sum-coincidence spectrum obtained with the sum gate set to select all two-step transitions from the capturing state to the ground state.

weaker peaks are caused by various spurious effects inherent in the sum coincidence method, such as triple summations.

Figure 2 shows the sum-coincidence spectrum for two-step transitions from the capturing state to the first excited state of Cr^{54} at 0.84 MeV. The sum gate was set at $8.6 < E < 9.0$ MeV. Here it was possible to measure the two correlations at 1.78 and 2.23 MeV. Rough correlation results were also obtained at 1.98 and 4.44 MeV. The 0.84- and 3.72-MeV peaks are spurious in this figure.

Figure 3 shows the ordinary coincidence spectrum obtained with a gate set to accept pulses from primary γ rays in the range $5.9 < E < 7.25$ MeV. In analyzing this spectrum by the usual spectrum-

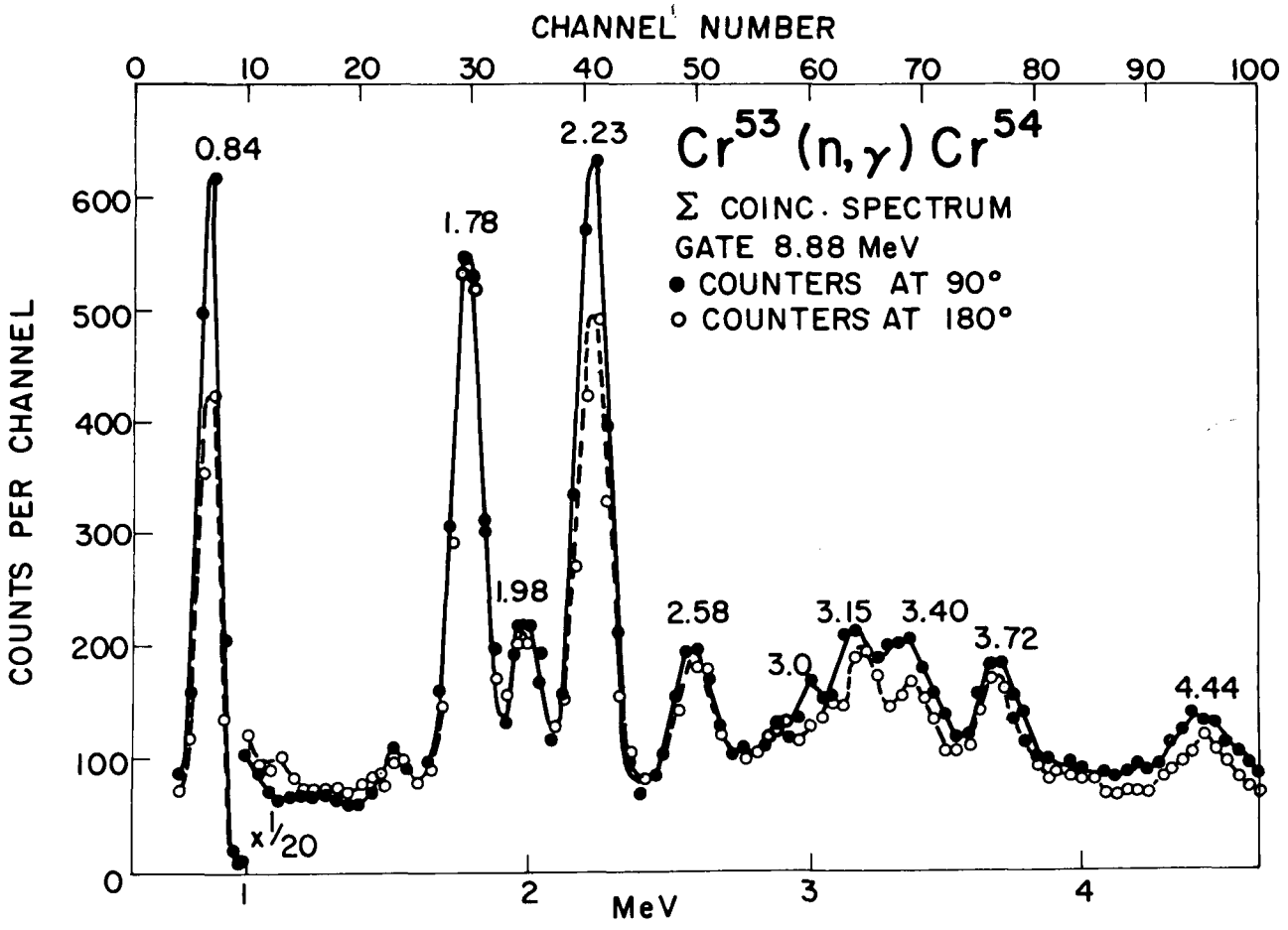

Fig. 2. Sum-coincidence spectrum for two-step transitions from the capturing state to the first excited state of Cr^{54} at 0.84 MeV.

unfolding procedure, we made use of standard γ-ray peak shapes measured with the same experimental arrangement. Correlations were measured for secondary γ rays at 3.72, 2.58, 2.23, and 1.78 MeV.

Figure 4 shows the spectrum in coincidence with the 0.84-MeV gamma ray at 90° and 180°. Measurements were also made at four intermediate angles. The insert shows the position of the gate $0.78 < E < 0.9$ MeV. A similar gate, set just above the 0.84-MeV gamma ray, was used to determine the background caused by pulses from the tails of high-energy γ rays falling in the 0.84-MeV gate. As in Fig. 3, a spectrum-unfolding analysis was carried out to determine the correlations of the individual lines.

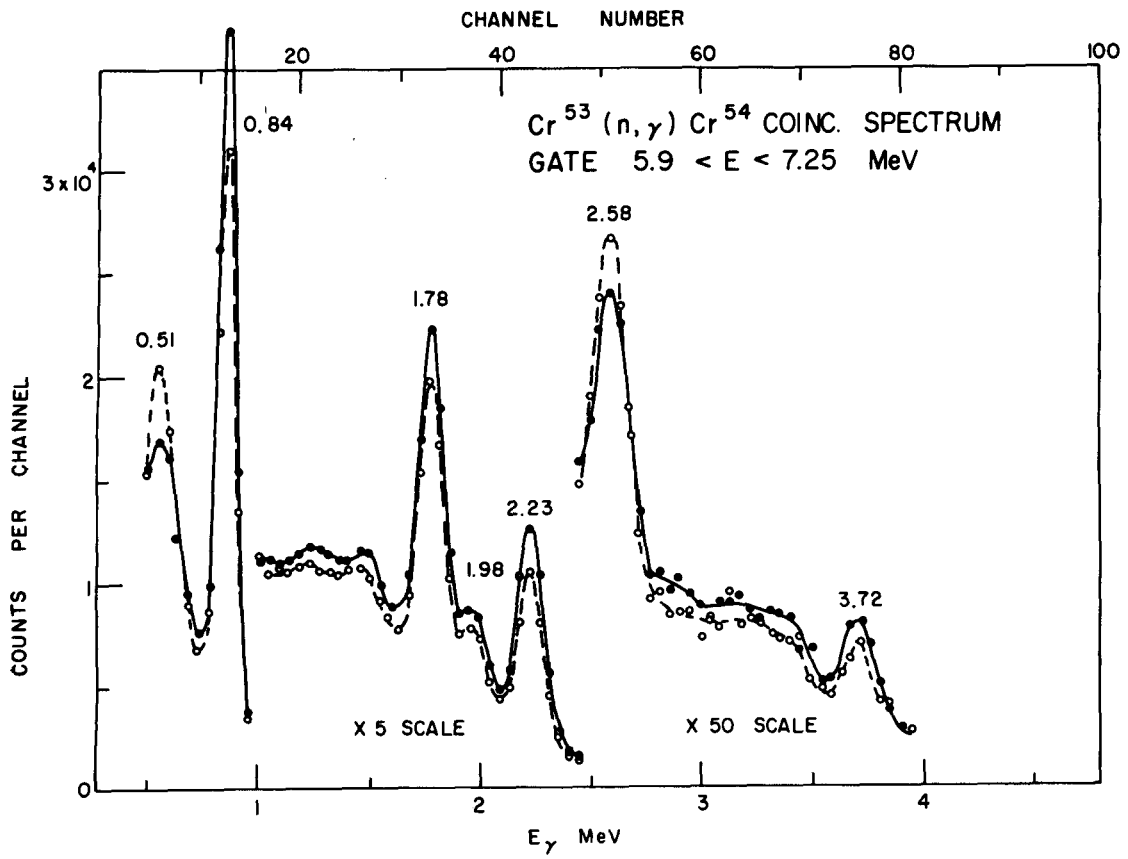

Fig. 3. Ordinary coincidence spectrum obtained with a gate set to accept pulses from primary gamma rays in the range $5.9 < E < 7.25$ MeV.

In Table I the results of the various correlations are expressed as coefficients A_2 and A_4 of the usual Legendre-polynomial expansion. In deriving these results, the observed counting rates in the total absorption peaks were first corrected for the effect of the finite diameter of the target and for absorption in the target.[3] The corrected counting rates were then used to deduce "raw" values for A_2 and A_4. These values were finally corrected for the finite length of the target and for detector solid angles[4] to obtain the values listed in the table.

---

[3] D. H. White, Nucl. Instr. and Methods 21, 209 (1963).

[4] A. M. Feingold and S. Frankel, Phys. Rev. 97, 1025 (1955).

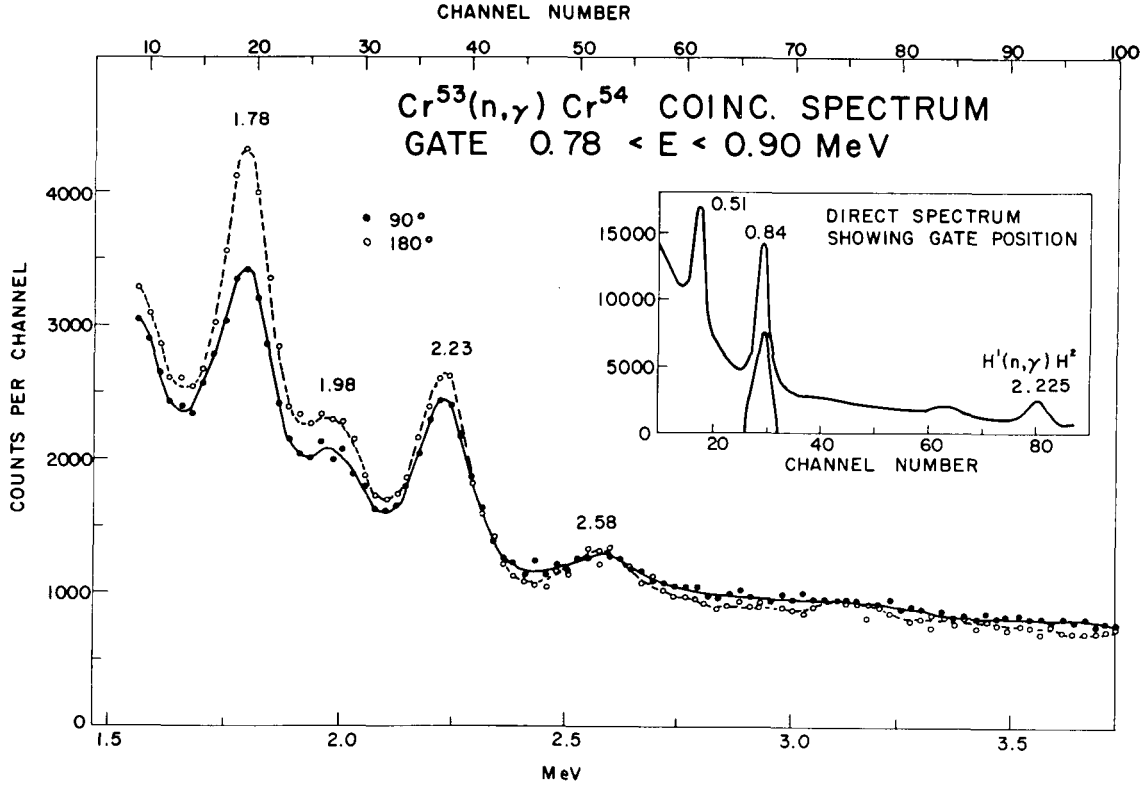

Fig. 4. Spectrum in coincidence with the 0.84-MeV gamma ray at 90° and 180°.

TABLE I. $Cr^{53}(n,\gamma)Cr^{54}$ Measured Correlations

Cascade MeV	Experiment	A_2	A_4	Angles
1.78 - 0.84	Present	0.39 ± 0.06	-0.02 ± 0.07	6
	White	0.500 ± 0.030	0.008 ± 0.060	3
1.98 - 0.84	Present	0.45 ± 0.15	0.47 ± 0.25	6
	White	0.299 ± 0.110	1.107 ± 0.22	3
2.23 - 0.84	Present	0.17 ± 0.05	0.06 ± 0.08	6
	White	0.178 ± 0.030	0.073 ± 0.068	3
2.58 - 0.84	Present	0.28 ± 0.10	-0.12 ± 0.20	6
	White	0.182 ± 0.080	-0.035 ± 0.180	3
8.88 - 0.84	Present	-0.22 ± 0.01		2
	White	-0.252 ± 0.006	-0.007 ± 0.015	3
7.10 - 1.78	Present	-0.02 ± 0.02		2
6.64 - 2.23	"	-0.18 ± 0.02		2
6.31 - 2.58	"	0.15 ± 0.05		2
6.00 - 3.72	"	-0.09 ± 0.02		2
4.86 - 4.86	"	-0.31 ± 0.05		2
4.44 - 4.44	"	-0.21 ± 0.03		2

The errors shown include statistical errors and also estimates of systematic errors which may arise principally in the background subtraction. The number of angles used to obtain each measurement is given in the last column.

The first five correlations in the table may be compared with the results of White.[2] The agreement is, in general, satisfactory. However, for the 1.98—0.84-MeV correlation our value of A_4 is considerably smaller than White's.

The values of A_2 for the last seven correlations listed in Table I were obtained with the assumption that M2 admixtures in E1 primary capture γ rays may be neglected. The assumption is supported by the observation that the ratios of reduced widths of primary γ rays conform roughly to the Weisskopf estimates for E1, M1, and E2 radiations.[5] On this basis the M2/E1 intensity ratio should be of the order of 10^{-5} for γ rays near 7 MeV. It may be deduced from (d, p) stripping measurements that the levels fed by the γ rays at 8.88, 7.10, 6.64, and 6.00 MeV all have even parity and therefore, since the capturing state is odd, these rays must all be E1. For the 6.31- and 4.86-MeV γ rays, E1 multipolarity has been inferred from the γ-ray intensities and the systematics of E1 and M1 γ-ray radiation strengths.[5]

Figure 5 shows a comparison of the observed coefficients with the theoretical predictions for various spin possibilities for the 2.62-MeV level. The γ rays involved in the two correlations measured and the various spin combinations are shown at the top of the figure. Since Cr^{53} is $\frac{3^-}{2}$, the capturing state is 1^- or 2^- or a mixture of both. The first excited state is known to be 2^+ from Coulomb excitation. The 7.10—1.78-MeV correlation is compared with theory in the upper row of diagrams and the 1.78—0.84-MeV correlation in the lower row. The coefficients

[5] G. A. Bartholomew, Ann. Rev. Nucl. Sci. 11, 259 (1961).

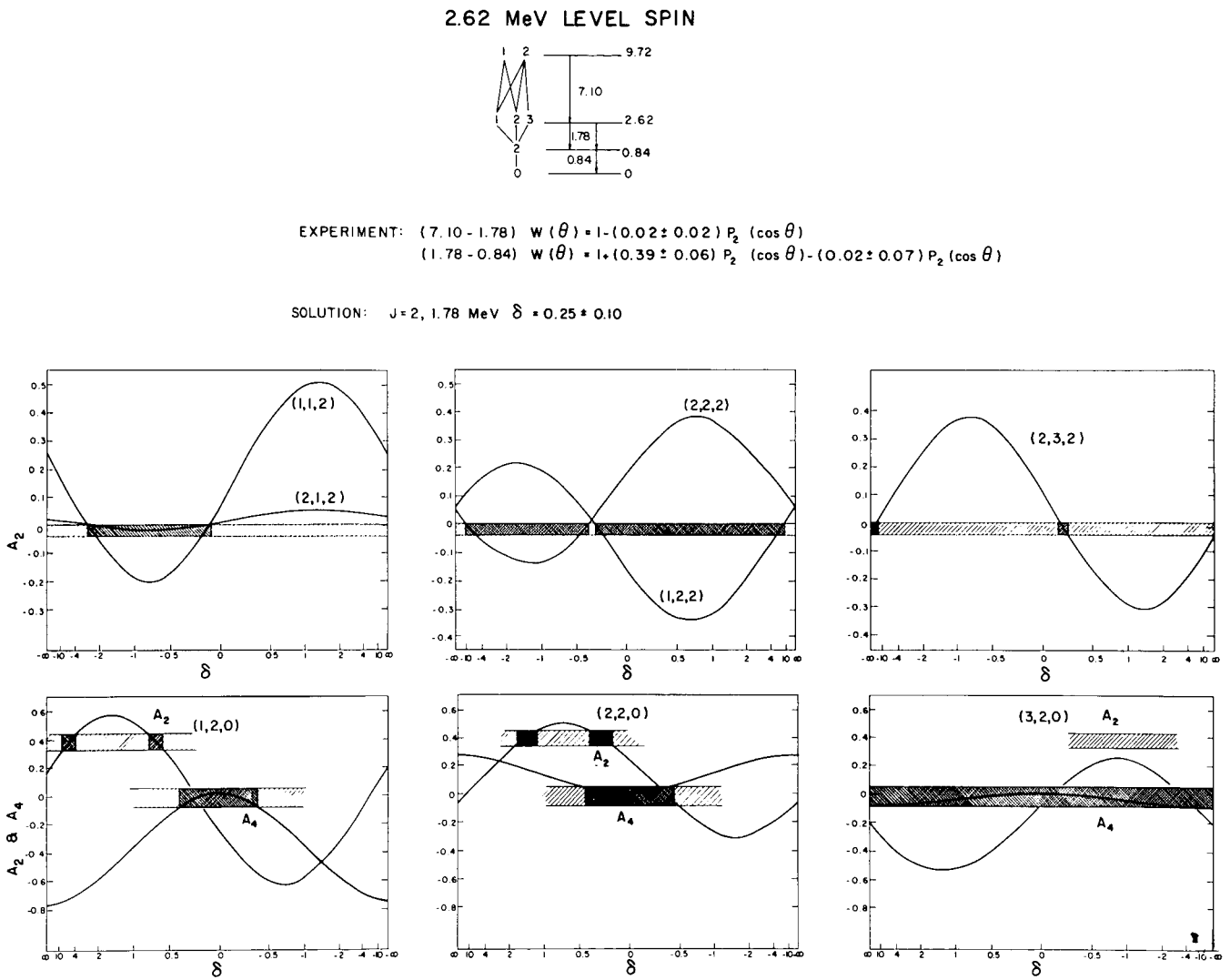

Fig. 5. Comparison of the observed coefficients with the theoretical predictions for various spin possibilities for the 2.62-MeV level.

are plotted as functions of δ for the 1.78-MeV gamma ray. (Note that by reversing the δ axis for the lower row of diagrams we have allowed for the sign change[6] that depends on the order of the γ rays in the cascade.) For the 7.10—1.78-MeV correlation, a large range of values of δ is allowed for the spin-1 and spin-2 possibilities because of the extra degree of freedom provided by the unknown spin mixture of the capturing state. It is clear, however, that spin 2 with $\delta = 0.25 \pm 0.10$ is the only spin consistent with all measurements.

Figure 6 gives a similar analysis for the 1.98—0.84-MeV correlation. The plots of A_2 and A_4 convincingly exclude the spin-1 and spin-3 possibilities. A solution is just possible for spin 2 with $\delta \approx 2$. The comparison for spin 0 is shown by the angular-correlation plot at the bottom of the figure. The least-squares fit to the observed points gives $A_2 = 0.45 \pm 0.15$ and $A_4 = 0.47 \pm 0.25$, as already mentioned. The value of A_4 is in poor agreement with the theoretical value for a (0, 2, 0) correlation, viz. $A_4 = 1.134$. However a superposition of the theoretical curve for (0, 2, 0) on the observed correlation suggests that much better agreement could result from only minor alterations in the positions of some of the points. When this fact is coupled with the observation that the 6.88—1.98-MeV correlation is apparently isotropic,[7] it would seem that we cannot definitely exclude the spin-0 possibility. Further measurements with better resolution would appear to be required to settle this point.

Table II summarizes all of the conclusions concerning spins and multipole mixtures. The 0.84-MeV level is known to be spin 2 and therefore the first entry adds no new information except possibly in the last column. The results for the next four levels are essentially in agreement with those of White. He concluded the spin of the 2.62-MeV level

---

[6] S. Ofer, Phys. Rev. 114, 870 (1959).

[7] This correlation was only measured roughly and is not recorded in Table I.

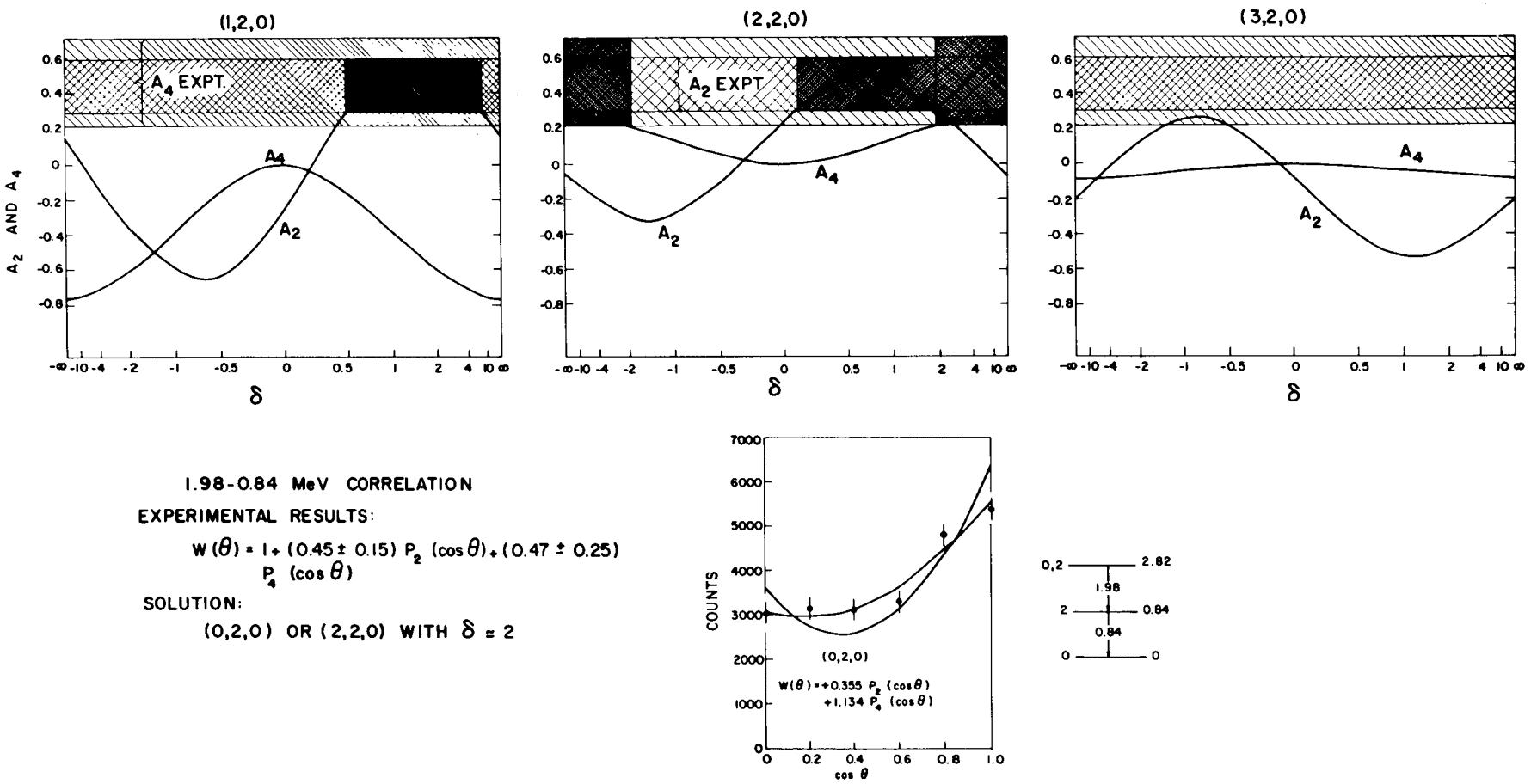

Fig. 6. Comparison of the observed coefficients with the theoretical predictions for various spin possibilities for the 1.98—0.84-MeV correlation.

TABLE II. $Cr^{53}(n,\gamma)Cr^{54}$ Results

Correlations MeV	Level MeV	J	γ-Ray MeV	δ	Capturing State Spin
8.88 - 0.84	0.84	1,2			mostly 1
1.78 - 0.84 7.10 - 1.78	2.62	2	1.78	0.25 ± 0.10	both 1 and 2
1.98 - 0.84 6.88 - 1.98	2.82	0,2	1.98		both 1 and 2
2.23 - 0.84 6.44 - 2.23	3.07	2,3			
2.58 - 0.84 6.31 - 2.58	3.41	2	2.58	0.00 ± 0.15	mostly 2
6.00 - 3.72	3.72	1,2			
4.86 - 4.86	4.86	1,2			mostly 1
4.44 - 4.44	5.28	> 0			

was 0 and not 2 and that that of the 3.41-MeV level was 1, 2, or 3. Our results in the last column show that both spin-1 and spin-2 resonances contribute appreciably to thermal capture and, as expected, the relative amounts vary with the primary transition. As mentioned above, our assignments for the 3.41- and 4.86-MeV levels depend on the assumption of E1 primary transitions and to this extent these assignments are tentative.

In Fig. 7 we show the Cr^{54} capture-γ-ray decay scheme with our spin assignments on the far left. Some branching-ratio information is also given on this diagram.

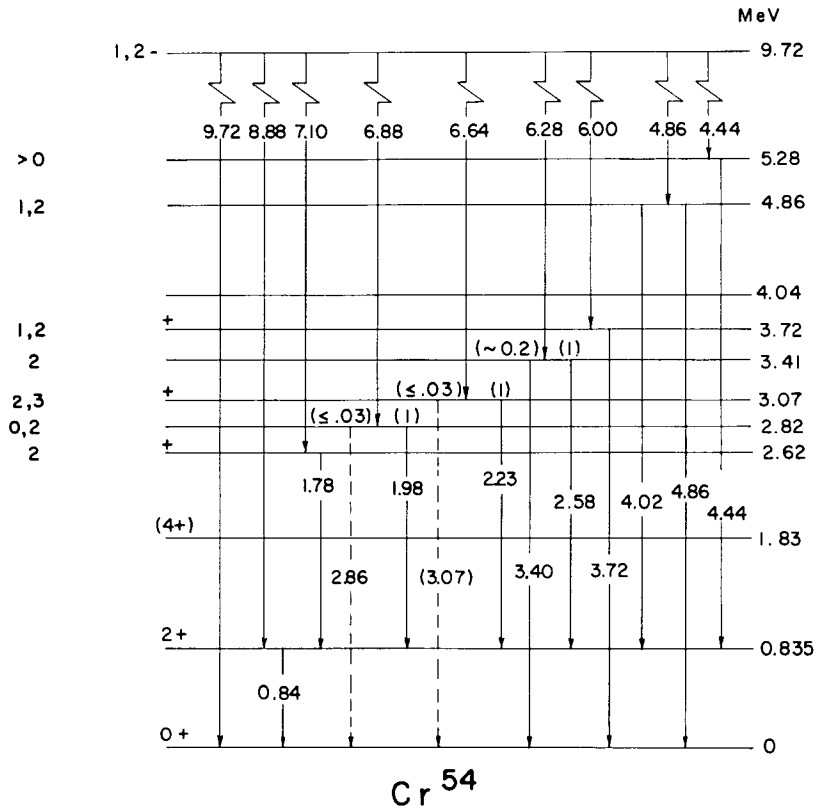

Fig. 7. Capture-gamma-ray decay scheme of Cr^{54}. Spin assignments are shown on the far left.

III-10. GAMMA-RAY ANGULAR CORRELATIONS IN Ca^{45}, Fe^{55}, Ni^{59}, Ni^{61}, and Ni^{63}. †

R. E. Coté, H. E. Jackson, Jr.,
L. L. Lee, Jr., and J. P. Schiffer

Argonne National Laboratory, Argonne, Illinois

The earlier measurements[1] on the angular correlations of cascade gamma rays in Ni^{59} and Ni^{61} have been extended to include a total of nine levels in Ca^{45}, Fe^{55}, Ni^{59}, Ni^{61}, and Ni^{63}. The observation of large anisotropies allows an unambiguous assignment of $J^{\pi} = \frac{3}{2}^{-}$ to be made for the well established $\ell = 1$ levels at 2.24 MeV in Ca^{45}, 0.880 MeV in Ni^{59}, and 0.158 and 0.528 MeV in Ni^{63}. The data for the levels at 0.418 MeV in Fe^{55}, 0.470 MeV in Ni^{59}, and 0.282 MeV in Ni^{61} indicate isotropy to within the statistical errors of less than 1.5%, a result that is consistent with an assignment of $J = \frac{1}{2}$ for these levels. The levels at 1.320 MeV in Ni^{59} and 1.008 MeV in Ni^{63} have also been assigned $J = \frac{1}{2}$ on the basis of an observed isotropy, although this assignment is somewhat uncertain because the statistical errors are about 12 and 7%, respectively. The results definitely show that the alleged separation of the levels associated with the $p_{\frac{3}{2}}$ and $p_{\frac{1}{2}}$ gross-structure groups is incomplete; $J = \frac{1}{2}$ levels exist within the $p_{\frac{3}{2}}$ group.

---

†Work performed under the auspices of the U. S. Atomic Energy Commission.

[1] R. E. Coté, H. E. Jackson, Jr., L. L. Lee, Jr., and J. P. Schiffer, Bull. Am. Phys. Soc. 7, 551 (1962).

III-11. VARYING THE ENERGY OF NEUTRON-CAPTURE GAMMA RAYS*

G. Ben-David, B. Arad, and I. Pelah

Israel Atomic Energy Commission, Soreq Research Establishment, Rehovoth, Israel

Resonant scattering of thermal-neutron-capture gamma rays will be discussed in the next paper (paper III-12) in this conference. A resonant condition is possible when the capture-gamma-ray peak energy happens to lie close to a suitable level in the target nucleus, after correcting for the target recoil energy. This is shown schematically in Fig. 1. Unless the resonance level has a particularly broad natural line

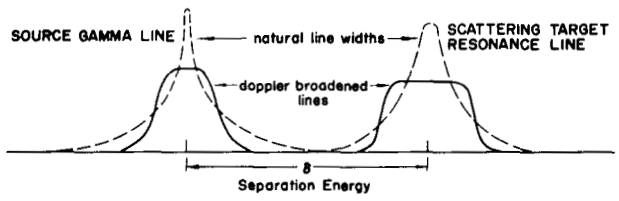

Fig. 1. Schematic diagram showing the possibility of resonance when the capture-gamma-ray peak happens to lie close to a suitable level in the target nucleus (after correction for the recoil energy of the target). No measurable resonance effects can be expected at separations δ greater than a few tens of electron volts.

width, the widths of both source and resonance line are governed predominantly by the thermal Doppler broadening, of the order of a few eV at normal temperatures. No measurable resonance effects could be expected at separations δ greater than a few tens of electron volts.

Variation of the separation energy δ could permit obtaining an exact resonance condition ($\delta = 0$) and a determination of the natural line width of the resonance level. Two methods for varying this separation energy suggest themselves.

The first is to use epithermal neutrons to produce the capture gamma rays, and thus alter their energy. The maximum energy change occurs for gamma rays emitted in the forward direction, and is

*Presented by G. Ben-David.

given by

$$E_{max} = Q - 535 \frac{E_\gamma^2}{A} + E\left(1 - \frac{1}{A}\right) + 46 \frac{E_\gamma}{A} E^{1/2}, \qquad (1)$$

where the neutron energies E and E_{max} are measured in eV, the gamma energy E_γ is in MeV, A is the mass number of the source nucleus, and Q is the energy difference corresponding to the gamma transition.

The second term in Eq. (1) is the normal recoil-energy term. For an 8-MeV gamma ray and a source-nucleus mass number of 50, this term totals 685 eV. The last two terms represent the additional energy given to the gamma ray because of the momentum of the incident neutron. Their sum E' is shown graphically in Fig. 2 as a function of neutron energy E. The maximum energy increase is unlimited, depending only on the available neutron energy, but the technique requires very

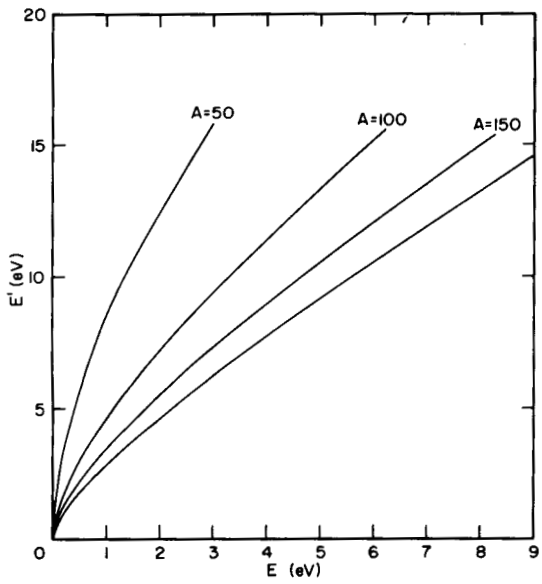

Fig. 2. Energy E' given to the gamma ray because of the momentum of the incident neutron, plotted as a function of the neutron energy E.

powerful sources of epithermal neutrons. One possible source is a pulsed neutron generator, neutron energies being measured by the time-of-flight technique.

A second method is to rapidly rotate the scattering target, using thermal-neutron-capture gamma rays. There is then a Doppler

shift in the gamma-ray energy seen by the scattering nucleus, the shift E_d being given by

$$E_d = E_\gamma \frac{v}{c}, \qquad (2)$$

where v is the rotation velocity and c the velocity of light.

The Doppler energy shift is limited by the maximum velocities attainable in practice. Taking a value of 600 m/sec as an upper limit, we find an energy shift in the range 15 — 20 eV for capture gamma rays in the energy range 6 — 9 MeV. This shift can be obtained in either a positive or negative sense by reversing the rotation direction.

These two methods have been compared,[1] taking as an example a high-flux pulsed reactor as a neutron source for the first method, and the available flux at the IRR1 thermal column in the second method. It was concluded that the latter method gives a far higher counting rate for achieving energy shifts up to 15 — 20 eV. Only the development of pulsed neutron sources having intensities several orders of magnitude larger than current ones would permit the production of useful amounts of capture gamma rays having energy shifts greater than 20 eV.

It was therefore decided to use the rotor technique in this laboratory. In a preliminary experiment, a steel-sheathed lead rotor of 20-cm diameter has been used to study the 7.28-MeV resonance in lead. The experimental setup is shown in Fig. 3. Initially it was possible to obtain peripheral speeds of 80 m/sec, giving an energy shift of about 2 eV in either sense. The change in counting rate under the resonance peak is shown in Fig. 4 as a function of velocity. These results confirm an energy separation of 8.5 ± 1 eV between the particular lead resonance level and the 7.28-MeV gamma ray produced in thermal-neutron

---

[1] G. Ben-David, B. Arad, and I. Pelah, Nucl. Instr. and Methods (in press, 1963).

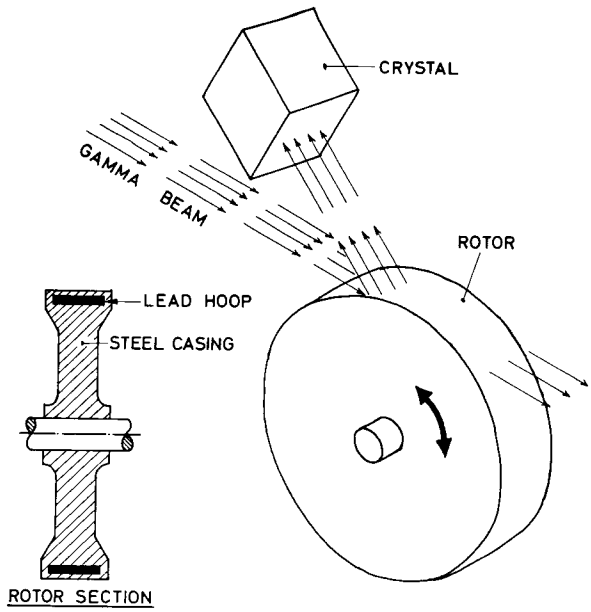

Fig. 3. Schematic diagram of the steel-sheathed lead rotor and associated equipment used to study the 7.28-MeV resonance in lead.

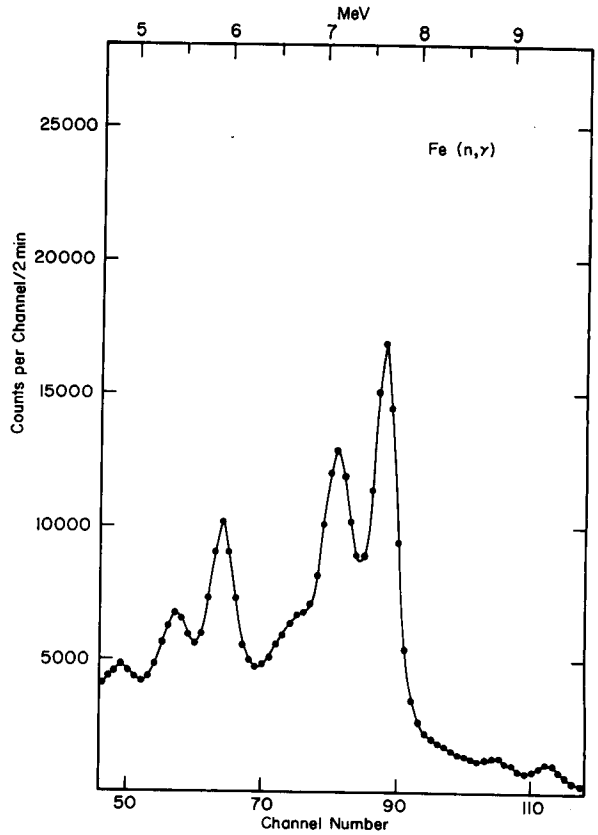

Fig. 4. Change in counting rate under the 7.28-MeV resonance peak in lead, plotted as a function of the rotor velocity. The results confirm an energy separation of 8.5 ± 1 eV between this lead level and the 7.28-MeV gamma ray from thermal-neutron capture in iron.

capture by iron. Rotors are being prepared with peripheral speeds of up to 600 m/sec, which will permit a systematic study of the resonance events to be reported in paper III-12 of this conference.

* * *

(The discussion was deferred to the end of paper III-12, which was also presented by Dr. Ben-David.)

III-12. NUCLEAR RESONANT SCATTERING OF THERMAL-NEUTRON-CAPTURE GAMMA RAYS*

B. Arad, G. Ben-David, I. Pelah, and Y. Schlesinger

Israel Atomic Energy Commission, Soreq Research Establishment
Rehovoth, Israel

A systematic survey of resonant scattering of thermal-neutron-capture gamma rays has been carried out at the Soreq Research Establishment. Nuclear resonant scattering has been reported previously in the particle threshold region (6—9 MeV) and above, using continuous spectra of gamma rays.[1—4] These experiments gave a measurement of the strength function averaged over a large number of levels, the energy resolution varying between a few hundred keV in the early experiments and 50 keV in those of highest resolution. In the present experiment we have a source emitting essentially monoenergetic capture gamma rays, the width being determined by the thermal Doppler broadening, of the order of a few eV at normal temperatures. This permits an investigation of individual levels in the energy region just below the particle threshold.

The experimental setup is shown in horizontal section in Fig. 1. The source of capture gamma rays is located in the side access

---

*Presented by G. Ben-David.

[1] Mary B. Stearns, Phys. Rev. 85, 706 (1952).

[2] E. G. Fuller and E. Hayward, Phys. Rev. 101, 692 (1956).

[3] K. Riebel and A. K. Mann, Phys. Rev. 118, 701 (1960).

[4] J. S. O'Connell, P. A. Tipler, and P. Axel, Phys. Rev. 126, 228 (1962).

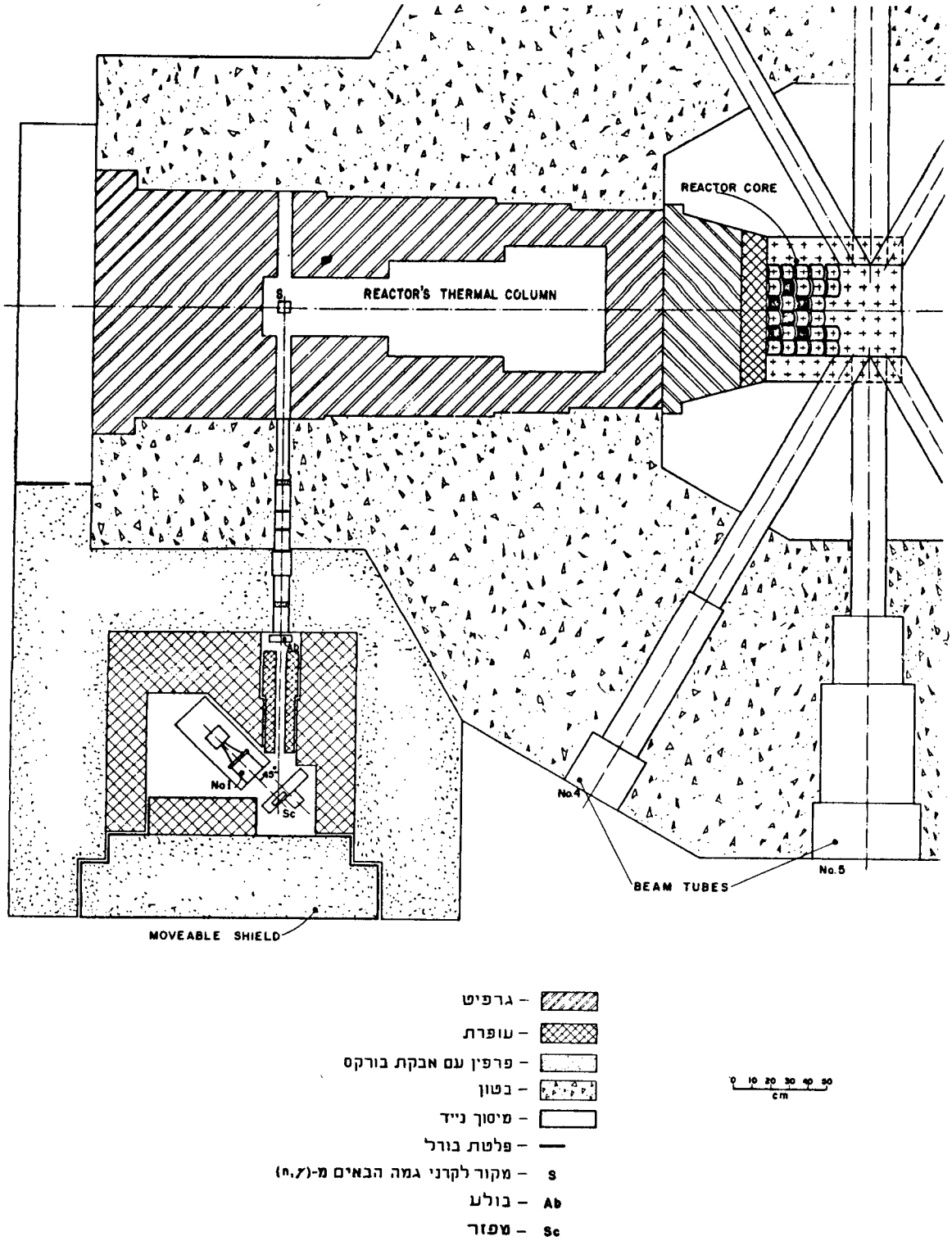

Fig. 1. Horizontal section of the experimental setup.

hole of the thermal column of the IRR1 reactor at a maximum flux position (10^{10} thermal neutrons cm^{-2} sec^{-1}). The gamma-ray beam is permitted to pass through a lead collimator to hit the scattering target at a distance of 2.5 m from the source. Boron and paraffin filters are used to remove thermal neutrons and residual epithermal neutrons from the beam. A NaI(Tl) crystal 5 in. thick and 5 in. in diameter is used to detect photons scattered at 135° with respect to the incident beam, the scattered spectrum being recorded in 200 channels of a multichannel analyzer. Considerable amounts of lead and paraffin shielding were used around the detector to reduce background counts due to stray radiation from the reactor and to cosmic radiation.

If the energy of a gamma line (corrected for source and target recoil) happens to coincide with a resonant level of the scattering nucleus, resonant scattering is possible.[5—7] Figure 2 shows the scattered spectra of iron capture gamma rays from similar targets of thallium and gold. There is clearly a resonant effect in thallium, the 7.65-MeV line responsible standing out clearly in both the scattered spectrum and the direct spectrum (Fig. 3).

Some fifty resonance events have so far been found in a survey involving twelve capture-gamma-ray sources and 51 scattering targets. The sources chosen were those giving appreciable intensities of capture gamma rays in the energy region of interest (6—9 MeV), namely Cl, Al, Co, Cr, Cu, Fe, Hg, Mn, Ni, Ti, Y, and V. Details of the scattering targets are in Table I, including the neutron numbers

---

[5] D. J. Donahue and C. S. Young, TID 12093 240.

[6] H. Fleischmann (thesis, Technischen Hochschule, München, 1961).

[7] G. Ben-David and B. Huebschmann, Phys. Letters 3, 87 (1962).

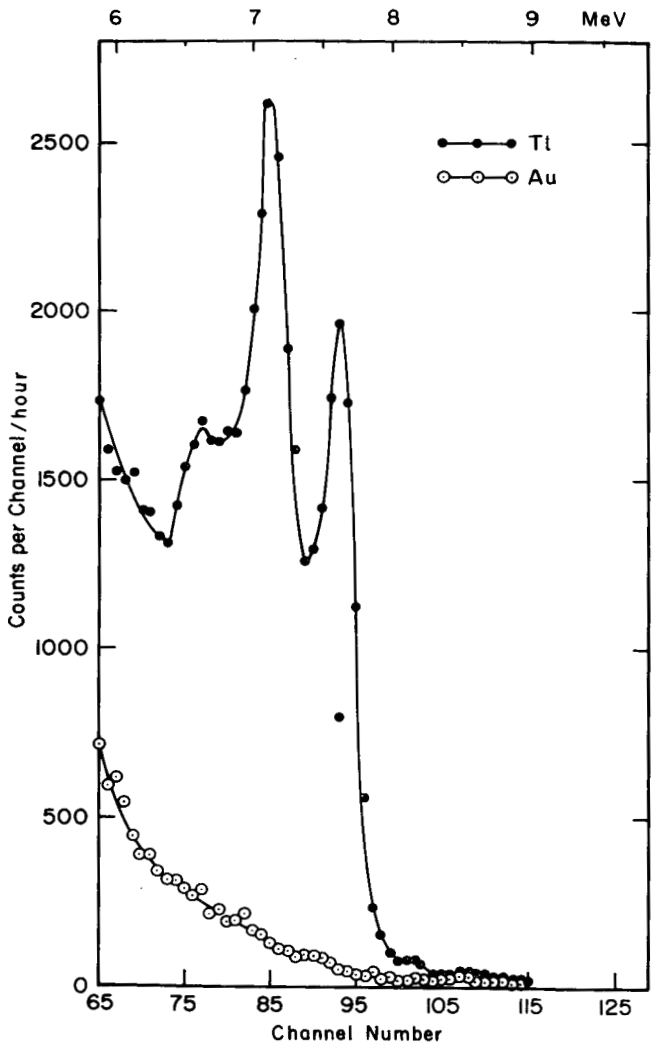

Fig. 2. Iron capture gamma rays scattered from similar targets of thallium and gold.

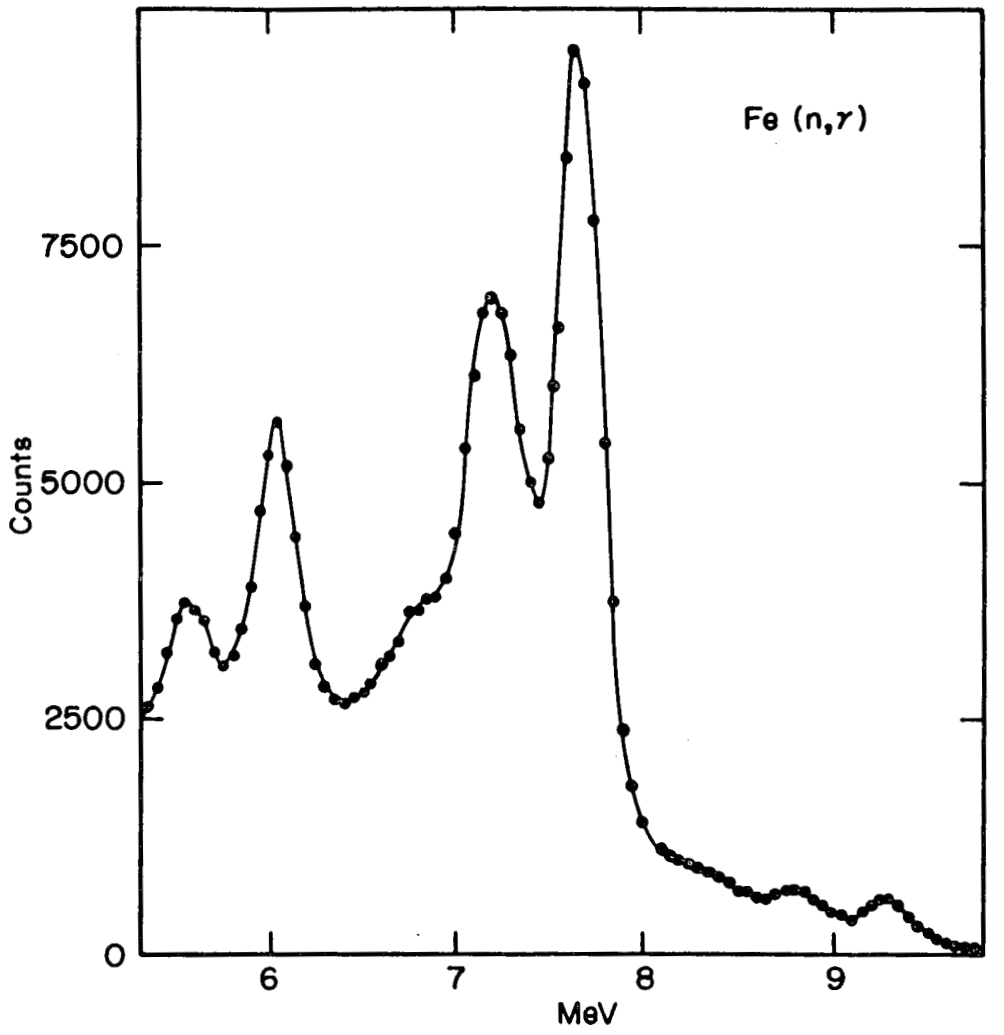

Fig. 3. Direct spectrum of gamma rays from capture in iron.

TABLE I. Details of scatterers.

Atomic charge Z	Element	Neutron number N (for naturally occuring isotopes)	Numbers of resonances found, with energies in MeV	Nearest closed shells for scatterers having one or more resonances	
11	Na	12	- -	-	-
12	Mg	12 13 14	- -	-	-
13	Al	14	- -	-	-
14	Si	14 15 16	- -	-	-
15	P	16	- -	-	-
16	S	16 17 18 20	- -	-	-
17	Cl	18 20	1 7.65	20N	-
19	K	20 22	-	-	-
20	Ca	20 22 23 24	-	-	-
22	Ti	24 25 26 27 28	1	28N,	20P
23	V	28	-	-	-
24	Cr	26 28 29 30	-	-	-
25	Mn	30	-	-	-
26	Fe	28 30 31 32	-	-	-
27	Co	32	-	-	-
28	Ni	30 32 33 34 36	1 7.639	28P	-
29	Cu	34 36	1 8.499	28P	-
30	Zn	34 36 37 38 40	-	-	-
34	Se	40 42 43 44 46 48	1 7.825	50N	-
35	Br	44 46	-	-	-
39	Y	50	-	-	-
40	Zr	50 51 52 54	1	50N	-
42	Mo	50 52 53 54 55 56 58	3 6.753, 7.14, 7.63	50N	-
47	Ag	60 62	-	-	-
48	Cd	58 60 62 63 64 65 66 68	5 6.474, 7.3, 7.65, 7.26	50P	-
50	Sn	62 64 65 66 67 68 69 70 72 74	2 6.508, 7.01	50P	-
51	Sb	70 72	-	-	
52	Te	68 70 71 72 73 74 76	1 7.575	50P	-
53	I	74	-	-	-
56	Ba	74 76 78 79 80 81 82	-	-	-
57	La	82	5 6.55, 8.505, 6.12, 7.63, 7.26	82N	-
58	Ce	78 80 82 84	1 5.646	82N	-
59	Pr	82	4 6.12, 6.69, 7.639, 8.881	82N	-
60	Nd	82 83 84 85 86 88	1 6.867	82N	-
62	Sm	82 86 87 88 90 92	1 8.997	82N	-
64	Gd	88 90 91 92 93 94 96	-	-	-
66	Dy	90 92 94 95 96 97 98	-	-	-
67	Ho	98	-	-	-
68	Er	94 96 98 99 100 102	-	-	-
70	Yb	98 100 101 102 103 104 106	-	-	-
72	Hf	102 104 105 106 107 108	-	-	-
73	Ta	108	-	-	-
74	W	108 109 110 112	1 6.413	-	-
78	Pt	112 114 116 117 118 120	1	-	-
79	Au	118	-	-	-
80	Hg	116 118 119 120 121 122 124	1 5.44	126N	82P
81	Tl	122 124	9 6.55, 7.65, 7.67, 7.69, 7.26, 7.63	126N	82P
82	Pb	122 124 125 126	11 6.98, 6.98, 7.149, 7.201, 7.261, 7.285, 7.3, 7.305, 7.32	126N	82P
83	Bi	126	1 6.996	126N	82P
90	Th	142	-	-	-
92	U	143 146	-	-	-

of the stable isotopes and the number of resonance events observed. The scatterers were of the natural isotopic abundance. Hence, except for those elements having one isotope only, it was not ordinarily possible to identify the particular isotope responsible for a given resonance. In the case of lead, where radio-lead is available, it was possible to show that most of the resonances occur in Pb^{208}.

One striking feature stands out on examination of Table I. There is clear grouping of the "resonant" events around nuclei possessing magic numbers of neutrons or protons. In fact, with one or two

exceptions, those elements showing resonance effects have isotopes within two nucleons of a closed shell of protons or neutrons. This effect is most pronounced at the closed shells 50 and 82 for neutrons and protons, and 126 for neutrons. Large numbers of resonances were found in the doubly-magic nucleus Pb^{208}, in neighboring Tl, and in the single-isotope elements Pr and La (both having 82 neutrons).

In nearly all cases the observed scattered spectra were consistent with being elastically scattered gamma rays only, with no signs of additional lower energy peaks which could be associated with inelastic scattering. However, in one case a second gamma line was found in the scattered spectrum from Mo (using capture gamma rays from copper). It has not yet been determined whether this is due to inelastic scattering or to resonant scattering occurring simultaneously for two of the gamma lines from copper.

There is quite clearly a connection between the occurrence of resonant scattering events and the presence of closed shells of nucleons. This may be explained by the high probabilities for the ground-state transition and by large values of branching ratios to the ground state, associated with the highly excited states of closed-shell nuclei.

Information on the individual resonances has been obtained by measuring the counting rate of scattered radiation as a function of the scatterer temperature. This modifies the Doppler broadening of the resonance level, and analysis of the temperature variation yields information on both the level width and the energy separation between this level and the gamma line. Independent information on the level width is obtained by carrying out a self-absorption experiment, an additional absorber of the resonance material being placed between the source and the scattering target. Results have been obtained for the 7.285-MeV resonance in lead ($\Gamma = 0.8$ eV), and the 7.639-MeV resonance

in nickel [$\Gamma = (1.6/a) \times 10^{-3}$ eV, where a is the fractional abundance of the isotope responsible for the resonance]. Similar measurements are being carried out for all the eight resonances discovered in lead.

It is of interest to mention the 7.3-MeV resonance in lead produced by capture gamma rays from mercury. No line of this energy has been reported in the spectrum of thermal-neutron-capture gamma rays from mercury.[8,9] However a line of 7.32 MeV has been reported[10] for resonance neutron-capture gamma rays in Hg^{201}. Preliminary measurements show the cross section for resonance scattering to be quite large, and an intensity of 0.01 gamma rays of this energy per 100 thermal neutrons captured in mercury would be sufficient to explain the observed resonance.

Variation in energy of the capture gamma rays would permit altering the separation between the gamma line and the resonance level, and thus of directly measuring this separation for thermal-neutron-capture gamma rays. This is discussed in the preceding paper in this conference (paper III-11). A Doppler shift is produced by rapid rotation of the scattering target.

* * *

P. AXEL, University of Illinois: That last remark you made would have concerned me more last summer when I was trying to find the 7.285-MeV level in lead by use of the gamma rays following the

---

[8] G. A. Bartholomew and L. A. Higgs, A.E.C.L. 699.

[9] L. V. Groshev, V. N. Lutsenko, A. M. Demidov, and V. I. Pelekhov, Atlas of Gamma-Ray Spectra from Radiative Capture of Thermal Neutrons (Pergamon Press, London and New York).

[10] R. T. Carpenter and L. M. Bollinger, Nucl. Phys. 21, 66 (1960).

capture of slow neutrons in iron. But you have come along now with three other levels near 7.3 MeV, and any of them could be the one we believe has a width of about 40 eV. I guess my favorite candidate at the moment is the gamma ray you could not see except after it has scattered from lead. A level 40 eV wide, such as we suspect, would cause the very large scattering needed to provide a measurable scattered gamma ray even though the gamma ray was too weak to be noticed in the direct unscattered beam.

More generally, I would like to supplement what you have said because I do not think you gave sufficient emphasis to the magnitude of the cross sections you get with this technique. You start with a peak cross section of about 150 b if you have a natural, unbroadened level. If the level is broadened, the peak cross section is lower, but it still is fantastically large for a nuclear photon-scattering cross section. Because of this, it is possible to find detectable scattering even with relatively poor energy overlap between the narrow incident gamma-ray beam and the narrow energy level.

Of course, the main limitation of the technique is that the gamma rays available from the capture of thermal neutrons are confined to a narrow, nonvariable energy range. One therefore must use many neutron capturers and many photon scatterers in order to find some levels. After a level is found, considerable additional work is needed to obtain its parameters. Furthermore, the most interesting implications of such experiments, the values of level spacings D and of average partial widths, depend on combining the results of very many experiments on individual levels. Fortunately, one can sometimes interpret the fragmentary results of these experiments by using what is already known from neutron resonance and from gamma-ray experiments made with poorer resolution.

This leads to the last part of my comment. I think you spoke of finding many levels near closed shells as though it were a rather puzzling shell effect. I do not feel it is quite so puzzling—and, in fact, predicted it. Briefly, one can say that away from closed shells the many levels which exist have only weak transitions to the ground state. Experiments on neutron-capture gamma-ray spectra indicate that the partial gamma-ray widths to low-lying states are only a small fraction of the total width. When you look at elastic scattering, you should expect to see large effects only when neutron-capture experiments indicate a high proportion of high-energy transitions. Thus, the reason for your finding levels mainly near closed shells is not different from the reason that strong high-energy neutron-capture gamma rays are found near closed shells.

H. MAIER-LEIBNITZ, Technischen Hochschule, Munich: First, did you use self-absorption measurements, such as were used by Fleischman who, I think, did the first work of that kind?

Second, is there any hope of determining the partial width of your excited level? Of course, in principle, there would also be the maximum cross section which depends upon spin; but that is hopeless, I think.

BEN-DAVID: I'm sorry I did not mention Fleischman's work. He was one of the early workers in this field—in addition to Donahue and Young. He discovered the resonance in mercury. We also use the self-absorption technique. This is useful since it enables us to compare the ground-state transition width with the full level width of the resonance level. We believe that in practically every case we are finding those levels that have a very strong ground-state transition ratio. In other words, if there is a strong transition to an intermediate level, the chance of elastic scattering would be less. We have found only one case among

the 50 resonances where there seems to be a second gamma ray which could come from a cascade. But even this case might of course be a double resonance, a resonance occurring with two of the capture gamma rays from the source. This will take us some time to decide, since coincidence experiments are quite difficult in this work.

J. JULIEN, Centre d'Etudes Nucleaires de Saclay: Prof. Axel suggested such experiments during his visit in Saclay last year. The main difficulty is not the intensity but the background. It is possible to select several resonances by time-of-flight techniques and to use detectors at different angles. Our multidimensional analyzer allows us to do such experiments. Our knowledge of neutron-capture gamma-ray experiments allows us to conclude that such experiments would be possible with a short flight path (5 m) and suitable nuclei. A few attempts have been made, but a decrease in the background is imperative.

BEN-DAVID: That is correct. Our calculations show that energy variation is better carried out with the rotor technique.

AXEL: I guess I missed the last point you made. I am not familiar enough with choppers to know about your fluxes, and hence cannot judge your intensity estimates with reactors. However, I think the Harwell linear accelerator clearly does have the necessary intensity. This view is shared by Dr. J. R. Bird who, although he is leaving Harwell, is well acquainted with the intensities available there. We would agree with Dr. Julien that the problem is background rather than intensity.

BEN-DAVID: Our calculations show that the counting rate would be far less with the accelerator. The number of counts you would get in the sodium iodide crystal would be negligibly small.

AXEL: I am not sure that I know what you are calculating. One of us seems to have made an error in estimating—an error that involves factors of 10. I doubt that we made the error because we did spend two

months last summer trying to set the experiment up. I think we did see the gamma rays resulting when iron captures neutrons with energies between 10 eV and 100 eV. If we had been able to see these gamma rays, our geometry was such that we could have seen scattering.

BEN-DAVID: Did you take into account the use of a very thin target to avoid too many gamma rays produced by scattered neutrons?

AXEL: It is not necessary to use a thin neutron capturer to avoid the errors introduced by neutron scattering. There are codes upon codes, which linear-accelerator researchers use to correct time-of-flight data for neutrons that interact after scattering. A thick target would spoil the time resolution somewhat; but I am not sure how good the resolution must be to see a level that is 10 eV wide.

BEN-DAVID: Our calculations show that even the low flux at the IRR1 thermal column would be a factor of 10 to 100 better than the accelerator type of experiment.

AXEL: The time-of-flight counting-rate estimate is increased considerably because one can record simultaneously events associated with all different neutron energies. A much greater energy spread can be tolerated with Doppler-broadened gamma-ray lines than is tolerable in the usual neutron resonance work. The time-of-flight technique also has the advantage that one can depend on passing over a level and, therefore, on being able to use the peak scattering cross section. In contrast, if one talks about the probability of detecting levels with thermal neutrons, it is necessary to make some assumption about how much below the peak cross section one will be (on the average) because of imperfect energy overlap.

R. E. SEGEL, Argonne National Laboratory: Then you have to make an assumption about how much (on the average) you can be away from it.

BEN-DAVID: We have published these calculations. I did not have time to explain them in detail. I have copies of this if anyone wants to study it.

AXEL: Because this conference probably has more people familiar with reactors than with linear accelerators, I would like to clarify this intensity question. If you ask which facility can give you a higher intensity of high-energy capture gamma rays from indiviudal neutron resonances, I think the answer is clearly that the linear accelerator has the higher intensity. I would like either Bollinger or someone else who has studied capture gamma rays to check me on this.

L. M. BOLLINGER, Argonne National Laboratory: If I have understood them correctly, this discussion between Axel and Ben-David has been somewhat confused because they have been talking about different things. Axel appears to have been asserting that the neutron intensity available from an electron Linac is greater than that from a fast-chopper time-of-flight neutron spectrometer. On the other hand, Ben-David has been asserting that a higher counting rate of resonantly scattered gamma rays is obtained by scattering thermal-neutron-capture gamma rays from a moving target than by the alternative approach in which the gamma rays resulting from resonant capture are scattered from a stationary target. I agree with both assertions.

Let me add a few further remarks to help clarify the comparisons between the two alternative methods of varying the effective energy of the resonantly scattered gamma rays. As Ben-David has said, the counting rates obtained by resonantly scattering thermal-neutron-capture gamma rays on a rotating target are several orders of magnitude greater than can be obtained, with existing sources, in the alternative experiment in which a variable neutron energy is used to control the energy of the capture gamma rays. On the other hand, the range of

energy that can be obtained by means of a moving target is very limited, say ± 30 eV, whereas in principle there is no such limitation on the range of variation obtainable by means of a variable neutron energy. My own evaluation of the experimental situation is that the scattering of thermal-neutron-capture gamma rays from a moving target is by far the better of the two methods at the present time. However, when much higher neutron intensities become available from pulsed sources, as will surely be the case some day, then the alternative method will be preferable.

III - 13. MEASUREMENT OF (γ, n) CROSS SECTIONS WITH NEUTRON-CAPTURE GAMMA RAYS*

L. Green and R. R. Hurst, Pennsylvania State University

and

D. J. Donahue, University of Arizona

In the experiments described here, γ rays produced by neutron capture have been used to measure (γ, n) cross sections at selected energies between threshold and 11 MeV. The (γ, n) cross sections have been studied mainly in experiments utilizing bremsstrahlung sources, and the interpretation of such experiments is quite complicated. Measurements with monoenergetic capture γ rays will provide a good check on previous results, and can possibly show some structure in the cross sections which was missed by the averaging process used to analyze bremsstrahlung measurements.

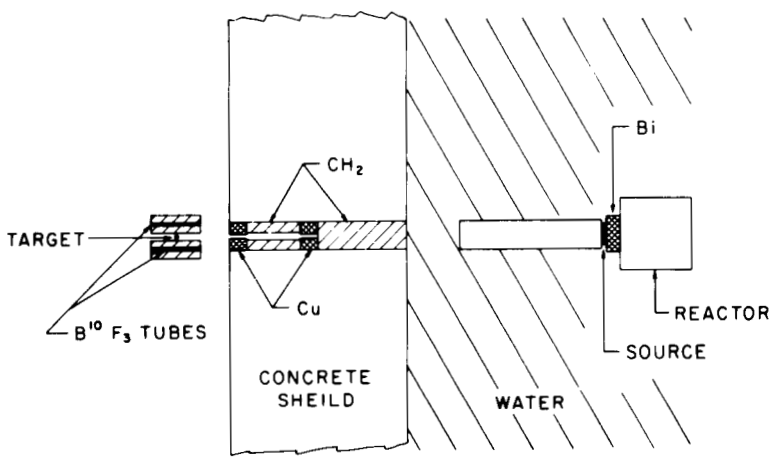

Fig. 1. Experimental arrangement.

The experimental arrangement used is shown in Fig. 1. The source of neutrons is the 200-kW pool reactor at Pennsylvania State University. Next to the reactor is a bismuth filter, and next to that is the source of γ rays. This source may consist of 1—2 kg of the capturing material. The γ rays produced in this source pass through filters and collimators to the target of material whose (γ, n) cross section is to

*Presented by D. J. Donahue.

be measured. The filter consists of approximately 4 ft of water and paraffin, which attenuates the neutrons in the beam by about a factor of 10^8 while reducing the γ-ray flux by only a factor of 20. Neutrons produced in the target are counted in a neutron detector which consists of four $B^{10}F_3$ tubes located symmetrically about the axis of the γ-ray beam. The distance of these counters from the beam axis was chosen so that the efficiency of the detector was approximately constant for neutrons with energies from 200 keV to 5 MeV. The efficiency of the detector was measured by use of a calibrated Am-Be neutron source.

The intensity of the γ-ray beam was measured with a NaI(Tl) crystal 4 in. in diameter by 6 in. long. The photofractions and photoefficiencies of Miller and Snow[1] were used to obtain the actual fluxes. Typical fluxes range from $2 \times 10^5/cm^2$-sec for an iron source to $5 \times 10^3/cm^2$-sec for a nitrogen source.

Before results are presented, one difficulty must be discussed. A source will ordinarily emit more than one group of γ rays with energies above the (γ, n) threshold of the target nuclei. For example, consider the case of γ rays coming from a nickel source and incident upon a tantalum target, which has a threshold of about 7.5 MeV. The nickel source emits γ rays with energies (and relative intensities) above this threshold of 7.8 MeV (0.2), 8.5 MeV (0.4), and 9.0 MeV (1.0). To obtain the cross section at 9.0 MeV, the following sequences is followed. First an aluminum source is used, which emits only 7.72-MeV γ rays above the Ta threshold. With this source, the cross section at 7.7 MeV is determined. Next, a chlorine source is used, which emits γ rays of 7.8 and 8.5 MeV above the (γ, n) threshold. From the cross section at 7.7 MeV, obtained with the aluminum source, the chlorine results give the cross section at 8.5 MeV. Finally, by use of the above-measured

[1] W. F. Miller and W. J. Snow, Argonne National Laboratory Report ANL-6318 (unpublished), and private communication.

cross sections at 7.7 and 8.5 MeV, the data obtained with the nickel source are used to deduce the (γ, n) cross section at 9.0 MeV.

Results obtained for the cross section of the reaction $Ta^{181}(\gamma, n)Ta^{180}$ are shown in Fig. 2. The smooth curve is the best fit

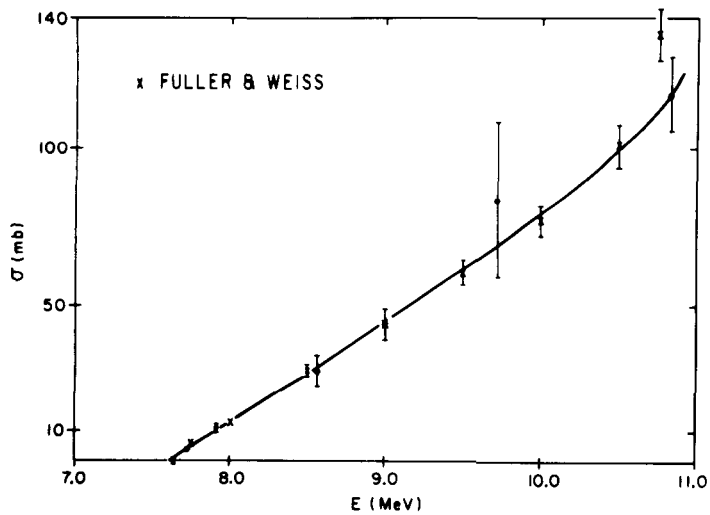

Fig. 2. The (γ,n) cross sections of Ta^{181}. The smooth curve is a fit to our data, and the points x are data of Fuller and Weiss.

to our data. Also illustrated in the figure are the results of Fuller and Weiss,[2] obtained by use of bremsstrahlung. The agreement is very good.

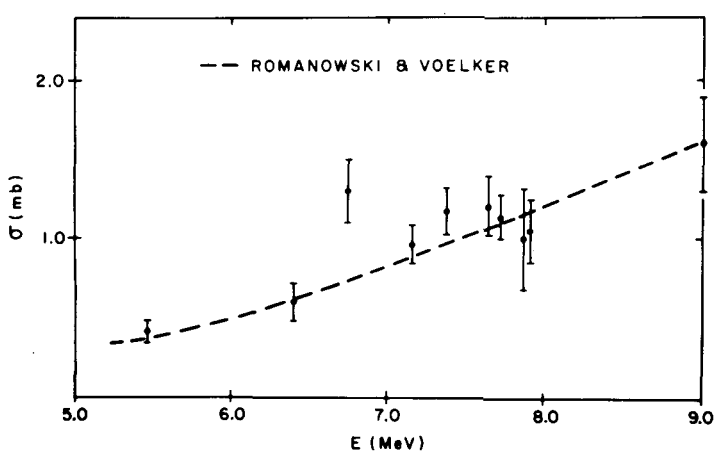

Fig. 3. The (γ,n) cross sections of Li^6. The dashed curve represents the results of Romanowski and Voelker.

Figure 3 illustrates the results for Li^6. The dashed curve represents the results of Romanowski and Voelker,[3] obtained with bremsstrahlung. There is an indication of structure in the Li^6 cross

[2] E. G. Fuller and M. S. Weiss, Phys. Rev. 112, 560 (1958).

[3] T. A. Romanowski and V. H. Voelker, Phys. Rev. 113, 886 (1959).

section near 6.7 MeV, but the lack of capture γ rays with appropriate energies makes this structure hard to investigate.

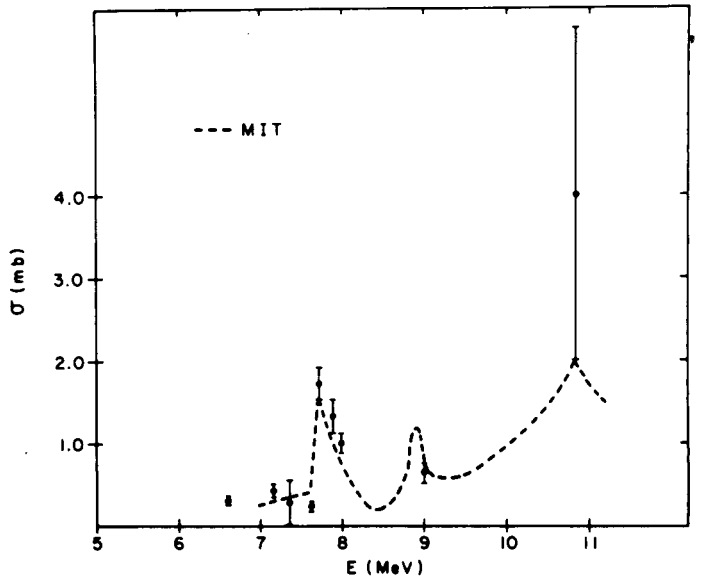

Fig. 4. The (γ,n) cross sections of C^{13}. The dashed curve represents results obtained at MIT.

Figure 4 compares our results for C^{13} with those obtained at MIT[4] by use of time-of-flight techniques. The agreement again is quite good.

Finally, to show the large number of cross sections which can be investigated with capture γ rays, the results illustrated in Fig. 5 are presented. This figure gives a plot of σ(γ,n) at 10.8 MeV vs the mass number A of the target. The smooth curve in the figure is a plot of an equation suggested by Axel,[5] which assumes that cross sections near threshold result from the tail of the giant resonance — which has a Lorentz shape.

The errors on the cross sections in Fig. 5 are about 10 — 15% and result almost entirely from uncertainties in the flux measurements.

---

[4] W. Turchinetz (private communication).

[5] Peter Axel, Phys. Rev. 126, 671 (1962).

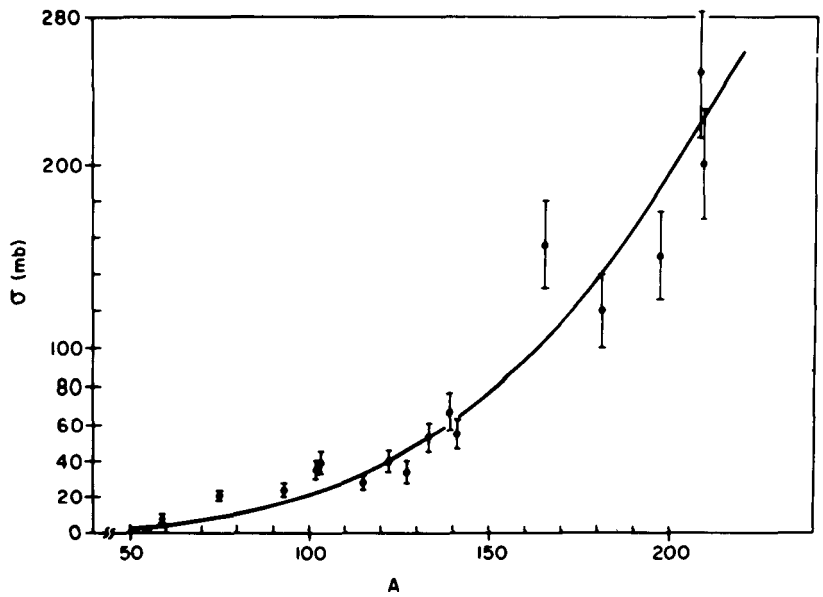

Fig. 5. The (γ,n) cross sections at 10.8 MeV vs the mass number A of the target. The curve is a plot of an equation taken from Axel (ref. 5).

* * *

G. BEN-DAVID, Israel Atomic Energy Commission, Soreq Research Establishment, Rehovoth: One thing that often puzzles me about this type of work is that presumably there are no resonance effects at all. If there be resonance effects similar to what I found in the scattering experiment, you cannot assume there is a steady curve.

DONAHUE: That is right.

BEN-DAVID: That is rather surprising.

DONAHUE: I could have shown you two other curves for lead and bismuth, and they do have resonance effects in them. For tantalum, once you get above the (γ, n) threshold the levels broaden out some. I am reasonably sure in the tantalum that the levels overlap so that they wash out the structure. In the corresponding graph for bismuth, there are some points well off the smooth curve. There are resonances in bismuth, I think.

A VOICE: What is the power of the reactor and what is the flux of the gammas?

DONAHUE: The power is 200 kW. At the target, 15 ft from the source, the flux from a good strong source is a few times 10^5 gamma rays per cm^2 per sec. It would be even higher except that the paraffin filter knocks down the intensity by a factor of 20.

III-14. TOTAL RADIATION WIDTHS FOR s-WAVE AND p-WAVE NEUTRON CAPTURE IN Nb^{93} †

H. E. Jackson

Argonne National Laboratory, Argonne, Illinois

I want to describe briefly an experiment in which we have measured the total radiation widths for p-wave and s-wave neutron capture in Nb^{93}. It will be brief, because the results are already published.[1] Recently here at Argonne we have been successful in using resonant-capture gamma-ray spectra to assign parities to resonances. This success makes possible a systematic study of resonance parameters for resonances excited by p-wave and s-wave capture.

The total radiation widths for s-wave and p-wave capture are of particular interest for two reasons. (1) They can possibly provide a source of information about the dependence of the electric-dipole radiation strength on the parity of highly excited radiation states. (2) Of more practical and immediate interest, for use in obtaining p-wave strength functions from average total capture cross sections, are the relative values of these total radiation widths. Until now, these widths have been assumed to be equal.[2]

The relative values of these widths have been determined for six resonances in Nb^{93}. In this particular case, accurate measurements of the radiation width are possible because for these resonances the neutron widths are very small. Thus one can make a standard transmission measurement of the total widths, make a small correction

---

†Work performed under the auspices of the U. S. Atomic Energy Commission.

[1] H. E. Jackson, Phys. Rev. Letters 11, 378 (15 October 1963).

[2] See, for example, the discussion of L. W. Weston, K. K. Seth, E. G. Bilpuch, and H. W. Newson, Ann. Phys. (New York) 10, 477 (1960).

for the neutron width, and obtain a precise value for the radiation widths. The results are shown in Table I. Also shown are the parity

TABLE I. Parameters for neutron resonances in niobium. The results for resonances at 35.9 eV and 42.2 eV are in agreement with those of Saplakoglu et al.[a] Because their results for resonances at higher energies are based on an assumed value $\Gamma_\gamma = 0.22$ eV for the radiation width, they will be subject to large corrections. The value of Γ_γ for the level at 194 eV is in strong disagreement with an older value of 0.34 ± 0.06 eV obtained in an indirect measurement by Rae.[b]

E_0 (eV)	Parity	Γ (10^{-3} eV)	$2g\Gamma_n$ (10^{-3} eV)	Γ_γ (10^{-3} eV)
35.9	-	215 ± 40	0.12 ± 0.01	215 ± 40
42.2	-	260 ± 20	0.09 ± 0.01	260 ± 20
94.3	-	215 ± 50	0.34 ± 0.03	215 ± 50
106	+	96 ± 50	0.05 ± 0.01	96 ± 50
119	+	113 ± 20	5.8 ± 0.6	107 ± 20
194	+	175 ± 25	41.7 ± 4	133 ± 30

[a] A. Saplakoglu, L. M. Bollinger, and R. E. Coté, Phys. Rev. 109, 1258 (1958).

[b] E. R. Rae in Proceedings of the International Conference on Peaceful Uses of Atomic Energy, Geneva, 1955 (United Nations, New York, 1956), Vol. 4, p. 110.

assignments arrived at from the study of the capture-gamma-ray spectra for these resonances.

In other nuclei, it is generally accepted that the radiation width for s-wave capture varies very little from resonance to resonance. If you look at these numbers, there is an obvious correlation between the parity of the resonance and the resonance width—in fact, you obtain a vale of 113×10^{-3} eV for the average s-wave radiation width and 230×10^{-3} eV for the average p-wave radiation width. Thus the data indicate a clear variation of the radiation with neutron angular momentum.

Now, if we restrict our discussion to electric-dipole

radiation, the radiation width for a resonance will be given by the expression

$$\Gamma_\gamma = \int_0^U \Gamma(U,E)\, \rho_{-\pi}(E)dE = \int_0^U \left\langle \frac{\Gamma(U,E)}{D_{J,\pi}(U)} \right\rangle \frac{\rho_{-\pi}(E)}{\rho_{J,\pi}(U)}\, dE,$$

$$\rho_{-\pi} = \sum_{J'=J-1}^{J+1} \rho_{J',-\pi}(E).$$

The bracketed quantity is the electric-dipole strength function for transitions from states at an excitation energy U to states at an excitation energy E, and $\rho_{J,\pi}(E)$ represents the density of states at excitation E and with spin J and parity π. The point I want to make is that a parity dependence of either the photon strength function or the ratio of level densities would explain the effect that we have observed. We have attempted to assess the effect of the difference of densities in states of opposite parity near the ground state to see if this would account for the difference. We find that the observed capture spectra indicate that this variation in density would not explain the magnitude of the difference in the radiation width. In the light of the discussion this morning, I do not think it is unreasonable to suggest that the variation is actually due to a variation in the photon strength function with the parity of the radiating state.

I should mention that in discussions in the hall yesterday, I learned that the French are also doing some measurements of this type. I think Dr. Julien wants to make a remark.

* * *

J. JULIEN, Centre d'Etudes Nucleaires de Saclay: The main difficulty in arriving at correct p-wave strength functions from individual resonance parameters is in identifying p-wave levels. In Saclay, Nb has been investigated up to around 1000 eV. Many weak levels

appear in transmission experiments. Below 100 eV, the small value of 2kR does not allow us to distinguish between s-wave and p-wave levels. Above 200 eV our high intensity allows us to use very thick samples and detect asymmetry in the transmission curve. In particular, we could definitely assign the p-wave character to the 243-eV resonance. In the data analysis, two groups of total radiation widths appeared. Neutron-capture experiments showed two groups of gamma-ray spectra similar to Jackson's experiments at Argonne. Resonances with strong high-energy gamma-ray transitions have a total radiation width equal to 230 ± 40 MeV. Since some resonances exhibiting such gamma-ray spectra have been identified as p-wave levels in transmission experiments, it can be confirmed that the total radiation width of a p-wave level differs from that of an s-wave level and that in examining gamma-ray spectra for very weak levels, one can distinguish between s-wave and p-wave levels.

Table II shows a few previous results obtained at Saclay

TABLE II. Saclay results on Nb^{93} + n.

E_0 (eV)	$2g\Gamma_n$ (10^{-3} eV)	Γ (10^{-3} eV)	Γ_γ (10^{-3} eV)
42.2	0.10 ± 0.15	230 ± 50	230 ± 50
119	4 ± 0.4	140 ± 20	136 ± 20
193	40 ± 5	175 ± 30	135 ± 30
243	2.1 ± 0.3	263 ± 50	263 ± 50
335	15 ± 2	165 ± 30	150 ± 30
379	97 ± 10	250 ± 30	153 ± 32

with a 3-nsec/m resolution ten months ago. Jackson's values agree well enough with our results for p-wave levels but our mean radiation width is 140 ± 20 MeV for s-wave levels. Complete results with a value for the p-wave strength function will be published very soon in Physics Letters.

The curve in Fig. 1 represents our experimental points

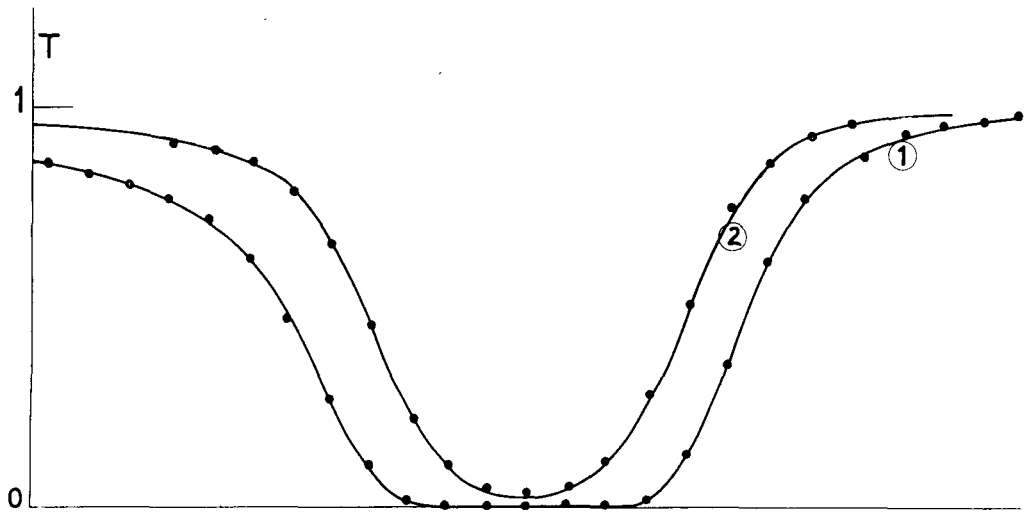

Fig. 1. Transmission curves for Nb at E_R = 118.8 eV. Solid curves were calculated with the parameters Γ = 140 MeV (resolution and Doppler effects included) and $g\Gamma_n$ = 2 MeV. The points are experimental values. Curve 1: thickness = 0.1515 atoms/barn. Curve 2: thickness = 0.046 atoms/barn.

fitted by the theoretical curve (resolution and Doppler effects included) for the 119-eV resonance.

K. K. SETH, Northwestern University: I would like to comment on your statement that up to this time it has been assumed that $(\overline{\Gamma}_\gamma)_s = (\overline{\Gamma}_\gamma)_p$. In fact, this is not so; the very first suggestion they might be different came from the (n,γ) cross-section work done at Duke University and published in the Annals of Physics (ref. 2). Since then the Russians, Popov and Fenin, analyzed their (n,γ) data on about ten different nuclei strictly on the basis of this suggestion. They conclude that ordinarily $\langle\Gamma_\gamma\rangle_s \neq \langle\Gamma_\gamma\rangle_p$ is indicated.

JACKSON: These are indirect measurements which can be analyzed

in terms of several alternative interpretations. Note added in proof: In reply to Dr. Seth's comment concerning $(\overline{\Gamma}_\gamma)_s = (\overline{\Gamma}_\gamma)_p$, I would like to cite the following quotation from the article (ref. 2) mentioned by him. The remark concerns the values of $(\overline{\Gamma}_\gamma/D_0)_s$ and $(\overline{\Gamma}_\gamma/D_0)_p$ which result from analysis of their data for Pd^{108}, a case in which these quantities differed significantly. Their analysis does not yield $(\overline{\Gamma}_\gamma)_s$ and $(\overline{\Gamma}_\gamma)_p$ directly. They say: "Assuming $(\overline{\Gamma}_\gamma/D_0)_p = 0.4\,(\overline{\Gamma}_\gamma/D_0)_s$ on the other hand results in an excellent fit. This result is not very surprising in view of the recent theoretical conjecture that parity effects may cause s- and p-wave level densities to differ to a much greater extent for an even-even target than for an odd-A target nucleus. $\overline{\Gamma}_\gamma$, of course, is not expected to differ appreciably for s- and p-wave neutrons."

SETH: In trying to explain their cross sections, the Russians find $(\overline{\Gamma}_\gamma)_s \neq (\overline{\Gamma}_\gamma)_p$ necessary. Of course, in our work we did not say that this is definitely indicated. We tried a few cases with $\langle\overline{\Gamma}_\gamma\rangle$ different for s- and p-wave capture and noticed that the fits were improved. We thus opened the possibility of such a variation of $\overline{\Gamma}_\gamma$.

P. AXEL, University of Illinois: I have a comment which leads to a question. It is misleadingly easy, once you have two letters like s and p, to think that the existence of two different total radiation widths would be explained by associating one with s and the other with p. The long formula Dr. Jackson wrote down for Γ_γ does not have anything in it to explain such a difference if it is the low-energy transitions that are responsible for most of Γ_γ. There is nothing in the present theory which would distinguish a cascade from a 1^- level from one from a 1^+ level.

We all know that there can be some differences between the decays of these levels. Until very recently, one had hoped that those differences were only associated with high-energy gamma rays that lead to low-lying energy levels of particular spin and parity. Such

high-energy transitions obviously depend on the parity of the initial state. But, if the first step of the cascade mainly involves 1—2-MeV gamma rays, we will have to reformulate the cascade calculation before it can explain the different Γ_γ values for the 1^- and the 1^+ states. At present, all you have at your disposal is the density of the final states and an energy-dependent transition probability. Nobody ever talks about a level density which depends on parity as well as on spin. Such a parity dependence would be needed to explain the difference between 1^- and 1^+ decays.

This leads to the question. Are you sure that the larger radiation widths cannot be associated with dominant high-energy transitions?

JACKSON: Yes, that is a certainty. The estimate we get is that something like 10% of this difference can be attributed to the transitions of energy greater than say 5 MeV.

AXEL: This is a clear sign that the cascade calculation must be refined. We just don't know enough about these 1-MeV or 2-MeV transitions. It will not help to add some magnetic-dipole or electric-quadrupole strength. You have to say that there is something different about the states reached in the first step of the cascade, depending on whether the initial state is 1^- or 1^+. We have seen plenty of evidence of such differences at energies as high as 3 MeV in a nucleus. For example, there are many 2^+ states but few, if any, 2^- states. If such parity dependence of the level density persists to much higher energies, someone will have to include such parity effects in a cascade calculation.

Session IV

NEUTRON CROSS SECTIONS

Wednesday afternoon, 16 October 1963

Presiding: J. A. Harvey

Scientific secretaries:
R. E. Coté
R. O. Lane

IV-1. STATISTICAL PROPERTIES OF NUCLEAR STATES AND TRANSITIONS*

Norbert Rosenzweig

Argonne National Laboratory, Argonne, Illinois

1. Introduction

I will attempt to summarize to a certain extent the statistical theory of neutron resonances, and I will be content if, in the course of the review, I succeed in making in some detail the following three points.

1. One and the same simple model, due to Wigner,[1] leads to a theory of both the energy-level fluctuations and the distribution of widths. The resulting economy in the number of assumptions is enough reason for making this point. However, there are also other reasons, as we shall see.

2. Even though the model is simple, it has not one or two but many consequences which can be compared with experiment.

3. Finally, the simple model, while very successful, naturally has its limitations which I want to discuss briefly. I must be brief because, aside from a couple of obvious limitations, the precise limits of the theory are not known. As is usual in a case like this, we will need to be guided by careful experiments.

Let me set the stage for these discussions by recalling what properties are under consideration. The best known statistical properties of a sequence of neutron resonance states are the distribution of neutron widths, which is well represented by the Porter-Thomas distribution[2]

---

*Invited paper.

[1] E. P. Wigner, Gatlinburg Conference on Neutron Physics by Time-of-Flight, Oak Ridge National Laboratory Report ORNL-2309, 1957, (unpublished), p. 59; Proceedings of the International Conference on Neutron Interactions with the Nucleus, Columbia University Report CU-175 (TID-7547), 1957 (unpublished), p. 49; Ann. Math. 65, 203 (1957); ibid. 67, 325 (1958).

[2] C. E. Porter and R. G. Thomas, Phys. Rev. 104, 483 (1956). For an extensive, recent analysis of the data see J. Garrison, Proceedings of the Symposium on Statistical Properties of Atomic and Nuclear Spectra, State University of New York at Stony Brook, May 1963.

$$P(y) = \frac{1}{\sqrt{2\pi}} \frac{e^{-\frac{1}{2}y}}{\sqrt{y}}, \qquad y = \frac{\Gamma}{\langle \Gamma \rangle}, \tag{1}$$

and the distribution of the spacings between adjacent levels having the same spin and parity which is well, though not perfectly, represented[3] by the Wigner surmise

$$P(x) = \frac{\pi}{2} x \exp(-\tfrac{1}{4}\pi x^2), \qquad x = \frac{s}{\langle s \rangle}. \tag{2}$$

The first, rather obvious, point which I want to make is that these two distributions by no means describe exhaustively the statistics of a number of successive resonances. Let me illustrate this with the help of Fig. 1.

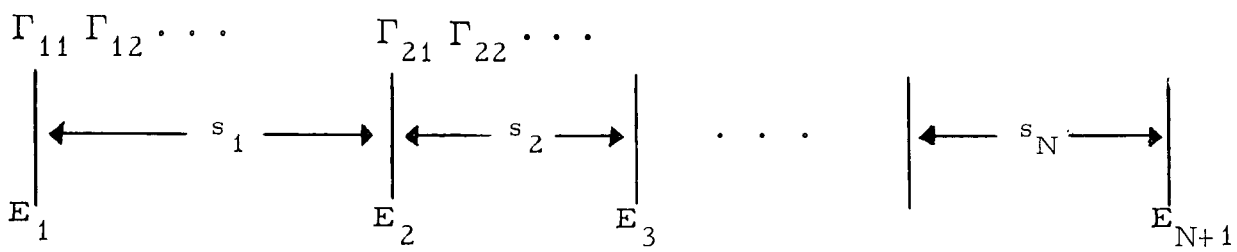

Fig. 1. Schematic drawing showing the positions of a series of successive neutron resonances of the same spin and parity and the associated partial widths. The first index of Γ_{ij} labels the compound state, the second identifies the final state.

In addition to inquiring about how the individual spacings $s_1, s_2, s_3, \cdots$ fluctuate about the mean value, one can, for example, ask about the joint distribution of two or more successive spacings; or about the joint distribution of two or more neutron widths; or, for a single level, for the joint distribution of two or more competing reaction widths. The most general object would evidently be the joint distribution of N spacings and all the widths associated with the N+1 levels, namely

[3] J. A. Harvey and D. J. Hughes, Phys. Rev. 109, 471 (1958). Very extensive results have been obtained at Columbia; see J. B. Garg, Proceedings of Stony Brook Symposium (Ref. 2).

$$P(s_1, s_2, \cdots, s_N; \Gamma_{11}, \Gamma_{12} \cdots ; \Gamma_{21}, \Gamma_{22} \cdots). \qquad (3)$$

II. Wigner's Random-Matrix Model

Next, I want to review a model which enables one to say quite a bit, though not everything, about the distributions which we have mentioned. Following Wigner,[1] one considers an ensemble of N-dimensional real symmetric matrices, defined by the probability distribution

$$\exp\left[-\mathrm{tr}\,(H - EI)^2 \right]. \qquad (4)$$

The volume element in the matrix space is naturally given by

$$dV_H = \prod_{i \leq j} dH_{ij}, \qquad i = 1, 2, \cdots, N. \qquad (5)$$

The following assumption is made concerning the relationship between the model and a nuclear spectrum. The behavior of n successive eigenvalues in the neighborhood of E is to be compared with the statistics of n successive energy levels of the same spin and parity $(n/N) \to 0$. The behavior of the corresponding eigenvectors is to be compared with the statistics of the corresponding compound states in the same limit.

The distribution is a plausible expression[4,5] of the idea that we give, in effect, a uniform weighting to the residual interaction $H - EI$. The residual interaction is arbitrary except for its magnitude $\mathrm{tr}\,(H - EI)^2$, which is essentially fixed.

While I do not wish to engage in an inconclusive discussion as to how, exactly, this remarkable model fits into the general scheme of things, I can underline two aspects, recognized by Wigner, which seem to play an essential role, and which make the success of the model understandable.

---

[4] F. J. Dyson, J. Math. Phys. 3, 140, 157, 166 (1962).

[5] N. Rosenzweig, Bull. Am. Phys. Soc. 7, 91 (1962); Brandeis University Lectures 1962 (W. A. Benjamin, Inc., New York, 1962).

1. Although we are ultimately concerned with the statistical properties of the levels and wave functions, it is essential to introduce a distribution of the matrices. I believe this is connected with the fact that this is the only natural way of expressing in quantum mechanics the effect of a known perturbation on a known model Hamiltonian.

2. The apparent validity of the conjecture that many of the statistical results will be largely independent of the precise form of the weighting function (5) has the practical result that even an approximate form gives many correct results.

III. Some Consequences of Wigner's Model[6]

The first step consists in transforming the volume element in the matrix space of eigenvalues and eigenvectors,[6] i.e.,

$$dV_H \rightarrow \prod_{i<j} |\lambda_i - \lambda_j| d\lambda_1 \cdots d\lambda_N \, dV_X . \tag{6}$$

Combining this with the weighting function (5), one obtains the distribution of eigenvalues

$$P(\lambda_1 \lambda_2 \cdots \lambda_N) \propto e^{-\sum \lambda_i^2} \prod_{i<j} |\lambda_i - \lambda_j| . \tag{7}$$

Several remarks are in order. (1) The cryptic symbol dV_X is an abbreviation for the distribution of eigenvectors, to which I will return later. (2) The distribution of eigenvalues contains the famous difference product which explains the "repulsion of levels." (3) The distribution of eigenvalues is independent of the distribution of eigenvectors. This implies, without any further calculation, that there is no correlation between widths and spacings.

[6] C. E. Porter and N. Rosenzweig, Suomalaisen Tiedeakatemian Toimituksia A VI, No. 44 (1960).

A similar conclusion will hold for any other ensemble that is invariant under an orthogonal change in basis. Dr. Seth informs me that examination of a lot of neutron-resonance data indicates that the correlation between a neutron width and a spacing is indeed quite small.

IV. Energy-Level Statistics

Let me first make some remarks about the distribution of spacings between neighboring levels of the same spin and parity (a "simple" sequence). You will remember that it was in this connection that the random-matrix model had its first striking success in the description of experimental results.[7,8] The success is of a kind which is well illustrated in Fig. 2, based on recent work at Saclay.[9]

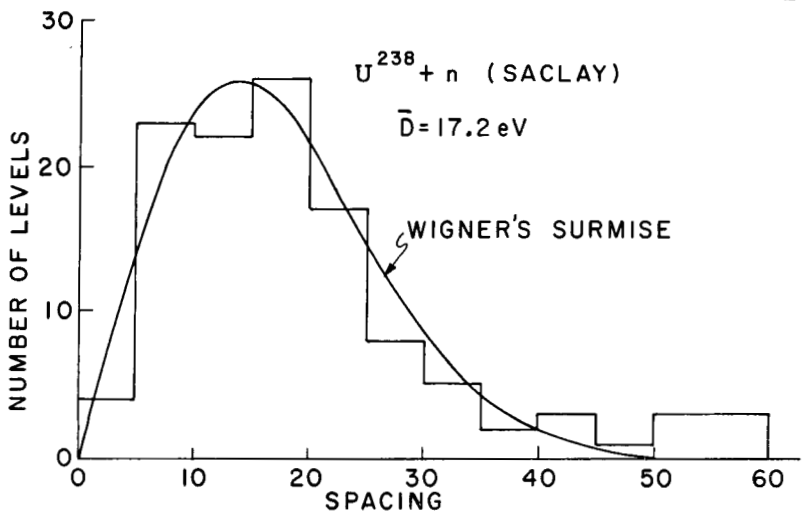

Fig. 2. Distribution of spacings between adjacent levels of the same spin and parity, observed at Saclay (Ref. 9) in the reaction U^{238} + n. These results confirm the earlier ones (Ref. 3) that the distribution is in accord with the statistical model, whose prediction is given to a good approximation by the Wigner distribution (solid curve).

The solid curve, known as the Wigner surmise, is a good (though not perfect) representation of the exact prediction of the model. It should be appreciated that according to the model the distribution of the spacing is given by an integration over all except two adjacent engenvalues

[7] S. Blumberg and C. E. Porter, Phys. Rev. 110, 786 (1958).

[8] N. Rosenzweig, Phys. Rev. Letters 1, 24 (1958).

[9] Private communication from J. Julien at this conference. See also C. Corge, Vinh-Dinh Huynh, J. Julien, J. Morgenstern, and F. Netter, Compt. Rend. 253, 859 (1961).

of the distribution (7). This formidable analytical problem was substatially solved by Mehta and Gaudin.[10]

The agreement between experiment and theory is apparently so good, in this particular case at least, that it makes sense to inquire whether there is any evidence of disagreement. In attempting to answer this question one must, of course, keep in mind that the theoretical result represents an average over the ensemble, whereas the particular set of levels is at best a fairly typical member of the ensemble. So, in order to answer the question reliably, one should calculate on the basis of the model what sort of deviations are reasonable. Such a calculation does not yet exist for the distribution of spacing. However, one can surely get an idea of the magnitude of the fluctuations by looking at one of the early Monte Carlo type calculations[8] leading to the theoretical distribution of spacings. This histogram, though based on 200 matrices of order 20, exhibits quite a few fluctuations (Fig. 3).

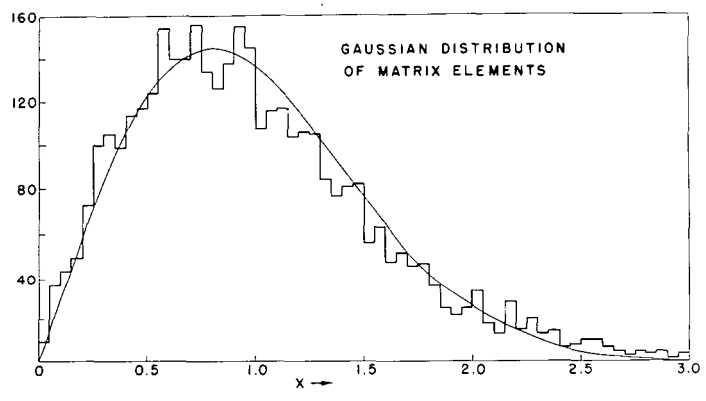

Fig. 3. Histogram representing a deduction (Ref. 15) of the spacing distribution from the statistical model with the help of a digital computer. The result is seen to be in good agreement with the simple analytical form proposed by Wigner, and therefore also with experiment. The histogram also gives an indication of the magnitude of the fluctuations away from a smooth curve, even though the histogram is based on as many as 4000 spacings.

---

[10] M. L. Mehta, Nucl. Phys. 18, 395 (1960); M. L. Mehta and M. Gaudin, Nucl. Phys. 18, 420 (1960); ibid. 22, 340 (1961). M. Gaudin, Nucl. Phys. 25, 447 (1961).

For the same reason one should probably be cautious in the interpretation of the interesting deviation (Fig. 4) observed by the Columbia group in Th^{232}

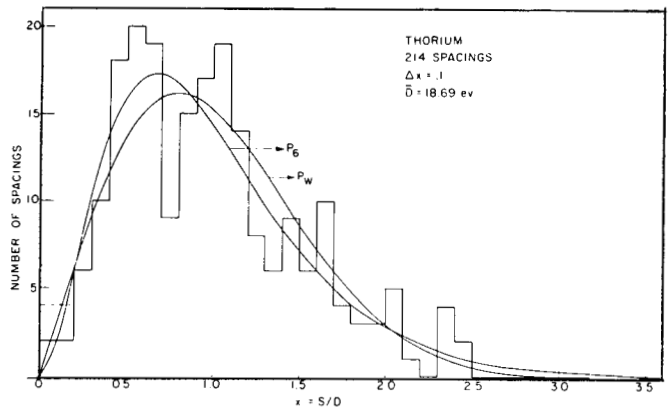

Fig. 4. Spacing distribution obtained by J. B. Garg at Columbia for Th^{232}.

Having displayed an appropriate conservatism, I want to stress right away that the discovery of deviations from the predictions of the simple model, and the explanation of deviations in terms of some general feature of a nuclear model is the most interesting and challenging aspect of the matter. This position was taken by Moldauer[11] at the recent symposium at Stony Brook where he attempted to discuss the dependence of the distribution of widths upon the nuclear model.

As a matter of fact, a few years ago we were able to illustrate this very thing, viz., deviations from the simple model in the case of complex atomic spectra.[12] Here also the deviations could be explained.

I would like to illustrate this with the help of Fig. 5, which still impresses me, even though it is three years old.[12] For the heavy elements, all the constants of the motion except total angular momentum and parity are practically washed out, and the observed spacing distribution is fairly close to the result of the simple asymptotic theory. For the light elements, which are rather close to L-S coupling, the observed result can be understood by superposing an appropriate set of independent

[11] P. A. Moldauer, Proceedings of the Stony Brook Symposium (see Ref. 2).

[12] N. Rosenzweig and C. E. Porter, Phys. Rev. 120, 1698 (1960); ibid. 123, 853 (1961).

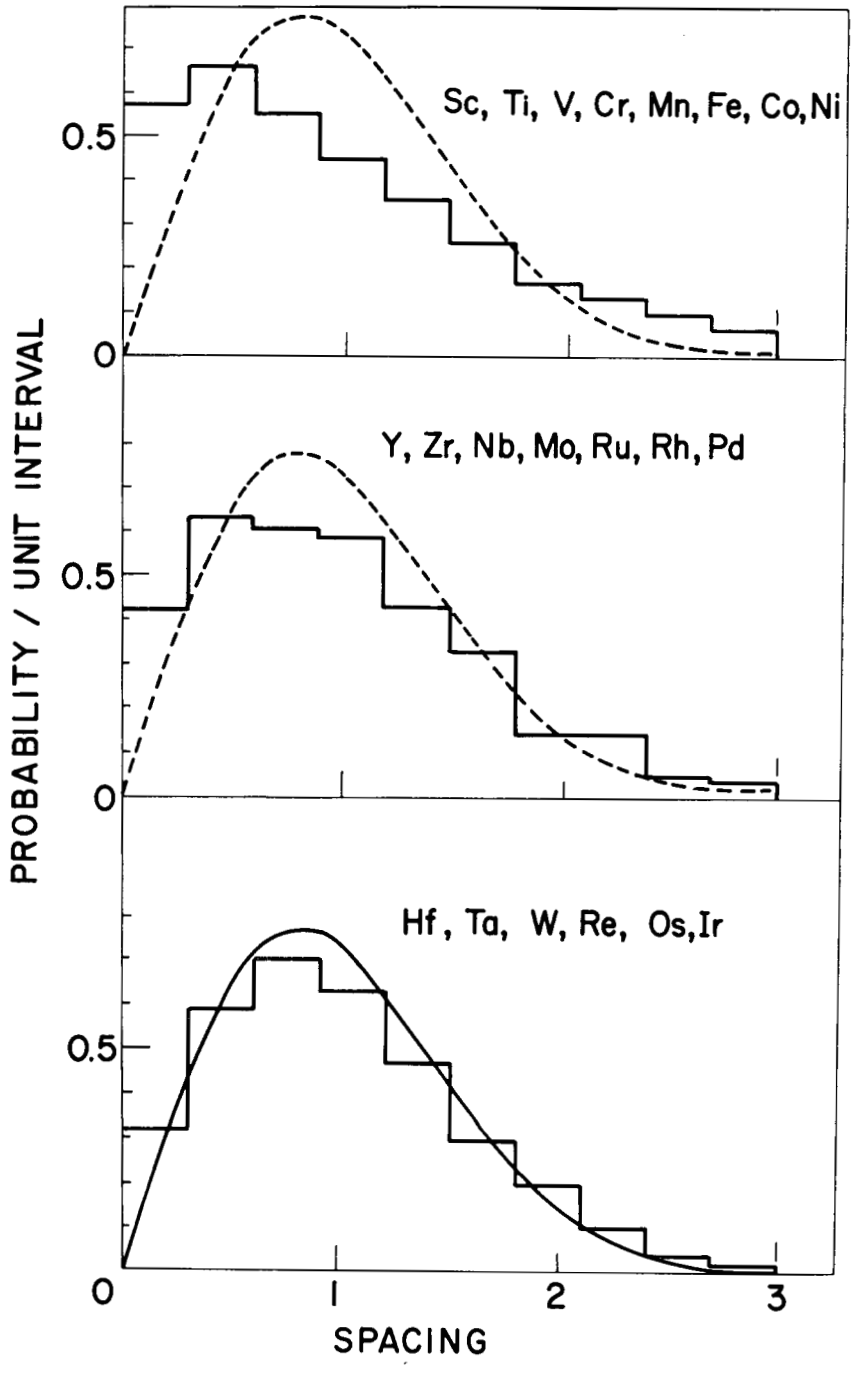

Fig. 5. Empirical distributions of nearest-neighbor spacings for the odd-parity levels of atomic spectra in the first, second, and third long periods. To obtain these figures, separate distributions were constructed for the J sequences of each element and then the results were combined. Comparison with the exponential and Wigner distributions (also shown) indicates that the degree of repulsion increases steadily as one goes from the first to the second and, finally, to the third period. This variation can be understood in terms of the corresponding increase in strength of the spin-dependent forces.

sequences, one for each S-L type. The intermediate case can be understood only if one assumes that the total orbital and total spin angular momentum are approximate constants of the motion. This can be expressed in the statistical theory by introducing a parameter which is essentially the ratio of the strength of the spin-orbit interaction to the residual electrostatic interaction. Even this simple model then provides a good qualitative explanation over an enormous range of atomic weights.

I now want to return definitely to the simple model and mention some of the other results which have been obtained.

Using the methods of Mehta, Gaudin, and Dyson, Peter Kahn[13] has calculated the distribution of the sum of two adjacent spacings in a simple sequence. His result differs very little from a preliminary estimate by Porter[14] using 3 X 3 matrices, and this enables me to use a graph (Fig. 6) which I happen to have, in which the theoretical result is compared with some data for Th^{232} obtained by Garg at Columbia. From such a calculation one also gets the correlation coefficient between two

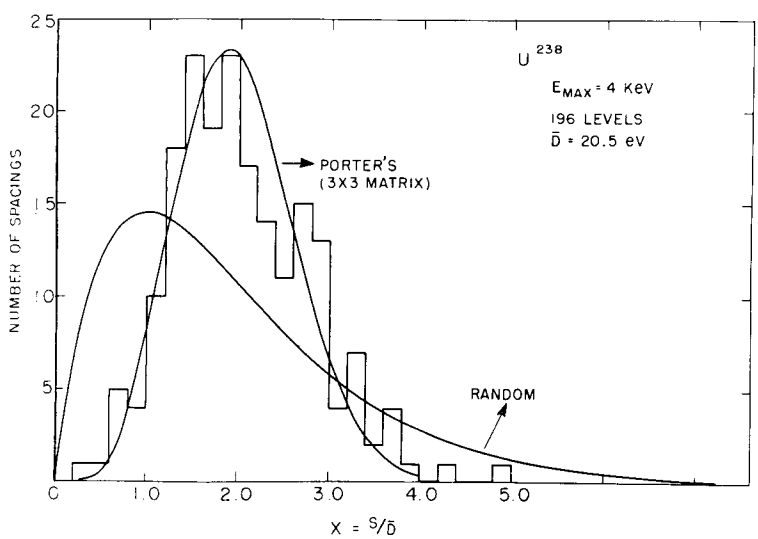

Fig. 6. Histogram representing the distribution of spacings between next-nearest neighbors, deduced at Columbia. The solid curve, which is in good agreement with the data, represents the prediction of the model obtained by Kahn (Ref. 13) and Porter (Ref. 14).

---

[13] P. Kahn, Nucl. Phys. 41, 159 (1963).

[14] C. E. Porter, Nucl. Phys. 40, 167 (1963).

adjacent spacings, which turns out to be -0.25. This can also be compared with results on Th^{232} obtained at Columbia (Fig. 7).

Dr. Seth has not only studied the available data for zero-spin target nuclei but also calculated the correlation coefficient from the data for odd targets as a function of the spin. These results can, in principle, be compared with the theoretical calculations carried out by Harvey Leff,[15] provided you know, or make assumptions about, the composition of the observed level sequence with respect to parity and spin.

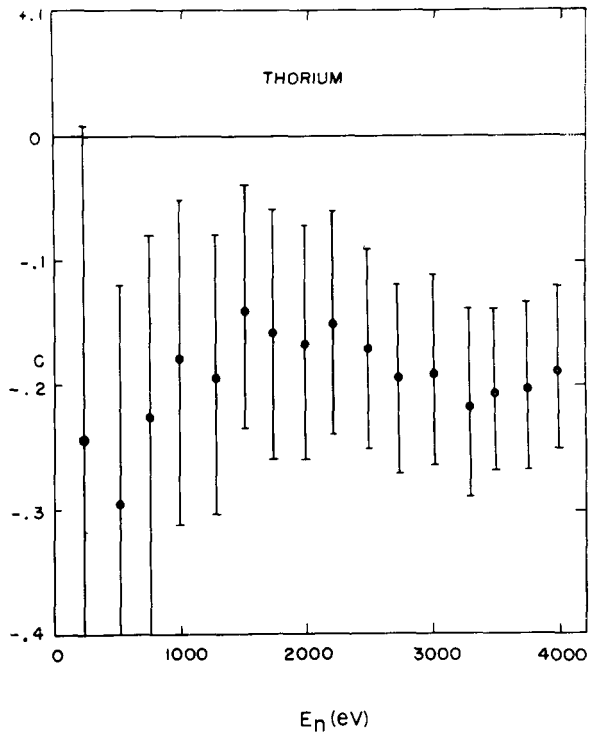

Fig. 7. A plot of the correlation coefficient between adjacent spacings as the number of levels included in the computation is increased. The theoretical result of -0.25 seems to be approached.

The distribution of the sum of two, three, four, and more adjacent spacings has been computed by Porter[16] who has recently continued with the early Monte Carlo studies. It should be remarked here that in spite of the considerable advances made in the analytical treatment of these problems,[17] there are many problems left which can only be handled on the computer, which may be employed with great power in these problems. On the other hand, one severe limitation of the computer should be noted: it is, of course, not possible to obtain rigorous asymptotic results as $N \to \infty$.

---

[15] H. Leff, Bull. Am. Phys. Soc. 8, 31 (1963); Ph.D. Thesis, University of Iowa, 1963 (unpublished).

[16] C. E. Porter, J. Math. Phys. 4, 1039 (1963).

[17] References 4 and 10, and a partial review in the Brandeis Lectures, Ref. 5.

Such analytical work as we have is very impressive, and I would like to illustrate the kind of result which has been obtained by describing one calculation by Dyson and Mehta.[18] They addressed themselves to the question already mentioned, viz., whether there is any evidence that the statistical model is not adequate for heavy nuclei. Consider a series of successive neutron resonance levels of the same spin and parity. Let N(E) be the number of levels having energy less than or equal to E. This leads to the familiar staircase (Fig. 8) which the experimenters for many years have used to determine the level density. (The level density will be just the slope of the straight line drawn through the staircase.)

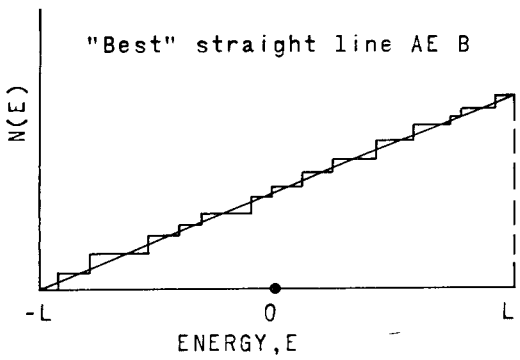

Fig. 8. A schematic drawing of the staircase observed in a typical neutron resonance experiment, and the straight line fitted to it according to the Dyson-Mehta least-squares criterion.

Dyson and Mehta define a statistic Δ which measures the total deviation of the staircase from the best straight line according to the least-squares criterion:

$$\Delta \equiv \min_{A,B} \left\{ \frac{1}{2L} \int_{-L}^{L} [N(E) - AE - B]^2 \, dE \right\}. \tag{8}$$

Solution of this minimum problem gives the experimentally observed value of Δ.

Dyson and Mehta are also able to calculate both $\langle \Delta \rangle$ and $\langle \Delta^2 \rangle$ from the statistical model. If a careful experiment contradicts

$$\Delta_{obs} \approx \langle \Delta \rangle \pm \sqrt{\langle \Delta^2 \rangle - \langle \Delta \rangle^2} \, , \tag{9}$$

[18] F. J. Dyson and M. L. Mehta (to be published).

then the theory is shown to be inadequate. Evidently, the smaller the variance of the statistic, the sharper is the test. This Δ is a very good statistic, since

$$\langle \Delta^2 \rangle - \langle \Delta \rangle^2 = \frac{1.169}{\pi^4} \quad \text{(independent of n!)} , \tag{10}$$

whereas,

$$\langle \Delta \rangle = \frac{1}{\pi^2} [\log n - 0.0687] . \tag{11}$$

Table I is a comparison between theory and experiment.

TABLE I. Preliminary comparison with the Columbia data [Dyson and Mehta (Ref. 18)] .

Nucleus	U^{238}	T^{181}	Th^{232}
Number of levels	57	68	154
Δ (observed)	1.278	1.437	3.123
Δ (theory)	0.40 ± 0.11	0.87 ± 0.22	0.50 ± 0.11

In interpreting the results, I make three comments. (1) The analysis is extremely sensitive to imperfections in the data. The absence of a few levels or misassignment of a few levels can change Δ by a factor of the order of 2. So at the moment it cannot be said whether the imperfection is in the data or the theory. (2) If the theory is perfect for both U^{238} and Th^{232}, then the data for Th are poorer than for U^{238}. (3) This Δ statistic is a measure of the long-range correlation of the series of levels.

The results of Dyson and Mehta indicate a rather stronger correlation between the positions of levels than one might have expected. This leads one to wonder to what degree a statistical predictive theory is feasible. For example, the spacing distribution has some, though not much, predictive value. Given a level at λ_1, it predicts the position of the next level according to the spacing distribution

$$P(\lambda_1 | \lambda_2)\, d\lambda_2 \approx \frac{\pi}{2} |\lambda_2 - \lambda_1| \exp\left[-\tfrac{1}{4}\pi(\lambda_2 - \lambda_1)^2\right] d\lambda_2 . \quad (12)$$

But now consider the conditional distribution

$$P(\lambda_1, \lambda_2, \cdots, \lambda_n | \lambda_{n+1})\, d\lambda_{n+1} \quad (13)$$

in which $\lambda_1, \lambda_2, \cdots, \lambda_n$ are the positions of n successive levels and P is the distribution of the next level λ_{n+1}. It seems obvious that (13) has more predictive value than (12) — but how much better it is, I do not know.

V. Distribution of Widths[1,6,19,20]

We will illustrate how the distribution of widths follows from the matrix ensemble (4) by considering the distribution of partial radiation widths. Let the (initial) compound states be denoted by $\psi_1, \psi_2, \cdots, \psi_N$ and the final states, after the emission of a single gamma ray, by $\phi_1, \phi_2, \cdots, \phi_n$. The partial radiation widths will be of the form

$$\Gamma_{i \to j} = (\psi_i, V\phi_j)^2. \quad (14)$$

---

[19] T. J. Krieger and C. E. Porter, J. Math. Phys. 4, 1272 (1963).

[20] N. Rosenzweig, Phys. Letters 6, 123 (1963).

One obtains a statistical model when the distribution of the ψ's is specified. The random-matrix model furnishes such a distribution on which a direct calculation of the distribution of widths can be based without any further assumption.[20] Let the ψ's be expanded in the same basis in which the matrices of the residual interaction were assumed to be constructed, i.e., let

$$\psi_i = \sum_{j=1}^{N} X_{ij} u_j, \tag{15}$$

where $u_1 \cdots u_N$ is this basis. The coefficients X_{ij} from an orthogonal matrix. In the random-matrix model, the orthogonal matrix $||X_{ij}||$ is distributed according to the invariant measure on the group of orthogonal matrices in N dimensions, dV_X. A physicist's view of this well known mathematical entity might be

$$dV_X \propto \prod_{i<j} \delta\left(\sum_k X_{ik}X_{jk}\right) \prod_i \delta\left(\sum_k X_{ik}^2 - 1\right) \prod_{i,j} dX_{ij}. \tag{16}$$

This represents a uniform distribution of N orthogonal unit vectors on the surface of the N-dimensional unit sphere. From this one also sees readily that the marginal distribution of a single compound state is given by

$$P(X_1, X_2, \cdots, X_N) \propto \delta\left[\sum X_i^2 - 1\right], \tag{17}$$

and this is all one needs in many, though not all, applications. [One might remark that distribution (17) is about the simplest distribution of a unit vector which there is, and is what one would naturally postulate also without the matrix ensemble. Indeed, Porter and Thomas, obtained the neutron-width distribution before the spacing distribution was discussed.]

Since one is usually interested only in a number of partial widths which is small compared with N (the number of statistically equivalent compound states), the "microcanonical ensemble" (17) may be replaced by the "canonical ensemble"

$$P(X_1, \cdots, X_n) \rightarrow \exp\left[-\tfrac{1}{2}N\sum_{i=1}^{n} X_i^2\right], \quad n \ll N. \tag{18}$$

At this point the calculation is almost finished, because the widths are just quadratic expressions in the X_i. The transformation of variables which leads to the distribution of widths is especially simple if one chooses the basis vectors wisely as follows. Let P denote the projection onto the space of the N compound states. Let the unit vector u_1 be defined through the relation

$$PV\phi_1 = |PV\phi_1|\, u_1. \tag{19}$$

Let the orthogonal unit vector u_2 be defined through the relation

$$PV\phi_2 = |PV\phi_2|\,[\alpha u_1 + \sqrt{1-\alpha^2}\, u_2]. \tag{20}$$

$$\vdots$$

Evidently,

$$\alpha = \frac{(PV\phi_1, PV\phi_2)}{|PV\phi_1|\,|PV\phi_2|}, \tag{21}$$

and so on.

The widths now are particularly simple quadratic expressions in the components of the random vector $\psi = \sum X_i u_i$:

$$\Gamma_1 = |PV\phi_1|^2 X_1^2, \tag{22}$$

$$\Gamma_2 = |PV\phi_2|^2 (\alpha X_1 + \sqrt{1-\alpha^2}\, X_2)^2, \tag{23}$$

$$\vdots$$

Substitution of (22) into the Gaussian (18) leads to a Porter-Thomas distribution (1) for the partial radiation width. The rather extensive measurements by Bollinger, Carpenter, Coté, and Marion[21] indicate that for the most part the distribution of a single partial radiation width is compatible with the Porter-Thomas distribution. However, the measurements are not yet so precise that deviations from the above theory are ruled out.

Substitution of (23) into the Gaussian distribution (18) leads to a correlated Gaussian distribution in the two width amplitudes. The correlation coefficient $\rho(\Gamma_1, \Gamma_2)$ between two partial radiation widths is best calculated in the space of X_1 and X_2 and has the transparent form

$$\rho(\Gamma_1, \Gamma_2) = \frac{(PV\phi_1, PV\phi_2)^2}{|PV\phi_1|^2 \, |PV\phi_2|^2} = a^2. \tag{24}$$

What matters is the overlap of $V\phi_1$ and $V\phi_2$ in the space of the compound states. Under many circumstances one would expect this to be a rather small number of order 1/N. However, the correlation coefficient in this model is definitely non-negative.

Application of the theory to a sum of partial radiation widths. In some experiments, what is measured is the sum of several partial radiation widths[22] (Fig. 9), namely

$$S = \Gamma_1 + \Gamma_2 + \cdots + \Gamma_n. \tag{25}$$

---

[21] L. M. Bollinger, R. T. Carpenter, R. E. Coté, and J. P. Marion, Phys. Rev. 132, 1640 (1963).

[22] D. J. Hughes, H. Palevsky, H. H. Bolotin, and R. E. Chrien in Proceedings of the International Conference on Nuclear Structure, Kingston, Canada, 1960, edited by D. A. Bromley and E. W. Vogt (University of Toronto Press, Toronto, 1960) p. 771; C. Corge et al., J. Phys. radium 22, 722 (1961).

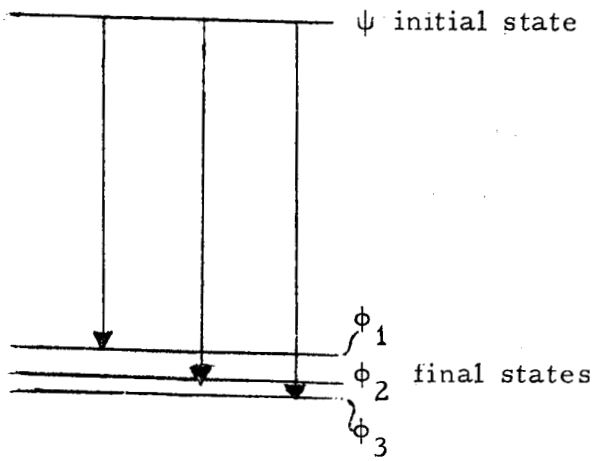

Fig. 9. A drawing to illustrate that a compound state may emit a gamma ray to one of several final states ϕ_1, ϕ_2, ϕ_3, ...

The distribution of this quantity may be determined experimentally by measuring the sum S for many initial (compound) states so that one can, for example, estimate the relative variance δ^2 given by

$$\delta^2 \equiv \frac{\langle S^2 \rangle - \langle S \rangle^2}{\langle S \rangle^2} . \tag{26}$$

On the other hand, on the basis of the foregoing theory, the inequality,

$$n \geqslant 2/\delta^2 \tag{27}$$

holds rigorously, where n is the number of final states. The inequality depends entirely on the fact that the relative variance of each partial width is 2, and that the correlation coefficients are non-negative, as implied by the statistical model.

When this inequality is confronted with some of the early measurements[22] on U^{238}, one gets a flat contradiction between experiment and theory. From the old data one would infer (assuming the theory to be applicable) that $n \geqslant 20$, whereas n is known to be about 5. Recent work by H. Jackson indicates that the discrepancy is certainty not as large as it seemed to be only a short time ago. Dr. Jackson will himself report on the present situation.[23]

[23] H. Jackson, paper IV-4 presented at this conference.

VI. Limitations of the Simple Random-Matrix Model

The model has two obvious limitations, one of which I have already alluded to. (1) The model describes a system which has a few exact constants of the motion, such as spin and parity, and no other quantum numbers which are even approximately constant. This obviously represents an oversimplified view of a real nucleus. (2) The model is a theory designed to explain fluctuations over a limited range in energy. Indeed, on a large scale the density of eigenvalues follows Wigner's semi-circle, which is, of course, not a realistic representation of the law of nuclear level densities.

Actually, the two limitations are not independent of each other because it seems obvious that the approximate quantum numbers (which arise from specific features of nuclear structure, such as collective or independent-particle effects) will frequently have effects extending over a large range in energy.

* * *

K. K. SETH, Northwestern University: You mentioned that only when all the quantum numbers except perhaps the spin and parity are washed out, then alone one expects distributions like Wigner's for level spacings and like Porter and Thomas's for neutron widths. Now, most of the examples which have been used so far to compare the theories of distribution functions have been obtained from heavy nuclei like uranium, thorium, and so on. We know these nuclei are rather strongly deformed. Doesn't this cast some sort of aspersion on the conclusions drawn from comparison between the theoretical distributions and such data?

ROSENZWEIG: The experimental evidence indicates that certain statistics (like the spacing distribution, which is an extremely local thing) are apparently not affected by specific features of the nuclear model. However, this may well be different for other statistics in which the wave

functions come in (e.g., for correlation coefficients between widths). However, I have no detailed insight into the matter.

SETH: In other words, you think that the spacing distribution will be less sensitive?

ROSENZWEIG: Yes, this is my impression.

P. AXEL, University of Illinois: I would like to extend the last question. Couldn't you turn the argument around to exclude some possibilities? For example, somebody might suggest a model for calculating energy levels near 7 MeV in a deformed nucleus. This model might postulate one class of levels associated with excitations along the long axis and another uncorrelated set of levels associated with excitations along the short axes. Couldn't you point to the observed level-spacing statistics as evidence that there are not two sets of levels like these? Would it not be fair to say that the observed level spacing tells us that there are not two distinct types of levels associated with the deformation?

ROSENZWEIG: Yes, it is fair with the following qualification. From the spacing distribution one could conclude that the motion which you mentioned does not correspond to an exact quantum number; or, if it is a rather good constant of the motion, then the two classes of excitation do not occupy overlapping energy ranges. But just how good it is, it is not possible to say from this particular statistic.

G. BEN-DAVID, Israel AEC Soreq Research Establishment: In the table of Dyson and Mehta, the experimental statistic Δ(obs) increases from U^{238} to Ta^{181} to Th^{232}, quite unlike the expected statistic. However, this observed statistic is nearly proportional to the number of levels used in the calculation. Has this calculation been carried out for the first 57 levels of each of the three nuclei to see if the statistic fit is better?

ROSENZWEIG: This has not yet been done. It should be done.

A. MICHAUDON, Centre d'Etudes Nucleaires de Saclay: About the distribution of level spacings in Th^{232} and the discrepancy between the Columbia results and the theory, I would like to say that recent measurements carried out with the Saclay linac show a level density about 30% higher than previously determined at Columbia and Harwell. This might change the experimental level-spacing distribution quite considerably.

J. JULIEN, Centre d'Etudes Nucleaires de Saclay: In U^{238}, the mean level spacing is 20 eV in the Columbia results and 17 eV in the Saclay results.

ROSENZWEIG: This sounds fascinating.

N. J. PATTENDEN, AERE Harwell: You mentioned that the Δ calculation by Dyson and Mehta was very sensitive to the number of levels missed in the experiment. Therefore it seems that this is a sensitive method of correcting experimental data for missed levels. Is that right?

ROSENZWEIG: This would seem to be the case. I think that experimenters should use the Δ statistic, which I regard as an unusually fine analytical achievement. It might be used as follows. If the data have a preliminary character, Δ might be used as an indication of the quality of the data. As the data became more perfect, Δ will serve to test the model.

IV-2. DISTRIBUTION OF PARTIAL RADIATION WIDTHS*†

L. M. Bollinger, R. E. Coté, R. T. Carpenter,‡ and J. P. Marion
Argonne National Laboratory, Argonne, Illinois

The gamma-ray spectra from the capture of neutrons in resonances of Hg^{199}, Pt^{195}, W^{183}, and Se^{77} have been studied in measurements extending over four years. A least-squares fitting of the spectra gives relative values of partial widths for various sets of high-energy radiative transitions. These widths are treated as statistical samples drawn from populations governed by a χ^2 distribution with ν degrees of freedom. A technique of hypothesis testing is used to derive unbiased values of ν from the small samples of experimental widths. The over-all result of the analysis is $\nu = 1.34 \pm 0.33 \pm 0.21$. The previously reported[1] partial radiation widths for resonances of Gd^{155}, Yb^{173}, Hf^{177}, and Hg^{201} are also analyzed. The result is $\nu = 1.14 \pm 0.44 \pm 0.21$. Thus, both sets of data are in good agreement with the value $\nu = 1$ expected from the Porter-Thomas description of the distribution of the widths associated with a single exit channel. A full description of the results will be given elsewhere.[2]

* * *

J. JULIEN, Centre d'Etudes Nucleaires de Saclay: I should like to know if the Argonne group agrees with the Saclay results on the spin assignments in Pt^{195} for the 154- and 150-eV resonances. We published our results one year ago and the Argonne group was still in disagreement with our values a few weeks ago.

---

*Work performed under the auspices of the U.S. Atomic Energy Commission.

† Read by title only.

‡ Now at State University of Iowa, Iowa City, Iowa

[1] R. T. Carpenter, Argonne National Laboratory Report ANL-6589, 1962 (unpublished).

[2] L. M. Bollinger, R. E. Coté, R. T. Carpenter, and J. P. Marion, Phys. Rev. 132, 1640 (1963).

BOLLINGER: The spin of the resonance in Pt^{195} at 151 eV is J = 1; the spin of the resonance at 154 eV is J = 0. The latter assignment was in error on the preprint of our paper that a few people received.

JULIEN: What is the spin assignment in the 980-eV resonance of Se^{77} for the Argonne group?

BOLLINGER: In Se^{77} we feel that there are two resonances at roughly 980 eV. One has spin 1 and the other resonance has spin 0. The resonance with spin 0 is the one that has the larger neutron width, but the resonance with spin 1 appears to be the one that produces the larger amount of capture — or, at least, an amount of capture that is roughly the same as that of the wider resonance.

JULIEN: Our resolution in Saclay is at least 10 times better and we only see one level. I don't understand how you can observe a little level so near this large resonance.

CHAIRMAN: I think that we can continue this discussion at coffee.

IV-3. RESONANCE NEUTRON COINCIDENCE CAPTURE GAMMA-RAY SPECTRA IN W^{184} †

J. A. Moore, J. L. Friedes, R. E. Chrien, and H. Palevsky

Brookhaven National Laboratory, Upton, L.I., New York

We have recently made additions to the fast chopper facility, operated jointly by B.N.L. and A.E.C.L., at the NRU reactor, Chalk River, Canada. A magnetic-tape recording system has been put into operation; the system includes both 1-parameter (time of flight) and 2-parameter (time of flight, pulse height) encoders. Secondly, a NaI crystal 8 in. in diameter × 6 in. long has been incorporated into the capture γ-ray spectrometer which, until now, consisted of an array of six 3 × 3-in. NaI crystals.

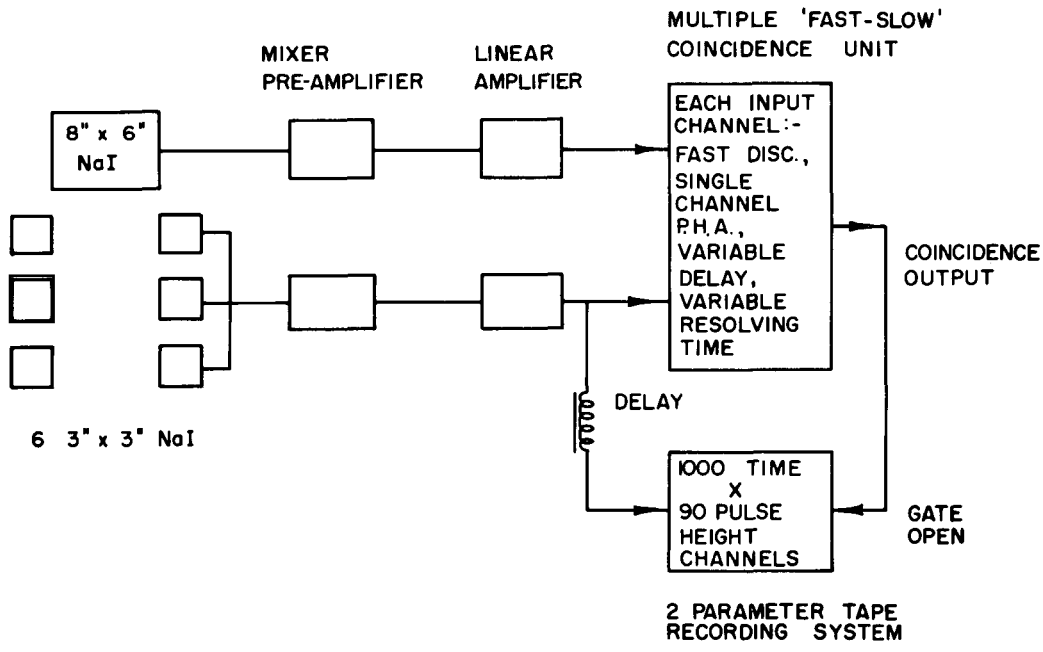

Fig. 1. Schematic diagram of the apparatus used for the measurement of coincidence capture γ-ray spectra.

Figure 1 is a schematic diagram of the system used for the measurement of resonance neutron coincidence capture γ rays. Coinci-

† Presented by J. A. Moore.

dences are formed between events in the 8 × 6-in. NaI detector (high-energy primary γ rays) and the corresponding low-energy γ rays detected in the six 3 × 3-in. NaI crystals, operated in parallel. The coincidence output opens the gate to permit the encoding of the time (neutron energy) and pulse height (γ-ray energy) of the event detected in the 3 × 3-in. crystals. The target was tungsten foil, 2.5 mil thick and 8 × 4-in. in area, inclined at 45° to both the beam direction and the faces of the 3 × 3-in. NaI crystals.

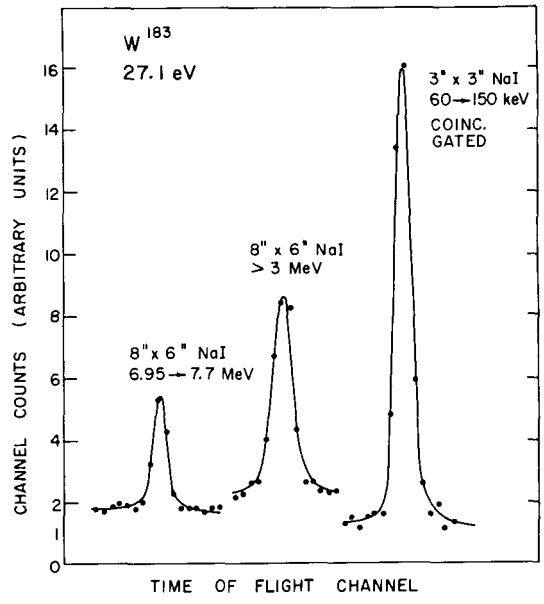

Fig. 2. The 27.1-eV resonance of W^{183} seen in time of flight by the NaI capture γ-ray detectors. The detectors used and the energy of the γ rays accepted for time-of-flight analysis label the three spectra shown. The 3× 3-in. events were in coincidence with γ rays of energy 2.5 to 8.0 MeV detected in the 8 × 6-in. NaI crystal. The three curves have not been normalized to the same ordinate scale.

Figure 2 shows, for comparison purposes, three time-of-flight spectra, observed by the NaI detectors, in the vicinity of the 27.1-eV resonance formed by neutron capture in W^{183}. Coincidence rates are less than the singles in the 8 × 6-in. NaI detector, due primarily to the solid angle of the 3 × 3-in. NaI array (15%) and to internal conversion of the low-energy γ rays. However, in this case, the disadvantage is partially compensated by the improved signal/background ratio of the coincidence events in the time-of-flight spectrum. This is evident from a comparison of the three spectra shown in Fig. 2.

Figures 3 and 4 show coincidence-gated low-energy γ-ray spectra, measured by the 3 × 3-in. array, from various resonances and isotopes of tungsten. The target was 2.5 mil natural tungsten and the pulse-height window of the 8 × 6-in. NaI coincidence input channel was set to accept γ rays between 2.5 and 8.0 MeV. Spectra observed from neutron capture in W^{183} (Fig. 3) show the characteristic radiation, 111 keV, which results from the depopulation of the first excited state in W^{184}, by the variety of cascades which are accepted by the coincidence circuit. Also evident in all resonances and isotopes, are tungsten K x rays (61 keV) resulting from internal conversion. With the exception of the 142-keV

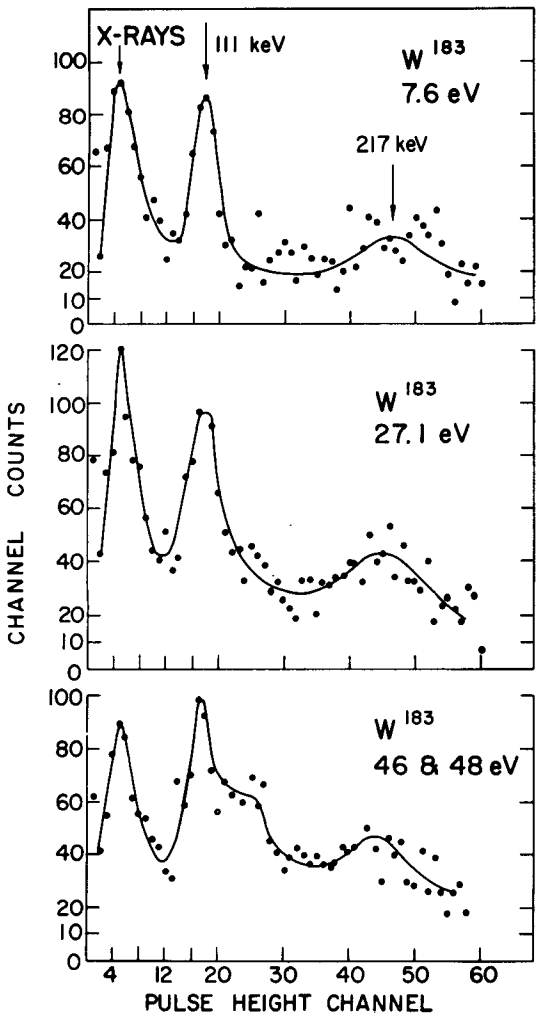

Fig. 3. Coincidence low-energy γ-ray spectra from resonances formed by capture in W^{183}. The 8 × 6-in. window was set at 2.5 to 8.0 MeV.

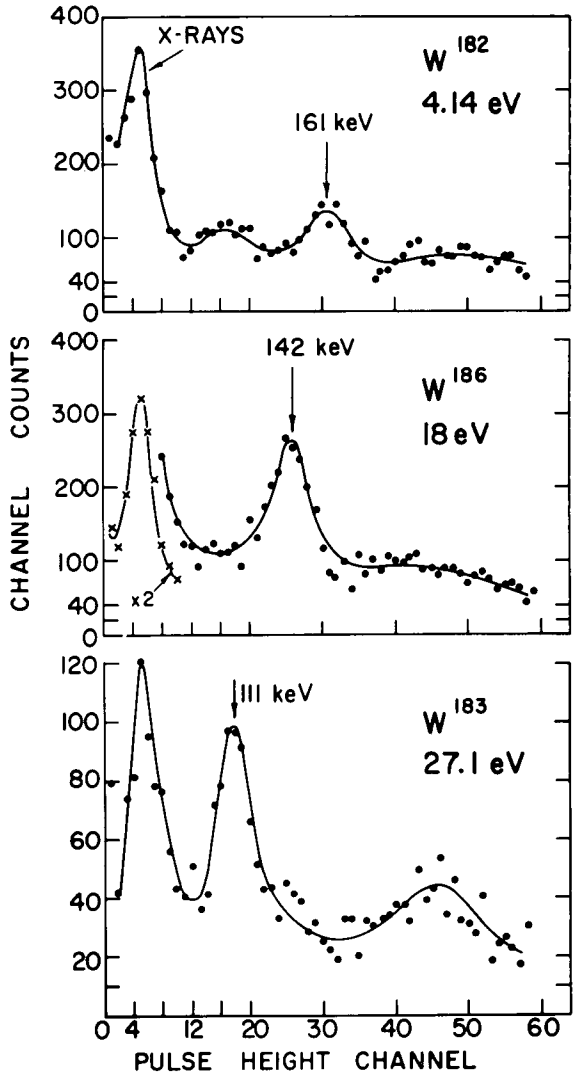

Fig. 4. Coincidence low-energy γ-ray spectra from resonances in various tungsten isotopes. The 8 × 6-in. window was set at 2.5 to 8.0 MeV.

radiation observed from capture in the 18-eV resonance of W^{186} and radiation of similar energy from the unresolved resonances (46 and 48 eV) in W^{183}, the observed low-energy γ rays can be attributed to known transitions in the corresponding compound nuclei. Detailed and accurate information is not available concerning low-lying levels in the compound nucleus W^{187}.[1] The 142-keV radiation observed from capture in the 46/48-eV neutron resonances in W^{183} is not explicable in terms of known transitions in W^{184}.

---

[1] Atlas of γ-Ray Spectra from Radiative Capture of Thermal Neutrons, edited by L. V. Groshev (Pergamon Press, London, 1959), p. 163.

The γ-ray spectra presented in Figs. 3 and 4 illustrate our ability to observe, correctly, the known details of γ rays resulting from transitions between low-lying states. We therefore used the coincidence technique to effectively resolve primary γ-ray transitions to the ground state and first excited state (111 keV) of W^{184}, and to measure the variation in the ratio $\Gamma_1/(\Gamma_1 + \Gamma_0)$ with neutron resonance, where Γ_0 and Γ_1 are the partial radiation widths for the primary γ-ray transitions to the ground state and first excited state, respectively. The width Γ_1 is proportional to the number of 111-keV gamma rays in coincidence with events in the 8 × 6-in. crystal whose pulse-height window (6.95 to 7.7 MeV) was set to accept only primary γ radiation to the ground state and first excited state of W^{184}. The sum $(\Gamma_0 + \Gamma_1)$ is proportional to the number of resonance-capture γ rays detected within the 8 × 6-in. window. These two quantities were measured simultaneously, using both the 2-parameter tape-recording system and the 1024-channel time analyzer. Figure 5 shows the low-energy spectra, in coincidence with γ rays (6.95 to 7.7 MeV) detected in the 8 × 6-in. NaI crystal, from neutron capture in W^{183} at 7.6, 27.1, and 46.2 eV. All these resonances are known[2] to have spin J = 1 and therefore they result in E1 radiation to the ground state and first excited state. Clearly, there is a large variation in the relative strength of the 111-keV radiation, i.e., the primary γ rays to the 111-keV state. For the 27.1-eV case, the peak-to-background ratio of the 111-keV radiation is better than 20:1, and the ratio of K x rays to 111-keV counts is, within experimental error, equal to the K-electron internal-conversion coefficient, 0.73. Since the K x rays are produced only by the 111-keV radiation, they are equally useful in labeling transitions to the 111-keV level in W^{184}. In the pulse-height spectra (Fig. 5), the background was assumed to be independent of pulse-height channel and was computed by averaging the counts from channel 24 to 56. Table I gives the results derived from the present measurement.

[2] D. J. Hughes, B. A. Magurno, and M. K. Brussel, Brookhaven National Laboratory Report BNL-325, 2nd edition, Supp. 1.

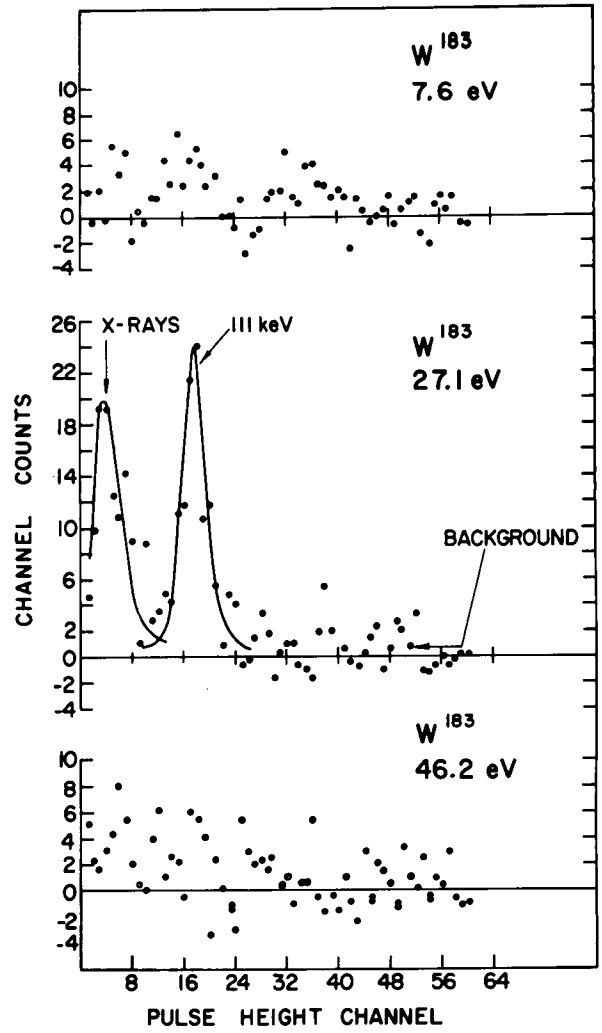

Fig. 5. Coincidence low-energy γ-ray spectra from the J=1 resonances formed by capture in W^{183}. The 8 × 6-in. window was set at 6.95 to 7.7 MeV.

Also included are data of the Argonne fast-chopper group,[3,4] which were obtained by careful measurement of the spectra in a single NaI detector and unfolding the complex spectra using an experimentally-determined line shape. There is reasonable agreement, within error, between the two sets of data.

---

[3] L. M. Bollinger, R. E. Coté, and T. J. Kennet, Phys. Rev. Letters 3, 376 (1959).

[4] L. M. Bollinger, R. E. Coté, R. T. Carpenter, and J. P. Marion, Phys. Rev. 132, 1640 (1963).

TABLE I. Variation in the ratio $\Gamma_1/(\Gamma_0 + \Gamma_1)$ with neutron resonance, normalized to a value of 1 at 27.1 eV. The widths Γ_0 and Γ_1 are partial radiation widths to the ground state and first excited state, respectively.

	Resonance		
	7.6 eV	27.1 eV	46.2 eV
Counts in 8 × 6-in. window			
$(\Gamma_0 + \Gamma_1)$	5360	3300	2580
Net counts: 111-keV + K x ray			
(Γ_1)	32.4 ± 9.5	187.9 ± 15.2	35.8 ± 10
$\Gamma_1/\Gamma_0 + \Gamma_1$	0.11 ± 0.03	1	0.24 ± 0.07[a]
	0.13 ± 0.04	1	0.26 ± 0.07[b]
	0.03 ± 0.04	1	0.29 ± 0.06[c]

[a]Present work.

[b]Argonne result, Ref. 3.

[c]Argonne result, Ref. 4.

In conclusion, we suggest that the disadvantage of low coincidence counting rates is likely, in a number of cases, to be more than compensated by the simplicity of the low-energy γ-ray spectra. The coincidence technique may therefore prove an excellent alternative approach to the continuing problem of measurement of partial radiation widths — an approach which has been rather neglected despite its use by Argonne in the case of manganese.[5]

[5] T. J. Kennet, L. M. Bollinger, and R. T. Carpenter, Phys. Rev. Letters 1, 76 (1958).

* * *

L. M. BOLLINGER, Argonne National Laboratory: Without meaning to be critical of the experiment reported by Moore, let me say that the reason the coincidence technique has not been widely used is that coincidence measurements are often not competitive with measurements of single gamma rays. For example, with our present equipment we could obtain a result of the same accuracy as that reported by Moore in about an hour, I would think. On the other hand, I would guess that the reported coincidence measurement took days or months.

MOORE: I agree that counting rates are low; our present running time was 100 hr. But the point that strikes me is that it is a very sensitive experiment and at least one can see the variation in the relative strength.

I agree that if you make very careful measurements, as you have done at Argonne, you would expect to arrive at the same result. But it seems that there is a possibility that in many cases one could accept the lower counting rate and be able to look and make a sensible measurement of the strength of these transitions to maybe one or more of the low-lying states in the compound nucleus — transitions which would otherwise be difficult to resolve.

P. AXEL, University of Illinois: I have a question about what you do experimentally. How many dimensions of data were you recording during the hundred hours of running you mentioned? In principle, if you had an adequate recording system, you could record all coincidences involving any two gamma rays.

MOORE: I'm sorry. Maybe I did not make that clear. Figure 5 showed the variation in the strengths of the 111-keV radiation. Those events were measured by gating the 8 × 6-in. crystal to accept primary radiations to the ground state or the first excited state.

AXEL: I think that you have explained clearly what you did. I wonder why you cannot record simultaneously coincidences involving other energies.

MOORE: In principle one can observe, simultaneously, transitions to many final states by observing the corresponding low-energy spectra. This we hope to do.

IV-4. FLUCTUATIONS IN PARTIAL RADIATION WIDTHS OF U^{239}

H. E. Jackson

Argonne National Laboratory, Argonne, Illinois

As you can see from the preceding talks, the study of the distribution of partial radiation widths has been a big problem in slow-neutron spectroscopy now for four years. I refer to the partial radiation widths for transitions from neutron resonances of a given spin and parity to a definite final state. To summarize the situation for most nuclei, there is general agreement among the various laboratories; the distribution which governs the statistics of the partial radiation widths is dominated by large fluctuations about the mean value.

Now, if the observed distribution is characterized by a number of degrees of freedom, ν, of a χ^2 distribution, as proposed in the theoretical treatment by Porter and Thomas, ν is generally accepted to be somewhere between 1 and 2. (I noticed that everyone at the conference is more or less assuming or talking in terms of a Porter-Thomas distribution.)

However, one striking anomaly has remained in U^{238}. In terms of its reduced width, the 4.06-MeV transition observed in the thermal capture of U^{238} is one of the strongest E1 transitions known. It was natural to attempt to study the distribution of the partial widths for this transition for a large number of resonances.

That was done several years ago by two laboratories, Brookhaven[1] and Saclay.[2] Their results indicated that the fluctuations of the partial widths about the mean value were only 11%. This is in very strong contrast to the results for all nuclei studied. Whereas ν is between 1 and 2 for all other nuclei, they[1] find the value of roughly 90 for U^{239}.

---

[1] D. J. Hughes, H. Palevsky, H. Bolotin, and R. Chrien, Proceedings of the International Conference on Nuclear Structure (University of Toronto Press, Toronto, Canada, 1960), p. 661.

[2] C. Corge, Vinh-Dinh Huynh, J. Julien, J. Morgenstern, and F. Netter, J. phys. radium 22, 722 (1961).

More recently it has become clear that the situation is quite complicated as far as this transition is concerned. Preliminary work here on the resonance-capture spectra and detailed work on the thermal-capture spectrum at Brookhaven[3] indicated that there are at least four lines involved in the peak at 4.06 MeV.

Furthermore, in our work we have found radiation at energies above this transition — transitions to states in the neighborhood of the ground state of U^{239}. However, even these facts do not explain the anomaly, since the older data employed at least 50 states, if individual widths are assumed to be uncorrelated.

In an attempt to confirm the anomaly, we measured twelve resonances in uranium. We measured transitions between 3.9 and 4.2 MeV for twelve resonances between 6.7 eV and 240 eV.

Figure 1 shows the experimental arrangement. The Argonne fast chopper was used to select neutrons of known energy by measuring the time of flight. The time-of-flight resolution of the system was about 80 nsec/m. Capture gamma rays were observed in a NaI(Tl) crystal, 8 in. in diameter and 6 in. deep. Each event consisting of a pulse height and a

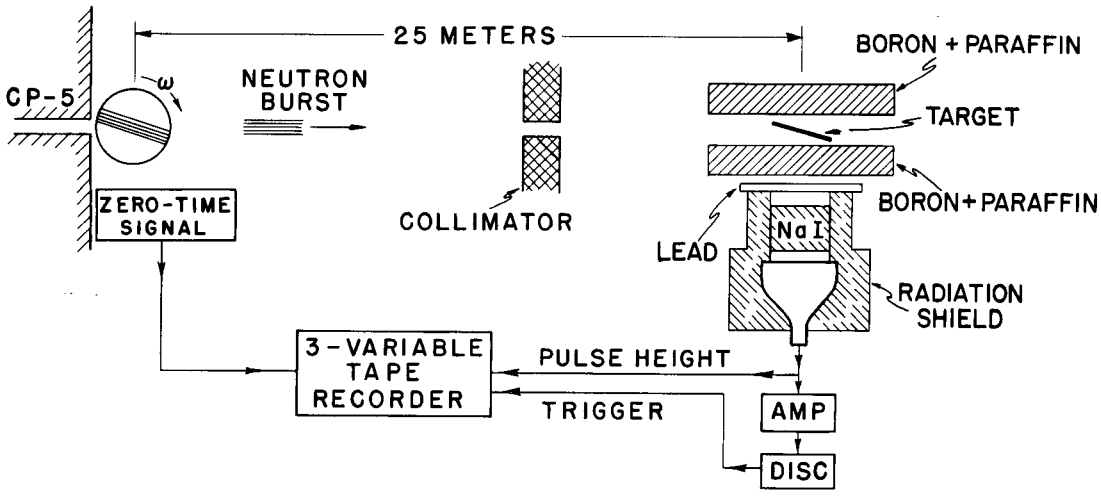

Fig. 1. Schematic diagram of experimental arrangement.

[3] N. F. Fiebiger, Bull. Am. Phys. Soc. 7, 140 (1962).

time of flight, was recorded and analyzed by means of the Argonne three-variable magnetic-tape recording system. With the exception of the resonance at 6.7 eV, all of the resonances were recorded in a single run under the same conditions of pulse-height gain and time-of-flight calibration. This feature is important inasmuch as it permits us to simultaneously analyze the resonance spectra using only a single set of line positions and a single response function. Thus it tends to minimize the systematic error in relative intensities of transitions from resonance to resonance.

We determined the response function of the crystal at two energies which span the energy range of interest in the uranium. This was accomplished by a coincidence measurement of the thermal-capture spectrum of Si^{28}, which is dominated by a two-step cascade through the 4.93-MeV state directly to the ground state. The line shapes for the 3.55-MeV photons and 4.49-MeV photons were restricted by restricting pulse heights in an identical crystal to the photopeak corresponding to the accompanying member of the cascade. The resulting line shapes are shown in Fig. 2.

One important effect (not really a difficulty, but a matter that has to be studied carefully) is the contribution of summing to the observed singles spectra. By summing I mean the observation of individual cascades in which two or more photons are observed in the crystal as a single pulse, and therefore mistakenly considered as a single gamma ray. This was observed in two auxiliary experiments. In the first experiment we looked at the 6.7-eV resonance with a detector solid angle which was 25% of the solid angle used in the final measurement, and could find no observable difference from the spectrum for the larger solid angle. In a more direct experiment, we performed the sum-coincidence measurement in which we added the pulse heights observed in two identical crystals, and thereby obtained a direct measure of the sum spectrum for each resonance, and again our results indicated that the contribution from summing was negligible.

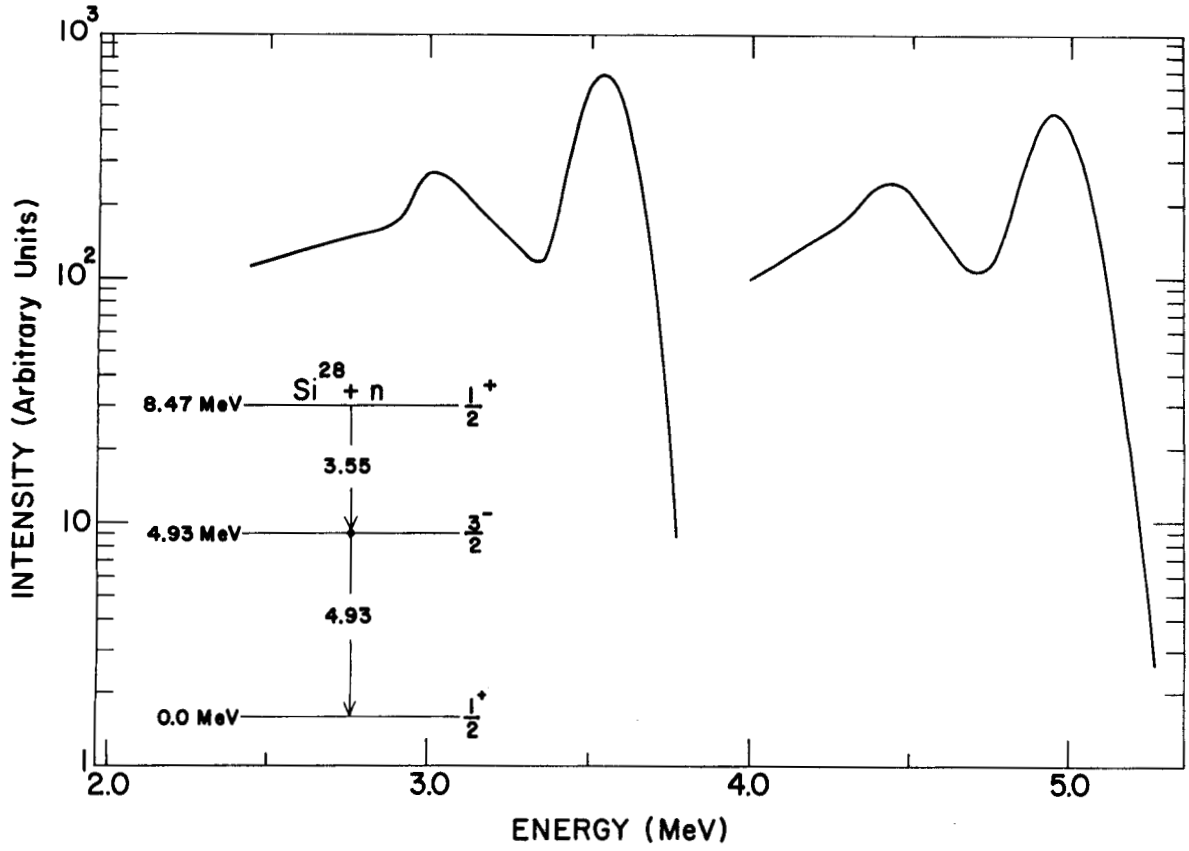

Fig. 2. Response functions of the NaI(Tl) crystal for photons with energies of 3.55 MeV and 4.93 MeV. The data were obtained by studies of the γ-ray cascade shown at the lower left.

Figure 3 shows a compilation of our spectra for twelve resonances with the background subtracted. The shaded area here represents the region of interest in previous experiments. The arrows indicate the positions of four lines of the level scheme which was proposed by Fiebiger of Brookhaven.

To get the intensities of these lines, a least-squares analysis was performed using the positions of the four lines shown in the figure and, in addition, two lines representing transitions to the neighborhood of the ground state. The line shape for each transition was generated by a linear extrapolation of the line shapes shown in Fig. 2. The resonance intensities were normalized by requiring the number of counts in the low-energy regions below 3 MeV to be equal in all cases. The intensities we

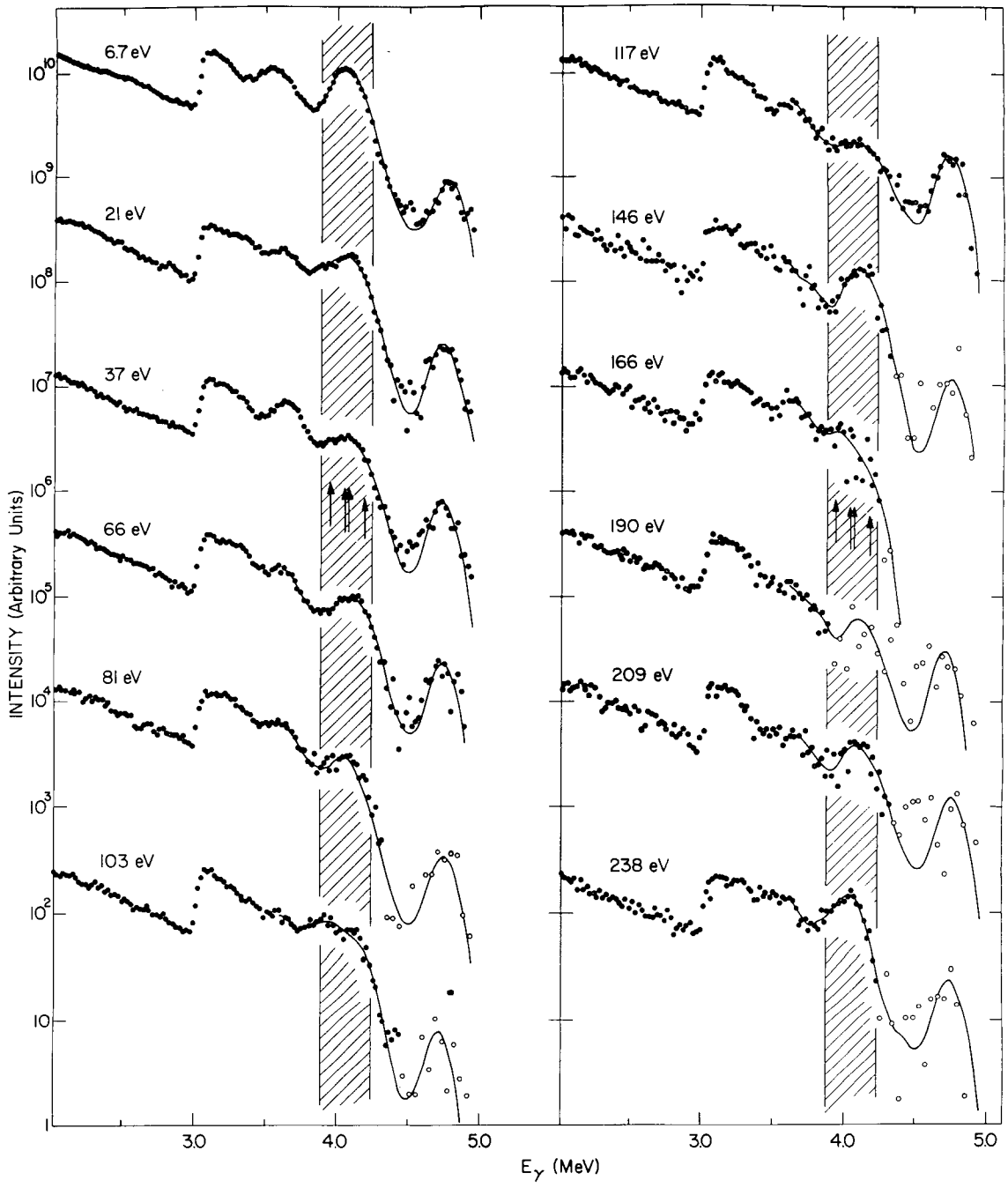

Fig. 3. Single-photon-capture spectra for neutron resonances in U^{239}. The shaded area indicates the region of interest in previous experiments. The arrows denote the energies of primary transitions observed in thermal-capture studies.

obtained for the four transitions in the neighborhood of 4 MeV were then added, and the distribution of this sum was used in a Monte Carlo calculation in which these results were compared with the results from mathematical samples in order to obtain a most probable value of ν. The results of this Monte Carlo calculation are shown in Fig. 4.

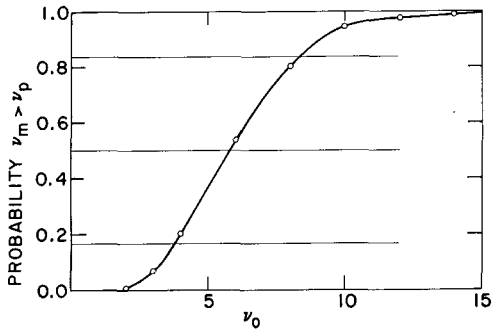

Fig. 4. Summary of the results of a Monte Carlo calculation of the most probable number of degrees of freedom.

Plotted here is the probability that the mathematical sample would give a ν_{meas} which is larger than the ν_{obs} for the sample. This probability is plotted against ν_0 for the various mathematical samples. This procedure is the one that was used in the paper IV-2 of this conference, and was used here in order to produce a result that could be directly compared with the other data. The most probable value for ν obtained from this treatment is 5.8 ± 2.3. In the talk by Dr. Rosenzweig, there was another relationship given for determining the number of lines present, as you remember, in terms of the variance of the observed widths; and if you use that relationship you find in that case that $\nu \gtrsim 6$.

This result, in contrast to the earlier experiment, is consistent with what we know about the nuclear structure of uranium and about the distribution of the width for other nuclei; namely, our results are consistent with 4 primary transitions of uncorrelated widths distributed according to a Porter-Thomas distribution.

* * *

I. BERGQVIST, Physics Division, Oak Ridge National Laboratory (on leave from Research Institute of National Defense, Stockholm): I have

seen the results of Fiebiger et al. on gamma rays from thermal-neutron capture as well as the (d, p) work of Middleton. It is quite evident that the spin and parity assignments of low-lying levels in U^{239} are inconclusive. Now we know about the fluctuations of intensities of transitions from various capturing states to the band of levels at an excitation energy of about 700 keV. I wonder if it is possible to take advantage of this fact and look for low-energy gamma rays in coincidence with the group of 4-MeV gamma rays. Due to the fluctuation from resonance to resonance of the various gamma rays having energies of about 4 MeV, one should be able to study the low-lying levels in greater detail.

JACKSON: Well, I think, it is an experiment worth thinking about. There are difficulties. We tried it very early in the game but did not go at it with too much effort. The main difficulty at the time was low-energy background radiation from the natural uranium target itself. We were forced to put lead in front of our counters to get this background down. Naturally, the low-energy response of the crystals was impaired. However, this approach to studying nuclear level structure is potentially very powerful. With sufficiently high resonance-neutron flux, the experiment on U^{238} should be possible.

R. E. CHRIEN, Brookhaven National Laboratory: The number $\nu = 90$ was reported by the Brookhaven group at the Kingston Conference in 1960. The analysis was in error because of two factors primarily. One error was that a biased sample was used. In other words, a resonance was omitted because the transition strength was small. The second point is that there was background radiation which we did not understand. We did not correct for it. We have made the analysis with the same data trying to make a correction for these two factors and got $\nu = 11$. Now, we hope to further investigate this problem by means of the coincidence technique that John Moore described to you because we feel this should shed considerable light on the problem.

JACKSON: Could you quote an error on your value of $\nu = 11$.

CHRIEN: I think it was 4: $\nu = 11 \pm 4$.

N. ROSENZWEIG, Argonne National Laboratory: Because of the great theoretical interest which attaches to any possible deviations from the simple model, I would like to ask you to amplify one of your statements. I presume you are referring mainly to the work of Bollinger, Coté, Carpenter, and Marion, that ν seems to be between 1 and 2. Do you mean it is sometimes 1 and sometimes 2 or do you mean it is 1 with an error that could make it 2?

JACKSON: The result comes from taking all of the data for a broad group of nuclei and treating them by the Monte Carlo method I have outlined here. The answer that you get from this calculation is 1.34, I believe. It is quoted in the program. The errors are large enough so that I think the only honest statement you can make is that the data imply that ν is somewhere between 1 and 2. In a sense this whole treatment is prejudiced because a specific group of distributions are being used to get a number to describe the experimental data. In a sense it is much better to use the variance figure you proposed in your talk because it does not imply any attempt to interpret or to make a prestatement about what the distribution is.

ROSENZWEIG: According to the simplest model, which I reviewed in my talk, a single partial radiation width is distributed according to the Porter-Thomas distribution, which is also a member of the χ^2 family, namely, the member with one degree of freedom ($\nu = 1$). If nature departs from the simple theory, then the correct distribution need not be describable by another member of the χ^2 family, although an approximate representation in terms of χ^2 functions may still be possible, especially if you admit ν as a continuous parameter. Needless to say, even if ν assumes a fractional value (such as 1.3) in such an analysis, there is still exactly one final state involved in the gamma-ray transition. I believe that it was in this sense that ν was employed as a parameter by Bollinger, Carpenter, Coté, and Marion.

I would like to make a remark about the sum of partial radiation widths observed in U^{239}, measured by Dr. Jackson. Of all nuclei known to man, this is one of the most complex, and if the simplest (asymptotic) model should be useful anywhere, then it should be for this nuclide. Yet, the disagreement between experiment and theory seemed so enormous that one could not simply dismiss it, and I therefore entertained the discrepancy in a recent study. However, we should be pleased if an alteration of the simple model is not necessary in this case.

All the same, deviations from the simple model are to be expected on general grounds. Their discovery and classification appear to me to be one of the most interesting aspects of the field, and I shall be looking forward to hearing about all sorts of deviations in the future.

J. A. MOORE, Brookhaven National Laboratory: This is just a point of information. In view of what Dr. Bollinger said earlier, how long did it take to run the data? Is it hours, days, or weeks?

JACKSON: Two and one-half weeks.

IV-5. RESONANCE REACTIONS AND THE NUCLEAR SHELL MODEL*

R. H. Lemmer

Massachusetts Institute of Technology

As most of you perhaps know, the advent of the unified theory of nuclear reactions which Feshbach[1] developed has resulted in an increased interest in trying to understand what sort of things go on when a nucleon hits a nucleus. By that I mean trying to take a closer and perhaps more detailed look at the sort of excitations that can occur, and even go so far as to try to calculate the cross sections that one might expect to get.

For example, within the framework of this theory, Block and Feshbach[2] have already discussed the neutron strength function; and the success of this very simple calculation makes one feel that really there is some point in trying to write down in more detail what goes on when a nucleon and nucleus get together to form a compound system.

Now most of the work thus far that has used this new approach has really just been concerned with pointing out general features that such a theory might have in it. I have already referred to the strength-function work of Block and Feshbach, for example. Now, I will discuss these general features, but I will also want to discuss with you the contents of a more detailed (perhaps you might feel unjustifiably detailed) calculation of the cross section for a specific nuclear reaction that we[3] recently have carried out. The purpose of this latter illustration will be to give you first of all a picture of the unified theory of nuclear reactions "in action," so to speak, and secondly to be able to write down some numbers that are specific to a specific nuclear reaction.

---

*Invited paper.

[1] H. Feshbach, Ann. Phys. (N.Y.) 5, 357 (1958); Ann. Phys. (N.Y.) 19, 287 (1962).

[2] B. Block and H. Feshbach, Ann. Phys. (N.Y.) 23, 47 (1963).

[3] R. H. Lemmer and C. M. Shakin, Ann. Phys. (New York) (to be published).

Now, let me do things in their proper order. First, I will write down some formulae just to have something to point to and then go on to discuss their contents. Let us call H the (A+1)-particle Hamiltonian and Ψ the wave function. Our formal problem then is to study the scattering states of

$$(E - H)\Psi = 0, \tag{1}$$

where E is the total energy. What follows now will be a discussion of how best to "solve" this innocent looking equation. In fact, if we could solve it as it stands we would have all the information we are looking for. Now of course we all know it is not as innocent as all that and a complete solution would invoke all the complexities of the many-body problem! But we cannot do this and so must lean (and quite heavily at that!) on some form of a model calculation.

However, before being too specific, let me at least say something about the structure of the T-matrix that we are going to use. To keep things simple, let us keep the energy E so low that only elastic encounters are possible. Then we can use Feshbach's breakup of the wave function Ψ into open and closed channels and write

$$\Psi = P\Psi + Q\Psi,$$

where P and Q are projection operators. They divide Ψ up into two orthogonal pieces such that

$$P\Psi \rightarrow (\text{incoming wave} + T\ \text{outgoing wave})\ \varphi_{g.s.}(A)$$
$$Q\Psi \rightarrow 0$$

as the separation between nucleon and target nucleus goes to infinity. Here $\varphi_{g.s.}(A)$ is the ground state of the target nucleus A and T is proportional to the T matrix for elastic scattering.

Thus if we are just doing elastic scattering (and from now on that's all we will be doing) a knowledge of $P\Psi$ is all we need to have a complete knowledge of the scattering properties of our system. Of

course, to get $P\Psi$ we have to go back to Eq. (1) which couples $P\Psi$ and $Q\Psi$ to each other so we really have to know $Q\Psi$ as well as an intermediate step. Writing Eq. (1) out as

$$(E - H_{PP})\, P\Psi = H_{PQ}\, P\Psi, \qquad H_{PQ} = PHQ, \text{ etc.} \tag{3}$$
$$(E - H_{QQ})\, Q\Psi = H_{QP}\, P\Psi,$$

and "solving" them a la Feshbach,[1] one gets the expression

$$T = T^{(p)} + \langle \psi_0^{(-)} H_{PQ} [E - H_{QQ} - W_{QQ}]^{-1} H_{QP} \psi_0^{(+)} \rangle, \tag{4}$$

with

$$W_{QQ} = H_{QP} \left(\frac{1}{E^{(+)} - H_{PP}} \right) H_{PQ} \tag{5}$$

for the T matrix. The $\psi_0^{(\pm)}$ are scattering solutions of

$$(E - H_{PP})\, \psi_0^{(\pm)} = 0 \tag{6}$$

with outgoing and incoming boundary conditions at infinity.

Now, let me discuss each of the terms in Eq. (4). The term $T^{(p)}$ is supposed to represent the transition matrix coming from just that part of H when the target is always in its ground state, that is to say, it is the scattering matrix related to Eq. (6). In other words $T^{(p)}$ is just that part of the transition matrix where the nucleon comes in and goes out without ever invoking the additional degrees of freedom of the target which it can excite. So this piece by its very definition should be a slowly varying function of energy, apart from possible potential resonances.

In contrast to $T^{(p)}$, the second piece in the transition matrix relates to the transition amplitude that comes about when the nucleus is actually excited. One sees this formally by noting the occurrence of the projection operator Q in the second term projecting always onto an

excited state of the target. It is in this second piece of the T matrix that the actual resonances arise that are due to resonance states of (A + 1).

Finally we note that the inverse operator $(E^{(+)} - H_{PP})^{-1}$ occurring in the definition of W_{QQ} is just the Green's function representing the propagation of the nucleon through the target nucleus without exciting the latter.

Well, I think we have enough formulas now to be able to talk a little more about the physics involved. Let us look at the resonant part of the T matrix first. Clearly the poles of this term in Eq. (4) will be connected with the resonances in the cross section. These poles are of course the eigenvalues of the operator $(H_{QQ} + W_{QQ})$. We might call them E_t and note that they are both complex and functions of the incident energy because of the presence of W_{QQ}.

Let us take the case where W_{QQ} is small. This will be so whenever the particle for one reason or another finds it hard to penetrate the nucleus. Then the eigenvalues E_t will be very close to the (real) eigenvalues ϵ_s of H_{QQ}, where

$$(\epsilon_s - H_{QQ})\, \Phi_s = 0. \tag{7}$$

The above expression forms a very convenient definition of what one might mean by a "compound state" in scattering. Notice that the state Φ_s has as yet no width for particle emission because H_{QQ} has no way of transferring its excitation energy to an outgoing particle, leaving the target in its ground state. The operator W_{QQ} must be present for this to happen. We can get the width of Φ_s in first order by just taking the diagonal element of W_{QQ} and looking at the imaginary part. Then we just get Feshbach's result, viz.

$$\Gamma_s = 2\pi \left| \langle \Phi_s\, H_{QP}\, \psi_0^{(+)} \rangle \right|^2 .$$

To understand the usefulness of this simple formula, some further remarks are necessary about the nature of H_{PP} and H_{PQ}. The first point I want to make is that since we said H_{PP} is connected with that part of the scattering amplitude which varies slowly with energy, it becomes almost irresistible to identify H_{PP} with the ordinary shell-model Hamiltonian which only contains potential resonances that would vary slowly over the much sharper resonances in H_{QQ}. Now if that is the case, i.e., if H_{PP} is identified with the shell-model Hamiltonian, then it is quite natural to identify H_{QP} (which in the above formulation is the interaction that takes you from the ground state to the excited states of the target) with what we call the residual interaction in shell-model language because it is only this part of the shell-model interaction which allows one to change the state of the target nucleus. Thus $H_{QP} = V_{QP}^{(res)}$ which is a sum of two-body interactions, so that out of Φ_s the width formula above picks up only the "2-particle 1-hole" component if we consider scattering from an even target nucleus, i.e., a 1-particle no-hole state. Thus the 2-particle 1-hole state plays the role of a "doorway." (Here we are using Feshbach and Block's word for this state.) Through it, all excitations must pass to go into the compound state Φ_s from the continuum — or vice versa. The investigation of the neutron strength function, for example, thus reduces to the very specific problem of estimating the amount of 2-particle 1-hole amplitude in Φ_s and the matrix elements $\langle \varphi^{(s)}(2p\text{-}1h)\, V_{QP}^{(res)}\, \psi_0^{(+)} \rangle$. How this may be done is shown by Feshbach and Block in their paper and I won't discuss this point further. Let me leave it with the remark that the results they get are very interesting and significant for further developments of this approach

Now let me take up the second topic I mentioned at the beginning of this talk, i.e., the structure of the scattering calculation for a specific nuclear reaction. We consider the scattering of low-energy nucleons by N^{15}, leading to compound states of N^{16} or O^{16} depending on whether the incident particle is a neutron or a proton. We describe N^{15}

by the shell model; then its ground state consists of a single $p_{1/2}$-hole state in the A=16 core. The incident channel in this case is then simply a particle-hole state with the particle in the continuum. The particle-hole interaction can then demote the $p_{1/2}$ hole to a $p_{3/2}$ hole and drop the incident nucleon into an unoccupied shell-model orbit at the same time. Such particle-hole excitations built on the $p_{3/2}$-hole state will be the "compound" states for N^{16} or O^{16} in this calculation. Let's discuss the nonresonant and resonant terms of the T matrix with this background. Now $T^{(p)}$ must describe a nucleon scattering off of N^{15} always in its ground state. We choose a Woods-Saxon well to describe this part of the scattering, adjusting the well so that it does give a $d_{3/2}$ single-particle resonance at about 2.6 MeV incident-nucleon energy. This is necessary in order to correctly reproduce the experimental phase shifts at this energy. Incidentally, the scattering wave functions we get in this manner are also required in order to construct the Green's function $(E^{(+)} - H_{PP})^{-1}$ which appears in W_{QQ}. To evaluate the resonant part of the T matrix, we use the eigenstates of H_{QQ} defined in Eq. (7). As we pointed out a few moments ago, these will be excitations of the 1-particle 1-hole state so we write

$$\Phi_s = \sum_{p,h \neq p_{1/2}^{-1}} A_{ph} |ph\rangle,$$

taking care to leave out the ground state $p_{1/2}^{-1}$ in the expansion. For simplicity we take $|ph\rangle$ to be a p-h excitation in an oscillator well, which means <u>all</u> our H_{QQ} states will be bound. This is, of course, an approximation — but all we are saying is that if we stick to the case of elastic scattering we are only interested in the bound states of H_{QQ} and that an expansion of Φ_s in oscillator orbitals will give a good representation for these. Note that the calculation of the ϵ_s and Φ_s is now just the usual shell-model problem with the $p_{1/2}^{-1}$ state removed.

Now we use the Φ_s as a basis in which to expand $[E - H_{QQ} - W_{QQ}]^{-1}$ so that

$$T = T^{(p)} + \sum_{s,s'} \langle \psi_0{}^{(-)} H_{PQ} \Phi_s \rangle \langle \Phi_s [E - H_{QQ} - W_{QQ}]^{-1} \Phi_{s'} \rangle \langle \Phi_{s'} H_{QP} \psi_0^{(+)} \rangle . \tag{8}$$

This presents us with a perfectly definite formula for T from which we can obtain the cross section without further ado. However, it is useful to have some inkling where the resonances are going to lie. We decide this as before by looking for the eigenvalues of $H_{QQ} + W_{QQ}$. However, perturbation theory is not in order now since W_{QQ} will be large whenever it involves the $d_{3/2}$ state near resonance, so we must diagonalize

$$\langle \Phi_s (H_{QQ} + W_{QQ}) \Phi_{s'} \rangle = \epsilon_s \delta_{ss'} + \langle \Phi_s W_{QQ} \Phi_{s'} \rangle \tag{9}$$

instead. This will give us the eigenvalues E_t referred to before. Since $E_t = E_t(E)$, the resonances in the cross section are expected near the roots of the transcendental equation

$$[E - \text{real part } E_t(E)] = 0. \tag{10}$$

Plotting this expression as a function of E yields a set of "trajectories" which intersect the energy axis at the resonance energies.

Figure 1 shows in (a) the incident particle on the hole in its ground state. Then in (b) the particle has been dropped in by the residual interaction and the hole has been demoted (or promoted, however you want to look at it!) to the $p_{3/2}^{-1}$ state. The broken curve shows that we approximate the situation (b) by using a harmonic-oscillator well. Then the initial state is repeated in (c).

Figure 2 is an example of the trajectories mentioned earlier. I merely show this to indicate what a single-particle potential resonance in H_{PP} can do for you. So long as you are off the single-particle resonance, you find trajectories which run smoothly with energy,

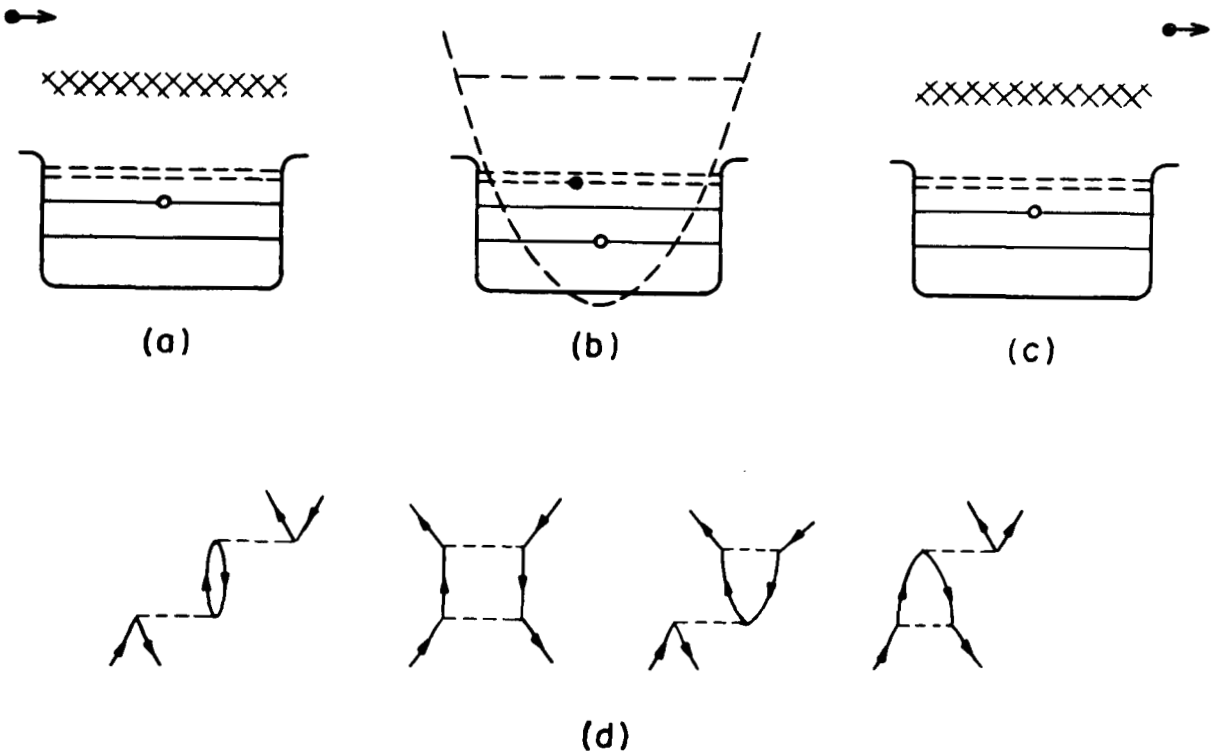

Fig. 1. Schematic picture of the calculation. (a) Nucleon (solid circle) incident on target nucleus in its ground state which is represented as a single hole state (open circle). Dashed horizontal lines show unfilled bound levels and the cross hatching indicates the presence of a potential-scattering resonance. (b) Situation in the closed channel. The hole has been excited and a particle appears in a previously unoccupied level. This particle can either be the incident nucleon or one of the target nucleons. The broken curve shows the harmonic-oscillator potential we use to generate the eigenstates of QHQ. (c) A nucleon leaves, with the target again in its ground state. (d) Diagramatic representation of the direct and exchange matrix elements that would describe the scattering process in lowest order perturbation theory. We, in effect, sum over all such diagrams since our calculation is nonperturbative.

and an intersection with the energy axis gives the position of a resonance. But the rather wild swing in trajectory No. 1 is brought about by the $d_{3/2}$ potential resonance at about 2.6 MeV. This shows that if you happen to get the intersections of the trajectories lying in the vicinity of the single-particle resonance, you can expect to get something rather strange.

Figure 3 shows the total cross section for $J = 1^-$, $T = 1$ states. The solid curve is the calculated cross section showing four

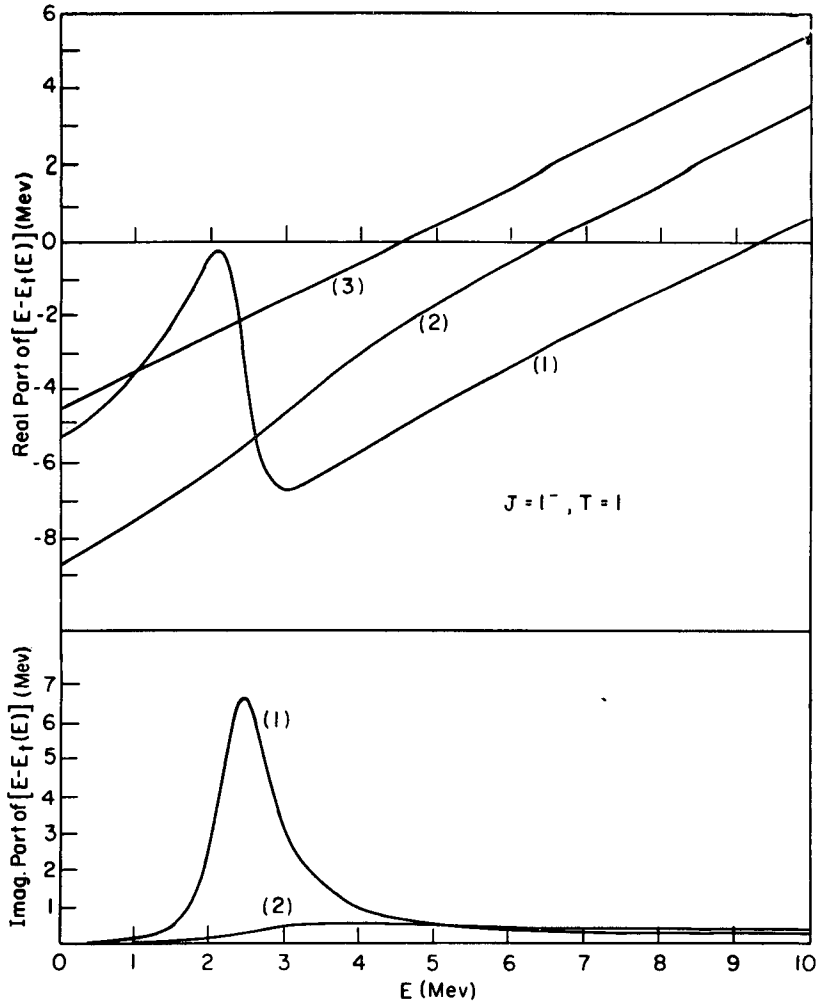

Fig. 2. Trajectories for J = 1 .

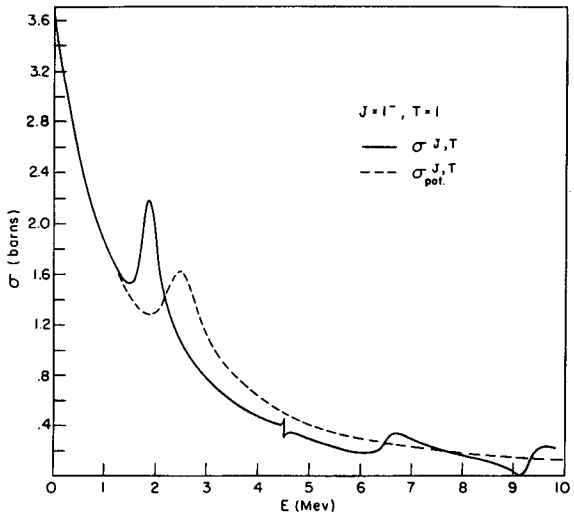

Fig. 3. Cross section for the $J=1^-$ channel as a function of the neutron energy E(c.m.). The dashed line shows the potential scattering alone. The resonances at 6.54 MeV (Γ = 800 keV) and 9.28 MeV (Γ = 580 keV) correspond to the two "giant dipole states" that are strongly excited in photoreactions involving O^{16} .

resonant states. Of course there are five dipole states in O^{16} (not four) but you do not see the lowest one because it is not open to particle decay. The other four are open. Let me just introduce you to the two well known upper members at 9.04 and 11.78 MeV excitation in N^{16}; they are the two "giant" dipole states of photonuclear fame.

You will notice that they are wide or "giant," also as far as particle decay is concerned, as well as for gamma-ray decay. The reason for the "giant" character in them lies more in the structure of the nuclear wave function than in the interaction that happens to be causing the decay. In this case of particle decay, they in fact compete favorably with the state at 4.35 MeV which has its origin mainly in the single-particle $d_{3/2}$ potential resonance.

The broken curve gives the elastic potential scattering from the Wood-Saxon well that we have used in H_{PP}. Notice that the particle interaction has shifted the single-particle $d_{3/2}$ resonance and has also narrowed it down; it has been mixed into the other dipole states.

Finally one notices the wide variety of widths one gets. There is a factor of nearly a hundred between the narrowest and widest dipole state on this figure. Yet all the resonances shown have the same basic particle-hole structure.

Figure 4 shows what can happen when one of the trajectories actually crosses the horizontal axis more than once. The broken curve represents the potential scattering as before. This is changed into the solid curve by the interaction and all sign of the potential resonance has disappeared. In its place appear several sharp resonances.

Another interesting fact, which is illustrated in Fig. 5, is that the positions of the resonances that we have gotten are very close to what an ordinary shell-model calculation would have predicted them to be. Let us look at the $J=1^-$ states as they are most familiar. The levels in column (c) are the results of our calculation, i.e., they are the resonant energies we have found by looking at the scattering problem.

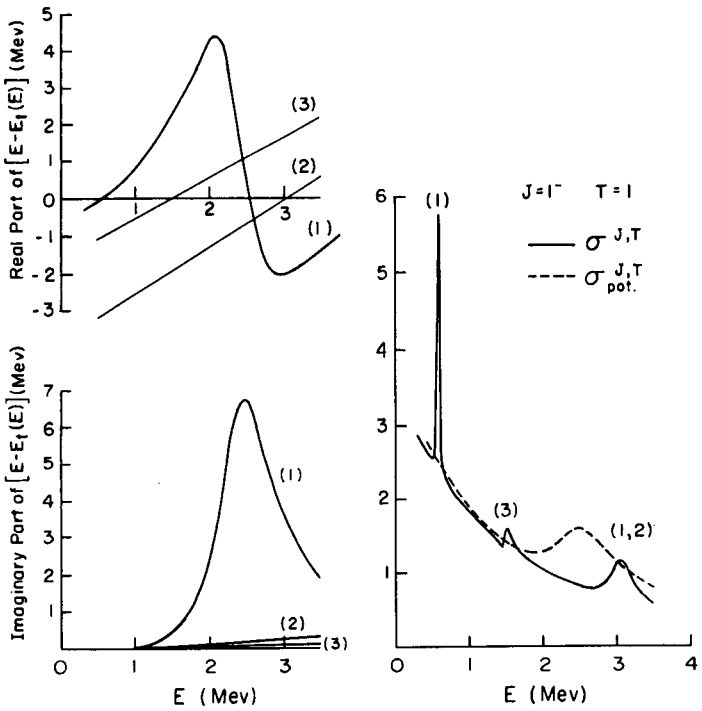

Fig. 4. Same as in Fig. 3 except that the particle-hole excitation energies have been set equal to the neutron separation energy in N^{16}. This places them at the zero of energy in this figure.

The next column (d) compares these results with those you get from doing the conventional shell-model calculation using the same interactions. It is very interesting to observe that the positions of the resonances, as calculated from a scattering theory and as calculated using an oscillator well for all states, agree quite well. This is rather nice evidence to have, namely, a shell-model calculation does indeed produce energy levels which are not going to be shifted around too much by the advent of a continuum. Of course, what does change is the fact that when you have a state that can decay, it also has a width and the width calculation is sensitive to what potential well you use in H_{PP}. In other words, the main difference as far as spectroscopy is concerned is that if you do a scattering calculation, you have a system which is much more sensitive (as far as the widths go) to the average potential that you pick than is the case of a bound-state calculation.

We have not tried a serious comparison with experiment yet. This is partly due to lack of sufficient data in the proper form and also because we have as yet ignored inelastic scattering which enters into

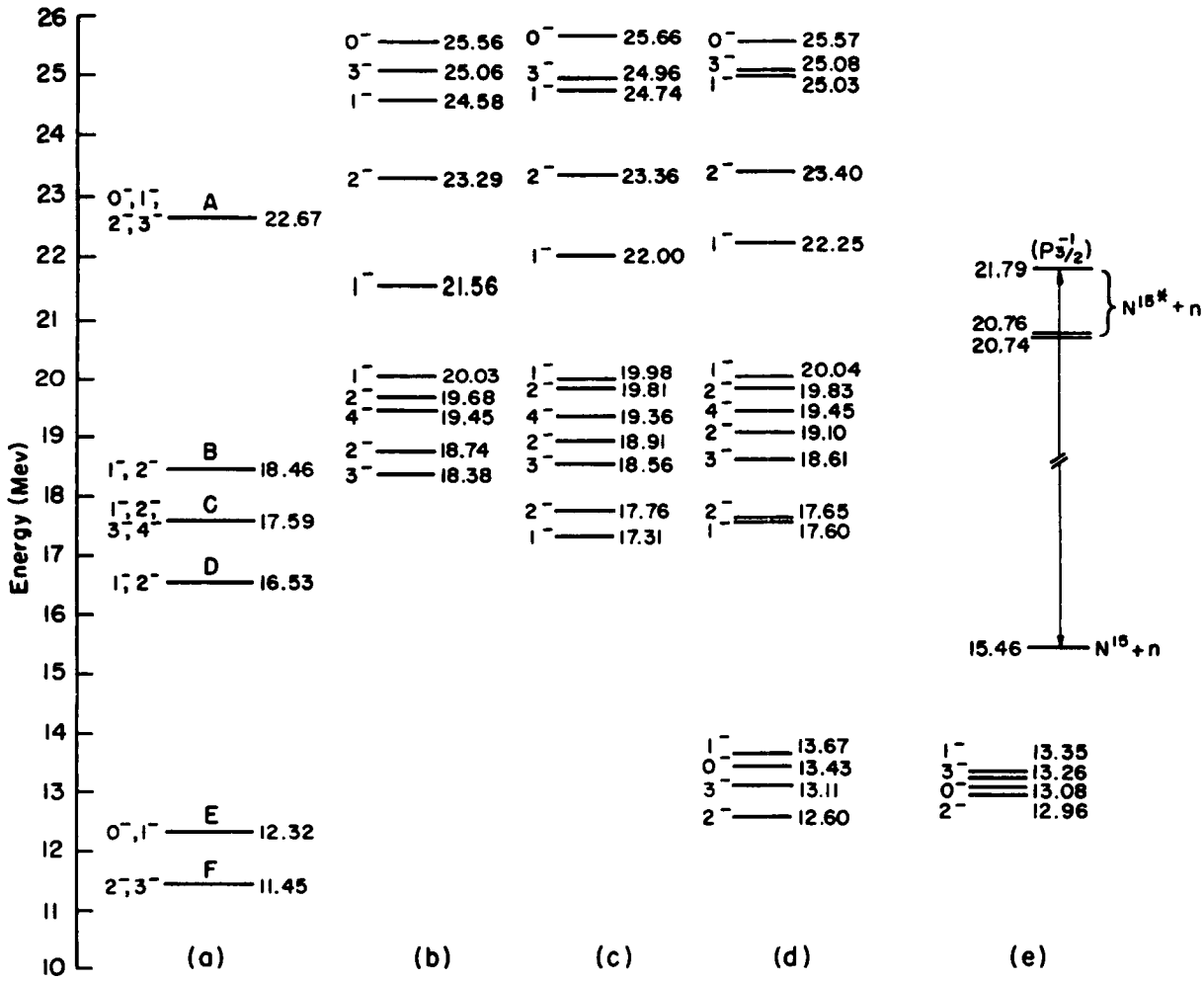

Fig. 5. Energy-level diagram: (c) calculated resonance energies, (d) energy levels obtained by a standard shell-model calculation.

the picture past about 6 MeV incident energy. All I want to say in this regard is that the size of the cross section and the magnitudes of the widths one gets are already of the correct order of magnitude. So I feel one can have some confidence in such an approach. Its spirit, as we have seen, is very close to that in the shell model and is not really a great deal harder to do. Finally, the calculated resonance energies and widths that one obtains using a particle-hole description for N^{16} are shown in Table I.

TABLE I. Calculated resonant energies and widths for the compound nucleus N^{16}.

J^{π}, T = 1	Neutron energy (c.m.) (MeV)	Γ (keV)	Excitation energy in N^{16} (MeV)
0^-	10.2	130	12.7
1^-	1.85	~300	4.35
	4.52	9	7.02
	6.54	800	9.04
	9.28	580	11.78
2^-	2.30	~800	4.80
	3.45	280	5.95
	4.35	80	6.85
	7.90	130	10.40
3^-	3.10	66	5.60
	9.50	21	12.00
4^-	3.90	0.6	6.40

* * *

F. COESTER, Argonne National Laboratory: I have a question about the definition of the two operators P and Q. In the Wigner-Eisenbud theory one has a surface separating an internal region and an external region. It does not matter too much where one places it as long as it is outside the nucleus. Now here there is no such surface. Instead we have the projections P and Q. In the shell model that you discussed, the

projection operators P and Q are well defined. But in the general theory there is a question: Are there general principles which give a unique definition for P and Q or is their definition arbitrary within some bounds?

LEMMER: I think that you have answered your own question. Your last statement is true. The division into P and Q is arbitrary, and in certain instances you may want to include in P not only the elastic scattering but maybe also the inelastic scattering to a few collective levels, and call Q whatever is left over.

The point is, that one has to be guided by the type of calculation he wants to carry out. In the shell model, of course, there is no difficulty in defining P, as the example that I have just discussed shows. This is a problem, however, in the general theory because the formulae that I wrote down defined both P and Q just asymptotically. That means that is all that you have said about them; and as far as our experience has indicated, that is perhaps all that you have to say. This point is still under investigation, and it may be possible to become more sophisticated about it.

However, I do want to make a comment about the nonoccurrence of a radius which plays such a central role in the Wigner-Eisenbud formulation. First of all, as Feshbach has shown, one can produce the Wigner-Eisenbud results by choosing an appropriate projection operator P which in effect introduces such a radius. Using a radius in a practical calculation, however, has the unpleasant result that your widths and your scattering cross sections start to depend explicitly on the radius you used at which to cut off. This does not happen in the present case at all. The boundary conditions are scattering boundary conditions at infinity. So we may say that the occurrence of a resonance in this way of writing down the scattering problem merely comes out as a by-product of the scattering calculation itself and is not presupposed in any way by setting up a matching boundary.

D. S. GEMMELL, Argonne National Laboratory: I would like to point out that the elastic scattering of protons on N^{15} was measured by a group of us at Harwell about a year ago. We measured the differential cross section from about 2 MeV to 10 MeV, in 20-keV steps I believe it was, at four or five angles. At the time, we did not make an analysis of the data because it was so complex, containing a vast amount of fine structure. I think in the light of what you have just said it would be interesting to re-examine these data.

T. FUKETA, Rensselaer Polytechnic Institute: I would like to ask you about the strength function. Taking the strength function as ordinate and the neutron energy as abscissa, you have a giant resonance in several MeV energy range from a single-particle picture. For example, if you make a three-quasi-particle-model calculation, the giant resonance in the strength function will split, and you may have on the order of a few hundred keV for the widths of the split peaks. With more complicated excitation modes, the peak might split into more peaks. Finally, in the actual nucleus would you expect or imagine that the fluctuation in strength function could occur in a very narrow energy range (for example, within a few hundred electron volts)? The reason why I ask you is this: according to my simple statistical check on published data for 9 nuclei, the data of 6 nuclei out of 9 showed a fluctuation of a local strength function out of an error based on the Porter-Thomas distribution of Γ_n^0 in a very narrow energy region.

LEMMER: It is true that within the framework presented here, such a possibility certainty exists. What will determine the eventual splitting up of the strength function will, of course, be the types and number of more complicated excitations that group together in such a case. It is certainty an interesting possibility.

H. JAHN, Kernforschungszentrum, Karlsruhe: Could you please write out again the expression for P?

LEMMER: Okay. What I said was that $P\Psi$ simply consisted of the incident nucleon on the target in the ground state, plus obviously some

scattering amplitude times the outgoing wave. All this is multiplied by the ground state of the target.

COESTER: I have one other question. You discussed here on this model specifically only elastic scattering. I wondered whether you have considered, or are planning to consider, also reactions or inelastic processes. Particularly if you calculate branching ratios, it seems to me that wave-function renormalization problems will arise. What are you doing about those?

LEMMER: The answer is yes, we are looking at inelastic scattering. In this case you end up with integral equations which we have not succeeded in solving properly yet. What one can do, however, and this we have done, is to use the schematic model of G. E. Brown, where you assume for the particle-hole interaction a separable matrix. If you do this, you can solve the problem in closed form, and you can identify the branching ratios. No difficulties seem to arise as far as wave-function normalization is concerned.

IV-6. OPTICAL-MODEL INTERPRETATION OF NEUTRON STRENGTH FUNCTIONS*†

P. A. Moldauer

Argonne National Laboratory, Argonne, Illinois

CONF-346-5
C-1-2264

The dependence of the s-wave neutron strength function on optical-model parameters is given[1] by

$$\frac{\bar{\Gamma}_n^0}{D} = \frac{2k}{\sqrt{E}} \quad \frac{M}{2\pi^2 \hbar^2} \quad \int_0^\infty |u(r)|^2 \; W(r)\, dr,$$

where u(r) is r times the optical-model radial wave function for s-wave neutrons in the limit of zero incident energy E, normalized to unit particle density, and W(r) is the imaginary part of the optical potential. Since neutron absorption is relatively weak, $|u(r)|^2$ is determined chiefly by the depth and size of the real part of the optical potential V(r), which fixes the positions of the size resonances. Thus the shape of the strength-function curve is determined chiefly by the magnitude and spatial distribution of W(r).

If W is distributed uniformly over the nuclear interior, the strength function depends mainly on the average magnitude of $|u|^2$ inside the nucleus. At resonance, u(r) has an antinode at the nuclear surface. In that case the amplitude of u inside the nucleus is comparable to that outside which, in turn, is proportional to the incident neutron wavelength, and hence the strength function is large. (That it is finite even

---

*Work performed under the auspices of the U. S. Atomic Energy Commission.

†Read by title only.

[1] C. E. Porter, Phys. Rev. 100, 935 (1955).

at zero energy is due to the limiting effect of W which produces a peak height proportional to W^{-1}.[2] If, on the other hand, u(r) has a node at the surface, then the interior amplitude of u is small compared to that outside the nucleus roughly in proportion to the ratio of interior to incident neutron wavelengths. Therefore the amplitude of u inside the nucleus is of the order of the interior neutron wavelength and the strength function is small and is, in fact, proportional to W/V. This familiar dependence of the strength function on the magnitude of the volume absorptive potential is shown in the top panel of Fig. 1. The extremely small values of W required to fit the strength-function data are, however, in conflict with the optical-model analysis of scattering experiments in the keV and MeV regions.

It has therefore been necessary to consider other spatial distributions of W—in particular, surface absorption. In that case the strength function depends on u not only through its interior amplitude but, more importantly, through its phase at the radius where W(r) is concentrated. Again an antinode at the surface produces a strength-function maximum, but now because of the coincidences of the radial peaks in W(r) and $|u(r)|^2$. Similarly, a node at the surface again produces a strength-function minimum. Moreover, by making the distribution of W(r) sufficiently narrow, the strength-function minimum can be made almost arbitarily small even for a large peak value of W. This is illustrated in the center panel of Fig. 1. It should be noted that the strength-function minimum in this family of curves decreases much more rapidly than does the width of the absorptive layer. Therefore the minimum will decrease with decreasing width even if W is increased so as to maintain W × b constant, in which case the strength-function maximum is maintained approximately constant.

---

[2] For a complete discussion see P. A. Moldauer, Nucl. Phys. 47, 65 (1963).

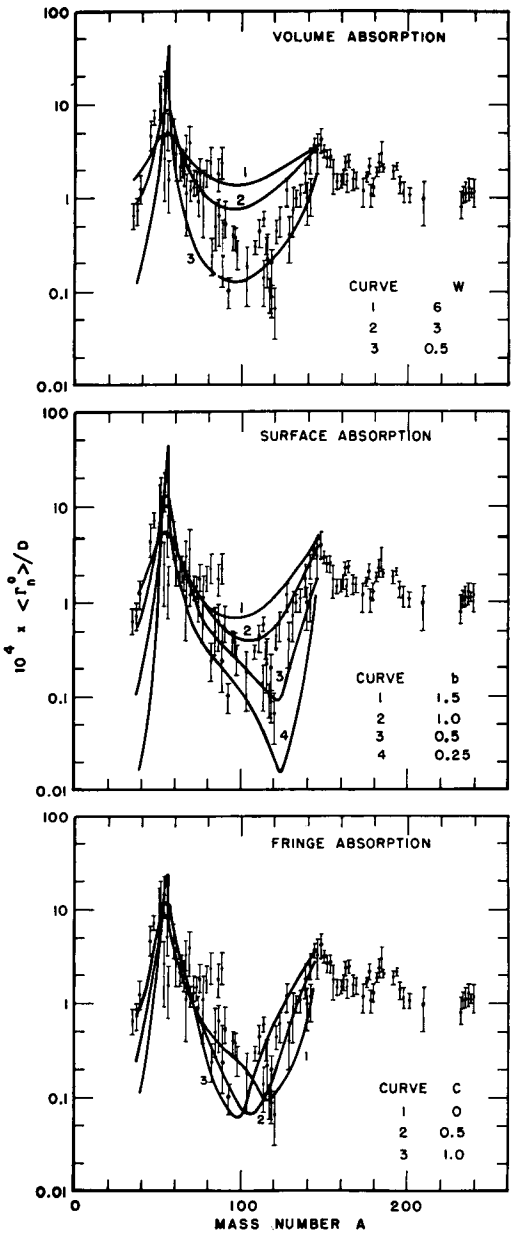

Fig. 1. Neutron strength functions for spherical nuclei according to optical models with parameters $V = 46$ MeV, $R = 1.3\ A^{1/3}$ fm, $a = 0.58$ fm, $W = 7$ MeV, $b = 0.5$ fm, $c = 0$ fm, except as specified differently in the figure. Experimental points are adapted from the summary of J. A. Harvey in Proceedings of the Symposium on Neutron Time-of-Flight Methods, Saclay, 1961, p. 23.

It is also clear that shifting the position of the absorptive peak with respect to the surface will shift the strength-function pattern; and in particular, if the absorptive peak is shifted outside the surface, the strength-function minimum is shifted while the maximum is virtually

unaffected. This phenomenon, which has been called fringe absorption,[3] is illustrated in the bottom panel of Fig. 1.

The large experimental uncertainties and pronounced scatter of presently available s-wave neutron strength-function data preclude anything approaching a unique optical-model fit. Moreover, to arrive at a meaningful multiparameter model it is necessary to fit a larger class of data. For these reasons an optical model has been obtained which gives a good account not only of strength functions and potential scattering radii but also of neutron elastic-scattering cross sections at energies below 1 MeV. The agreement with the data is indicated in Figs. 2 and 3. The model is specified by

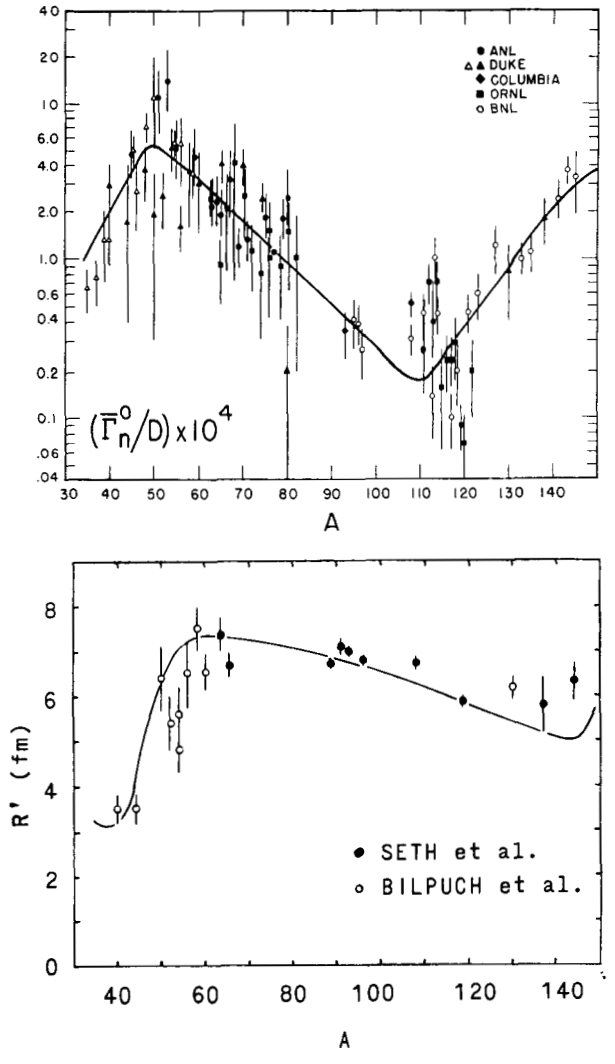

Fig. 2. Neutron strength functions and potential-scattering radii for spherical nuclei according to the optical model specified in the text.

[3] P. A. Moldauer, Phys. Rev. Letters 9, 17 (1962).

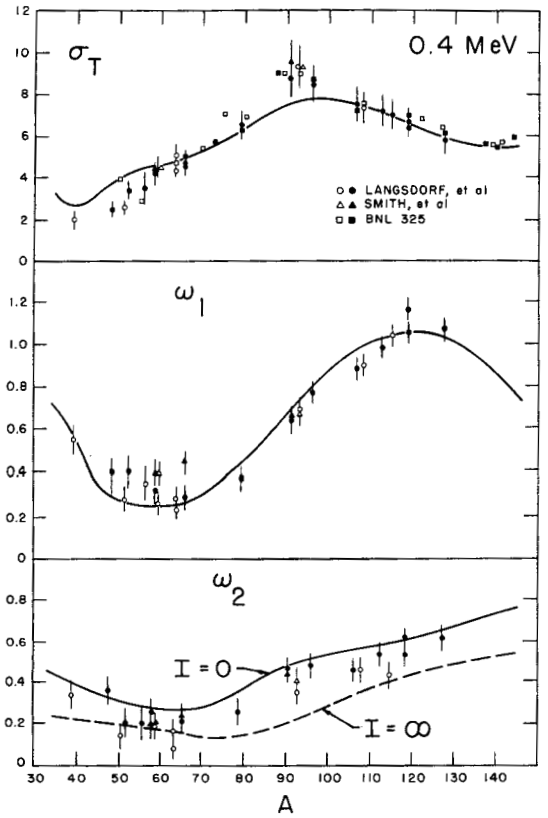

Fig. 3. Neutron total cross sections and Legendre coefficients of the elastic-scattering angular distribution, assuming no inelastic scattering according to the optical model in the text and for 0.4 MeV neutrons.

$$- V \left[1 + \exp\left(\frac{r - R}{a}\right)\right]^{-1} - iW \exp\left[-\left(\frac{r - R - c}{b}\right)^2\right],$$

where V = 46 MeV, W = 14 MeV, $R = 1.16\ A^{1/3} + 0.6$ fm, a = 0.62 fm, b = 0.5 fm, c = 0.5 fm. This model is in qualitative agreement with theoretical predictions[4] and with the results of optical-model fits of nucleon-scattering data at higher energies.[5]

---

[4] G. L. Shaw, Ann. Phys. (New York) 8, 509 (1959); L. C. Gomes, Phys. Rev. 116, 1226 (1959).

[5] F. Perey and B. Buck, Nucl. Phys. 32, 353 (1952); J. S. Nodvick, C. B. Duke, and M. A. Melkanoff, Phys. Rev. 125, 975 (1962).

IV-7. SPIN OF SOME LOW-ENERGY NEUTRON RESONANCES BY RESONANCE SCATTERING*

F. Poortmans and H. Ceulemans

SCK - CEN, Mol, Belgium

A method was developed to measure the ratio Γ_n/Γ of low-energy neutron resonances by means of a crystal spectrometer and a scattering chamber. The method and some results obtained with it have been published previously.[1,2] We have further applied this method to some resonances in Sm^{149}, Sm^{147}, Ir^{193}, and Gd^{157}.

The results are summarized in Table I. From the measured value of Γ_n/Γ and the published values of $g\Gamma_n$ (or σ_0) and Γ, the statistical factor g (and consequently the spin value) is deduced.

Ir^{193}

Si(111) was used as monochromator for two reasons: (1) to avoid scattering of the second-order neutrons by the 5.36-eV resonance in Ir^{191}, and (2) since high resolution was not required because the samples used were rather thick. The measured transmission at the resonance energy was T = 0.326. The parameters σ_0 and Γ of this resonance were taken from a paper of Landon *et al.*[3]

Sm^{149}

Our evaluation of the spin of the first resonance at 0.096 eV has already been communicated.[1] The result (J = 3) being in disagreement

---

*Oral report presented by Paul Fettweis.

[1] H. Ceulemans and F. Poortmans, Bull. Am. Phys. Soc. 8, 70 (1963).

[2] H. Ceulemans, M. Nève de Mévergnies, and F. Poortmans, Nucl. Instr. and Methods 17, 342 (1962).

[3] H. H. Landon, Phys. Rev. 100, 1414 (1955).

TABLE I. Spin values of slow-neutron resonances.

Target nuclide	Target spin, I	Resonance energy (eV)	$100(\Gamma_n/\Gamma)$	g (exp.)	g_+(theor.)	g_-(theor.)	$J = I \pm \frac{1}{2}$ This work	$J = I \pm \frac{1}{2}$ Previous results
Ir^{193}	3/2	1.303	0.84 ± 0.13	0.618 ± 0.09	0.625	0.375	2	
Sm^{149}	7/2	0.87	1.8 ± 0.2	0.38 ± 0.05	0.56	0.44	3	4[a]
Gd^{157}	3/2	0.0314	$\leqslant 0.48$	$\geqslant 0.574$	0.625	0.375	2	2[b,c]
Sm^{147}	7/2	3.4	3.3 ± 0.5	0.20 ± 0.04	0.56	0.44	(3)	

[a] H. Marshak et al. Phys. Rev. 128, 1287 (1962).

[b] G. A. Bartholomew (private communication).

[c] A. Stolovy, Phys. Rev. (to be published).

with those of Marshak et al.,[4] Brockhouse,[5] and Roberts,[6] we have repeated this measurement with another monochromator [Be($10\bar{1}1$) instead if Cu(111)] and with other samples but we found the same result within the experimental error.

Marshak et al. have measured the spin states of the following resonances in Sm^{149}: 0.096 eV (J = 4), 0.87 eV (J = 4), 4.93 eV (J = 4), and 8.9 eV (J = 4) using polarized neutrons and a polarized target. Considering that the absolute value of the spin obtained by this method might be questionable, but that the relative values are not, we have measured also the spin of the 0.87-eV resonance; we found (J = 3). In this experiment, we used Be($10\bar{1}1$) as monochromator and measured the scattering counting rate between 2 eV and 0.65 eV (Fig. 1) to be sure that there were no disturbing effects as, for example, from higher order scattered neutrons or from impurities in the sample.

Some information about the spin of the capturing state in (Sm^{149} + n) can be obtained from the study of the reactions Sm^{149} (thermal n, α) Nd^{146},[7,8] and $Sm^{149}(n,\gamma)Sm^{150}$.[9,10] We think that with the available results the conclusions are not clear[11] and that further work on these reactions is necessary.

---

[4] H. Marshak, H. Postma, V. L. Sailor, F. J. Shore, and C. A. Reynolds, Phys. Rev. 128, 1287 (1962).

[5] B. N. Brockhouse, Can. J. Phys. 31, 432 (1953).

[6] L. D. Roberts, Phys. Rev. 95, 105 (1954).

[7] R. D. Macfarlane and I. Almodovar, Phys. Rev. 127, 1665 (1962).

[8] E. Cheifetz, J. Gilat, A. I. Yavin, and S. G. Cohen, Phys. Letters 1, 289 (1962).

[9] R. K. Smither, Bull. Am. Phys. Soc. 6, 316 (1962).

[10] E. Bieber, T.v. Egidy, and O. W. B. Schult, Z. Physik 170, 465 (1962).

[11] H. Ceulemans, F. Poortmans, and M. Nève de Mévergnies, Colloque de Physique Nucléaire, Orsay, 2-4 mai 1963. To appear in Journal de Physique et le Radium.

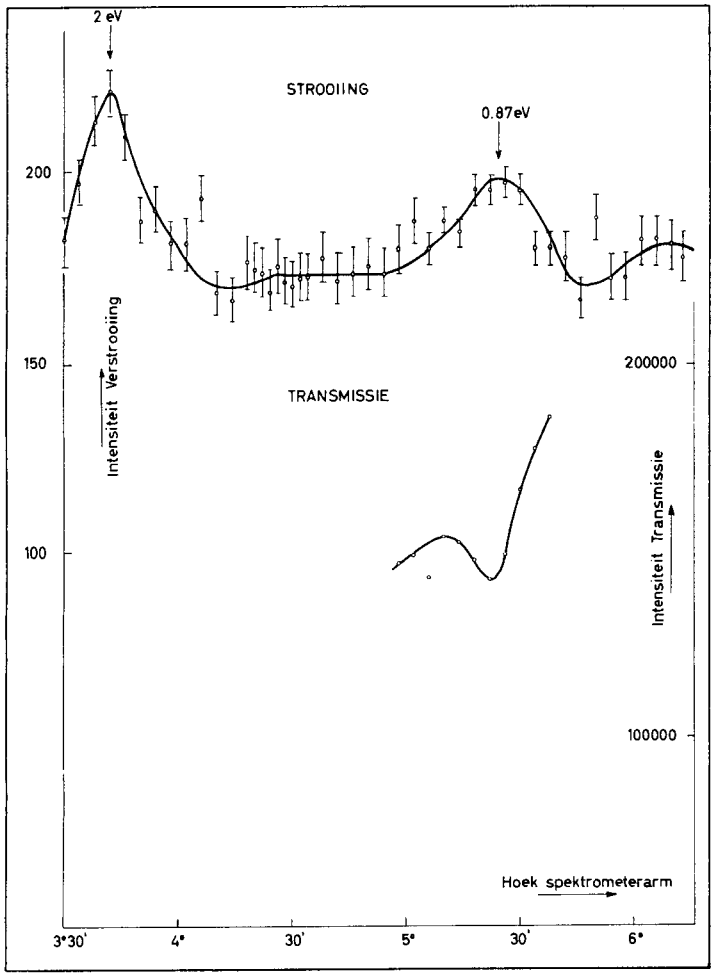

Fig. 1. Counting rates for neutrons scattered (upper curve, left-hand scale) and transmitted (lower curve, right-hand scale) by Sn^{149}.

Gd^{157}

For the 0.034-eV resonance we quote an upper limit for Γ_n/Γ because we have taken the calculated value of $n\sigma_p$ (where n is the number of atoms per cm^2 and σ_p is the potential-scattering cross section) as the contribution for nonresonant scattering.

There might be an additional contribution due to impurities in the sample; this is quite improbable, but even if it was the case, the value of g would be higher. The result is in agreement with previous measurements (see Table I).

Sm^{147}

The alpha decay of the compound nucleus formed by capture of a thermal neutron by Sm^{147} is very similar to that of $Sm^{149}(n,\alpha)Nd^{146}$,[7,8] so the study of ($Sm^{147}$ + n) might help in solving the problem of (Sm^{149} + n) mentioned above.

Up to now we have only preliminary results for the first resonance at 3.4 eV. The published values of σ_0 and Γ, needed to calculate g, are not accurate so that it is still difficult to give a firm result for the spin of this resonance. Better transmission measurements are needed to confirm this.

* * *

A. I. YAVIN, University of Illinois: In the last New York meeting, your laboratory presented data which disagreed with several experiments on the assignment of the spin of the first resonance of Sm^{149}. At that time I mentioned that (n, α) experiments done with the Israel Research Reactor and published last year in Physics Letters also indicated $J^{\pi} = 4^-$ for this resonance, in disagreement with your laboratory. Your assignment of J = 3 for the second resonance in Sm^{149} again disagrees with experiments done by Marshak et al. in Brookhaven. As to Sm^{147}, we found on the basis of our (n, α) work that our data are consistent with a 4^- level very close to $E_n = 0$ and we therefore felt that the first resonance at 3.4 eV has $J^{\pi} = 4^-$. The data which you presented tentatively claim that this level has J = 3. If this is the case, I feel that there is probably a bound state with $J^{\pi} = 4^-$ very close to $E_n = 0$. This state would then be the main contributor to the absorption cross section of thermal neutrons.

H. E. JACKSON, Argonne National Laboratory: In capture-gamma-ray experiments here at Argonne, R. T. Carpenter[12] has studied the capture spectra for the resonances in Sm^{149} at 0.096, 0.87, and 4.93 eV.

[12] R. T. Carpenter, "The Electric-Dipole Gamma-Ray Strength Function for Heavy Even-Even Nuclei," Argonne National Laboratory Report ANL-6589, August 1962.

He finds that the intensity of the primary transition from the capture state to the 2^+ first excited state of Sm^{150} is zero within statistics for each of these resonances. If the capture state were 3^-, de-excitation to the first excited state of Sm^{150} by electric-dipole radiation would be observed. It is highly unlikely that fluctuations in the partial widths would result in unobservably small intensities for all three of these resonances. This strongly suggests that if the spins of these three resonances are the same as indicated by measurements with polarized neutrons and targets, then the spin value is 4^- and not 3^-.

IV-8. SMALL-SAMPLE TRANSMISSION MEASUREMENTS ON Pu^{241}, USING AN ELECTRON-LINAC PULSED-NEUTRON-SOURCE TIME-OF-FLIGHT SPECTROMETER*

N. J. Pattenden and S. Bardsley

A.E.R.E., Harwell, Berks., England

In comparing the relative merits of reactors and pulsed accelerators as neutron sources for slow-neutron time-of-flight spectrometers, there is considerable agreement that, in the region below a few electron volts, reactors have more advantages, and in the region above a few hundred electron volts, pulsed machines have a clear advantage. Also, pulsed machines have some advantage in many partial-cross-section applications. However, in the field of transmission measurements on small samples of separated isotopes in the region between a few eV and a few hundred eV, it is still considered that choppers on reactors are superior to pulsed accelerators. This paper describes the use of a pulsed machine with a subcritical fast reactor target (booster) for such an experiment. It can thus be considered as a combination of both techniques.

The Harwell 28-MeV electron linear accelerator and neutron booster target used as a pulsed neutron source have already been described.[1] The small-sample time-of-flight spectrometer utilizes one of the beam positions from the booster target, and the experimental arrangement is shown in Fig. 1. The beam dimensions are progressively reduced along the flight path from the 25 cm square of the water moderator tank to one of a range of sizes at the sample position, the smallest size being 1.8 mm in diameter. The flight path from source to detector is about 14.6 m. The detector is located about 1 m from the sample, and consists of a lithium glass scintillator (Nuclear Enterprises NE.905) with 7.3% lithium, enriched

*Presented by N. J. Pattenden.

[1] M. J. Poole and E. R. Wiblin, Proc. 2nd Geneva Conference 14, 266 (1958).

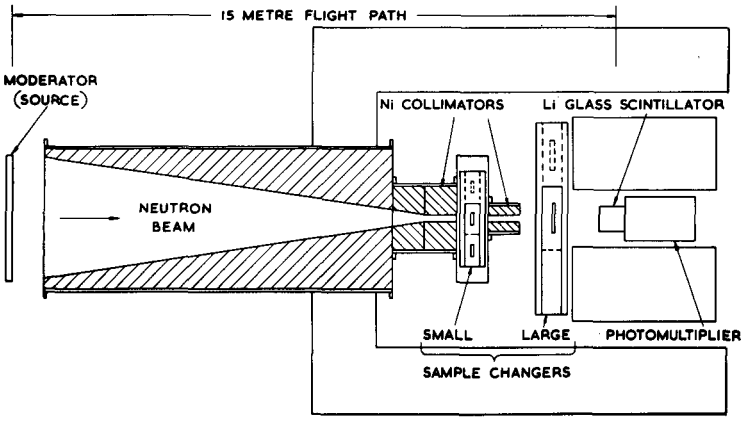

Fig. 1. Experimental arrangement of small-sample transmission measurement.

to 96% Li^6, 1.3 cm in diameter and 1.3 cm thick. The scintillator is mounted on a E.M.I. 9524B photomultiplier. A resolution of about 16% was obtained on the width of the neutron peak.

The detector pulses are fed to a time analyzer system consisting of an on-line 16-track tape recorder, and an off-line 1024-channel analyzer.[2] In this application, the system was coded to provide 4096 channels for each of the four combinations of sample-changer positions. A typical observed neutron time spectrum is shown in Fig. 2.

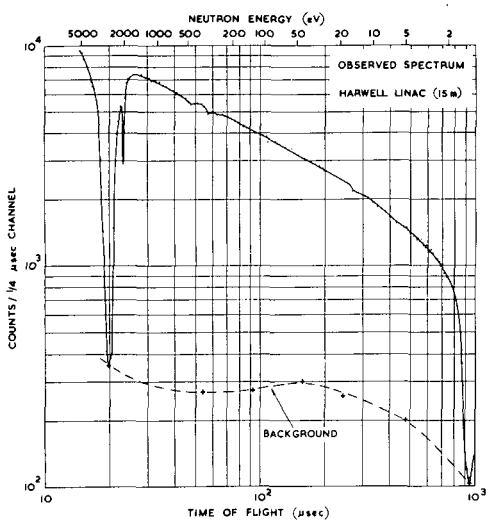

Fig. 2. Observed neutron time spectrum and background rate.

A boron filter is kept in the beam to avoid overlapping of pulses. The background curve shown in the figure was obtained by inserting a range of filters with "black" resonances. The observed counting rate at 100 eV was about 20 counts per minute per resolution width per cm^2 beam area at the sample, with a background of about 8%.

The energy resolution of the spectrometer can be approximately represented by

[2] J. R. Waters and J. R. Bird, Nucleonics 19, No. 3, 70 (1961).

$$\frac{\Delta E}{E} = 2\sqrt{\left(\frac{\Delta t}{2}\right)^2 + \left(\frac{\Delta \ell}{\ell}\right)^2},$$

where E, t, and ℓ denote energy, time, and distance, respectively, and ΔE, Δt, and $\Delta \ell$ denote the uncertainties in these quantities. The width at half height of the unmoderated neutron burst was considered to be about 0.23 μsec, the channel width was 0.25 μsec, and all other time jitters appeared to be small compared to these. Therefore Δt was taken to be 0.25 μsec. Because of the size of the neutron source and the fact that the flight path was not perpendicular to the source, the geometrical distance uncertainty was about 4 cm. To this must be added an effective distance uncertainty due to the moderation time, and an effective value of $\Delta \ell$ of 4.3 cm was taken. These give values for the resolution of 17 nsec/m in the high-energy region where the distance uncertainty was negligible, and $\Delta E/E = 0.6\%$ in the low-energy region where the time uncertainty was negligible. The two effects are equal at about 150 eV. The above estimates of the spectrometer resolution are consistent with experimental data which have been obtained on thorium resonances.

The Pu^{241} samples were prepared by D. Boreham (Chemistry Division, A.E.R.E.) from two batches of material enriched by the A.E.R.E. electromagnetic separator HERMES. The isotopic analyses of these two batches shortly after separation are shown in Table I. Altogether 380 mg of plutonium was available. Oxide powder samples of four different thicknesses were prepared, the thicknesses being shown in Table I.

In the transmission measurements, a sufficient time was spent on each sample to give at least 4000 counts per channel between resonances, except for the thickest sample, for which at least 1000 counts per channel were obtained. The observed total cross section per PuO_2 molecule is shown in Figs. 3, 4, 5, and 6, covering the ranges 3 to 15 eV, 15 to 39 eV, 39 to 87 eV, and 70 to 5000 eV, respectively.

TABLE I. Pu^{241} samples.

(a) Isotopic analysis.

Batch No.	Atoms per cent				Date of measurement
	239	240	241	242	
HB41	0.93 ± 0.01	2.67 ± 0.02	95.7	0.7 ± 0.006	9 March 62
HB50	1.08 ± 0.02	5.49 ± 0.03	93.02	0.41 ± 0.01	24 May 62

(b) Thickness. (The estimated error in thickness is ± 3%.)

Batch No.	Area (cm^2)	Weight of PuO_2 (mg)	Thickness (Pu atom/barn)
HB41 + HB50	0.117	117 ± 3 + 248 ± 4	8.01×10^{-3}
HB50	0.117	248 ± 4	4.67×10^{-3}
HB41	0.317	173 ± 3	1.21×10^{-3}
HB50	0.895	235 ± 2	5.79×10^{-4}

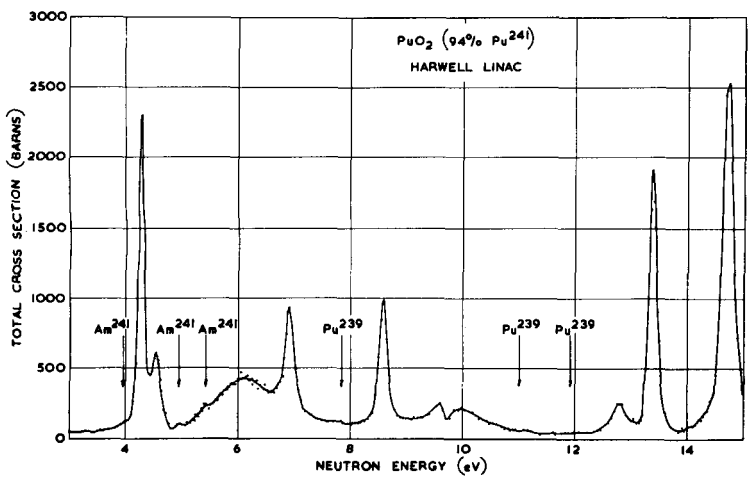

Fig. 3. Observed total cross section of PuO_2 (about 94% Pu^{241}) from 3 to 15 eV.

The Pu^{241} total cross section has been previously measured by Simpson and Schuman[3] with poorer resolution and a less pure sample. Our data may be compared with the Doppler-broadened cross

[3] O. D. Simpson and R. P. Schuman, Nucl. Sci. and Eng. 11, 111 (1961).

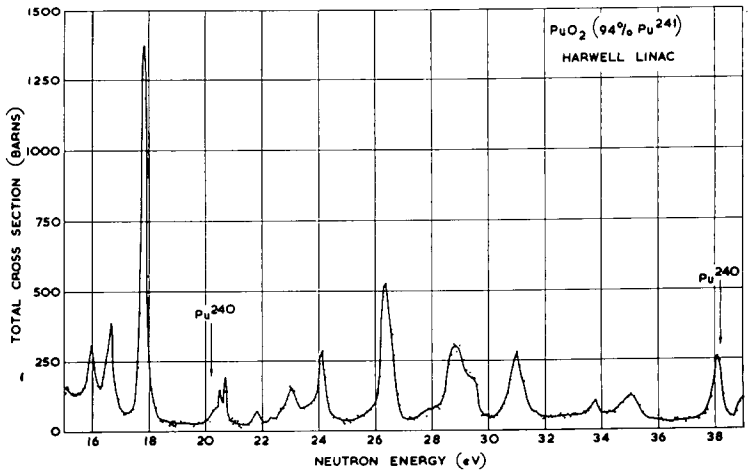

Fig. 4. Observed total cross section of PuO_2 (about 94% Pu^{241}) from 15 to 39 eV.

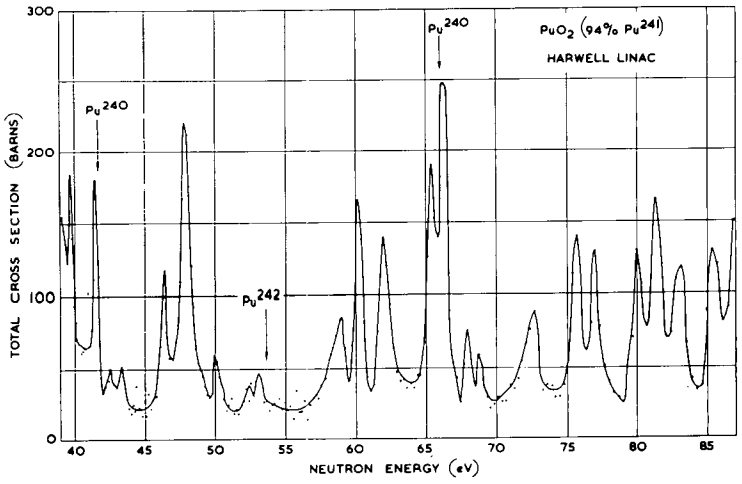

Fig. 5. Observed total cross section of PuO_2 (about 94% Pu^{241}) from 39 to 87 eV.

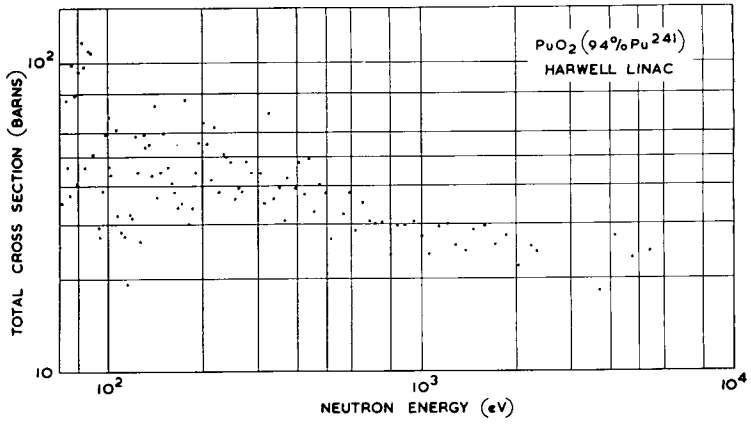

Fig. 6. Observed total cross section of PuO_2 (about 94% Pu^{241}) from 70 to 5000 eV.

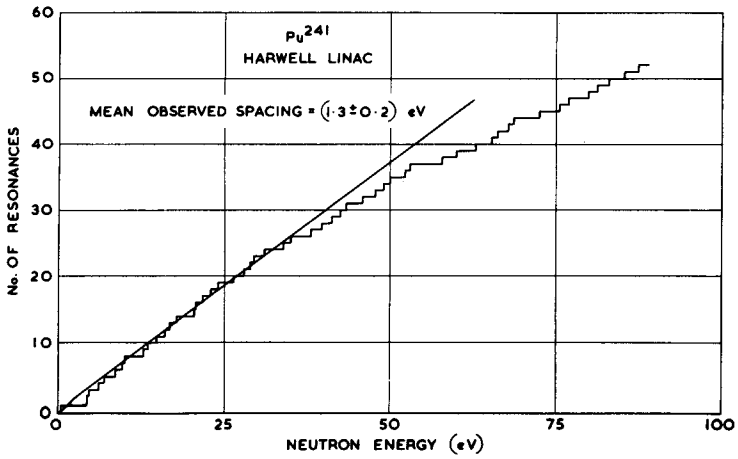

Fig. 7. Number of Pu^{241} resonances against energy.

section calculated from the resonance parameters which they have obtained in the region below 11 eV.[4] In the regions between resonances, the agreement is within 4% and frequently much better, but on the peaks of narrow resonances our observed values are considerably higher than their values for the cross section with Doppler broadening corresponding to 27°C, and sometimes higher than their un-Doppler-broadened values. In general, the energy scales of the two measurements are in good agreement.

Figure 7 shows a plot of the number of observed resonances against energy. From this it appears that most of the resonances below 50 eV have been observed, and the mean observed spacing is 1.25 ± 0.2 eV. A multilevel analysis of the resonances below 50 eV is proceeding.

[4] O. D. Simpson and N. H. Marshall, IDO-16679 (1961).

* * *

L. M. BOLLINGER, Argonne National Laboratory: At the risk of being impolite to a guest, I would like to compare the counting rates given by the speaker with what one can obtain with a chopper. At the same energy, namely 100 eV, with a resolution that is slightly worse, perhaps 22 nsec/m, we obtained a counting rate of about 140 counts/min per resolution width. We appear to be better off by a factor of 5 than this high-power accelerator.

PATTENDEN: Could you mention what your background rate is?

BOLLINGER: I cannot state it accurately. However, the background rate is, I would think, in the neighborhood of 5% at 100 eV.

F. B. SIMPSON, Phillips Petroleum Co.: How does the area of the sample compare in the two experiments?

BOLLINGER: The area is the same, 1 cm^2.

M. S. MOORE, Phillips Petroleum Co.: I wanted to remark that the sample measurements that you referred to were taken with a sample slightly too thick on the resonance peaks.

K. K. SETH, Northwestern University: Did you do the analysis for the widths, and could you quote a strength-function value?

PATTENDEN: This has not been done as yet, but we shall do this.

IV-9. A TIME-SHARED COMPUTER-CENTERED DATA-COLLECTION SYSTEM AT THE BROOKHAVEN GRAPHITE RESEARCH REACTOR*†

R. E. Chrien, S. Rankowitz, and R. J. Spinrad

Brookhaven National Laboratory, Upton, New York

BNL-7396
C 12-20-63

The increasing complexity of the data of nuclear physics has led to widespread interest in the possibility of utilizing a digital computer for on-line data collection. Through the combined efforts of the Instrumentation Division of the Neutron Physics group at Brookhaven, such a system has been placed into operation. Several features of this system are believed to be unique and of interest to research groups centered about a major facility like a reactor or an accelerator.

The system provides for effectively simultaneous data collection for two physically unrelated neutron time-of-flight experiments at the Brookhaven Graphite reactor. For the fast neutron chopper, the computer provides a 1024-channel time-of-flight analyzer for total or partial neutron cross-section experiments, three auxiliary clocks, three total-events scalers, and two monitor scalers. The 1024 channels can be split into halves to permit recording of data obtained in sample-cycling operations. At the same time a 256-channel time analyzer, a clock, a total-events scaler, and a monitor scaler are provided for slow-neutron-chopper experiments dealing largely with "cold" neutron scattering from solids, liquids, and gases. Completely independent operation of both experiments is always maintained.

A general-purpose, transistorized, digital computer[1] of a 2048 24-bit-word memory is the heart of this system. The computer possesses a "priority interrupt" feature making it especially useful for time-shared operation. A signal on any one of 16 interrupt lines forces the

*Work supported by the U.S. Atomic Energy Commission.

†Presented by R. E. Chrien.

[1] The SDS-910, manufactured by Scientific Data Systems, Inc., Santa Monica, California.

computer to suspend its current operation and enter a special subroutine determined by the interrupt line which was signaled. Appropriate action is taken by the computer; e.g., incrementing a scaler, incrementing the contents of a time-of-flight channel, responding to a typewriter request, etc. The interrupt system is hierarchical in nature, each line being ordered as to time of execution. Thus simultaneous requests are processed in order according to their priority assignments. The computer also accepts 24-bit parallel input into its memory and is able to send out 24-bit parallel-output information. Accordingly, binary encoded data may be easily transferred to and from the machine.

The data words are encoded by external circuitry using conventional modular logic cards.[2] Immediately following an interrupt request, an encoded time-of-flight address is presented to the input terminals of the computer, and it is subsequently accepted by the interrupt-initiated subroutine. The data-taking subroutine takes 96 μsec for execution; however, a computer modification is available which will reduce this to 16 μsec.

A block diagram of the entire system is presented in Fig. 1. To facilitate connection of external analog-to-digital converters, a matrix type of connection board is employed.[3] The insertion of pins in this board assigns the significance of the bit patterns transferred between the computer and the external equipment, and also assigns the significance of the various interrupt lines. Figure 2 shows a photograph of the boards employed in the present system.

The program package placed in the computer memory utilizes the computer typewriter keyboard for control of the data-taking operation. Sixteen 4-letter mnemonic codes are available to the user for starting and stopping runs, printing scaler readings, generating data tapes,

---

[2] Computer Control Corporation, Framingham, Massachusetts (S-Pac Series).

[3] "Sealectoboard," manufactured by Sealectro Corporation, Mamaroneck, New York.

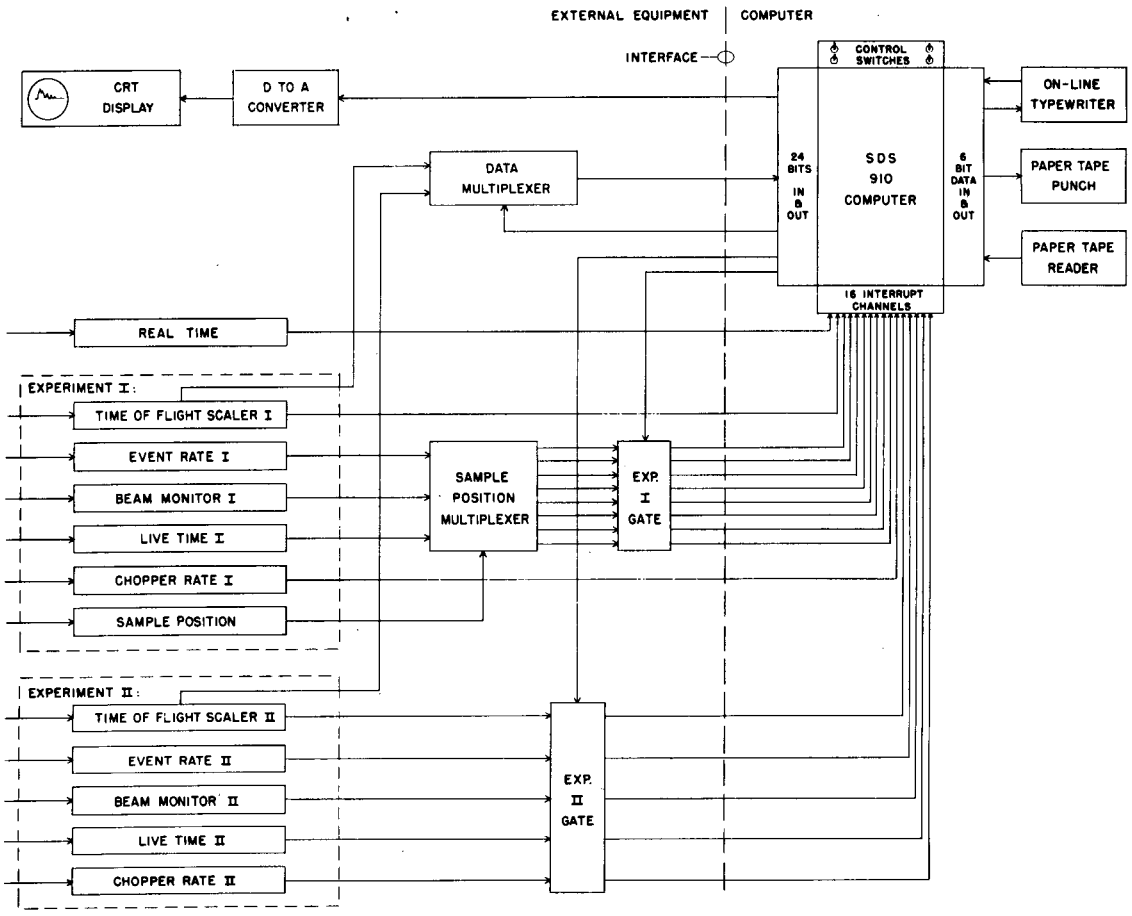

Fig. 1. A block diagram of the time-shared data-collection system.

and so on. For example, the code "FPUN" typed by the operator causes the following sequence of events:

(1) Data taking with the fast-chopper analyzer is terminated.

(2) The computer types, with headings, the following:

(a) a master-clock reading

(b) the accumulated live times for sample-in, sample-out and background,

(c) the total number of detected events for sample-in, sample-out, and background time periods,

(d) beam-monitor readings during sample-in and sample-out times, and

(e) a calculation of the rotor speed in rpm.

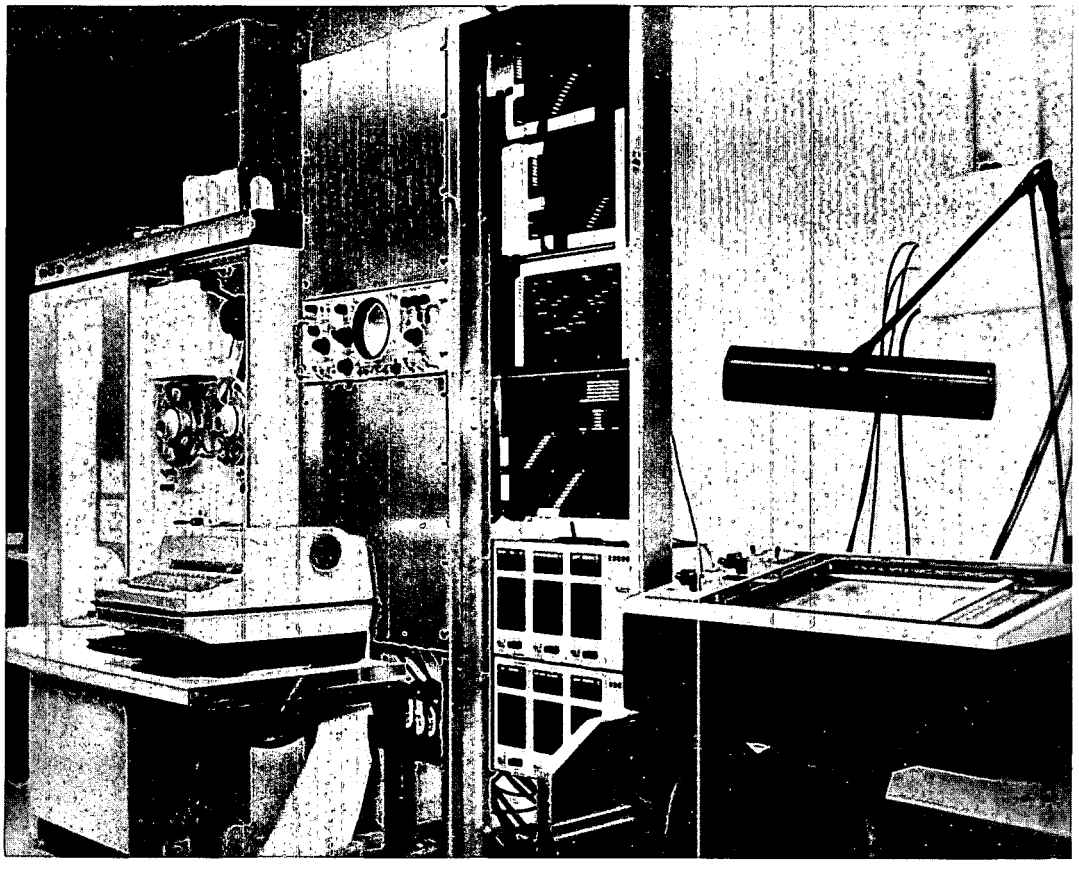

Fig. 2. A photograph of the time-shared data-collection system showing the "Sealectoboard" connection board for data transfer between the computer and peripheral equipment.

(3) The computer generates a perforated tape containing the 1024-channel contents preceded by a readable array of holes denoting the absolute time as a tape identifier.

None of the above operations affect slow-chopper data taking in any way except for a slight increase in deadtime (about 0.3%) during punchout. Similar commands exist for data typeouts, scaler and clock typeouts, data-taking terminations and initiations, etc. The time out occupied in input-output and data-taking is used in generating a display, which to the visual observer appears to be continuous. The display is maintained at all times with a switch controlling the choice of spectrum presented. The typed commands and corresponding responses from the

computer constitute a permanent experimental log. Figure 3 shows a section of that log, illustrating several operations and formats.

The basic program package of dual analyzer simulation and typewriter control, output routines, binary-decimal conversion, etc. occupies approximately 700 words. With 1296 words of computer memory devoted to scalers and data channels, little room is available for on-line data processing programs in the remaining memory. Provision will be made for reading in special processing programs when desired from a spool of punched program tape. The time-shared data-taking ability of the computer can be maintained during these operations, with only typewriter control to be given up. When normal operation is to be resumed after data processing is completed, the operator will be able to read back in the normal program system.

Memory expansion to 4096 words and the addition of a magnetic tape deck will greatly enhance the power of the present system. Ultimately, the computer will act as a multiparameter analyzer on both slow-chopper and fast-chopper experiments and will perform on-line data processing when required.

The versatility of the computer data-taking system provides a built-in protection against obsolescence. In a sense, the capabilities of these systems are limited only by the ingenuity of the programmer and user. We expect to see a rapid increase in the use of these systems in the near future and believe that the use of time-shared computers will become common practice among research teams using a large facility such as a nuclear reactor or an accelerator.

* * *

R. C. BLOCK, Oak Ridge National Laboratory: That is all nice, Bob, but how much does it cost? That is one thing you did not mention.

CHRIEN: Well, the price is a nebulous factor because costs are coming down. For example, we could have made a significant reduction in price had we waited.

```
SONN     ABS. TIME: Ø1504

         SLOW:   TIME          TOTALS        MONITOR       RPM
                 ØØØØØ         ØØØØ3         ØØØØØ         Ø5781


FPUN     ABS. TIME: Ø1511

         FAST:   TIME          TOTALS        MONITOR       RPM
SAMPLE IN        Ø1139         ØØ387         Ø2757         Ø9566
NO SAMPLE        ØØØ37         ØØØØ3         ØØØØØ
BACKGROUND       ØØØ37         ØØØØ5


FOON N G

SCON     ABS. TIME: Ø1542

         SLOW:   TIME          TOTALS        MONITOR       RPM
                 ØØØØØ         ØØØØ4         ØØØ42         Ø6875


FCLR     ABS. TIME: Ø1661

         FAST:   TIME          TOTALS        MONITOR       RPM
SAMPLE IN        Ø1139         ØØ387         Ø2757         Ø9595
NO SAMPLE        ØØØ37         ØØØØ3         ØØØØØ
BACKGROUND       ØØØ37         ØØØØ5


FONN     ABS. TIME: Ø1694

         FAST:   TIME          TOTALS        MONITOR       RPM
SAMPLE IN        ØØØØØ         ØØØØØ         ØØØØØ         ØØ176
NO SAMPLE        ØØØØØ         ØØØØØ         ØØØØØ
BACKGROUND       ØØØØØ         ØØØØØ


FCLR     ABS. TIME: Ø1724

         FAST:   TIME          TOTALS        MONITOR       RPM
SAMPLE IN        ØØØ26         ØØØØØ         ØØØ61         Ø9663
NO SAMPLE        ØØØØØ         ØØØØØ         ØØØØØ
BACKGROUND       ØØØØØ         ØØØØØ


FONN     ABS. TIME: Ø1729  <--- 1700  Sept 20  1963

         FAST:   TIME          TOTALS        MONITOR       RPM
SAMPLE IN        ØØØØØ         ØØØØØ         ØØØØØ         ØØØ19
```

Fig. 3. A segment of the experimental log sheet automatically produced by the typewriter program package. Several of the mnemonic codes are shown. Also shown is the effect of typing an incorrect code which results in the typewriter producing the characters N G.

The price of the basic computer is about $45 000. The input-output units (the punch and the typewriter) are extra. When you add this peripheral equipment, the price comes to $62 000. The ADC units and the sealectoboards I showed you provide a flexible input-output connection and cost another $12 000. So the entire system, as you saw it, costs about $77 000.

However, the prices keep coming down all the time, and it is a little hard to give you a price quotation because I think it is rather meaningless.

L. M. BOLLINGER, Argonne National Laboratory: It wasn't clear to me from what you said what you think you will achieve ultimately in the way of a simple time analyzer. Could you state briefly the characteristics that you think you will have achieved: the number of channels, capacity per channel, channel width, counting rates, and that sort of thing?

CHRIEN: Are you referring to the present system, or do you want to include the multiparameter analysis that we hope to be doing later on?

BOLLINGER: I am asking about what you are aiming at by the time you have added the peripheral equipment—which I would guess was not included in the cost that you just gave. I would want you to include that equipment in your projection of what you would achieve in the way of a simple time analyzer. In other words, what I am getting at is this: It seems that what you have now described is not a very useful device as a simple time analyzer. But this does not say that you cannot achieve it with some further complication.

CHRIEN: It is an extremely useful device because it is easy to control. It is flexible and it is very reliable, which is something that we have not had at Brookhaven over the past ten years or so. I didn't mention this, but I will bring it up at the present time. Since this system has been in operation (and this represents some months of operation), we have had only one failure of the computer. This failure was attributable

to somebody pushing the wrong switch on a voltage control somewhere. This is one important feature that I did not stress in my talks, but it is a very important one, i.e., reliability.

We have also freed by essentially doing all our data collection in one system. We have freed several analyzers because there is an essential duplication of effort within our group; that is, we are doing two experiments with two different time analyzers. Essentially, we have wasted most of the time because of the counting rates, which are not very high.

This system enables us to more efficiently use our electronics, I would say. But the present system represents no particular advance in the number of time channels, or the number of time delays, or the channel-width selection that we have. We have a rather wide selection of channel widths.

This system gives no particular advance in these sorts of features. I am not sure that I have answered your question.

BOLLINGER: Well, let me put it in a slightly different way. If you wanted to attack the problem in the way you have described, could you come up with an analyzer that has in the neighborhood of 4000 to 10 000 channels, that could accept 1000 counts/sec, and that has a wide range of channel widths?

CHRIEN: Certainly, I do not see any reason why not.

BOLLINGER: At a reasonable price?

CHRIEN: Well, I do not see any reason why not.

Let me add one more point, because I forgot to mention this. The present data-handling subroutine in the present system takes 96 μsec for its execution. This is not the shortest time that could be achieved in storing a band. We can get down to about 16 μsec; but it is the shortest time that is simply achieved without buying computer modifications. This is adequate for our present counting rates and probably adequate for all our experiments in the near future, but it does represent a limitation on certain kinds of experiments, I would imagine.

IV-10. SLOW-NEUTRON CROSS SECTION OF He^3, B, AND Au; AND A He^3 PROPORTIONAL COUNTER FOR THE ABSOLUTE DETERMINATION OF NEUTRON BEAM INTENSITY*

J. Als-Nielsen, A. Bahnsen, and O. Dietrich

Research Establishment Risø, Roskilde, Denmark

This paper describes a method for the measurement of the density of neutrons in a beam by means of He^3.

The first requirement for the method is that the $He^3(n, p)$ cross section is known and obeys the (1/v) law. If so, the determination of neutron density is converted to a measurement of the number of (n, p) processes taking place in a "thin" known amount of the (1/v) absorber He^3. The (1/v) dependence and the absorption cross section have been measured by a total-cross-section measurement of He^3 in the energy region from 0.0003 eV to 11 eV.

The monochromatization was done on a single-axis spectrometer, using mica, Be (1, 0, 0), and Be (1, 2, 1) as monochromator crystals. Higher order contamination was completely avoided by means of a velocity selector up to 0.05 eV and corrected for at higher energies.

The He^3 was contained in an Al box with dimensions of approximately 5 × 12 × 36 cm. The box could be turned so that three values of N (number of He^3 atoms/cm^2 along the neutron path) could be obtained with the same He^3 filling of approximately $\frac{1}{2}$ atm, yielding transmissions between 6% and 90% in the energy region 0.0003 eV — 11 eV.

In this energy region no deviation from the (1/v) law can be found from the data. The cross section at 2200 m/sec was found to be $\sigma(He^3) = 5327^{+10}_{-9}$ barns. As an instrumental check, the cross sections of natural boron and of gold were also measured; the results agree with the most accurate existing data. The absorption cross sections at 2200 m/sec were found to be $\sigma_a(B) = 759.1 \pm 2.0$ barns and $\sigma_a(Au) = 98.6 \pm 0.2$ barns. The results are shown in Figs. 1—3.

*Read by title only.

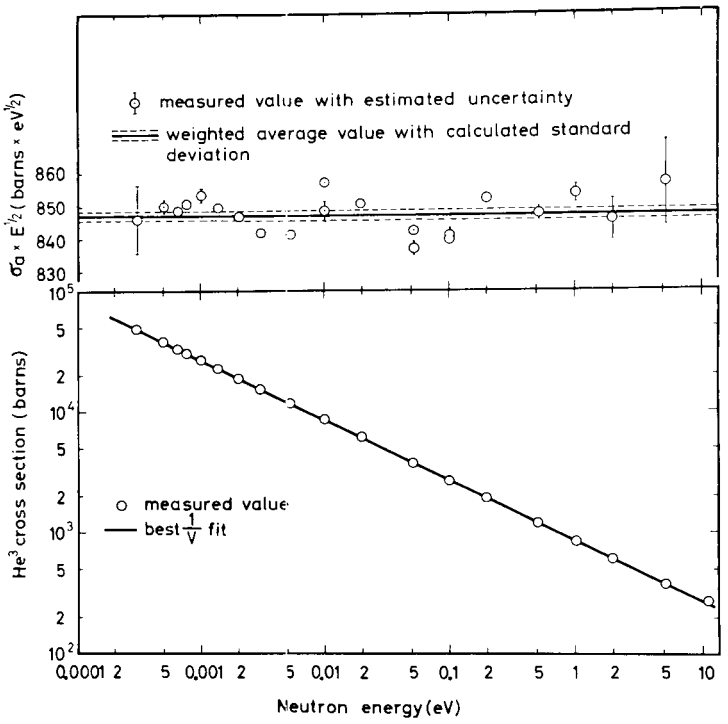

Fig. 1. The total cross section σ_{tot} of He^3 versus neutron energy E. From the (1/v) fit, it is concluded that $\sigma_{tot} = \sigma_a$ within the accuracy of the data. $\sigma_a\sqrt{E}$ vs E is also shown. It is noted that the estimated uncertainties are only used in the weighing procedure to find the average value, the standard deviation of which is calculated from the actual spread of the data.

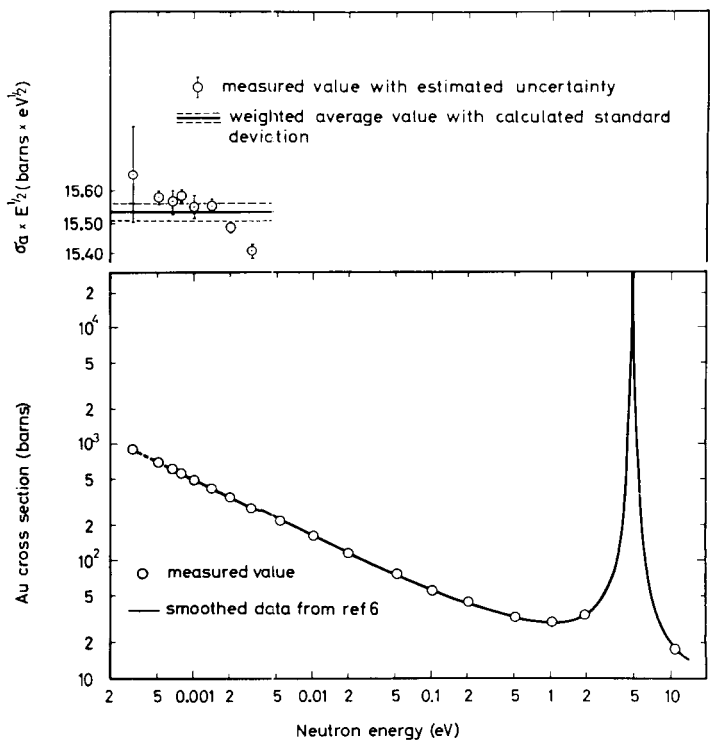

Fig. 2. The total cross section σ_{tot} of Au versus neutron energy E. The absorption cross section σ_a is deduced from σ_{tot} for $E < 0.005$ eV. The curve of $\sigma_a \cdot \sqrt{E}$ vs E is also shown. Reference 6 is D. J. Hughes and R. G. Schwarz, "Neutron Cross Sections," BNL-325 (1958).

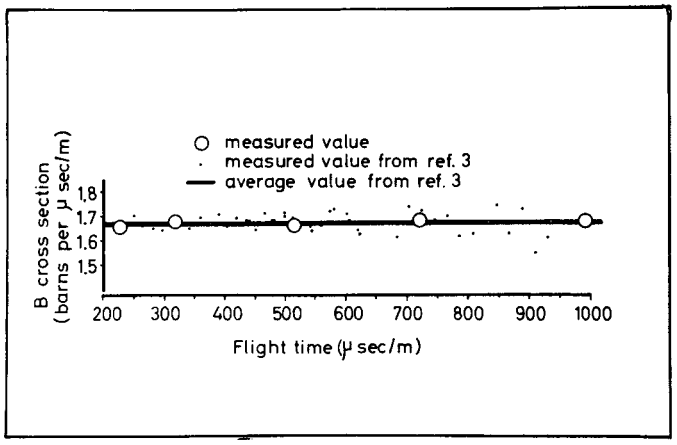

Fig. 3. Reproduction of part of Fig. 8 in "Ref. 3" [A. Deruytter et al., "Measurement of the Thermal Neutron Absorption Cross Section of Boron by Means of a Time of Flight Technique," EUR. 12.e (1962)] together with the authors' measured values of the boron cross section.

For the purpose of measuring the number of (n, p) reactions taking place in a given amount of He^3, a proportional counter of well-known detection efficiency was developed. The counter has a rectangular cross section, and the anode wire is perpendicular to the beam, which can then traverse either the short (3 cm) or the long (5 cm) dimension of the counting chamber (Fig. 4). In both cases, the maximum energy loss

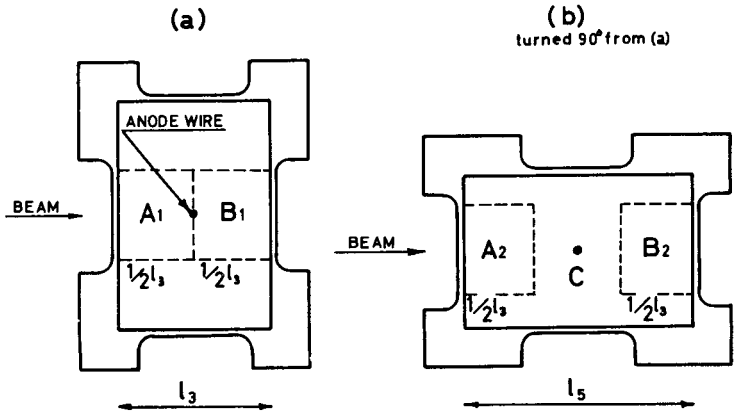

Fig. 4. Cross section of the He^3 counter, shown with a neutron beam traversing the short (a) and the long (b) directions. The track distribution for region $A_1 + B_1$ will be equal to that for region $A_2 + B_2$, which leaves region C as a "wall-less" counter.

from ionization tracks (shortened at the walls) will be $\frac{3}{4}Q$, reaction particles being expelled in opposite directions. All (n, p) reactions will therefore be counted with a discriminator level below $\frac{1}{4}Q$.

Detailed calculations of the wall-effect spectrum exhibit a step at $\frac{1}{4}Q$; and this is clearly demonstrated by the measurements, which also show it is possible to discriminate effectively against background.

Spectra, recorded at 1 and 2 atm gas pressure, agree very well with the calculated ones, and the difference between the spectra for the two counter lengths is very close to that expected from a wall-less counter, indicating that conditions in the counter are close to ideal (Fig. 5). The ratio between the counting rates of the long and the short dimensions of the counter was compared to the ratio between the physical lengths, and good agreement was found. It is concluded that detection efficiency, i.e., the ratio between the number of counts and the number of (n, p) reactions, is equal to 1.000 with an uncertainty of ± 0.4% for both counter orientations.

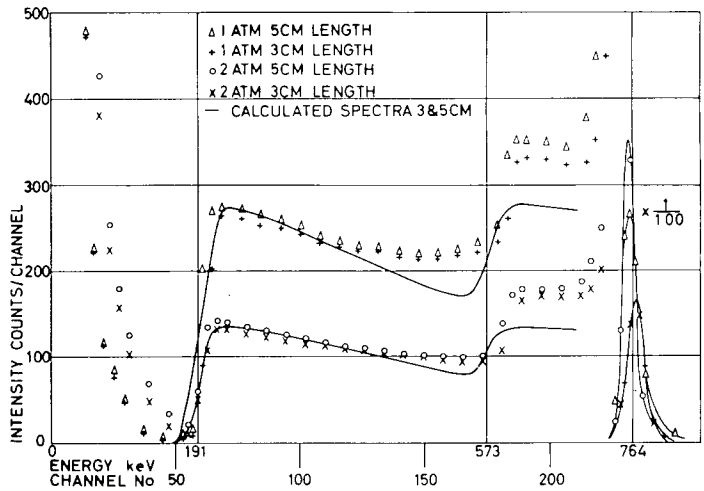

Fig. 5. Spectra of the H^3 counter with the beam traversing the short and long directions, and with a gas pressure of 1 and 2 atm (absolute). The background has been subtracted, and the spectra at 1 and 2 atm correspond to the same integrated number of counts.

A comparison between the usual gold foil activation method and the He^3 method sketched above for determination of the neutron density in a beam will be completed in the near future.

IV-11. Withdrawn at the request of the authors.

IV-12. RADIOMETRIC DETERMINATION OF THE NEUTRON-CAPTURE CROSS SECTION OF 35-HR Rh^{105} †*

L. E. Glendenin and H. C. Griffin

Argonne National Laboratory, Argonne, Illinois

and

R. A. Schmitt

General Dynamics/General Atomic, San Diego, California

The activation cross section for capture of reactor neutrons by 35-hr Rh^{105} has been measured by radiometric assay of the induced activities of 30-sec Rh^{106} and 2.2-hr Rh^{106}. Carrier-free targets of Rh^{105} (2-60 μCi) were prepared by radiochemical separation from neutron-irradiated ruthenium and exposed in a TRIGA reactor (pulsed operation) for production of 30-sec Rh^{106} and in the CP-5 reactor for production of 2.2-hr Rh^{106}. A selective γ-γ coincidence method was used for counting the induced Rh^{106} activities in the presence of Rh^{105} and extraneous activities resulting from contaminants. Values of 14 000 ± 2000 b and 5800 ± 1200 b were obtained for production of 30-sec and 2.2-hr Rh^{106}, respectively, relative to a value of 36 b for neutron capture by Co^{59}. This yields a combined cross section of 20 200 ± 3000 b for capture of reactor neutrons. A cadmium ratio of ≥ 6 was observed for the formation of the 30-sec isomer. No determination was made in the case of the 2.2-hr isomer, since this activity was produced in a flux with a small fast component.

---

†Work performed under the auspices of the U.S. Atomic Energy Commission.

*Read by title only.

IV-13. ANGULAR DISTRIBUTION OF GAMMA RAYS FROM (n, n'γ) REACTIONS PRODUCED BY FAST NEUTRONS FROM A REACTOR*

R. D. Roberts, Pennsylvania State University

and

D. J. Donahue, University of Arizona

Using a statistical assumption concerning the intermediate states involved in nucleon inelastic scattering, Satchler[1] has obtained an equation to describe the angular distribution of γ rays emitted after inelastic-scattering events. The experiments described here were performed to see if a nuclear reactor could be used as a source of neutrons with which to study these angular distributions, and to check the validity of Satchler's equation.

The experimental arrangement used is shown in Fig. 1. Fast neutrons from the 200-kW Pennsylvania State University reactor pass through various collimators in the reactor shield, and are incident upon a target located about 15 ft from the reactor. Gamma rays produced by inelastic scattering in the target are detected by a 3-in.-diameter by 3-in.-long NaI(Tl) crystal, and recorded in a 128-channel pulse-height analyzer. The angle between the incident neutrons and detected γ rays could be varied from 100° to 165°. The targets used were thin enough so that less than 7% of the incident neutrons suffered an elastic collision, and no corrections were made for multiple neutron scattering.

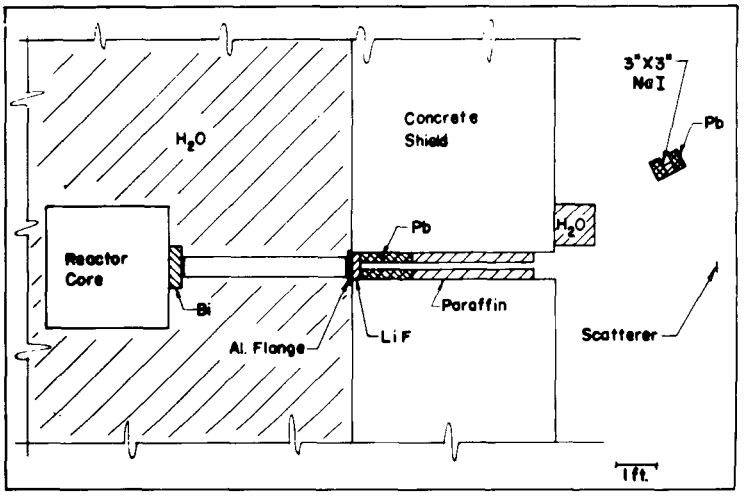

Fig. 1. Experimental arrangement.

*Presented by D. J. Donahue.

[1] G. R. Satchler, Phys. Rev. 104, 1198 (1956); ibid. 111, 1747 (1958).

A complication which must be considered in using the neutron beam from a reactor results from the fact that this beam contains neutrons with all energies up to about 10 MeV, whereas the theoretical equation depends on the energy of the neutrons producing the reactions. Two facts allow one to say something about the energy of neutrons which produce the observed reactions.

First, the shape of the cross section for inelastic scattering through a particular nuclear state rises rapidly from threshold to an approximately constant value. Second, the energy distribution of neutrons in the beam decreases exponentially. Thus, the product $\sigma(E)\phi(E)$ has a maximum. This is illustrated in Fig. 2 for the case of scattering from the 2.6-MeV 3^- state in Pb^{208}. From this curve we find that (a) the median energy of neutrons producing the state is 4.2 MeV and (b) 70% of all reactions are produced by neutrons with energies between 3.2 and 6.0 MeV. This is rather poor energy resolution, but as will be shown, it is sufficiently good to allow comparison between our experiments and theory.

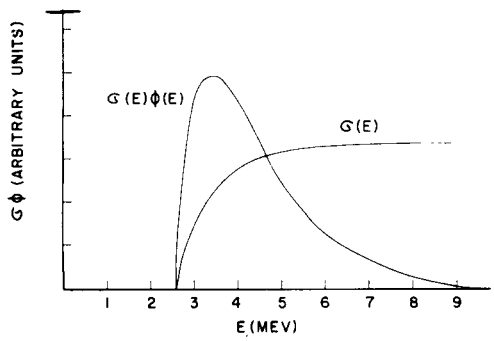

Fig. 2. A curve showing the product $\sigma(E)\phi(E)$ as a function of neutron energy.

The results for the angular distribution of γ rays from the 2.6-MeV 3^- state in Pb^{208} are shown in Fig. 3. The points are experimental results. Curves A, B, and C are calculated from Satchler's equation for incident neutron energies of 3.5, 4.1, and 6.0 MeV, respectively, assuming that the quantum number of the state is 3^-. Curve D is calculated for 4.1-MeV neutrons, assuming quantum numbers for the state of 2^+. For all calculations, the transmission coefficients of Beyster et al.[2] were used. From Fig. 3 we conclude: (a) the energy dependence of the theory

[2] J. R. Beyster, R. G. Schrandt, M. Walt, and E. W. Salmi, Los Alamos Scientific Laboratory Report LASL-2099 (1957).

is sufficiently small so that the energy spread used in these experiments can be tolerated; (b) the experimental points agree very well with the calculated curves; and (c) the calculated curves are sufficiently dependent on the quantum numbers of the state so that a 3^- state can easily be differentiated from a 2^+ state.

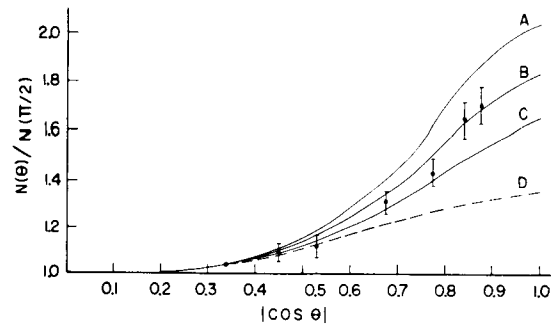

Fig. 3. Angular distribution of 2.6-MeV γ rays from $Pb^{208}(n, n'\gamma)Pb^{208}$ reactions. The various curves are explained in the text.

To determine whether or not agreement with calculations could be obtained for low-A nuclei, the angular distribution of 1.37-MeV γ rays from (n, n') reactions in Mg^{24} was measured. The median energy of neutrons producing this reaction was calculated to be 2.4 MeV. The results are shown in Fig. 4. The circles are our experimental results, and the curves are calculated distributions for incident neutron energies of 2 and 3 MeV, obtained by assuming that the quantum number of the state is 2^+. The squares are results of Boring and McEllistrem,[3] obtained using neutrons produced by particles from an accelerator. Again, our results are in excellent agreement with the calculations.

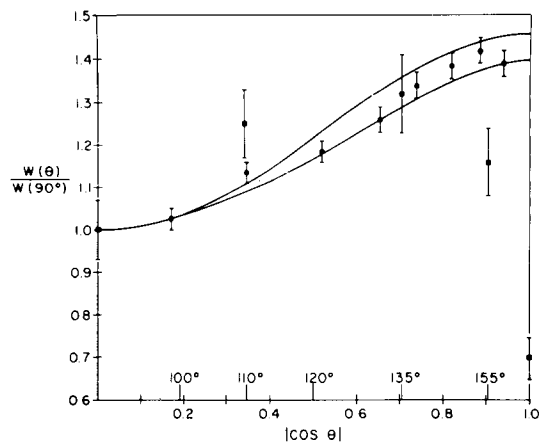

Fig. 4. Angular distribution of 1.37-MeV γ rays from the $Mg^{24}(n, n'\gamma)Mg^{24}$ reaction. The squares are from Boring and McEllistrem (Ref. 3).

---

[3] J. W. Boring and M. T. McEllistrem, Phys. Rev. 124, 1531 (1961).

Angular distributions of the 0.85-MeV γ rays from the $2^+ \rightarrow 0^+$ transition in Fe^{56} and of the 1.24-MeV γ rays from the $4^+ \rightarrow 2^+$ transition in Fe^{56} have also been measured. In all cases good agreement with calculated distributions was obtained. Thus it seems reasonable to conclude that inelastic-scattering experiments using neutrons from a reactor, together with Satchler's angular-distribution equation, can be used to investigate the quantum numbers of the nuclear states involved in the reactions.

* * *

J. A. HARVEY, Oak Ridge National Laboratory: On your first figure on lead, you showed a peak at 2.2 and then you did not go into that anymore. You worked on the 2.6-MeV gamma ray. Do you know where the 2.2 is?

DONAHUE: I think it was 2.1. That would be the first escape from the 2.6.

P. MOLDAUER: Argonne National Laboratory: Your coefficient involves a knowledge of the neutron transmission coefficients over the range of the average. What did you use for those?

DONAHUE: I should have mentioned that. We used the transmission coefficients that are tabulated in the Los Alamos report.

IV-14. COHERENT NUCLEAR SCATTERING AMPLITUDES AND CROSS SECTIONS AS DETERMINED BY NEUTRON-DIFFRACTION TECHNIQUES*

M. H. Mueller, S. S. Sidhu, L. Heaton,
R. L. Hitterman, and H. W. Knott

Argonne National Laboratory, Argonne, Illinois

CONF-346-6
C-1-22-64

The scattering of slow neutrons has been employed for the study of unknown crystal structures in much the same way as x rays. Whereas x-ray scattering factors f are functions of atomic number and can be calculated with a fair degree of accuracy, this is not the case as yet for thermal-neutron scattering amplitudes b.

The nuclear scattering amplitude consists of two parts, potential scattering and resonance scattering. In the case of the potential scattering, the nucleus behaves as an impenetrable sphere in which the magnitude increases only slowly with atomic mass number A, and is proportional to $A^{1/3}$; in the case of resonance scattering it seems to vary in a random fashion from element to element and may be of the same or opposite sign (180° phase difference) as the potential scattering. This leads to an increase or decrease of the total scattering amplitude. The value of b may well be different for the different isotopes of an element since their nuclei may have different energy levels and hence vary considerably in resonance scattering.

Therefore, in order to obtain a working set of neutron scattering amplitudes for use in crystal structure analysis, a known crystal structure may be employed to obtain the coherent nuclear scattering properties of the nuclei of an element or an isotope which makes up the structure. The amplitude b and cross section σ may be obtained for elements and isotopes by several different diffraction techniques: (1) powder pattern using a Ni powder sample as an external standard; (2) a powder pattern using one of the elements as an internal standard; (3) single-crystal data together with a standard reference crystal; and (4) single-crystal

*Presented by M. H. Mueller.

data using one element as an internal standard.

From time to time we at Argonne have made coherent scattering measurements on a number of different samples in order to obtain data on elements or isotopes not previously determined or to obtain data to recheck previously reported results. A brief description of the techniques and a summary of some of the results is given below.

In order to carry out the powder diffraction method[1] the integrated intensity $P_{hk\ell}$ from a set of $hk\ell$ planes is

$$P_{hk\ell} = k^2 \frac{\rho'}{\rho_0} N_c^2 \frac{m_{hk\ell}}{\sin^2\theta \cos\theta} F_{hk\ell}^2 (0) e^{-2W} A(\theta), \qquad (1)$$

in which $P_{hk\ell}$ is the integrated intensity, k is a constant, ρ'/ρ_0 is the ratio of the measured density to the true density of the solid, N_c is the number of unit cells per cubic centimeter, F(0) is the structure factor at $(\theta/\lambda) = 0$, W is the Debye-Waller temperature factor, and $A(\theta)$ is the absorption correction.

In practice k is determined from a known substance such as Ni, and then after running the unknown under identical experimental conditions this k can be used to obtain the value for $F_{hk\ell}$ which consists of the scattering factor b and a trigonometric term related to the atom positions in the crystal. Details of the method for obtaining b and the calculation for σ were described in an earlier paper[1] in which for a bound atom, $\sigma^b_{coh} = 4\pi b^2$; and for a free atom $\sigma^f_{coh} = \mu^2 \sigma^b_{coh}$, where μ is the reduced mass.

All of the results shown in Table I for Zr, Tc^{99}, Os, and the Os isotopes were obtained using method (1) in which neutron powder patterns were obtained for the material under study together with a nickel powder standard using b_{Ni} as 1.03×10^{-12} cm. Patterns were obtained

[1] S. S. Sidhu, L. Heaton, and M. H. Mueller, J. Appl. Phys. 30, 1323 (1959).

TABLE I. Summary of coherent-nuclear-scattering data.

Element or isotope	Data from	b (10^{-12} cm)	σ^b_{coh} (barns)	σ^f_{coh} (barns)
Zr	metal	0.70	6.16	6.13
Tc^{99}	metal	0.68	5.81	5.79
Os	metal	1.07	14.39	14.49
Os^{188}	metal	0.78	7.65	7.70
Os^{189}	metal	1.10	15.21	15.31
Os^{190}	metal	1.14	16.33	16.44
Os^{192}	metal	1.19	17.80	17.92
K	chloride	0.34	1.45	1.41
K^{39}	chloride	0.37	1.72	1.66
Rb	chloride	0.85	9.08	9.02
Rb^{85}	chloride	0.83	8.66	8.60
Ir	oxide	1.06	14.12	14.22
Mg	oxide	0.48	2.90	2.72

from samples $\frac{1}{4}$ in. in diameter and the integrated intensities for the reflections were then used in the Busing-Levy[2] least-squares crystallographic computer program for evaluating the best value for the scattering amplitude. The value of b_{Zr} is considerably higher than 0.62×10^{-12} cm previously reported,[3] but is in agreement with recent results of others.

The results shown in Table I for K, K^{39}, Rb, and Rb^{85} were also obtained initially by the powder technique of method (1). However, they were also checked by method (2) in which $b_{Cl} = 0.99 \times 10^{-12}$ cm was used as an internal standard. In method (2) the value of k shown in Eq. (1) need not be evaluated and a set of relative values of F for the

[2] W. R. Busing and H. A. Levy, Oak Ridge National Laboratory Report 59-4-37 (1959).

[3] International Tables for X-Ray Crystallography (The Kynock Press, 1962), Vol. III, pp. 229-231.

various choices of hkℓ may be used directly in the least-squares computer program. The scattering amplitude b for K is in agreement with the previous value reported,[3] but the K^{39} results are new. The value $b_{Rb} = 0.85 \times 10^{-12}$ cm is considerably higher than the previous value[3] of 0.55×10^{-12} cm and the value for Rb^{85} has not been reported before.

A value for b_{Ir} was obtained from a powder pattern of IrO_2. Since IrO_2 is tetragonal, $a_0 = 4.49$ Å and $c_0 = 3.14$ Å. There are a limited number of resolved lines in the forward reflecting region. Therefore, method (2) was employed, using the oxygen as an internal standard. The relative intensities from five resolved reflections were usedin the least-squares program[2] in which the scale factor, b_{Ir}, and the positional parameter x in the xx0 position for oxygen were treated as variables. The results are shown briefly in Table I.

The results shown in the table for Mg were obtained from neutron intensities from a single crystal of MgO which was being used for instrument alignment. Intensity data were obtained from approximately 150 hkℓ which occurred in three octants of reciprocal space. These intensities were then used in the least-squares program in which the scale factor and temperature factor were treated as variables. A calculation was then tried in which b_{Mg} was also allowed to vary and considerable improvement was noted in the agreement factor. It was then concluded,on the basis of method (4) described above, that the previous value of 0.54×10^{-12} cm for b_{Mg} was too high and a value of 0.48×10^{-12} cm shown in Table I is more nearly correct. It has also been reported recently[4] that powder diffraction data for MgO give a value of 0.516×10^{-12} cm for b_{Mg}.

---

[4] T. M. Sabine and J. D. Browne, Acta Cryst. 16, 834 (1963).

IV-15. NMR OF SHORT-LIVED NUCLIDES BY POLARIZED NEUTRON CAPTURE AND β-DECAY ANISOTROPY*

D. W. Connor, T. Tsang, and D. L. Davis

Argonne National Laboratory, Argonne, Illinois

Introduction

In this paper we shall discuss briefly the nuclear polarization resulting from the capture of polarized neutrons, the relaxation processes which tend to destroy the nuclear polarization, the spatial anisotropy of β-particle emission from polarized nuclei, and the experimental techniques which we have used. These matters, and particularly the nuclear magnetic resonance (NMR) aspects, are treated more fully in a forthcoming paper[1] where references to related work will be found.

1. Nuclear Polarization

Since the capture of polarized neutrons gives a net angular momentum to the target, it is intuitively evident that some nuclear polarization must result. In fact, for capture into the higher spin compound state, positive values of the magnetic quantum number are emphasized, as shown in Fig. 1. For capture into the lower spin state, the reverse is true. The resultant polarization of the compound state is:

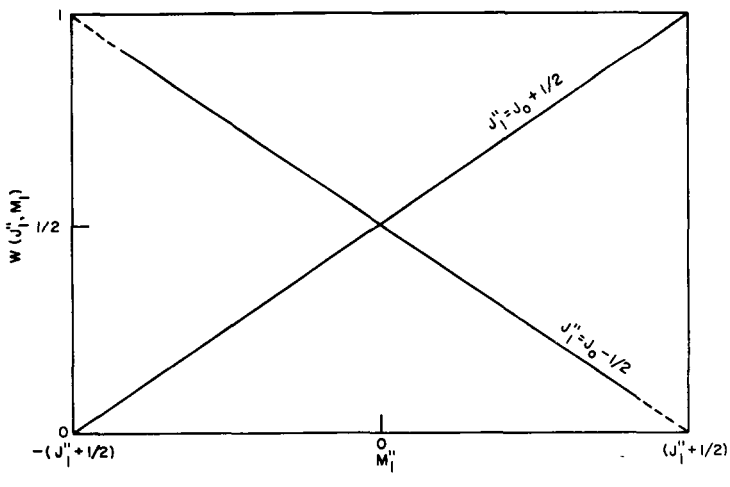

Fig. 1. Relative probabilities $W(J_1'', M_1'')$ of the states formed from the capture of polarized slow neutrons by unpolarized nuclei of spin J_0.

---

*Presented by D. W. Connor.

[1] T. Tsang and D. Connor, Phys. Rev. 132, (fall 1963).

$$\text{For } J_1'' = J_0 + \tfrac{1}{2}, \qquad P = (1 + J_1'')/3J_1''.$$

$$\text{For } J_1'' = J_0 - \tfrac{1}{2}, \qquad \begin{cases} P = -1/3 & (J_1'' \neq 0). \\ P = 0 & (J_1'' = 0). \end{cases}$$

The labeling of the several states is given in Fig. 2.

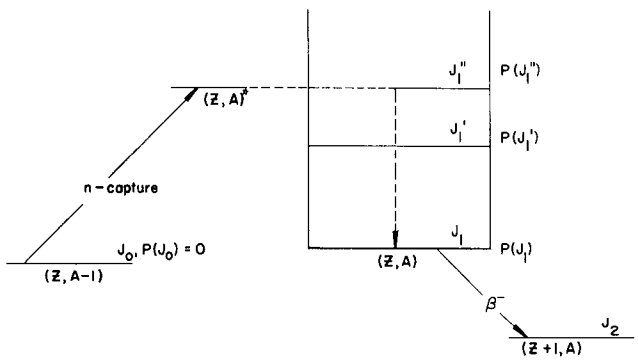

Fig. 2. Diagram illustrating the process of neutron capture and subsequent β decay.

The emission of capture gammas in the transition to the ground state (g.s.) generally reduces the ground-state polarization but, typically, not by a large factor. This can be treated exactly, of course,[2] but since neither the capture-gamma scheme nor the spins of the intermediate levels are usually known well enough, the calculation seems unprofitable. If the g.s. spin differs by only one or two units from that of the compound states, the g.s. polarization should usually be between 0.05 and 0.5. Since the two compound states give opposite polarization, the possibility of accidental cancellation exists but it is probably rare that the two capture cross sections are so neatly balanced.

2. Relaxation Processes

These tend to reduce the initial g.s. polarization to the much smaller value corresponding to statistical equilibrium, typically a few parts per million in kilogauss magnetic fields. In order that the nuclear polarization be observable via an anisotropy in β decay, it is necessary that the relaxation time (τ_1 in conventional NMR usage) be at least comparable to the half-life. Of the two relaxation processes which are

[2] F. D. Shapiro, Uspekhi Fiz. Nauk. 65, 133 (1958).

significant in usual NMR experiments, that of relaxation via paramagnetic impurities is insignificant in our work since the near-zero concentration of product nuclei ($\approx 10^{-19}$ cm^{-3}) inhibits the process of spin diffusion (transfer of angular momentum between neighboring like nuclei) which normally couples a nucleus to a distant impurity. The other well known process, quadrupolar relaxation, does occur whenever the nuclear quadrupole moment is appreciable. It may be inhibited only by reducing the sample temperature T ($\tau_1 \propto T^{-2}$) and, to some degree, by choice of target compound. We have been able to study Li^8 and F^{20} at room temperature because the quadrupole moments are fortuitously small. In the case of B^{12}, relaxation is not negligible at 80°K even though the half-life is only 0.02 sec.

3. β-Decay Anisotropy

For allowed transitions, the angular distribution is $W(\theta) = 1 + (v/c)PA \cos\theta$, where the coefficient A depends on the spin change in the β transition (see Table I). Detecting the betas with a pair of similar counters, each subtending at the source a cone of half-angle θ_1 about the polarization axis, the relative difference in counting rates is

TABLE I. Asymmetry coefficient A for allowed β emission with angular momentum change $J_2 - J_1$.

ΔJ	A	
1	$J_1/(1 + J_1)$	
-1	-1	
0	$-1/(1 + J_1)$	(pure G-T)
0	0	(pure Fermi)

$$(N_1 - N_2)/(N_1 + N_2) = (a/2)\sin^2\theta_1/(1 - \cos\theta_1),$$

$$a \equiv (v/c)PA.$$

We have source and counters in a strong magnetic field so that $\theta_1 \approx \pi/2$ and

$$(N_1 - N_2)/(N_1 + N_2) \approx a/2$$

4. Nuclear Magnetic Resonance

An overly simplified description will suffice to illustrate the experiment. In an applied magnetic field H_0 (parallel to the polarization axis), the nuclear Zeeman levels are separated in energy by the amount $\Delta E = \mu H_0/J_1$. If the nuclei are irradiated with photons of angular frequency $\omega_L = \gamma H_0$, where γ is the gyromagnetic ratio (macroscopically an rf magnetic field of this frequency), transitions among the Zeeman levels will destroy the polarization. Experimentally, one varies ω or H_0 and looks for a decrease in the β-decay asymmetry. From a determination of γ, one may obtain the nuclear g factor $g \equiv \mu/\hbar J_1$ from the relation $g = \gamma\hbar/\beta_N$, where β_N is the nuclear magneton.

By providing a circularly polarized rf field, we have been able to determine the sign of the magnetic moment.[3]

5. Experimental

The arrangement is shown schematically in Fig. 3.

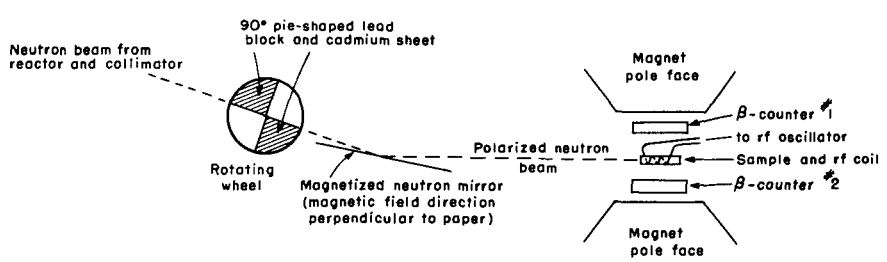

Fig. 3. Experimental layout.

[3] D. Connor and T. Tsang, Phys. Rev. 126, 1506 (1962).

Reactor neutrons pass through a slow chopper, are polarized by reflection from a magnetic mirror, and irradiate a sample held in the gap of a large electromagnet. Chopping the beam allows (half-time) counting free from interference by capture gammas.

A typical room-temperature sample-holder is shown in Fig. 4. The boron nitride end pieces serve to collimate the polarized neutron beam, thereby minimizing radioactive background due to capture of stray neutrons by nearby objects such as the counters. The rf magnetic field is generated by passage of the appropriate current through the coil surrounding the sample.

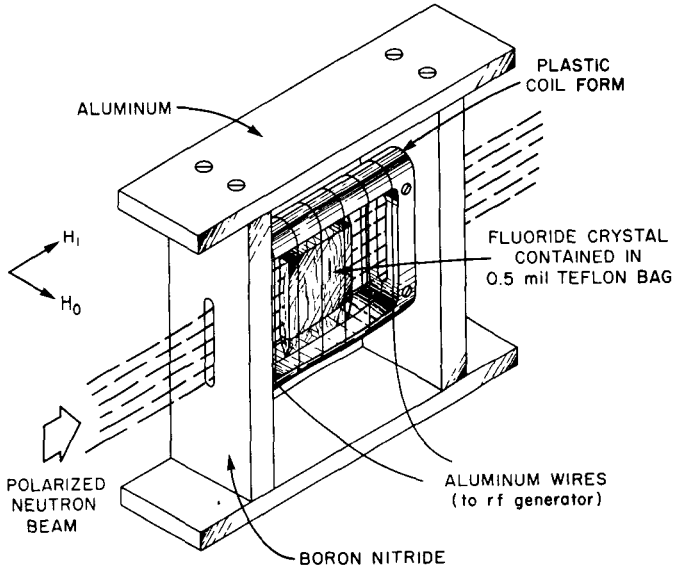

Fig. 4. Target/coil-form assembly. Neutron and nuclear polarization are parallel to H_0.

The experimental procedure is usually the following. The β-emission asymmetry for the nuclide under study is determined by comparing the rates of the two counters with the neutron beam alternately polarized and unpolarized. This comparison frees us from the difficult task of providing absolutely symmetrical counters and experimental conditions. If the asymmetry is large enough (a few per cent) to make observation of the resonance feasible, a search for the resonance is made by turning on the rf field and measuring the asymmetry during systematic variation of either ω or H_0. The search may be very tedious and we have sometimes been able to shorten it by modulating H_0 at an audio frequency, thereby artificially

broadening the NMR line. Once the resonance has been located, a careful point-by-point study readily gives γ or g to within a few hundredths of a per cent. Some resonance data for F^{20} appear in Fig. 5.

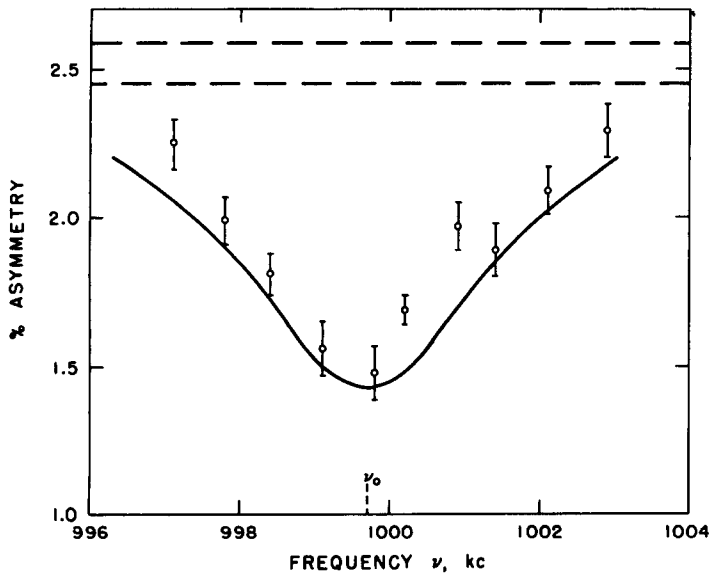

Fig. 5. Experimental NMR asymmetry data for F^{20} in a CaF_2 single crystal. H_0 = 1253 Oe parallel to the 110 axis; H_1 = 5.3×10^{-3} Oe. The solid curve was calculated from a model discussed in Ref. 1. The dotted lines indicate the asymmetry (with experimental uncertainty) obtained in the absence of rf field.

6. Discussion

We believe that this method will permit observation of the NMR for some fifty radionuclides for which neither conventional NMR nor the atomic-beam method is feasible. Cross sections of a few millibarns have sufficed for the work to date and it appears that the sensitivity can be improved considerably by careful reduction of background. However, in most cases a sample temperature in the liquid-helium range will be required in order to extend the quadrupolar relaxation time sufficiently. At low temperature, it may be possible to observe the quadrupole splitting. This would permit an unambiguous determination of the spin and probably fairly good estimates of the quadrupole moment.

Acknowledgment

Experiments of this type were first suggested by T. B. Novey and V. L. Telegdi, with whom we enjoyed many helpful discussions in the early phases of the work.

* * *

H. MAIER-LEIBNITZ, Technischen Hochschule, Munich: I think that I first should say that I have always thought it was one of the nicest experiments in the field in the last few years.

Secondly, I would like to ask you whether you have thought of applying this to the fission process — I mean, looking at some fast-decaying beta matter and looking for some polarization that you get from fission by polarized neutrons. It might be an interesting application. I don't suppose it is too easy.

CONNOR: Let me answer, first, by thanking you for the comment and acknowledging that the original notion for this experiment is due to Ted Novey of Argonne and Valentine Telegdi of the University of Chicago.

The nicest thing about this is thinking of it, but I did not do that. Secondly, we simply have not thought about it, primarily because I am not really a nuclear physicist any more.

I would be delighted to have anyone apply the technique to anything useful. I am not going any further with it myself.

Session V

THE FISSION PROCESS

Thursday morning, 17 October 1963

Presiding: J. S. Fraser

Scientific secretary:
V. E. Krohn

V-1. THE THEORY OF FISSION*

Lawrence Wilets

University of Washington, Seattle, Washington

Pub. lit CONF-346-3 C-1-2064

Next autumn will mark a quarter of a century since the appearance of the now classic paper by Niels Bohr and John Wheeler entitled "The Mechanism of Nuclear Fission." This was the first detailed theory of the phenomenon, and it invoked the liquid-drop model suggested by Meitner and Frisch.

The liquid-drop model has a certain esthetic beauty of its own, apart from any relevance it may have to the fission process. The assumptions upon which it rests are of the greatest simplicity: Statics (1) uniform nuclear and charge density (sharp surface), (2) surface energy proportional to surface area. Dynamics (1) no viscosity, irrotational flow. We will return to a critique of these assumptions later.

In spite of its simplicity, the implications of the model have been maddeningly difficult to ascertain. An expansion of the static energy about the spherical shape in terms of Legendre coefficients has been useful, but undoubtedly fails to converge in regions of great interest. Beginning with the numerical calculations of Frankel and Metropolis, the potential surface has been surveyed by several workers until now, thanks to the definitive calculations of Cohen and Swiatecki, the nature of the saddle-point configurations is well understood: the saddle point configurations are symmetric in shape, and are stable against small asymmetric deformations.

The situation with respect to dynamics is less clear. Beyond the small-deformation region, numerical calculations must be invoked; and for this we have only the fragmentary results of D. L. Hill. Without a dynamical calculation, such important questions as mass asymmetry cannot be settled. Even without the dynamics, however, several failures of the simple liquid-drop model are evident.

---

*Invited paper.

(1) Most fission thresholds lie systematically 5–10 MeV higher than the liquid-drop model predicts. Although this is a large discrepancy, it is true that it is small compared with the individual Coulomb and surface terms contributing to the deformation energy. The saddle point determines the threshold energy, independent of the dynamics.

(2) The experimental value of the kinetic energy of the fragments (in thermal and spontaneous fission) corresponds to the Coulomb energy of touching or separated spheres; the kinetic energy is especially low in the region of symmetric fission. Both the small magnitude of the kinetic energy and the fact that it does not increase with increasing excitation energy is rather difficult (but not impossible) to understand on the basis of a viscosity-free model.

(3) The mass-yield curves are clearly connected with nuclear shell structure. The preference for preserving the 50-proton 82-neutron core (and possibly the 50-neutron core) is outside the domain of the liquid-drop model.

What can we do with the liquid drop model? We could systematically raise the level of sophistication of each of the four assumptions listed above. Statics: (1) take the nuclear density as given by the electron-scattering experiments, (2) let the surface energy depend upon factors other than surface area (such as curvature and nuclear shell structure), as suggested by Terrell, Vandenbosch, and Fong. Dynamics: (1) allow for viscosity, thus admitting the transfer of energy from collective motion into internal (nucleonic) excitation, and (2) use an alternative description for calculating the flow (i.e., the Inglis "cranking model").

The logical successor to the liquid-drop model is the adiabatic model. Like the liquid-drop model, it can be defined crisply. It meets some of the failings of the liquid-drop model but not all. The prescription of the adiabatic model is that the stationary states of the many-body system are calculated subject to a small number of constraints. These constraints specify the amount of deformation intrinsic in the nucleus,

for example, the quadrupole, octupole, etc. moments of the mass distribution:

$$(H - \underset{\sim}{\alpha} \cdot \underset{\sim}{Q}) \Psi_i (\underset{\sim}{\alpha}) = \epsilon_i (\underset{\sim}{\alpha}) \Psi_i (\underset{\sim}{\alpha}) , \qquad (1)$$

where $\underset{\sim}{Q}$ is the set of operators whose expectation value is specified, $\underset{\sim}{\alpha}$ is the corresponding set of Lagrangian multipliers, and the $\epsilon_i(\underset{\sim}{\alpha})$ are the adiabatic energy levels. These constraints, in turn, become the dynamical variables of collective motion. In order to carry out a calculational program for the adiabatic model, one must utilize at least moderately realistic two-body interactions; the simplified pairing-plus-quadrupole interaction used so successfully by the Copenhagen group for studying low-lying excitations would be inadequate here.

Even though the complete adiabatic model is not likely to be calculated in the near future, we can nevertheless deduce (and speculate on) several interesting features of the model. There is a definite prescription for calculating each of the required generalizations of the liquid-drop model listed above. The incorporation of the shell model is a natural consequence. Viscosity — the transfer of collective energy to internal excitation — can be calculated in principle, and has been estimated numerically under simplifying assumptions. In general, these nonadiabatic processes are found to be very large. The distance in excitational energy space over which diffusion occurs during transit of one unit in β is roughly

$$0.5 \langle (V_0^3 A T_\beta)^{\frac{1}{4}} \rangle ,$$

where V_0 is the depth of the nuclear potential, T_β is the kinetic energy of collective (β-) motion, and $\langle\,\rangle$ denotes some appropriate average. Taking $T_\beta \approx \frac{1}{2}$ MeV, this number turns out to be about 22 MeV. The exception appears to be that the lowest intrinsic states are at least

partially isolated from higher states. That is to say, statistical equilibrium may well be established among states of high excitation, but these will not feed the lowest states. Furthermore, if the nucleus passes over the saddle point only in the lowest excitational states, it may not thermalize by the time of scission.

At this point it is appropriate to make some comments about the concept of channels. The number of exit channels (or degrees of freedom in the final state) is in the order of billions. On the other hand, the measures which we use for the number of channels turn out to be small. The resolution of this minor paradox is that at some point in the fission process there is a "bottle neck," namely the saddle configuration, through which the nucleus must pass. The few (intermediate) states at the saddle configuration are interpreted as the channels.

There are currently two measures for the number of channels. The first, due to Bohr and Wheeler, is given by

$$\nu_1 = \frac{2\pi \langle \Gamma_f \rangle}{D} = \sum f_a \ . \tag{2}$$

Here f_a may be interpreted, roughly, as the penetrability through the fission barrier. Thus $f_a \leq 1$, where a denotes the channel.

The other measure is based upon the fluctuations in the fission widths,

$$\nu_2 = \frac{2\langle \Gamma_f \rangle^2}{\langle \Gamma_f^2 \rangle - \langle \Gamma_f \rangle^2} = \frac{(\sum f_a)^2}{\sum f_a^2} \ . \tag{3}$$

This expression yields the Porter-Thomas value of the channel number when there are (say) ν_2 degrees of freedom, all of which are equally available (equal penetrability). However, the formula has a broader interpretation. If the channels do not participate equally (unequal penetrabilities),

the distribution of fission widths will not, in general, be of the Porter-Thomas form nor need ν_2 be an integer. The physical interpretation of ν_2 is expressed by $(\sum f_a)^2/\sum f_a^2$.

One finds from Eqs. (2) and (3) that

$$\frac{\nu_1}{\nu_2} = \frac{\sum f_a^2}{\sum f_a} < 1 . \tag{4}$$

This inequality is well verified experimentally, where for thermal-neutron fission ν_1 is the order of tenths and ν_2 is the order of ones. Indeed, the ratio ν_1/ν_2 is anomalously small. The f_a appear to be small in a region where the penetrabilities should indicate at least one open channel. An explanation of the anomaly is afforded by the isolation of the low-lying adiabatic states. A small value for f_a can be attributed not only to a low penetrability, but also (or instead) to the inability of reaching the state.

The question of whether thermal equilibrium is reached at or near the time of scission is of crucial importance to Fong's statistical model of fission. The available theoretical apparatus — in terms of small deviations from the adiabatic model — is probably adequate to answer the question, but no one has yet come forward with the results. However, the implications of the preceding discussion are that the conditions necessary for the validity of the Fong model may not be met for the thermal fissioners, but that at several MeV above threshold the statistical conditions may well be valid.

At this point I would like to defend Fong in one area of attack. Newton has proposed an alternative formulation of the statistical model. Both the Fong and the Newton expressions for the mass yield may be written

$$Y(Z_1A_1Z_2A_2) = \text{const.} \int_0^{E_T} dE_k \int_0^{E_T-E_k} d\epsilon_1 (R_s P_s) \mu^2 E_k W_1(\epsilon_1) W_2(E_T-E_k-\epsilon_1) ,$$

where E_T is the total energy, E_k is the kinetic energy of a fragment, W is the level density, μ is the reduced mass of a fragment, and R_s and P_s are the channel radius and penetrability.

The factors R_s and P_s do not appear in Fong's expression. The distinction between the two cases is that in Fong's expression the quantities are evaluated at scission and in Newton's they are evaluated at infinite separation. In the classical limit where P is a step function of the kinetic energy, the formulae differ only in the factor E_k; but then Fong is clearly correct, for only the scission configuration values are relevant. The basic assumption in the Fong model is clear: thermal equilibrium at scission. The Newton assumption of equal reduced widths is not so clear in that case. Furthermore, Newton's calculations are not free of scission effects — as claimed — because they enter into R_s and P_s in the form of nuclear deformation and polarizability.

Although the statistical model once held promise of being free of arbitrary parameters, its predictions are so sensitive to the input data — especially the form and energy arguments of the level-density formulae — that a "first-principle" calculation loses much of its meaning.

In conclusion, I would like to state two basic theoretical questions which can be studied profitably with some refinement of current techniques: (1) The question of establishing thermodynamic equilibrium between the saddle point and scission. (2) The scission process itself — that final tearing of the nucleus. A detailed calculation of the adiabatic model, while very important, is a far more ambitious enterprise.

* * *

J. J. GRIFFIN, Los Alamos Scientific Laboratory: I wonder if you could repeat, a little more slowly, the point about the limiting situation (the step-function case) where the Newton model is inapplicable but the Fong model would be applicable.

WILETS: In the classical limit, the penetrability becomes a step function of E_k(scission), jumping from zero to unity at the barrier energy. What happens beyond the point of scission can be of no consequence to us whatever! Now Fong's formula contains the fragment KE level density and the velocity factor E_k(scission). Newton has the factor $E_k(\infty) = E_k$(scission) + E(Coulomb). This is the only way the formulae differ. These factors are quite distinct: Fong's factor begins from zero and increases linearly with E_k(scission); Newton's formula also increases linearly with E_k(scission), but because of the large constant Coulomb energy it is relatively insensitive to E_k(scission).

GRIFFIN: Let me just ask about the penetrability. Is this the penetrability for two fragments coming together? What is the penetration factor that Newton uses?

WILETS: It is derived from the Coulomb wave functions and is equal to one minus the reflection coefficient. It is the probability that two fragments coming from infinity will actually penetrate over or through the Coulomb barrier.

N. ROSENZWEIG, Argonne National Laboratory: Someone once told me that a long time ago Kramers considered a Brownian-motion model to describe statistically a certain portion of the dynamical aspect. I have never found a paper that says anything about this. Do you know anything about it?

WILETS: No, I am afraid I don't. But now that I have you "on the phone," let me make a comment concerning a question which we discussed earlier. I think that one might be able to put the question of these various penetrabilities, at least, in a language which is similar to the one you use. You had on the board yesterday the expression for the transition rate which determines the width — an expression $\langle \Psi, V\Phi \rangle$ where, as I recall, Φ was an exit channel, Ψ was a member of the ensemble, and V was a potential operator which, however, is a constant. This is not to be

identified with the off-diagonal matrix elements but is a constant. (Is it not a constant. Is it statistical also?)

ROSENZWEIG: In the example I used for the radiation width, it would obviously be something like a dipole operator for dipole radiation width.

WILETS: Yes, but would it not be essentially of constant strength over all of the various final states Φ?

ROSENZWEIG: It is defined independently of Φ. In the case which I discussed, it is just an operator causing a transition. In the case of fission I don't really know what to write down, and perhaps you will tell us.

WILETS: What I was going to suggest is that in the case of fission it may not be so easy to write it in this form, but one would make an identification with a V which is also a function of the final state and could vary in strength to simulate in some way the fact that these various states have different penetrabilities. That would, I think, lead to expressions quite similar to those that I put on the board.

ROSENZWEIG: I don't want to let this point go by since it is right here in front of us. Maybe when this is done Bohr's idea of why the fission width shows so much fluctuation can then be expressed in terms of the language which I like by showing why the correlation coefficient (which is expressed in terms of scalar products of this kind) is so strongly positive.

WILETS: Fine!

P. MOLDAUER, Argonne National Laboratory: I am afraid I didn't understand that last point. Clearly, if you are talking about two different channels, therefore two different Φ, there is no need for supposing that one will get the same value of the ensemble average $\langle \Psi, V\Phi \rangle$ for both channels. It is precisely these differing averages which yield the different transmission coefficients for different channels, even though we use the same V; and it is these transmission coefficients which

determine ν_1. What determines ν_2 is essentially the fluctuations about the average as one varies the members of the ensemble Ψ.

WILETS: Actually I am sure there are different ways of looking at it, and I was trying to use a language similar to Rosenzweig's. The point is that it is very difficult to write down this expression in this picture — to write down a Ψ, and a Φ, and a V in between. I was saying, let us take the Φ's as being a nondescript set of wave functions which do not have any peculiar characteristics in them, and let us put the blame on some potential operator. What you are saying is that the Φ's are peculiar and one can build peculiar behavior into $\langle \Psi, V\Phi \rangle$ that way; I think it probably doesn't matter which way you build it in as long as it is built in.

P. FONG, Cornell University: I would like to make a point concerning statistical equilibrium. We can estimate the time a nucleus takes from the saddle point to the moment of scission. This turns out to be about 10 times as long as the time required for a nucleon to move across the nucleus, which is comparable to the time to move a mean free path. The relaxation time of a gas is of the order of magnitude of the latter. As long as the time is longer than the relaxation time we have good reason to believe that, in the gas model, statistical equilibrium will be established. On the other hand, in the adiabatic approximation one requires a much longer time for the approximation to be valid. The estimated time does not seem to be long enough to justify the adiabatic treatment.

WILETS: You can't have it both ways. A long time for collective motion implies adiabatic motion. I expressed it here in terms of β rather than in terms of time. You do get very rapid diffusion in energy space; in other words, thermalization rates. But all of the approximations just break down when you have the very special case of the ground state or first few excited states, which are highly correlated with important deviations from the gas model. I think that as soon as one is at an energy above this point, so that one has many states available where the pairing

has broken down, then your estimates are probably right and I should think that this would be a good place for the statistical model to be valid once more.

FONG: In order that the ground state go by an adiabatic approximation, I think it would take a much longer time. This is a point which is determined by perturbation theory and is independent of any nuclear model.

WILETS: I think it depends very much on the nuclear model.

FONG: The nuclear model tells you the intrinsic frequency and the perturbation theory tells you that the time involved must be much longer than the intrinsic period, to apply the adiabatic approximation.

WILETS: But you already said that that was right. Didn't you say that the time from saddle to scission is 10 times longer than the intrinsic period?

FONG: Well, this is not long enough to justify the adiabatic approximation.

WILETS: Gee, 10 times is pretty good!

V-2. STATISTICAL THEORY OF FISSION AND KINETIC ENERGY DISTRIBUTION

Peter Fong

Cornell University, Ithaca, New York

Phys Rev, 122, 1543-4 (June 1, 1961)
C 6-15-61

I have just remarked (see discussions following paper V-1) on the theoretical justification of taking a statistical approach to the fission problem. In addition, I wish to point out the empirical evidence that supports this view. The mass distribution curves of all fissioning nuclides coincide in the heavy-fragment region where the fission fragments have closed shells of 50 protons and 82 neutrons. The prompt-neutron distribution curves of all fissioning nuclides seem to coincide and the relation to closed shells is again evident. These results seem to indicate that the fission process is determined by the fission products instead of by the fissioning nuclides. In other words, the process is determined by the final condition instead of by the initial condition. In any dynamical theory the results are determined by the initial condition; the physical system has no way of knowing its future and does not adjust itself in anticipation of the final condition. On the other hand, in a statistical theory we may regard the fission process as a quasi-static process in which equilibrium is established instantaneously. The relative probability is determined by the statistical weight at the moment equilibrium is last established, i.e., at the moment of scission. The results are thus determined by the final condition. Because of these arguments, one tends to regard the discrepancy between the statistical theory and the experimental results as most likely due to the deficiency of the physical data used in the theory rather than the basic assumption itself. I will illustrate this point by discussing three problems.

The first is the mass distribution. It was found that the statistical theory works well with U^{235} but not with Pu^{239}. The predicted mass distribution curve for Pu^{239} has four peaks instead of two. The

difficulty was traced to the use of an atomic mass formula based on experimental data prior to 1951. Calculations carried out by making use of several later mass formulas show that in every case the curve has two peaks instead of four.

The second is the energy dependence of the mass distribution. When the bombarding energy of the incident particle is increased, we find an increase of the yields of fission products in the valley and in the wings of the double-humped mass distribution curve. This may be explained by the statistical theory but the theory predicts that the valley and the wings will increase by about the same amount. Experimentally the valley increases much faster than the wings and eventually we have symmetric fission. This discrepancy probably may be attributed to a nuclear shell effect on the energy-level density function which was not considered in the previous treatment. It is known that the shell effect is strongest for the ground states, and becomes weaker and weaker for higher excitation states. It is possible that at a sufficiently high energy the shell effect becomes vanishingly small and the nucleus would behave like one without shells, i.e., a liquid drop. In this case one would expect symmetric fission.

The third is the kinetic energy and the prompt neutron distributions. It is now well established that the curve of total kinetic energy vs mass ratio has a large dip in the symmetric-fission region and the curve of number of prompt neutrons vs fragment mass has a saw-tooth structure with an apparent break in the symmetric-fission region. These facts are contrary to the predictions of the statistical theory as worked out in an earlier paper.[1] The difficulty is traced to a nuclear shell effect on the deformability of the nucleus which was not known at the time of the earlier paper but has been made known later by the collective-model studies of nuclear structure. The earlier calculation on deformation

---

[1] Peter Fong, Phys. Rev. 102, 434 (1956).

energy is based on the liquid-drop model which shows no shell effect. Now we can calculate deformation energy without the liquid-drop model by making use of experimental information obtained in Coulomb-excitation analysis which includes the shell effect. On this basis the calculation of kinetic-energy and prompt-neutron distributions is repeated; the results of thermal-neutron fission of U^{235} agree well with the experimental results. This work has been reported at the Washington meeting[2] early this year and will be published in the next issue of Physical Review Letters [Phys. Rev. Letters 11, 375 (15 October 1963)].

Since the Washington meeting, additional calculations have been made in two extreme cases: the deuteron fission of Ra^{226} and the spontaneous fission of Cf^{252}. The kinetic energy distribution is shown in Fig. 1. The agreement is not as close as in U^{235}. This is not

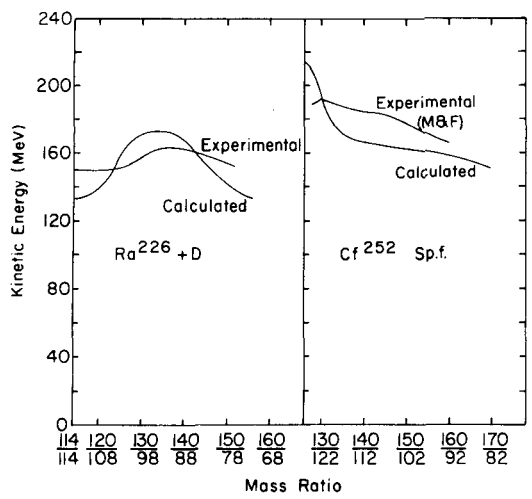

Fig. 1. Calculated kinetic-energy distribution curves for deuteron fission of Ra^{226} and spontaneous fission of Cf^{252} compared with experimental results.

surprising because in these calculations we made use of the same set of extrapolated deformation-energy parameters (the spring constant) as in U^{235}, which is merely an approximation. Nevertheless the results bring out the experimentally established fact that the peak of the kinetic-energy distribution curve moves towards symmetric fission as the mass of the fissioning nucleus increases, and reaches symmetric fission near

[2] Peter Fong, Bull. Am. Phys. Soc. 8, 385 (1963).

Cf^{252}. The deformation-energy curves of the three isotopes are plotted together in Fig. 2. They show the saw-tooth shape and they coincide

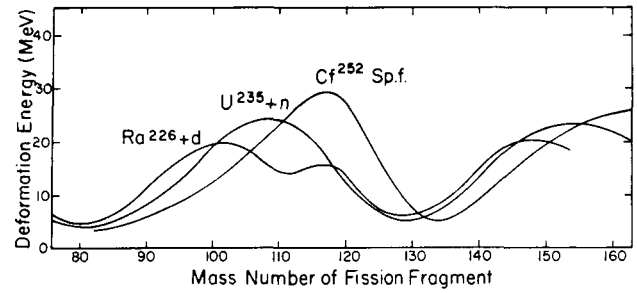

Fig. 2. Deformation energy of fission fragment as a function of fragment mass for U^{235}, Ra^{226}, and Cf^{252}.

fairly closely in the heavy-fragment region though not quite as closely in the light-fragment region. This result may be related to the approximate universality of Terrell's neutron distribution curve.[3] In the symmetric-fission region where the curves do not coincide closely, there is no experimental information for comparison.

On the basis of the new information on nuclear deformability, we have calculated the width of the total-kinetic-energy distribution curve for a pair of fission fragments with a fixed mass ratio. In the earlier work[1] the half-width at half-maximum for the most probable modes of fission of U^{235} is calculated; the value is about 5 MeV, which is smaller than the then known experimental value of 7 MeV. The value from the present calculation is 6.3 MeV, which agrees much better. Later experimental results do not agree among themselves. Stein's width is close to the previously known value of 7 MeV, while Milton and Fraser's is much larger.[4] Regarding the variation of the width with respect to the mass ratio, we plot the calculated width for thermal-neutron fission of U^{235} as a function of the mass ratio in Fig. 3. The width increases from 5.3 MeV in the symmetric-fission region to the maximum of 6.3 MeV in the mass-ratio region of 1.3 to 1.5. It then decreases to 4.1 MeV at mass ratio 2.2.

---

[3] James Terrell, Phys. Rev. 127, 880 (1962).

[4] W. E. Stein, Phys. Rev. 108, 94 (1957); J. C. D. Milton and J. S. Fraser, Can. J. Phys. 40, 1626 (1962).

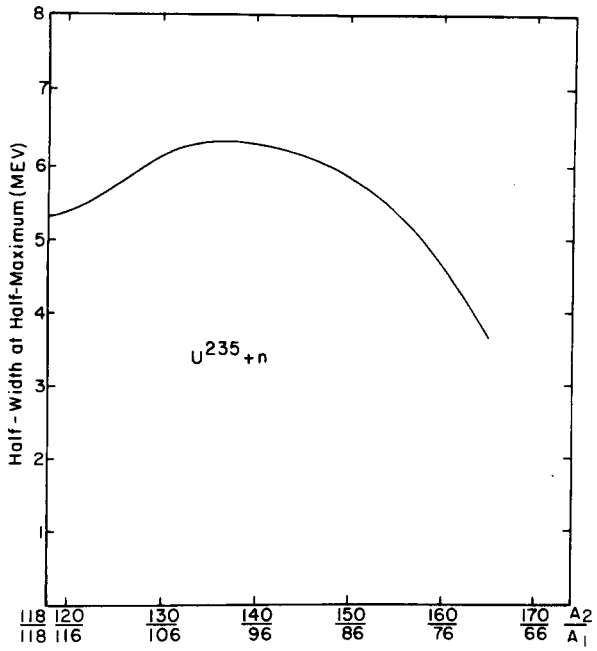

Fig. 3. Half-width at half-maximum of the total-kinetic-energy distribution curve for thermal-neutron fission of U^{235} as a function of the mass ratio of the two fragments.

The predicted variation of the width with respect to the mass ratio is just opposite to the experimental results of Milton and Fraser[4] which show a minimum in the most probable modes. They mentioned that their observed increase in width in the far asymmetric-fission region could be instrumental in origin. Gibson and Thomas[5] have established that their observed increase in width in the symmetric-fission region, at least in the case of U^{233}, is definitely instrumental in origin and the corrected curve actually shows a dip at symmetric fission. Huizenga et al.[6] determined the width as a function of the mass ratio in a number of isotopes (U^{235} not included) for high-energy fission. Their results show that the trend of variation is similar to that of the calculated result, thus contradicting Milton and Fraser.

In conclusion, we remark that the detailed application of the statistical theory requires physical information on nuclear masses, on nuclear level density, and on nuclear deformability; and that nuclear shell structure affects all three. The relation of the shell effect on nuclear masses to the fission process has been recognized and investigated in the earlier paper.[1] The shell effects on the level-density function and

[5] W. M. Gibson and T. D. Thomas (private communication).

[6] J. A. Huizenga (private communication).

on nuclear deformability have not been completely investigated; their application to the fission problem has just begun. Qualitatively many of the mysterious facts in fission may be explained by the three kinds of shell effects. On the other hand, a conclusive study by the statistical theory still awaits a detailed investigation of all aspects of the shell effect and much remains to be done.

* * *

N. ROSENZWEIG, Argonne National Laboratory: Some years ago I studied the question as to how rapidly the shell-structure effects on the level density decrease with increasing excitation energy. Although the model I used was not very realistic, one impressive fact emerged. The effects decline rather slowly, essentially because of the appearance of a correction Δ in the exponential

$$\text{density} \propto e^{a\sqrt{E - \Delta}} .$$

Of course, if it is untrue in nature that the shell-model levels themselves move about as the energy is increased, then the main assumption on which my insight is based collapses.

I would also like to ask a question. I think Dr. Wilets said that the fission yield depends very strongly on the level-density law. If this is so, why not turn things around and use fission to give information about the level density?

FONG: I have not come to this point yet. My effort so far has been to try to convince people that the statistical theory is correct in fission.

With regard to the statement preceding Dr. Rosenzweig's question, I would guess that without any shell effect the nuclear level scheme would change slowly from one nuclide to its neighboring ones. When the shell

effect is introduced, I would suspect that the low-lying levels are pushed down to a larger extent than the higher excited levels and the lowering of the level becomes smaller and smaller as the energy increases; when the energy is sufficiently high the change becomes very small and the shell effect is washed out. This is my guess. If we take this, then we can explain the change of the fission yields with respect to incoming energy.

ROSENZWEIG: I think we merely disagree about the energy at which the level density becomes independent of the shell effect. I seem to think that this energy is higher than you think.

FONG: If you look at the data concerning the energy dependence of fission yields, one suspects that the energy at which the shell effect is washed out is something like 40 MeV, so the energy is certainly high.

ROSENZWEIG: This does not sound so different from what one gets on the basis of the simple model which I studied in 1957. Naturally, the result depends on atomic weight. For the same energy, shell effects disappear more quickly for heavy nuclei.

P. MOLDAUER, Argonne National Laboratory: I would like to make a comment on the question of how the appropriateness of different theoretical concepts depends on excitation energy. At low energies in neutron fission, we know (from the fact that the resonances are well isolated) that the period of collective motion up to the saddle point is long compared with the period of motion of the internal degrees of freedom of the nucleus and therefore that the adiabatic description of the fission process is valid at least up to the saddle point. Whether it is also valid to the scission point will depend on whether the time required in going from the saddle point to the scission point is also long. From experience with other reaction processes, I would say that the factor of ten mentioned by Dr. Fong is plenty to make the adiabatic description valid. However, as the energy increases, one must expect this factor of ten to decrease; and as it does, the statistical aspect of the description will become more

important. Eventually, when resonances overlap, even the period of motion to the saddle point becomes smaller than the internal period and the collective description becomes problematical even up to the saddle point. Therefore, at these higher energies a statistical description is probably more appropriate. It might also be worthwhile to mention that in this limit of overlapping resonances the transmission coefficients for the important fission channels can be expected to approach unity. Hence, for energies above the saddle point the number of channels can be appropriately described by Wilet's ν_1 as determined by the fission cross section.

V-3. EXPERIMENTS ON FISSION USING THERMAL NEUTRONS*

H. Maier-Leibnitz

Technischen Hochschule, Munich

The usefulness of reactor neutrons in studies of the fission process may be seen in two fields. First, the excitation energy of the compound nucleus can be varied in very small steps if neutrons in the resonance region are used. This may also be achieved using moderated neutrons from a linear accelerator. Second, a reactor is quite unique in producing a maximum of fission processes in a sample. Thus, in the few cases where fission can be effected by slow neutrons, a very detailed investigation of the fission process can be made. In the present paper, we shall disregard the work using resonance neutrons and shall instead try to discuss what are the possibilities and limits in gaining complete experimental data on the fission process in the few examples that correspond to the capture of thermal neutrons. It will be seen that, apart from certain side fields, currently available methods will allow one to obtain all data that can possibly be measured so that we may expect that the experimental knowledge may be complete in a few years.

After scission, there will be two nuclei with atomic weights A_p and $(236 - A_p)$, atomic numbers Z and (92 - Z) (in the case of U^{235} fission), total kinetic energy T, and excitation energies E_1 and E_2. The probability distribution $W_p(A_p, Z, T, E_1, E_2)$ contains the full knowledge of the primary fission process with the following exceptions. First, additional particles may be emitted, especially alpha particles and probably a small fraction of primary neutrons.[1] These particles are emitted while there is still an interaction between the two fission products, and thus will

---

*Invited paper.

[1] H. W. Schmitt, J. H. Neiler, F. J. Walter, and A. Chetham-Strode, Phys. Rev. Letters 9, 427 (1962).

furnish interesting information on the latest stage of scission. Second, if the fissioning nuclei are aligned, the fission products may be emitted anisotropically with respect to the original symmetry axis in the uranium nuclei.[2] There is also a possibility that W_p will be angle dependent. Third, after fission, there may be some polarization of the fission products with respect to their direction of flight. This might show up in an anisotropy, in the moving system, of neutron and gamma emission.[3] In what follows, we shall not treat any of these effects.

Among the variables in W_p, only Z can be measured and that is very difficult to do. All the others are unmeasurable because of the prompt neutrons. After their emission, there is a probability distribution

$$W_s(A_1, A_2, Z, T_1, T_2, \vec{p}_1, \cdots, \vec{p}_n, E_{\gamma 1}, E_{\gamma 2}) ,$$

where $\vec{p}_i$ is the momentum of the ith neutron, and $E_{\gamma 1}$ and $E_{\gamma 2}$ are the excitation energies after neutron emission. Of the variables in W_s, not many can be measured simultaneously in a single fission. Therefore, there will always be an inherent uncertainty in the determination of the variables in W_p from measurements on W_s and the task of the experimenter is fulfilled if the experimental errors are smaller than these basic uncertainties.

Mass and Energy Distribution

The greatest number of measurements has so far been made on the distribution of mass and energy.[4,5] The time-of-flight method has

---

[2] L. D. Roberts, F. J. Walter, J. W. T. Dabbs, G. W. Parker, and J. O. Thomson, Proc. Seventh International Conference on Low Temperature Physics, edited by G. M. Graham and A. C. H. Hallet (University of Toronto Press, Toronto, 1961), p. 174.

[3] S. S. Kapoor and R. Ramanna (abstract V-6 of this conference).

[4] J. S. Fraser, J. C. D. Milton, H. R. Bowman, and S. G. Thomson (private communication).

[5] F. J. Walter, H. W. Schmitt, and J. H. Neiler (paper V-5 of this conference).

reached an accuracy of 0.5% and may be still further improved (e.g., by introducing quadrupole lenses to make long flight paths feasible). The old double ionization chamber has been abandoned in favor of solid-state detectors which measure the energy of the fission products to ± 1.5 MeV. It will probably be difficult to improve much over the latter figure because most of the uncertainty seems to be due to fluctuations in the energy that goes into collisions with atoms instead of into ionization while the fission products are being slowed down.

Impressive results have been obtained both by time of flight and by energy measurements, combining these with the known data on the average number and energy of the prompt neutrons. However, there is still an uncertainty of about 2 amu and an equivalent amount in energies; so individual fluctuations are not very clearly seen, and the theoretical limit of our knowledge has not been reached. The curves of Fig. 1 show an example of this work. The total kinetic energy of the fragments is lower for symmetric fission than for asymmetric fission, and recently some fine structure has been seen in these curves.

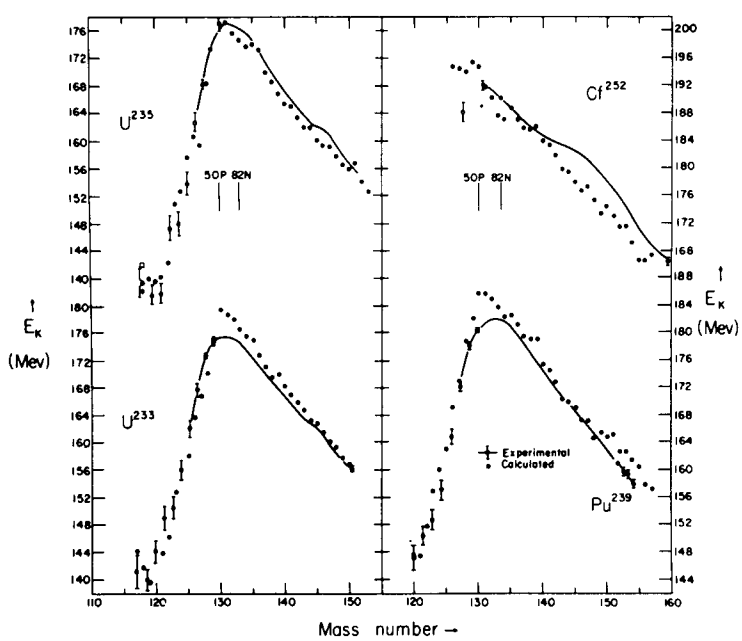

Fig. 1. The average total kinetic energy as a function of the mass of the heavy fragment. In the mass region 130 — 150, the experimental curve is determined by over 20 points, each with a statistical error of less than 0.25 MeV.

An optimum measurement would include accurate determination of A_1 and A_2 and of the velocities or kinetic energies of both products. Then the numbers of neutrons (n_1 and n_2) would be known and they could be attributed to A_1 and A_2 so as to make the momenta on both sides approximately equal. From many such measurements, a distribution $W(A_1, A_2, T, n_1, n_2)$ will be obtained, subject to some uncertainty associated with the lack of knowledge of the neutron momenta. From this, one will obtain a distribution $W_p(A, T)$ and a neutron distribution $W(A, T, n_1, n_2)$ which is a rather good indication for the excitation energies E_1 and E_2.

One method of achieving our aim is to measure the velocity of both fission products by time of flight, and their energy with solid-state detectors. This experiment seems quite feasible and could even be done with the fission rates available in accelerator experiments. Since the determination of A_1 and A_2 is not unambiguous, the distribution $W(A_1, A_2, T, n_1, n_2)$ will take more unfolding than was explained above and the final distribution will be less accurate. An experiment of this type is in progress at Oak Ridge.

Recently, it has become possible to apply stronger methods. Ewald[6] has constructed an outsize Mattauch-Herzog type mass spectrometer that separates masses by e/m and has both space and velocity focusing, but with the velocity resolved to 1 — 2%. Figure 2 shows this instrument which allows the determination of $W(A_i, T_i)$ with exactly separated masses. The intensity is still somewhat low. We are agreed that it would be better to use a double-focusing parabola-type mass spectrometer, with electric and magnetic deflections at right angles to one another. In such an instrument a parabola is obtained for each e/m, and every point on the parabola corresponds to a velocity. The detection efficiency at a given A and T would be about 10^{-6}. Such an instrument can be combined (using a through-tube in the reactor) with a time-of-flight method to obtain the

---

[6] H. Ewald, E. Konecny, and H. Opower, Advances in Mass Spectrometry (Pergamon Press, London, 1963), Vol. 2, p. 189.

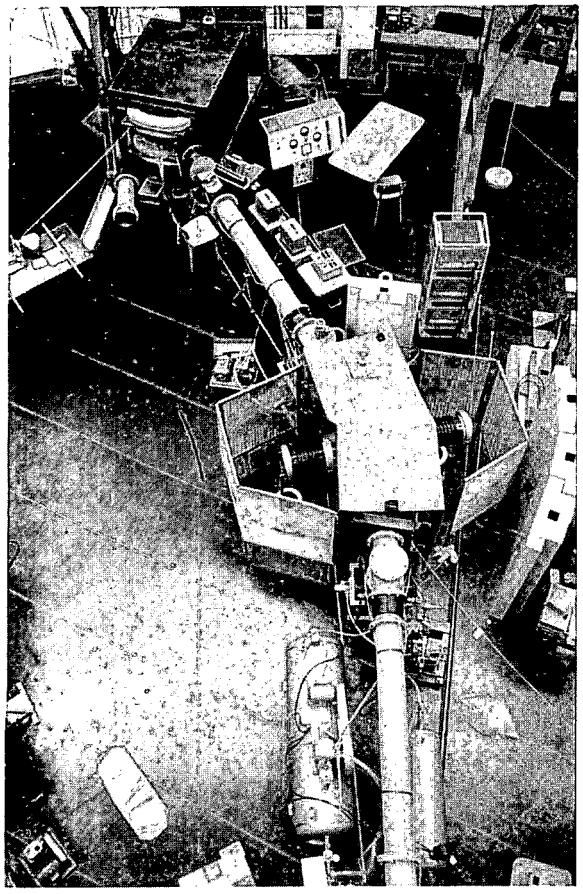

Fig. 2. Large Mattauch-Herzog type mass spectrometer constructed by H. Ewald.

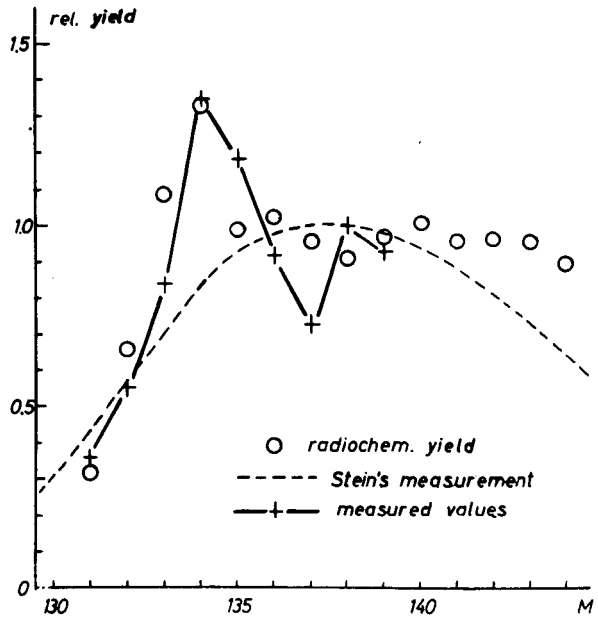

Fig. 3. Mass yield of U^{235} fission products for mass value of 131 — 138.

velocity, and a solid-state detector to measure the energy of the second particle. It would even be feasible to use two parabola spectrometers in coincidence. In this case, however, it would be necessary to have several detection systems on each side or the experiment would take a very long time.

One of the first achievements with this instrument is given in Fig. 3 which shows the mass yield, at one velocity, in the neighborhood of A = 134. The dip adjacent to the well-known peak in the yield curve suggests that the peak is caused by a variation in the emission of neutrons after primary fission.

Mass-Charge-Energy Distribution

Until last year all information on the charge distribution for various masses (primary yields) came from radiochemical data[7]

[7] For a recent example, see A. C. Wahl, R. L. Ferguson, D. R. Nethaway, D. E. Troutner, and K. Wolfsberg, Phys. Rev. 126, 1112 (1962).

which were not very satisfactory because low half-lives are so difficult to investigate using radiochemical methods. The knowledge of the average atomic number $\overline{Z}(A)$ and also of the Z dependence of $W_p(A, Z, T)$ is of fundamental importance to the understanding of the fission process. Recently a number of new methods have been applied or have become available.

(a) Coarse mass separation of the fast fission products in a helium-filled region in a magnetic field, as was first done by B. Cohen at Oak Ridge. Armbruster and Meister[8] have done this using the arrangement shown in Fig. 4. The method depends upon the fact that the equilibrium charge on a fission fragment is proportional to the velocity so that a mass separation is achieved, even from a thick target. The fission products are collected on a foil and the number and energies of the β rays are measured over a long time. Thus, the average number of decays and the average beta-decay energy per fission product are

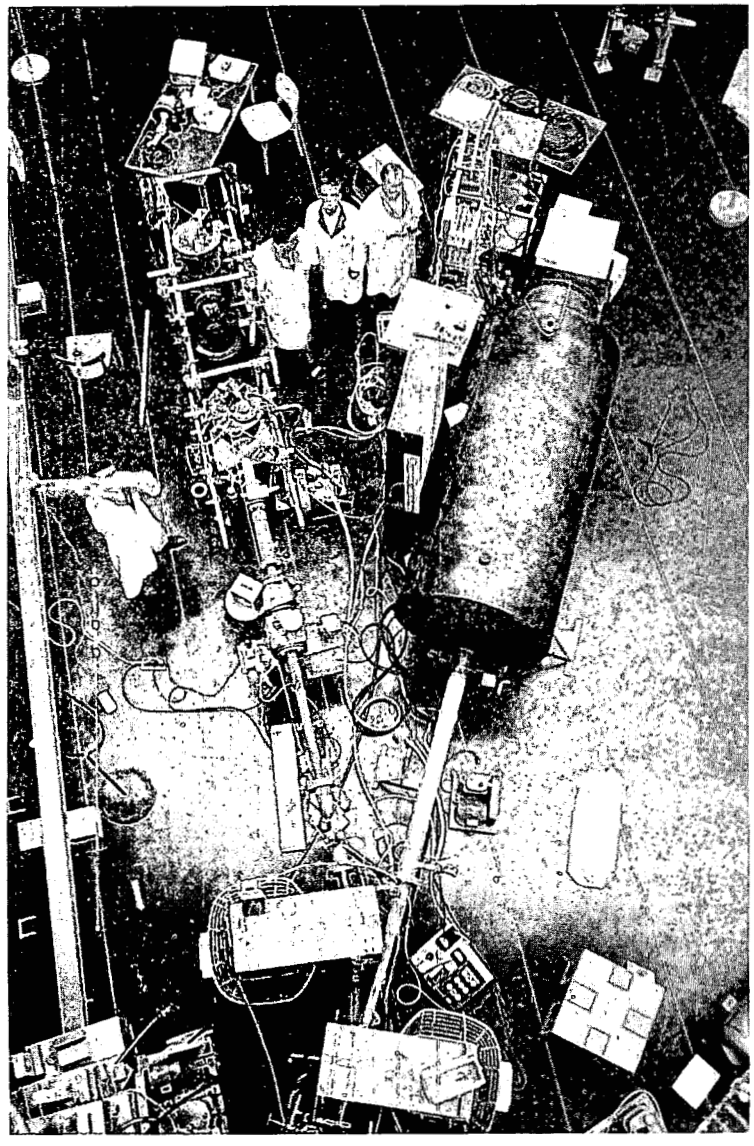

Fig. 4. Arrangement used by Armbruster and Meister to separate fast fission products in a helium-filled region in a magnetic field.

[8] P. Armbruster and H. Meister, Z. Physik 170, 279 (1962).

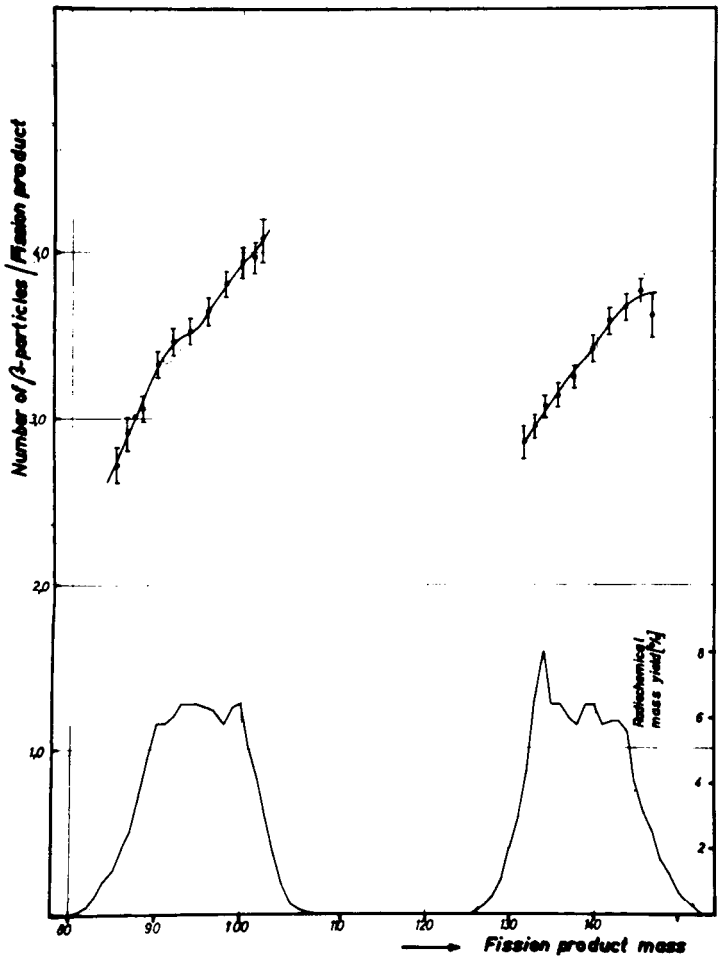

Fig. 5. Upper curves: Mass dependence of the number of β particles per fission product. These curves are the result of four different sets of data. Lower curves: Mass distribution from radiochemical data.

obtained for various values of A not too far from the yield maximum. Figure 5 gives the results that were obtained in this way. One sees that the heavier atoms, both in the light and in the heavy fraction of the fission products, emit more beta rays than the lighter atoms. This is strong evidence for the validity of the Whetstone model, because the neck connecting the heavy and the light fragment prior to scission would contain a high neutron excess as a result of Coulomb repulsion; and any fragment receiving a large part of the neck would tend to emit a large number of betas, in agreement with these results.

(b) Using the same arrangement for separation, efforts can be made to investigate low-half-life decays with beta-gamma coincidence techniques and thus increase our knowledge of the decay chains and independent yields. We may note here that more Q-value measurements are desirable in order to obtain mass values for fission isotopes. These are important for the fission energy balance.

(c) Again using Cohen's arrangement, the production of the L x rays of fission products passing through matter has been observed.[9] From the average L-x-ray energies, $\bar{Z}$ is found as a function of A.

(d) During the rearrangement of the electronic shells which takes place after fission, K x rays are emitted in about 10% of the fission events. These have been detected[10] with a proportional counter in coincidence with a double ionization chamber observing the fission products. The resolution so far obtained was 11% for the x rays, but an improvement of nearly a factor of two would seem possible. In this case, the x rays from consecutive atomic numbers among the light fission fragments would be nearly separated, and W(Z, A) could be observed. Solid-state detectors would be used, of course, in the future for the fission products. The method has one drawback. Coincident K x rays are also formed by the internal conversion of prompt gamma rays. This may enhance the yield irregularly for a number of nuclides.

(e) By converting Ewald's spectrometer to a parabola spectrometer and using it with a reactor of flux somewhat higher than 10^{13} neutrons $cm^{-2} sec^{-1}$, enough fission products accurately separated by mass could be collected to perform a complete analysis of their beta decays and obtain independent yields and Q values. Each such measurement would be done at one energy, and then finally W(A, Z, T) would be obtained.

(f) An attempt, that may or may not succeed, to obtain the same result with less neutron intensity consists in collecting the fission products in a sandwich of two nuclear emulsions (which is opened for a very short time in the beam of the spectrometer) and then counting the number of beta particles connected with each fission track.

(g) With modern mass spectrometers, the resolution may be as good as 10^{-5}. Thus, using Ewald's instrument, it should be possible

---

[9] H. Specht, A. Vollmer, and P. Armbruster (paper V-9 of this conference).

[10] H. Hohmann, Z. Physik 172, 143 (1963).

in principle to obtain a fine structure in the lines for each A, with a peak for each Z. The intensity, however, would be very low if such accuracy is wanted and it would be difficult to keep voltages and magnetic fields sufficiently constant. Considering the good chance that we see now to observe the same data by other methods, the high-resolution mass spectrograph may not be necessary.

(h) With most of the methods mentioned so far, the investigation of the low-yield fission products will still be a problem. Therefore, we want to emphasize the importance of radiochemical work. There may be still more possibilities for the fast separation of fission products. For instance, short irradiations using a pulsed reactor may make it possible in many instances to analyze the growth and decay of isotopes to obtain independent yields of precursors.

Excitation of the Primary and Secondary Fission Products

The greatest part of the excitation energy of the primary fission products will appear in neutron emission, and the number of neutrons emitted will be a good indicator of this energy. In the foregoing we have indicated a method that should allow one to determine this number and its fluctuations as a function of A and T, approximately separated for the heavy and light fragment. There also exist measurements of the average number of neutrons as a function of A, indicating that the number of neutrons increases with mass, both in the light and in the heavy fraction.[11,12] This is shown in Fig. 6 and we note that this result seems to agree with the beta-decay data of Fig. 5. In near-symmetrical fission,

---

[11] J. Terrell, Phys. Rev. 127, 880 (1962).

[12] For a recent measurement on Cf^{252}, see H. R. Bowman, J. C. D. Milton, S. G. Thompson, and W. J. Swiatecki, Phys. Rev. 129, 2133 (1963).

the total number of neutrons is definitely higher than in asymmetric fission. This can be seen from the experimental points of Fig. 7.[13]

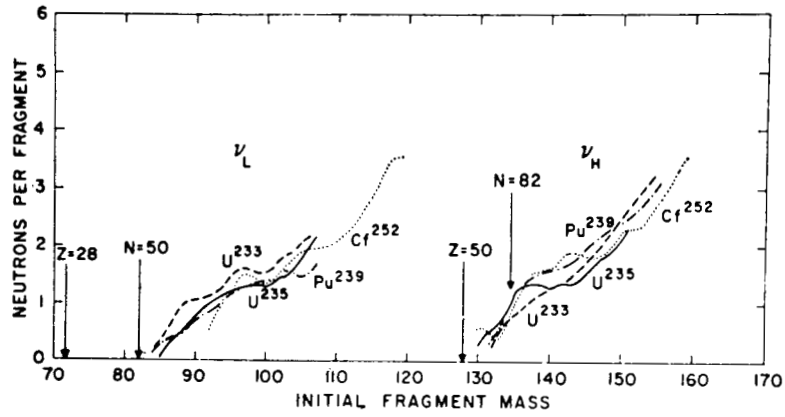

Fig. 6. Summary of neutron yields derived from cumulative mass yields, as functions of initial fragment mass. The approximate initial fragment masses corresponding to various magic numbers are shown (based on constant charge-to-mass ratio for initial fragments).

The energy distribution of the gamma radiation (Fig. 8) has been measured[14] as a function of the mass ratio A_1/A_2 using a double-ionization-chamber technique. Recent results from Trombay show the asymmetry with respect to the direction of the light (or heavy) fragments. This could be used along with solid-state detectors

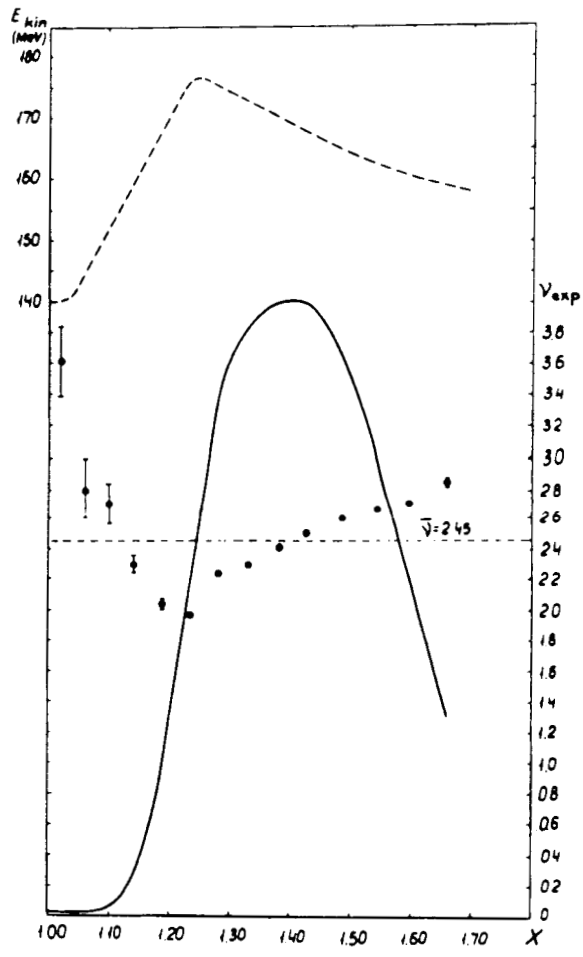

Fig. 7. Measurement of the number of fission neutrons against the fragment mass ratio. The dots are experimental points. The solid line denotes the experimental distribution of the fragment mass ratio and the dashed line denotes the total kinetic energy of the fragments.

[13] V. F. Apalin, Yu N. Gritsyuk, I. E. Kutikov, F. I. Lebedev, and L. A. Mikaetyan, Nucl. Phys. 41, 92 (1963).

[14] F. Rau, Ann. Physik 10, 252 (1963).

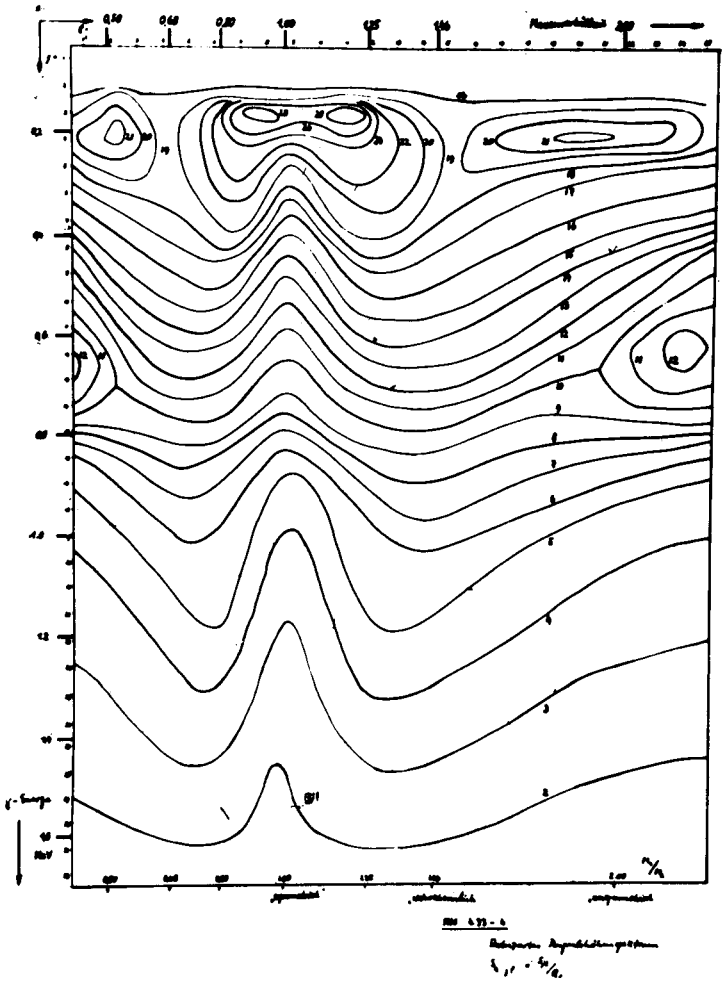

Fig. 8. Energy distribution of the gamma radiation, plotted as a function of the mass ratio A_1/A_2. These data were measured by a double-ionization-chamber technique.

for the fission products to measure the average gamma excitation energies $E_{\gamma 1}$ and $E_{\gamma 2}$ of the light and heavy fragments as a function of A and T.

From such data, along with the use of the energy balance for each A, Z, T to determine the total excitation energy, a fair knowledge will be available of the excitation energy of the two primary fission products.

* * *

A. I. YAVIN, University of Illinois: When two fission fragments are observed in coincidence and their energies are added, how many events are found in which the sum of the energies is less than 50— 60 MeV?

MAIER-LEIBNITZ: I am afraid that I cannot answer that question. You should ask Mr. Armbruster.

A. I. YAVIN: The reason I am asking the question is that is has to do with a fascinating process. There is 200 MeV of kinetic energy

involved in a fission event, which is a strong-interaction event. Since the mass of a pion is only 140 MeV, the question is raised whether pions can be emitted in fission. I do not know what the model for the creation of a pion might be, although I can think of several very unlikely ways. The trouble is that the kinetic energy comes from the Coulomb energy and is contributed by the separation of the fragments; and once separated, it is hard to expect that the short-range nuclear force would still be effective. Nevertheless, I feel that the possibility, though remote, is fascinating enough to merit an experimental check. As I implied before, it might be possible to observe a pion by looking for an increase in the low-energy side of the kinetic energy distribution below 60 MeV.

MAIER-LEIBNITZ: The trouble, of course, is that we are all working on the line that just before fission there is very, very little excitation energy left at all. That is where we get the magic-number effects. It would be quite complicated.

J. S. FRASER, Chalk River Nuclear Laboratory: There was once an experiment done to look for pions or shower-producing radiation from a reactor, but with negative results.

D. R. INGLIS, Argonne National Laboratory: It would seem that this question might remind us of the difficulty of concentrating fission energy into one small event and in an extreme case — much more extreme than those we have considered in other connections. For example, earlier in the conference there was a discussion of the possibility that if neutrons come out, maybe we could have four of them emerging at once if the tetraneutron were stable. Here, too, is a question of concentrating energy in one event, rather than having it diffused in several events in the general statistics of what is going on in the fission process.

I would like to relate this and a few of the other things that we have been hearing at this conference. The beautiful experiment Prof. Maier-Leibnitz has just told us about (giving the number of betas as a function of fragment mass distributed over the light group of nuclear

fragments, rising to heavier fragments, and again over the heavy group of fragments) is an indication of the validity of the picture that Professor Wilets drew on the board — a small fragment and a large fragment with a neck between. The experiment seems to show that the neck contains more than its share of neutrons.

This is related to Professor Fong's picture in the previous talk in which we saw the number of neutrons as a function of fragment number, a similar plot, compared with the expectation from the statistical model. This plot showed none of this tendency, but rather a symmetrical peak across each fragment group. This is an illustration of how the experimentalist can show us that the statistical model does not give the whole story.

To get back to the tetraneutrons, it seems from the graphs that Professor Maier-Leibnitz showed that there might be an excess of one or two neutrons in the neck. It is not a pure neutron neck by any means, but has a value of N/Z somewhat larger than is found in normal nuclear matter, closer to 2/1 than to 1/1. This is not large enough to make it tempting to think that if a droplet of it should snap out, it would be apt to be a tetraneutron. It makes it more apt to be a triton than an alpha particle; but an alpha is observed in more cases, presumably because of its much greater binding energy.

One other thing. On the graph showing the number of neutrons as a function of symmetry of fission, for symmetric fission the number went up, if I read the ordinate correctly, to 3.6 neutrons per fission. If the idea of the neck snapping off is valid, it would be tempting to think that these are all from the fragment that receives the neck, thereby identifying this as a rare extreme case of the heavy end of the light-fragment distribution. This fragment might thereby receive all of the excess neutrons and most of the energy of deformation — either to boil off the neutrons or perhaps, in this snapping process before thermalization, to snap out not 3.6 but in the exceptional case 4 neutrons, <u>if</u> the tetraneutron should exist.

MAIER-LEIBNITZ: Well, I think we have now gotten accustomed to considering all the processes around the symmetric fission as a different process. You have much excitation energy left over, and that leads to more neutron emission. Now, whether that is realistic, that is a pragmatic approach. There are several arguments for it. We think that the symmetric fission is something else than the things we discussed today.

V-4. INSTRUMENTATION FOR FISSION-FRAGMENT ENERGY CORRELATION EXPERIMENTS WITH PILE-UP REDUCTION CAPABILITIES*

C. W. Williams, H. W. Schmitt, F. J. Walter, and J. H. Neiler†

Oak Ridge National Laboratory, Oak Ridge, Tennessee

Experiments have been performed at the Oak Ridge National Laboratory in which the kinetic energies of correlated fragment pairs from thermal- and resonance-neutron-induced fission have been measured. In addition, a three-parameter ternary-fission experiment has been performed in which the energies of correlated fragments were measured in coincidence with the energy of a third particle, usually a long-range alpha particle. The detectors used were large-area silicon surface-barrier detectors.

The multiparameter data-acquisition system associated with these experiments, shown in Fig. 1, includes an inspection system

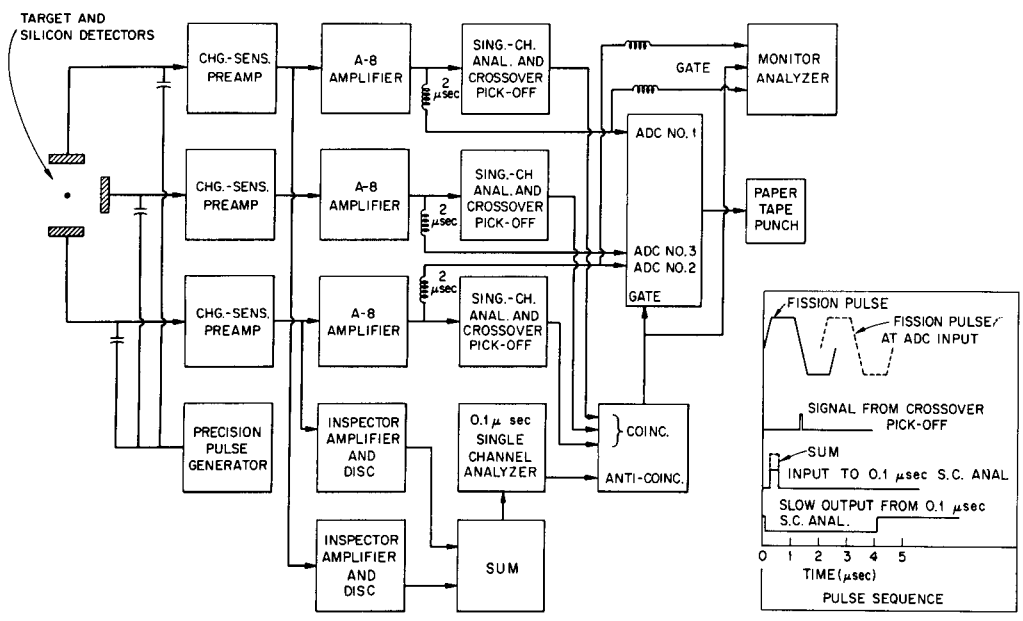

Fig. 1. Block diagram for fission-energy correlation measurements.

---

*Presented by C. W. Williams.

†Now with Oak Ridge Technical Enterprises Corporation.

for reducing spectrum distortion caused by pile-up (multiple pulses arriving within the amplifier resolving time). Inspection is performed now on only two parameters but may be expanded to three parameters.

The straightforward approach of detecting pile-up pulses by examining the pulses for shape change cannot be used in this application because of the inaccuracies in the present timing methods. The method employed here consists of clipping the preamplifier pulses with a 20-nsec clipping line, then triggering a fast discriminator with these pulses. A 4-μsec inhibit pulse is generated for each "single" event. Proper delay of the linear signals makes it possible to reject coincident events, distorted by the "single" event, within ± 2 μsec of the "single" event. This logic is well suited to multiple-detector systems, and an alternative method, for use with a single semiconductor or scintillation detector, is shown in the block diagram of Fig. 2. This system utilizes

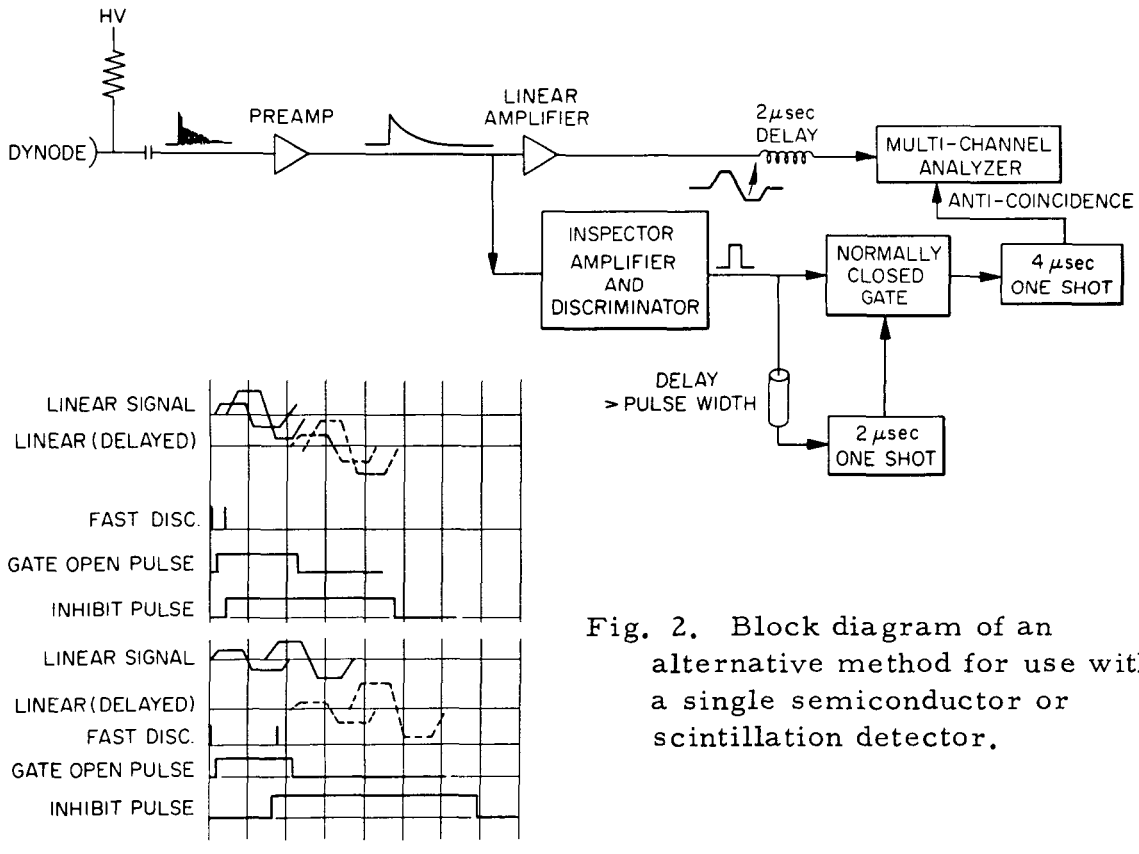

Fig. 2. Block diagram of an alternative method for use with a single semiconductor or scintillation detector.

a normally closed gate and two one-shot multivibrators to obtain the inhibit requirement necessary to remove the distorted events.

The method used in testing for pile-up in this system utilizes a pulser and a monoenergetic alpha-particle source and provides rapid accumulation of easily interpreted data. Results of these tests show that the inspection system reduces the effective resolving time of each amplifier from 3.3 ± 0.1 μsec to 0.55 ± 0.03 μsec.

V-5. CORRELATED FRAGMENT-ENERGY MEASUREMENTS FOR LOW-ENERGY NEUTRON-INDUCED FISSION*

F. J. Walter, H. W. Schmitt, and J. H. Neiler†

Oak Ridge National Laboratory, Oak Ridge, Tennessee

I would like to begin by giving a very brief description of the experimental equipment for the benefit of those who are not familiar with this type of experiment. For the sake of brevity, I shall not make any attempt to describe the rather lengthy and involved computer operations which are required to transform the raw data into mass distributions, mass-energy correlations, etc. I will also confine my discussion of the results to what can be learned from the mass distributions. This is done primarily because of time limitations, although there is the additional reason that there still remain some minor questions about the energy calibrations of the detectors; these should be settled before we attempt to draw conclusions which depend on precise energy calibrations.

Figure 1 shows the source, detector, and vacuum-chamber arrangement used for most of these experiments. Since many of the details shown here are convenience features rather than essential elements in the system, we will not take time to discuss them. The target is a very thin layer of a fissionable isotope deposited on a 50-$\mu g/cm^2$ nickel foil or on a 20-$\mu g/cm^2$ carbon foil by vacuum evaporation. The two 4-cm^2 surface-barrier detectors are located on opposite sides of the source and outside of the high-intensity neutron beam. In the case of a 3-particle fission experiment, the third detector is located in the region above the target.

---

*Presented by F. J. Walter.

†Now at Oak Ridge Technical Enterprises Corporation.

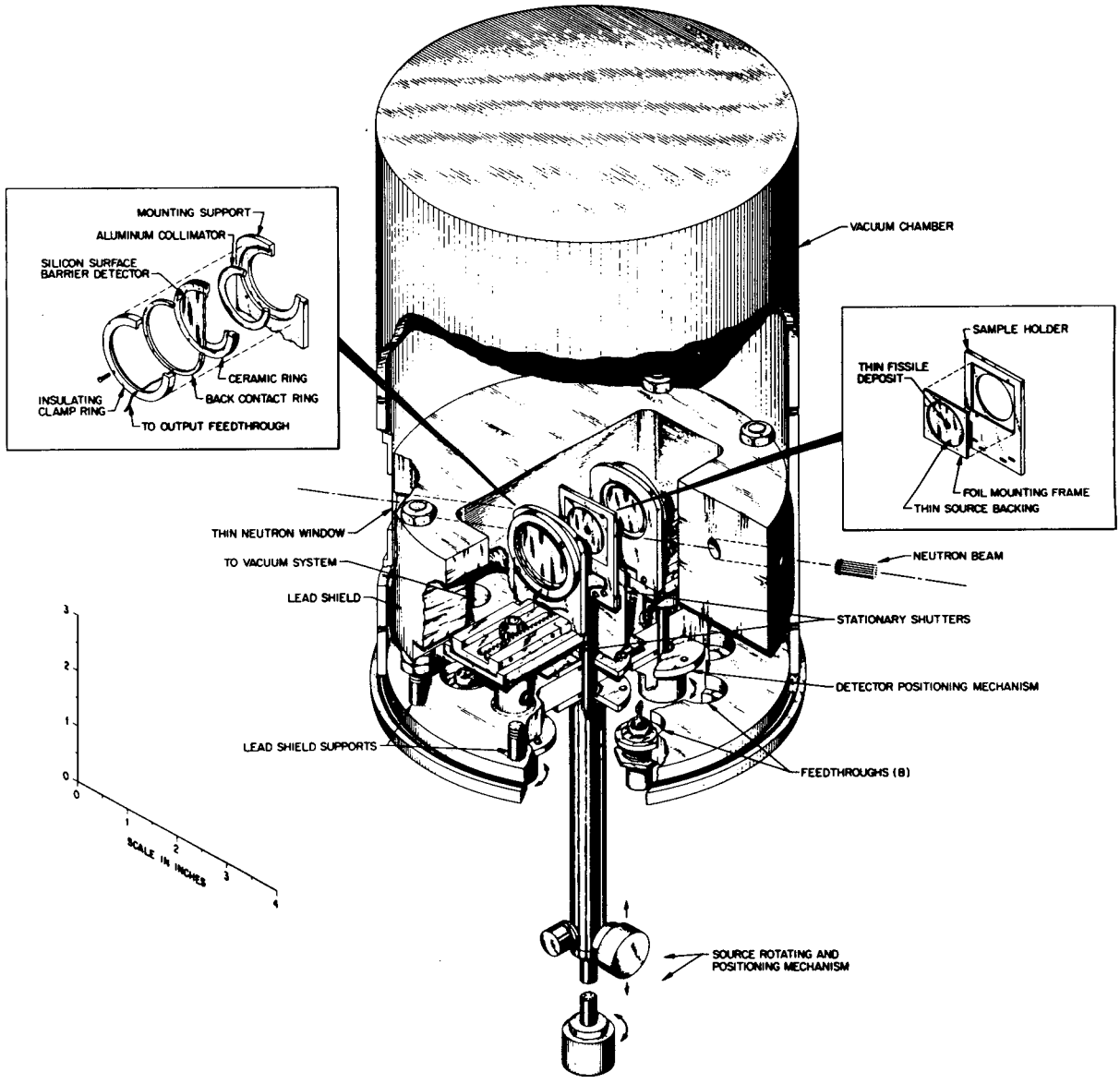

Fig. 1. Source-detector chamber for fission-fragment energy-correlation measurements.

The information obtained from these experiments is in the form of two or three correlated pulse heights recorded (event by event) on punched paper tape. This information, when properly sorted, produces an array of the type shown in Fig. 2. This is an array for thermal-neutron-induced fission of U^{235}. In this figure, the pulse heights have been converted to fragment energies, and lines of constant mass and constant total kinetic energy have been added. We feel that much of what can be learned from these experiments is dependent on our ability to obtain

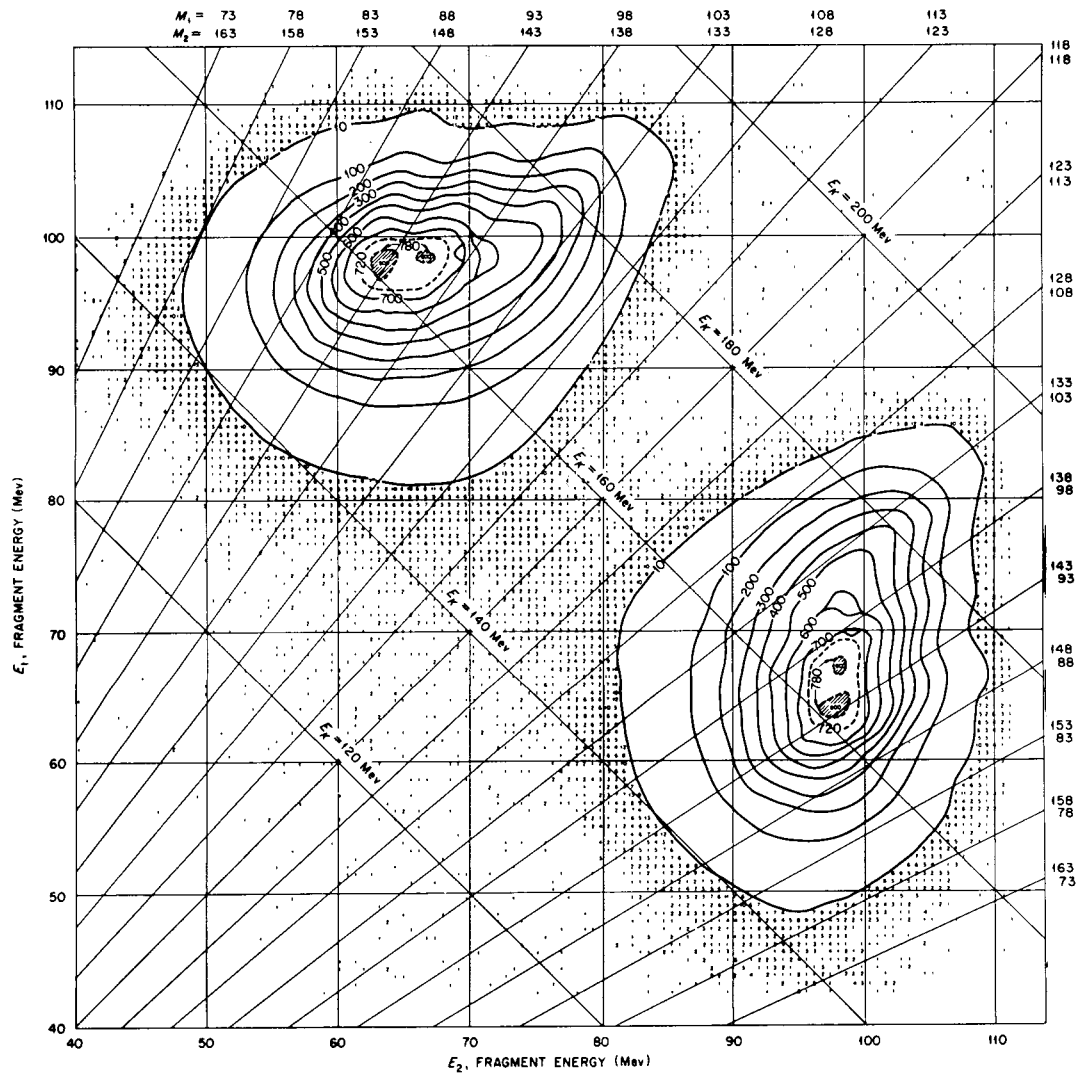

Fig. 2. Contour diagram representing the correlation of fragment energies in the thermal-neutron-induced fission of U^{235}.

high resolution in measurements of very good statistical accuracy. Consequently, on observing one of these arrays, one can begin to appreciate our concern about such things as small amounts of pile-up or accidental coincidences. Since there are more than 2 decades between the highest contours and the lower ones, even a small amount of tailing (from poor collimation), or the occurrence of extraneous pulses where they don't belong, can significantly change the peak-to-valley ratio in the mass distribution. In addition, it does not take very much loss in energy resolution to change the appearance of the fine structure. These problems are particularly acute in an experiment such as that in which we measured relatively small changes in the peak-to-valley ratio for an alpha-active plutonium isotope as a function of incident-neutron energy.[1]

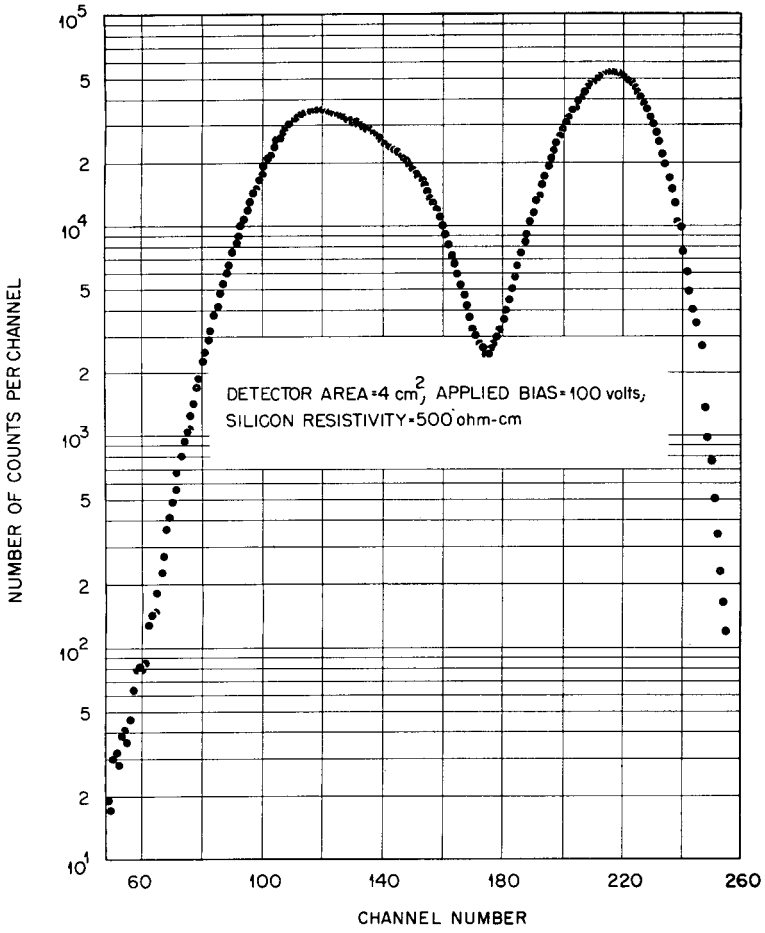

Fig. 3. Pulse-height spectrum for fission fragments from thermal-neutron-induced fission of U^{235}.

Figure 3 shows a typical single-side energy spectrum for

[1] F. J. Walter, J. H. Neiler, and H. W. Schmitt, Bull. Am. Phys. Soc. 8, 369 (1963).

U^{235}. This is, of course, obtained by summing the data in Fig. 2 along lines of constant E_1 or E_2, and the mass distribution is obtained by appropriate transformation and summing of the data. The spectrum is clean and sharp 3 decades down from the peak. The peak-to-valley ratio of 22/1 shown here is, incidentally, a very sensitive indicator of energy resolution.

Figure 4 is a comparison of our mass distribution for Pu^{239} to the radiochemical and mass spectrometric results. Since the latter results are essentially post-neutron-emission mass distributions, we expect them to be shifted to lower mass values, as is indeed observed. The saw-tooth shape of the neutron-emission curve is clearly evident in this comparison, i.e., the neutron-emission probability is large in the 105—115-amu and 140—160-amu regions and small in the 85—100-amu and 125—135-amu regions. The other fissionable isotopes show essentially this same result.

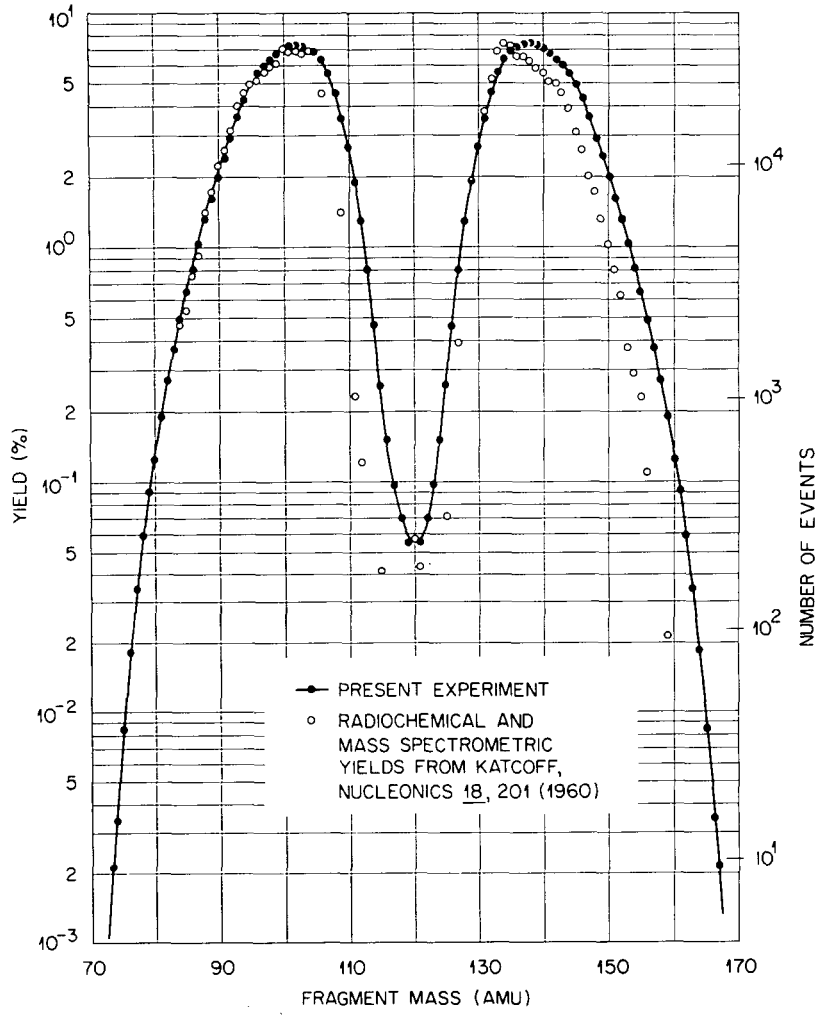

Fig. 4. Fission-fragment mass yield for Pu^{239} thermal-neutron-induced fission.

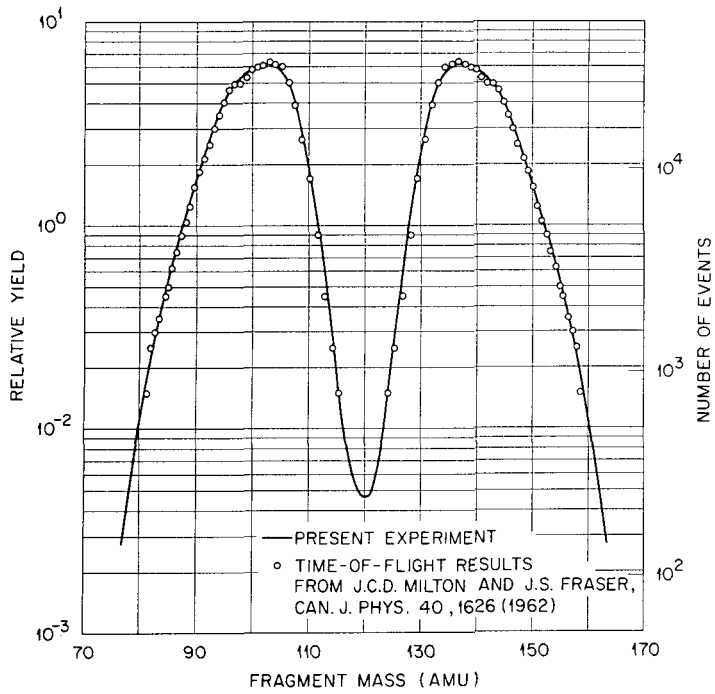

Fig. 5. Comparison of time-of-flight and correlated energy measurements of the fragment mass yield for Pu^{239} thermal-neutron-induced fission.

Figure 5 is a comparison of the same Pu^{239} data with the time-of-flight data of Milton and Fraser.[2] In general, agreement is good.

Figure 6 shows a comparison of the Pu^{239} results with those for Pu^{241}. It is of interest to observe that the two-neutron increase in the compound system appears predominantly in the light fragment for near-symmetric fission but appears to be shared between the light and heavy fragments for more asymmetric fission. This result is consistent with the cluster model of fission[3] in which the stability of closed-shell structures fundamentally influences the fragment mass and energy distributions at low excitation energies. For these cases, one expects that the low-mass edges of the heavy-fragment peaks should occur in the region of Z = 50 and/or N = 82, where masses are in the range 128— 135 amu. This effect is illustrated somewhat more effectively in Fig. 7 in which

[2] J. C. D. Milton and J. S. Fraser, Can. J. Phys. 40, 1626 (1962).

[3] K. Wildermuth and H. Faissner, Proceedings of the International Conference on Nuclear Structure, edited by D. A. Bromley and E. W. Vogt (University of Toronto Press, Toronto, 1960), p. 972; Phys. Letters 2, 212 (1962).

we have compared the mass distributions of Pu^{239}, Pu^{241}, and U^{235} binary fission and U^{235} three-particle fission.

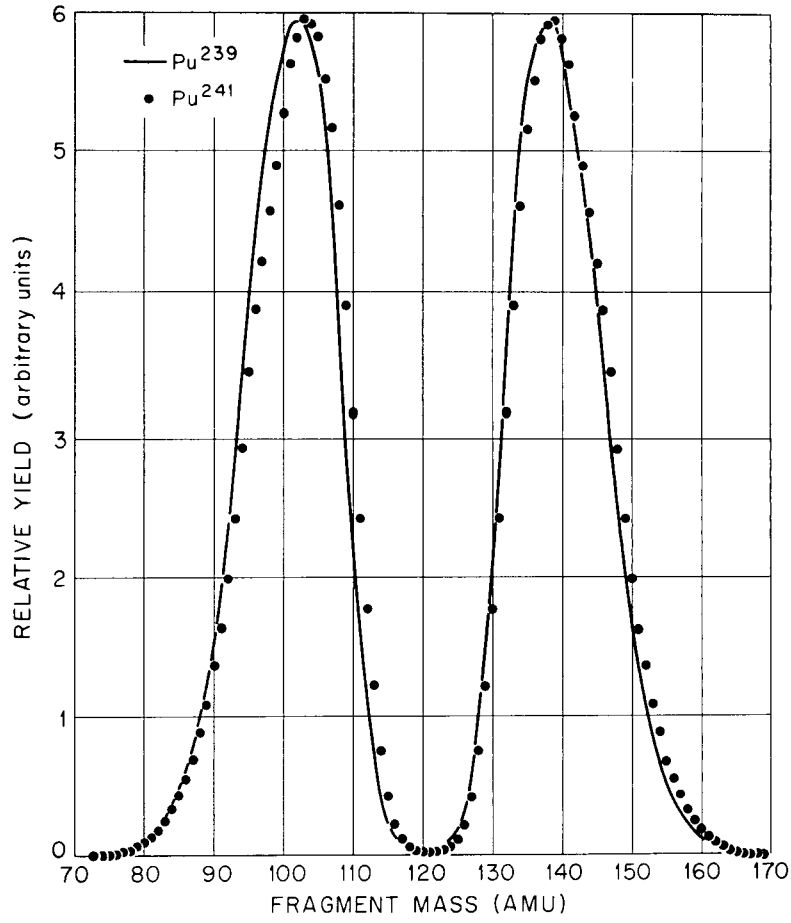

Fig. 6. Comparison of fission-fragment mass distributions for thermal-neutron-induced fission of Pu^{239} and Pu^{241}.

Fig. 7. Comparison of fission-fragment mass distributions.

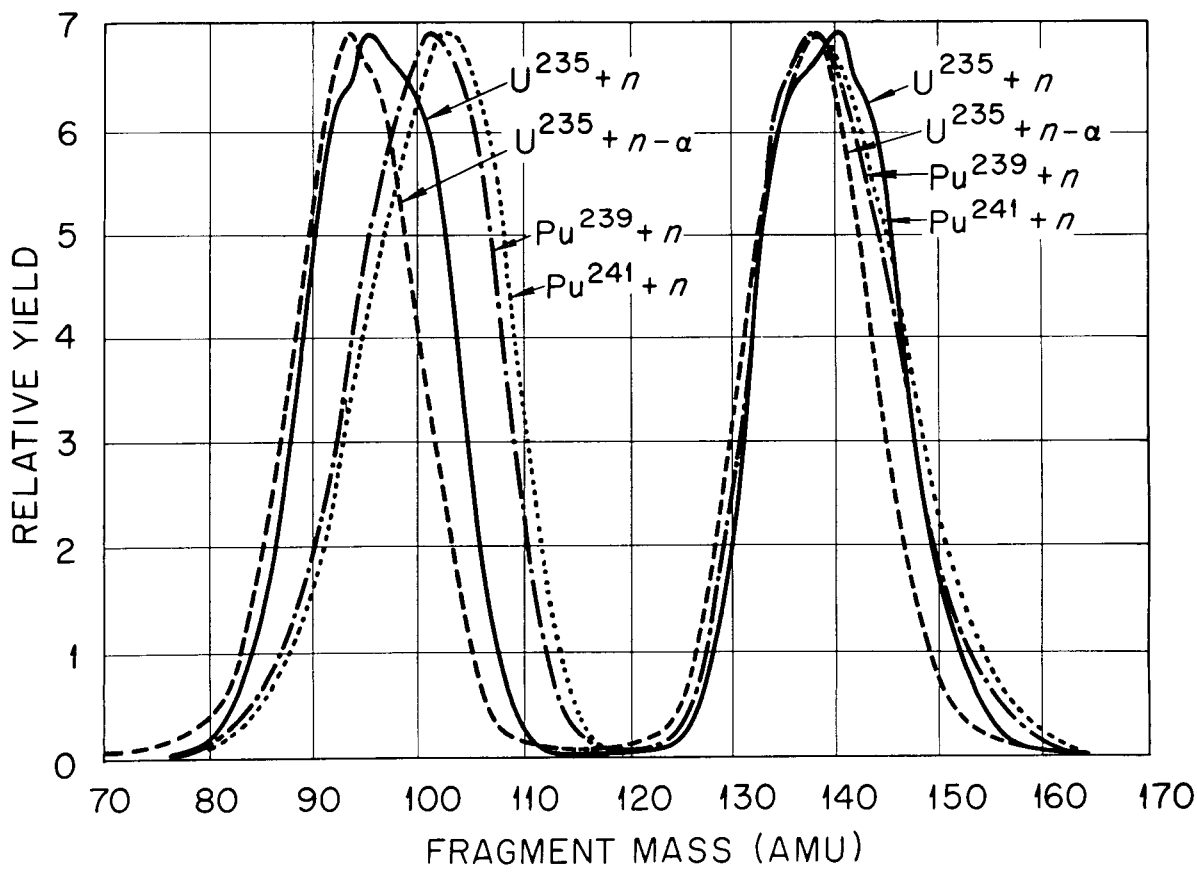

* * *

L. B. BORST, State University of New York at Buffalo: In Fig. 2 you seemed to have some double-valued contour lines. What does that mean? How can you have two contours of the same value?

WALTER: We believe these are real. If one tries to obtain a physical picture of the topology involved here, you can visualize the main peak as a mountain with a rather smooth top, but with two rather abrupt protrusions corresponding to the two shaded areas. The double-valued contour lines part way down the side can be thought of as a fairly level "putting green" sliced out of the side of the mountain. We have done auxiliary experiments in which we looked very carefully, and with very good statistics, at the regions containing the peaks and we have been able to reproduce the fine structure shown in Fig. 2.

N. J. PATTENDEN, AERE, Harwell: In your abstract you mentioned that you have done some work with filtered neutrons that applied particularly to the 0.3 eV resonance of Pu^{239}.

WALTER: That experiment was reported in some detail at the Washington APS meeting.[1] We measured the mass distributions for thermal-neutron-induced fission of Pu^{239} and for fission resulting primarily from the 0.3-eV resonance. We did see a definite difference in the relative peak-to-valley ratios, which agreed with the previous radiochemical measurements of Regier *et al.*,[4] within the accuracy of the experiments.

---

[4] R. B. Regier, W. H. Burgess, R. L. Tromp, and B. H. Sorensen, Phys. Rev. 119, 2017 (1960).

V-6. EMISSION OF PROMPT GAMMA RAYS IN THE THERMAL-NEUTRON FISSION OF U^{235} †

S. S. Kapoor and R. Ramanna

Atomic Energy Establishment, Trombay, Bombay, India

The angular distributions of prompt fission gamma rays with respect to the direction of selected fission fragments in the thermal neutron fission of U^{235} have been studied for two different gamma energy groups using a gridded ionization chamber-scintillation detector assembly and time-of-flight method for eliminating fission neutron background. From the measured angular distributions with respect to the direction of the selected light fragments, the values of the laboratory anisotropy $\{N(0^{\circ}) - N(90^{\circ})\}/N(0^{\circ})$ for gamma rays of energies greater than 180 keV and 510 keV are found to be 14.9% and 12.2%, respectively. The measured ratio of the intensities of the gamma rays nearly along the direction of motion of the light and the heavy fragments suggests that the heavy fragments emit more gamma rays than the light fragments. These measurements definitely show the existence of a significant anisotropy of emission of the gamma rays in the emitting fragment system after making allowance for the motion of the fragments. The anisotropy of emission is explained as arising due to the polarized angular momenta of the fission fragments, which also lead to an enhancement of the gamma-ray emission. The emission of the gamma rays in fission is discussed with respect to the observed number and the spectrum of the gamma rays.

---

† Read by title only.

V-7. DIRECT AND ABSOLUTE MEASUREMENT OF AVERAGE YIELD OF NEUTRONS FROM THERMAL FISSION OF U^{235} †‡

A. DeVolpi and K. Porges

Argonne National Laboratory, Argonne, Illinois

CONF-346-7
C - 2-11-64

The yield of neutrons from thermal fission of U^{235} is a quantity of interest both to basic fission studies and also to reactor physics. At the present time the best value is derived indirectly from η, the number of fission neutrons per neutron captured, and relative fission-to-capture cross sections, as well as by comparison with Cf^{252} measurements recently reported. Because of various possibilities for systematic error in these experiments, a precise direct determination of $\bar{\nu}$ has been under way for some time. Great importance has been attached to having results independent of detector efficiencies, neutron leakage, fission energy spectra, cross-section values, background subtractions, counting statistics, and other adjustments. Otherwise, the experiment is being performed in such a manner as to have small dependence on factors which cannot be directly removed from influencing data. In consequence, the over-all experiment is composed of several important stages, each of which is required to exhibit precision in the order of $\frac{1}{2}$%. Moreover, constant review, improvement, and repetition of technique are required, resulting in a lengthy experiment aimed at attaining 1% accuracy in $\bar{\nu}$.

The measurement may be considered to consist in two independent phases: (1) absolute determination of neutron intensity and (2) evaluation of fission rate. A simultaneous measurement of neutron and fission rate is adjusted according to absolute calibrations determined in the two separate phases.

---

†Work performed under the auspices of the U.S. Atomic Energy Commission.

‡Presented by A. DeVolpi.

The source of fission neutrons is a well-moderated beam emerging from the Argonne CP-5 thermal column. As indicated in Fig. 1, the beam is directed into the beam channel through the shielding tank and into the fission chamber located at the center of the manganese

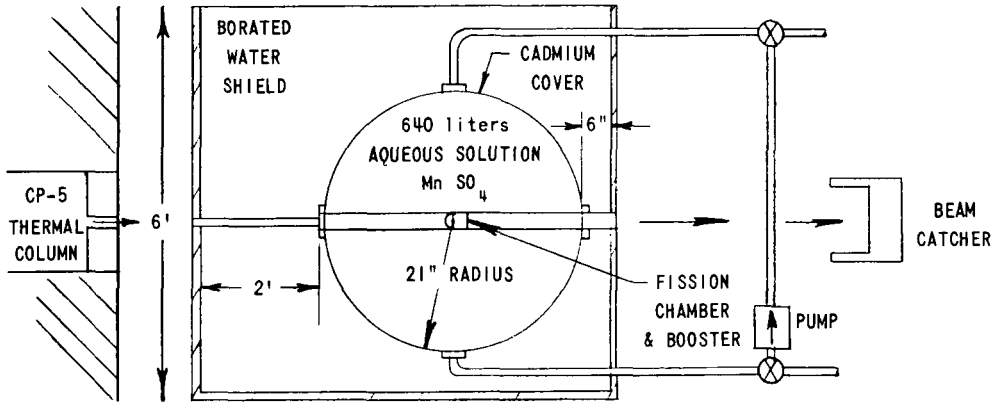

Fig. 1. Diagram of experimental arrangement for epoxy-coated aluminum slowing-down sphere.

bath sphere. Transmitted thermal neutrons in the beam pass through the remainder of the collimator and are stopped in an external beam catcher. The beam tube is lined with cadmium to keep scattered thermal neutrons out of the slowing-down sphere. Fission neutrons from the U^{235} coating of the fission chamber undergo scattering and absorption in both the hydrogen and manganese of the aqueous solution of manganous sulfate.

The thermal neutron beam is monitored by four fission counters located near the beam hole. The fission counter located at the center of the sphere has a sufficiently thin coating to permit long-term operation on a flat plateau. Adequate source rate is obtained by adding a "booster foil" consisting of additional enriched uranium placed in the shadow region of the chamber coating. Fission fragments from the booster are not counted in the ionization counter, but fission neutrons do augment the activation.

After mixing the solution by closed-loop circulation with a pump, samples are withdrawn for counting of the 2.6-hr Mn^{56} activity. To permit accurate counting of weakly activated solutions of $Mn^{56}SO_4$, a

two-stage counting facility has been developed.[1] Two-liter aqueous solutions are counted directly in a gamma-gamma coincidence arrangement which features relatively high efficiency and long-term stability. An electronic delay, mixing, splitting, and repeating technique is used to allow full utilization of radiation detected in both NaI(Tl) crystals while only two single-channel analyzers are required. This system is calibrated on an absolute scale through another unit which counts small aliquots of a strongly activated sample mixed with liquid scintillator in a 4π beta-gamma coincidence mode. Otherwise incompatible requirements of convenience, stability, efficiency, and accuracy are satisfied by using this two-stage process of direct counting backed up by calibration.

The largest correction that must be made is for thermal absorption of neutrons in water in direct competition with manganese capture. For a typical 200-g/liter solution of manganous sulphate, only about 30% of the fission neutrons yield Mn^{56}, the remainder being lost chiefly in hydrogen. A computed correction for this loss requires precise knowledge of the thermal and epithermal cross sections for manganese and hydrogen, as well as a satisfactory theory of slowing down in a hydrogenous medium. This problem is circumvented through an independent experimental evaluation of the relative manganese/hydrogen capture in the medium used with the actual sources. The slowing-down sphere used is of sufficient diameter to reduce leakage from fission sources down to less than 1%. Thus, counting the activity induced by a fixed source in the manganous sulfate at different concentrations determines the energy- and space-weighted manganese/hydrogen cross-section ratio. Small corrections are required for the sulphur/manganese cross-section ratio, for leakage, for (n, α) and (n, p) reactions, for the beam-tube cadmium liner, and for other factors. Special attention is given to the problem of preventing the Szilard-Chalmers reaction from causing precipitation of Mn^*O_2.

---

[1] A. DeVolpi and K. G. Porges, Argonne National Laboratory Report 6760 (to be published).

An independent calibration of the fission counter is carried out as follows. The U^{235} was fabricated into a hemispherical cap and placed back-to-back with the U^{235}-coated electrode of a fission chamber of hemispherical shape. A well-collimated beam from a reactor covers both. Fission neutrons are counted with a "Hornyak button" in coincidence with fission events in the chamber. The hemispherical shape of the latter averages out the angular correlations between neutrons and detectable fission fragments; delayed neutrons are eliminated by pulse-height selection in the single neutron channel. Rise times of the order of 10 ns throughout the counting system allow relaible fast coincidences at an acceptable true/accidental ratio when the fission-channel counting rate is of the order of 10^4 sec^{-1}. Counting losses are avoided through use of fast electronics throughout, including 100-Mc/sec scaling. The two singles, the prompt, and the delayed coincidence counts provide enough information to compute the ratio of absolute fission rate to fission-channel counting rate.

A pulse-shape recognition scheme has been developed which can eliminate a very large fraction of the gamma pulses in "Hornyak buttons" without integration. This scheme may be used either to abstract fast pulses, for possible coincidence counting of fast neutrons, or to precede an integration stage, thus extending the degree of gamma discrimination by several orders of magnitude. Circuits and results of a number of tests have been reported elsewhere.[2]

At the present time improvements are being made on the counting and calibration equipment so that higher long-term stability may be derived. Improved electronic techniques have been adapted to allow

---

[2] A. DeVolpi and K. G. Porges, "Rejection of Gamma Background Radiation Pulses in Hornyak Buttons," IRE Transactions on Nuclear Science NS-9 (3), 320-326 (1962).

more reliable counting systems; in particular, a single current amplifier following the direct output of the fission chamber into 50-ohm cable can be used, since it provides 3-nsec over-all rise time and has feedback stabilization. Recent developments in counting-system regulation with the aid of external pulse generators may be applied. A transistorized version of the Hornyak-button background-suppression circuit is now available. Finally, considerable experience has been accumulated in operation of the Mn^{56} counting facility, indicating improved accuracy and reproducibility. After some experiments with Cf^{252}, a return to the U^{235} determination at the thermal column will be scheduled.

V-8. NEW METHOD FOR THE DETECTION OF SHORT-LIVED FISSION PRODUCTS*

D. Hovestadt and P. Armbruster

Laboratorium für Technische Physik der Technischen Hochschule München, Munich, Germany

Using mass spectrometric separation devices, it is possible to investigate the short-lived fission products without radiochemical separation methods. The separation time amounts to about 1 μsec. Half-lives, Q values, and the genetics of the decay chains can be investigated.

A helium-filled magnetic mass separator[1,2] has been used to separate the fission products of U^{235}. The number of fission products in a maximum-yield chain amounts to 10^4 min^{-1}; the resolution of the instrument is ± 4 atomic mass units. Fission products are stopped in a stopping foil which is transported in times of about 0.1 sec into a β-γ coincidence counting setup. The stopping foil is a discontinuously moving film which is irradiated by fission products for a certain variable time. Simultaneously, the foregoing irradiation is counted in the β-γ coincidence setup. The γ spectrum coincident with β particles is registered by a TMC multichannel analyzer. Known γ lines of isotopes with a half-life of about 10 min have been used to calibrate the magnet-current scale in amu and to determine the mass resolution of the instrument. Figure 1 gives a schematic view of the experimental arrangement. Figure 2 gives the mass yield distribution of the mass separator and the calibration curve. The mass of an isotope can be determined to an accuracy of about ± 0.5 amu.

---

*Presented by H. Maier-Leibnitz.

[1] C. Fulmer and B. L. Cohen, Nucl. Phys. 6, 547 (1958).

[2] P. Armbruster, Nukleonic 3, 188 (1961).

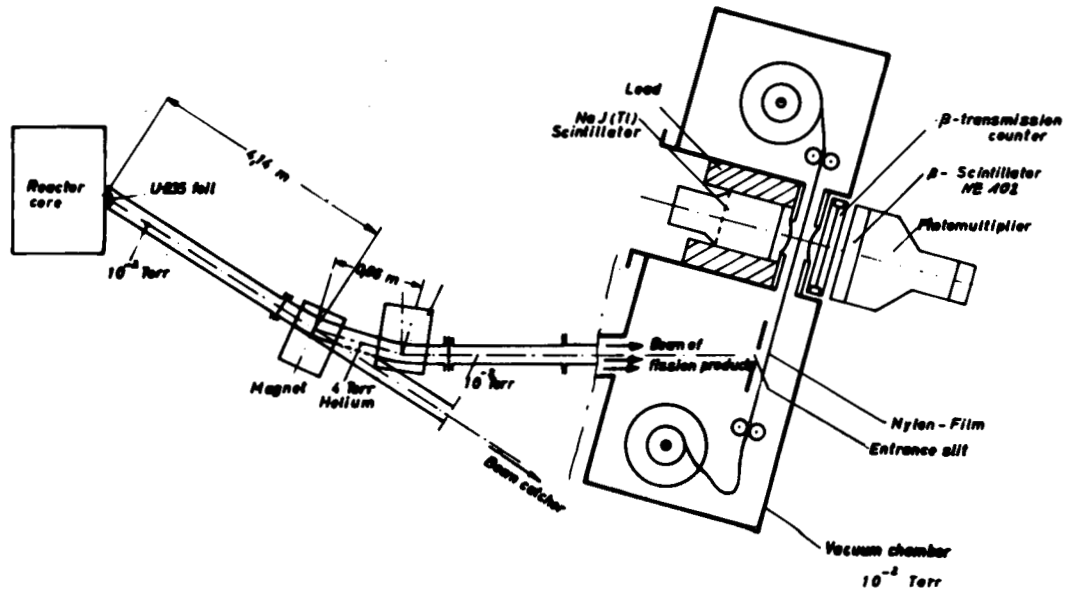

Fig. 1. Experimental setup for the measurement of β-γ coincidences of short-lived fission products.

A 4-channel time analysis and 64-channel γ-spectrum analysis has been used to give a rough determination of the mass of the emitting isotope, of the energy of the γ lines, and the half-life (Fig. 3). The strongest unknown γ line, a 1.42-MeV γ line which has been found in the light group of fission fragments, has been used to demonstrate the new technique. All other γ lines which have been found have not been identified until now.

Figure 4 gives the mass determination of the 1.42-MeV line. The mass has been determined to be $A = 94 \pm 0.05$. Exactly at the same position in the mass scale the 0.92-MeV gamma line of Y^{94}, with a half-life of about 20 min, has been found. A two-dimensional 16-channel time and 64-channel γ-spectrum analysis (Fig. 5) has been used for the half-life determination. The measured half-life of 72 ± 7 sec is in good agreement with the known half-life[3] of Sr^{94}, namely 78 sec. Thus the 1.42-MeV gamma line could be definitely identified as coming from the $Sr^{94} \rightarrow Y^{94}$ decay.

[3] J. D. Knight and D. C. Hoffmann, J. Inorg. Nucl. Chem. 10, 18 (1959).

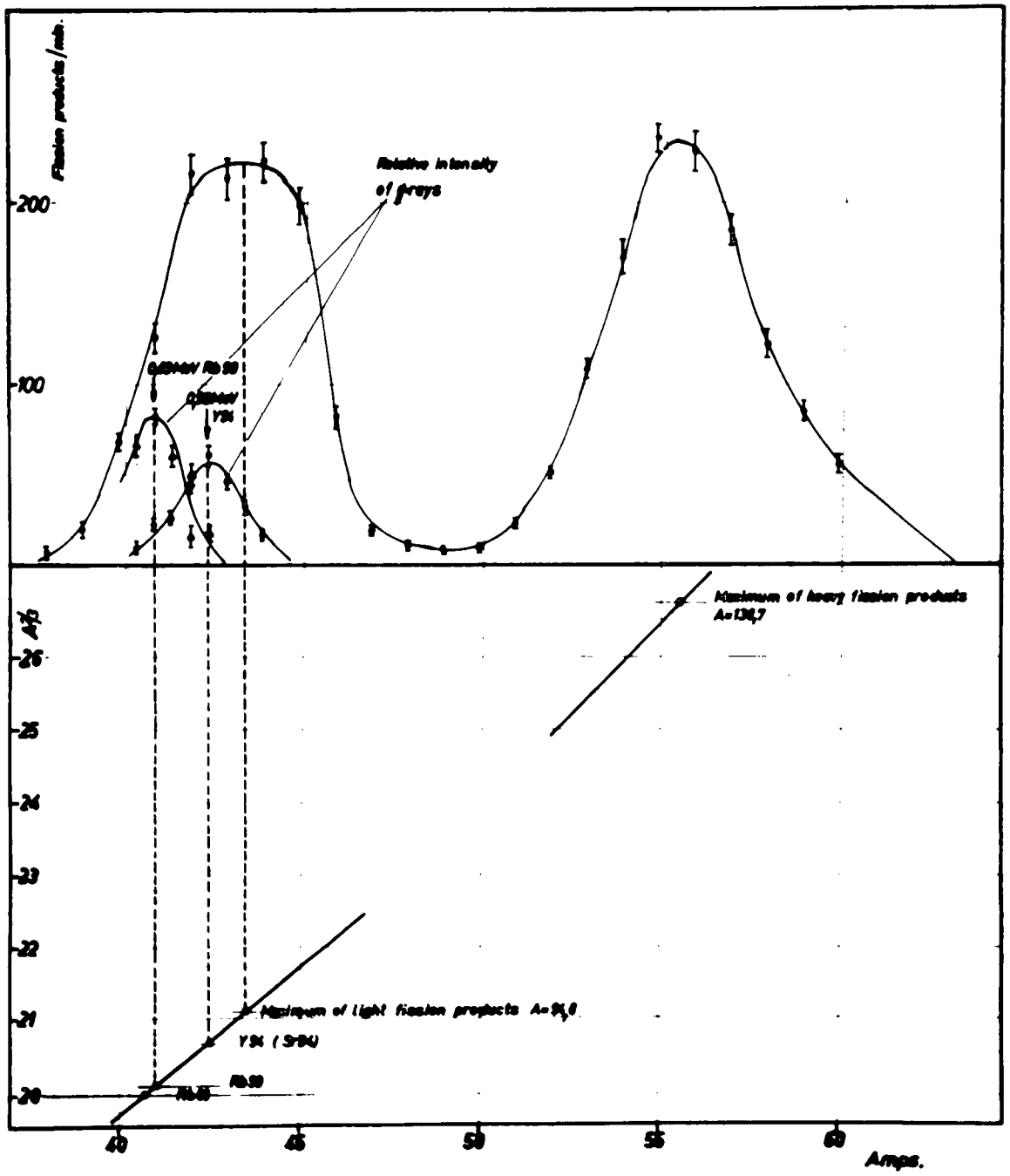

Fig. 2. Calibration of mass separator by known γ lines (Rb^{88}, Rb^{90}, and Y^{94}). The straight line in the lower portion shows the theoretical $I \propto A^{2/3}$ dependence.

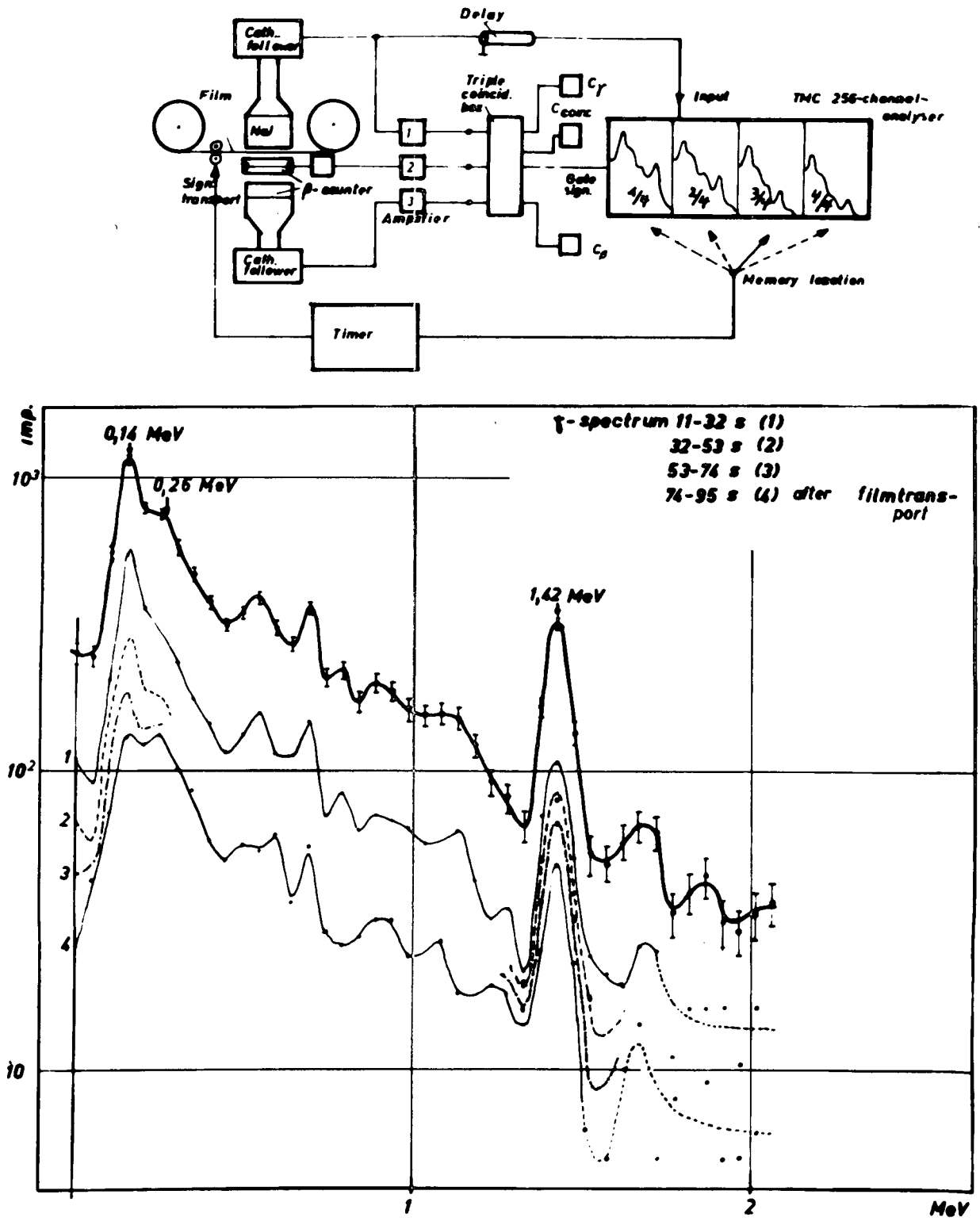

Fig. 3. The 1.42-MeV gamma line and its decay in a 4-channel time and 64-channel γ-spectrum analysis.

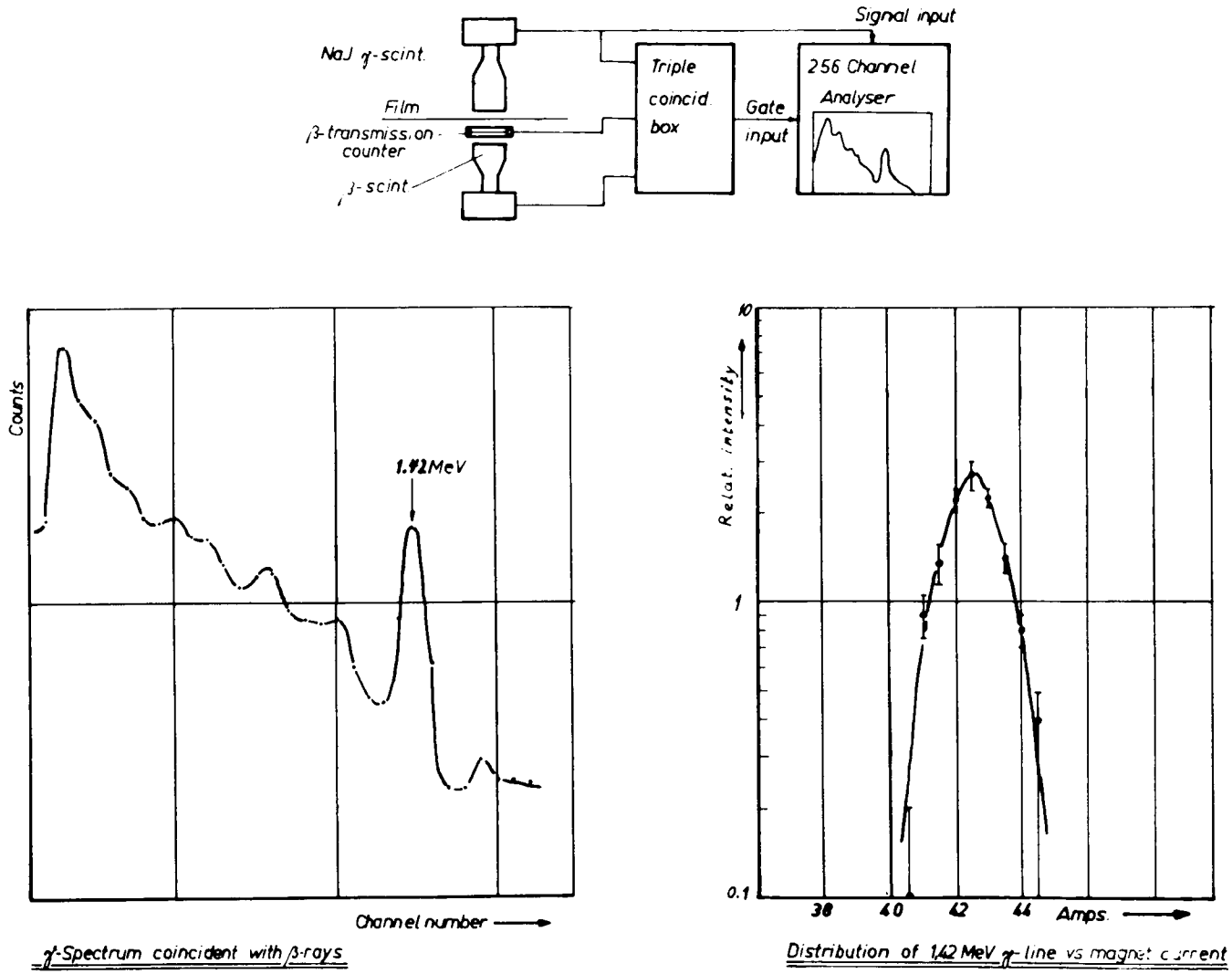

Fig. 4. Distribution of 1.42-MeV gamma line vs magnet current for a mass determination of the 1.42-MeV gamma line.

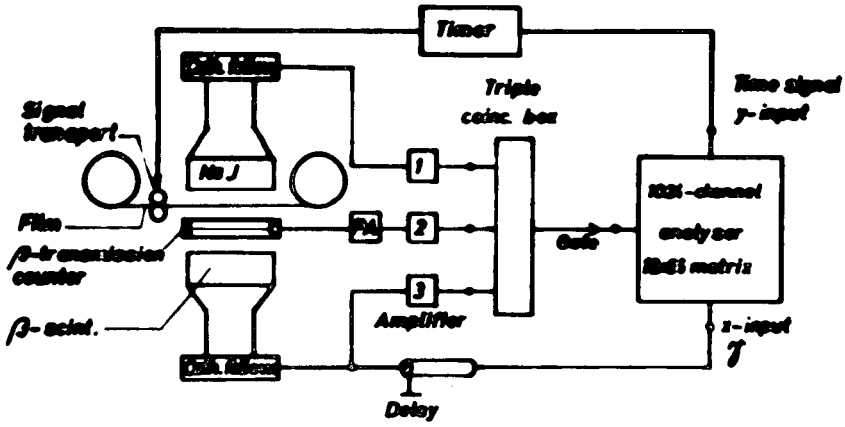

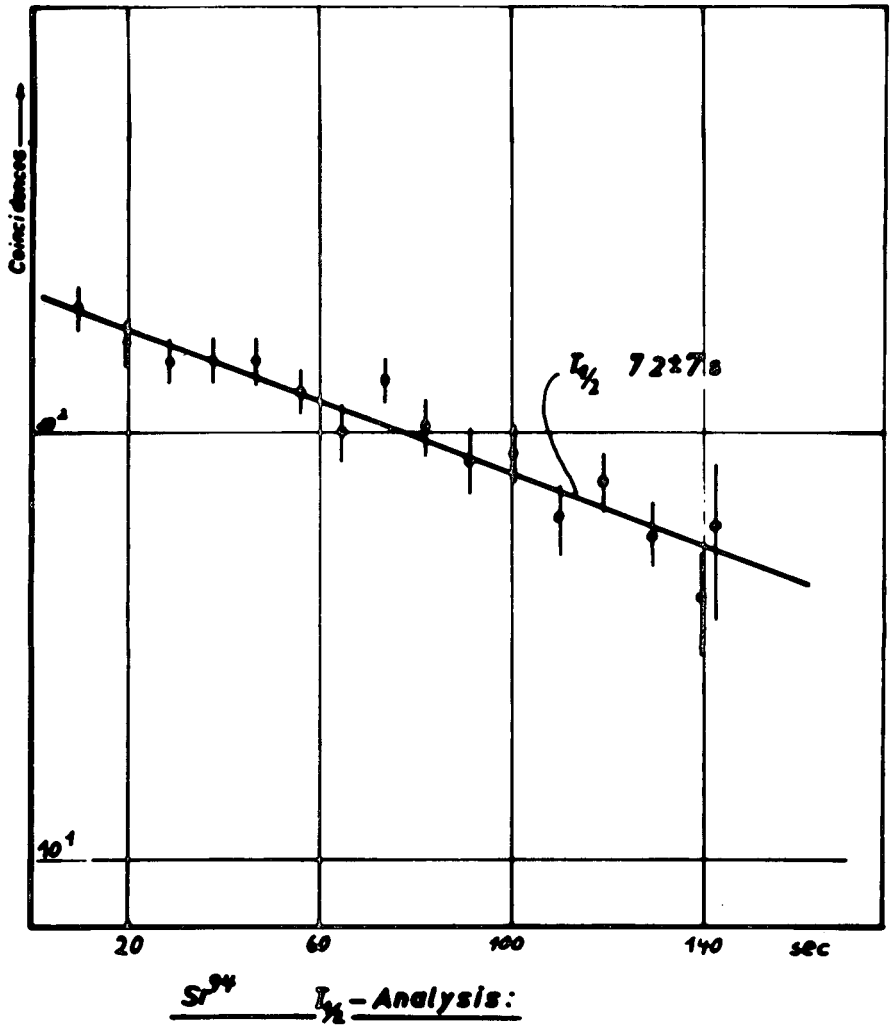

Fig. 5. Half-life analysis of the 1.42-MeV gamma line of Sr^{94} in a 16-channel time and 64-channel γ spectrum analysis.

The Q value of the $Sr^{94} \rightarrow Y^{94}$ decay has been measured by a two-dimensional 16×64 β-γ spectrum analysis (Fig. 6). The maximum energy of the β spectrum coincident with the 1.42-MeV gamma line amounts to 2.05 ± 0.1 MeV. It has been proved by a triple β-γ-γ coincidence experiment and by a two-dimensional 32×32 γ-γ spectrum analysis that no other γ line is coincident with the 1.42-MeV gamma. The Q value of the $Sr^{94} \rightarrow Y^{94}$ decay amounts to 3.45 ± 0.1 MeV.

Figure 7 gives the decay schemes of several even-even nuclides in the A = 90 region. The spin and parity assignment of the excited state of Y^{94} is unambiguous and is determined by the ft value of the β decay.

The investigation of the $Sr^{94} \rightarrow Y^{94}$ decay is the first result of a new method for the investigation of fission-product decays. The method is not restricted by any separation times, and in principle all half-lives might be investigated.

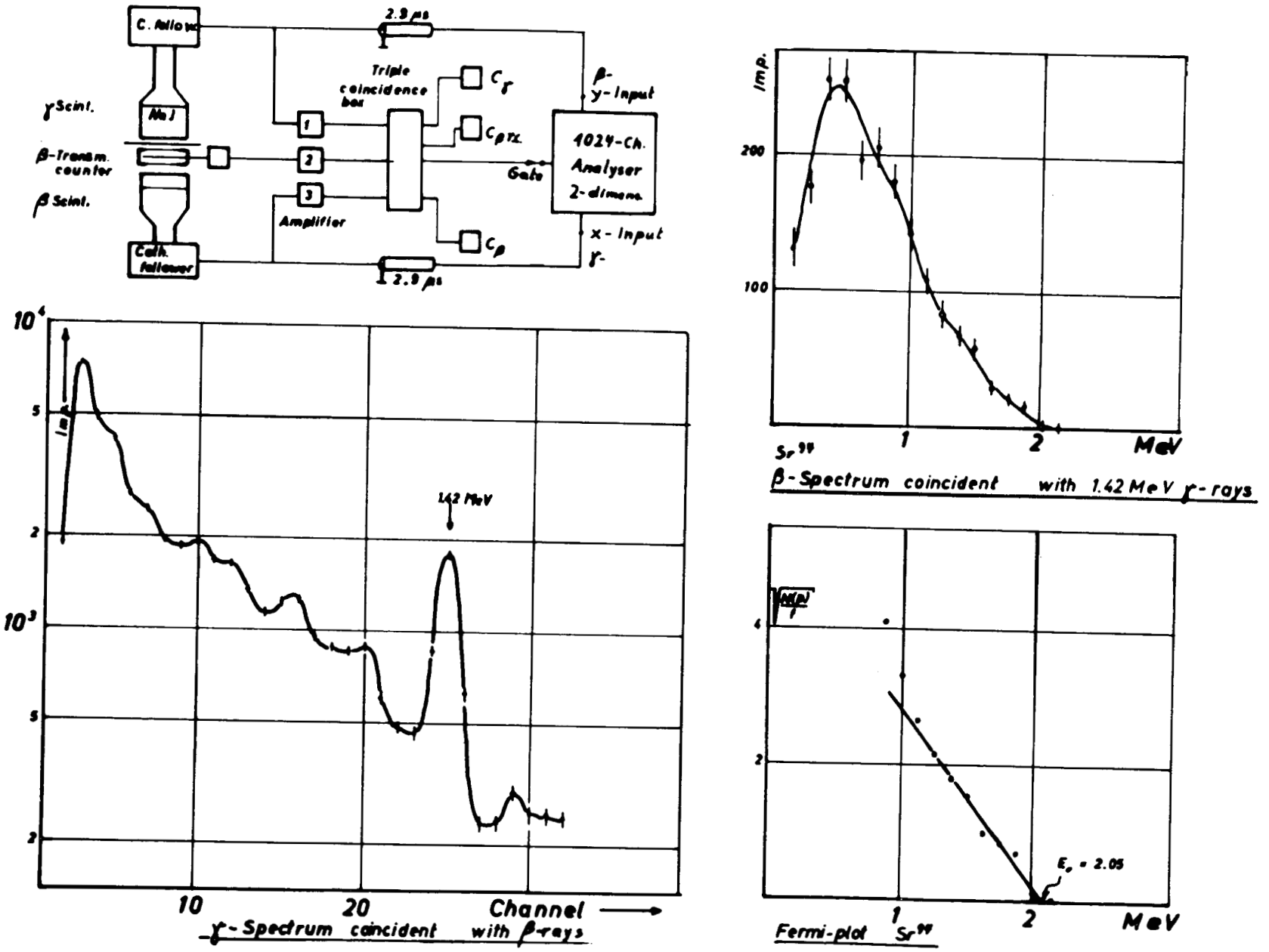

Fig. 6. Two-dimensional analysis of β-γ coincidence spectrum of Sr^{94}.

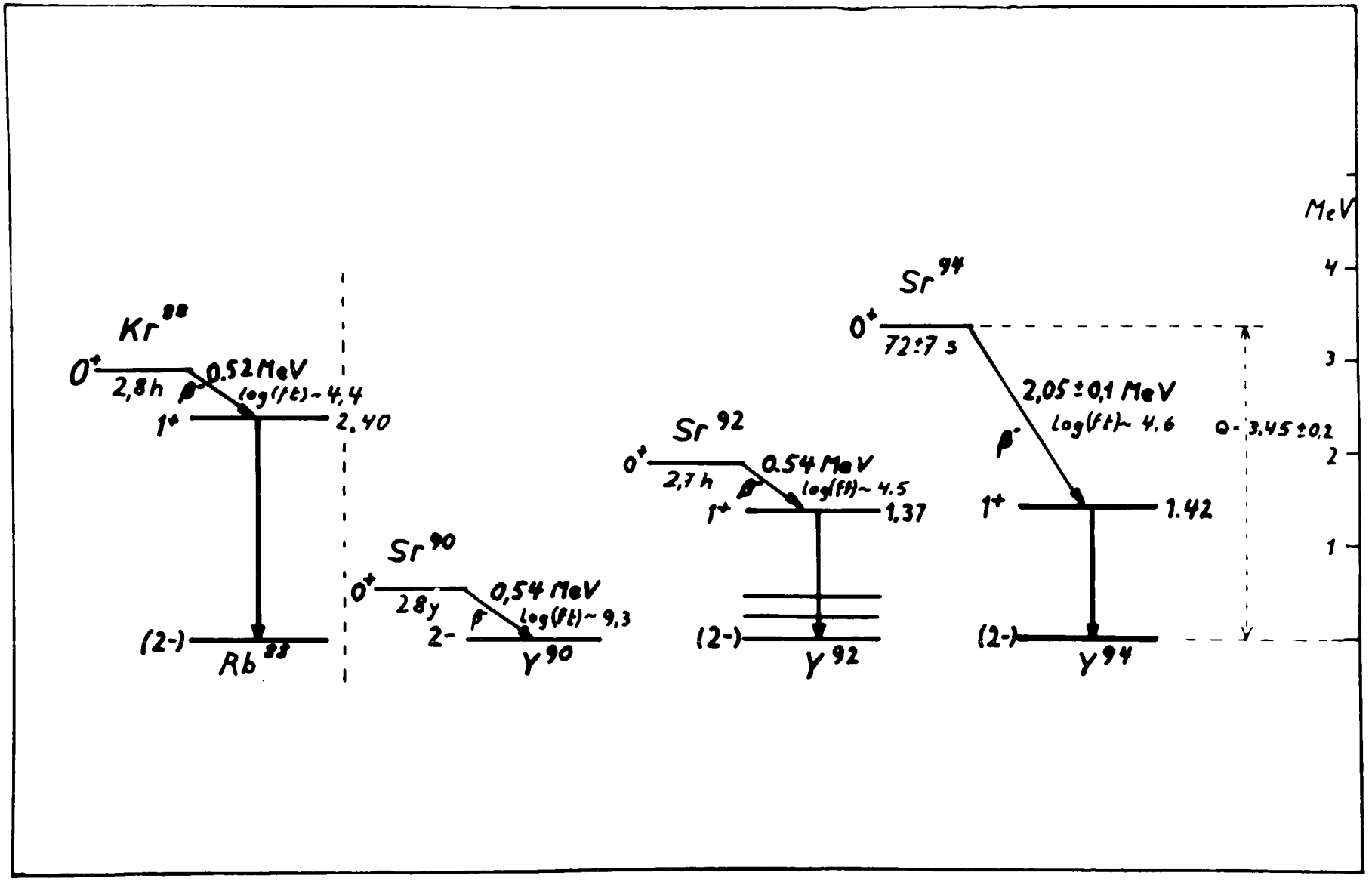

Fig. 7. Decay schemes of even-even isotopes in the mass region A ≈ 90.

V-9. INVESTIGATION OF QUASI-ADIABATIC ATOMIC COLLISIONS BY FISSION PRODUCTS*

P. Armbruster, H. Specht, and A. Vollmer

Laboratorium für Technische Physik der Technischen Hochschule München, Munich, Germany

The excitation mechanism of the inner-shell ionization has been investigated using fission products as a source of heavy ions. The excitation of L x rays when fission products are slowed down can be used to determine the primary charge of the fission products. On the other hand, fission products (heavy ions in the energy range of 10 — 100 MeV) are an excellent new means to investigate the collision mechanism in nearly adiabatic collisions.

These collisions are characterized by a disturbance of the electron orbits, which is slow compared to the velocity of the electrons in the disturbed orbits. Nearly adiabatic excitation processes are rare events. The cross section for these collisions is small and decreases rapidly with the relative velocity of the colliding atoms and the ionization energy of the electrons. Ionization of the inner electron shells by nearly-adiabatic collisions has been investigated by proton and α-particle bombardment. The work in this field has been reviewed by E. Merzbacher and H. Lewis.[1] Nearly adiabatic collisions of fast heavy ions constitute a new field. The excitation of L x rays when fission products are slowed down has been found by P. Armbruster.[2] Characteristic x rays of the target atom as well as x rays of the fission products could be detected.

---

*Presented by H. Maier-Leibnitz.

[1] E. Merzbacher and H. W. Lewis, Handb. f. Physik 34, Springer Verlag (1958).

[2] P. Armbruster, Z. Physik 166, 341 (1962).

The helium-filled magnetic mass separator,[3,4] which has been installed at the Munich 1-MW swimming-pool reactor, gives a beam of mass-separated fission products. The number of fission products is counted by a low-pressure (5 mm Hg) methane-flowed transmission proportional counter. The fission products are stopped in various stopping materials after they have passed this transmission counter. The x ray quanta produced by inner-shell ionization processes are detected by a high-resolution proportional counter. Coincidences between the fission-product signal in the transmission counter and the x-ray quanta gate a TMC multichannel analyzer in which the x-ray spectrum is registered. Figure 1 shows the experimental setup.

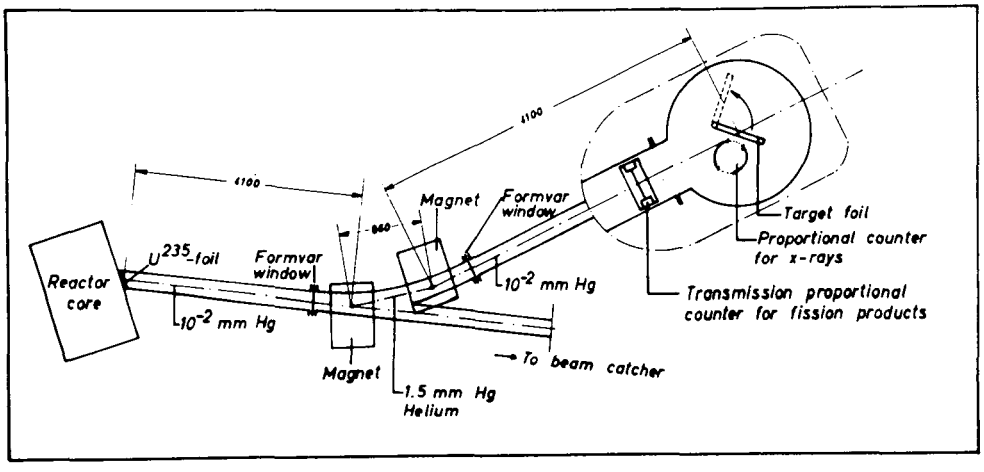

Fig. 1. Experimental setup for measurement of L x rays from fission products.

The cross section for inner-shell ionization depends on the energy of the fission pro duct, the nuclear charge of the fission product, the atomic number of the target atom, and the ionic charge of the fission product. All these parameters can easily be varied in the experimental setup.

The energy dependence of the number of detected L x ray quanta from light and heavy fission products has been measured for several

[3] C. Fulmer and B. L. Cohen, Nucl. Phys. 6, 547 (1958).

[4] P. Armbruster, Nukleonik 3, 188 (1961).

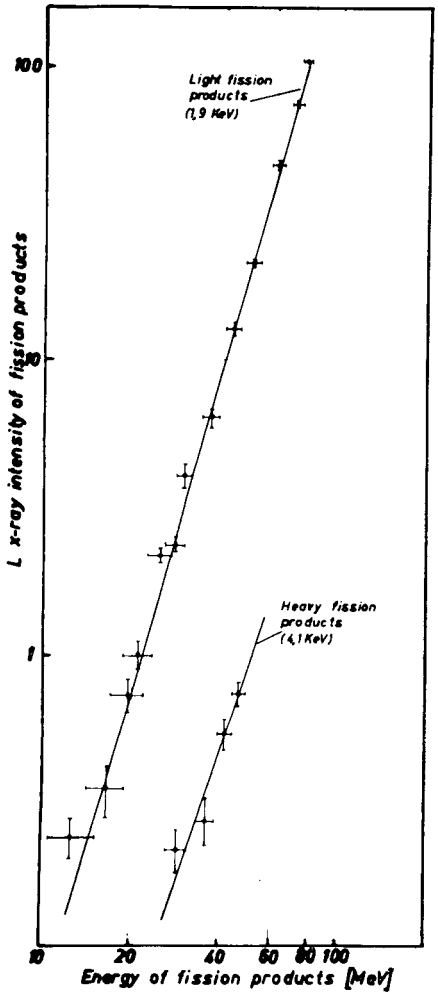

Fig. 2. Energy dependence of L-shell ionization for light and heavy fission products and a beryllium target. The L-x-ray energies of the two groups amount to 1.9 keV and 4.1 keV. The intensity is given in a relative scale.

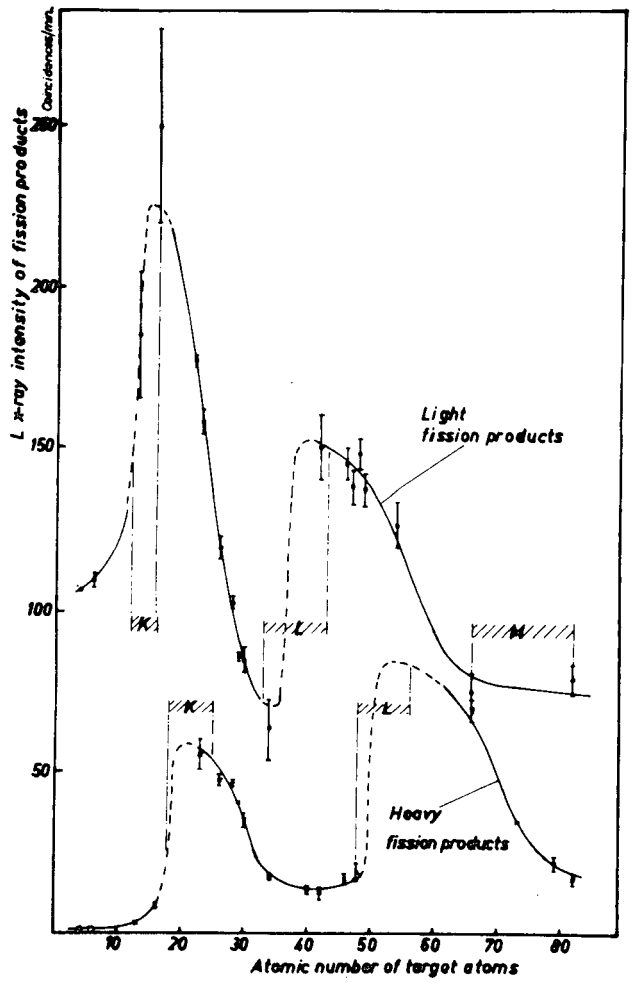

Fig. 3. L-shell ionization on a relative scale vs atomic number of stopping target for light and heavy fission products. In the shadowed regions, L x rays of fission products cannot be separated from the target radiation.

targets. Figure 2 gives the energy dependence for a beryllium target. The excitation cross section decreases rapidly with the energy of the fission products. A decrease with a high power (the third or fourth) of the fission-product energy has been found for all investigated targets.

The number of L x-ray quanta from light and heavy fission products has been measured for a constant fission-product energy (78 MeV

for the light fragment and 46 MeV for the heavy fragment) and a great number of stopping materials. Figure 3 gives the variation of the cross section for the two fission-product groups, when the atomic number of the target is varied over the periodic system. Characteristic discontinuities have been found in certain regions of the periodic system. The cross section increases if electrons in the target atoms are available which have the same energy as the L electrons of the fission products. Electron-exchange phenomena in the quasi-molecule configuration of the electron shells during the nearly-adiabatic collision seem to be responsible for the increase of the cross section.

The energy of the L x-ray quanta from 78-MeV light fission products and 46-MeV heavy fission products have been compared for a beryllium and a copper target. No dependence of the energy of the quanta on the atomic number of the stopping material was expected. Nevertheless, it has been found that the energy of the x-ray quanta of the fission products is (5.5 ± 2)% smaller in a beryllium target than in a copper target for both the fission-product groups. A definite explanation of this effect cannot be given. It might be possible that the outer screening of the Coulomb field of the nuclei, which depends on the ionic charge, is different in the two stopping materials. A calculation of the screening and its dependence on the ionic charge will decide whether the different outer screening in the two materials might be responsible for the energy difference of the x-ray quanta.

* * *

W. V. PRESTWICH, McMaster University: You mentioned that in studying fission products separated by mass, you obtain a charge distribution [Z = f(A)] from the L-x-ray energies and that this agrees with results obtained by counting betas. Have you compared your results with the radiochemical values of Wahl?

MAIER-LEIBNITZ: I think that the charge values that we get are somewhat different from all the radiochemical data that have been obtained before. From Wahl's data, the distribution looked different than what we got. It is very difficult to do a thing like that from radiochemical analysis alone.

ATTENDANCE AT THE INTERNATIONAL CONFERENCE ON NUCLEAR PHYSICS WITH REACTOR NEUTRONS

Visitors

R. Lee Aamodt
Los Alamos Scientific Laboratory
Los Alamos, New Mexico

D. B. Adler
University of Illinois
Urbana, Illinois

F. T. Adler
Physics Department
University of Illinois
Urbana, Illinois

Peter Axel
Physics Department
University of Illinois
Urbana, Illinois

George L. Ball
Physics Group
Atomic Power Development
Associates, Inc.
1911 First Street
Detroit 26, Michigan

G. A. Bartholomew
Atomic Energy of Canada Limited
Chalk River
Ontario, Canada

George B. Beard
Physics Department
Wayne State University
Detroit 2, Michigan

Gerald Ben-David
Israel Atomic Energy Commission
Yavne, Israel

Ingvar L. Bergqvist
Research Institute of National Defense
Stockholm, Sweden

Robert C. Block
Oak Ridge National Laboratory
Oak Ridge, Tennessee

Lyle B. Borst
Hochstetter Hall
State University of New York
Administration Road
Buffalo, New York

Charles D. Bowman
Lawrence Radiation Laboratory
Berkeley, California

David M. Brink
Department of Physics
Clarendon Laboratory
University of Oxford
Parks Road
Oxford, England

Harold C. Britt
Los Alamos Scientific Laboratory
Los Alamos, New Mexico

David L. Bushnell
Northern Illinois University
Department of Physics
DeKalb, Illinois

Raymon T. Carpenter
Department of Physics and
Astronomy
State University of Iowa
Iowa City, Iowa

Robert E. Carter
Los Alamos Scientific Laboratory
Los Alamos, New Mexico

R. S. Carter
National Bureau of Standards
Washington, D.C.

Robert E. Chrien
Brookhaven National Laboratory
Upton, L.I., New York

David D. Clark
Cornell University
Ithaca, New York

John W. T. Dabbs
Oak Ridge National Laboratory
Oak Ridge, Tennessee

Horace R. Danner
University of Missouri
Columbia, Missouri

William C. Dickinson
Lawrence Radiation Laboratory
Livermore, California

Dwight R. Dixon
Brigham Young University
Provo, Utah

Douglas J. Donahue
Department of Physics
University of Arizona
Tucson, Arizona

P. Fettweis
Oak Ridge National Laboratory
Oak Ridge, Tennessee

Roger W. Finlay
Ohio University
College of Arts and Sciences
Department of Physics
Athens, Ohio

David E. Fischer
Cornell University
Department of Engineering
Nuclear Reactor Laboratory
Ithaca, New York

Peter Fong
Laboratory of Nuclear Studies
Cornell University
Ithaca, New York

J. S. Fraser
Chalk River Laboratories
Chalk River
Ontario, Canada

Joseph L. Friedes
Brookhaven National Laboratory
Upton, L.I., New York

Toyojero Fuketa
Rensselaer Polytechnic Institute
Troy, New York

John D. Garrison
Brookhaven National Laboratory
Upton, L.I., New York

Newell S. Gingrich
Department of Physics
University of Missouri
Columbia, Missouri

Murrey D. Goldberg
Sigma Center
Brookhaven National Laboratory
Upton, L.I., New York

Norwood B. Gove
Nuclear Data Project
NAS-NRC
2101 Constitution Avenue
Washington, D.C.

James J. Griffin
Los Alamos Scientific Laboratory
Los Alamos, New Mexico

G. Hardie
Illinois Institute of Technology
Research Institute
3300 S. Federal
Chicago, Illinois

Kenneth Hartt
University of Missouri
Physics Department
Columbia, Missouri

John A. Harvey
Oak Ridge National Laboratory
Oak Ridge, Tennessee

Mazhar Hasan
Physics Department
Northern Illinois University
DeKalb, Illinois

E. N. Hatch
Department of Physics
Iowa State University
Ames, Iowa

Darleane C. Hoffman
Los Alamos Scientific Laboratory
Los Alamos, New Mexico

Marvin M. Hoffman
Los Alamos Scientific Laboratory
Los Alamos, New Mexico

Christoph Hofmeyer
Laboratorium für Technische Physik
Technische Hochschule
Arcisstrasse 21
Munich, Germany

Heinz Horstmann
Oak Ridge National Laboratory
Oak Ridge, Tennessee

Leonard Hughes
Department of Physics
McMaster University
Hamilton
Ontario, Canada

Hidetsugu Ikegami
Brookhaven National Laboratory
Upton, L.I., New York

Helmut Jahn
Kernforschungszentrum
Karlsruhe
7500 Karlsruhe
Postfach 947
Fernsprecher Linkenheim 81
Germany

Walter John, Jr.
Lawrence Radiation Laboratory
Livermore, California

M. W. Johns
Department of Physics
McMaster University
Hamilton
Ontario, Canada

Jean Julien
Centre D'Etudes Nucleaires de Saclay
Service de Physique Nucleaire de Basse Energie
Boite Postale No. 2
Gif-sur-Yvette (Seine-et-Oise)
France

Edward T. Jurney
Los Alamos Scientific Laboratory
Los Alamos, New Mexico

Walter R. Kane
Brookhaven National Laboratory
Upton, L.I., New York

Selig Kaplan
Lawrence Radiation Laboratory
University of California
Berkeley, California

T. J. Kennett
McMaster University
Hamilton
Ontario, Canada

E. D. Klema
Northwestern University
Evanston, Illinois

J. Warwick Knowles
Chalk River Laboratories
Chalk River
Ontario, Canada

George A. Kolstad
Physics & Mathematics Branch
USAEC
Washington, D.C.

Harry H. Landon
National Bureau of Standards
Washington, D.C.

Richard H. Lemmer
Department of Physics
Massachusetts Institute of Technology
Cambridge, Massachusetts

Marvin Lubert
DIG Nuclear Analysis
Bldg. E6, Room 219
General Electric Company
Knolls Atomic Power Laboratory
Box 1072
Schenectady, New York

Ronald D. MacFarlane
McMaster University
Hamilton
Ontario, Canada

F. C. Maienschein
Neutron Physics Division
Oak Ridge National Laboratory
Post Office Box X
Oak Ridge, Tennessee

Heinz Maier-Leibnitz
Technischen Hochschule
Arcisstrasse 21
Munich 2, Germany

S. Marshall
Rockford College
Rockford, Illinois

Rudolf Meier
Eidgenossischen Institut für
Reaktorforschung
Wuerenlingen/AG
Switzerland

Walfried Michaelis
Nuclear Spectroscopy Group
Kernforschungszentrum
Karlsruhe
7500 Karlsruhe
Postfach 947
Fernsprecher Linkenheim 81
Germany

André Michaudon
French Atomic Energy Commission
Saclay, France

Sergio Monaro
Brookhaven National Laboratory
Upton, L.I., New York

John A. Moore
Brookhaven National Laboratory
Upton, L.I., New York

M. S. Moore
Phillips Petroleum Company
Materials Testing Reactor
Idaho Falls, Idaho

Steven Moszkowski
Department of Physics
University of California
Los Angeles 24, California

Henry Motz
Los Alamos Scientific Laboratory
Los Alamos, New Mexico

C. O. Muehlhause
National Bureau of Standards
Washington, D.C.

M. Luis Muga
Chemistry Department
University of Florida
Gainesville, Florida

Herve Nifenecker
Centre d'Etudes Nucleaires de
Saclay
Boite Postale No. 2
Gif-sur-Yvette (Seine-et-Oise)
France

Sam Nilsson
Forskningsradens Laboratorium
Studsvik
Nykojseng, Sweden

Karl Ott
Kernforschungszentrum
Karlsruhe
7500 Karlsruhe
Postfach 947
Fernsprecher Linkenheim 81
Germany

L. Passell
Brookhaven National Laboratory
Upton, L.I., New York

Norman J. Pattenden
Nuclear Physics Division
Bldg. 418
AERE, Harwell
Didcot, Berks.
England

J. Reid Patterson
Department of Physics
Rockford College
Rockford, Illinois

Daniel Paya
Oak Ridge National Laboratory
Oak Ridge, Tennessee

W. V. Prestwich
McMaster University
Hamilton
Ontario, Canada

J. H. Reed
Illinois Institute of Technology
Research Institute
3300 S. Federal
Chicago, Illinois

George Rogosa
Physics & Mathematics Branch
USAEC
Washington, D.C.

Brice M. Rustad
Brookhaven National Laboratory
Upton, L.I., New York

V. L. Sailor
Brookhaven National Laboratory
Upton, L.I., New York

R. I. Schermer
Brookhaven National Laboratory
Upton, L.I., New York

Josef Johannes Schmidt
Kernforschungszentrum
Karlsruhe
7500 Karlsruhe
Postfach 947
Fernsprecher Linkenheim 81
Germany

I. G. Schröder
Brookhaven National Laboratory
Upton, L.I., New York

Otto W. B. Schult
OS/RA/Reactor DR-3
Research Establishment Risø
Roskilde, Denmark

G. Schupp
U. S. Rubber Company

K. K. Seth
Department of Physics
Northwestern University
Evanston, Illinois

F. B. Simpson
Phillips Petroleum Company
Materials Testing Reactor
Idaho Falls, Idaho

Willard Skolnik
Knolls Atomic Power Laboratory
Schenectady, New York

G. G. Slaughter
Physics Division
Oak Ridge National Laboratory
Oak Ridge, Tennessee

T. Soda
University of Chicago
Chicago, Illinois

R. R. Spencer
Phillips Petroleum Company
Materials Testing Reactor
Idaho Falls, Idaho

Daniel Sperber
Illinois Institute of Technology
Research Institute
3300 S. Federal
Chicago, Illinois

Louis G. Stang, Jr.
Hot Laboratory Division
Brookhaven National Laboratory
Upton, L.I., New York

William E. Stein
Los Alamos Scientific Laboratory
Los Alamos, New Mexico

Martin O. Stern
General Atomics
P. O. Box 608
San Diego 12, California

Richard H. Stokes
Los Alamos Scientific Laboratory
Los Alamos, New Mexico

Warren F. Stubbins
Nuclear Science and Engineering
University of Cincinnati
The Graduate School
Cincinnati 21, Ohio

George C. Summerfield
College of Engineering
University of Michigan
Ann Arbor, Michigan

R. H. Tabony
Duke University
Durham, North Carolina

W. L. Talbert
Department of Physics
Iowa State University
Ames, Iowa

C. W. Terrell
Illinois Institute of Technology
Research Institute
3300 S. Federal
Chicago, Illinois

C. L. Thader
Atomic Energy Establishment
Trombay
Apollo Pier Road
Bombay, India

R. M. Thaler
Department of Physics
Case Institute of Technology
Cleveland 6, Ohio

Clifford W. Tompson
University of Missouri
Columbia, Missouri

William F. Vogelsang
College of Engineering
University of Wisconsin
1513 University Avenue
Madison 5, Wisconsin

Richard H. Vogt
U.S. Naval Research Laboratory
Washington, D.C.

F. J. Walter
Oak Ridge National Laboratory
Oak Ridge, Tennessee

Oren A. Wasson
Physics Department
Yale University
New Haven, Connecticut

Donald H. White
University of California
Lawrence Radiation Laboratory
Livermore, California

Lawrence Wilets
Department of Physics
University of Washington
Seattle, Washington

C. W. Williams
Oak Ridge National Laboratory
Oak Ridge, Tennessee

Claude S. Williamson
Nuclear Physics Department
University of Washington
Seattle, Washington

S. G. Wogulis
Atomics International
Box 309
Canoga Park, California

A. I. Yavin
University of Illinois
Urbana, Illinois

R. C. Young
Phillips Petroleum Company
Materials Testing Reactor
Idaho Falls, Idaho

D. J. Zaffarano
Department of Physics
Iowa State University
Ames, Iowa

Argonne Staff

L. M. Bollinger
Herbert H. Bolotin
Thomas H. Braid
Merle T. Burgy
S. B. Burson
Dorothy Carlson
William Childs
Fritz Coester
Stanley Cohen
Donald W. Connor
Robert E. Coté
D. L. Davis
Alexander DeVolpi
Charles Eggler
Hans Ekstein
Alexander Elwyn
C. A. Engelbrecht
John Erskine
P. R. Fields
A. M. Friedman
Donald S. Gemmell
L. E. Glendenin
L. S. Goodman
Henry C. Griffin
Melvin Hack
Morton Hamermesh
H. S. Hans
L. Heaton
Juergen Heberle
C. T. Hibdon
R. E. Holland
J. R. Huizenga
D. R. Inglis
Harold E. Jackson
C. N. Kelber
H. W. Knott
A. B. Krisciunas
Victor Krohn
Dieter Kurath
Raymond O. Lane
Alexander Langsdorf, Jr.
Robert Lawson
Linwood L. Lee
H. J. Lipkin
Frank J. Lynch
Malcolm Macfarlane
Allen P. Magruder
Amnon Marinov
J. P. Marion
Leon Markheim
Luise Meyer
Peter A. Moldauer
James Monahan
F. P. Mooring
M. H. Mueller
Arthur Namenson
Gilbert Perlow
Murray Peshkin
K. G. Porges
Richard Preston
Sol Raboy
W. C. Redman
G. R. Ringo
Norbert Rosenzweig
John P. Schiffer
R. E. Segel

E. Brooks Shera
S. S. Sidhu
P. P. Singh
A. B. Smith
R. K. Smither
E. P. Steinberg
J. C. Taylor
G. E. Thomas
F. E. Throw
Carroll C. Trail
H. K. Vonach
W. G. Vonach
Dieter von Ehrenstein
James Wing
Jan L. Yntema